UNIVERSIDADE FEDERAL DE MINAS GERAIS

Tese de Doutorado em Microbiologia

OCORRÊNCIA, ABUNDÂNCIA E EXPRESSÃO DE GENES ASSOCIADOS A VIAS DE TRADUÇÃO EM *MIMIVÍRUS* E EM TUPANVÍRUS, OS MAIS NOVOS GIGANTES DE AMEBAS CARACTERIZADOS

Lorena Christine Ferreira da Silva

Belo Horizonte

2017

Lorena Christine Ferreira da Silva

OCORRÊNCIA, ABUNDÂNCIA E EXPRESSÃO DE GENES ASSOCIADOS A VIAS DE TRADUÇÃO EM *MIMIVÍRUS* E TUPANVÍRUS, OS MAIS NOVOS GIGANTES DE AMEBAS CARACTERIZADOS

Tese de Doutorado apresentada ao Programa de Pós-Graduação em Microbiologia da Universidade Federal de Minas Gerais, como requisito parcial para a obtenção do título de Doutor em Microbiologia.

Orientador: Jônatas Santos Abrahão
Coorientador: Flávio Guimarães da Fonseca
Supervisor: Bernard La Scola

Belo Horizonte
2017

DEDICATÓRIA

A Deus, Nossa Senhora Aparecida e minha família...

Percebe e entende que os melhores amigos
São aqueles que estão em casa, esperando por ti
Acredita, nos momentos mais difíceis da vida
Eles sempre estarão por perto pois só sabem te amar
E se por acaso a dor chegar, ao teu lado vão estar
Pra te acolher e te amparar.
Pois, não há nada como um lar

Tua família, volta pra ela
Tua família te ama e te espera.
Para ao teu lado sempre estar
Tua família

Às vezes muitas pedras surgem pelo caminho
Mas em casa alguém feliz te espera, pra te amar
Não, não deixe que a fraqueza tire a sua visão
Que um desejo engane o teu coração
Só Deus não é ilusão
E se por acaso a dor chegar, ao teu lado vão estar
Pra te acolher e te amparar
Pois não há nada como o lar.

Tua família volta pra ela
Tua família te ama e te espera
Para ao teu lado sempre estar
Tua família
Nossa família

(Tua família – Anjos de Resgate).

AGRADECIMENTOS

A Deus e Nossa Senhora Aparecida em primeiro lugar. Obrigada por terem me guiado durante todo o caminho. Quando eu fraquejei e tive medo foi Deus que me levantou. Amadureci muito na fé durante estes quatro anos, principalmente enquanto estive na França. Só Deus para dar força, calma, paciência e sabedoria para seguir em frente, superar os obstáculos e as dificuldades, sempre me iluminando em direção a mais esta conquista. E Nossa Senhora sempre cuidando de mim, como minha mãe sempre diz "Quando eu não posso cuidar, Ela cuida!". Pode esperar minha tese na Sala das Promessas ano que vem, mãezinha. ".... Tudo é do Pai, toda Honra e toda Glória... É dele a vitória alcançada em minha vida!"

Aos meus pais e meu irmão, pela força, paciência e amor incondicional. Por terem suportado meu stress, pela ajuda financeira, pela palavra amiga nos momentos que mais precisei, por sempre terem acreditado em mim, por serem os que mais torceram por esta vitória. Um ano longe durante o Doutorado sanduíche foi difícil, mas vencemos e fortificamos mais ainda os nossos laços. Amo vocês!

Ao professor Dr. Jônatas Abrahão, além de orientador, um amigo! Obrigada pela brilhante orientação desde a Especialização, Jonska! Nosso tempo juntos na França também foi incrível! Obrigada por todo conhecimento e crescimento que me proporcionou. Sempre paciente, amigo e tão presente no dia-a-dia dos alunos. Uma grande inspiração para todos nós. Espero um dia poder inspirar pessoas como vocês faz!

Aos membros da banca, por terem aceitado fazer parte e contribuírem para o enriquecimento do trabalho.

Aos demais professores do Laboratório de Vírus: Prof. Erna, Prof. PP, Prof, Cláudio, Prof. Gi e Prof. Betânia. Obrigada por toda orientação, incentivo e até mesmo broncas. Obrigada pela preocupação em formar pessoas!!! Esse Laboratório é especial demais, meu orgulho!!! Vou levar o nome dele pra onde for...

Aos amigos do Laboratório de Vírus. Tantas personalidades diferentes, às vezes nos desentendemos, mas no fim, acaba sendo bom demais estar com vocês todos os dias!! Tenho um carinho especial por cada um. Sem citar nomes, mas cada um sabe quão especial é pra mim. Enquanto estive fora aprendi a dar ainda mais valor a nossa convivência no Laboratório... Nossos cafés, reuniões, festinhas... Lá fora nunca será igual!!! Amo ser Labvírus!!! Pra sempre!!!

Aos colegas do laboratório francês, em especial Issam (meu chouchou) e Lina. E ao meu orientador Bernard La Scola! Obrigada pela convivência e toda ajuda durante o meu sanduíche. Merci beaucoup!

A todos os funcionários do ICB e UFMG por toda ajuda!

As agências de fomento pelo apoio financeiro!

A todos os mestres que tive durante toda minha vida estudantil e acadêmica! Amo demais meus professores! Foram e são fundamentais para o meu sucesso neste caminho que escolhi.

Aos meus professores de línguas, inglês e francês! Thank you e Merci beaucoup!

À minha grande família querida, que sempre esteve comigo. Tias, tios, primos, avó, padrinhos, meu afilhado lindo... Obrigada por me fortaleceram com suas orações e apoio.

Aos amigos da vida que tornam tudo mais leve. Amo vocês!!! Os amigos aqui do Brasil e agora, os amigos estrangeiros... Cada um contribuiu a sua maneira para que eu chegasse até aqui... Obrigada!

"Aqueles que passam por nós, não vão sós, não nos deixam sós. Deixam um pouco de si, levam um pouco de nós."

Antoine de Saint-Exupéry

EPÍGRAFE

"A percepção do desconhecido é a mais fascinante das experiências. O homem que não tem os olhos abertos para o misterioso passará pela vida sem ver nada."

Albert Einstein

RESUMO

Nos últimos anos, vários vírus gigantes de DNA foram identificados nos mais diversos ambientes. A presença de características peculiares e distintas daquelas vistas na maioria dos vírus até então conhecidos despertaram grande interesse por parte da comunidade científica em relação a este grupo. Em 2003, *Acanthamoeba polyphaga mimivirus* (APMV) foi identificado e surpreendentemente, alguns dos genes codificados por seu grande genoma são relacionados com processos de tradução protéica. Tais genes nunca haviam sido observados em outros vírus na ocasião da descoberta, sendo considerados exclusivos de organismos celulares e até o momento sem o significado biológico para APMV elucidado. Atualmente, sabe-se que outros isolados de vírus gigantes apresentam também arsenal gênico que codifica elementos envolvidos com tradução. Diante disso, este estudo teve o objetivo de prospectar e caracterizar novos isolados de vírus gigantes em amostras ambientais, bem como aumentar a compreensão acerca do papel de genes relacionados à tradução nestes e em mimivírus já isolados. Para isso, foi utilizada a plataforma de isolamento em amebas e os isolados obtidos foram caracterizados biologicamente e geneticamente. Dois vírus com estrutura única nunca antes observada foram isolados e chamados de Tupanvirus. Tais vírus apresentam um capsídeo associado a uma longa cauda podendo atingir 2.3μm, sendo, portanto, a mais longa partícula viral já observada. Um dos isolados mostrou a capacidade de se multiplicar em um amplo espectro de células de protozoários, como várias espécies dentro do gênero *Acanthamoeba*, *Vermoamoeba vermiformis*, entre outras, algo nunca descrito na literatura, uma vez que os vírus gigantes conhecidos apresentam um espectro de hospedeiro muito restrito. Para análises genéticas, o sequenciamento completo dos genomas das duas amostras foi feito, revelendo genomas com ~1,4 mega pares de bases e permitindo a análise dos genes relacionados à tradução que estão presentes em abundância nestes isolado, que parecem ter sido adquiridos de forma independente de organismos celulares, como ressaltam as análises filogenéticas. Os tupanvirus apresentaram o mais completo conjunto de genes de tradução da virosfera, com 20 aminoacil-tRNA sintetase, ~70 tRNAs e dezenas de outros fatores associados a tradução protéica. Por fim, a análise da expressão de genes relacionados à tradução em diferentes mimivírus, realizada por PCR em tempo real, indicou que estes são diferencialmente expressos de acordo com as condições de infecção e diferenças genéticas entre diferentes isolados. Os dados aqui apresentados contribuem para uma melhor compreensão acerca da origem, abundância, diversidade e expressão de genes associados à tradução, presente nos mimivírus e tupanvírus.

Palavras chave: *Mimiviridae.* Isolamento. Caracterização. RNA transportadores. Aminoacil tRNA sintetases. Tradução.

ABSTRACT

In recent years, several DNA giant viruses have been identified. The presence of peculiar and distinct characteristics not seen in most previously known viruses, aroused interest in the scientific community regarding this group. In 2003, *Acanthamoeba polyphaga mimivirus* (APMV) was identified and interestingly some of the genes encoded by its large genome are related to translation process. These genes were considered exclusive of cellular organisms and have never been observed in other viruses. The biological relevance of their expression to APMV is still unknown. Currently, it is known that other giant virus isolates also present genes encoding elements involved in translation. Thus, this study aimed to prospect and characterize new giant viruses isolates in environmental samples and to increase the comprehension about the role of translation-associated genes in both new and previously isolated mimivíruses. Two viruses with morphology never seen were observed and called Tupanvirus. These viruses presenting a capsid associated to a long tail, being able to reach 2.3 µm, being the longest viral particle already observed. One of the isolates possesses the ability to multiply in a broad spectrum of protozoa cells, as some species from the *Acanthamoeba* genus, *Vermoamoeba vermiformis* and others, something never described in the literature, since the known giant viruses have a very restrict host spectrum. Full genome sequencing of the two isolated Tupanviruses was performed and showed genomes with ~1,4 mega pair bases and allowed to analyse translation-associated genes, present in abundance in these isolates. Our phylogenetic analysis emphasize that they were acquired independently of cellular organisms. Tupanviruses present the most complete set of translation-associated genes in the virosphere, with 20 aminoacyl-tRNA synthetases, 70 tRNAs and dozens of other factors associated with translation. Finally, the expression of translation-associated genes after infection with different mimivírus was assessed by real-time PCR and indicated that these are differentially expressed according to the infection conditions and genetic variances between different isolates. The data presented here contribute to a better understanding about the origin, abundance, diversity and expression of genes associated with translation, present in mimivírus and tupanvirus.

Key words: *Mimiviridae*. Isolation. Characterization. Tranfers-RNA. Aminoacyl-tRNA synthetases. Translation.

LISTA DE TABELAS

TABELA 1: RESUMO DE DIFERENTES VÍRUS GIGANTES ASSOCIADOS A AMEBAS ISOLADOS NOS ÚLTIMOS ANOS. 13

TABELA 2: ELEMENTOS RELACIONADOS À TRADUÇÃO EM ISOLADOS REPRESENTATIVOS DE CADA GRUPO OU FAMÍLIA 23

TABELA 3: COLEÇÃO DE AMOSTRAS PARA PROSPECÇÃO 35

TABELA 4: RESULTADO DA PROSPECÇÃO EM DIFERENTES AMEBAS 48

TABELA 5: PERFIL DE PERMISSIVIDADE DE TPVSL EM DIFERENTES CÉLULAS DE PROTOZOÁRIOS. 57

TABELA 6: GENES DE ELEMENTOS RELACIONADOS À TRADUÇÃO PRESENTES EM TPVDO 62

TABELA 7: SEQUÊNCIAS DOS INICIADORES DESENHADOS PARA PCR EM TEMPO REAL 68

LISTA DE ILUSTRAÇÕES

FIGURA 01: PARTÍCULAS DE APMV NO INTERIOR DE UMA AMEBA DE VIDA LIVRE. 05

FIGURA 02: APMV VISUALIZADO ATRAVÉS DE MICROSCOPIA ELETRÔNICA DE TRANSMISSÃO. 06

FIGURA 03: VIRÓFAGO NA PARTÍCULA DE ACMV VISUALIZADO ATRAVÉS DE MICROSCOPIA ELETRÔNICA DE TRANSMISSÃO. 07

FIGURA 04: IMAGEM OBTIDA ATRAVÉS DE PROJEÇÃO COMPUTACIONAL BASEADA EM CRIO-MICROSCOPIA ELETRÔNICA EVIDENCIA A ESTRUTURA DE APMV. 09

FIGURA 05: CICLO DE MULTIPLICAÇÃO DE APMV EM *A. CASTELLANII*. 11

FIGURA 06: MORFOLOGIA DE *MARSEILLEVIRUS MARSEILLEVIRUS*. 15

FIGURA 07: MORFOLOGIA DE MIMIVÍRUS, PANDORAVÍRUS, PITHOVÍRUS E MOLLIVIRUS SIBERICUM. 16

FIGURA 08: MORFOLOGIA DE FAUSTOVIRUS E12, KAUMOEBAVIRUS E PACMANVIRUS. 18

FIGURA 09: MORFOLOGIA DO CEDRATVIRUS. 18

FIGURA 10: ANÁLISE FILOGENÉTICA DOS KLOSNEUVÍRUS. 20

FIGURA 11: ISOLADOS DE SOLOS DE LAGOAS ALCALINAS VISUALIZADOS POR MICROSCOPIA DE CONTRASTE NEGATIVO. 49

FIGURA 12: ISOLADO DE SOLO OCEÂNICO VISUALIZADO POR MICROSCOPIA DE CONTRASTE NEGATIVO. 50

FIGURA 13: COLORAÇÃO HEMACOLOR® EM AMEBAS. 51

FIGURA 14: PARTÍCULA DE TUPANVIRUS SODA LAKE. 53

FIGURA 15: CICLO DE MULTIPLICAÇÃO DE TUPANVIRUS SODAL LAKE EM *A. CASTELLANII* VISUALIZADO POR MET. 54

FIGURA 16: CICLO DE MULTIPLICAÇÃO DE TPVSL EM *A. CASTELLANII* POR IF. 55

FIGURA 17: ECP DE TPVSL EM DIFERENTES CÉLULAS. 58

FIGURA 18: RIZOMA DO GENOMA DE TUPAN VIRUS DEEP OCEAN. 59

FIGURA 19: FILOGENIA PARA O GENE DA DNA POLIMERASE B. 60

FIGURA 20: ANÁLISE DE REDES: RNA TRANSPORTADORES. 61

FIGURA 21: ANÁLISE DE REDES: AMINOACIL-TRNA SINTETASES. 61

FIGURA 22: ANÁLISE DE REDES: FATORES ENVOLVIDOS EM BIOSSÍNTESE PROTÉICA. 64

FIGURA 23: ANÁLISE COMPARATIVA DE USO DE CÓDONS E AMINOÁCIDOS POR DIFERENTES MIMIVÍRUS E *A. CASTELLANII*. 65

FIGURA 24: CURVAS-PADRÃO PARA TRNA. 67

FIGURA 25: CURVAS-PADRÃO PARA AARS. 65

FIGURA 26: NÍVEL DE MRNA DE RNA HELICASE VIRAL POR DIFERENTES MIMIVÍRUS EM AMEBAS INFECTADAS SOB DIFERENTES CONDIÇÕES NUTRICIONAIS. 69

FIGURA 27: NÍVEL DE MRNA DE TRNA POR DIFERENTES MIMIVÍRUS EM AMEBAS INFECTADAS EM DIFERENTES CONDIÇÕES NUTRICIONAIS. 71

FIGURA 28: NÍVEL DE MRNA DE AARS POR DIFERENTES MIMIVÍRUS EM AMEBAS INFECTADAS SOB DIFERENTES CONDIÇÕES NUTRICIONAIS. 73

FIGURA 29: EXPRESSÃO DE AARS POR DIFERENTES MIMIVÍRUS EM AMEBAS INFECTADAS SOB DIFERENTES CONDIÇÕES NUTRICIONAIS. 74

FIGURA 30: MULTIPLICAÇÃO DE MIMIVÍRUS EM AMEBAS CULTIVADAS EM CONDIÇÕES NUTRICIONAIS DISTINTAS. 76

FIGURA 31: REPRESENTAÇÃO ESQUEMÁTICA DO GENE R663 (ARGINIL-RS) EM DIFERENTES MIMIVÍRUS. 77

LISTA DE ANEXOS

ANEXO 01: RECEITA PYG 109

ANEXO 02: RECEITA PAS 110

ANEXO 03: RECEITA TS 111

ANEXO 04: TABELA DE CÓDONS E SIGLAS DE AMINOÁCIDOS 112

ANEXO 05: TABELA DE ANTICÓDONS PARA OS TRNA DE TUPANVIRUS DEEP OCEAN 115

ANEXO 06: ANÁLISES FILOGENÉTICAS DAS AARS DE TUPANVÍRUS 117

ANEXO 07: POLIMORFISMOS APRESENTADOS NOS GENES DE TRNA E AARS DE APMV, APMV M4, SMBV, KROV E OYTV 137

ANEXO 08: ARTIGOS PUBLICADOS DURANTE O DOUTORADO 144

LISTA DE SIGLAS E ABREVIATURAS

µm - micrômetro

aaRS – aminoacil-tRNA-sintetase

Acanthamoeba castellanii - *A. castellanii*

Acanthamoeba griffini - *A. griffini*

Acanthamoeba micheline - *A. micheline*

Acanthamoeba polyphaga - *A. polyphaga*

Acanthamoeba royreba - *A. royreba*

Acanthamoeba sp E4 - *A. sp E4*

ACMV – *Acanthamoeba castellanii mamavirus*

AMZV – *Amazonia virus*

APMV - *Acanthamoeba polyphaga mimivirus*

APMV M4 - *Acanthamoeba polyphaga mimivirus* M4

AVL – amebas de vida livre

cDNA – DNA complementar

Dictyostelium discoideum - *D. discoideum*

ECP – efeito citopático

GEPVIG – grupo de estudo e prospecção de vírus gigantes

h.p.i – horas pós infecção

IF – Imunofluorescência

Kb – kilo pares de bases

KROV – Kroon virus

Mb – mega pares de bases

m.o.i.- multiplicidade de infecção

MET – microscopia eletrônica de transmissão

MPAA – microorganismos patogênicos associados a amebas

mRNA – RNA mensageiro

m.o.i – mulplicidade de infecção

NCLDV - Vírus grandes núcleo-citoplasmáticos de DNA

NYMV – Niemeyer virus

ORF – fase aberta de leitura

OYTV – Oyster virus

PAS – solução salina para amebas

PBS – solução salina fosfatada

PCR – reação em cadeia da polimerase

PYG – meio protease peptona extrato de levedura e glicose

SFB – soro fetal bovino

SMBV – Samba virus

Tetrahymena hyperangularis - *T. hyperangularis*

TF – fator de tradução

TGH – transferência gênica horizontal

TPV – Tupanvirus

TPVdo – Tupanvirus deep ocean

TPVsl – Tupanvirus soda lake

Trichomonas tenax - *T. tenax*

tRNA – RNA transportador

Vermoamoeba vermiformis - *V. vermiformis*

Willaertia magna - *W. magna*

SUMÁRIO

DEDICATÓRIA ..... **III**

AGRADECIMENTOS ..... **IV**

EPÍGRAFE ..... **VI**

RESUMO ..... **VII**

ABSTRACT ..... **VIII**

LISTA DE TABELAS ..... **IX**

LISTA DE ILUSTRAÇÕES ..... **X**

LISTA DE ANEXOS ..... **XIII**

LISTA DE SIGLAS E ABREVIATURAS ..... **XIV**

I- INTRODUÇÃO **1**

1.1 Vírus grandes núcleo-citoplasmáticos de DNA 1

1.2 Amebas de vida livre e outros protozoários 2

1.3 Família *Mimiviridae* 4

1.4 Estrutura, genoma e ciclo de multiplicação: características dos mimivírus 8

1.5 Outros vírus gigantes isolados recentemente 12

1.6 Elementos relacionados à tradução em vírus gigantes 20

II- JUSTIFICATIVA **27**

III- OBJETIVOS **29**

3.1 Objetivo geral 29

3.2 Objetivos específicos 29

3.2.1 Prospecção e caracterização de vírus gigantes *29*

3.2.2 Modulação do nível de mRNA de genes relacionados à tradução em resposta a disponibilidade nutricional durante a infecção de mimivírus em A. castellanii *29*

IV- FLUXOGRAMAS DE TRABALHO **31**

V- MATERIAIS E MÉTODOS **32**

5.1 Prospecção e caracterização de vírus gigantes 32

5.1.1 Sistemas celulares *32*

5.1.2 Multiplicação e purificação viral (Abrahão et al. 2014; Abrahão et al. 2016) *33*

5.1.3 Titulação viral (Reed e Muench, 1938) *33*

5.1.4 Processamento de amostras *34*

5.1.5 Tentativa de isolamento *35*

5.1.6 Caracterização inicial: microscopia de contraste negativo e Hemacolor® *36*

5.1.7 Microscopias *36*

5.1.8 Permissividade em outros sistemas celulares *37*

5.1.9 Análises de genoma *37*

5.1.10 Análises de redes *38*

5.1.11 Análises filogenéticas *39*

5.2 MODULAÇÃO DO NÍVEL DE MRNA DE GENES RELACIONADOS À TRADUÇÃO EM RESPOSTA A DISPONIBILIDADE NUTRICIONAL DURANTE A INFECÇÃO DE MIMIVÍRUS EM *A. CASTELLANII* 39

5.2.1 Sistemas celulares *39*

5.2.2 Vírus *40*

5.2.3 Multiplicação e purificação viral (Abrahão et al. 2014; Abrahão et al. 2016) *40*

5.2.4 Titulação viral (Reed e Muench, 1938) *41*

5.2.5 Uso de códons e aminoácidos *41*

5.2.6 Padronização de PCR em tempo real *41*

5.2.7 Infecções em diferentes condições nutricionais *42*

5.2.8 Extração de RNA, transcrição reversa e PCR em tempo real *43*

5.2.9 Curva de ciclo único *44*

5.2.10 Análise de polimorfismos em tRNA e aaRS de mimivírus *44*

5.2.11 Análises estatísticas *45*

VI- RESULTADOS **46**

6.1 PROSPECÇÃO E CARACTERIZAÇÃO DE VÍRUS GIGANTES 47

6.1.1 Prospecção e isolamento *47*

6.1.2 Caracterização inicial das amostras positivas *48*

6.1.3 Tupanvirus soda lake: morfologia *52*

6.1.4 Tupanvirus soda lake: ciclo de multiplicação *53*

6.1.5 Tupanvirus soda lake: Permissividade de diferentes células de protozoários ao novo vírus *56*

6.1.6 Tupanvirus deep ocean: características do genoma *58*

6.1.7 Tupanvirus deep ocean: análise de genes envolvidos com tradução *61*

6.1.8 Aminoacil-tRNA sintetases em vírus gigantes: análises filogenéticas *66*

6.2 MODULAÇÃO DO NÍVEL DE MRNA DE GENES RELACIONADOS À TRADUÇÃO EM RESPOSTA A DISPONIBILIDADE NUTRICIONAL DURANTE A INFECÇÃO DE MIMIVÍRUS EM *A. CASTELLANII* 66

6.2.1 Perfil de utilização de códons e aminoácidos em Mimiviridae *66*

6.2.2 Padronização de PCR em tempo real *68*

6.2.3 Expressão do nível de mRNA de elementos relacionados à tradução em Mimiviridae *71*

6.2.4 Perfil de multiplicação de mimivírus em diferentes condições nutricionais *75*

6.2.5 Polimorfismos em genes envolvidos em tradução em mimivírus *77*

VII- DISCUSSÃO 78

VIII- CONCLUSÕES 90

IX- ATIVIDADES DESENVOLVIDAS NO PERÍODO 92

9.1 Doutorado sanduíche 92

9.2 Eventos 92

9.3 Artigos completos publicados em periódicos (Anexo 8) 92

9.4 Capítulo de livro publicado 94

REFERÊNCIAS BIBLIOGRÁFICAS 95

ANEXOS 110

Anexo 1 – Receita PYG 110

Anexo 2 – Receita PAS 111

Anexo 3 – Receita TS 112

Anexo 4 – Tabela de códons e siglas de aminoácidos. 113

Anexo 5 – Tabela de anticódons para os tRNA de Tupanvirus deep ocean. 116

Anexo 6– Árvores filogenéticas para as aaRS presentes em tupanvírus.. 117

Anexo 7–Polimorfismos apresentados nos genes de tRNA e aaRS de APMV, APMV M4, SMBV, KROV e OYT 137

Anexo 8– Artigos publicados durante o doutorado. 144

I- INTRODUÇÃO

1.1 Vírus grandes núcleo-citoplasmáticos de DNA

Os vírus são organismos parasitas intracelulares obrigatórios, tradicionalmente conhecidos por apresentarem pequenas dimensões e pequenos genomas codificadores de algumas poucas dezenas de proteínas. No entanto, um grupo especial de vírus, denominado vírus grandes núcleo-citoplasmáticos de DNA (NCLDV, do inglês *Nucleo-cytoplasmic large DNA viruses*), criado em 2001, possui representantes com genomas de DNA dupla fita especialmente extensos, com capacidade de codificação para centenas de proteínas. Dentre as famílias de vírus incluídas neste grupo, tem-se: *Poxviridae, Phycodnaviridae, Iridoviridae, Asfarviridae, Mimiviridae* e mais a recente, *Marseilleviridae* (LA SCOLA et al., 2003; LA SCOLA et al., 2008; YUTIN et al., 2009; ETTEN, LANE e DUNIGAN, 2010; COLSON et al., 2013d). Mais recentemente foram isolados vários outros vírus gigantes, e embora estes ainda não tenham sido classificados em nenhuma família, são considerados como membros do grupo, dentre eles: Faustovirus E12, Pandoravirus salinus, Phitovirus sibericum e Mollivirus sibericum (PHILIPPE et al., 2013; LEGENDRE et al., 2014; LEGENDRE et al., 2015; RETENO et al., 2015). Com o isolamento destas várias amostras de vírus gigantes, vem sendo proposta a criação de uma nova ordem, *Megavirales*, na qual seriam englobados todos os NCLDV (COLSON et al., 2013a; COLSON et al., 2012).

Os vírus deste grupo são capazes de infectar vários grupos de animais (vertebrados e invertebrados), algas e eucariotos unicelulares. Eles demonstram relativa independência diante do sistema transcricional de seus hospedeiros, pois codificam genes para várias proteínas necessárias ao processo, como DNA polimerases, helicases e topoisomerases (RAOULT et al., 2004; YUTIN et al., 2009; KOONIN e YUTIN, 2010). Neste contexto, é importante destacar também a presença de genes envolvidos no processo de tradução, previamente não encontrados em outros vírus, como aminoacil-tRNA sintetases (aaRS), o que sugere também uma certa independência do sistema traducional do seu hospedeiro por parte destes vírus. Há ainda a presença de genes que codificam para RNA transportadores (tRNA) e outros fatores de tradução (FT) (iniciação, elongação e liberação da cadeia polipeptídica) (RAOULT et al., 2004; ABERGEL et al., 2007; LEGENDRE et al., 2010).

A limitação técnica foi um dos motivos para que mais vírus gigantes não tenham sido detectados há mais tempo, pois procedimentos de isolamento viral clássicos, como a filtração em filtros microbiológicos de 0,2 micrômetros (μm), causavam a retenção da maioria dos vírus gigantes. Além disso, a seleção dos sistemas celulares representava um problema, uma vez que alguns vírus gigantes de DNA apresentam espectro de hospedeiros muito restrito. Sendo assim, a maioria dos vírus gigantes de DNA foram inicialmente detectados com o auxílio de dados metagenômicos. Muitos outros vírus interessantes e incomuns podem estar ainda espalhados pelos mais diversos ambientes. Sendo assim, a descoberta e caracterização dos NCLDV se mostra um campo vasto e aberto (GHEDIN e CLAVERIE, 2005; CLAVERIE et al., 2006; ETTEN, LANE e DUNIGAN, 2010).

1.2 Amebas de vida livre e outros protozoários

As amebas de vida livre (AVL) são um grupo de protozoários extremamente ubíquos, e já foram isoladas em ambientes aquáticos, solo, ar, sistemas de tratamento de esgoto, ambientes hospitalares, sistema de ventilação e ar condicionado e em lentes de contato. Podem ser encontradas como parte da microbiota normal de alguns animais, incluindo o homem. As AVL são extremamente resistentes a extremos de pH e temperatura, e são altamente estáveis após tratamento com desinfetantes (SILVA e ROSA, 2003; CROZETTA, 2007; DUARTE, 2010). Estas amebas são caracterizadas por apresentarem duas fases em seu clico de vida: trofozoítica, ativa, que se alimenta e se reproduz e, cística, que se desenvolve em situações de condições desfavoráveis, não sendo capazes de se reproduzirem (CROZETTA, 2007). As AVL podem causar doenças graves e crônicas, entre as quais, tem-se: encefalite amebiana granulomatosa, acantamebíase cutânea, ceratite amebiana e a meningoencefalite amebiana primária (CROZETTA, 2007).

As amebas do gênero *Acanthamoeba e Vermoamoeba* pertencem ao grupo das AVL. Em relação à *Acanthamoeba,* até o momento, já foram descritas aproximadamente vinte e quatro espécies para o gênero, sendo as mais estudadas: *A. polyphaga*, *A. castellanii, A. culbertsoni, A. rhysodes e A. divionensi*, geralmente associadas a doenças em indivíduos imunodebilitados (CROZETTA, 2007). Algumas destas espécies podem estar associadas a doenças graves e crônicas, entre as quais encefalite amebiana granulomatosa, acantamebíase cutânea, ceratite amebiana e a meningoencefalite amebiana primária (CROZETTA, 2007). *V vermiformis* também pode apresentar potencial patogênico ao homem, além da capacidade de

abrigar bactérias patogênicas. *A. castellanii* e *V. vermiformis* vêm sendo utilizadas como plataformas celulares para o isolamento de vírus gigantes (RETENO et al., 2015). *Dictyostelium* é um outro gênero de eucariotos de vida livre, conhecido como "ameba social" não patogênica com aproximadamente 10-20 µm de diâmetro que pode ser encontrado no solo, onde se alimenta através de fagocitose de bactérias e possui um ciclo de vida que alterna entre fases unicelular (fase de crescimento) e multicelular (fase de desenvolvimento em condições adversas). Devido a essas características, tem sido utilizada como modelo de estudo para processos biológicos como divisão e diferenciação, por exemplo (KESSIN, 2000). O gênero *Willaertia* foi descrito pela primeira vez em 1984. *Willaertia magna* é uma especíe dentro deste gênero, uma ameba termófila e não patogênica, encontrada em amostras de água e que se alimenta por fagocitose. Ela possui atividade biocida de forma que ao contrário de muitas AVL, a fusão do fagolisossomo não é inibida por bactérias parasitárias, como *Legionella pneumophila* (DE JONCKHEERE et al., 1984; SÖDERBOM e LOOMIS, 1998).

Tetrahymena é um gênero de protozoário ciliado de vida livre encontrado em água doce, onde se alimenta de bactérias e outros microorganismos por fagocitose e que não é considerado patogênico. Exemplos de espécies deste genero são *T. hyperangularis*, *T. vorax*, *T. pigmentosa*, *T. thermophila* e *T. Pyriformis* (DIAS et al., 2003). *Trichomonas tenax* é tricomonadídeo, um protozoário flagelado, fagocítico e anaeróbio facultativo, comensal da microbiota bucal do homem, apesar de não ser considerado patogênico, quando encontrado indica higiene bucal precária (MARTY et al., 2017).

Os microorganismos patogênicos associados a amebas (MPAA) representam agentes causadores de pneumonia que ganharam destaque nos últimos anos (GREUB e RAOULT, 2004). Fazem parte dos MPAA microorganismos dos gêneros *Legionella*, *Parachlamydia*, *Mycobacterium*, dentre outros (GREUB e RAOULT, 2004; LA SCOLA et al., 2005). Embora ainda seja debatido o quão importante são estes patógenos em termos de números absolutos de casos de pneumonia, uma parte da comunidade científica acredita que os MPAA estão associados a muitos casos nosocomiais de infecção pulmonar (GREUB e RAOULT, 2004).

Análises realizadas por diversos grupos de pesquisa demonstram que os MPAA são patógenos que mesmo após serem fagocitados por amebas, resistem ao ambiente intracelular, e muitas vezes conseguem se multiplicar e produzir progênie numerosa (GREUB e RAOULT, 2004; LA SCOLA et al., 2005). Desta forma, é possível que diferentes gêneros de AVL funcionem como plataformas biológicas de amplificação e propagação de MPAA

(FRITSCHE et al., 1993; GREUB e RAOULT, 2004; LA SCOLA et al., 2005). Este dado ganha importância quando são considerados diversos estudos realizados em pequenas, médias e grandes instituições de saúde, que revelaram a presença de AVL em objetos e no piso de diversos ambientes hospitalares, como unidades de terapia intensiva (UTI), centro cirúrgico, berçário, cozinha, emergência e setor de doenças infecciosas (SILVA e ROSA, 2003; CARLESSO et al., 2007).

Todavia, apesar de toda atenção e importância que vem sendo atribuída às AVL e aos MPAA nos últimos anos, uma descoberta recente chamou atenção da comunidade científica e agregou ainda mais valor aos MPAA: o isolamento e caracterização dos mimivírus (LA SCOLA et al., 2003). Sabe-se que material genético de mimivírus já foi detectado em amostras clínicas humanas relacionadas a casos de pneumonia e em áreas de ambientes hospitalares, sendo que neste último caso, o isolamento viral também foi possível. Além disso, alguns estudos já tiveram sucesso no isolamento de vírus gigantes à partir de amostras como fezes e sangue. E por fim, foi demonstrado que mimivírus é capaz de se multiplicar em células fagocíticas humanas e nelas modular a ação do sistema interferon. Todos esses achados fortalecem a teoria de que vírus gigantes asssociados a amebas podem ter importância clínica (COLSON et al., 2013b; GHIGO et al., 2008; POPGEORGIEV et al., 2013; SAADI et al., 2013; SANTOS-SILVA et al, 2015; SILVA et al., 2014).

1.3 Família *Mimiviridae*

A descoberta do primeiro mimivírus aconteceu a partir de estudos de caracterização de MPAA relacionados a surtos de pneumonia nosocomial, sendo este presente em amostra de água de uma torre de resfriamento de um hospital em Bradford, Inglaterra. Esta amostra de água foi coletada em 1992, e o estudo aprofundado deste material aconteceu no início dos anos 2000. O grupo de pesquisa francês coordenado pelos Drs. Didier Raoult e Bernard La Scola (Aix-Marseille Université, França) percebeu a presença de um microorganismo crescendo em amebas e que se assemelhava a pequenos cocos Gram-positivos frente à coloração de Gram do material coletado em Bradford (Fig 01). (LA SCOLA et al., 2003).

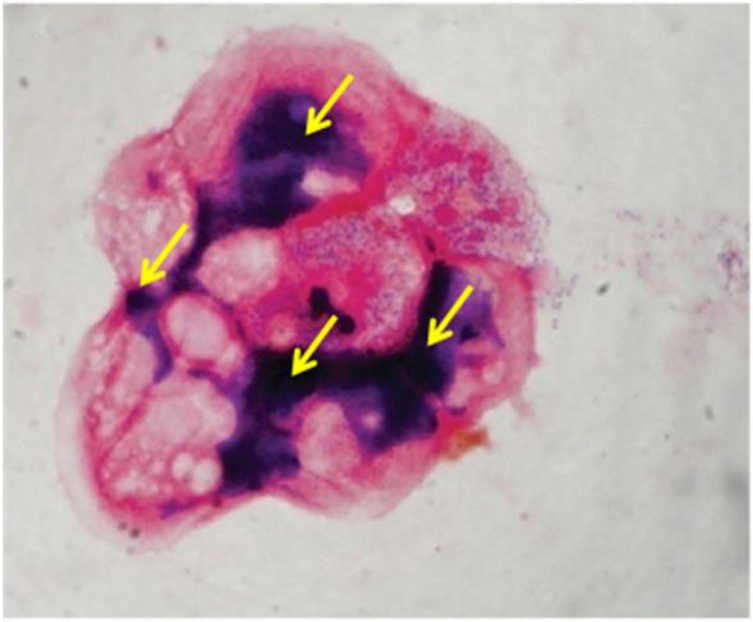

Figura 01: Partículas de APMV no interior de uma ameba de vida livre. O vírus é corado de violeta através da coloração de Gram, e assim pode ser visualizado por microscopia óptica. **Fonte:** Raoult, 2005.

Embora este MPAA apresentasse dimensões bacterianas e características de um Gram-positivo, não respondia a nenhuma classe de antibióticos. Após diversas tentativas malsucedidas de caracterização deste microorganismo, os pesquisadores decidiram fazer microscopia eletrônica do material e, surpreendentemente, foram visualizadas estruturas com morfologia muito semelhante a alguns vírus. Estudos genéticos posteriores revelaram que os "cocos de Bradford", como foram inicialmente chamados, eram, de fato, um novo vírus, então denominado *Acanthamoeba polyphaga mimivirus* (APMV) (Fig. 02) (LA SCOLA et al., 2003).

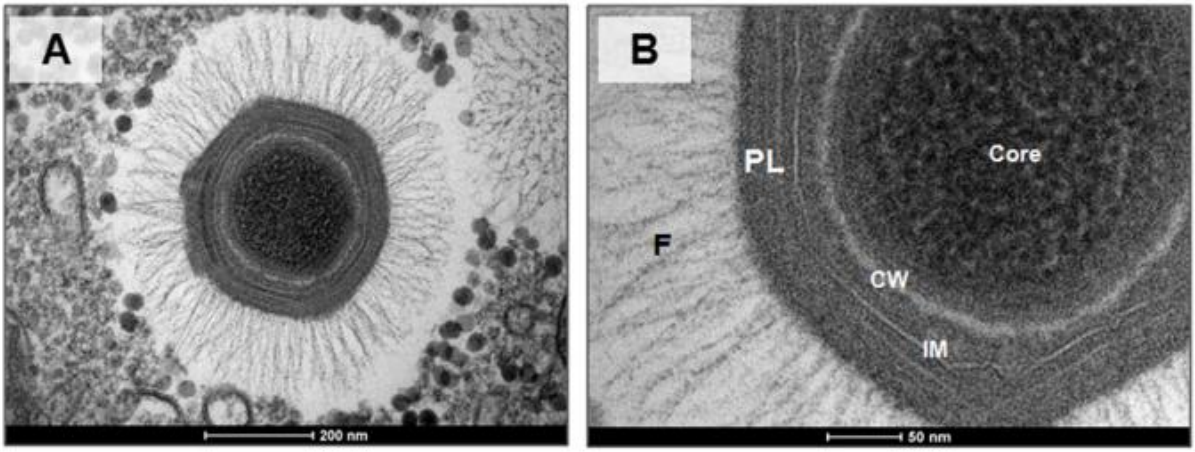

Figura 02: APMV visualizado através de microscopia eletrônica de transmissão. (A) É possível observar a estrutura do vírus gigante: capsídeo proteico circundado por fibrilas e presença de membrana interna, que envolve o nucleocapsídeo; (B) F: fibrilas; PL: camada protéica do capsídeo; CW: camada que protege o cerne; IM: membrana interna; Core: cerne. **Fonte:** Abrahão et al., 2014.

Na ocasião da descoberta, por apresentar características diferenciais que não permitiam sua classificação em uma família viral já existente, a família *Mimiviridae* foi criada para incluir APMV (DESNUES e RAOULT, 2010). Atualmente, a família compreende o gênero *Mimivirus*, que possui como única espécie APMV e o gênero *Cafeteriavirus*, que possui também uma única espécie, *Cafeteria roenbergensis virus*, um vírus marinho capaz de infectar flagelados heterotróficos (ICTV, 2017).

Após cinco anos da descoberta do APMV, uma nova amostra viral foi isolada de uma torre de resfriamento em Paris, *Acanthamoeba castellanii mamavirus* (ACMV) (LA SCOLA et al., 2008). Este vírus possui morfologia e propriedades genéticas muito semelhantes às de APMV (COLSON et al., 2011b). Com o isolamento de ACMV, descobriu-se uma das características diferenciais mais intrigantes de alguns vírus gigantes da família *Mimiviridae*, que corresponde a sua associação estreita com outro vírus menor, denominado *Sputnik virus*. Este pequeno vírus é capaz de parasitar ACMV, quando este é encontrado multiplicando-se em uma ameba. Este processo de coinfecção leva a formação de partículas anormais e uma diminuição significativa na lise amebiana. Tal descoberta levou a criação do termo "virófago", ou seja, vírus que infectam outros vírus (Fig. 03) (LA SCOLA et al., 2008; DENUES e RAOULT, 2010). Desde então, outros virófagos já foram isolados: Sputnik 2, coisolado com Lentillevirus, mimivírus da linhagem A; Mavirus, coisolado com *C. roenbergensis virus*; Rio Negro virus, primeiro virófago brasileiro coisolado com Samba virus

(SMBV); Zamilon, coisolado com um mimivírus da linhagem C a partir de uma amostra de solo tunisiana. Zamilon é capaz de infectar mimivírus da linhagem B e C, mas não da linhagem A (COHEN et al., 2011; FISHER e SUTTLE, 2011; CAMPOS et al., 2014; GAIA et al. 2014). Através de análises de metagenômica, muitos outros virófagos já foram detectados, embora ainda não isolados (AHERFI et al., 2016). De toda forma, isso tem contribuído para o estabelecimento desta nova classe de organismo.

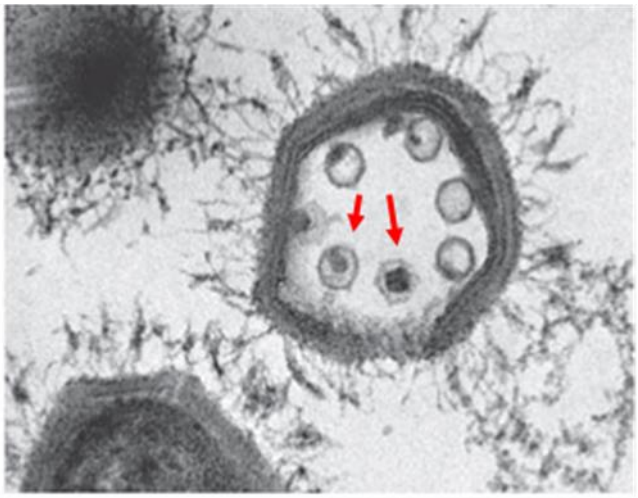

Figura 03: Virófago na partícula de ACMV visualizado através de microscopia eletrônica de transmissão. É possível observar vírus menores, virófagos Sputinik virus, identificados pela seta vermelha no interior do capsídeo do vírus gigante. **Fonte:** Fonte: La Scola et al., 2008

Atualmente, a família *Mimiviridae* possui cerca de 90 isolados (AHERFI et al., 2016). Embora estes ainda não tenham sido oficialmente inseridos na família, aumentam o conhecimento acerca da diversidade e peculiaridades dos mimivírus. Dentre estes isolados, tem-se: Megavirus chilensis, isolado a partir de uma amostra de água coletada na costa do Chile (ARSLAN et al., 2011); Acanthamoeba polyphaga moumouvirus, isolado de amostra ambiental (LA SCOLA et al., 2010); Megavirus LBA111, isolado em amostra respiratória de paciente com infecção pulmonar (SAADI et al., 2013); Lentillevirus, isolado à partir de uma solução de lavagem de lentes de contato (DESNUES et al., 2012); SMBV, Oyster virus (OYTV), Kroon virus (KROV) Amazonia virus (AMZV) e Niemeyer virus (NYMV), isolados brasileiros (CAMPOS et al., 2014; ANDRADE et al., 2015; ASSIS et al., 2015; BORATTO et al., 2015). De acordo com características genéticas e filogenéticas diferenciais, os diferentes isolados de mimivírus são atualmente subdivididos em três linhagens propostas:

A, que tem como representante o protótipo APMV; linhagem B, que tem como representante o Acanthamoeba polyphaga moumouvirus e linhagem C, representada por Megavirus chilensis (FISHER et al., 2010; ARSLAN et al., 2011; COLSON et al., 2011a; ICTV, 2017).

1.4 Estrutura, genoma e ciclo de multiplicação: características dos mimivírus

Os estudos de caracterização do primeiro mimivírus, APMV, evidenciaram a descoberta de um vírus extremamente diferenciado e com características muito peculiares. Estruturalmente (Fig. 04), este vírus apresenta partículas maduras de diâmetro maior que 600 nm, com um capsídeo de simetria icosaédrica de aproximadamente 500 nm, no qual em um dos eixos forma-se uma depressão central, denominada de *stargate.* Esta região permite a liberação do genoma viral no citoplasma da célula hospedeira. Ocorre também a presença de uma membrana interna envolvendo o genoma que parece estar imerso em uma matriz fibrosa (ZAUBERMAN et al., 2008; XIAO et al., 2009; KUZNETSOV et al., 2013). As partículas virais não apresentam envelope externo, mas são revestidas por fibrilas de aproximadamente 130 nm, as quais estão imersas em uma camada de peptideoglicano. As funções destas fibrilas ainda não foram totalmente elucidadas, mas sabe-se que elas são importantes para a adesão viral em diferentes organismos, inclusive em hospedeiros protistas, e é possível que estejam envolvidas na proteção dos vírus contra radiação ultra-violeta e altas temperaturas, bem como responsáveis por atuar como atrativos para amebas (LA SCOLA et al., 2003; RAOULT, LA SCOLA e BIRTLES, 2007; CLAVERIE, ABERGEL e OGATA, 2009; XIAO et al., 2009; RODRIGUES et al., 2015). A estrutura da partícula de APMV pode ser um reflexo de transferência gênica horizontal (TGH), principalmente no ambiente intracelular de uma ameba. A associação do genoma com uma matriz fibrosa se assemelha à estrutura dos grandes genomas eucariotos; a liberação do genoma por mecanismo de *stargate* é análogo ao mecanismo presente em certos tipos de bacteriófagos; e por fim, a matriz de peptideoglicano que envolve as fibrilas externas pode ter sido derivada de bactérias (MOREIRA e BROCHIER-ARMANET, 2008).

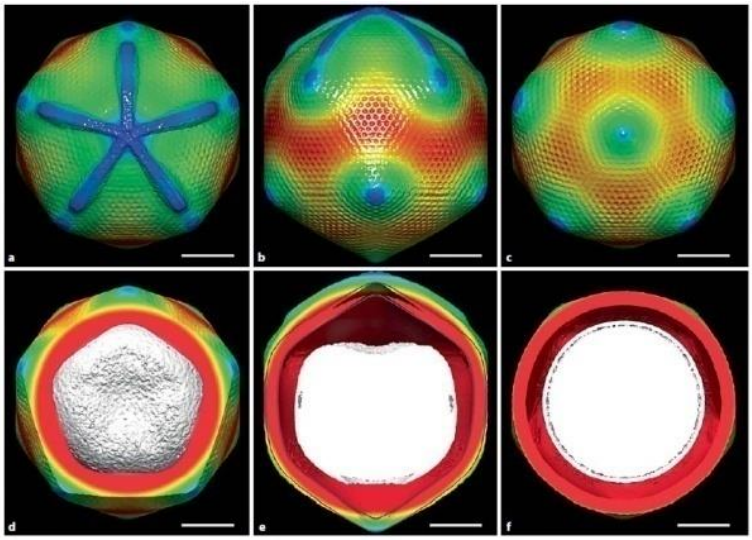

Figura 04: Imagem obtida através de projeção computacional baseada em crio-microscopia eletrônica evidencia a estrutura de APMV. A-C: Diferentes ângulos da estrutura externa do capsídeo viral com simetria icosaédrica evidencia a presença do *stargate*, canal através do qual o genoma viral é liberado no citoplasma da célula hospedeira. D-F: Estrutura interna do capsídeo. É possível verificar a membrana interna que envolve o genoma. **Fonte:** Klose et al., 2010.

Geneticamente, APMV apresenta um genoma de DNA dupla fita de aproximadamente 1,2 Mb que codifica em torno de 1000 proteínas, muitas ainda sem função conhecida e outras nunca antes observadas em outros vírus na ocasião da descoberta (RAOULT et al., 2004; LEGENDRE et al., 2011). Dentre estas, merecem destaque genes que codificam proteínas envolvidas em reparo do DNA; motilidade celular e biogênese de membranas. Além disso, são importantes as proteínas envolvidas em processo de tradução protéica, como as tRNA, aaRS, além de fatores de iniciação, elongação e terminação da cadeia polipeptídica (RAOULT et al., 2004; ABERGEL et al., 2007; LEGENDRE et al., 2010). Dentre os componentes do sistema transcricional codificados por APMV destacam-se duas subunidades maiores de RNA polimerase II (R501 e L244) e quatro subunidades menores Rpb3/Rpb11 (R470), Rpb5 (L235), Rpb6 (R209), Rpb7/E (L376). O vírus também possui sua própria poli (A) polimerase (R341) e diversos fatores de transcrição (L250, R339, R350, R429, R450, R559) (LEGENDRE et al., 2011). Esse grande arsenal gênico pode ser importante por permitir que APMV utilize sua própria maquinaria em paralelo com os elementos análogos celulares para replicação de seu genoma e formação de progênie (SUHRE, 2005; COLSON et al., 2011b; COLSON et al., 2013c).

Um estudo que avaliou as alterações genéticas em APMV mantido em cultura axênica de amebas (sistema alopátrico), sem as fontes principais para a troca gênica, como bactérias e outros microorganismos associados a amebas e verificou que após 150 sucessivas passagens em *A. castellanii*, o tamanho do genoma de APMV diminuiu e alterações morfológicas ocorreram. Nessas condições ocorrem deleções no genoma, principalmente nas regiões terminais não conservadas. A perda de certos genes afetou a expressão de proteínas das fibrilas e também sua glicosilação, hipoteticamente porque nas condições de cultivo alopátrico estas não são necessárias, uma vez que não há competição com outros microorganismos, por exemplo. Supostamente, isso ainda influencia na capacidade do vírus em se associar com virófagos e na capacidade antigênica da partícula que está associada às fibrilas (BOYER et al., 2011). Análises do perfil de transcrição, expressão e variabilidade gênica em APMV após sucessivas passagens em amebas em comparação com o tipo selvagem evidenciaram que 77% dos genes permaneceram intactos e 23% apresentaram variabilidade na sequência nucleotídica. Destes, um total de 10% dos genes se tornaram inativos. A maioria dos genes que sofreram variações e inativação ao longo das passagens eram menos transcritos e expressos no início do cultivo alopátrico. Já para os genes com altos níveis transcricionais, e também de expressão, observou-se que a maioria permaneceu intacta. O fato de genes fracamente transcritos e expressos em sua maioria serem inativados sugere que em condições alopátricas não há pressão de conservação para genes pouco utilizados, levando à sua perda. Além disso, sabe-se que ocorre reparo de DNA em regiões ativamente transcritas e isso pode explicar por que os genes com menores níveis transcricionais sofreram mais variações, uma vez que não são alvos de reparação e essas variações observadas correspondem a erros de sequência que permanecem (COLSON e RAOULT, 2012).

Para se multiplicar, APMV penetra em amebas do gênero *Acanthamoeba* através de fagocitose, sendo o ciclo completamente realizado no citoplasma destas células (Fig. 05) (MUTSAFI et al., 2010; KUZNETSOV et al., 2013). O início do ciclo de multiplicação é marcado por uma fase de eclipse típica, na qual partículas virais não são detectadas na célula (SUZAN-MONTI et al., 2007; LA SCOLA et al., 2008; CLAVERIE e ABERGEL, 2009; LEGENDRE et al., 2010). Nos estágios iniciais de multiplicação, partículas virais fagocitadas podem ser detectadas dentro de fagossomos na célula hospedeira onde ocorre a abertura do *stargate* e fusão entre membranas, viral e endossomal, com posterior liberação do genoma no citoplasma da célula hospedeira (ZAUBERMAN et al., 2008; MUTSAFI et al., 2010).

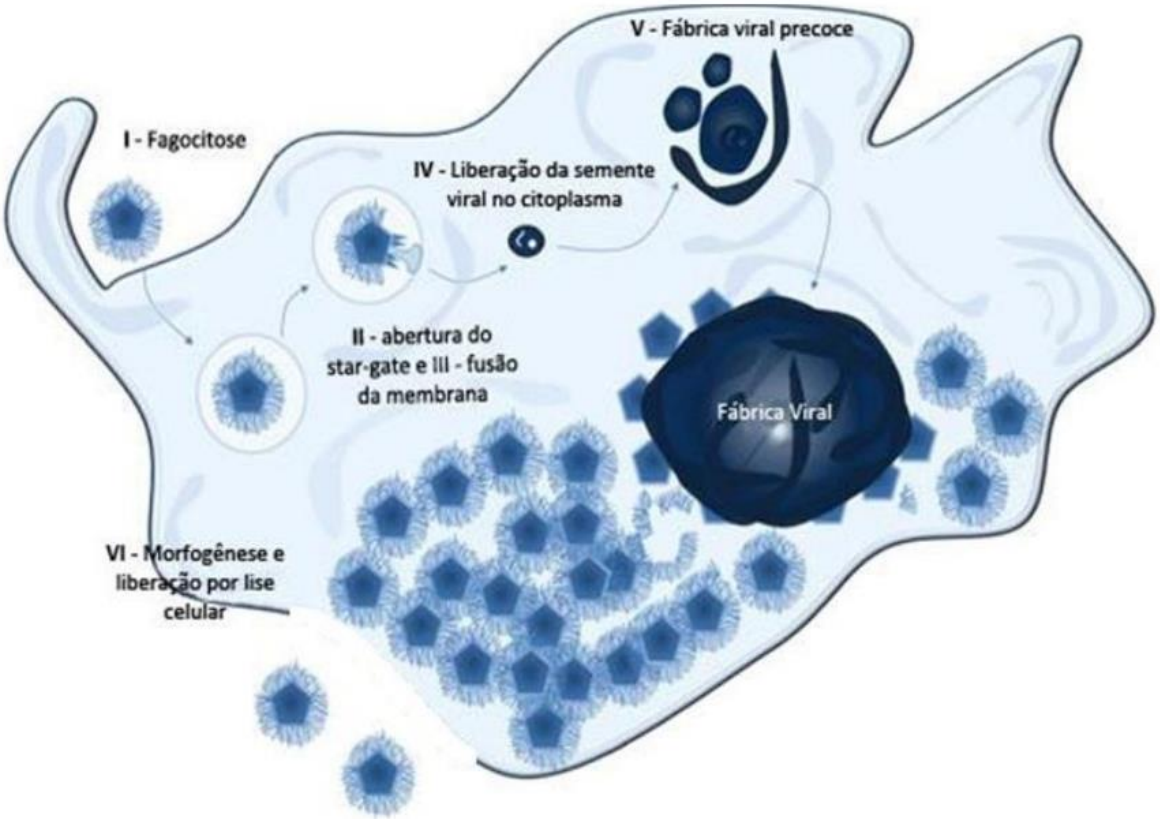

Figura 05: Ciclo de multiplicação de APMV em *A. castellanii*. Desenho esquemático que mostra a penetração do vírus na ameba pelo processo de fagocitose (I). Ocorre abertura do *stargate* e o genoma viral é liberado no citoplasma após fusão de membranas (II e III). Ocorre a replicação do genoma e produção viral nas chamadas fábricas virais (IV). Partículas virais maduras são liberadas com a lise da célula hospedeira (V). **Fonte:** Adaptado de Abrahão et al., 2014.

O genoma é desnudado e se estabiliza sob a forma de núcleos esféricos livres (sementes virais), ao redor dos quais se formam as chamadas fábricas virais, onde ocorre a replicação e transcrição do genoma, após uma fase de eclipse típica. Embora esse processo ocorra no citoplasma, não se pode afirmar que fatores nucleares não estejam presentes. (SUZAN-

MONTI et al., 2007; XIAO et al., 2009; ETTEN, LANE e DUNIGAN, 2010; MUTSAFI et al., 2010; KUZNETSOV et al., 2013). Foi demonstrado que cerca de 2 horas após a infecção de amebas por APMV, inicia-se o aparecimento de várias vesículas transportadoras, as quais a origem ainda é desconhecida, mas suspeita-se que derivem de membrana nuclear ou do retículo endoplasmático rugoso próximo ao núcleo. Essas vesículas são apontadas como responsáveis por carrear fatores nucleares para estes locais (KUZNETSOV et al., 2013). A transcrição dos genes ocorre de uma forma temporal: transcrição de genes iniciais, intermediários e tardios (SUHRE, AUDIC e CLAVERIE, 2005; LEGENDRE et al., 2010). Após a expressão de genes tardios ocorre um aumento da fábrica viral e proteínas estruturais são sintetizadas, dando início ao processo de morfogênese viral. Na superfície das fábricas virais, acumulada com proteínas, inicia-se a montagem dos capsídeos e *stargate*, seguido do empacotamento do material genético. Ocorre uma grande acumulação de partículas virais na fase final de morfogênese, sendo liberados na superfície da fábrica viral, onde adquirem uma camada de tegumento e uma camada de fibras superficiais, como etapa final antes da liberação da progênie viral mediada por lise celular (SUZAN-MONTI et al., 2007; MUTSAFI et al., 2010; KUZNETSOV et al., 2013).

1.5 Outros vírus gigantes isolados recentemente

O estudo de prospecção e caracterização de novas amostras de vírus gigantes vem crescendo nos últimos anos e vários novos isolados têm sido descobertos nos mais diferentes ambientes e espécimes. Estes isolados estão sumarizados na tabela 01 (PAGNIER et al., 2013).

Tabela 1. Resumo de diferentes vírus gigantes associados a amebas isolados nos últimos anos.

Família/Família putativa	Linhagem	Isolado	Plataforma de isolamento
Mimiviridae	A	*Acanthamoena polyphaga mimivirus*	*Acanthamoeba polyphaga*
		Acanthamoeba castellanii mamavirus	*Acanthamoeba castellanii*
		Samba virus	*Acanthamoeba castellanii*
		Kroon virus	*Acanthamoeba castellanii*
		Niemeyer virus	*Acanthamoeba castellanii*
		Amazonia virus	*Acanthamoeba castellanii*
		Lentille virus	*Acanthamoeba castellanii*
	B	Acanthamoeba polyphaga moumouvirus	*Acanthamoeba castellanii*
	C	Megavirus chilensis	*Acanthamoeba castellanii*
		Megavirus LBA 111	*Acanthamoeba castellanii*
Marseilleviridae	A	*Marseille marseillevirus*	*Acanthamoeba castellanii*
		Cannes8 virus	*Acanthamoeba castellanii*
		Fointaine Saint-Charles virus	*Acanthamoeba castellanii*
		Senegalvirus	*Acanthamoeba castellanii*
		Giant blood Marseillevirus	*Acanthamoeba castellanii*
	B	Lausannevirus	*Acanthamoeba castellanii*
	C	Tunisvirus	*Acanthamoeba castellanii*
		Insectomime virus	*Acanthamoeba castellanii*
	D	Brazilian Marseillevirus	*Acanthamoeba castellanii*
Pandoraviridae		Pandoravirus salinus	*Acanthamoeba castellanii*
		Pandoravirus dulcis	*Acanthamoeba castellanii*
		Pandoravirus inopinatum	*Acanthamoeba castellanii*

Pithoviridae	Pithovirus sibericum	*Acanthamoeba castellanii*
	Pithovirus massiliensis	*Acanthamoeba castellanii*
Faustoviridae	Faustovirus E12	*Vermoamoeba vermiformis*
	Kaumoebavirus	*Acanthamoeba castellanii*
	Pacmanvirus	*Acanthamoeba castellanii*
Molliviridae	Mollivirus sibericum	*Acanthamoeba castellanii*
Cedratviridae	Cedratvirus	*Acanthamoeba castellanii*
Klosneuviridae	Klosneuvirus	-
	Catovirus	-
	Indivirus	-
	Hokovirus	-

Marseillevirus marseillevirus também foi isolado em amebas de vida livre a partir de amostras de água de uma torre de resfriamento de Paris. Este vírus apresenta características genéticas muito distintas de APMV e ACMV e foi incluído na nova família *Marseilleviridae* em 2013 (BOYER et al., 2009; RAOULT e BOYER, 2010; ICTV, 2017). É um vírus de simetria icosaédrica, com capsídeo de aproximadamente 250 nm e genoma de aproximadamente 370 kb (Fig. 06) (BOYER et al., 2009). Atualmente existem vários marseillevírus isolados e divididos em quatro linhagens: A, B, C e D de acordo com diferenças genéticas e filogenéticas (AHERFI et al., 2014; DORNAS et al., 2016). A linhagem A é composta pelo vírus protótipo, *Marseillevirus marseillevirus*, e pelos Cannes8 virus, Fointaine Saint-Charles virus, Senegalvirus, Giant blood Marseillevirus e Melbournevirus (LAGIER et al., 2012; AHERFI et al., 2013; COLSON et al., 2013b; DOUTRE et al., 2014). Lausannevirus é o único isolado inserido na linhagem B e a linhagem C contém Tunisvirus e Insectomine virus. Estes isolados foram obtidos a partir de diferentes amostras e localidades (BOUGHALMI et al., 2013; AHERFI et al., 2014). Um dos marseillevírus mais recentemente isolado é o Tokyovirus, obtido a partir de água coletada em um rio localizado em Tokyo, Japão (TAKEMURA, 2016). Atualmente, a criação da linhagem D foi proposta após o isolamento e caracterização do primeiro marseillevírus isolado no Brasil, Brazilian Marseillevirus (DORNAS et al., 2016). Recentemente, etapas o ciclo de multiplicação de marseillevírus em *A. castellanii* foram desvendadas. Foi possível concluir que devido ao tamanho menor de sua partícula, ao contrário de outros vírus gigantes, as partículas virais isoladas dos marseillevírus não estimulam a fagocitose, mas penetram por

meio de endocitose mediada por receptor. Além disso, foi demonstrado que os marseillevírus podem formar vesículas gigantes, contendo de centenas a milhares de partículas virais, promovendo a penetração por fagocitose (ARANTES et al., 2016).

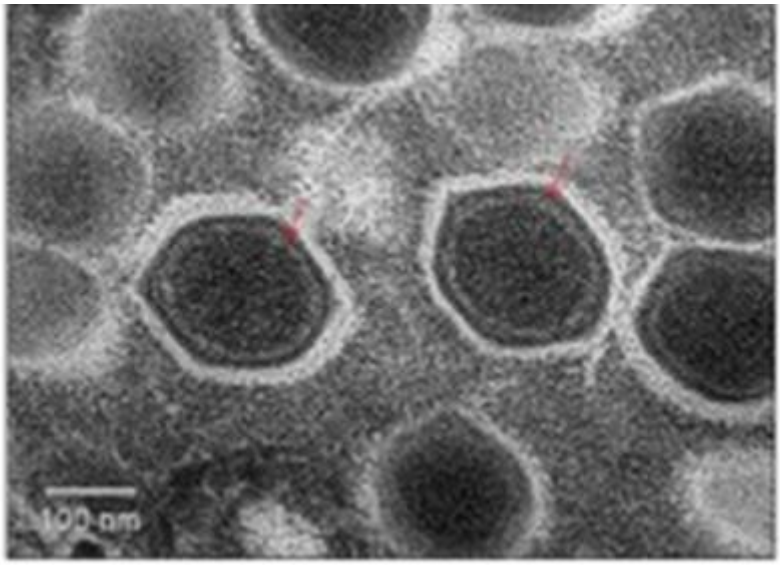

Figura 06: Morfologia de *Marseillevirus marseillevirus*. Imagem de microscopia eletrônica demonstra a estrutura de *Marseillevirus*, o vírus apresenta simetria icosaédrica e é relativamente menor que os mimivírus, com partícula de aproximadamente 250 nm. **Fonte:** Adaptado de Arantes et al., 2016

Isolados recentes demonstram que a diversidade dos vírus gigantes pode ser muito grande. Por exemplo, Pandoravirus salinus e P. dulcis, foram isolados de amostras do Chile (sedimentos de um rio) e Austrália (lama de uma lagoa), respectivamente (PHILIPPE et al., 2013). Os pandoravírus apresentam morfologia diferenciada, as partículas virais são ovóides e apresentam três camadas proteicas, podendo o vírus alcançar 1 µm de comprimento. Os genomas são complexos com tamanho de 2,5 Mb para P. salinus e 1,9 Mb para P. dulcis (PHILIPPE et al., 2013). Por meio de sequenciamento, em 2015 foi demonstrado que um organismo descrito em 2008 como endossimbionte de amebas trata-se na verdade de um pandoravírus, sendo este novamente classificado e denominado P. inopinatum (ANTWERPEN et al., 2015). O quarto pandoravírus descrito corresponde a um isolado brasileiro proveniente de uma amostra de água coletada na Lagoa da Pampulha em Belo Horizonte (DORNAS et al., 2015). Em relação ao ciclo de multiplicação dos pandoravírus nas amebas, sabe-se que também se inicia através de fagocitose. O ciclo de multiplicação ocorre

no citoplasma da ameba, mas fatores nucleares parecem estar envolvidos, uma vez que ocorre uma marcante reorganização do núcleo hospedeiro. A replicação do material genético viral e a morfogênese de partículas ocorrem ao mesmo tempo, sendo as partículas maduras liberadas aproximadamente após 10 horas de infecção (PHILIPPE et al., 2013).

Em 2014, Pithovirus sibericum foi isolado de uma amostra de *permafrost* coletada na Sibéria (LEGENDRE et al., 2014; LEGENDRE et al., 2015). A morfologia deste isolado é semelhante à dos pandoravírus, porém a partícula apresenta um poro apical em uma das extremidades, estrutura que é ausente em pandoravírus. Além disso, as partículas do Pithovirus sibericum são ainda maiores que as dos pandoravírus, com cerca de 1,5 μm de comprimento, sendo considerado até o momento o maior vírus já isolado. Apesar do tamanho da partícula, o genoma é menos complexo e apresenta tamanho de 610 Kb. O Pithovirus massiliensis é o mais novo representante deste grupo, isolado a partir de amostras de esgoto da cidade Francesa de La Ciotat (LEVASSEUR et al., 2016). Mollivirus sibericum também foi isolado a partir da amostra de *permafrost* da Sibéria. Este isolado apresenta uma partícula esférica de aproximadamente 600 nm e genoma de DNA linear de aproximadamente 650 Kb (LEGENDRE et al., 2015). Os phitovírus apresentam um ciclo de multiplicação semelhante ao dos pandoravírus, porém não são observadas alterações na organização do núcleo celular (LEGENDRE et al., 2014). As partículas de pandoravírus, phitovírus e M. sibericum estão representadas na figura 07 em comparação com mimivírus.

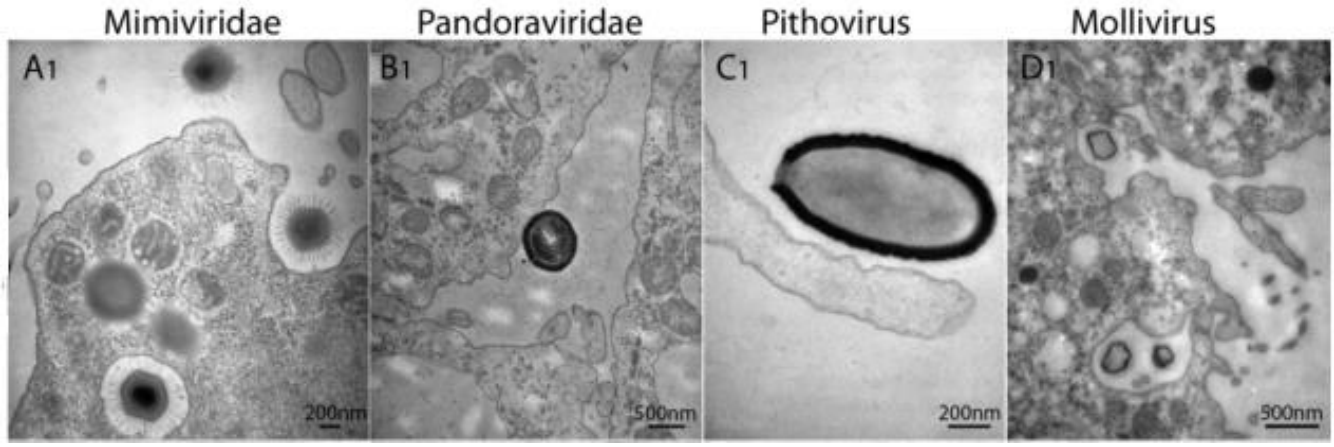

Figura 07: Morfologia de mimivírus, pandoravírus, pithovírus e mollivírus. Imagens de microscopia de varredura evidenciam a morfologia particular destes quatro diferentes grupos de vírus gigantes. (A) mimivírus (B) pandoravirus, partícula ovóide; (C) P. sibericum, partícula ovóide com poro

apical em uma das extremidades; (D) M. sibericum, com estrutura esférica. **Fonte:** Adaptado de Abergel, Legendre e Claverie, 2015

Faustovirus E12 foi o primeiro vírus gigante isolado em uma ameba de gênero diferente, *Vermoamoeba vermiformis*. Ele foi isolado a partir de amostras de esgoto de Marseille, França (RETENO et al., 2015). Morfologicamente, apresenta um capsídeo icosaédrico com dupla camada, cerca de 200 nm de diâmetro e sem fibrilas. Possui um genoma de DNA dupla fita circular e de 466 Kb (RETENO et al., 2015). O ciclo dos faustovírus aparentemente inicia-se através de fagocitose em *V. vermiformis* e ocorre de forma semelhante à de outros vírus gigantes, porém é mais lento, sendo que apenas entre 18 e 20 horas após a infecção é possível observar a liberação de partículas virais maduras (RETENO et al., 2015). Atualmente, existem outros faustovírus isolados no mundo. Um segundo representante deste grupo foi também isolado em *V. vermiformis,* Kaumoebavirus. O isolamento foi a partir de amostra de esgoto da cidade de Jeddah, Arábia Saudita (BAJRAI et al., 2016). Este isolado apresenta morfologia semelhante à de Faustovirus E12, sendo um pouco maior. Seu genoma também é de DNA circular com 350 Kb. Um terceiro representante deste grupo é o Pacmanvirus, isolado a partir de uma amostra ambiental coletada na Argéria. Neste caso, o isolamento foi em *A. castellanii* (ANDREANI et al., 2017). Análises genéticas e filogenéticas após a expansão do grupo dos faustovírus, juntamente com Kaumoebavirus e Pacmanvirus vêm levando a proposição da relação destes novos isolados com a família *Asfarviridae* (ANDREANI et al., 2017). Os vírus deste grupo estão representados na figura 08.

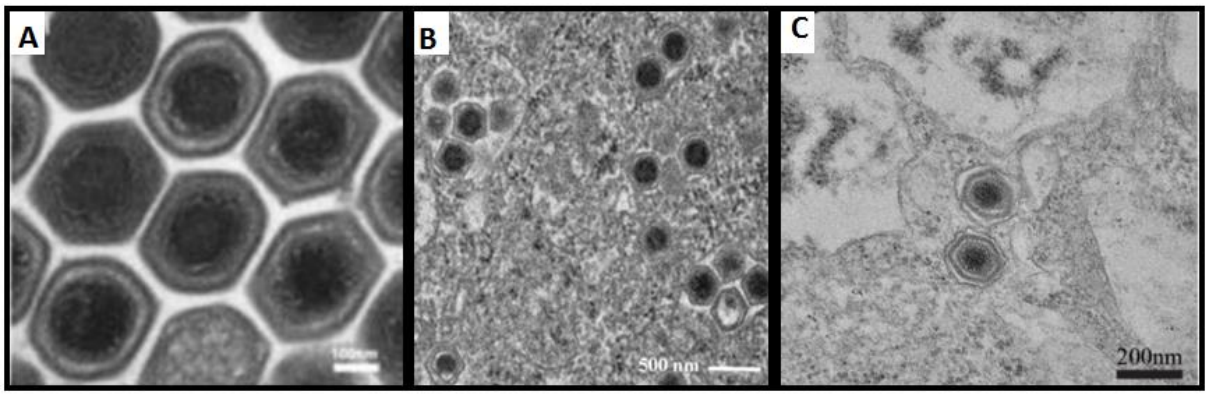

Figura 08: Morfologia de Faustovirus E12, Kaumoebavirus e Pacmanvirus. Imagens de microscopia de eletrônica evidenciam a estrutura destes isolados relacionados. (A) Faustovirus E12; (B) Kaumoebavirus; (C) Pacmanvirus. **Fonte:** Adaptado de Reteno et al., 2015; Bajrai et al., 2016 e Andreani et al., 2017.

Através de prospecção em amostras coletadas em quatro regiões da Argélia foi isolado o Cedratvirus, um vírus de 1,2 µm e com morfologia semelhante à dos pithovírus, porém com poros apicais nas duas extremidades da partícula. Geneticamente, apresenta um genoma circular de aproximadamente 589 Kb e apresenta um ciclo de multiplicação típico de outros vírus gigantes já supracitados (Fig. 09).

Figura 09: Morfologia do Cedratvirus. Microscopia eletrônica de transmissão evidencia as partículas do Cedratvírus com destaque para os poros apicais nas duas extremidades indicados pelas setas vermelhas. **Fonte:** Adaptado de Andreani et al., 2016.

Recentemente, foi publicada a identificação genética de novos vírus através de análises metagenômicas, sendo estes filogeneticamente relacionados a outros vírus gigantes (Fig. 10). Embora não isolados, os novos vírus em questão chamaram a atenção devido ao conteúdo genético. Os dados foram obtidos a partir de análise metagenômica de uma usina de tratamento de esgoto, localizada em Klosterneuburg, no leste da Áustria, sendo identificados genomas para quatro novos vírus gigantes, sendo o grupo destes novos vírus denominado Klosneuvírus. Foram identificados: o Indivirus com genoma de 0,86 Mb; o Hokovirus, com genoma de 1,33 Mb; o Catovírus, com genoma de 1,53 Mb e o Klosneuvirus, com genoma de 1,57 Mb. A análise do sequenciamento destes genomas revelou a presença de genes relacionados à tradução nunca anteriormente verificados em outros vírus, com genes codificadores de vários tRNA, aaRS e outros TF (SCHULZ et al., 2017).

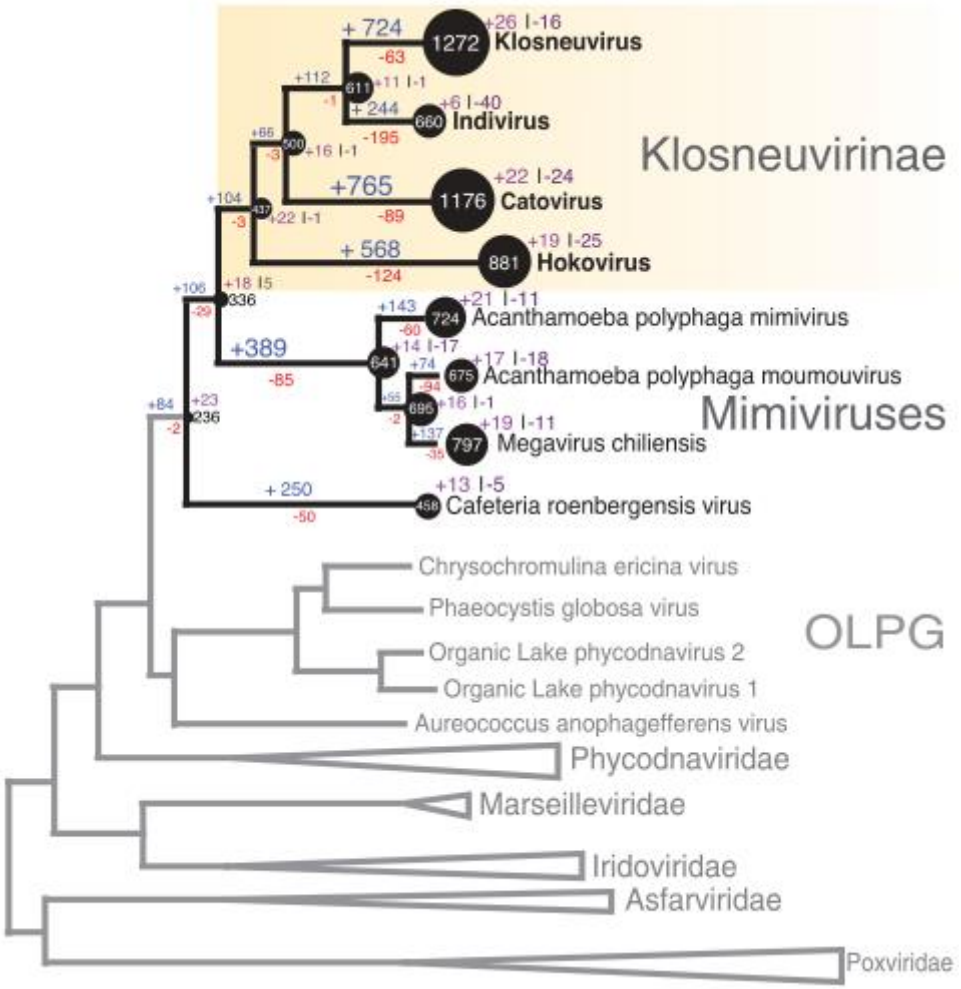

Figura 10: Análise filogenética dos Klosneuvírus. Árvore de máxima verossimilhança evidencia a relação dos klosneuvírus com outros grupos de vírus gigantes. **Fonte:** Adaptado de Schulz et al., 2017.

1.6 Elementos relacionados à tradução em vírus gigantes

Desde a sua descoberta, os vírus são considerados um verdadeiro quebra-cabeça, especialmente para aqueles que estudam evolução. Devido à sua natureza como entidades na fronteira entre os vivos e os não-vivos, o debate sobre sua origem tem sido constante e recentemente ganhou um impulso sem precedentes com a descrição dos genomas de vírus gigantes. Há mais de duas décadas, Carl Woese propôs a divisão dos seres vivos em três Domínios: *Eukarya*, *Bacteria* e *Archaea* (WOESE, KANDLER e WHEELIS, 1990;

MOREIRA E BROCHIER-ARMANET, 2008, RUIZ-SAENZ e RODAS, 2010; WILLIAMS, EMBLEY e HEINZ, 2011). Sempre foi considerado que os genomas da maioria dos vírus não contêm informações suficientes que suportem a classificação dos mesmos em um Domínio próprio. Porém, surpreendentemente, NCLDV apresentam genes que eram tradicionalmente considerados como marcadores de organismos celulares. Para alguns pesquisadores, este fenômeno os coloca na mesma definição de vida que é atribuída a esses Domínios (RAOULT et al., 2004; RAOULT e FORTERRE, 2008; RUIZ-SAENZ e RODAS, 2010; WILLIAMS, EMBLEY e HEINZ, 2011; RAOULT, 2013). Estudos recentes indicaram a existência de um sistema de glicosilação independente da ameba hospedeira presente em APMV. Análises filogenéticas indicaram que o gene L136 deste sistema foi adquirido por evolução independente e não por TGH (PIACENTE et al., 2012). Em relação ao colágeno, uma das proteínas mais abundantes em seres vivos, foi descrito um novo tipo de glicosilação em APMV, mostrando pela primeira vez que modificações pós-traducionais do colágeno não estão restritas aos clássicos domínios da vida (LUTHER et al., 2011).

Dentre as fases abertas de leitura (ORFs), ORFans (ORF sem homologia com nenhuma sequência disponível nos bancos de dados) e proteínas hipotéticas codificadas pelos mimivírus, o que mais chamou atenção dos virologistas e evolucionistas em relação ao genoma foi, sem dúvida, a presença de regiões codificadoras de elementos envolvidos em tradução protéica. Nenhum genoma viral, até então descrito, apresentava arsenal gênico tão complexo capaz de codificar vários fatores de iniciação/elongação/liberação peptídica, tRNA e aaRS, sendo, portanto, obrigados a utilizar de forma direta ou indireta os correspondentes celulares para a síntese de suas proteínas. Isto sugere que um controle rígido deste complexo traducional é necessário para multiplicação dos mimivírus e que estes fatores apresentam de certa forma pressão de conservação, pois são encontrados em todos os membros descritos até o momento (RAOULT et al., 2004; ABERGEL et al., 2007; LEGENDRE et al., 2010).

A tradução de RNA mensageiros (mRNA) em proteínas se dá através de um processo complexo que ocorre no citoplasma celular e consiste em três etapas principais: iniciação, elongação e liberação peptídica, participando do processo o mRNA, ribossomos, tRNA e um variado aparato enzimático. Neste contexto, as aaRS são essenciais, pois são as enzimas responsáveis por promover a correta interação dos tRNA com seus aminoácidos cognatos através de formação de ligações covalentes, processo denominado aminoacilação. Dessa forma, uma vez formada a ligação, o complexo reconhece seu respectivo códon no mRNA e

promove a tradução da informação genética para uma cadeia polipeptídica (IBBA e SÖLL, 2004; WALSH e MOHR, 2011).

Genes celulares que codificam elementos envolvidos com a maquinaria de tradução são regulados por diferentes mecanismos. Alguns destes mecanismos envolvem a regulação da expressão de aaRS e são bem caracterizados em bactérias e eucariotos unicelulares (RYCKELYNCK et al., 2005). A expressão de aaRS em *Escherichia coli*, por exemplo, é regulada de uma maneira dependente da taxa de crescimento, mas também por mecanismos específicos induzidos em resposta a baixa concentração do aminoácido cognato em questão, como também ocorre em *Bacillus subtilis* (PUTZER e LAALAMI, 2000; RYCKELYNCK et al., 2005). Já para algumas leveduras, sob baixa concentração de aminoácidos, ocorre a estimulação de um ativador transcricional, GCN4, que ativa a expressão de aaRS (RYCKELYNCK et al., 2005). Todo este controle é necessário para garantir o equilíbrio entre as concentrações intracelulares de tRNA carregados e não carregados para permitir o ajuste fino da tradução e do metabolismo celular como um todo, em resposta às condições nutricionais no ambiente extracelular. Vários elementos de vias de biossíntese de aminoácidos específicos estão envolvidos na regulação da expressão de aaRS. Muitos mecanismos reguladores diferentes permitem tanto o controle específico do gene em questão quanto o controle global da expressão de genes envolvidos na tradução de proteínas (NEIDHARDT et al., 1975; PUTZER e LAALAMI, 2000).

De uma forma geral, o número de regiões codificadoras de elementos relacionados à tradução varia em relação à quantidade e à natureza entre os vírus gigantes até então caracterizados (Tabela 2). O APMV e ACMV, por exemplo, codificam seis moléculas de tRNA: cistenil-tRNA, histidinil-tRNA, triptofanil-tRNA e três leucinil-tRNA; e quatro de aaRS: cisteinil-RS, metionil-RS, arginil-RS, e tirosil-RS (RAOULT et al., 2004; COLSON et al., 2013c). O genoma de Megavirus chilensis codifica três tRNA: duas leucinil-tRNA e uma triptofanil-tRNA, além de sete aaRS, todas essas presentes em APMV, além de isoleucinil-RS, asparaginil-RS e triptofanil-RS (ARSLAN et al., 2011). A análise do genoma do SMBV, a primeira amostra de mimivírus isolada no Brasil, revelou a presença de seis tRNA e quatro aaRS, iguais aos identificados em APMV (CAMPOS et al., 2014). Outro isolado brasileiro, NYMV, apresenta, de forma interessante, as quatro aaRS presentes em APMV, porém, três dessas são duplicadas: arginil-RS, tirosil-RS e metionil-RS (BORATTO et al., 2015). Por fim, os pandoravírus, apesar de seus genomas serem quase duas vezes maiores do que dos

mimivírus, apresentam somente 3 tRNA: prolinil-tRNA, metionil-tRNA e triptofanil-tRNA, e duas aaRS: triptofanil-RS e tirosil-RS (PHILIPPE et al., 2013). Estas duas aaRS parecem ter sido adquiridas por TGH a partir de *Acanthamoeba*, diferentemente do observado para mimivírus (PHILIPPE et al., 2013). De forma interessante, alguns desses elementos não são encontrados em *M. marseillevirus*, Faustovirus E12 e P. sibericum (AHERFI et al., 2014; LEGENDRE et al., 2014; RETENO et al., 2015).

Recentemente, a descrição dos Klosneuvírus renovou as discussões acerca dos elementos envolvidos em tradução em vírus gigantes, uma vez que os membros deste grupo apresentam o mais complexo arsenal de tradução já verificado em um genoma viral até então. Dentro do grupo, Catovirus apresenta quinze aaRS, três tRNA e nove TF; Hokovirus apresenta treze aaRS e dez TF; Indivirus apresenta três aaRS, oito tRNA e um único TF e por fim, de forma surpreendente Klosneuvirus apresenta dezenove aaRS, vinte e três tRNA e doze TF (SCHULZ et al., 2017).

Tabela 2. Elementos relacionados à tradução em isolados de vírus gigantes representativos de cada grupo ou família.

Grupo/Vírus	AaRS	tRNA	TF
Mimivírus Linhagem A			
APMV	ArgRS, CisRS, MetRS, TirRS	Leucina (3x), Histidina, Cisteína, Triptofano	IF4A, IF4E, SUI1, eF-TU, eRF1
Mamavirus	ArgRS, CisRS, MetRS, TirRS	Leucina (3x), Histidina, Cisteína, Triptofano	IF4A, IF4E, SUI1, eF-TU, eRF1
Lentille	ArgRS, CisRS, MetRS, TirRS	Leucina (3x), Histidina, Cisteína, Triptofano	IF4A, IF4E, eF-TU, eRF1
Hirudovirus	ArgRS, CisRS, MetRS, TirRS	Leucina (3x), Histidina, Cisteína, Triptofano	IF4A, IF4E, SUI1, eF-TU, eRF1
SMBV	ArgRS, CisRS, MetRS, TirRS	Leucina (3x), Histidina, Cisteína, Triptofano	IF4A, IF4E, SUI1, eF-TU, eRF1
OYTV	ArgRS (2x), CisRS, MetRS, TirRS	Leucina (3x), Histidina, Cisteína, Triptofano	IF4A, IF4E, SUI1, eF-TU, eRF1
KROV	ArgRS, CisRS, MetRS, TirRS	Leucina (3x), Histidina, Cisteína	IF4A, IF4E, eF-TU, eRF1
AMZV	CisRS, TirRS	Leucina (3x), Histidina, Cisteína, Triptofano	IF4A, IF4E, SUI1, eF-TU, eRF1

NYMV	ArgRS, CisRS (2x), MetRS (2x), TirRS (2x)	Leucina (2x), Histidina, Cisteína	IF4A, IF4E, SUI1, eF-TU, eRF1
Terra2	-	Leucina (3x), Histidina, Cisteína, Triptofano	IF4A, IF4E, SUI1, eF-TU, eRF1
Bombay	ArgRS, CisRS, MetRS, TirRS	Leucina (3x), Histidina, Cisteína, Triptofano	IF4A, IF4E, SUI1, eF-TU, eRF1
Mimivírus Linhagem B			
Moumovirus	ArgRS (4x), CisRS, IleRS, MetRS, TirRS	Leucina, Histidina, Cisteína	IF4E, SUI1, eF-TU, eRF1
Goulette	CisRS, MetRS	Leucina (3x), Histidina, Cisteína	IF4E, SUI1, eF-TU, eRF1
Monve	ArgRS (2x), AsnRS, CisRS, IleRS (2x), MetRS, TirRS	Leucina, Histidina, Cisteína	IF4A, IF4E (2x), SUI1, eRF1
Saudi moumouvirus	MetRS, IsoRS, AspRS (x2), ArsRS(x2), CistRS(x2), TyrRS	Cisteínas, Histidina	IF4E, IF4a, SUI1, eRF1
Mimivírus Linhagem C			
Megavirus chilensis	ArgRS, AsnRS, CisRS, IleRS, MetRS, TrpRS, TirRS	Leucina (2x), Triptofano	IF4A, IF4E, SUI1, eF-TU, eRF1
Terra1	-	Leucina, Triptofano	IF4A, IF4E, SUI1, eF-TU, eRF1
LBA111	ArgRS, AsnRS, CysRS, IleRS, MetRS, TrpRS, TyrRS	Leucina (2x), Histidina, Cisteína, Triptofano	IF4A, IF4E, SUI1, eF-TU, eRF1
Courdo7	IleRS, TirRS	Leucina (3x), Triptofano	IF4A (2x), IF4E, SUI1, eRF1
Courdo11	ArgRS, AsnRS (2x), CysRS, IleRS, MetRS, TrpRS, TyrRS	Leucina (3x), Histidina, Cisteína, Triptofano	IF4A (2x), IF4E, SUI1, eRF1
Mimivírus grupo II			
Cafeteria roenbergensis virus	IleRS	Leucina (9x), Serina (5x), Tirosina, Asparagina, Lisina	IF4A, IF4E, SUI1
Phaeocystis globosa virus	-	Leucina (3x), Asparagina (2x), IsoLeucina, Arginina, Glutamina	IF4E
Organic Lake Phycodnavirus	-	Leucina, IsoLeucina, Tirosina, Asparagina, Arginina	IF4E
Outros vírus gigantes			
Marseillevirus marseillevirus	-	-	eIF5, SUI1, EF1α, eRF1
Faustovirus E12	-	-	SUI1
Pandoravirus salinus	TyrRS, TrpRS	Prolina, Metionina, Triptofano	IF4E
Pandoravirus dulcis	TyrRS	Prolina	IF4E
Pandoravirus inopinatum	-	Prolina	IF4E
Mollivirus sibericum	-	Leucina, Metionina, Tirosina	IF4E

Catovirus	CisRS, IleRS, MetRS, AnsRS, ArsRS, TyrRS, TrpRS, LeuRS, LysRS, ProRS, HisRS, GlnRS, ThrRS, GlyRS, ValRS	Cisteína, Glicina, Triptofano	IF1A, IF2A, IF2beta, IF2gama, IF4E, eIF-4A-III, eIF4G, eRF1
Indivirus	IleRS, MetRS, AsnRS	Asparagina	IF1A, IF2beta, IF2gama, IF4E, IF5B, eIF2a-4, eIF4G
Hokovirus	IleRS, MetRS, AnsRS, ArsRS, TyrRS, TrpRS, SerRS, LysRS, ProRS, HisRS, GlnRS, ThrRS, LeuRS	-	IF1A, eIF2a, IF2beta, IF2beta2, IF2gama, IF4E, eIF-4A-III, eIF4G, eEF1, eRF1
Klosneuvirus	AlaRS, ArRS, AsnRS, AspRS, ArgRS, PheRS, GlyRS, GluRS, HisRS, IsoRS, LeuRS, LisRS, MetRS, ProlRS, SerRS, TirRS, ThrRS, TrpRS, ValRS	Ácido Glutâmico, Leucina (x3), Serina, Tirosina, Triptofano, Prolina (x3), Histidina, Glutamina, Asparagina, Aspartato, Cisteína, Isoleucina (x2), Metionina, Arginina,Valina	IF1, IF1A, IFA2, IF2beta, IF2beta2, IF2gama, IF4E, eIF-4A-III, eIF4G, IF5a, eEF1, eRF1

Sabe-se que de forma geral, tRNA e aaRS presentes em vírus gigantes não são pseudogenes, uma vez que são distintos de genes celulares e também por serem expressos durante todo o ciclo de replicação, nos estágios inicial, intermediário e tardio. Alguns destes genes são expressos em altos níveis nos diferentes tempos de infecção, sugerindo que eles são envolvidos no processo de tradução do início ao fim do ciclo de multiplicação viral (LEGENDRE et al., 2010). Além disso, duas aaRS codificadas por APMV, tirosil-RS e metionil-RS demonstraram possuir atividade enzimática genuína (ABERGEL et al., 2007; LEGENDRE et al., 2010).

A presença de genes relacionados à tradução em vírus gigantes ajuda a incitar a discussão sobre a sua origem e suporta a teoria de ancestralidade comum para estes vírus (CLAVERIE et al., 2006). A discussão se dá principalmente entre a teoria de que os vírus gigantes derivam de um ancestral celular comum que sofreu degradação do genoma progressivamente até se adaptar ao estilo de vida parasitário e a teoria contrária que acredita na expansão do genoma a partir de um ancestral viral simples (MOREIRA e LOPEZ-GARCIA, 2005; CLAVERIE et al., 2006; FILÉE et al., 2008; YUTIN et al., 2014). Curiosamente, APMV M4, obtido após várias passagens de APMV em *A. castellanii* sob condições alopátricas, perdeu várias ORFs, incluindo aquelas envolvidas na síntese de triptofanil-tRNA e tirosil-RS, sugerindo que estas ORFs não sejam essenciais nestas condições de cultivo. Assim, hipotetiza-se que os genes deletados após as sucessivas

passagens seriam importantes somente em condições de crescimento simpátrico e, de alguma forma, os mimivírus são capazes de competir melhor com outros microorganismos associados a amebas quando possuem tais ORFs. Todavia, não foram realizados experimentos que demonstrem a importância isolada destes genes no contexto da infecção (BOYER et al., 2011; COLSON e RAOULT, 2012). Algum tempo depois, foi então proposta uma terceira teoria de modelo evolucionário para os vírus gigantes, do tipo “sanfona”, que acredita na expansão ou redução do genoma viral como uma forma de adaptação às alterações ambientais e aos diferentes hospedeiros (FILÉE et al., 2015). A atual identificação dos klosneuvírus fortalece a teoria de aquisição de genes a partir de um ancestral viral mais simples, levando a aumento significativo do genoma, de forma a ser possível identificar tais vírus com aparato de tradução consideravelmente complexo (SCHULZ et al., 2017).

II- JUSTIFICATIVA

Os vírus gigantes de DNA surgiram como uma fascinante linha de pesquisa, principalmente por suscitarem importantes questionamentos sobre sua relação com seus hospedeiros e evolução. Ao longo de mais de 15 anos de estudos, vários novos isolados de vírus gigantes foram identificados em diferentes amostras e espécimes. Assim, as descobertas científicas atuais permitem novas discussões sobre a natureza e dinâmica biológica dos vírus, restabelecendo até mesmo a polêmica sobre o que deve ser considerado "vivo" ou não. A complexidade estrutural e genômica dos vírus gigantes recentemente isolados e caracterizados é intrigante. Estruturalmente, é possível notar que a diversidade entre os isolados está cada vez maior. Muitos de seus genes codificam proteínas/RNA não observadas (ou raramente observadas) anteriormente em outros vírus, como por exemplo, RNA transportadores e aminoacil-tRNA-sintetases envolvidos no processo de tradução. Desta forma, a prospecção de vírus gigantes continua sendo um campo de estudo importante na busca de novos isolados que possam ajudar a montar o quebra-cabeça na compreensão da diversidade biológica dos vírus deste grupo, bem como possível papel ecológico, espectro de hospedeiros e aspectos evolutivos. Recentemente, análises metagenômicas identificaram vírus gigantes inseridos em um grupo denominado de Klosneuvírus que apresentam o aparato traducional mais complexo já detectado entre vírus até o momento. No entanto, o isolamento de vírus deste tipo ainda é um ponto importante e necessário, pois poderia esclarecer características biológicas relacionadas aos mesmos. Desta forma, este estudo se faz necessário, uma vez que busca isolar novos vírus gigantes em amostras ambientais brasileiras, a fim de aumentar a compreensão em relação à diversidade biológica e genética dos vírus gigantes, bem como seus aspectos de evolução com o emprego de abordagens genéticas que permitam elucidar dúvidas acerca da origem, presença, abundância e possível papel de elementos envolvidos em tradução, possivelmente presentes em novos isolados. Além disso, este trabalho também se faz importante por propor a prospecção e avaliação funcional destes elementos em mimivírus isolados anteriormente. Estes elementos, quando presentes nestes vírus, intrigam em relação à sua essencialidade e importância biológica. Por que investir genoma e energia para a biossíntese de elementos presentes em abundância nas células hospedeiras? Seriam estas proteínas virais essenciais para a multiplicação viral? Qual impacto destes elementos na

adaptabilidade viral? E por fim: seriam estes elementos capazes de ampliar a versatilidade e espectro de hospedeiros? Estas e várias outras questões permanecem sem resposta e a busca por novos isolados que possam apresentar um complexo aparato traducional, bem como a avaliação destes elementos em diferentes isolados já conhecidos poderão levar à elucidação do possível papel destes genes na virulência, multiplicação e evolução viral, uma vez que o significado biológico da frequência e essencialidade desses genes ainda é desconhecido.

III- OBJETIVOS

3.1 Objetivo geral

Este trabalho tem por objetivo prospectar e caracterizar novos isolados de vírus gigantes em amostras ambientais, bem como aumentar a compreensão acerca do papel de genes relacionados à tradução em diferentes mimivírus já isolados.

3.2 Objetivos específicos

3.2.1 Prospecção e caracterização de vírus gigantes

- Prospectar vírus gigantes em amostras ambientais;

- Caracterizar biologicamente um novo isolado de vírus gigante;

- Caracterizar geneticamente um novo isolado de vírus gigante;

- Analisar o uso de códons/aminoácidos nos novos vírus isolados;

- Analisar o arsenal de genes relacionados à tradução presentes nestes novos vírus isolados;

- Analisar as relações filogenéticas de aaRS presentes nos novos vírus isolados.

3.2.2 Modulação do nível de mRNA de genes relacionados à tradução em resposta a disponibilidade nutricional durante a infecção de mimivírus em *A. castellanii*

- Analisar a modulação do nível de mRNA de elementos relacionados à tradução em APMV, APMV M4, SMBV, KROV e OYTV durante a infecção de *A. castellanii* sob condições nutricionais diversas;

- Analisar o perfil de multiplicação de APMV, APMV M4, SMBV, KROV e OYTV durante a infecção de *A. castellanii* sob condições nutricionais diversas;

- Analisar possíveis polimorfismos em genes de tRNA e aaRS de APMV, APMV M4, SMBV, OYTV, KROV.

IV-FLUXOGRAMAS DE TRABALHO

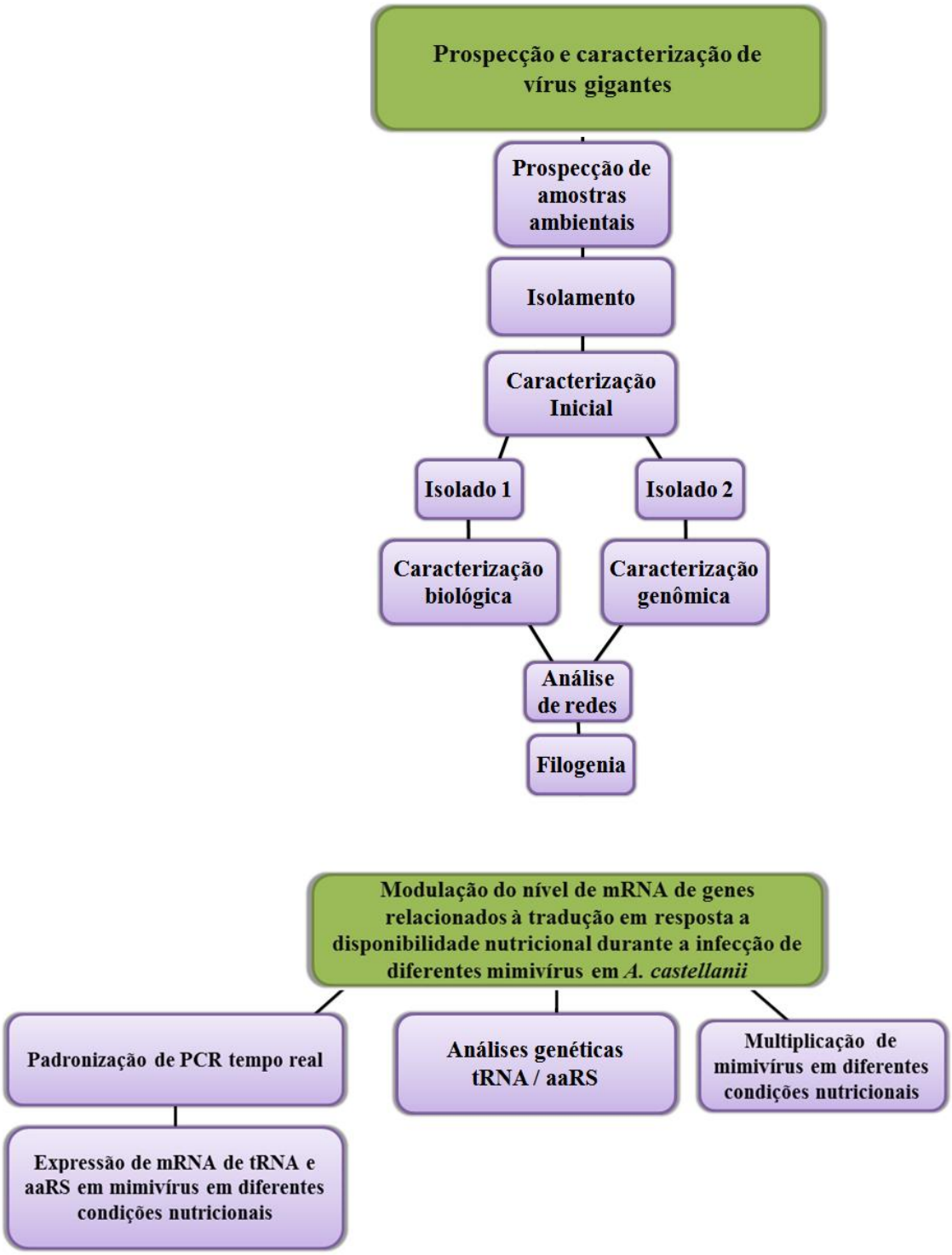

V- MATERIAIS E MÉTODOS

5.1 Prospecção e caracterização de vírus gigantes

5.1.1 Sistemas celulares

Para tentativa de isolamento, produção de vírus e realização de experimentos foram utilizados diferentes suportes celulares: *A. castellanii* (ATCC 30010), *Vermoamoeba vermiformis* (ATCC 20237), *A. polyphaga* (ATCC 50998), *A. griffini* (ATCC 50702), *A. micheline, A. royreba* (ATCC 30884), *A. sp E4*, *Dictyostelium discoideum*, *Willaertia magna* (ATCC 30273), *Tetrahymena hyperangularis* (ATCC 30273) e *Trichomonas tenax* (ATCC 30273). Estas células foram utilizadas no Laboratório de Amebas da equipe do Professor Bernard La Scola, na Aix Marseille Université, França. As diferentes espécies de amebas foram cultivadas em meio específico para cada célula em questão: meio protease peptona extrato de levedura e glicose (PYG) (Anexo 1), para *A. castellanii*, *A. polyphaga*, *A. griffini, A. micheline, A. royreba, A. sp E4*, *Willaertia magna, Tetrahymena hyperangularis;* solução salina para amebas (PAS) (Anexo 2), para *Dictyostelium discoideum* ou TS (Anexo 3), para *V. vermiformis* e *T. tenax*. As amebas foram cultivadas em garrafas de cultura de tamanho médio (TPP, Suíça). Os meios foram suplementados com gentamicina (50 µg/mL), penicilina potássica (200 U/mL) e anfotericina B (fungizona) (2,5 µg/mL). A maioria das células foi mantida à 30ºC, sendo as garrafas completamente vedadas. Apenas *Trichomonas tenax* foi mantida à 35ºC e sob uma atmosfera anaeróbia. Os subcultivos foram realizados três vezes por semana ou de acordo com a necessidade, sendo a monocamada celular desprendida da superfície da garrafa de cultura através de leves batidas nas mesmas. Após este procedimento, as células foram observadas ao microscópio óptico invertido para garantir o desprendimento total da monocamada celular. O conteúdo celular foi coletado, sendo 100 µL deste conteúdo utilizado para realizar uma diluição 1:10 das células em 900 µL de solução salina tamponada (PBS) em um tubo de 1,5 mL. Esse conteúdo foi homogeneizado e 10 µL utilizados para montagem em câmara de Neubauer, sendo as células contadas através de observação ao microscópio. A partir do número obtido, foi realizado o cálculo (número de células/4 x 10 x fator de diluição) e dessa forma utilizou-se um volume contendo aproximadamente $3x10^6$ células de amebas para subcultivo em garrafas novas completadas para 20 mL de meio fresco final.

5.1.2 Multiplicação e purificação viral (Abrahão et al. 2014; Abrahão et al. 2016)

Para a produção de vírus gigantes, garrafas de cultura de 175-cm^2 contendo monocamada de amebas da espécie *A. castellanii* ou *V. vermiformis* apresentando cerca de 90% de confluência foram inoculadas com o vírus na multiplicidade de infecção (m.o.i.) de 0,01. Para isto, o meio das garrafas foi descartado e a solução viral em PBS 1X foi cuidadosamente adicionada sobre a monocamada e adicionou-se um volume de 25 mL de meio PYG 7% SFB. As garrafas contendo os inóculos virais foram mantidas a 30ºC, completamente vedadas. Após a observação de ECP satisfatório, o sobrenadante e o lisado celular foram coletados, transferidos para um tubo cônico de 50 mL, e mantidos sob resfriamento. Após centrifugação a 900 *g*, por 5 min, a 4°C em centrífuga *Sorvall RI 6000B*, o sobrenadante foi transferido para outro tubo cônico, e o sedimento foi submetido a 3 ciclos de congelamento e descongelamento, visando a liberação de partículas eventualmente aprisionadas em trofozoítos não lisados. Ainda com este intuito, o lisado foi ressuspendido em 5-10 mL de PBS 1X e então submetido a 2 ciclos de lise no homogeneizador do tipo "Douncer" (Wheaton, E.U.A.) por 50 vezes. Em seguida, o sobrenadante e o sedimento foram filtrados em filtros de 2 µm (Millipore, E.U.A.) para a retenção de lisado celular. Este filtrado foi então vagarosamente gotejado sobre 10 mL de uma solução de sacarose a 22% (Merck, Alemanha), em tubos próprios para a ultra centrífuga *Combi Sorvall* (Rotor *AH-629va*). A amostra foi, então, ultra centrifugada em *Combi Sorvall* à 14000 r.p.m, por 30 min, entre 4^{o}C e 8^{o}C, para a sedimentação das partículas virais. Por fim, o sobrenadante foi descartado e o sedimento ressuspendido em PBS 1X. As alíquotas virais foram identificadas e estocadas à -80ºC.

5.1.3 Titulação viral (Reed e Muench, 1938)

Placas de 96 poços (TTP, Suíça) contendo $4x10^4$ trofozoítos de amebas *A. castellanii* por poço foram utilizadas para titulação de vírus gigantes pelo método de diluição limitante (REED e MUENCH, 1938). As amostras a serem tituladas sofreram três ciclos de congelamento e descongelamento com nitrogênio líquido, em seguida foram centrifugadas a 900 *g* por 5 min, a 4ºC. O sobrenadante foi diluído seriadamente em PBS, na razão de 10 (10^{-1} a 10^{-11}). Um total de 50 µL de cada diluição foi inoculado em cada poço, em quadruplicata. As placas foram completamente vedadas, incubadas a 30 ºC e a infecção monitorada por até

quatro dias para observação de ECP e cálculo do título pelo método de Reed-Muench, dado em $TCID_{50}$/mL.

5.1.4 Processamento de amostras

Foram prospectadas neste estudo 17 amostras pertencentes à coleção de amostras do grupo de estudo e prospecção de vírus gigantes (GEPVIG). Dentre estas, doze amostras de solo de lagoas alcalinas coletadas em Pantanal da Nhecolândia, Pantanal, Brasil em 2014 por Ivan Bergier (Embrapa Pantanal). E, cinco amostras de solo oceânico coletadas em uma profundidade de 450-2500 metros, coletadas na Bacia de Campo (RJ), no ano de 2012 por um submarino remoto em parceria com a Petrobras. Estas amostras foram numeradas de 1-17 (Tabela 3) e foram submetidas a um pré-tratamento: foram transferidas para tubos cônicos de 15 mL e adicionadas de 5 mL de PAS. O sistema foi mantido por 24 h à 4ºC para decantação do sedimento. Após este tempo, o sobrenadante foi submetido a três etapas de filtração: filtração em filtro de café, filtração em filtro de 5 μm e por último filtro de 0.8 μm para remover partículas grandes de sedimento e concentrar os possíveis vírus gigantes ali presentes. O conteúdo filtrado foi conservado à 8ºC e utilizado para tentativa de isolamento em células de amebas.

Tabela 3. Coleção de amostras para prospecção.

Número da Amostra	Tipo de Amostra	Origem
1	Solo	Lagoa Cascavel II (Pantanal)
2	Solo	Lagoa Santa Rosa (Pantanal)
3	Solo	Lagoa Mineira (Pantanal)
4	Solo	Lagoa Gabinete (Pantanal)
5	Solo	Lagoa STF IV (Pantanal)
6	Solo	Lagoa Burro B (Pantanal)
7	Solo	Lagoa Jati I (Pantanal)
8	Solo	Lagoa Jati II (Pantanal)
9	Solo	Lagoa STF III (Pantanal)
10	Solo	Lagoa Cascavel I (Pantanal)
11	Solo	Lagoa Coração (Pantanal)
12	Solo	Lagoa STF I (Pantanal)
13	Solo	Bacia de Campo (Rio de Janeiro)
14	Solo	Bacia de Campo (Rio de Janeiro)
15	Solo	Bacia de Campo (Rio de Janeiro)
16	Solo	Bacia de Campo (Rio de Janeiro)
17	Solo	Bacia de Campo (Rio de Janeiro)

5.1.5 Tentativa de isolamento

Para o processo de isolamento foram utilizadas amebas *A. castellani* e *V. vermiformis* inicialmente. Aproximadamente $5x10^5$ células foram implantadas em placas de 24 poços, em meio PAS (*A. castellanii)* ou TS (*V. vermiformis*), suplementados com um coquetel de antibióticos: ciprofloxacino (20 μg/mL; Panpharma, Z.I., França), vancomicina (10 μg/mL; Mylan, França), imipenem (10 μg/mL; Panpharma, Z.I., França doxiciclina (20 μg/mL; Panpharma, Z.I., França) e voriconazol (20 μg/mL; Mylan, França). Um total de 100 μL de cada amostra filtrada e concentrada foi inoculado nos respectivos poços (01-17), sendo um poço separado para controle negativo sem amostra, apenas meio de cultura. A placa foi incubada a 30ºC em câmara úmida. Diariamente, os poços foram observados em microscópio óptico para acompanhamento de presença de possível ECP. Após três dias, novas passagens

das amostras inoculadas foram realizadas da mesma maneira: 50 µL das culturas infectadas na primeira passagem, incluindo o controle negativo foram coletados e inoculados em novas placas com amebas frescas, sendo incubadas a 30ºC e observadas diariamente em microscópio óptico. Este procedimento foi realizado até completar-se a terceira passagem, na qual os poços com ECP e lise foram considerados positivos, coletados e utilizados para produção e análise dos possíveis isolados.

5.1.6 Caracterização inicial: microscopia de contraste negativo e Hemacolor®

Na tentativa de iniciar a identificação de possíveis vírus isolados, as amostras positivas foram analisadas por meio de duas diferentes técnicas. Para a microscopia de contraste negativo, aproximadamente 100 µl de cultura de amebas inoculadas e identificadas como positivas foram coletados e fixados com 100 µl de solução de glutaraldeído 2.5%. Uma gota da suspensão viral fixada foi aplicada sobre uma grade específica para microscópio eletrônico. Os vírus foram corados imediatamente com uma gota de molibdato de amónio a 1% (1-800-ACROS, EUA) durante 5 min. O excesso foi retirado com papel de filtro seco. Eletromicrografias foram realizadas em microscópio eletrônico de transmissão Tecnai G20 operado a 200 Kev no Centro de Microscopia da Aix-Marseille Université. Para coloração por Hemacolor®, 100 µl de cultura de amebas inoculadas e identificadas como positivas foram coletados e processados em centrífuga para citocentrifugação do tipo Shandon Cytospin 4 (Thermo Electron Corporation) a 800 rpm por 10 min. As lâminas obtidas foram fixadas com metanol e após secagem foram coradas manualmente com imersão sequencial em três soluções reagentes (1, 2, 3) por 30 seg cada (Hemacolor®, Merck, Alemanha). Após secagem, as lâminas foram montadas com lamínulas, sendo as fábricas e partículas virais observadas em microscópio óptico Olympus BX40 (USA), em óleo de imersão com aumento de 1000x.

5.1.7 Microscopias

Para avaliar a morfologia, bem como o ciclo de multiplicação dos novos isolados, duas técnicas foram utilizadas, microscopia eletrônica de transmissão (MET) e imunofluorescência (IF). Garrafas de cultura de 25-cm^2 com 1x10^7 células *A. castellanii* ou *V. vermiformis* foram infectadas com os isolados na m.o.i de 1 e incubados a 30ºC por 0, 2, 4, 6, 8, 12, 16, 18 e 24 h. Para MET, as células foram coletadas após os tempos indicados, lavadas em meio PAS e centrifugadas a 900 *g* por 10 min, sendo o sedimento obtido fixado em 1 mL de solução de glutaraldeído 2.5% à 4ºC. A inclusão das amostras, secções ultrafinas e eletromicrografias

foram realizadas no Centro de Microscopia da Aix-Marseille Université. O microscópio eletrônico de transmissão utilizado foi Tecnai G20 operado a 200 Kev. Já para IF, 100 µL de células infectadas foram coletados após os tempos determinados e processados em centrífuga para citocentrifugação do tipo Shandon Cytospin 4 (Thermo Electron Corporation) a 800 rpm por 10 min. As lâminas foram fixadas com metanol e após secagem a marcação foi realizada. Basicamente, as lâminas foram saturadas com solução de PBS Tween 0,1% por 15 min à temperatura ambiente; em seguida as lâminas foram incubadas com anticorpo primário anti-Tupanvirus produzido em camundongo (os anticorpos foram produzidos por técnico francês responsável pela plataforma de experimentação animal, sendo o vírus utilizado para tal produzido durante este estudo) diluído 1:500 em solução de BSA 3%/PBS tween 0,1% por 1 h à 37ºC. Após este tempo as lâminas foram lavadas três vezes com PBS tween 0,1%, por 5 min cada lavagem sob agitação. As lâminas foram incubadas com anticorpo secundário anti-camundongo conjugado com FITC diluído 1:500 em solução de BSA 3%/PBS tween 0,1% por 1 h à 37ºC. As lâminas foram novamente submetidas a três ciclos de lavagem em PBS sob agitação e após secagem foram adicionadas de Fluoroprep e montadas com lamínulas para observação em microscópio de fluorescência.

5.1.8 Permissividade em outros sistemas celulares

Garrafas de cultura de 25-cm^2 com aproximadamente 1x10^7 de diferentes células de protozoários do Laboratório de Amebas da Aix-Marseille Université (*A. castellanii*, *V. vermiformis, A. polyphaga*, *A. griffini, A. micheline, A. royreba, A. sp E4, D. discoideum*, *W. magna, T. hyperangularis* e *T. tenax*) mantidas em meio de cultivo específico de crescimento para cada célula de acordo com o item 5.1.1, foram infectadas com o vírus isolado na m.o.i de 1, sendo as garrafas completamente vedadas e incubadas em estufa a 30ºC ou 35º, de acordo com a célula em questão. Após o tempo de adsorção e após 24 h de infecção (sabidamente o tempo para ciclo de multiplicação completo), amostras das células infectadas foram coletadas e utilizadas para verificar o aumento do título viral por PCR em tempo real e titulação em *A. castellanii* conforme descrito no item 5.1.3.

5.1.9 Análises de genoma

Quatro produções diferentes de cada vírus isolado foram realizadas em *A. castellanii* e *V. vermiformis*, partindo de 20 garrafas cada conforme item 5.1.2.1, para sequencial obtenção de vírus purificado para sequenciamento. Os vírus produzidos e purificados foram enviados a

plataforma de genômica de Aix Marseille Université, sendo as etapas de extração, sequenciamento, análise de sequências obtidas e montagem do genoma realizadas pela equipe responsável. Para a predição de ORFs, com o auxílio do programa ARTEMIS (CARVER et al., 2012), ORFs menores que 50 aminoácidos foram descartadas e regiões intergênicas com mais de 1.000 nt foram checadas para avaliar a presença de ORFs hipotéticas. As sequências de aminoácidos obtidas foram exportadas pelo programa e utilizadas para caracterização funcional das ORFs por meio da ferramenta BlastP do *National Center for Biotechnology Information* (NCBI). Foram considerados os *Best hits* sequências que seguiram os seguintes parâmetros: *hit* estatisticamente significativo com valores de identidade >30%; cobertura >70%; E-value < 10^{-3} (ASSIS et al., 2015); ORF sem similaridade com sequências disponíveis no banco de dados não redundante de proteínas do NCBI, bem como qualquer sequência que não apresentou *hit* estatisticamente significativo dentro dos parâmetros exigidos na análise foram consideradas ORFans. Para a predição de tRNA, os genomas dos novos isolados foram submetidos ao *software* online ARAGORN (LASLETT e CANBACK, 2004). A anotação resultante do genoma de TPVdo foi utilizada para montar bancos de dados que foram utilizados no *software* CIRCOS (KRZYWINSKI et al., 2009) para obtenção de ideograma circular para análise deste genoma em relação a possível origem dos genes virais. Para comparar o genoma dos novos isolados com sequências de outros vírus gigantes descritos foi realizado o cálculo do conteúdo G-C e análise do uso de códons, utilizando também o programa ARTEMIS (CARVER et al., 2012).

5.1.10 Análises de redes

Para a análise de redes de elementos envolvidos em tradução em vírus gigantes, foram analisadas três categorias: tRNA, aaRS e TF. Elementos destas diferentes categorias foram pesquisados nos genomas disponíveis em bancos de dados para diferentes mimivírus das linhagens A, B e C; *Cafeteria roenbergensis virus*, Klosneuvirus, *A. castellanii*, *Encephalitozoon cuniculi*, *Nanoarchaeum equitans*, *Candidatus Carsonella ruddii* e os novos isolados de Tupanvirus. Estes dados serviram como base para a montagem de dois bancos de dados necessários para obtenção dos grafos através de importação para programa Gephi 0.9.1 (BASTIAN, HEYMANN e JACOMY, 2009). Foi criada uma planilha de Excel (Microsoft Oficce) contendo todos os elementos a serem avaliados no programa e uma segunda planilha contendo as conexões destes elementos com seus vírus ou organismos celulares. Uma vez importados, o *software* forneceu grafos (rede de conexões obtidas com o conjunto de dados)

que foram submetidos ao algorítimo de layout de *Fruchterman-Reingold*, que se baseia no princípio de direcionamento por força entre os elementos do grafo de acordo com o grau de conexão para gerar a conformação final. Após, os grafos foram manualmente editados e ajustados para melhor visualização dos dados.

5.1.11 Análises filogenéticas

Para tentar compreender a relação evolutiva entre aaRS presentes nos novos vírus gigantes isolados e em outros já descritos, foram realizadas análises filogenéticas utilizando as sequências de aminoácidos para cada uma das 20 aaRS. Para gerar os alinhamentos, foram utilizadas sequências preditas para os genes correspondentes aos novos isolados, bem como seus 100 primeiros *best hits* obtidos em bancos de dados através de análise de BlastP. As sequências de aminoácidos obtidas foram formatadas em FASTA e alinhadas pelo método ClustalW através do programa MEGA 7.0 (KUMAR, STECHER e TAMURA, 2016). A partir deste alinhamento, foram geradas árvores filogenéticas através do método de máxima verossimilhança com 1000 replicatas de bootstrap. Análises filogenéticas também foram realizadas para o gene da DNA Polimerase B, um gene conservado em vírus gigantes, na tentativa de compreender a posição dos novos isolados em relação a outros vírus gigantes já conhecidos. Para isso, as sequências nucleotídicas desta proteína nos tupanvírus e outros vírus foram obtidas através do banco de dados do NCBI. As sequências foram organizadas em FASTA e alinhadas pelo método ClustalW através do programa MEGA 7.0 (KUMAR, STECHER e TAMURA, 2016). A partir deste alinhamento, foram geradas árvores filogenéticas através do método de máxima verossimilhança com 1000 replicatas de bootstrap.

5.2 Modulação do nível de mRNA de genes relacionados à tradução em resposta a disponibilidade nutricional durante a infecção de mimivírus em *A. castellanii*

5.2.1 Sistemas celulares

Para a produção de vírus e realização de experimentos foram utilizadas células de *A. castellanii* provenientes da *American Type Culture Collection* (ATCC 30010) (Maryland, E.U.A.), gentilmente cedidas pelo Laboratório de Amebíases do Instituto de Ciências

Biológicas (ICB), da Universidade Federal de Minas Gerais (UFMG). As amebas foram cultivadas em garrafas de cultura de tamanho médio contendo meio PYG suplementado com 7% de soro fetal bovino (SFB) (Cultilab) de acordo com item 5.1.1.

5.2.2 Vírus

Cinco vírus diferentes foram utilizados nesta parte do trabalho. O estoque inicial de APMV, vírus protótipo da família *Mimiviridae* (LA SCOLA et al., 2003), foi gentilmente cedido por Dr. Didier Raoult (Aix-Marseille Université, França). Estoques virais posteriores foram produzidos e titulados, de acordo com a necessidade, em células de *A. castellanii*. APMV M4 é um clone obtido após 150 passagens de APMV em cultivo de amebas *A. castellanii*. Após esse número sucessivo de passagens, o clone obtido apresentou várias diferenças genéticas, morfológicas e biológicas em relação ao protótipo APMV (BOYER et al., 2011). O estoque inicial de APMV M4 foi gentilmente cedido por Dr. Bernard La Scola (Aix Marseille Université, França). Estoques virais posteriores foram produzidos e titulados, de acordo com a necessidade, em células de *A. castellanii*. SMBV foi o primeiro vírus gigante brasileiro isolado e caracterizado pelo GEPVIG. A amostra foi isolada de uma amostra de água coletada no Rio Negro, Amazonas, em 2011 (CAMPOS et al., 2014). Estoques virais foram produzidos e titulados de acordo com a necessidade em células de *A. castellanii*. Kroon virus (KROV) é uma amostra de vírus gigante brasileiro isolado e caracterizado pelo GEPVIG. O vírus foi isolado de uma amostra de água coletada na Lagoa Central do município de Lagoa Santa, Minas Gerais, em 2012 (ASSIS et al., 2015). Estoques virais foram produzidos e titulados, de acordo com a necessidade, em células de *A. castellanii*. OYTV é uma amostra de vírus gigante brasileiro isolado e caracterizado pelo GEPVIG. Foi isolado a partir de uma amostra de ostra coletada na orla da cidade de Florianópolis, SC, em 2013 (ANDRADE et al., 2015). Estoques virais foram produzidos e titulados, de acordo com a necessidade, em células de *A. castellanii*.

5.2.3 Multiplicação e purificação viral (Abrahão et al. 2014; Abrahão et al. 2016)

Para a produção dos vírus gigantes utilizados nesta parte do trabalho, células de amebas da espécie *A. castellanii* foram utilizadas para infecção e o protocolo de produção, seguido de purificação se deu como descrito no item 5.1.2.

5.2.4 Titulação viral (Reed e Muench, 1938)

Para a titulação de vírus produzidos ou de amostras provenientes de experimentos nesta parte do trabalho foi utilizado a titulação pelo método de diluição limitante (REED e MUENCH, 1938) e o protocolo se deu como descrito no item 5.1.3.

5.2.5 Uso de códons e aminoácidos

Para investigar o perfil de utilização de códons e aminoácidos em diferentes mimivírus e compará-los entre si, bem como entre os vírus e o hospedeiro *A. castellanii*, as sequências proteicas preditas de APMV (Genbank: HQ336222.2), APMV M4 (Genbank: JN036606.1), SMBV (Genbank: KF959826.2), KROV (Genbank: KM982402), OYTV (Genbank: KM982401) e *A. castellanii* (Genbank: AHJI00000000.1) foram obtidas a partir do banco de dados do GenBank/NCBI e submetidos a cálculo do uso de códons e composição de aminoácidos usando o programa ARTEMIS. Os perfis de utilização foram expressos em porcentagem e refletiram a contribuição de cada códon/aminoácido separadamente.

5.2.6 Padronização de PCR em tempo real

Oito pares de iniciadores foram desenhados para a amplificação de oito genes alvos relacionados à tradução em mimivírus (leucinil-tRNA, histidinil-tRNA, cisteinil-tRNA, triptofanil-tRNA, metionil-RS, cisteinil-RS, tirosinil-RS e arginil-RS) por PCR em tempo real. Os iniciadores foram desenhados com base no genoma completo de APMV disponível (Genbank: HQ336222.2) e utilizando a plataforma online do NCBI. Os iniciadores em solução estoque foram diluídos na concentração de 200 μM, sendo o estoque de trabalho à 10 μM. Foi realizado um teste para avaliar a concentração ideal de iniciadores a ser utilizada nas reações, sendo ao final estas realizadas em placas de 48 poços, em duplicata, utilizando 0,1 μM de iniciadores específicos *forward* e *reverse*, 5 μL de SYBR Green Master Mix, 1 μL de amostra (Applied Biosystem, EUA) e água em concentrações ajustadas para 10 μL de reação. Controles negativos foram realizados nas mesmas condições, sendo a amostra substituída por 1 μL de água.As reações foram feitas no aparelho StepOne (Applied Biosystem, EUA) seguindo as condições térmicas padrão do mesmo. Com a reação funcionando, foram construídas curvas padrão para cada gene avaliado em questão. O DNA de APMV foi extraído através do método PCI, no qual basicamente 10 μL de vírus purificado foi adicionado de 450 μL de PBS, este conteúdo foi acrescido (v/v) de solução fenol/clorofórmio/álcool

isoamílico 25:24:1 e homogeneizado por inversão, em seguida foi centrifugado em microcentrífuga *Eppendorf 5415R* a 12000*g* por 5 min. A fase aquosa foi então recuperada e transferida para um novo tubo livre de DNase. Na etapa de precipitação, foram adicionados solução de acetato de sódio (1/10 v/v) e etanol 96°GL gelado (2x v/v), seguido de incubação no gelo por 5 min. Em seguida, a solução foi centrifugada a 12000 *g* por 5 min à 4°C. O sobrenadante foi então descartado e o sedimento incubado a 37°C para secagem e em seguida, ressuspendido em 50 μL de água livre de nuclease para a solubilização do DNA. O DNA extraído dosado e em seguida submetido a PCR em tempo real para amplificação de cada um dos 8 alvos de trabalho, em duplicata, sendo realizado também dois poços para controle negativo de reação. Após, cada 20 μL de produto de PCR obtido foi coletado e diluído seriadamente em água livre de nuclease em 10 pontos (10^{-1}-10^{-10}), sendo os pontos de 10^{-3}-10^{-7} de cada alvo utilizados como pontos da curva padrão durante todo o estudo. Estas curvas foram avaliadas quanto à eficiência (estabelecida entre 80-110%) para garantir a qualidade das análises a serem realizadas durante o estudo.

5.2.7 Infecções em diferentes condições nutricionais

Para investigar o nível de mRNA de genes relacionados à tradução em mimivírus sob diferentes condições nutricionais, placas de 24 poços contendo $1x10^5$ amebas por poço em volume de 500 μL de meio específico, foram infectadas quando as monocamadas atingiram 90% de confluência. As infecções foram realizadas em duplicata, com APMV, APMV M4 e os isolados brasileiros (SMBV, KROV e OYTV) na m.o.i de 10. As três diferentes condições de infecção utilizadas foram: PAS (um meio salino simples usado para manutenção de amebas), PYG (o meio comumente utilizado para cultivo de amebas em laboratório), sendo em uma condição complementado com 7% de SFB e em outra sem SFB. Para infecção, cada meio de cultura específico foi retirado dos poços com amebas, e então adicionados de 100 μL de solução viral para cada vírus na m.o.i de 10, em duplicata. Controles de células foram realizados em duplicata, com adição de 100 μL de PBS 1X. As placas foram vedadas e incubadas por uma hora a 30ºC, com agitação a cada 10 min. Após o tempo de adsorção, as placas foram retiradas da estufa e o inóculo viral foi cuidadosamente retirado dos poços com auxílio de pipeta de 100 μL (no caso, os poços não foram lavados com PBS 1X, pois este procedimento implica no descolamento de amebas da monocamada, levando a perda), sendo os poços preenchidos com novos 500 μL de meio fresco específico. As placas foram incubadas a 30ºC, totalmente vedadas. Após 8 h de infecção, tempo em que ocorre o pico de

multiplicação destes vírus, sobrenadante e células foram coletados, sendo as placas observadas em microscópio óptico invertido antes da coleta para observação da morfologia das células infectadas e das células controle, bem como após a coleta, para garantir que todas as células foram desprendidas da monocamada e recuperadas. O conteúdo coletado foi centrifugado a 900*g* por 5 min a 4ºC. O sobrenadante foi descartado e o sedimento obtido utilizado para extração de RNA total, transcrição reversa e PCR em tempo real conforme item 5.2.8.

5.2.8 Extração de RNA, transcrição reversa e PCR em tempo real

A extração de RNA total foi feita a partir de alíquotas coletadas durante os ensaios de infecção em diferentes condições nutricionais utilizando o kit RNeasy (Qiagen, Alemanha), de acordo com as recomendações do fabricante. O processo consistiu, resumidamente, nas seguintes etapas: lise celular e inativação de RNAses com 700 µL tampão de guanidina, desnaturação e precipitação dos complexos proteicos com 700 µL de etanol 70%, e passagem das amostras por uma coluna de afinidade, seguido de centrifugação à 8000*g* por 30 seg. O conteúdo líquido foi descartado. Em seguida, foi realizada lavagem com 700 µL de tampão de lavagem RW1, seguido de centrifugação à 8000*g* por 30 seg. O conteúdo líquido foi descartado. Após, foram realizados mais dois ciclos de lavagem com 500 µL de tampão RPE seguido de centrifugação à 8000*g* por 30 seg e 1 min em cada ciclo. O conteúdo líquido foi descartado. Por fim, a eluição do RNA extraído foi realizada com 50 µL água livre de nuclease. Após centrifugação à 8000*g* por 1 min, o RNA obtido foi dosado e estocado em -80ºC. A obtenção de DNA complementar (cDNA) foi feita tendo como molde 1 µg de RNA extraído das culturas de células. As reações foram feitas utilizando-se a enzima MMLV (Promega, Madison, WI, USA), tampão 5X, dNTP, oligo-dT e DTT nas concentrações indicadas pelo fabricante e água q.s.p. para 20 µL de reação. O RNA e oligo-dT foram incubados a 70°C por 5 min e depois incubados em gelo por 5 min. Os outros componentes da reação foram adicionados e os tubos incubados a 42°C por uma hora e a 72°C por 15 min. O cDNA resultante foi diluído 1:10 e foi utilizado como molde para PCR em tempo real. Estas foram feitas em placas de 48 poços, em duplicata, utilizando 0,1 µM de iniciadores específicos, 5 µL de SYBR Green Master Mix e água em concentrações ajustadas para 10 µL de reação. As reações foram feitas no aparelho StepOne, seguindo as condições térmicas padronizadas do mesmo. Os resultados foram obtidos a partir de valores arbitrários dados às curvas padrão padronizada conforme o item 5.2.6. Os gráficos de amplificação obtidos foram

analisados quanto à qualidade através de parâmetros como C_T, curva de dissociação, curva padrão, eficiência e os resultados foram exportados para realização dos cálculos. Análises de expressão relativa de nível de mRNA para os elementos envolvidos em tradução foram realizadas utilizando o método ΔΔCt e normalizadas para 18S ribossomal amebiano (18S rDNA).

5.2.9 Curva de ciclo único

Células *A. castellanii* foram implantadas em placas de 6 poços ($1x10^6$ células por poço) em volume de 1 mL de meio específico. Ao atingirem aproximadamente 90% de confluência, as células foram infectadas. Para infecção, o meio de cultura foi retirado dos poços com amebas, e então adicionados de 400 μL de solução viral para cada vírus analisado na m.o.i de 10, em duplicata para cada tempo estabelecido. Controles de células foram realizados em duplicata, com adição de 400 μL de PBS 1X. As placas foram vedadas e incubadas por uma h à 30ºC, com agitação a cada dez min. Após o tempo de adsorção, as placas foram retiradas da estufa e o inóculo viral retirado dos poços com auxílio de pipeta de 1000 μL (no caso, os poços não foram lavados, pois este procedimento implica no descolamento de amebas da monocamada, levando a perda), sendo os poços preenchidos com novo 1 mL de meio fresco específico. As placas foram incubadas a 30ºC, totalmente vedadas. Após diferentes períodos de infecção: 0 (1 h após a adsorção); 2; 4; 8; 24 h, sobrenadante e células foram coletados, sendo as placas observadas em microscópio óptico invertido antes da coleta para observação da morfologia das células infectadas e das células controle, bem como após a coleta, para garantir que todas as células foram desprendidas da monocamada e recuperadas. O conteúdo coletado foi centrifugado a 900*g* por 5 min a 4ºC. O sobrenadante foi descartado e o sedimento ressuspendido em PBS 1X, a partir do qual foi verificado o perfil de multiplicação viral por titulação em amebas *A. castellanii* pelo método de diluição limitante de Reed-Muench (REED e MUENCH, 1938) conforme descrito no item 5.1.3.

5.2.10 Análise de polimorfismos em tRNA e aaRS de mimivírus

Para investigar possíveis polimorfismos entre os genes relacionados à tradução presentes nos mimivírus analisados, as sequências de tRNA e aaRS de APMV, APMV M4, SMBV, KROV e OYTV foram obtidas através do genoma completo depositado no banco de dados do Genbank. As sequências foram analisadas quanto à posição dos promotores, sítios de poliadenilação e éxons. Essas sequências foram organizadas em formato FASTA e

alinhadas através do método ClustalW com posterior curação manual utilizando MEGA *software* versão 5.2 (Arizona State University, Phoenix, AZ, USA). Após o alinhamento, as sequências foram analisadas e comparadas manualmente para verificar similaridade, perfil de sequência de promotores, sítios de poliadenilação e *gaps*.

5.2.11 Análises estatísticas

Análises estatísticas foram realizadas através do programa GraphPad Prism 5.0 (CA, USA). A análise de significância foi realizada comparando a média dos resultados obtidos. Os valores foram submetidos em diferentes combinações a análises por testes de One-way ANOVA e Bonferroni (intervalos de confiança de 95%). Diferenças entre grupos foram consideradas significativas quando os valores de p foram menores que 0,05.

VI- RESULTADOS

Em Dezembro de 2013, teve início o projeto de doutorado contemplado nesta Tese e este foi inicialmente pensado como um estudo da importância biológica de elementos relacionados à tradução em vírus gigantes. Desta forma, no primeiro ano, foi realizado um trabalho para verificar a modulação da expressão destes elementos em diferentes vírus da família *Mimiviridae*. Esta primeira parte do trabalho resultou na padronização de ensaio de PCR em tempo real direcionado a 8 elementos relacionados a tradução em mimivírus, bem como a avaliação da modulação da expressão gênica destes elementos pelos diferentes vírus em estudo quando infectando amebas em condições nutricionais distintas. Os resultados desta primeira parte do projeto foram publicados em 2015 (Anexo 08) e geraram novos questionamentos que levaram a perspectiva de continuação do estudo utilizando a técnica de silenciamento destes genes, como uma complementação aos dados já alcançados e publicados.

Desde 2011, através do início de uma colaboração com o grupo francês coordenado pelos professores Didier Raoult e Bernard La Scola, o grupo de estudo e prospecção de vírus gigantes (GEPVIG), coordenado pelo professor Jônatas Santos Abrahão, tem trabalhado na prospecção e caracterização de vírus gigantes em diferentes biomas brasileiros. Neste contexto, no segundo semestre de 2015, várias amostras coletadas em lagoas alcalinas no Pantanal foram triadas no Laboratório de Vírus pela aluna Thalita Arantes de Souza, sendo observado para uma delas, um efeito citopático (ECP) diferenciado em amebas da espécie *A. castellanii*. Foi confirmada por microscopia de varredura a presença de um novo isolado de vírus gigante na amostra, com uma morfologia peculiar, nunca vista até então. Desta forma, com o objetivo de acelerar a caracterização deste novo isolado, as amostras originais foram levadas à Marseille, para serem também trabalhadas durante o período de doutorado sanduíche. Na tentativa de expandir os resultados obtidos no Brasil, as amostras foram novamente triadas no laboratório francês. Após o re-isolamento, foram preparadas grandes produções para análises gênomica, proteômica, análise de ciclo de multiplicação, bem como análise de espectro de hospedeiros. Estes resultados são apresentados nesta Tese e, diante deste histórico, para facilitar a compreensão, os resultados serão divididos em dois tópicos.

6.1 Prospecção e caracterização de vírus gigantes

6.1.1 Prospecção e isolamento

Foram triadas doze amostras de solo de lagoas salinas do Pantanal e cinco amostras de solo oceânico do Rio de Janeiro. As amostras foram submetidas a um processo de pré-tratamento e em seguida foram triadas através de um processo de inoculação e passagens em amebas *A. castellanii* e *V. vermiformis*. Após três passagens, quatro amostras foram positivas, apresentando ECP e lise celular (Fig. 17A): 7, 10, 12 (amostras de solo de lagoas do pantanal) e 15 (amostra de solo oceânico). As amostras 7, 12 e 15 foram inicialmente positivas apenas em *V. vermiformis*. Já a amostra 10 apresentou ECP em *A castellanii* e, de forma surpreendente, também em *V. vermiformis*, as duas plataformas testadas (Tabela 4). Este resultado foi promissor, pois até aquele momento nunca havia sido isolado um vírus gigante capaz de gerar ECP em duas células de amebas de gêneros diferente.

Tabela 4. Resultado da prospecção de amostras ambientais em diferentes amebas.

Número da Amostra	***A. Castellanii***	***V. vermiformis***
1	-	-
2	-	-
3	-	-
4	-	-
5	-	-
6	-	-
7	-	+
8	-	-
9	-	-
10	+	+
11	-	-
12	-	+
13	-	-
14	-	-
15	-	+
16	-	-
17	-	-

6.1.2 Caracterização inicial das amostras positivas

Diante do resultado promissor, as amostras positivas foram rapidamente expandidas em suas respectivas células de isolamento e uma tentativa de caracterização rápida foi feita através de microscopia eletrônica, utilizando a técnica de contraste negativo, e também através de coloração por Hemacolor®. O contraste negativo revelou que as quatro amostras positivas apresentavam uma morfologia similar: um vírus gigante, com capsídeo clássico de mimivírus, sendo ligado a ele, uma estrutura cilíndrica, semelhante a uma "cauda" (Fig. 11 e 12). Esse resultado foi interessante, pois mostrou que o isolado 10 aparentemente era capaz de infectar duas células diferentes, *A. castellanii* e *V. vermiformis*, uma vez que, pelo menos morfologicamente, os vírus isolados nestas duas plataformas celulares, eram muito parecidos.

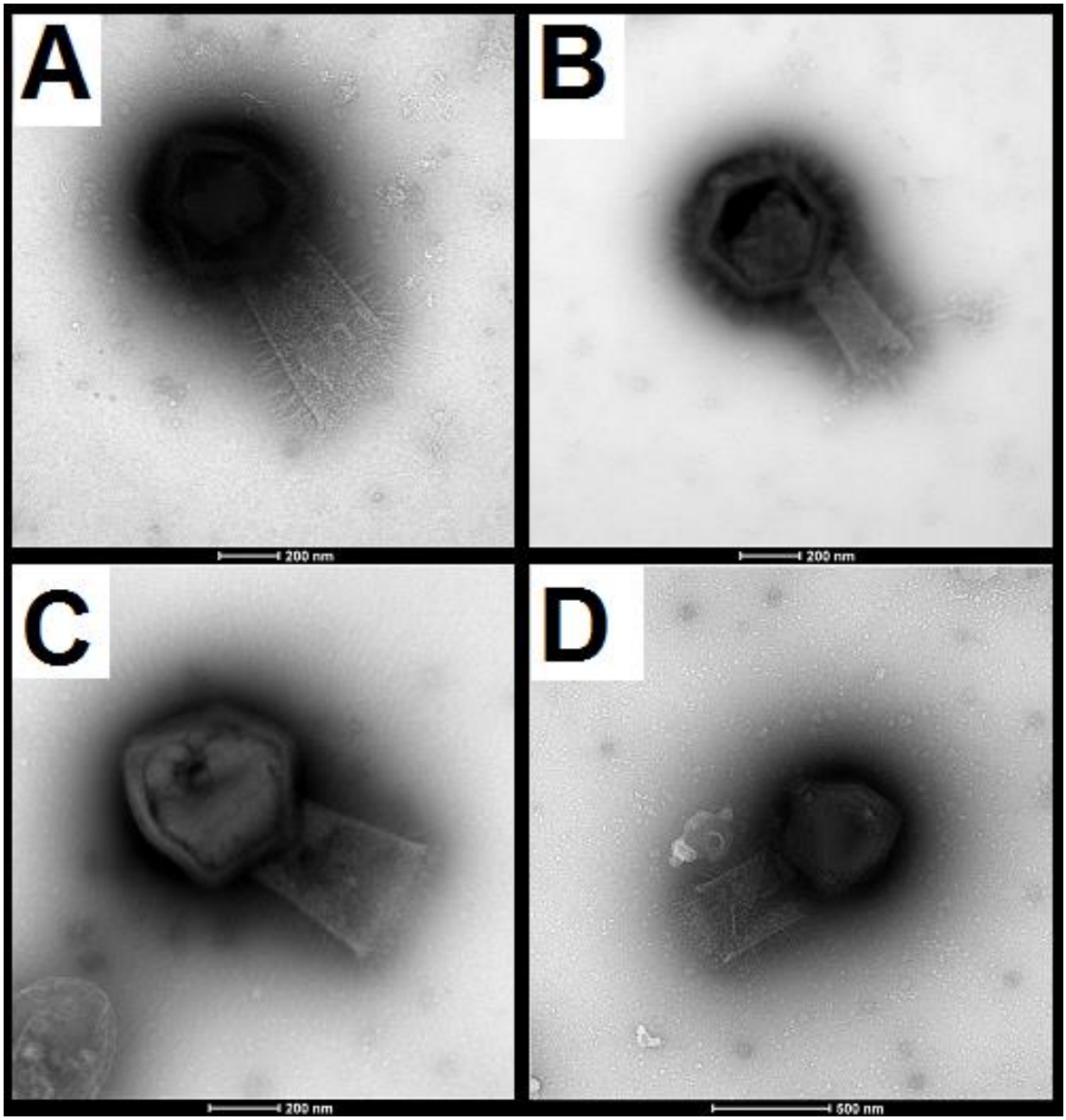

Figura 11: Isolados de solos de lagoas alcalinas visualizados por microscopia eletrônica de contraste negativo. (A) amostra 7 em *V. vermiformis*; (B) amostra 12 em *V. vermiformis*; (C) amostra 10 em *A. castellanii*; (D) amostra 10 em *V. vermiformis.* É possível notar que os novos isolados apresentam um capsídeo icosaédrico típico de mimivírus, porém a estrutura da cauda ligada a este capsídeo torna a estrutura destes vírus muito peculiar. Os isolados correspondentes à amostra 10 (em C e D) foram isolados em duas amebas de gêneros diferentes.

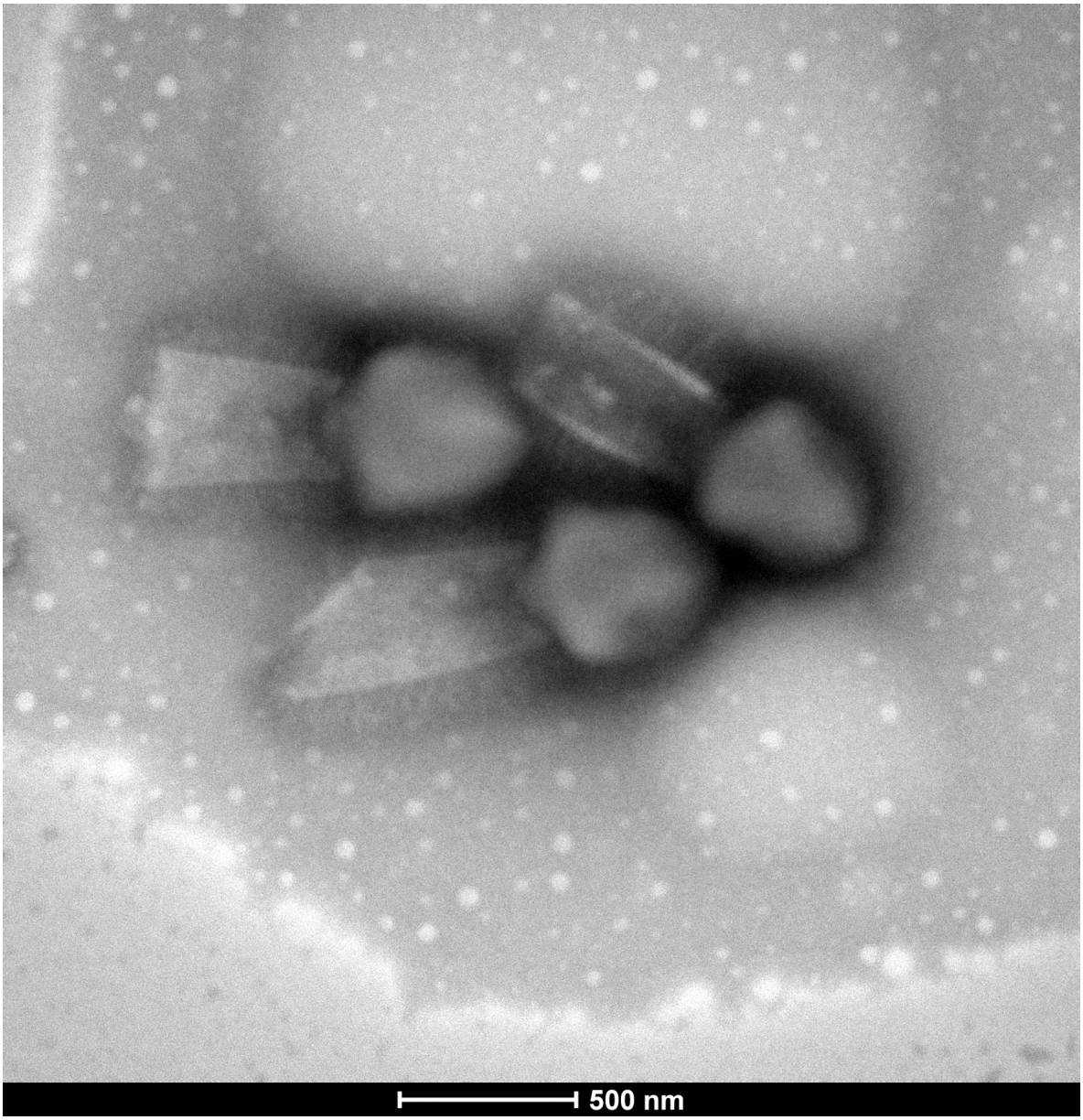

Figura 12: Isolado de solo oceânico visualizado por por microscopia eletrônica de contraste negativo. Amostra 15 em *V. vermiformis.* É possível notar que o novo isolado apresenta um capsídeo icosaédrico típico de mimivírus, porém com a estrutura de uma cauda ligada a este capsídeo.

Já a coloração por Hemacolor® permitiu a visualização de partículas e fábricas virais típicas de vírus gigantes nas amebas infectadas. (Fig. 13).

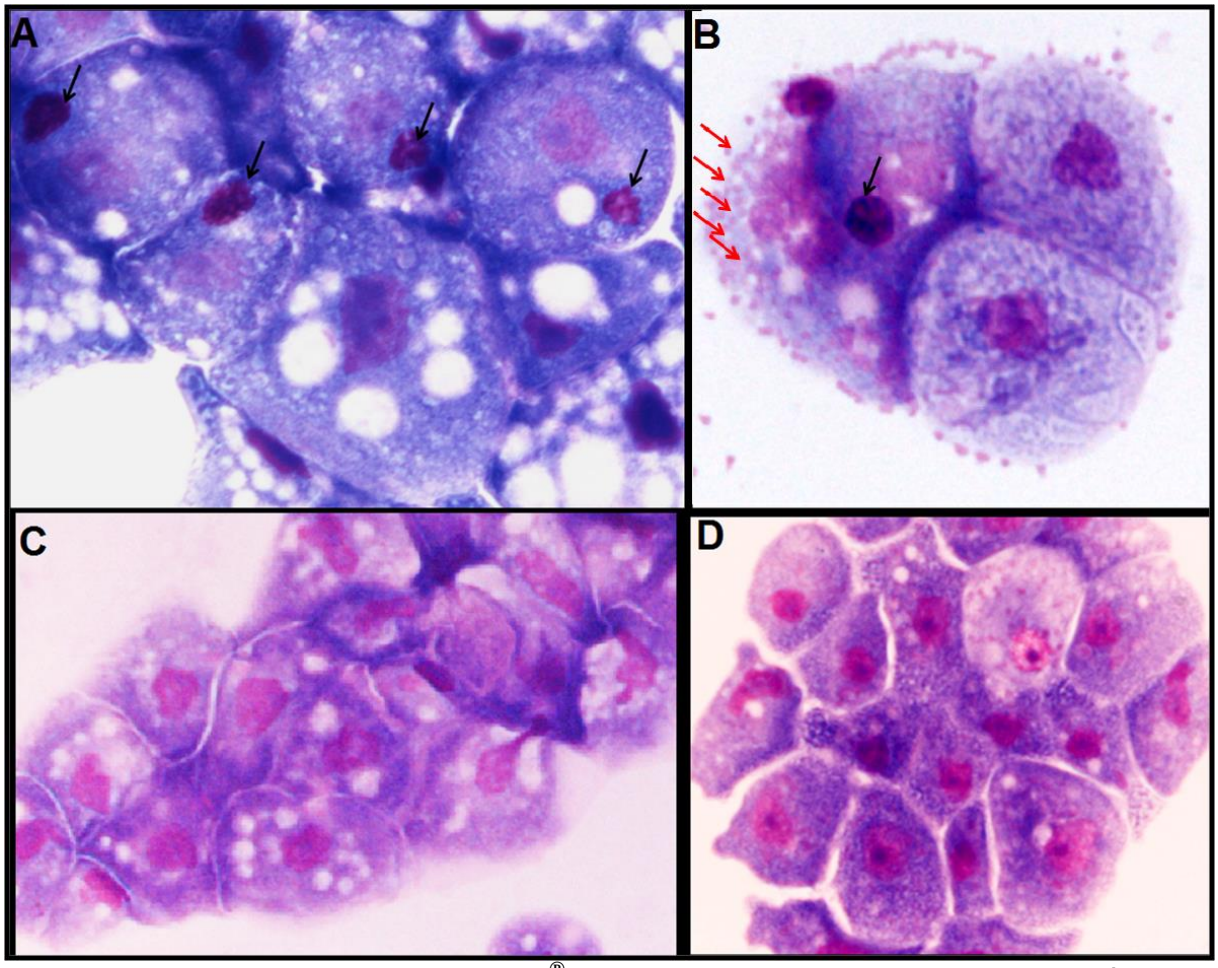

Figura 13: Coloração Hemacolor® em amebas. (A) amostra 10 em *A. castellanii*. É possível observar fábricas virais típicas (formato circular-disforme) de vírus gigantes indicadas pelas setas pretas. Próximo às fábricas é possível visualizar o núcleo celular; (B) amostra 10 em *V. vermiformis*. É possível observar uma fábrica viral próxima ao núcleo celular indicada pela seta preta. As setas vermelhas indicam partículas virais como pontos aleatórios dentro do citoplasma da célula hospedeira; (C e D) amebas *A. castellanii* e *V. vermiformis*, respectivamente, não infectadas. É possível ver o núcleo das células, bem como a presença de um número maior vacúolos (aparecem em menor número nas células infectadas). Aumento de 1000 vezes.

Das amostras positivas, optou-se por trabalhar com a amostra 10, isolada a partir de amostras de solo de lagoas alcalinas do Pantanal em duas plataformas celulares diferentes e com a amostra 15, isolada a partir de solo oceânico em *V. vermiformis*. Os novos isolados foram então denominados de Tupanvirus (TPV), sendo o isolado proveniente do Pantanal, denominado Tupanvirus soda lake (TPVsl) e o isolado proveniente de solo oceânico, Tupanvirus deep ocean (TPVdo). A fim de otimizar o estudo dos novos isolados, optou-se por trabalhar com TPVsl na plataforma de caracterização biológica (a parte de anotação do

genoma deste isolado foi realizada por outro aluno) e com o TPVdo na plataforma genômica. É importante ressaltar que as amostras 7, 12 e 15, isoladas incialmente apenas em *V. vermiformis* foram expandidas após isolamento e novamente inoculadas em *A. castellanii* e, desta forma, mostraram-se capazes de infectar também está célula, assim como a amostra 10, apesar do resultado negativo inicial.

6.1.3 Tupanvirus soda lake: morfologia

Imagens de microscopia eletrônica evidenciaram uma morfologia diferente para TPVsl (Fig. 14). A partícula apresenta um capsídeo similar ao de outros mimivírus com aproximadamente 450 nm e com presença de *stargate* (Fig. 14C). No entanto, o que chamou mais atenção foi a presença de uma grande estrutura cilíndrica ligada na base do capsídeo, como uma cauda, com aproximadamente 550 nm de extensão e 450 nm de diâmetro, incluindo fibrilas e preenchida com pequenas estruturas eletrodensas. Dessa forma, o vírion completo possui um tamanho médio de aproximadamente 1 µm, embora algumas partículas possam atingir mais de 2 µm, devido a variações de tamanho desta cauda. (Fig. 14G). O conteúdo interno da cauda é menos eletrondenso que do capsídeo e não preenche toda a cauda (há um compartimento vazio na parte inferior). As imagens analisadas sugerem ainda que o capsídeo e cauda não estão firmemente ligados (Fig. 13Ae F).

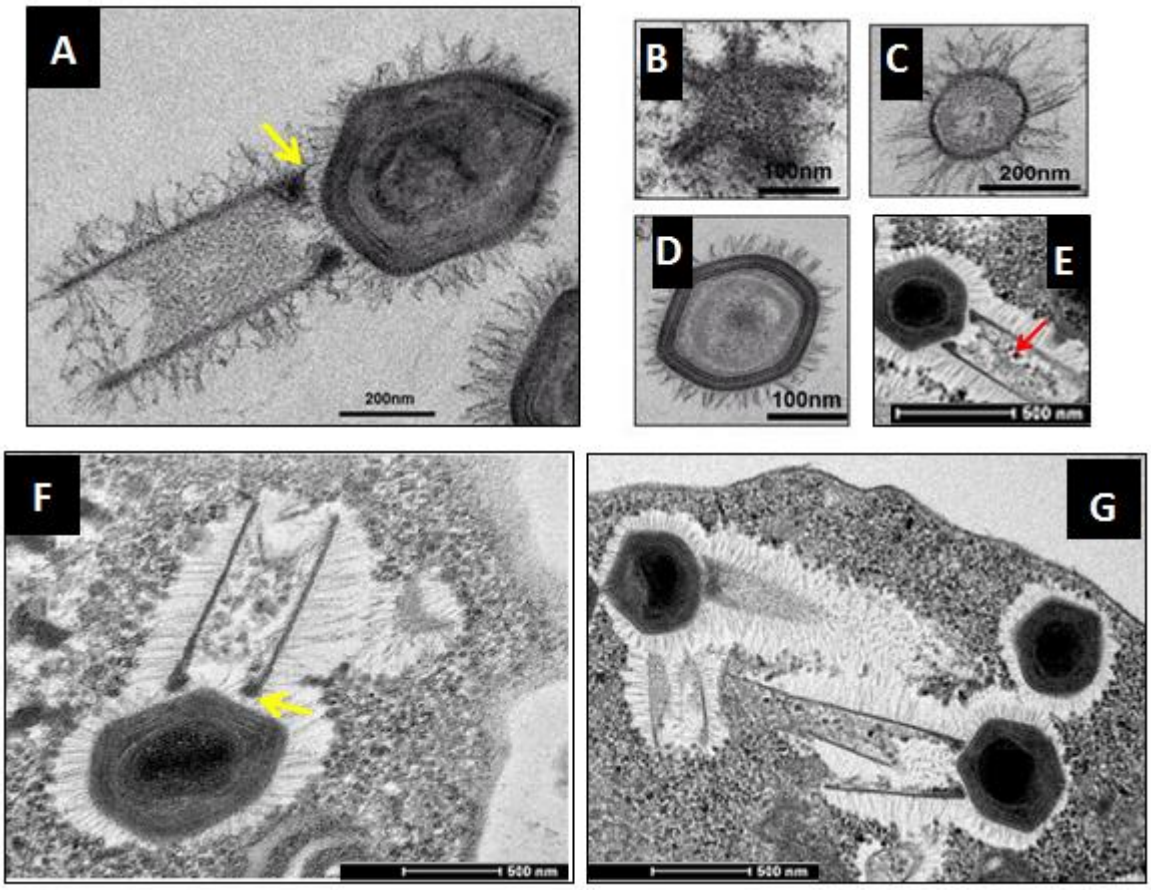

Figura 14: Partícula de Tupanvirus soda lake. Imagens de microscopia eletrônica de transmissão que evidenciam as características e peculiaridades do novo isolado. (A) Uma partícula de TPVsl em *A. castellani*, é possível ver claramente o capsídeo típico de mimivírus ligado a uma cauda, sendo as duas estruturas circundadas por fibrilas. A seta amarela evidencia que a cauda é frouxamente ligada ao capsídeo (B) *Stargate* de TPVsl; (C) Corte transversal da cauda de TPV; (D) Capsídeo de TPVsl ainda sem a cauda ligada, evidenciando a presença de fibrilas externas no capsídeo; (E) Partícula de TPVsl que exibe uma cauda preenchida com pequenas estruturas eletrodensas indicados pela seta vermelha; (F) Uma partícula de TPVsl em *V. vermiformis*. A seta amarela evidencia que a cauda é frouxamente ligada ao capsídeo; (G) Detalhe de partículas com caudas maiores. As imagens A, B, C, D foram obtidas no Centro de Microscopia da UFMG e as imagens E, F e G foram obtidas no Centro de Microscopia de Aix Marseille Université.

6.1.4 Tupanvirus soda lake: ciclo de multiplicação

O ciclo viral de TPVsl observado por MET em *A. castellanii* e *V. vermiformis* revelou um perfil de multiplicação similar em ambas as células (Fig. 15). As partículas são internalizadas através de fagocitose e mantidas dentro de fagossomos (1-2 h.p.i) (Fig. 15A e B). Neste passo, o genoma é liberado através da abertura do *stargate* pela fusão da membrana interna do capsídeo com a membrana do fagossomo. Curiosamente, a abertura do *stargate* pode ser precedida ou seguida pela fusão de membrana da cauda também com o fagossomo, causando a liberação do conteúdo da cauda no citoplasma das amebas (Fig. 15C e D). Ocorre uma fase de eclipse típica. Aproximadamente 10 h.p.i foi possível visualizar a formação de fábricas virais do tipo "vulcão", uma espécie de "cratera" que toma parte do citoplasma da ameba e ejeta as partícula virais maduras (Fig. 15E). A morfogênese viral revelou que a cauda

é ligada ao capsídeo após a formação e fechamento do mesmo, sendo o processo associado a fábrica viral (Fig. 15F). Em tempos tardios, 24 h.p.i, o citoplasma da ameba é preenchido com partículas virais maduras, seguido da lise celular e liberação dos vírus.

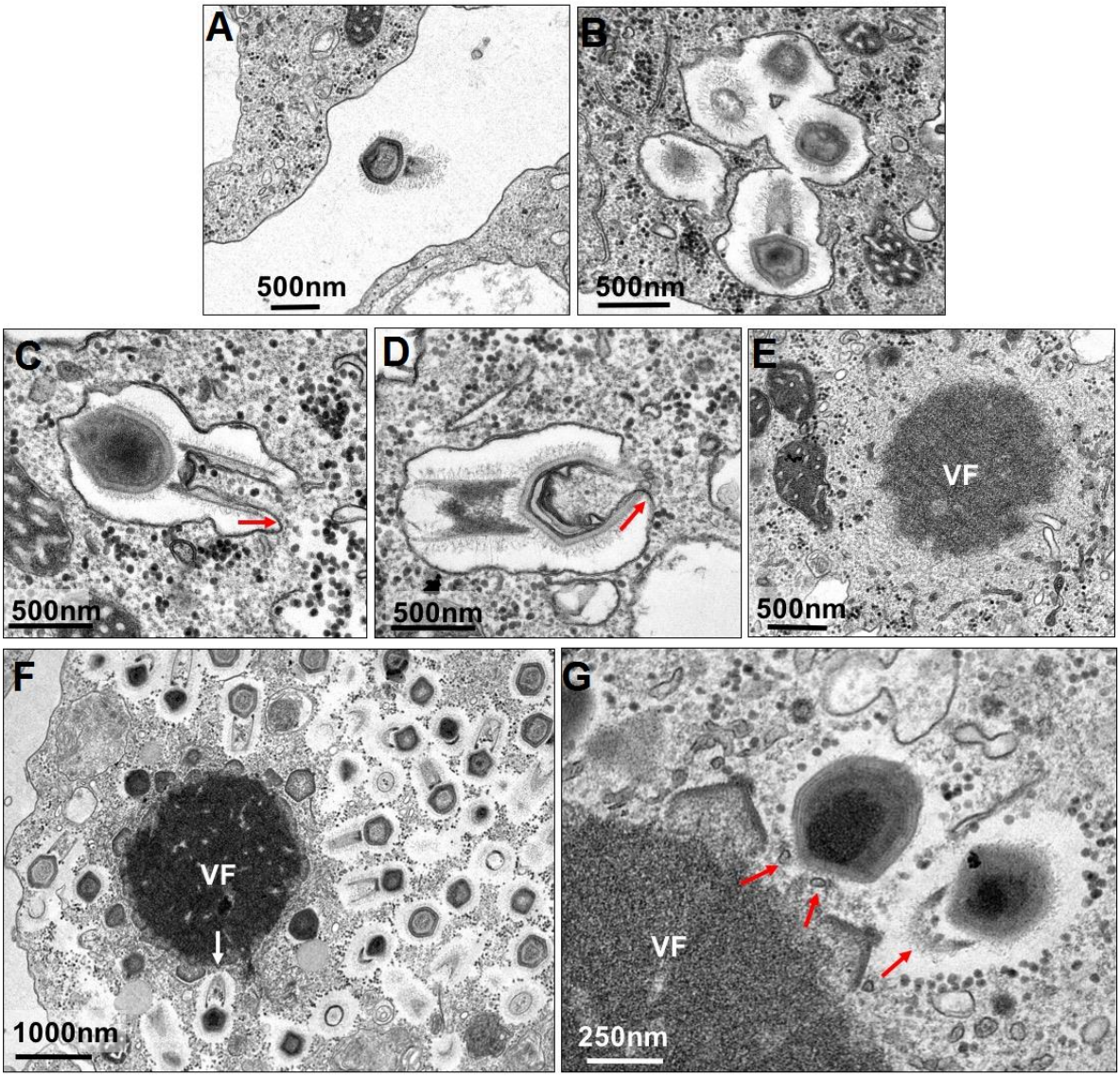

Figura 15: Ciclo de multiplicação de Tupanvirus sodal lake em *A. castellanii* visualizado por MET. (A) As partículas são internalizadas através de fagocitose; (B) As partículas se mantêm dentro de fagossomos; (C) Pode ocorrer fusão de membrana da cauda com o fagossomo, causando a liberação do conteúdo da cauda no citoplasma amebiano; (D) O genoma é liberado através da abertura do *stargate* e pela fusão da membrana interna do capsídeo com o fagossomo; (E) Formação de fábricas virais; (F) Fase de morfogênese; (G) A cauda é ligada ao capsídeo após a formação e fechamento do mesmo, sendo o

processo associado à fábrica viral. Imagens obtidas no Centro de Microscopia da UFMG em colaboração com os alunos de Doutorado do grupo GEPIVIG/Laboratório de Vírus, Thalita Arantes e Rodrigo Araújo.

Anticorpos policlonais foram produzidos em camundongos e o ciclo completo de TPVsl em *A. castellanii* foi observado também por IF. Foi possível visualizar a penetração do vírus nas células (2 h.p.i), fase de eclipse (4-8 h.p.i), formação da fábrica viral (10-12 h.p.i), multiplicação intensa e morfogênese (16-18 h.p.i), e liberação das partículas virais maduras (24 h.p.i) (Fig. 16).

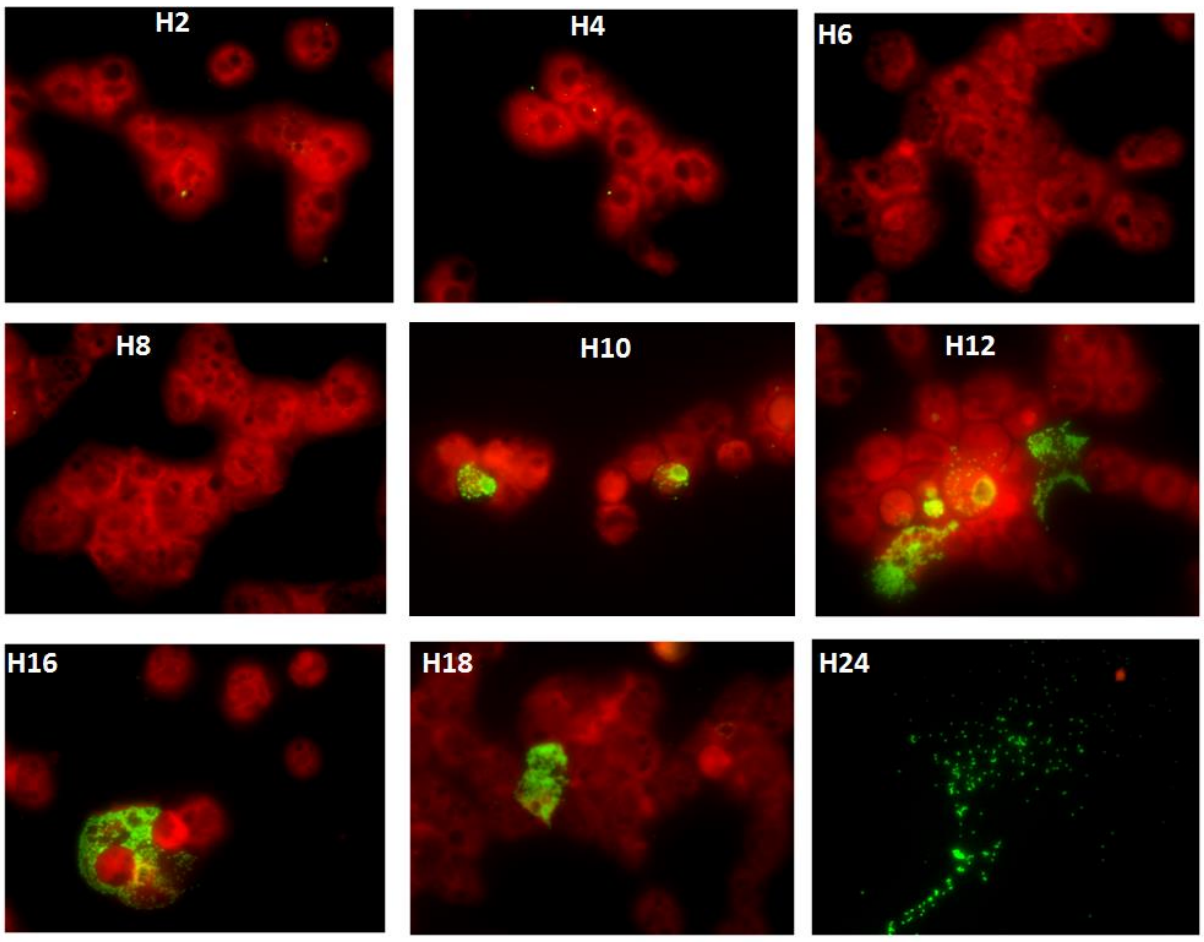

Figura 16: Ciclo de multiplicação de TPVsl em *A. castellanii* por IF. É possível visualizar a entrada do vírus nas células (2 h.p.i), fase de eclipse (4-8 h.p.i), formação da fábrica viral (10-12 h.p.i), morfogênese (16-18 h.p.i) e liberação das partículas virais (24 h.p.i). Células de amebas *A. castellanii* em vermelho e TPVsl como pontos verdes. Aumento de 1000 vezes.

6.1.5 Tupanvirus soda lake: Permissividade de diferentes células de protozoários ao novo vírus

Foi testada a permissividade de um largo painel de protozoários ao TPVsl. Foram testadas: *A. polyphaga, A. griffini, A. micheline, A. royreba, A. sp E4, D. discodium, W. magna, T. hyperangularis* e *T. tenax***,** sendo estas infectadas com TPVsl, na m.o.i. de 1, e o título viral calculado após 24 horas. Observou-se ECP característico de TPVsl em todas as células infectadas, exceto *T. tenax* (Tabela 5 e Fig. 17). Para a maioria das células (*V. vermiformis, A. polyphaga, A. griffini, A. sp E4, D. discoideum, W. magna*) foi possível verificar um aumento do título viral em aproximadamente 1 log 24 h.p.i, embora em *A. castellanii* este aumento tenha sido de 3 log. Para algumas células, *A. sp. micheline, A. royreba*, apesar do ECP visualizado, o aumento do título viral 24 h.p.i não foi observado, porém, foi observada a replicação do genoma viral. Já no caso de *T. hyperangularis*, apesar do ECP apresentado durante a infecção com TPVsl, não houve aumento de título viral, nem replicação do genoma.

Tabela 5. Perfil de permissividade de TPVsl em diferentes células de protozoários.

Protozoário	ECP	Aumento do título viral	Replicação do genoma viral
Acanthamoeba castellanii	+	$3\log_{10}$, após 24 horas	5 x $3\log_{10}$, após 24 horas
Acanthamoeba sp. E4	+	$1\log_{10}$, após 24 horas	6 x $3\log_{10}$, após 24 horas
Acanthamoeba sp. micheline	+	Não	2 x $1\log_{10}$, após 24 horas
Acanthamoeba polyphaga	+	$1\log_{10}$, após 24 horas	4 x $1\log_{10}$, após 24 horas
Acanthamoeba royreba	+	Não	2 x $1\log_{10}$, após 24 horas
Acanthamoeba griffini	+	$1{,}5\log_{10}$, após 24 horas	7 x $1{,}5\log_{10}$, após 24 horas
Vermoamoeba vermiformis	+	$1\log_{10}$, após 24 horas	6 x $1\log_{10}$, após 24 horas
Dictyostelium discoideum	+	$1\log_{10}$ após 48 horas	2 x $1\log_{10}$ após 48 horas
Willaertia magna	+	$0{,}5\log_{10}$ após 24 horas	$0{,}8\log_{10}$ após 24 horas
Tetrahymena hyperangularis	+	Não	Não
Trichomonas tenax	-	Não	Não

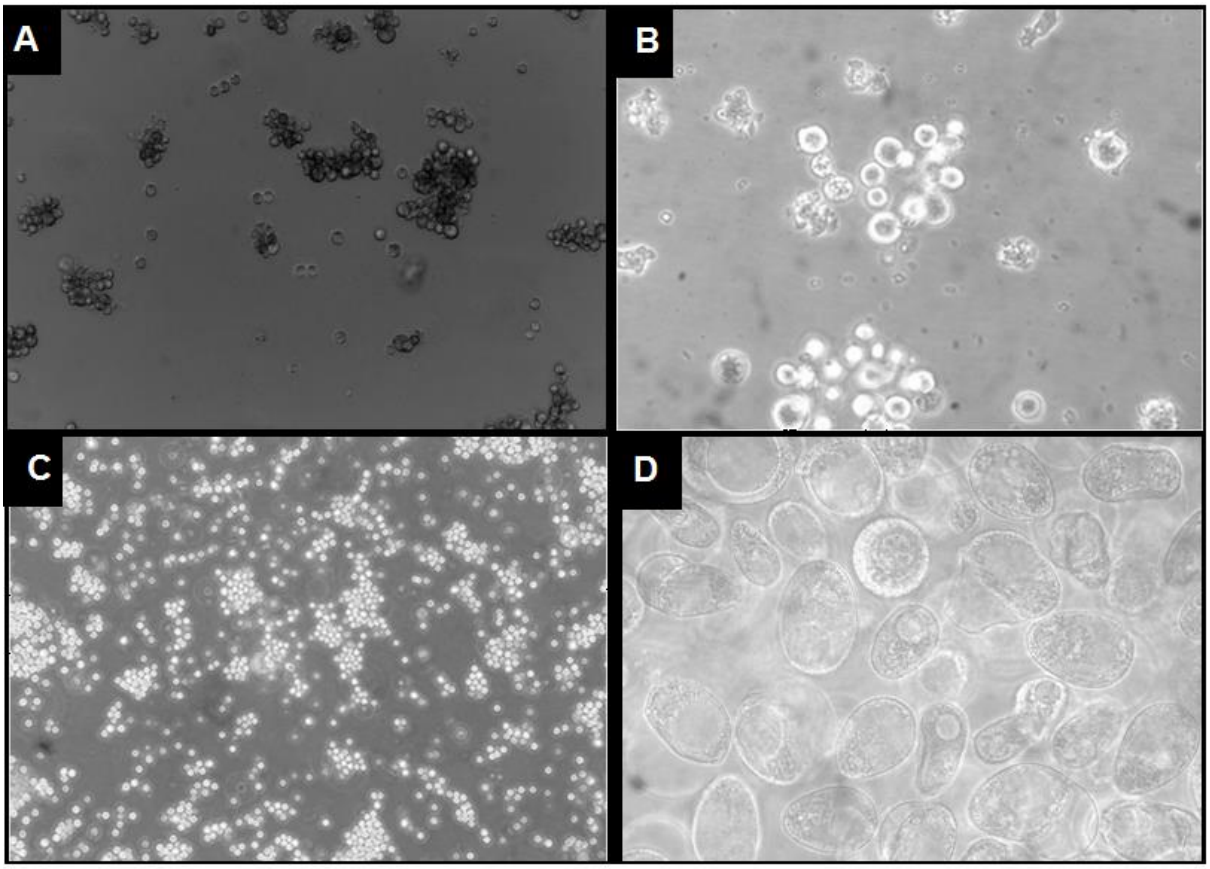

Figura 17: ECP de TPVsl em diferentes células. É possível visualizar ECP típico de mimivírus em algumas células infectadas, como arredondamento de células e lise celular. Por outro lado, a infecção por TPVsl leva a agregação de células amebianas formando "cachos de uva" conforme visualizado em A, B e C. (A) ECP em amebas do gênero *Acanthamoeba;* (B) ECP em *V. vermiformis*; (C) ECP em *D. discoideum*; (D) *T. hyperangularis*, células perderam a mobilidade. Aumento de 100 vezes.

6.1.6 Tupanvirus deep ocean: características do genoma

O sequenciamento de TPVdo revelou um genoma de DNA dupla fita de 1.516.267 pares de bases, com conteúdo de CG de 29,1%. A predição revelou um total de 1.359 ORFs, das quais 378 (~27%) são ORFans (ORF sem nenhuma correspondência em bancos de dados públicos). Os *best hits* para as ORFs de TPVdo são principalmente relacionados às linhagens de mimivírus: A (~10%), B (~18%) e C (~15%). Cerca de 30% das ORFs restantes são relacionadas a outros organismos, incluindo *Eukaria* (12%), *Archaea* (0,5%) e *Bacteria* (9%) e outros vírus gigantes, incluindo o grupo dos Klosneuvírus (8%) (Fig. 18)

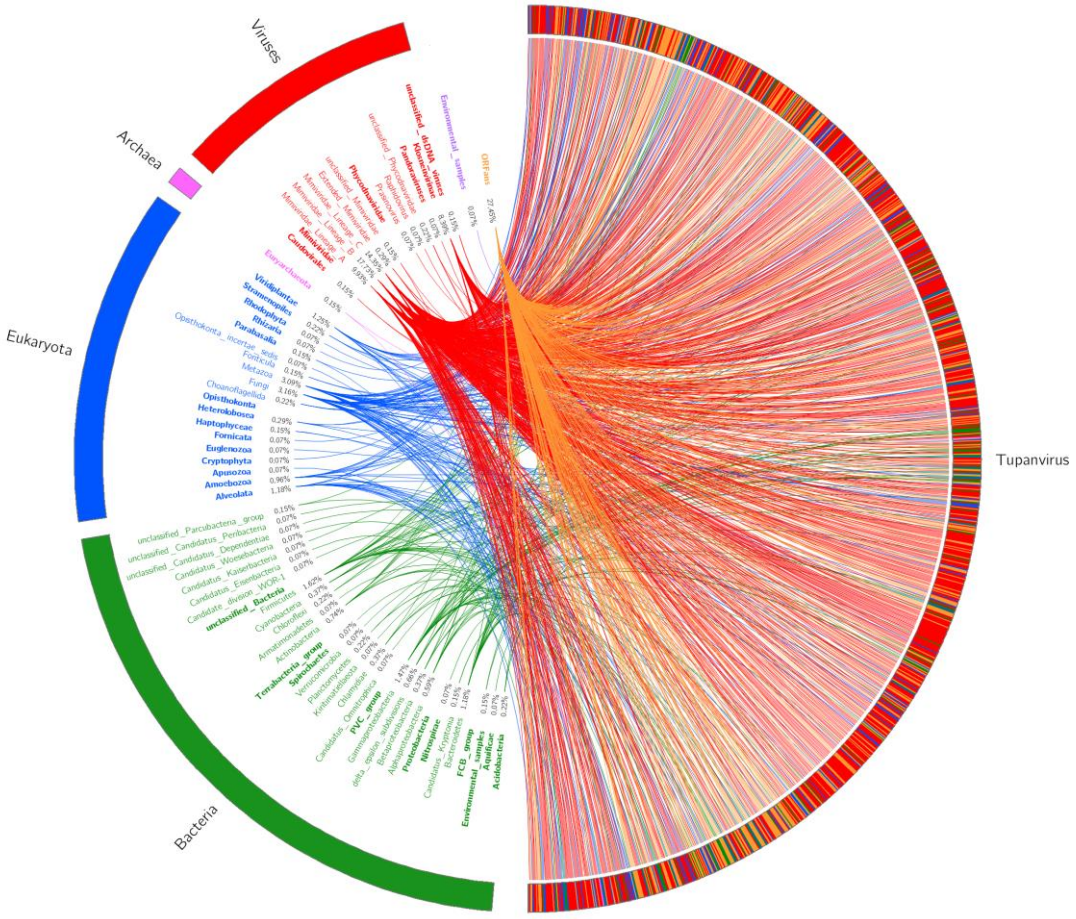

Figura 18: Rizoma do genoma de Tupanvirus deep ocean. Nesta figura é possível verificar que os *best hits* para TPVdo estão principalmente relacionados a mimivírus, embora correspondências com *Archaea*, *Eukaria*, *Bacteria* também estejam presentes.

A análise filogenética para o gene da DNA polimerase B mostrou os tupanvírus em uma posição relacionada à dos mimivírus, sugerindo um novo gênero dentro de *Mimiviridae*. (Fig. 19). A análise de uso de códons e aminoácidos para o genoma de TPVdo em comparação TPVsl e a célula hospedeira *A. castellanii*, revelou perfil de uso semelhante entre si, enquanto difere do uso de códons e aminoácidos pela célula hospedeira (Fig. 20).

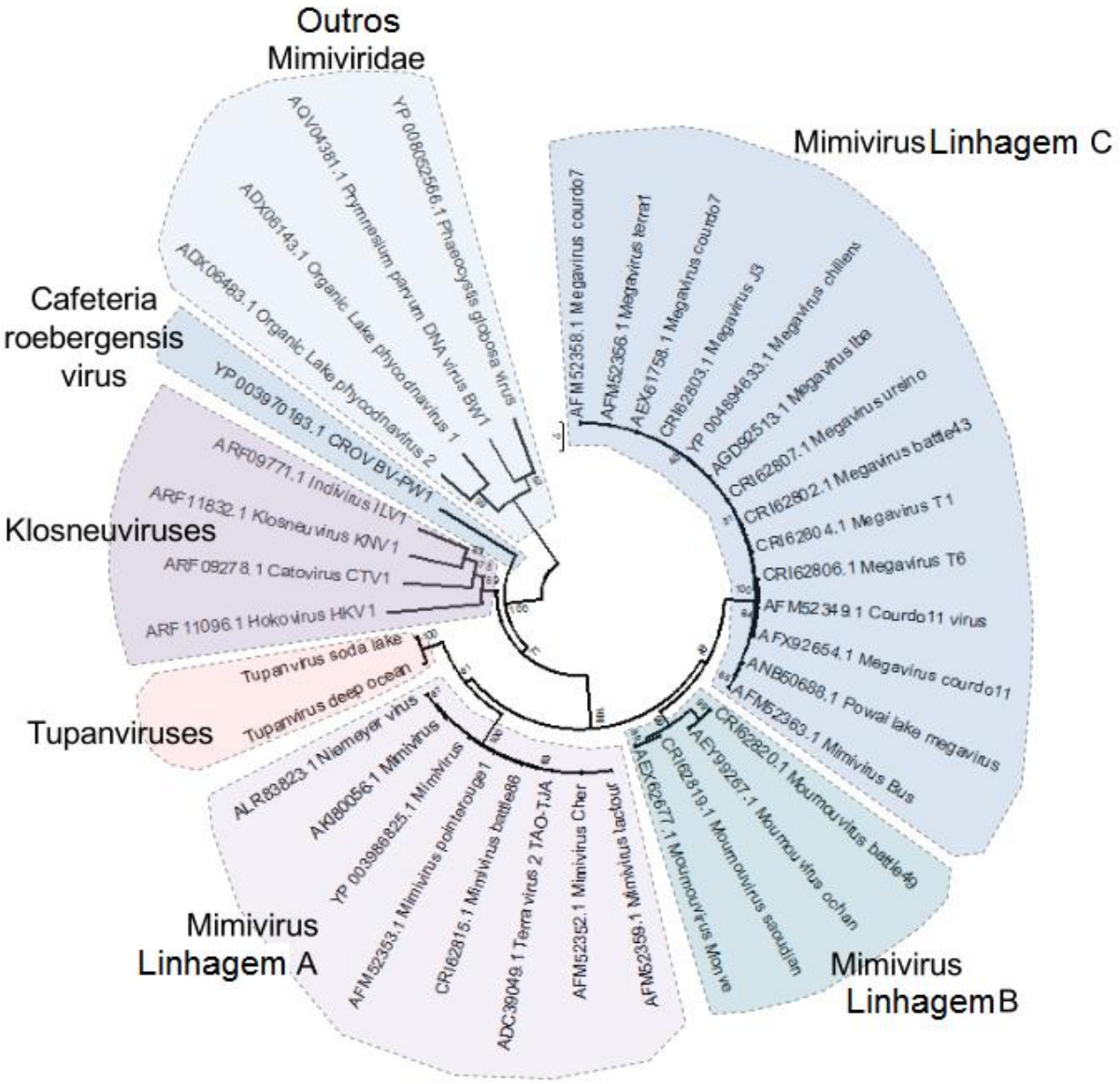

Figura 19: Filogenia para o gene da DNA polimerase B. A análise filogenética deste marcador molecular clássico em vírus gigantes mostra que os tupanvírus são próximos dos mimivírus.

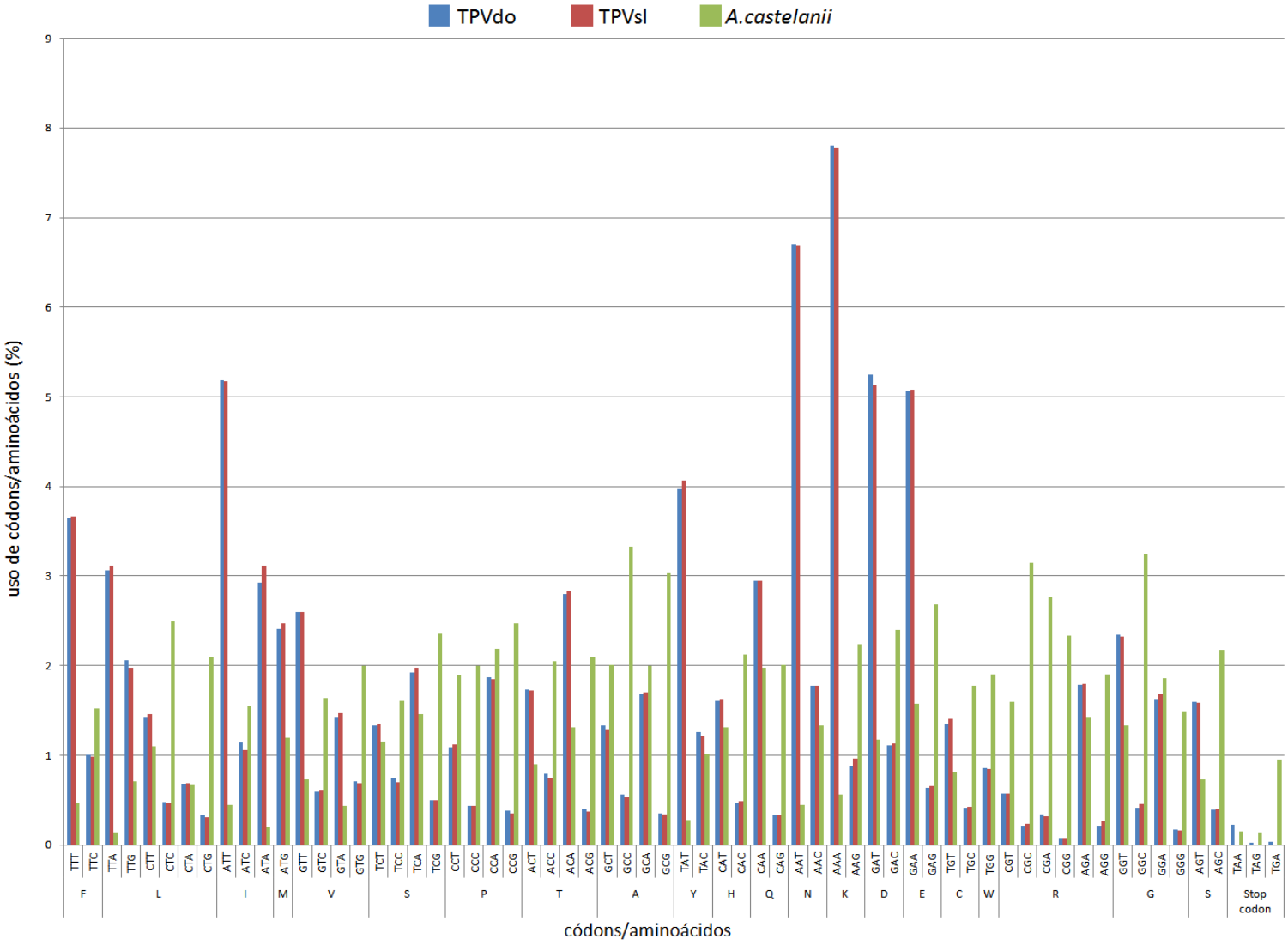

Figura 20: Utilização de códons e aminoácidos por tupanvirus. É possível observar que o perfil de uso de códons/aminoácidos é semelhante entre os dois isolados de tupanvírus, enquanto difere do perfil de uso por *A. castellanii*. A identificação dos códons e aminoácidos utilizados de acordo com a figura está no anexo 4.

6.1.7 Tupanvirus deep ocean: análise de genes envolvidos com tradução

A anotação do genoma de TPVdo revelou um grande conjunto de genes relacionados à tradução: ORFs relacionadas a aaRS e tRNA para 20 aminoácidos, sendo ausente unicamente genes relacionados à selenocisteína. Além das aaRS codificadas pelos outros vírus gigantes, no TPVdo foi encontrado um gene relacionado a uma glutamato/prolil-RS bifuncional. Além disso, TPVdo codifica 70 tRNAs, que correspondem a 48 códons (Anexo 5). Vários genes relacionados a fatores de biossíntese proteica foram também encontrados em TPVdo, sendo envolvidos em todas as etapas da tradução. Um total de nove genes para fatores de iniciação (IF2alfa, IF5, IF4e, IF5a (2 cópias), IF2 subunidade beta, IF2 subunidade gama, SUI1, IF4a), um fator de elongação (eF2) e um fator de terminação (ERF1) (Tabela 6).

Tabela 6. Genes de elementos relacionados à tradução presentes em TPVdo.

aaRS	tRNA	TF
Alanil-RS, Arginil-RS, Asparagil-RS, Aspartil-RS, Cisteinil-RS, Fenilalanil-RS, Glicil-RS, Glutamato/prolil-RS, Glutaminil-RS, Histidinil-RS, Isoleucina-RS, Leucil-RS, Lisil-RS, Metionil-RS, Prolil-RS, Seril-RS, Tirosinil-RS, Treonil-RS, Triptofanil-RS, Valinil-RS	Metionil-tRNA, Lisinil-tRNA, Aspartatil-tRNA, Triptofanil-tRNA, Glutaminil-tRNA, Cisteinil-tRNA, Leucinil-tRNA, Arginil-tRNA, Ácido glutaminil-tRNA, Prolinil-tRNA, Treoninil-tRNA, Alaninil-tRNA, Serinil-tRNA, Valinil-tRNA, Isoleucinil-tRNA, Glicinil-tRNA, Tirosinil-tRNA, Histidinil-tRNA, Asparaginil-tRNA, Fenilalanil-tRNA	**Fatores de Iniciação:** IF2alfa, IF5, IF4e, IF5a, eIF5A, IF2 subunidade beta, IF2 subunidade gama, SUI1, IF4a **Fatores de elongação:** eF2 **Fator de terminação:** ERF1

A comparação entre os genes relacionados à tradução compartilhada pelos tupanvírus com outros mimivírus das linhagens A, B e C e com organismos celulares revelou que os tupanvírus apresentam um conjunto de genes mais rico do que outros vírus gigantes e organismos celulares quando se trata de tRNA. Os tupanvírus apresentam mais tRNA do que *E. cuniculi*, um organismo eucariótico, por exemplo (Fig. 21). Já em relação às aaRS, os tupanvírus apresentam enzimas para 20 aminoácidos conhecidos, assim como visto para célula hospedeira e para *E. cuniculi* (Fig. 22). E em relação a outros fatores envolvidos com tradução, de forma geral, os tupanvírus e mimivírus, bem como pequenos organismos celulares apresentam um conjunto muito menor destes genes em relação à célula *A. castellanii* (Fig 23).

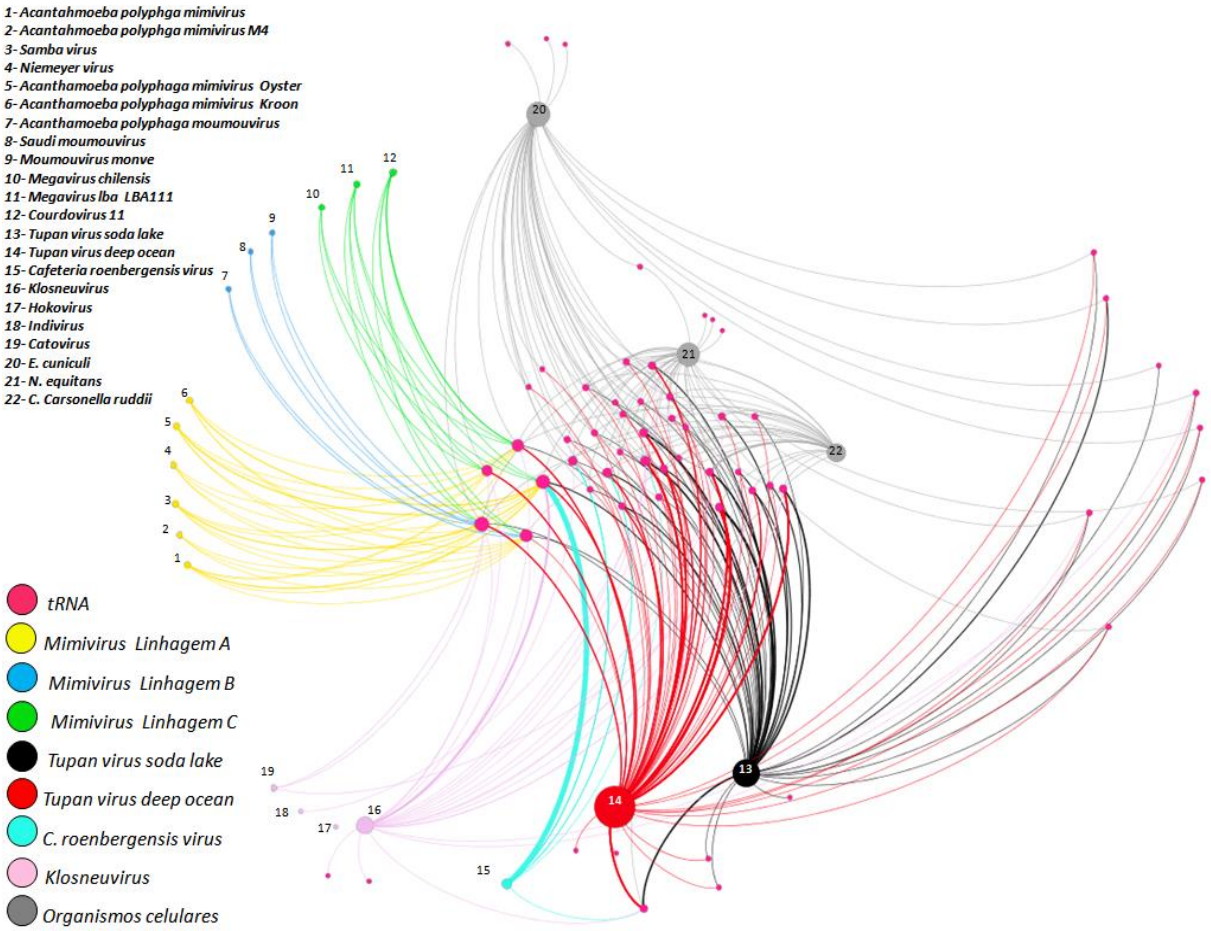

Figura 21: Análise de redes: RNA transportadores. Presença de tRNA (rosa) em mimivírus das linhagens A (amarelo), B (azul) e C (verde); tupanvírus (preto e vermelho); *C. roenbergensis virus* (azul turquesa), Klosneuvírus (rosa claro) e organismos celulares dos grupos *Archaea*, *Eukaria* e *Bacteria* (cinza). O diâmetro dos círuculos é proporcional ao número de tRNA e a espessura das linhas se refere ao número de cópias de um mesmoo tRNA em determinado organismo. É possível observar que TPVdo apresenta o maior conteúdo de tRNA dentre os grupos representados nesta rede de conexões.

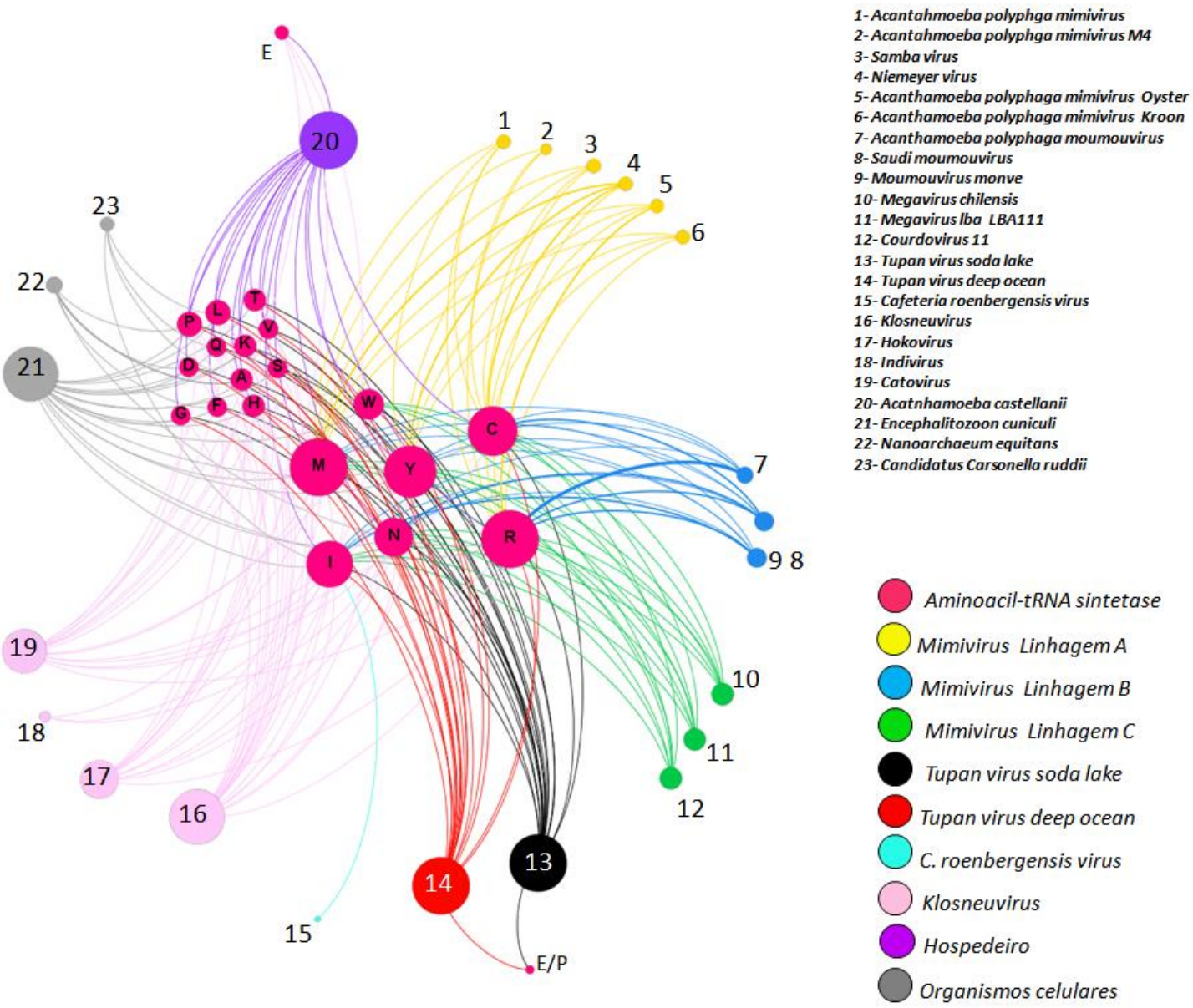

Figura 22: Análise de redes: Aminoacil-tRNA sintetases. Presença de aaRS (rosa) em mimivírus das linhagens A (amarelo), B (azul) e C (verde); tupanvírus (preto e vermelho); *C. roenbergensis virus* (azul turquesa), Klosneuvírus (rosa claro), *A. castellanii* (roxo) e organismos celulares dos grupos *Archaea*, *Eukaria* e *Bacteria* (cinza). O diâmetro dos círuculos é proporcional ao número de aaRS e a espessura das linhas se refere ao número de cópias de um mesmoo aaRS em determinado organismo. É possível observar que os tupanvírus apresentam conteúdo de aaRS equivalente ao da célula hospedeira e outros organismos celulares e mais significativo em relação aos demais vírus.

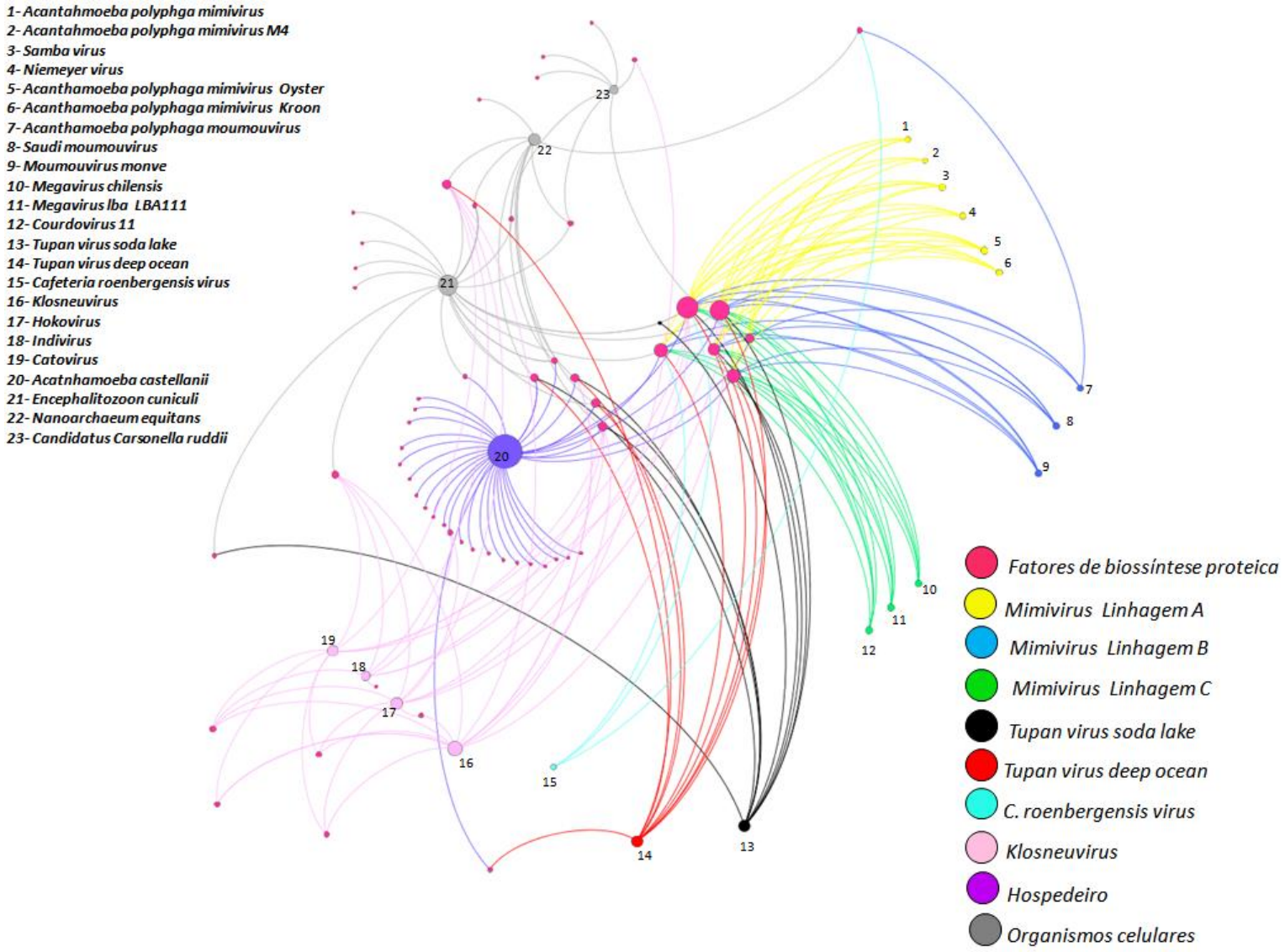

Figura 23: Análise de redes: Fatores envolvidos em biossíntese protéica. Presença de outros fatores associados à tradução (rosa) em mimivírus das linhagens A (amarelo), B (azul) e C (verde); tupanvírus (preto e vermelho); *C. roenbergensis virus* (azul turquesa), Klosneuvírus (rosa claro), *A. castellanii* (roxo) e organismos celulares dos grupos *Archaea*, *Eukaria* e *Bacteria* (cinza). O diâmetro dos círuculos é proporcional ao número de aaRS e a espessura das linhas se refere ao número de cópias de um mesmoo aaRS em determinado organismo. É possível observar que de forma geral, os vírus e pequenos organismos celulares analisados nesta rede apresentam menor conteúdo destes fatores em relação à célula hospedeira, *A. castellanii*.

6.1.8 Aminoacil-tRNA sintetases em vírus gigantes: análises filogenéticas

Para as análises filogenéticas das aaRS dos tupanvírus, foram construídas árvores baseadas no alinhamento das sequências de aminoácidos que codificam para cada uma das 20 aaRS presentes nos genomas destes vírus, nos 100 primeiros *best hits* obtidos através de análise destas sequências na plataforma BlastP do NCBI, Klosneuvírus e alguns representantes de Amoebozoa. As análises, de forma geral evidenciaram uma origem independente para a maioria das aaRS presentes nestes vírus, exceto fenilalanil-RS, prolil-RS, seril-RS, tirosil-RS, treonil-RS e valil-RS (Anexo 6).

6.2 Modulação do nível de mRNA de genes relacionados à tradução em resposta a disponibilidade nutricional durante a infecção de mimivírus em *A. castellanii*

6.2.1 Perfil de utilização de códons e aminoácidos em *Mimiviridae*

Ao analisarmos o uso de códons e de aminoácidos por cinco isolados de mimivírus investigados neste trabalho e o hospedeiro *A. castellanii*, foi possível observar claramente um perfil distinto entre os dois grupos, enquanto a comparação apenas entre os vírus evidencia um perfil muito similar, exceto em alguns códons utilizados diferencialmente pelo KROV (Fig. 24).

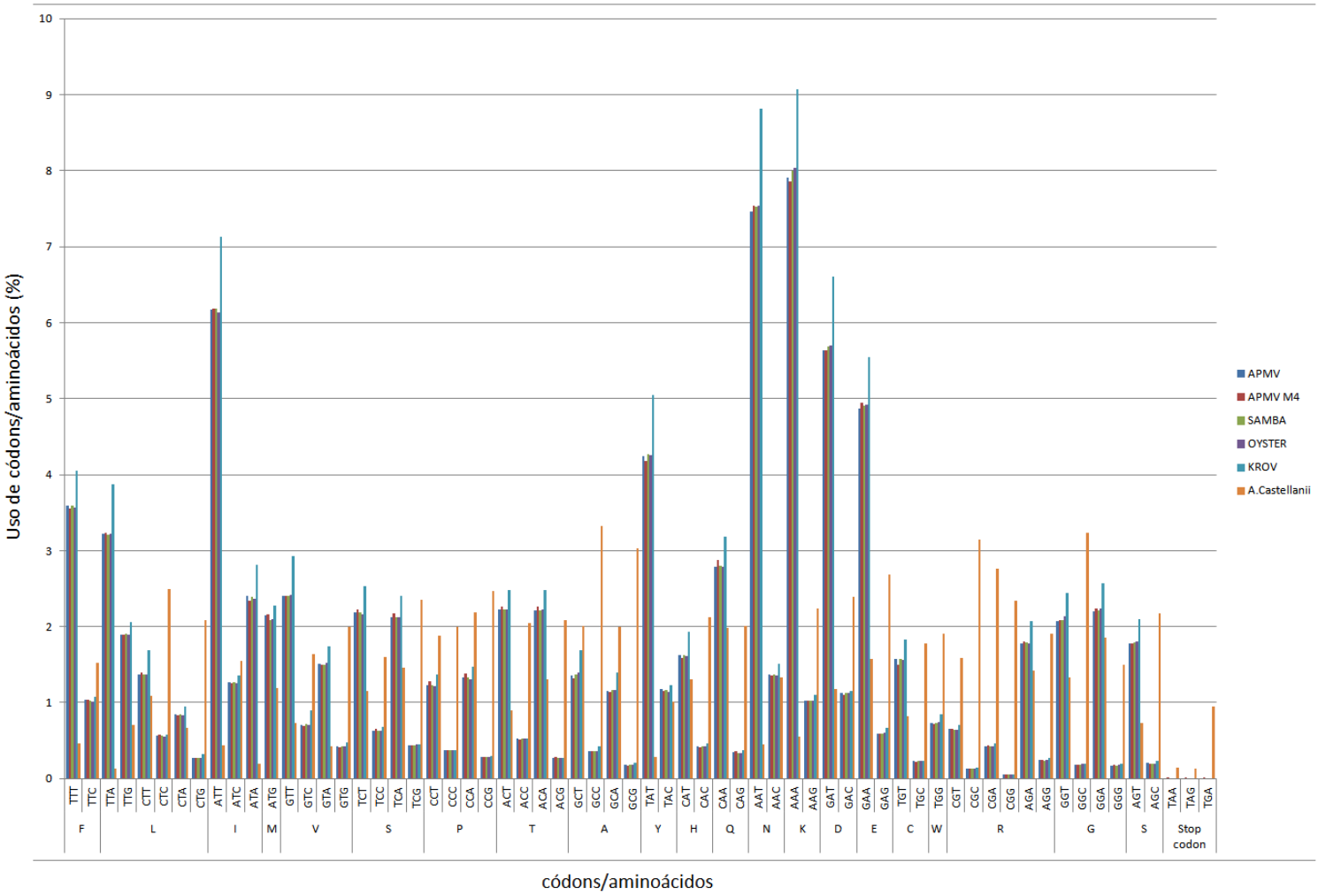

Figura 24: Análise comparativa de uso de códons e aminoácidos por diferentes mimivírus e *A. castellanii*. O perfil de utilização de códons e aminoácidos em mimivírus brasileiros (SMBV, OYTV e KROV), APMV, APMV M4 e *A. castellanii* foi calculado através do programa ARTEMIS. É possível observar que os vírus apresentam um perfil semelhante no uso de códons e aminoácidos, mas este difere em relação ao uso pela célula hospedeira. A identificação dos códons e aminoácidos utilizados de acordo com a figura está no anexo 4.

6.2.2 Padronização de PCR em tempo real

Para o estudo da expressão do nível de mRNA de elementos envolvidos em tradução em mimivírus, primeiramente foi necessária a realização de uma padronização de PCR em tempo real para avaliação da expressão de 8 genes: 4 tRNA (leucinil-tRNA, histidinil-tRNA, cisteinil-tRNA, triptofanil-tRNA) e 4 aaRS (metionil-RS, cisteinil-RS, tirosinil-RS e arginil-RS) presentes em *Mimiviridae*. Oito pares de iniciadores foram desenhados (Tabela 7). O desenho foi realizado utilizando a plataforma *online* do NCBI e tendo como base o genoma completo de APMV disponível. A padronização englobou avaliação de condições ideais de reação e a construção de curvas-padrão para a reação de cada gene em estudo (Fig. 25 e Fig. 26), bem como normalizações utilizando genes constitutivos celular (18S rDNA de *A. castellanii)* e viral (helicase) (Tabela 7). Para este último gene, os resultados demonstraram que as condições nutricionais de infecção diferentes a serem testadas não influenciaram na expressão deste gene constitutivo em mimivírus (Fig. 27).

Tabela 7. Sequências dos iniciadores desenhados para PCR em tempo real.

Iniciador	**Sequência *Forward***	**Sequência *Reverse***
Leucinil tRNA	GGGATTCGAACCCACGACAT	ATAAGCAAAGGTGGCGGAGT
Histidinil tRNA	TTAGTGGTAGAACTACTGTTTGTGG	TTTTCAAAAATGACCCGTACAGGAA
Cisteinil tRNA	ACAGTCAACTGGATCGTTAGC	AGGATCGTATCAGAATTGAACTGA
Triptofanil tRNA	GTGCAACAATAGACCTGTTAGTTTA	ACCGGAATCGAACCAGTATCA
Metionil RS	TGATTGGCGTGAATGGCTGA	ACCAATCACACTAGCCGGAA
Arginil RS	GTGGGTGATTGGGGAACTCA	TGATACGGTCTCCAATCGGG
Tirosil RS	TTTGGCAAACCAATCGGCAA	TGGTTTTGAACCTAGTGGTCGT
Cisteinil RS	TGCCAACCAGGTACACCAAA	TGCTCTTTGGAAAGGTCGATCA
18S rDNA	TCCAATTTTCTGCCACCGAA	ATCATTACCCTAGTCCTCGCGC
Helicase APMV	ACCTGATCCACATCCCATAACTAAA	GGCCTCATCAACAAATGGTTTCT

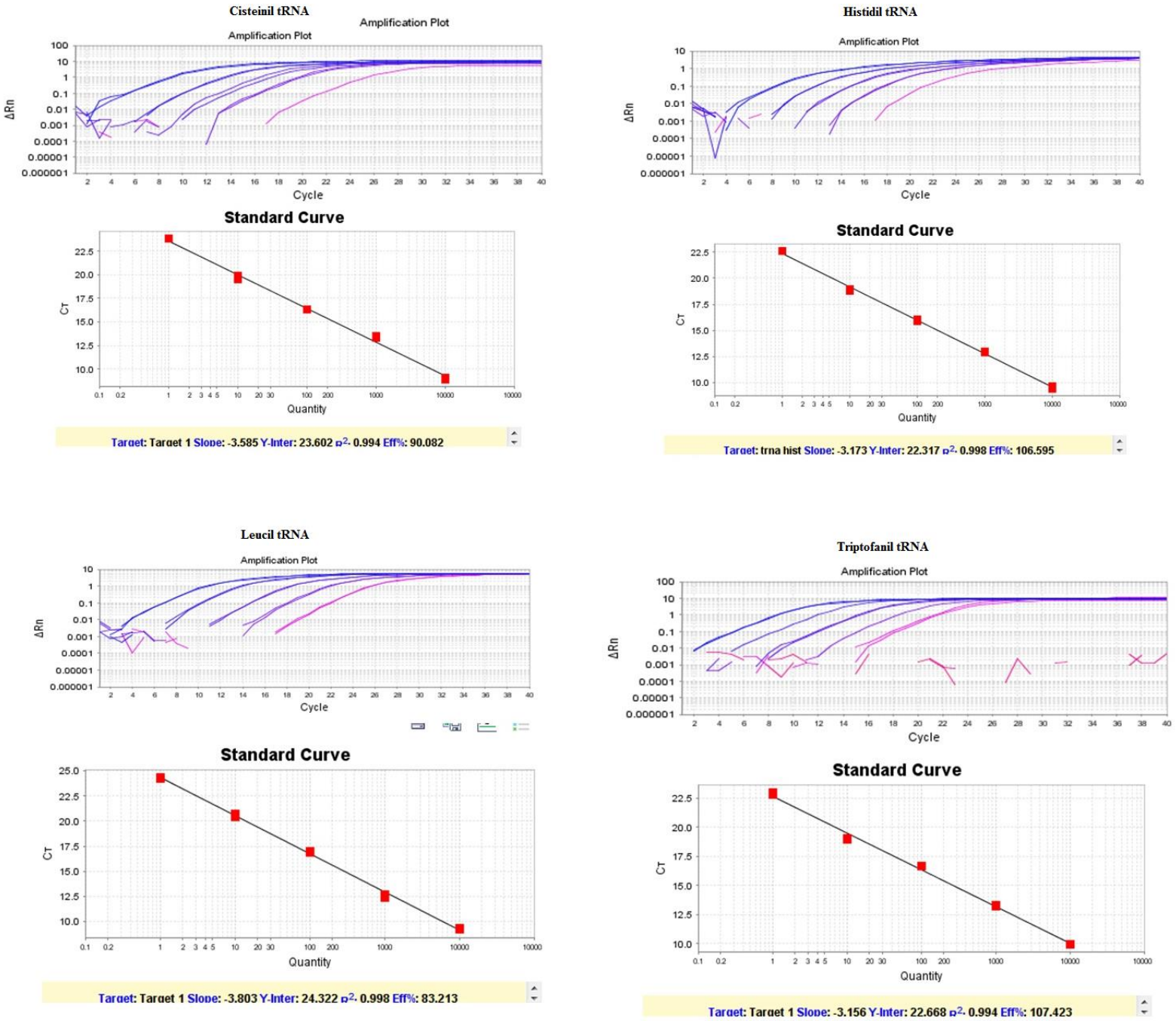

Figura 25: Curvas-padrão para tRNA. Curvas padrão construídas para utilização nas PCR em tempo real para avaliação do nível de mRNA de genes de tRNA em mimivírus: (A) curva padrão para amplificação do gene cisteinil-tRNA; (B) curva padrão para amplificação do gene histidinil-tRNA; (C) curva padrão para amplificação do gene leucinil-tRNA; (D) curva padrão para amplificação do gene triptofanil-tRNA. A porcentagem de eficiência estabelecida para as curvas padrão foi de 80-110%.

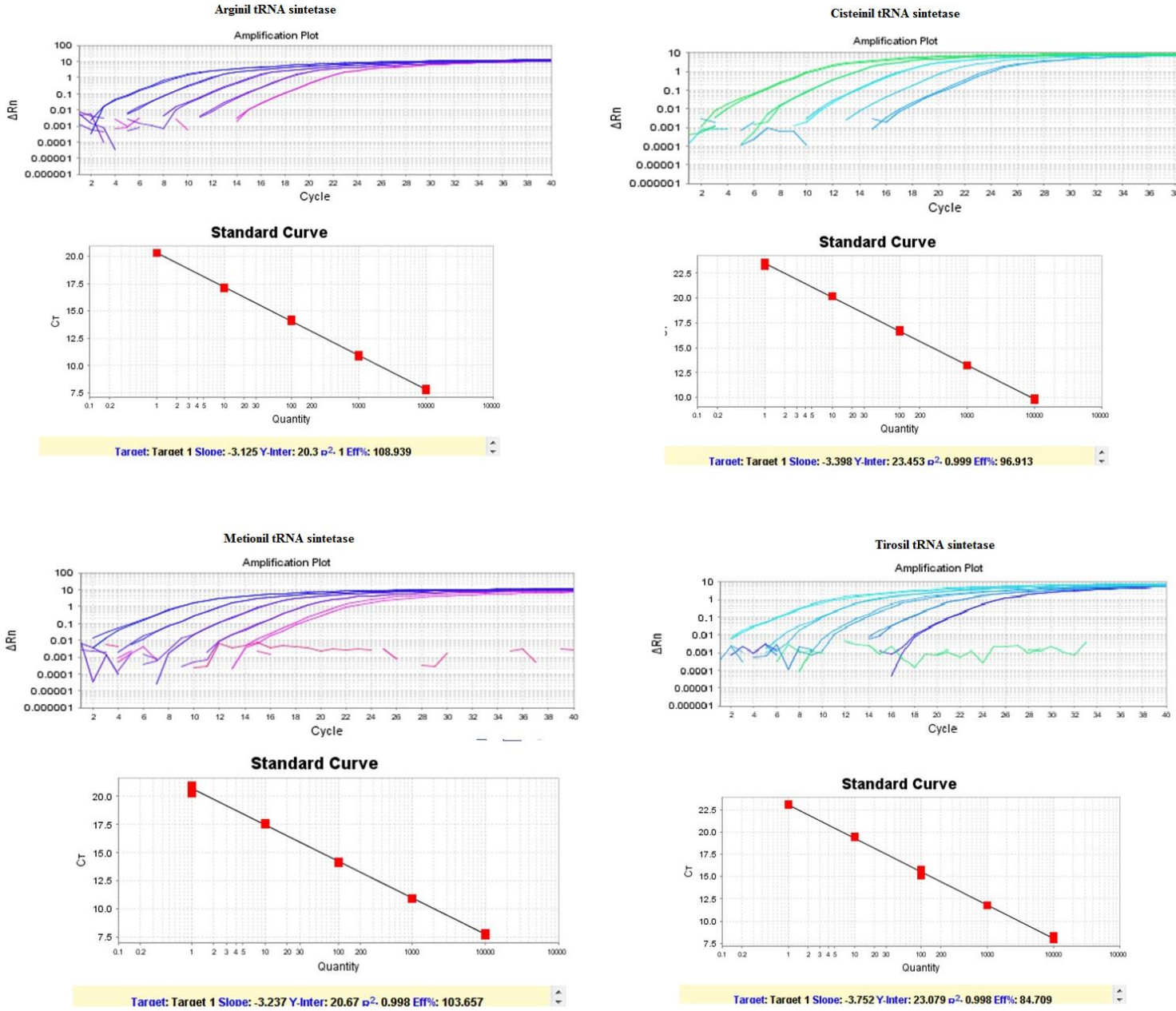

Figura 26: Curvas-padrão para aaRS. Curvas padrão construídas para utilização nas PCR em tempo real para avaliação do nível de mRNA de genes de aaRS em mimivírus: (A) curva padrão para amplificação do gene arginil-RS; (B) curva padrão para amplificação do gene cisteinil-RS; (C) curva padrão para amplificação do gene metionil-RS; (D) curva padrão para amplificação do gene tirosinil-RS. A porcentagem de eficiência estabelecida para as curvas padrão foi de 80-110%.

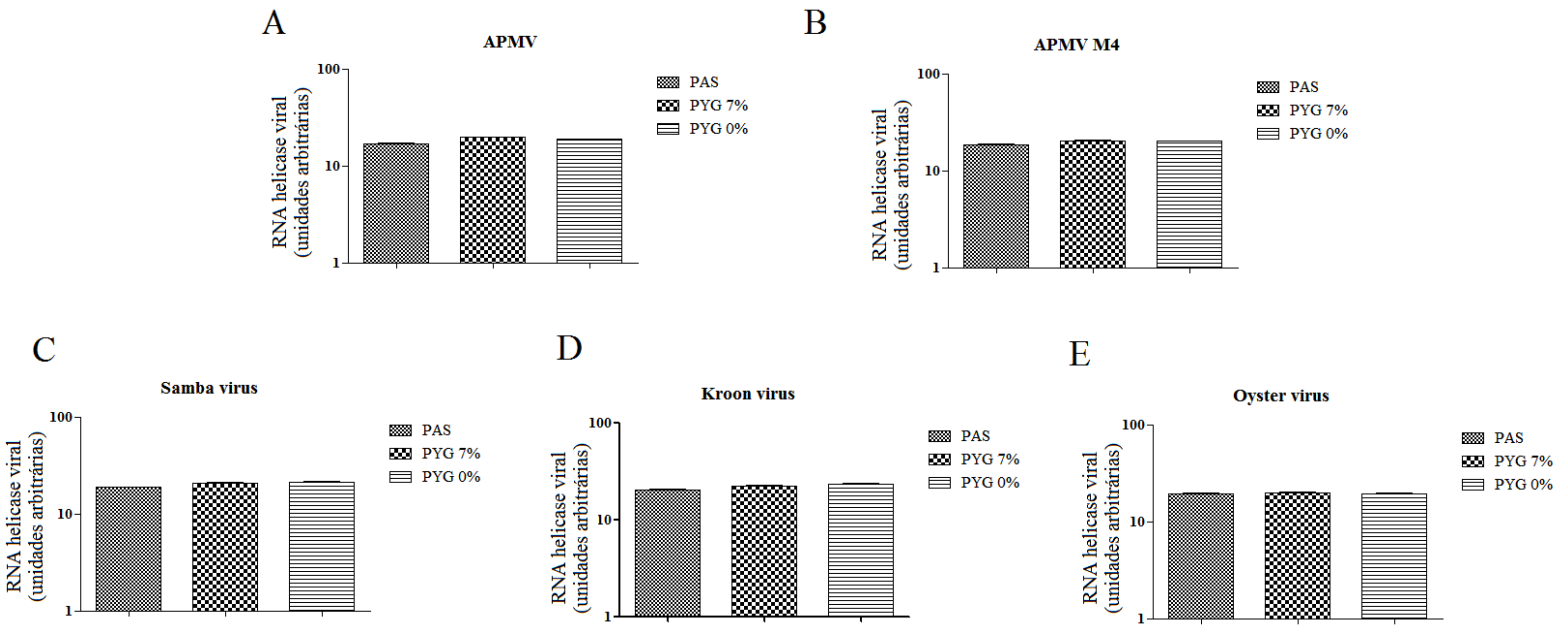

Figura 27: Nível de mRNA de RNA helicase viral por diferentes mimivírus em amebas infectadas sob diferentes condições nutricionais. Células de *A. castellanii* cultivadas em três diferentes meios de cultura foram infectadas por 8 horas com diferentes mimivírus. As células infectadas foram coletadas, submetidas à extração de RNA total, transcrição reversa e o cDNA resultante utilizado como molde para PCR em tempo real. (A) APMV; (B) APMV M4; (C) SMBV; (D) KROV; (E) OYTV. É possível observar que o nível de mRNA para o gene de RNA helicase não varia entre os diferentes mimivírus independente do meio de cultivo empregado na infecção das amebas.

6.2.3 Expressão do nível de mRNA de elementos relacionados à tradução em *Mimiviridae*

Uma vez padronizada as PCR de trabalho e o perfil de utilização de códons/aminoácidos verificado para os vírus e célula hospedeira, para avaliar se o nível de mRNA dos elementos relacionados à tradução variava entre os mimivírus testados e em diferentes condições nutricionais de infecção, amebas foram infectadas com os diferentes isolados (APMV, APMV M4, SMBV, KROV, OYTV) e em diferentes meios de cultivo (PAS, PYG 0%, PYG 7%) por oito horas, processadas e analisadas por PCR em tempo real. As análises de expressão relativa para os quatro tRNA e as quatro aaRS avaliadas neste trabalho revelaram que os mimivírus analisados foram capazes de modular diferencialmente a expressão do nível de mRNA destes genes, e que essa expressão varia ainda de acordo com a disponibilidade de nutrientes (PAS, PYG 0% ou PYG 7%) durante a infecção da célula amebiana (Fig. 28 e 29). De modo geral, o nível de mRNA destes genes em células infectadas

em meio com alta concentração de nutrientes (PYG 7%) foi significativamente menor em comparação a células infectadas sob condições nutricionais mais pobres, PYG 0% e PAS, no qual foi possível verificar o maior nível de mRNA viral para todos os genes analisados ($p<0.01$ ou $p<0.001$) (Fig. 28 e 29). Os diferentes mimivírus mostraram também uma variação no perfil do nível de mRNA destes genes entre si. Por exemplo, observou-se um perfil de expressão distinto para a arginil-RS e metionil-RS codificadas por KROV em relação aos demais vírus, em todas as condições testadas (Fig. 28 B e Fig. 29 A, D). Além disso, KROV e APMV M4 não apresentaram níveis detectáveis de triptofanil-tRNA, o que já era esperado, devido à ausência do gene correspondente nessas duas amostras (Fig. 28 D). Da mesma forma, APMV M4 também não codifica tirosil-RS (Fig. 29 B).

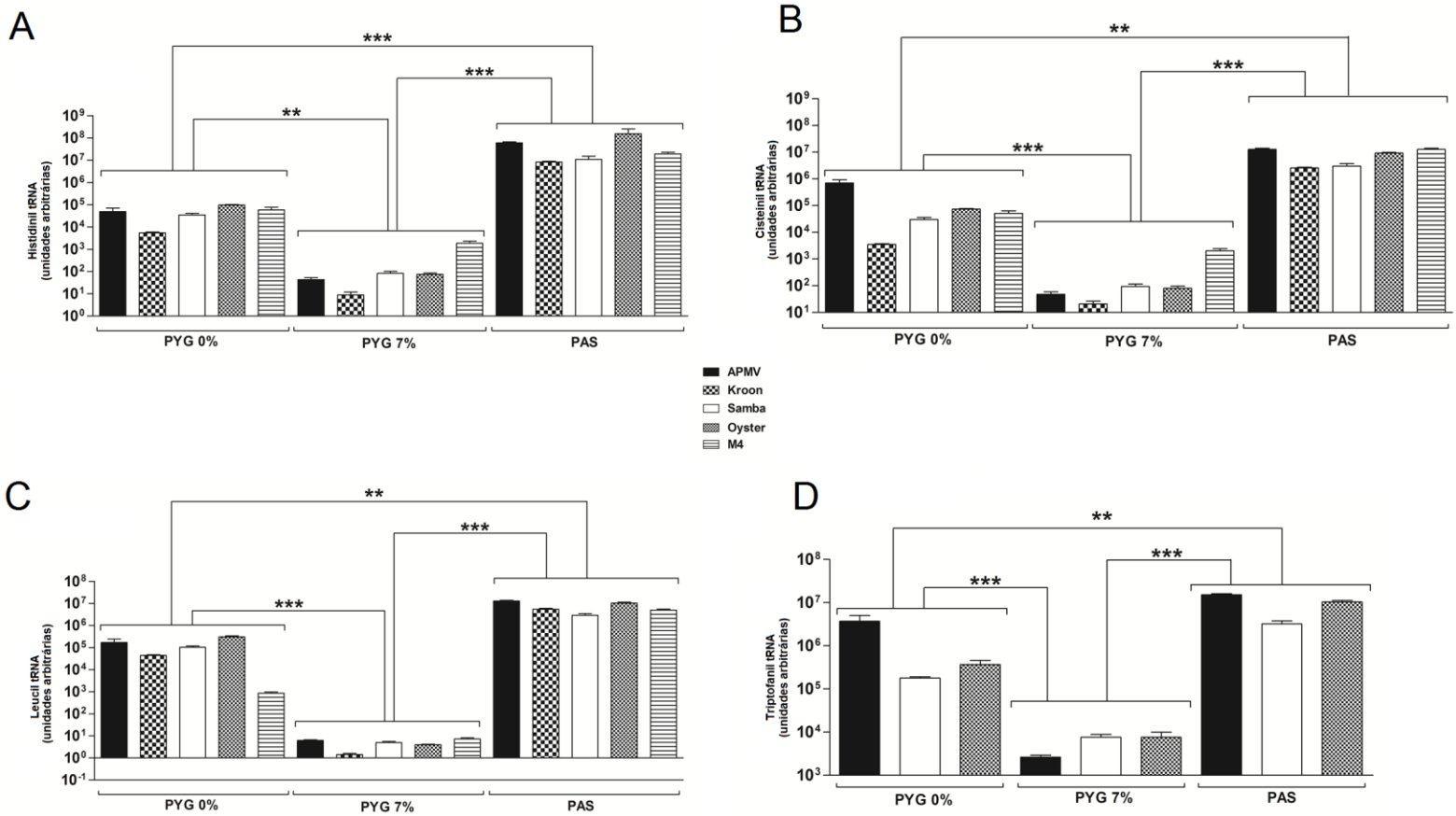

Figura 28: Nível de mRNA de tRNA por diferentes mimivírus em amebas infectadas em diferentes condições nutricionais. Células de *A. castellanii* cultivadas em três diferentes meios de cultivo foram infectadas por 8 horas com cinco isolados de mimivírus. As células infectadas foram coletadas, submetidas à extração de RNA total, transcrição reversa e o cDNA resultante utilizado como molde para PCR em tempo real. (A) Histidinil-tRNA; (B) Cisteinil-tRNA; (C) Leucinil-tRNA; (D) Triptofanil-tRNA. É possível observar que os mimivírus testados apresentam uma modulação diferenciada no nível de mRNA de genes que codificam tRNA em resposta às condições nutricionais de infecção.

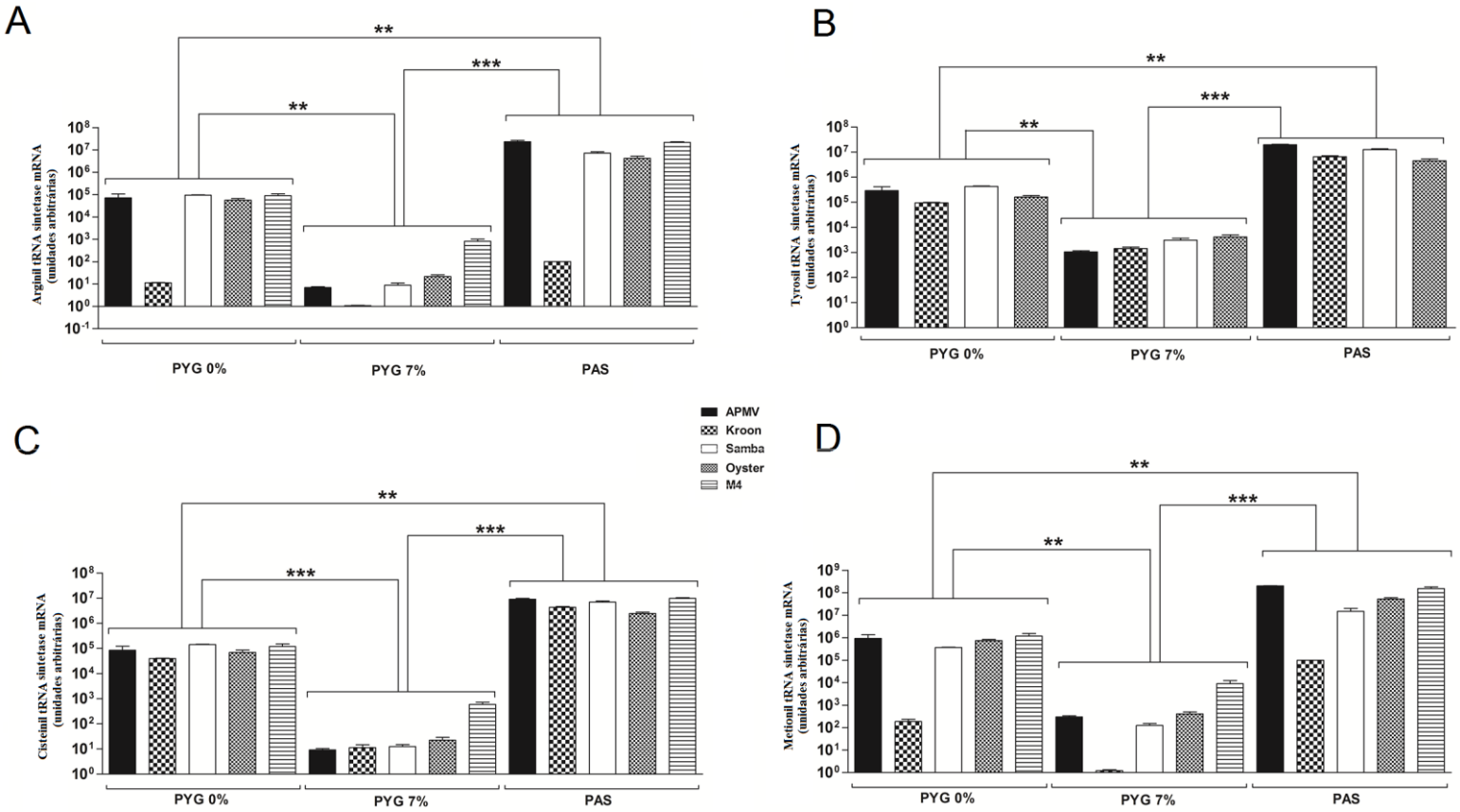

Figura 29: Nível de mRNA de aaRS por diferentes mimivírus em amebas infectadas sob diferentes condições nutricionais. Células de *A. castellanii* cultivadas em três diferentes meios de cultivo foram infectadas por 8 horas com cinco isolados mimivírus. As células infectadas foram coletadas, submetidas à extração de RNA total, transcrição reversa e o cDNA resultante utilizado como molde para PCR em tempo real. (A) Arginil-tRNA-sintetase; (B) Tirosil-tRNA-sintetase; (C) Cisteinil-tRNA-sintetase; (D) Metionil-tRNA-sintetase. É possível observar que os mimivírus testados apresentam uma modulação diferenciada no nível de mRNA de genes que codificam aaRS em resposta às condições nutricionais de infecção.

6.2.4 Perfil de multiplicação de mimivírus em diferentes condições nutricionais

Para avaliar se a diferença observada no nível de mRNA dos genes relacionados à tradução em cada condição nutricional aplicada poderia ser devido a uma diferença no perfil de multiplicação destes vírus nestas diferentes condições, cada mimivírus (APMV, APMV M4, SMBV, KROV e OYTV) foi submetido a uma curva de ciclo único em amebas *A. castellanii* na presença de PAS, PYG 0% ou PYG 7%. Os resultados mostraram que os cinco mimivírus avaliados foram capazes de infectar e se multiplicar normalmente em amebas cultivadas nas diferentes condições (Fig. 30). Todos os isolados mostraram aumento do título viral 4 horas pós infecção (h.p.i), com pico em aproximadamente 8 h.p.i, sendo este mantido até 24 h.p.i (Fig. 30). Não houve diferença significativa entre o título viral nas curvas de ciclo único dos mimivírus testados em infecção realizada em PYG 0% ou PYG 7% (Fig. 30 A e B). Ao contrário, o título viral foi aproximadamente 1.000 vezes menor na infecção realizada em PAS (Fig. 30 C).

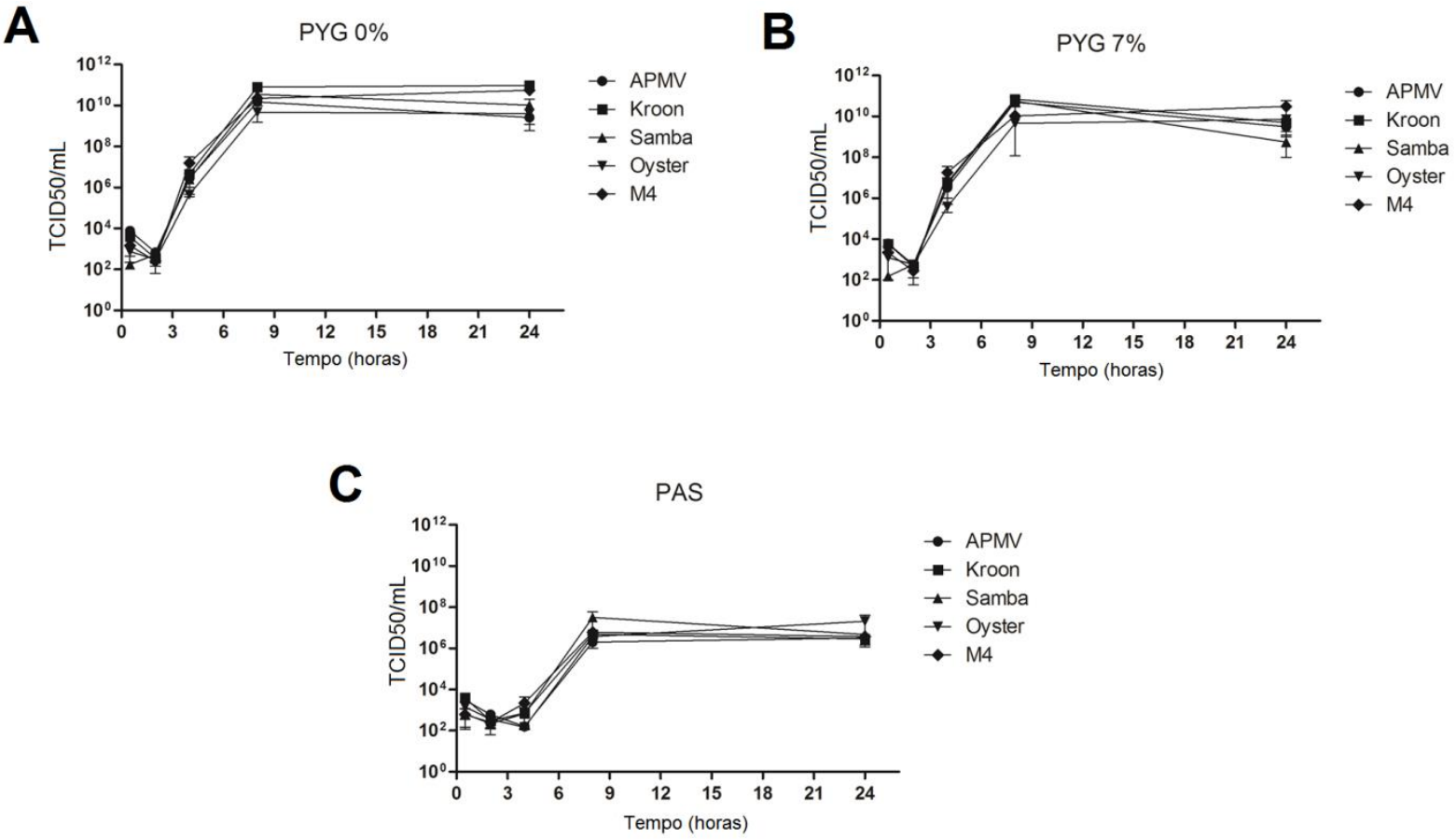

Figura 30: Multiplicação de mimivírus em amebas cultivadas em condições nutricionais distintas. As células de *A. castellanii* cultivadas em três meios distintos foram infectadas com mimivírus. As células infectadas foram coletadas em tempos determinados e submetidas à titulação. (A) PYG 0%SFB; (B) PYG 7%SFB; (C) PAS.

6.2.5 Polimorfismos em genes envolvidos em tradução em mimivírus

Para avaliar se as diferenças na expressão de genes relacionados à tradução durante infecção por diferentes mimivírus, além da condição nutricional, poderiam estar associadas com polimorfismos nestes genes nos diferentes mimivírus estudados, foram analisadas as sequências dos oito genes em questão através de alinhamento manual utilizando o *software* MEGA 5.2. O genoma de APMV, protótipo de *Mimiviridae* serviu como base para a comparação com a sequência dos genes dos outros mimivírus analisados. A comparação mostrou que em APMV e SMBV todos os genes apresentam 100% de similaridade (Anexo 7). Dos oito genes analisados, seis exibem 100% de similaridade entre APMV e APMV M4, com exceção de tirosil-RS e triptofanil-tRNA que foram perdidos em APMV M4 após as sucessivas passagens em *A. castellanii* (Anexo 7). Vários polimorfismos foram também detectados durante a comparação dos genes entre APMV e dois mimivírus brasileiros, KROV e OYTV (Anexo 7). KROV apresentou os polimorfismos mais marcantes, incluindo ausência do gene de triptofanil-tRNA (Anexo 7). Além disso, KROV e OYTV apresentam vários polimorfismos nas regiões promotoras e sítios de poliadenilação, com modificações de nucleotídeos em genes como cisteinil-tRNA, metionil-RS e arginil-RS devido à presença de *gaps* e substituições nestas regiões (Anexo 7 e Fig. 31).

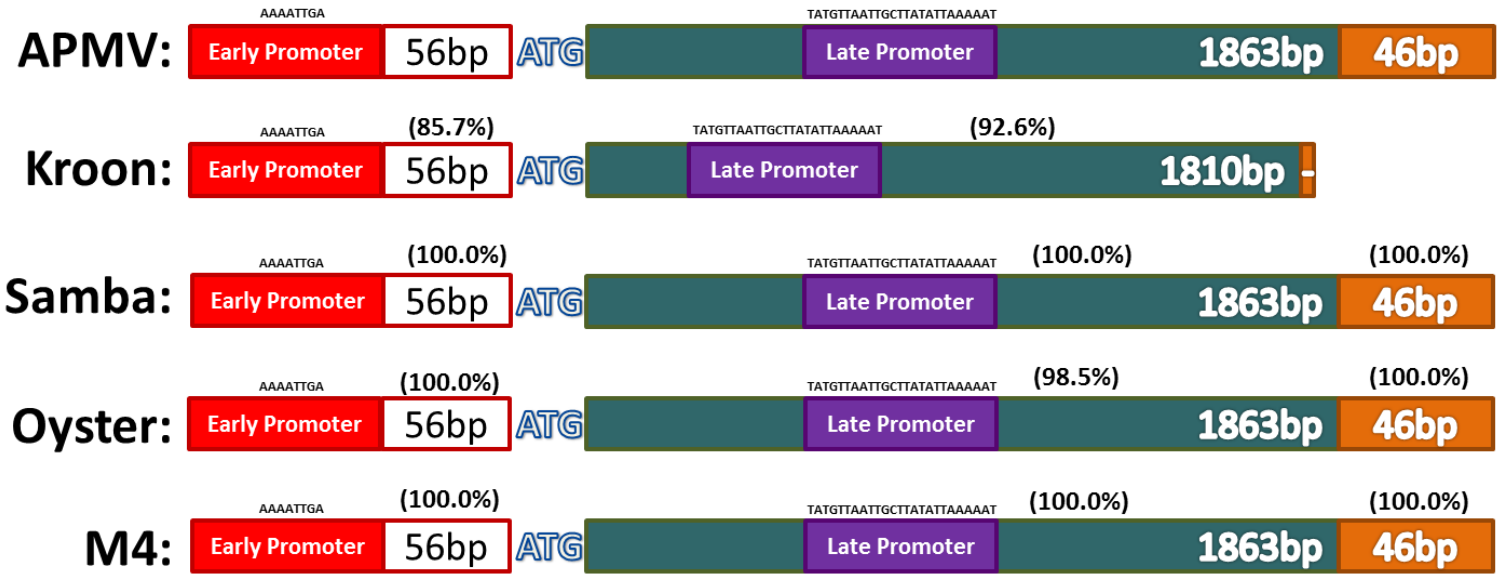

Figura 31: Representação esquemática do gene R663 (arginil-RS) em diferentes mimivírus. KROV é o isolado que apresenta o gene com menor similaridade dentre os isolados analisados.

VII- DISCUSSÃO

Desde o isolamento de APMV no início dos anos 2000, os vírus gigantes vêm despertando interesse devido a sua complexidade estrutural e genômica. São feitos questionamentos acerca de sua relação com seus hospedeiros, sua evolução, sua posição no mundo microbiano, bem como sobre a natureza e dinâmica biológica dos vírus em geral, restabelecendo a polêmica sobre o que deve ser considerado "vivo" ou não. Nestes mais de 15 anos de estudo, vários outros vírus gigantes foram isolados, como os Marseillevírus, pandoravírus, phitovírus, dentre outros, aumentando o conhecimento sobre a diversidade deste grupo. Muitos outros vírus interessantes e incomuns podem estar espalhados pelos mais diversos ambientes, sendo assim, a descoberta e caracterização destes vírus está em sua fase inicial e pode representar um grande desafio (GHEDIN e CLAVERIE, 2005; CLAVERIE et al., 2006; ETTEN, LANE e DUNIGAN, 2010). Sabe-se que, classicamente, os vírus dependem exclusivamente da maquinaria de síntese proteica da célula hospedeira para a tradução de suas proteínas. No entanto, a descoberta de vírus gigantes que codificam genes relacionados à tradução foi bastante surpreendente (RAOULT et al., 2004; MOREIRA e BROCHIER-ARMANET, 2008). Atualmente a presença destes elementos em vírus gigantes se mostra cada vez mais diversa. Recentemente, o grupo dos Klosneuvírus foi descrito e embora não isolados, a análise metagenômica revelou vírus gigantes com aparato de tradução com cerca de 19 aaRS, 23 tRNA e outros fatores associados (SCHULZ et al., 2017). Acredita-se que estes elementos não sejam pseudogenes, uma vez que são distintos dos análogos correspondentes celulares e são expressos durante todo o ciclo de multiplicação (LEGENDRE et al., 2010). E, também baseado na demonstração de atividade enzimática genuína para duas aaRS codificadas por APMV (ABERGEL et al., 2007). Porém, a real essencialidade destes elementos em vírus gigantes é desconhecida e sua posição no contexto da origem/evolução dos vírus gigantes permanece em debate. Neste contexto, nossos resultados apresentam o isolamento de novos vírus gigantes em amostras de ambientes especiais e a investigação do complexo traducional nestes novos isolados, traz novos dados acerca da relação de mimivírus anteriormente isolados e seus elementos envolvidos em tradução.

A prospecção de dezessete amostras provenientes de lagoas salinas e solo oceânico proporcionou o isolamento de novos isolados virais que foram investigados. As lagoas alcalinas são ambientes aquáticos considerados extremófilos nos quais é possível mimetizar

condições de vida primordiais devido a salinidade e pH extremamente elevados (SOROKIN et al., 2014). Os solos oceânicos por sua vez aqui utilizados para prospecção são de regiões pouco exploradas na virologia, regiões afóticas e abissais (3000m de profundidade). Foi possível obter dois isolados em duas plataformas celulares diferentes, *A. castellanii* e *V. vermiformis,* a partir de uma das amostras proveniente de uma lagoa alcalina bdo Pantanal (Tabela 4). E um isolado em *V. vermiformis* a partir de uma amostra de solo oceânico (Tabela 4). O isolamento foi feito através de observação de ECP nas células infectadas. Além do clássico ECP de vírus gigantes que corresponde a arredondamento das amebas, bem como lise, foi observado um padrão diferenciado de agregação das células amebianas, formando o que chamamos de "cachos de uva", tipo de ECP não observado nos nossos estudos de prospecção até aquele momento (Fig. 17A). Para a amostra do Pantanal, os resultados iniciais indicaram que poderíamos ter isolado dois vírus diferentes a partir de uma mesma amostra, uma vez que na ocasião da descoberta o único vírus gigante já isolado em *V. vermiformis* havia sido o Faustovírus E12 (RETENO et al., 2015). Porém, a análise microscópica de contraste negativo evidenciou que parecia tratar-se de um mesmo isolado viral capaz de se multiplicar em duas células de gêneros diferente, pois pelo menos morfologicamente eram parecidos (Fig. 11). Esse resultado foi diferente do observado para outros vírus isolados apenas em células do gênero *Acanthamoeba,* como mimivírus, phitovírus e pandoravírus ou apenas no gênero *Vermoamoeba* como faustovírus e kaumoebavírus (LA SCOLA et al., 2008; PHILIPPE et al., 2013; LEGENDRE et al., 2014; RETENO et al., 2015; BAJRAI et al., 2016). O isolado de solo oceânico também foi observado por microscopia de contraste negativo e, assim como os isolados do Pantanal, mostrou uma estrutura diferenciada em relação a outros vírus gigantes conhecidos até o momento: um vírus com capsídeo icosaédrico, típico de mimivírus, porém associado a este uma espécie de cauda (Fig. 11 e Fig. 12). Além disso, a análise da presença de fábricas virais em amebas infectadas evidenciou a presença de fábricas típicas de vírus gigantes nas células amebianas utilizadas para isolamento (Fig. 13). O isolamento a partir da amostra de solo oceânico inicialmente apenas em *V. vermiformis* nos parece algum viés experimental, uma vez que após isolamento e expansão deste isolado, foi realizada nova tentativa de inoculação em *A. castellanii*, com sucesso. Os novos isolados foram nomeados de Tupanvirus. O vírus isolado a partir de amostra do Pantanal foi denominado de Tupanvirus soda lake (TPVsL) e o vírus isolado a partir de amostra de solo oceânico foi denominado Tupanvirus deep ocean (TPVdo). Tupan foi um nome escolhido em alusão as tribos indígenas ribeirinhas que habitam na região do Pantanal e consideram Tupã o Deus do trovão.

Nossos resultados de caracterização biológica de TPVsl, por meio de análises de microscopia eletrônica, revelaram sua estrutura *sui generis* (Fig. 14): um capsídeo semelhante ao de mimivírus com *stargate* em uma das faces e circundado por fibrilas, sendo estas visualizadas também na região deste canal, mesmo que em pequenas quantidades, o que difere de outros mimivírus (XIAO et al., 2009). No entanto, a presença de uma cauda ligada ao capsídeo nos isolados nos parece o grande diferencial de TPVsl em relação a outros vírus gigantes descritos até então. Os mimivírus chamaram a atenção por apresentarem capsídeo icosaédrico grande associado a fibrilas; já os pandoravírus, cedratvírus e phitovírus na ocasião de suas descobertas evidenciaram uma morfologia ovoide, são vírus bem grandes e ainda apresentam poros apicais. Porém, em nenhum destes foi observado qualquer estrutura que se assemelhasse a de uma cauda (LA SCOLA et al., 2003; PHILIPPE et al., 2013; LEGENDRE et al., 2014). Além disso, esta cauda aumenta as dimensões do vírus para cerca de 1,0 μm, embora algumas partículas possam atingir até 2,3 μm, devido à plasticidade no tamanho desta cauda, podendo ser consideradas as partículas virais mais longas descritas até então, passando o tamanho dos phitovírus e cedratvírus (Fig. 14) (PHILIPPE et al., 2013; LEGENDRE et al., 2014). A análise microscópica sugeriu que o capsídeo e a cauda não estão firmemente ligados, o que nos levou a especular se a conexão entre estes elementos seria promovida pelas fibrilas (Fig.14 A e F). Nosso grupo tentou realizar a separação da cauda e capsídeo quimicamente através de tratamento enzimático sequencial (bromelina, lisozima e proteinase K), todavia, mesmo observando a degradação das fibrilas, não foi possível separar estes elementos. Além disso, existe uma membrana lipídica dentro do capsídeo icosaédrico e provavelmente na cauda cilíndrica, relacionada à fusão com a membrana celular e liberação do conteúdo do capsídeo e do conteúdo da cauda (Fig.14).

O ciclo de multiplicação de TPVsd em *A. castellanii* foi estudado em detalhes através de microscopia eletrônica. Nossas análises revelaram que as partículas se ligam à superfície da célula hospedeira e penetram através do processo de fagocitose (Fig.15). As membranas internas do capsídeo e da cauda se fundem com a membrana de fagossomo, liberando o conteúdo do genoma e partículas, respectivamente (Fig.15). A fábrica viral do tipo "vulcão" é formada e nela ocorre a morfogênese, como descrito para outros mimivírus (Fig.15) (SUZAN-MONTI et al., 2007). Durante este passo, a cauda do vírion é ligada ao capsídeo após a sua formação e fechamento. Foi possível observar também em várias imagens a incorporação de ribossomos amebianos na cauda viral, como descrito para arenavírus (MURPHY e WHITFIELD, 1975). Nos tempos tardios (16-24 h.p.i.), o citoplasma de amebas

é preenchido por várias partículas virais, seguido de lise celular e liberação de partículas (Fig.15). O mesmo perfil de multiplicação também foi observado por microscopia de imunofluorescência e de forma geral, nossos resultados evidenciaram um ciclo de multiplicação típico como observado em outros vírus gigantes de DNA (Fig.16) (LA SCOLA et al., 2008).

Além de multiplicação de TPVsd em *A. castellanii* e *V. vermiformis*, nossos resultados evidenciaram que diferentemente de outros vírus gigantes, TPVsl foi capaz de infectar uma ampla gama de organismos protistas (Tabela 5). Para a maioria das células testadas foi possível verificar ECP e lise, embora menor e mais tardia do que a lise observada em *A. castellanii* infectada com TPVsl (Fig.17). Para *T. hyperangularis*, após a infecção, foi possível observar que as células, normalmente intensamente móveis em condições saudáveis, haviam perdido a motilidade. Para a maioria das células (*V. vermiformis, A. polyphaga, A. griffini, A. sp E4, D. discoideum, W. magna*) foi possível verificar um aumento do título viral em aproximadamente 1 log 24 h.p.i, embora em *A. castellanii* este aumento tenha sido de 3 log. Para *A. sp. Micheline* e *A. royreba* apesar do ECP visualizado, o aumento do título viral não foi observado, porém, houve replicação do genoma viral, o que pode indicar um ciclo de multiplicação abortivo para o vírus nessas células. Já no caso de *T. hyperangularis*, apesar do ECP apresentado durante a infecção com TPVsl, não houve aumento de título viral, nem replicação do genoma, o que pode indicar que o vírus seria de alguma forma apenas tóxico para essas células, o que ainda necessita de investigação mais profunda. O vírus não causou ECP, aumento do título viral ou da quantidade de material genético apenas para *T. tenax*. Dessa forma, foram observados quatro perfis distintos de infectividade: 1) ciclo produtivo em células permissíveis; 2) ciclo abortivo; 3) células refratárias; e 4) células não hospedeiras que apresentam um fenótipo citotóxico na presença de TPVsl sem multiplicação, uma circunstância nunca relatada.

Nossos resultados de caracterização genômica para o isolado de solo oceânico, TPVdo, revelaram que seu genoma de 1,5 Mb fica atrás dos pandoravírus, que possuem genoma variando entre 1,9-2,5 Mb (PHILIPPE et al., 2013). O rizoma do TPVdo revelou que seus genes estão principalmente relacionados a família *Mimiviridae*. Em conjunto com a análise filogenética para o gene da DNA Polimerase B, este achado sugere que os tupanvírus são próximos de *Mimiviridae,* porém estão em uma posição filogenética mais próxima do ancestral dos mimivírus, anteriormente à ramificação das três linhagens (Fig. 18 e 19). Além

disso, TPVdo apresenta vários genes com origem relacionada com os grupos *Eukaria* e *Bacteria*. E, além disso, o rizoma indicou a relação de genes de TPVdo com o novo grupo dos Klosneuvírus. Estes, por sua vez, também compartilham a maioria de seus genes com *Mimiviridae*. Porém, de forma interessante, dos 355 genes compartilhados com o grupo *Eukaria*, apenas 12 foram encontrados nos quatro genomas dos representantes deste grupo (Catovíus, Indivírus, Hokovírus e Klosneuvírus) enfatizando uma dinâmica evolutiva complexa e um possível distinto espectro de hospedeiros para cada um dos diferentes representantes. Análises genéticas comparativas entre TPVdo e TPVsl poderiam ajudar a compreender melhor este cenário. De forma geral, outros vírus gigantes recentemente isolados demonstram um complexo perfil de origem de genes, evidenciando a diversidade entre eles. Por exemplo, dentre os phitovírus, vemos representantes que apresentam alta porcentagem de ORFans em seus genomas (mais de 60%), sugerindo ausência de parentes próximos anteriormente sequenciados. Dos genes com órtologos em bancos de dados relacionados a vírus, *P. sibericum* apresenta maior compartilhamento de genes com os Marseillevírus, assim como visto em Cedratvirus, um phitovírus relacionado (LEGENDRE et al., 2014; ANDREANI et al., 2016). Já os representantes dos faustovírus apresentam muitos genes relacionados à família *Asfarviridae* (RETENO et al., 2015). *M. sibericum* é mais relacionado aos pandoravírus (LEGENDRE et al., 2015). *P. salinus* apresenta uma porcentagem impressionante de ORFans em seu genoma (93%). Das ORFs preditas com *matchs* em bancos de dados há relação com *Eukaria*, *Bacteria* e outros vírus, porém, a maioria apresenta baixo nível de similaridade, evidenciando que há ausência de organismos sequenciados que sejam próximos dos pandoravírus e que eles são evolucionariamente distantes de microorganismos conhecidos até então, inclusive outros vírus gigantes (PHILIPPE et al., 2013). E por fim, os marseillevírus apresentam um alto grau de mosaicismo em seus genomas, fruto de TGH durante a multiplicação destes vírus no ambiente simpátrico amebiano, juntamente com outros vírus, bactérias e eucariotos. Além disso, essa troca engloba também genes hospedeiros (BOYER et al., 2009). O uso de códons e aminoácidos para o genoma de TPVdo em comparação com TPVsl e a célula hospedeira *A. castellanii*, revelou, como já evidenciado anteriormente por Colson e colaboradores (2013c) que o uso de códons e aminoácidos entre vírus gigantes de um mesmo grupo é muito semelhante entre si, enquanto difere do uso de códons e aminoácidos pela célula hospedeira (Fig. 20). Este perfil fortalece a teoria de que as amebas deste gênero não são os hospedeiros naturais dos vírus gigantes (COLSON et al., 2013c).

Surpreendentemente, a anotação do genoma de TPVdo revelou o maior conjunto de genes envolvidos em tradução conhecido para um vírus até o momento, ultrapassando até mesmo os Klosneuvírus recentemente descrito por SCHULZ e colaboradores (2017). Nosso novo isolado apresenta genes que codificam 20 ORFs relacionadas à aaRS, 70 tRNA que correspondem a um total de 48 códons (Tabela 6 e anexo 5), sendo ausentes apenas genes relacionados com selenocisteína, como também observado em muitas outras células (GONZALES-FLORES et al., 2014). Vários genes relacionados à TF foram também encontrados em TPVdo. Um total de nove genes para fatores de iniciação, um fator de elongação e um fator de terminação (Tabela 6). Alguns destes fatores são novidades na virosfera (comparação entre Tabela 2 e 05). Embora aminoácidos como leucina, arginina, prolina, treonina e serina, com um grande número de isoaceptores, ou seja, tRNA com diferentes anticódons que podem ligar-se a um mesmo aminoácido (Anexo 5), estejam relacionados com os tRNA de TPVdo, foram observadas várias duplicações, triplicações ou mesmo quadruplicações para os aminoácidos com poucos isoaceptores, como tirosina, asparagina e glutamina. De forma interessante, foi observada a alta correlação entre isoaceptores de tRNA de TPVdo e a maioria dos códons utilizados por ele, considerando separadamente cada aminoácido (Fig.20). Assim, para a maioria deles, o genoma de TPV apresenta isoaceptores de tRNA relacionados a alta abundância de códons (ou a soma deles).

Análises de redes para os genes relacionados à tradução em vírus gigantes permitiu a visualização de um panorama geral destes nos tupanvírus em relação aos outros vírus gigantes isolados até o momento, bem como organismos celulares. Foi analisada a presença destes elementos em representantes das três linhagens de mimivírus, *Cafeteria roenbergensis virus*, Klosneuvírus, *A. castellanii*, bem como *Encephalitozoon cuniculi*, representante de *Eukaria*, *Nanoarchaeum equitans*, representante de *Archaea* e *Candidatus Carsonella ruddii*, representante de *Bacteria*. Estes três foram selecionados por serem os representantes com menor genoma dentro destes grupos e também por serem parasitas intracelulares obrigatórios, como os vírus. Os grafos de conexões obtidos para análise de tRNA nestes representantes evidenciaram que os tupanvírus apresentam mais desses elementos em relação aos mimivírus e outros vírus gigantes relacionados e até mesmo em relação aos pequenos organismos celulares dos três domínios da vida, sendo TPVdo o vírus mais completo em relação a tRNA nesta análise, com 70 no total (Fig. 21). Não foi possível analisar o conteúdo de tRNA no hospedeiro, uma vez que não existem dados disponíveis confiáveis em relação a esses elementos em *A. castellanii*. Em

relação às aaRS, foi possível observar que o número de aaRS nos tupanvírus se compara com o conteúdo desses elementos em *A. castellanii* e *E. cuniculi* e é maior que o número de aaRS na maioria dos outros vírus gigantes analisados. Porém, os novos Klosneuvírus apresentam também um número significativo destes elementos, embora ligeiramente menor que o dos tupanvírus (Fig. 22). Ainda neste contexto, nossas análises acerca da origem evolutiva dos genes codificadores de aaRS em tupanvírus revelou que a maioria de suas aaRS, exceto fenilalanil-RS, prolil-RS, seril-RS, tirosil-RS, treonil-RS e valil-RS não parece ter sido adquirida recentemente de organismos celulares. A maioria das árvores apresentou um padrão no qual os tupanvírus aparecem como grupo externo (Anexo 6). Todavia, é importante salientar que a filogenia de aaRS é extremamente complexa, uma vez que estes genes são muito antigos, e uma grande instabilidade entre clados celulares canônicos é frequentemente observada (ABRAHÃO et al., 2017). Em relação aos outros fatores relacionados à síntese proteica, pode-se observar através dos grafos que são os elementos menos presentes nos vírus gigantes em geral, sendo o maior número destes observados nos Klosneuvírus, mas sem ultrapassar o conteúdo dos organismos celulares, sendo o arsenal mais completo nesta categoria presente em *A. castellanii* (Fig. 23). Provavelmente, a pressão evolutiva relacionada à conservação ou perda destes genes varia em diferentes grupos de vírus gigantes, algo que pode estar ligado a diferentes ambientes e espectro de hospedeiros de cada grupo ao longo do tempo (ABRAHÃO et al., 2017). Nossos resultados do panorama geral de elementos relacionados à tradução nos novos isolados, mostram que eles apresentam o maior complexo traducional entre vírus gigantes descritos até então, deixando para trás inclusive os recém descritos Klosneuvírus (SCHULZ et al., 2017). O grande número de tRNA, muitas vezes presentes em várias cópias no genoma, bem como 20 aaRS, número equivalente à presença destas enzimas em organismos celulares, sugere que estes novos vírus poderiam ter uma maior independência das células hospedeiras em relação a esses elementos, porém, em relação a outros TF ligados a tradução de proteínas, seu pequeno número nos genomas virais leva a acreditar que etapas cruciais do processo ainda são totalmente dependentes de correspondentes celulares. No entanto, estudos mais detalhados devem ser realizados para provar essa teoria, bem como entender o equilíbrio entre utilização da maquinaria de tradução viral e/ou celular durante a infecção.

Como supracitado, dados prévios demonstraram que o uso de códons/aminoácidos em vírus gigantes é muito similar, mas difere em relação ao uso em *A. castellanii*, a célula hospedeira (COLSON et al., 2013c). A avaliação do uso de códons/aminoácidos por cinco

diferentes isolados de mimivírus da linhagem A (APMV, APMV M4, SMBV, OYTV e KROV) e por *A. castellanii* confirmou estes dados. (Fig. 24). Apenas para alguns poucos códons, vemos um perfil um pouco diferente em KROV em relação aos demais mimivírus da linhagem A, sendo KROV, dentre estes mimivírus analisados, o que mais apresenta pequenas diferenças biológicas e genéticas. Este isolado brasileiro apresenta um genoma um pouco maior em relação ao mimivírus brasileiros da linhagem A; possui uma camada a mais em seu capsídeo e fibrilas com um perfil um pouco diferenciado (BORATTO et al., 2017). Já é conhecido que 48% dos tRNA presentes em mimivírus são codificados por um dos 10 códons mais utilizados em seu genoma, enquanto 84% deles são codificados pelos códons menos utilizados em amebas (COLSON et al., 2013c). Considerando os tRNA e aaRS analisados neste trabalho, hipotetiza-se de que os aminoácidos mais utilizados, como leucina (L) e tirosina (Y), são importantes para a maquinaria viral. Assim, todos os mimivírus analisados possuem um gene de leucinil-tRNA, sendo L codificada pelo códon TAA (anticódon TTA), comum entre estes mimivírus, mas pouco frequente em *A. castellanii*, que codifica este tRNA principalmente pelos códons CTG (anticódon CAG) e CTC (anticódon GAG) (COLSON et al., 2013c). Sabe-se, que de forma geral, leucinil-tRNA está presente em vários outros vírus gigantes e muitas vezes em múltiplas cópias (COLSON et al., 2013c). Arginina (R) e metionina (M) são menos utilizados pelos vírus, mas podem ser importantes porque R é amplamente utilizado por *A. castellanii* e a variedade de códons é grande nos dois grupos, enquanto M é o aminoácido de iniciação, e mesmo que pouco utilizado, estes mimivírus codificam genes para metionil-RS e arginil-RS, também codificados pela ameba. Histidina (H) e a cisteína (C) também são mantidos na maquinaria viral e hospedeira, embora sejam menos usados, mas podem ser importantes para o processo de infecção de outros hospedeiros, uma vez que estes mimivírus codificam genes para histidinil-tRNA (GTG-CAC), cisteinil t-RNA (GCA-TGC) e cisteinil-RS. Finalmente, o uso de triptofano (W) não é frequente, o que explicaria a baixa pressão de manutenção deste aminoácido na maquinaria viral, uma vez que o gene que codifica triptofanil-tRNA (CCA-TGG) é ausente em KROV e APMV M4. A diferença no uso de códons/aminoácidos entre estes mimivírus e a célula hospedeira, reforça a hipótese de que talvez amebas do gênero *Acanthamoeba* não sejam seus hospedeiros naturais, porém novas análises e estratégias de estudo necessitam ser realizadas para comprovar tal teoria (COLSON et al., 2013c). Essa teoria é reforçada pela indicação de que os mecanismos da expressão destes genes em mimivírus variam durante todo o ciclo de multiplicação e que os transcritos de tRNA virais são incorporados nas partículas virais maduras formadas ao final do ciclo, incitando que não são pseudogenes e que podem tornar a partícula viral mais

independente ao uso de códons/aminoácidos da célula amebiana. Mesmo se não forem seu hospedeiro natural, fica claro que os mimivírus se adaptaram a essas células e ao seu perfil de uso de códons/aminoácidos, e vice-versa (LEGENDRE et al., 2010; COLSON et al., 2013c).

Nossa padronização de PCR em tempo real permitiu a obtenção de reações otimizadas e confiavéis para a avalição do nível de mRNA de elementos envolvidos em tradução em mimivírus por meio de expressão relativa. Estas análises revelaram que os mimivírus analisados foram capazes de modular a expressão de genes relacionados à tradução de acordo com a disponibilidade de nutrientes durante a infecção da célula amebiana (Fig. 28 e 29). De modo geral, em condições de supressão de nutrientes, como por exemplo, nas infecções realizadas em meio PAS ou PYG0%, a indução do nível de mRNA de tRNA e aaRS codificadas por mimivírus foi mais alta em relação ao nível de mRNA destes genes em amebas infectadas na presença de PYG7%, meio com alta concentração de nutrientes. Esta indução da expressão destes genes em condições nutricionais pobres se assemelha à indução de aaRS celulares sob a mesma condição de crescimento em bactérias e *Saccharomyces cerevisae*, como anteriormente observado (RYCKELYNCK et al., 2005). Na levedura, a baixa disponibilidade de aminoácidos é detectada pela proteína quinase GCN2 que é ativada por tRNA não carregados. GCN2 fosforila o fator de iniciação eIF2, inibindo sua função na iniciação da tradução. A inativação de eIF2 leva à tradução de GCN4, que por sua vez é um ativador de transcrição que ativa a transcrição de aaRS por ligação aos promotores dos genes que as codificam (RYCKELYNCK et al., 2005). Se este mesmo sensor de disponibilidade de aminoácidos opera em *A. castellanii* ainda necessita de investigação, mas poderia explicar a indução destes genes virais após oito horas de infecção da célula amebiana. Seria possível a existência de uma interação entre a detecção da disponibilidade de nutrientes da ameba e a estimulação dos genes de tRNA e aaRS virais.

Considerando a menor multiplicação viral em células infectadas com a condição nutricional mais pobre, meio PAS, em relação à multiplicação viral em meio PYG, com ou sem SFB, conforme demonstrado pelos experimentos de curva de ciclo único (Fig. 30C), pode-se formular a hipótese de que contornar a disponibilidade limitada de nutrientes é fundamental ou muito importante para a propagação de mimivírus em populações de amebas. Embora os isolados tenham mostrado uma menor multiplicação viral nesta condição, a baixa de nutrientes pode ser responsável por induzir a alta expressão dos genes relacionados à tradução nesta condição se comparado aos resultados obtidos nas infecções em PYG com ou

sem SFB (Fig. 28 e 29). Assim, isso pode indicar que na baixa presença de nutrientes, com a multiplicação mais lenta das amebas, os vírus necessitariam compensar a expressão gênica desses elementos e dessa forma garantir o sucesso da infecção, algo talvez não necessário em condições mais ricas, como meio PYG suplementado, por exemplo, na qual ele poderia usufruir mais facilmente dos genes relacionados à tradução expressos normalmente também pelo seu hospedeiro. Assim, a maquinaria de tradução própria dos vírus gigantes poderia ser útil em condições adversas e em determinados casos poderia ser necessária de uma maneira que muitas vezes não pode ser realizada pela maquinaria homóloga celular. De toda forma, a expressão destes genes na célula hospedeira em diferentes condições de infecção é um ponto que deve ser investigado.

Alguns dos mimivírus analisados apresentaram diferenças no nível de mRNA de alguns genes relacionados a tradução em comparação com outros isolados. Diferenças genéticas entre estes isolados foram descobertas através de análises das sequências nucleotídicas preditas para os mesmos, revelando polimorfismos nas regiões promotoras destes genes, o que poderia explicar esse fenômeno. Os polimorfismos foram detectados em alguns genes codificados por OYTV e com alta frequência em KROV (Anexo 7). Uma análise cuidadosa das sequências desses dois isolados brasileiros, especialmente o KROV, demonstrou substituições de nucleotídeos nas regiões promotoras e sinais de poliadenilação de alguns genes e a ausência dessas sequências reguladoras em outros genes, incluindo leucinill-tRNA, cisteinil-tRNA, cisteinil-RS, metionil-RS e arginil-RS (Anexo 7). Para o gene codificador de arginil-RS que apresentou os níveis de mRNA mais baixos durante a infecção pelo KROV em todas as condições nutricionais testadas, observou-se uma diferença de aproximadamente 15% na sequência de nucleotídeos entre o promotor precoce e o códon de iniciação, além de uma diferença de aproximadamente 8% na região contendo o promotor tardio. Além disso, estão ausentes aproximadamente 46 pb na extremidade 3' do gene em comparação com o ortólogo codificado por APMV (Fig. 31). Propomos que essas diferenças possam ajudar a explicar os diferentes níveis de mRNA de genes relacionados à tradução por KROV em comparação com os outros mimivírus (Fig. 28, Fig. 29 e Anexo 7). APMV M4, um clone que foi obtido após sucessivas passagens de APMV em condições alopátricas, sem as fontes principais para a troca gênica (bactérias, eucariotos e outros micro-organismos amebianos) perdeu vários ORFs em seu genoma, incluindo aquelas que codificam o triptofanil-tRNA e o tirosil-RS, os quais não tiveram níveis detectáveis de mRNA neste estudo. Portanto, sugere-se que esses genes são provavelmente importantes apenas em

condições de crescimento simpátrico, nas quais APMV poderia competir melhor com outros microorganismos associados a amebas, codificando essas ORFs e expressando os genes de tradução de acordo com a disponibilidade de nutrientes (BOYER et al., 2011; COLSON e RAOULT, 2012). Isso nos leva a sugerir que a evolução da maquinaria de tradução em diferentes isolados de vírus gigantes pode ser fruto da adaptabilidade de cada isolado ao longo de sua história, considerando diferentes espectros de hospedeiros e condições ambientais.

A estrutura e genoma mais complexos dos vírus gigantes, como verificado atualmente garantiriam maior versatilidade e capacidade adaptativa frente a diferentes hospedeiros e condições ambientais. Isso é claramente observado nos nossos resultados de modulação dos elementos envolvidos em tradução em infecções com diferentes condições nutricionais. Dessa forma, propomos que o aparato traducional presente em vírus gigantes poderia atuar como uma vantagem adaptativa, além de permitir a estes vírus maior versatilidade de hospedeiros, como verificado no caso do novo isolado, TPVsl, claramente capaz de multiplicar-se em células de diferentes gêneros e apresentando o maior número de elementos envolvidos em tradução já conhecido para vírus gigantes, verificado em análises genéticas em conjunto com o outro representante do grupo, TPVdo. No contexto evolutivo, dados recentemente publicados, juntamente com os obtidos neste trabalho ajudam no debate sobre a origem dos vírus gigantes. A presença de um complexo arsenal de tradução nos Klosneuvírus (SCHULZ et al., 2017), identificados apenas metagenomicamente, e também nos tupanvírus, aqui demonstrados através de caracterização biológica e genômica, sugere que estes vírus possuem um ancestral comum. Existem várias teorias para este caminho evolutivo complexo: no primeiro modelo, os mimivírus possuiriam um ancestral comum mais simples que foi adquirindo genes ao longo dos tempos; a teoria que preconiza a existência de um ancestral comum genomicamente mais complexo, que foi sofrendo degradação genômica; e a teoria da sanfona que acredita que estes vírus evoluem ganhando ou perdendo genes de acordo com as condições seletivas de um determinado momento (MOREIRA e LOPEZ-GARCIA, 2005; CLAVERIE et al., 2006; FILÉE et al., 2008; YUTIN et al., 2014; FILÉE et al., 2015; SCHULZ et al., 2017). Por fim, com todos os dados em conjunto, nós acreditamos que os tupanvírus, assim como os Klosneuvírus, possam ser considerados vírus gigantes arcaicos que dividem um ancestral comum com vírus da família *Mimiviridae.* Este ancestral provavelmente tinha um estilo de vida mais generalista, podendo infectar uma grande variedade de hospedeiros, como demonstramos para o TPVsl. Nesta visão, o ancestral seria um vírus gigante complexo que ao iniciar a adaptação em amebas passou a sofrer principalmente uma

evolução genômica redutiva, usual entre os parasitas intracelulares obrigatórios (SMITH, 2009; MERHEJ e RAOULT, 2011; NUNES e GOMES, 2014). Nestes casos, os organismos perdem genes relacionados à tradução e produção de energia, sendo uma das principais razões do seu estilo de vida parasitário. No entanto, no caso específico dos mimivírus, somente a perda de genes associados à tradução pode ser analisada, pois em todos os mimivírus, incluindo tupanvírus e Klosneuvírus, os genes associados à produção de energia são muito escassos. A prospecção de novos vírus gigantes, em ambientes ainda não explorados, parece ser um passo essencial para que os conhecimentos acerca da evolução dos mimivírus sejam aprimorados. Os esforços feitos pelo nosso grupo ao longo dos últimos anos mostraram que novos e fantásticos vírus estão na natureza, aptos a serem isolados e prontos para nos contarem novas histórias. Neste trabalho de Tese, optamos por avançar nos fatores de tradução dos tupanvírus e outros mimivírus, mas certamente, aspectos biológicos, filogenéticos e estruturais permanecem a ser explorados.

VIII- CONCLUSÕES

- Foram isolados dois novos vírus gigantes, denominados de Tupanvirus (TPV). O isolado de amostra de solo de lagoa alcalina coletada no Pantanal, foi denominado Tupanvirus soda lake (TPVsl) e o isolado de amostra de solo oceânico da Bacia De Campo foi denominado Tupanvirus deep ocean (TPVdo).

- TPVsl apresentou morfologia totalmente nova para vírus gigantes e a incrível capacidade de multiplicar-se em mais de uma célula de protozoário;

- A análise do genoma de TPVdo revelou que o aparato relacionado à tradução nos tupanvírus é o mais complexo entre os vírus gigantes conhecidos até então, sendo algumas vezes mais complexo do que o aparato traducional de pequenos organismos celulares;

- As análises filogenéticas das aaRS dos tupanvírus revelaram que a maioria delas parecem ter sido adquiridas independentemente de organismos celulares conhecidos.

- O perfil de uso de códons/aminoácidos entre APMV, APMV M4, SMBV, KROV e OYTV é muito similar, enquanto se mostra diferente quando comparado ao perfil de uso de aminoácidos pela célula hospedeira *A. castellanii*. O mesmo perfil também foi observado para os tupanvírus;

- O nível de mRNA para alguns tRNA e aaRS virais é diferentemente modulado pelos mimivírus durante a infecção em amebas. Diferenças genéticas entre os diferentes isolados podem explicar esse fenômeno. Por exemplo, a presença de polimorfismos encontrados na análise destes genes;

- A condição de cultivo das amebas *A. castellanii* infectadas também é um fator importante para modulação do nível de mRNA destes genes em mimivírus, uma vez que em amebas mantidas em meio nutricionalmente mais pobre (PAS), a expressão destes genes foi maior se comparada às células infectadas na presença de um meio mais rico (PYG);

- Os diferentes mimivírus analisados foram capazes de se multiplicar produtivamente em amebas mantidas nos três meios de cultivo testados, embora na presença de PAS, o título viral final tenha sido menor em relação às células infectadas mantidas em PYG;

IX- ATIVIDADES DESENVOLVIDAS NO PERÍODO

9.1 Doutorado sanduíche

- Período de um ano em Aix Marseille Université, Marseille/França (Agosto/2015 – Agosto/2016).

9.2 Eventos

- XXV Congresso Brasileiro de Virologia, 2014, Ribeirão Preto: Hélio Gelli Pereira Award - Melhor trabalho na categoria Pós Graduação (mestrado) e 2 resumos

- I Simpósio de Microbiologia da UFMG (2014): 5 Resumos

- III Simpósio de Microbiologia da UFMG (2016)

9.3 Artigos completos publicados em periódicos (Anexo 8)

ABRAHAO, J.S.; **SILVA, L.C.F**; SILVA, L.K.S.; KHALIL, J.Y.B.; RODRIGUES, R.A.L.; ARANTES, T.S.; ASSIS, F.L; BORATTO, P.V.M.; ANDRADE, M.; KROON, E.G.; RIBEIRO, B.; BERGIER, I.; SELIGMANN, H.; GHIGO, E.; COLSON, P.; LEVASSEUR, A.; KROEMER, G.; RAOULT, D.; LA SCOLA, B. Tailed giant Tupanvirus possesses the most complete translational apparatus of the virosphere. Nature Communications, 2018.

SILVA, LORENA C. F.; ALMEIDA, GABRIEL M. F.; ASSIS, FELIPE L.; ALBARNAZ, JONAS D.; BORATTO, PAULO V. M.; DORNAS, FÁBIO P.; ANDRADE, KETYLLEN R.; LA SCOLA, BERNARD; KROON, ERNA G.; DA FONSECA, FLÁVIO G.; ABRAHÃO, JÔNATAS S. Modulation of the expression of mimivírus-encoded translation-related genes in response to nutrient availability during Acanthamoeba castellanii infection. Frontiers in Microbiology (Online), v. 06, p. 1-8, 2015.

ALMEIDA, GABRIEL MAGNO DE FREITAS; **SILVA, LORENA C. FERREIRA**; COLSON, PHILIPPE; ABRAHAO, JONATAS SANTOS. Mimivíruses and the Human Interferon System: Viral Evasion of Classical Antiviral Activities, But Inhibition By a Novel Interferon-β Regulated Immunomodulatory Pathway. Journal of Interferon & Cytokine Research, v. 37, p. 1-8, 2017.

BORATTO, PAULO V. M.; ARANTES, THALITA S.; **SILVA, LORENA C. F.**; ASSIS, FELIPE L.; KROON, ERNA G.; LA SCOLA, BERNARD; ABRAHÃO, JÔNATAS S. Niemeyer Virus: A New Mimivírus Group A Isolate Harboring a Set of Duplicated Aminoacyl-tRNA Synthetase Genes. Frontiers in Microbiology (Online), v. 6, p. 1256, 2015.

ANDRADE, KÉTYLLEN R.; BORATTO, PAULO P. V. M.; RODRIGUES, FELIPE P.; **SILVA, LORENA C. F.**; DORNAS, FÁBIO P.; PILOTTO, MARIANA R.; LA SCOLA, BERNARD; ALMEIDA, GABRIEL M. F.; KROON, ERNA G.; ABRAHÃO, JÔNATAS S. Oysters as hot spots for mimivírus isolation. Archives of Virology, v. 160, p. 477-482, 2015.

DORNAS, FÁBIO P.; RODRIGUES, FELIPE P.; BORATTO, PAULO V.M.; **SILVA, LORENA C.F.** ; FERREIRA, PAULO C.P.; BONJARDIM, CLÁUDIO A.; TRINDADE, GILIANE S.; KROON, ERNA G.; LA SCOLA, BERNARD; ABRAHÃO, JÔNATAS S. Mimivírus Circulation among Wild and Domestic Mammals, Amazon Region, Brazil. Emerging Infectious Diseases (Print), v. 20, p. 469-472, 2014.

DORNAS, FÁBIO P.; **SILVA, LORENA C. F.**; DE ALMEIDA, GABRIEL M.; CAMPOS, RAFAEL K.; BORATTO, PAULO V. M.; FRANCO-LUIZ, ANA P. M.; LA SCOLA, BERNARD; FERREIRA, PAULO C. P.; KROON, ERNA G.; ABRAHÃO, JÔNATAS S. Acanthamoeba polyphaga mimivirus Stability in Environmental and Clinical Substrates: Implications for Virus Detection and Isolation. Plos One, v. 9, p. e87811, 2014.

CAMPOS, RAFAEL K; BORATTO, PAULO V; ASSIS, FELIPE L; AGUIAR, ERIC RGR; **SILVA, LORENA CF**; ALBARNAZ, JONAS D; DORNAS, FABIO P; TRINDADE, GILIANE S; FERREIRA, PAULO P; MARQUES, JOÃO T; ROBERT, CATHERINE; RAOULT, DIDIER; KROON, ERNA G; LA SCOLA, BERNARD; ABRAHÃO, JÔNATAS S. Samba virus: a novel mimivírus from a giant rain forest, the Brazilian Amazon. Virology Journal, v. 11, p. 95, 2014.

ABRAHÃO, JÔNATAS S; DORNAS, FÁBIO P; **SILVA, LORENA CF**; ALMEIDA, GABRIEL M; BORATTO, PAULO VM; COLSON, PHILLIPE; LA SCOLA, BERNARD; KROON, ERNA G. Acanthamoeba polyphaga mimivirus and other giant viruses: an open field to outstanding discoveries. Virology Journal, v. 11, p. 120, 2014.

ABRAHÃO, JÔNATAS S.; BORATTO, PAULO; DORNAS, FÁBIO P.; **SILVA, LORENA C.F**; CAMPOS, RAFAEL K.; ALMEIDA, GABRIEL M.F.; KROON, ERNA G.; LA SCOLA, BERNARD. Growing a Giant: Evaluation of the Virological Parameters for Mimivírus Production. Journal of Virological Methods, v. 207, p. 6-11, 2014.

9.4 Capítulo de livro publicado

Abrahão, Jônatas Santos; Oliveira, Graziele Pereira; **Ferreira da Silva, Lorena Christine**; dos Santos Silva, Ludmila Karen; Kroon, Erna Geessien; La Scola, Bernard. Mimivíruses: Replication, Purification, and Quantification. Current Protocols in Microbiology. 41. ed. John Wiley & Sons, Inc., 2015. v. 1.

REFERÊNCIAS BIBLIOGRÁFICAS

ABERGEL, C.; LEGENDRE, M.; CLAVERIE, J.M. The rapidly expanding universe of giant viruses: Mimivírus, Pandoravirus, Pithovirus and Mollivirus. FEMS Microbiology Reviews, fuv037, 39, 2015, 779–796. 2015. doi: 10.1093/femsre/fuv037

ABERGEL, C.; RUDINGER-THIRION, J.; GIEGÉ, R.; CLAVERIE, J.M. Virus-encoded aminoacyl-RNA synthetases: structural and functional characterization of mimivírus TirRS and MetRS. Journal of virology, E.U.A., v. 81, n. 22, p.12406-17, 2007.

ABRAHÃO, J.S.; ARAÚJO, R.; COLSON, P.; LA SCOLA, B. The analysis of translation-related gene set boosts debates around origin and evolution of mimivíruses. PLoS Genet. 13(2):e1006532. 2017. doi: 10.1371/journal.pgen.1006532.

ABRAHÃO, J.S.; DORNAS, F.P.; SILVA, L.C.; ALMEIDA, G.M.; BORATTO, P.V.; COLSON, P.; LA SCOLA, B.; KROON, E.G. Acanthamoeba polyphaga mimivirus and other giant viruses: an open field to outstanding discoveries. Virol J, v.11, n.120, 2014. doi: 10.1186/1743-422X-11-120.

ABRAHÃO, J.S.; OLIVEIRA, G.P.; FERREIRA DA SILVA, L.C.; DOS SANTOS SILVA, L.K.; KROON, E.G.; LA SCOLA, B. Mimivíruses: Replication, Purification, and Quantification. Curr Protoc Microbiol. 41:14G.1.1-14G.1.13, 2016. doi: 10.1002/cpmc.2.

AHERFI, S.; COLSON, P.; LA SCOLA, B.; RAOULT, D. Giant Viruses of Amoebas: An Update. Front Microbiol., 2016. doi: 10.3389/fmicb.2016.00349.

AHERFI, S.; LA SCOLA, B.; PAGNIER, I.; RAOULT, D.; COLSON, P. The expanding family Marseilleviridae. Virology. v.466, n.467, p. 27-37. 2014. doi: 10.1016/j.virol.2014.07.014.

AHERFI, S.; PAGNIER, I.; FOURNOUS, G.; RAOULT, D.; LA SCOLA, B.; COLSON, P. Complete genome sequence of Cannes 8 virus, a new member of the proposed family "Marseilleviridae". Virus Genes, v.47, n.3, p.550-5. 2013. doi: 10.1007/s11262-013-0965-4.

ANDRADE, K.R.; BORATTO, P.P.; RODRIGUES, F.P.; SILVA, L.C.; DORNAS, F.P.; PILOTTO, M.R.; LA SCOLA, B.; ALMEIDA, G.M.; KROON, E.G.; ABRAHÃO, J.S. Oysters as hot spots for mimivírus isolation. Arch Virol, v. 160, n.2, p.477-82, 2015. doi: 10.1007/s00705-014-2257-2.

ANDREANI J.; BOU KHALIL, J.Y.; SEVVANA, M.; BENAMAR, S.; DI PINTO, F.; BITAM, I.; COLSON, P.; KLOSE, T.; ROSSMANN, M.G.; RAOULT, D.; LA SCOLA, B. Pacmanvirus, a new giant icosahedral virus at the crossroads between Asfarviridae and Faustoviruses. J Virol. pii: JVI.00212-17. 2017. doi: 10.1128/JVI.00212-17.

ANDREANI, J.; AHERFI, S.; BOU KHALIL, J.Y.; DI PINTO, F.; BITAM, I.; RAOULT, D.; COLSON, P.; LA SCOLA, B. Cedratvirus, a Double-Cork Structured Giant Virus, is a Distant Relative of Pithoviruses. Viruses. v.3;8(11). 2016. doi:10.3390/v8110300

ANTWERPEN, M.H.; GEORGI, E.; ZOELLER, L.; WOELFEL, R.; STOECKER, K.; SCHEID, P. Whole-genome sequencing of a pandoravirus isolated from keratitis-inducing acanthamoeba. Genome Announc. v.3(2). 2015. pii: e00136-15. doi: 0.1128/genomeA.00136-15.

ARANTES, T.S.; RODRIGUES, R.A.; DOS SANTOS SILVA, L.K.; OLIVEIRA, G.P.; DE SOUZA, H.L.; KHALIL, J.Y.; DE OLIVEIRA, D.B.; TORRES, A.A.; DA SILVA, L.L.; COLSON, P.; KROON, E.G.; DA FONSECA, F.G.; BONJARDIM, C.A.; LA SCOLA, B.; ABRAHÃO, J.S. The Large Marseillevirus Explores Different Entry Pathways by Forming Giant Infectious Vesicles. J Virol. v.90(11), p.5246-55, 2016. doi: 10.1128/JVI.00177-16.

ARSLAN, D.; LEGENDRE, M.; SELTZER, V.; ABERGEL, C.; CLAVERIE, J.M. Distant mimivírus relative with a larger genome highlights the fundamental features of *Megaviridae*. PNAS, E.U.A., v. 108, n. 42, p. 17486-91, 2011.

ASSIS, F.L.; BAJRAI, L.; ABRAHAO, J.S.; KROON, E.G.; DORNAS, F.P.; ANDRADE, K.R.; BORATTO, P.V.; PILOTTO, M.R.; ROBERT, C.; BENAMAR, S.; SCOLA, BL.; COLSON, P. Pan-Genome Analysis of Brazilian Lineage A Amoebal Mimivíruses. Viruses, v.7, n.7, p.3483-99, 2015. doi: 10.3390/v7072782.

BAJRAI, L.H.; BENAMAR, S.; AZHAR, E.I.; ROBERT, C.; LEVASSEUR, A.; RAOULT, D.; LA SCOLA, B. Kaumoebavirus, a New Virus That Clusters with Faustoviruses and Asfarviridae. Viruses. v.8 (11). p. 278. 2016. doi:10.3390/v8110278.

BASTIAN, M.; HEYMANN, S.; JACOMY, M. Gephi: an open source software for exploring and manipulating networks.International AAAI Conference on Weblogs and Social Media. 2009.

Blast website. Disponível http://blast.ncbi.nlm.nih.gov/Blast.cgi

BORATTO, P.V.M.; DORNAS, F.P.; **SILVA, L.C.F**; RODRIGUES, R.A.L.; OLIVEIRA, G.P; CORTINES, J.R.; DRUMOND, B.P.; ABRAHÃO, J.S. The analysis of KV mimivirus major capsid gene and its transcript highlights a distinct pattern of gene evolution and splicing among mimiviruses. Journal Of Virology, 2017. doi:10.1128/JVI.01782-17.

BORATTO, PV.; ARANTES, T.S.; SILVA, L.C.; ASSIS, F.L.; KROON, E.G.; LA SCOLA, B.; ABRAHÃO, J.S. Niemeyer Virus: A New Mimivírus Group A Isolate Harboring a Set of Duplicated Aminoacyl-tRNA Synthetase Genes. Front Microbiol, v. 10, n. 6, 2015. doi: 10.3389/fmicb.2015.01256.

BOUGHALMI, M.; SAADI, H.; PAGNIER, I.; COLSON, P.; FOURNOUS, G.; RAOULT, D.; LA SCOLA, B. High-throughput isolation of giant viruses of the *Mimiviridae* and *Marseilleviridae* families in the Tunisian environment. Environmental Microbiology, Inglaterra, v.15, n.7, p. 2000–7, 2013.

BOYER , M.; AZZA, S.; BARRASSI, L.; KLOSE, T.; CAMPOCASSO, A.; PAGNIER, I.; FOURNOUS, G.; BORG , A.; ROBERT, C.; ZHANG, X.; DESNUES, C.; HENRISSAT, B.; ROSSMANN, M.G.; LA SCOLA, B.; RAOULT, D. Mimivírus shows dramatic genome reduction after intraamoebal culture. PNAS, E.U.A., v. 108, n. 25, p. 10296-301, 2011.

BOYER, M.; YUTIN, N.; PAGNIER, I.; BARRASSI, L.; FOURNOUS, G.; ESPINOSA, L.; ROBERT C.; AZZA, S.; SUN, S.; ROSSMANN, M.G.; SUZAN-MONTI, M.; LA SCOLA, B.; KOONIN, E.V.; RAOULT, D. Giant Marseillevirus highlights the role of amoebae as a melting pot in emergence of chimeric microorganisms. PNAS, v.106, n.51, p. 21848–21853, 2009. Doi: 10.1073/pnas.0911354106.

CAMPOS, R.K.; BORATTO, P.V.; ASSIS, F.L.; AGUIAR, E.R.; SILVA, L.C.; ALBARNAZ, J.D.; DORNAS, F.P.; TRINDADE, G.S.; FERREIRA, P.P.; MARQUES, J.T.; ROBERT, C.; RAOULT, D.; KROON, E.G.; LA SCOLA, B.; ABRAHÃO, J.S. Samba virus: a novel mimivírus from a giant rain forest, the Brazilian Amazon. J. Virol, v. 14, n. 11:95. doi: 10.1186/1743-422X-11-95. 2014.

CARLESSO, A.M.; SIMONETTI, A.B.; ARTUSO, G,L.; ROTT, M.B.Isolation and identification of potentially pathogenic free-living amoebae in samples from environments in a public hospital in the City of Porto Alegre, Rio Grande do Sul. Revista da Sociedade Brasileira de Medicina Tropical. 40(3):316-320, 2007.

CARVER, T.; HARRIS, S.R.; BERRIMAN, M.; PARKHILL, J.; MCQUILLAN, J.A. Artemis: an integrated platform for visualization and analysis of high-throughput sequence-based experimental data. Bioinformatics. 15;28(4):464-9. 2012. doi: 10.1093/bioinformatics/btr703.

CLAVERIE, J.M.; ABERGEL, C. Mimivírus and its virophage. Annu Rev Genet, v.43, p.49-66, 2009. doi: 10.1146/annurev-genet-102108-134255.

CLAVERIE, J.M.; ABERGEL, C.; OGATA, H. Mimivírus. Current topics in microbiology and immunology, Alemanha, v. 328, p. 89-121, 2009.

CLAVERIE, J.M.; OGATA, H.; AUDIC, S.; ABERGEL, C.; SUHRE, K.; FOURNIER, P.E. Mimivírus and the emerging concept of "giant" virus. Viruses Research, Países Baixos, v. 117, n. 1, p.133-44, 2006.

COHEN, G.; HOFFART, L.; LA SCOLA, B.; RAOULT, D.; DRANCOURT, M. Ameba-associated Keratitis, France. Emerg. Infect. Dis., v.17, p. 1306–1308, 2011.

COLSON, P., DE LAMBALLERIE, X., YUTIN, N., ASGARI, S., BIGOT, Y., BIDESHI, D.K., CHENG, X.W., FEDERICI, B.A., VAN ETTEN, J.L., KOONIN, E.V., LA SCOLA, B., RAOULT, D. "Megavirales", a proposed new order for eukaryotic nucleocytoplasmic large DNA viruses. Arch Virol. 158(12):2517-21. doi: 10.1007/s00705-013-1768-6, 2013a.

COLSON, P.; DE LAMBALLERIE, X.; FOURNOUS, G.; RAOULT, D. Reclassification of giant viruses composing a fourth domain of life in the new order *Megavirales*. Intervirology, Suíça, v.55, n. 5, p. 321-32, 2012.

COLSON, P.; FANCELLO, L.; GIMENEZ, G.; ARMOUGOM, F.; DESNUES, C.; FOURNOUS, G.; YOOSUF, N.; MILLION, M.; LA SCOLA, B.; RAOULT, D. Evidence of the megavirome in humans. Journal of clinical virology, Países Baixos, v. 57, n. 3, p.191-200, 2013b.

COLSON, P.; FOURNOUS, G.; DIENE, S.M.; RAOULT, D. Codon usage, amino acid usage, transfer RNA and amino-acyl-tRNA Synthetases in mimivíruses. Intervirology, Suíça, v. 56, n. 6, p.364-75, 2013c.

COLSON, P.; GIMENEZ, G.; BOYER, M.; FOURNOUS, G.; RAOULT, D. The giant *Cafeteria roenbergensis virus t*hat infects a widespread marine phagocytic protist is a new member of the fourth domain of Life. PLoS One, E.U.A., v. 6, n. 4, p. 01-11, 2011a.

COLSON, P.; PAGNIER, I.; YOOSUF, N.; FOURNOUS, G.; LA SCOLA, B.; RAOULT, D. '*Marseilleviridae*', a new family of giant viruses infecting amoebae. Archives of virology, Áustria, v. 158, n.4, p. 915-20, 2013d.

COLSON, P.; YUTIN, N.; SHABALINA, S.A.; ROBERT, C.; FOURNOUS, G.; LA SCOLA, B.; RAOULT, D.; KOONIN, E.V. Viruses with more than 1,000 Genes: *Mamavirus*, a new *Acanthamoeba polyphaga mimivirus* strain, and reannotation of mimivírus genes. Genome biology and evolution, Inglaterra, v. 3, p. 737–42, 2011b.

COLSON, P.; RAOULT, D. Lamarckian evolution of the giant mimivírus in allopatric laboratory culture on amoebae. Frontiers in cellular and infection microbiology [electronic resource], Suíça, v.,2, n.91, 2012. Disponível em <http://www.ncbi.nlm.nih.gov/pubmed/22919682>.

CROZETTA, M.A.S. Identificação morfológica e molecular de amebas de vida livre do gênero Acanthamoeba isoladas em poeira de ambiente hospitalar. 2007. 46p. Dissertação (Mestrado em Ciências Biológicas), Universidade Federal do Paraná, Curitiba. 2007.

DE JONCKHEERE, J.F.; DIVE, D.; PUSSARD, M.; VICKERMAN, K. Willaertia magna gen. nov., sp. nov. (Vahlkampfiidae), a thermophilic amoeba found in different habitats. Protistologica 20: 5–13. 1984.

DESNUES, C.; LA SCOLA, B.; YUTIN, N.; FOURNOUS, G.; ROBERT, C.; AZZA, S.; JARDOT, P.; MONTEIL, S.; CAMPOCASSO, A.; KOONIN, E.V.; RAOULT, D. Provirophages and transpovirons as the diverse mobilome of giant viruses. PNAS, E.U.A., v. 109, n. 44, p. 18078-83, 2012.

DESNUES, C.; RAOULT, D. Inside the lifestyle of the virophage. Intervirology, Suíça, v. 53, n.5, p. 293-303, 2010.

DIAS, N.; AMARAL, A.; FERREIRA, E.; LIMA, N. Automated image analysis to improve bead ingestion toxicity test counts in the protozoan Tetrahymena pyriformis. Letters Applied Microbiology. (37) 230-233. 2003.

DORNAS, F.P.; ASSIS, F.L.; AHERFI, S.; ARANTES, T.; ABRAHÃO, J.S.; COLSON, P.; LA SCOLA, B. A Brazilian Marseillevirus Is the Founding Member of a Lineage in Family Marseilleviridae. Viruses, v. 8, n.3, p. 76, 2016. doi: 10.3390/v8030076.

DORNAS, F.P.; KHALIL, J.Y.; PAGNIER, I.; RAOULT, D.; ABRAHÃO, J.; LA SCOLA, B. Isolation of new Brazilian giant viruses from environmental samples using a panel of protozoa. Front Microbiol. 2015:1086. doi: 10.3389/fmicb.2015.01086. eCollection

DOUTRE, G.; PHILIPPE, N.; ABERGEL, C.; CLAVERIE, J. M. Genome analysis of the first Marseilleviridae representative from Australia indicates that most of its genes contribute to virus fitness. J. Virol, v. 88, n.24, p.14340–14349, 2014. doi:10.1128/JVI.02414-14

DUARTE, J.L. Caracterização morfológica, molecular e fisiológica de isolados clínicos e ambientais de Acanthamoeba. 2010. 85p. Dissertação (Mestrado em Parasitologia), Universidade Federal do Paraná, Curitiba. 2010.

ETTEN, J.L.V.; LANE,L.C.; DUNIGAN, D.D. DNA viruses: the really big ones (giruses). Annual review of microbiology, E.U.A., v. 13, n. 64, p. 83–99, 2010.

FILÉE, J. Genomic comparison of closely related Giant Viruses supports an accordion-like model of evolution. Front Microbiol. v.16, p.593, 2015. doi: 10.3389/fmicb.2015.00593.

FILÉE, J.; POUGET, N.; CHANDLER, M. Phylogenetic evidence for extensive lateral acquisition of cellular genes by Nucleocytoplasmic large DNA viruses. BMC Evol Biol. v. 8. p320. 2008. doi: 10.1186/1471-2148-8-320.

FISCHER, M.G.; ALLEN, M.J.; WILSON, W.H.; SUTTLE, C.A. Giant virus with a remarkable complement of genes infects marine zooplankton. PNAS, v. 107, n. 45, p. 19508-13, 2010. doi: 10.1073/pnas.1007615107.

FISCHER, M.G.; SUTTLE, C.A. A virophage at the origin of large DNA transposons Science, v. 332, p. 231–234, 2011.

FRITSCHE, T.; GAUTOM, R.K.; SEYEDIRASHTI, S.; BERGERON,D.L.; LINDQUIST, T.D. Occurrence of bacterial endosymbionts in Acanthamoeba spp. isolated from corneal and environmental specimens and contact lenses. J. Clin. Microbiol. 31:1122–1126. 1993.

GAIA, M.; BENAMAR, S.; BOUGHALMI, M.; PAGNIER, I.; CROCE, O.; COLSON, P.; RAOULT, D.; LA SCOLA, B. Zamilon, a novel virophage with Mimiviridae host specificity. PLoS ONE, v.9, n.4, e94923. doi:10.1371/journal.pone.0094923. 2014.

Genbank website. Disponível em: http://www.ncbi.nlm.nih.gov/genbank/

GHEDIN, E.; CLAVERIE,J.M. Mimivírus relatives in the Sargasso sea. Virology Journal, Inglaterra, v. 2, p. 62-69, 2005.

GHIGO, E.; KARTENBECK, J.; LIEN, P.; PELKMANS, L.; CAPO, C.; MEGE, J.L.; RAOULT, D. Ameobal pathogen mimivirus infects macrophages through phagocytosis. PLoS Pathogens, E.U.A., v. 4, n. 6, p. 01-17, 2008.

GONZALES-FLORES, J. N.; SHETTY, S. P.; DUBEY, A.; COPELAND, P.R. The molecular biology of selenocysteine. Biomol Concepts. 4, 349-65. 2014.

GREUB, G., RAOULT, D. Microorganisms resistant to free-living amoebae. Clin Microbiol Rev.17(2):413-433. 2004.

IBBA, M.; SÖLL, D. Aminoacyl tRNA: setting the limits of the genetic code. Genes Dev, v.18, n.7, p. 731–738, 2004. doi: 10.1101/gad.1187404.

Internacional Commitee On Taxonomy Of Viruses (ICTV). Master Species List 2017. Disponível em <http://www.ictvonline.org>.

KESSIN, RH. Evolutionary biology. Cooperation can be dangerous. Nature. 408(6815):917, 919. 2000.

KLOSE, T.; KUZNETSOV, Y.G.; XIAO, C.; SUN, S.; MCPHERSON, A.; ROSSMANN, M.G. The Three-Dimensional Structure of Mimivírus. Intervirology, Suíça, v. 53, n. 5, p. 268-73, 2010.

KOONIN, E.V.; YUTIN, N. Origin and evolution of eukaryotic large nucleo-cytoplasmic DNA viruses. Intervirology, Suíça, v. 53, p. 284–92, 2010.

KRZYWINSKI, M.I.; SCHEIN, J.E.; BIROL,I.; CONNORS, J.; GASCOYNE, R.; HORSMAN, D.; JONES, S.J.; MARRA, M.A. Circos: An information aesthetic for comparative genomics. Genome Res. 2009. doi:10.1101/gr.092759.109

KUMAR, S.; STECHER, G.; TAMURA, K. MEGA7: Molecular Evolutionary Genetics Analysis Version 7.0 for Bigger Datasets. Mol Biol Evol. 33(7):1870-4. 216. doi: 10.1093/molbev/msw054. Epub 2016 Mar 22.

KUZNETSOV, Y.G.; KLOSE, T.; ROSSMANN, M.; MCPHERSON, A. Morphogenesis of mimivírus and its viral factories: an atomic force microscopy study of infected cells. Journal of virology, E.U.A., v. 87, n. 20, p. 11200-13, 2013.

LA SCOLA, B.; AUDIC, S.; ROBERT, C.; JUNGANG, L.; DE LAMBALLERIE, X.; DRANCOURT, M.; BIRTLES, R.; CLAVERIE, J.M.; RAOULT, D. A giant virus in amoebae. Science, E.U.A., v. 299, n. 5615, p. 2033, 2003.

LA SCOLA, B.; CAMPOCASSO, A.; N'DONG, R.; FOURNOUS, G.; BARRASSI, L.; FLAUDROPS, C.; RAOULT, D. Tentative characterization of new environmental giant viruses by MALDI-TOF mass spectrometry. Intervirology, Suíça, v. 53, n. 5, p. 344-53, 2010.

LA SCOLA, B.; DESNUES, C.; PAGNIER, I.; ROBERT, C.; BARRASSI, L.; FOURNOUS, G.; MERCHAT, M.; SUZAN-MONTI, M.; FORTERRE, P.; KOONIN, E.; RAOULT, D. The virophage as a unique parasite of the giant mimivírus. Nature, Inglaterra, v. 455, n. 7209, p. 100-4, 2008.

LA SCOLA, B.; MARRIE, T.J.; AUFFRAY, J.P.; RAOULT, D. Mimivírus in pneumonia patients. Emerging infectious diseases, E.U.A., v. 11, n. 3, p. 449–52. 2005.

LAGIER, J. C.; ARMOUGOM, F.; MILLION, M.; HUGON, P.; PAGNIER, I.; ROBERT, C.; BITTAR, F.; FOURNOUS, G.; GIMENEZ, G.; MARANINCHI, M.; TRAPE, J.F.; KOONIN, E.V.; LA SCOLA, B.; RAOULT, D. Microbial culturomics: paradigm shift in the human gut microbiome study. Clin. Microbiol. Infect, v. 18, n.12, p. 1185–1193, 2012. doi:10.1111/1469-0691.12023.

LASLETT, D.; CANBACK, B. ARAGORN, a program to detect tRNA genes and tmRNA genes in nucleotide sequences. Nucleic Acids Research. 32 (1). 2004. DOI: 10.1093/nar/gkh152

LEGENDRE, M.; AUDIC, S.; POIROT, O.; HINGAMP, P.; SELTZER, V.; BYRNE, D.; LARTIGUE, A.; LESCOT, M.; BERNADAC, A.; POULAIN, J.; ABERGEL, C.; CLAVERIE, J.M. mRNA deep sequencing reveals 75 new genes and a complex transcriptional landscape in Mimivírus. Genome Research, E.U.A., v. 20, n.5, p. 664-74, 2010.

LEGENDRE, M.; BARTOLI, J.; SHMAKOVA, L.; JEUDY, S.; LABADIE, K.; ADRAIT, A.; LESCOT, M.; POIROT, O.; BERTAUX, L.; BRULEY, C.; COUTÉ, Y.; RIVKINA, E.; ABERGEL, C.; CLAVERIE, J.M. Thirty-thousand-year-old distant relative of giant icosahedral DNA viruses with a pandoravirus morphology. PNAS, E.U.A, v.111, n.11, p. 4274-9, 2014. doi: 10.1073/pnas.1320670111.

LEGENDRE, M.; LARTIGUE, A.; BERTAUX, L.; JEUDY, S.; BARTOLI, J.; LESCOT, M.; ALEMPIC, J.M.; RAMUS, C.; BRULEY, C.; LABADIE, K.; SHMAKOVA,

L.; RIVKINA, E.; COUTÉ, Y.; ABERGEL, C.; CLAVERIE, J.M. In-depth study of Mollivirus sibericum, a new 30,000-y-old giant virus infecting Acanthamoeba. PNAS, E.U.A, v.112, n.38:E5327-35. doi: 10.1073/pnas. 2015.

LEGENDRE, M.; SANTINI, S.; RICO, A.; ABERGEL, C.; CLAVERIE, J.M. Breaking the 1000-gene barrier for Mimivírus using ultra-deep genome and transcriptome sequencing. Virol J., 2011. doi: 10.1186/1743-422X-8-99.

LEVASSEUR, A.; ANDREANI, J.; DELERCE, J.; BOU KHALIL, J.; ROBERT, C.; LA SCOLA, B.; RAOULT, D. Comparison of a Modern and Fossil Pithovirus Reveals Its Genetic Conservation and Evolution. Genome Biol Evol. v.8(8), p.2333-9. 2016. doi: 10.1093/gbe/evw153.

LUTHER, K.B.; HÜLSMEIER, A.J.; SCHEGG, B.; DEUBER, S.A.; RAOULT, D.; HENNET, T. Mimivírus collagen is modified by bifunctional lysyl hydroxylase and glycosyltransferase enzyme. The Journal of biological chemistry, E.U.A., v. 286, n. 51, p.43701-9, 2011.

MARTY, M.; LEMAITRE, M.; KÉMOUN, P.; MORRIER, J.J.; MONSARRAT, P. Trichomonas tenax and periodontal diseases: a concise review. Parasitology. 144(11):1417-1425. doi:10.1017/S0031182017000701. 2017.

MERHEJ, V.; RAOULT, D. Rickettsial evolution in the light of comparative genomics. Biol Rev Camb Philos Soc. 86, 379-405. 2011.

MOREIRA, D.; BROCHIER-ARMANET, C. Giant viruses, giant chimeras: the multiple evolutionary histories of mimivírus genes. BMC Evolutionary Biology, Inglaterra, v. 8, n. 12, p. 01-10, 2008.

MOREIRA, D.; LÓPEZ-GARCÍA, P. Comment on "The 1.2-megabase genome sequence of Mimivírus". Science v.308. p.5725. 2015.

MURPHY, F.A.; WHITFIELD, S.G. Morphology and morphogenesis of arenaviruses. Bull World Health Organ, v.52, n4-6, p.409-19, 1975.

MUTSAFI, Y.; ZAUBERMAN, N.; SABANAY, I.; MINSKY, A. Vaccinia-like cytoplasmic replication of the giant Mimivírus. PNAS, E.U.A., v. 107, n. 13, p.5978–82, 2010.

NEIDHARDT, F. C.; PARKER, J.; MCKEEVER, W. G. Function and regulation of aminoacyl tRNA synthetases in prokaryotic and eukaryotic cells. Annu. Rev. Microbiol, v.29, p. 215-50, 1975. doi: 10.1146/annurev.mi.29.100175. 001243.

NUNES, A.; GOMES, J.P. Evolution, phylogeny, and molecular epidemiology of Chlamydia. Infect Genet Evol. 23, 49-64. 2014.

PAGNIER, I.; RETENO, D.G.; SAADI, H.; BOUGHALMI, M.; GAIA, M.; SLIMANI, M.; NGOUNGA, T.; BEKLIZ, M.; COLSON, P.; RAOULT, D.; LA SCOLA, B. A Decade of improvements in *Mimiviridae* and *Marseilleviridae* isolation from amoeba. Intervirology, Suíça, v.56, n. 6, p. 354-63, 2013.

PHILIPPE, N.; LEGENDRE, M.; DOUTRE, G.; COUTÉ, Y.; POIROT, O.; LESCOT, M.; ARSLAN, D.; SELTZER, V.; BERTAUX, L.; BRULEY, C.; GARIN, J.; CLAVERIE, J.M.; ABERGEL, C. Pandoraviruses: amoeba viruses with genomes up to 2.5 Mb reaching that of parasitic eukaryotes. Science, E.U.A., v. 341, n. 6143, p. 281-6, 2013.

PIACENTE, F.; MARIN, M.; MOLINARO, A.; DE CASTRO, C.; SELTZER, V.; SALIS, A.; DAMONTE, G.; BERNARDI, C.; CLAVERIE, J.M.; ABERGEL, C.; TONETTI, M. Giant DNA virus mimivírus encodes pathway for biosynthesis of unusual sugar 4-amino-4,6-dideoxy-D-glucose (Viosamine). The Journal of biological chemistry, E.U.A., v. 287, n. 5, p. 3009-18, 2012.

POPGEORGIEV, N.; BOYER, M.; FANCELLO, L.; MONTEIL, S.; ROBERT, C.; RIVET, R.; NAPPEZ, C.; AZZA, S.; CHIARONI, J.; RAOULT, D.; DESNUES, C. Giant blood Marseillevirus recovered from asymptomatic blood donors. The Journal of infectious diseases, E.U.A., v. 208, n. 7, p. 1042-50, 2013.

PUTZER, H.; LAALAMI, S. Regulation of the Expression of Aminoacyl tRNA Synthetases and Translation Factors. In: Madame Curie Bioscience Database [Internet]. Austin, TX: Landes Bioscience, 2000. Disponível em: http://www.ncbi.nlm.nih.gov/books/NBK6026.

RAOULT, D. The journey from Rickettsia to Mimivírus. ASM News, E.U.A., v. 71, n. 6, p. 278-84. 2005.

RAOULT, D. TRUC or the need for a new microbial classification. Intervirology., v.56, n.6, p.349-53, 2013. doi: 10.1159/000354269.

RAOULT, D.; AUDIC, S.; ROBERT, C.; ABERGEL, C.; RENESTO, P.; OGATA, H.; LA SCOLA, B.; SUZAN, M.; CLAVERIE, J.M. The 1.2-megabase genome sequence of Mimivírus. Science, E.U.A., v. 306, n. 5700, p. 1344-50, 2004.

RAOULT, D.; BOYER, M. Amoebae as genitors and reservoirs of giant viruses. Intervirology, Suíça, v. 53, n. 5, p. 321-29, 2010.

RAOULT, D.; FORTERRE, P. Redefining viruses: lessons from Mimivírus. Nat Rev Microbiol, v.6, n.4:315-9, 2008. doi: 10.1038/nrmicro1858.

RAOULT, D.; LA SCOLA, B.; BIRTLES, R. The discovery and characterization of Mimivírus the largest known virus and putative pneumonia agent. Clinical infectious diseases, E.U.A., v. 45, n. 1, p. 5-102, 2007.

REED, L.J.; MUENCH, H. A simple method of estimating fifty per cent end points. American journal of epidemiology, E.U.A., v. 27, p. 493–97, 1938.

RETENO, D.G.; BENAMAR, S.; KHALIL, J.B.; ANDREANI, J.; ARMSTRONG, N.; KLOSE, T.; ROSSMANN, M.; COLSON, P.; RAOULT, D.; LA SCOLA, B. Faustovirus, an asfarvirus-related new lineage of giant viruses infecting amoebae. J Virol, v.89, n.13, p.6585-94, 2015.

RODRIGUES, R.A.; DOS SANTOS SILVA, L.K.; DORNAS, F.P.; DE OLIVEIRA, D.B.; MAGALHÃES, T.F.; SANTOS DA COSTA, A.O.; DE MACÊDO FARIAS, L.; MAGALHÃES, P.P.; BONJARDIM, C.A.; KROON, E.G.; LA SCOLA, B.; CORTINES, J.R.; ABRAHÃO, J.S. Mimivírus Fibrils Are Important for Viral Attachment to the Microbial World by a Diverse Glycoside Interaction Repertoire. J Virol., v.89, n. 23, p.11812-, 2015. doi: 10.1128/JVI.01976-15.

RUIZ-SAENZ, J.; RODAS, J.D. Viruses, virophages, and their living nature. Acta virologica. Eslováquia, v. 54, n. 2, p. 85-90, 2010.

RYCKELYNCK, M.; MASQUIDA, B.; GIEGÉ, R.; FRUGIER, M. An intricate RNA structure with two tRNA-derived motifs directs complex formation between yeast aspartyl-tRNA synthetase and its mRNA. J. Mol. Biol., v. 354, n.3, p.614–629, 2005. doi: 10.1016/j.jmb.2005.09.063.

SAADI, H.; RETENO, D.G.; COLSON, P.; AHERFI, S.; MINODIER, P.; PAGNIER, I.; RAOULT, D.; LA SCOLA, B. *Shan virus*: a new mimivírus isolated from the stool of a Tunisian patient with pneumonia. Intervirology, Suíça, v. 56, n. 6, p. 424-9, 2013.

SANTOS-SILVA, L. K.; ARANTES, T. S.; ANDRADE, K. R.; LIMA RODRIGUES, R. A.; MIRANDA BORATTO, P. V.; DE FREITAS ALMEIDA, G. M.; KROON, E. G.; LA SCOLA, B.; CLEMENTE, W. T.; SANTOS ABRAHAO, J. High positivity of mimivirus in inanimate surfaces of a hospital respiratory-isolation facility, Brazil. J Clin Virol. v. 66, p. 62-65, 2015.

SCHULZ, F.; YUTIN, N.; IVANOVA, N.N.; ORTEGA, D.R.; LEE, T.K.; VIERHEILIG, J.; DAIMS, H.; HORN, M.; WAGNER, M; JENSEN, G.J.; KYRPIDES, N.C.; KOONIN, E.V.; WOYKE, T. Giant viruses with an expanded complement of translation system components. Science. 7;356(6333):82-85. 2017. doi: 10.1126/science.aal4657.

SILVA, L.C.F.; ALMEIDA, G.M.F.; OLIVEIRA, D.B.; DORNAS, F.P.; CAMPOS, R.K.; LA SCOLA, B.; FERREIRA, P.C.P.; KROON, E.G.; ABRAHÃO, J.S. A resourceful giant: APMV is able to interfere with the human type I interferon system. Microbes and Infections. v.16, n. 3, p. 187-195, 2013.

SILVA, M.A.; ROSA, J.A. Isolation of potencially pathogenic free-living amoebas in hospital dust. Rev Saúde Pública. 37(2):242-246. 2003.

SMITH, J.E. The ecology and evolution of microsporidian parasites. Parasitology. 136, 1901-14. 2009.

SÖDERBOM, F; LOOMIS, W.F. Cell-cell signaling during Dictyostelium development. Trends Microbiol. (10):402-6. 1998.

SOROKIN, D.Y.; BERBEN T.; MELTON, E.D.; OVERMARS, L.; VAVOURAKIS, C.D.; MUYZER, G. Microbial diversity and biogeochemical cycling in soda lakes. Extremophiles. 18, 791-809. 2014.

SUHRE, K. Gene and genome duplication in *Acanthamoeba polyphaga mimivirus.* Journal of Virology, E.U.A., v. 79, n. 22, p.14095–101, 2005.

SUHRE, K.; AUDIC, S.; CLAVERIE, J.M. Mimivírus gene promoters exhibit an unprecedented conservation among all eukaryotes. PNAS, E.U.A., v. 102, n. 41, p. 14689-93, 2005.

SUZAN-MONTI, M.; LA SCOLA, B.; BARRASSI, L.; ESPINOSA, L.; RAOULT, D. Ultrastructural characterization of the giant volcano-like virus factory of *Acanthamoeba polyphaga mimivirus*. PLoS One, E.U.A., v. 2, n. 3, p. 01-11, 2007.

TAKEMURA, M. Draft Genome Sequence of Tokyovirus, a Member of the Family Marseilleviridae Isolated from the Arakawa River of Tokyo, Japan. Genome Announc, v.9, n.4, 2016. pii: e00429-16. doi: 10.1128/genomeA.00429-16.

WALSH, D.; MOHR, I. Viral subversion of the host protein synthesis machinery. Nat. Rev. Microbiol, v. 9, n. 12, p. 860–875, 2011. doi: 10.1038/nrmicro2655.

WILLIAMS, T,A.; EMBLEY, T.M.; HEINZ,E. Informational Gene Phylogenies Do Not Support a Fourth Domain of Life for Nucleocytoplasmic Large DNA Viruses. PNAS, E.U.A., v.6, n. 6, p. 01-11, 2011.

WOESE, C.R.; KANDLER, O.; WHEELIS, M.L. Towards a natural system of organisms: proposal for the domains Archaea, Bacteria, and Eucarya. PNAS, v.87, n.12, p.4576-9, 1990.

XIAO, C.; KUZNETSOV, Y.G.; SUN, S.; HAFENSTEIN, S.L.; KOSTYUCHENKO, V.A.; CHIPMAN, P.R.; SUZAN-MONTI, M.; RAOULT, D.; MCPHERSON, A.; ROSSMANN, M.G. Structural studies of the giant Mimivírus. PLoS Biology, E.U.A., v. 7, n. 4, p. 958-66, 2009.

YUTIN, N.; WOLF, Y.I.; KOONIN, E.V. Origin of giant viruses from smaller DNA viruses not from a fourth domain of cellular life. Virology. v.466, p.38-52. 2014. doi: 10.1016/j.virol.2014.06.032.

YUTIN, N.; WOLF, Y.I.; RAOULT, D.; KOONIN, E.V. Eukaryotic large nucleo-cytoplasmic DNA viruses: clusters of orthologous genes and reconstruction of viral genome evolution. Virology Journal, Inglaterra, v. 6, n. 223, p. 01-13, 2009.

ZAUBERMAN, N.; MUTSAFI, Y.; HALEVY, D.B.; SHIMONI, E.; KLEIN, E.; XIAO, C.; SUN, S.; MINSKY, A. Distinct DNA exit and packaging portals in the virus Acanthamoeba polyphaga mimivirus. PLoS Biol, v.13, n. 6, 2008. e114. doi: 10.1371/journal.pbio.0060114.

ANEXOS

Anexo 1 – Receita PYG

O meio de cultura extrato peptona glicose (PYG) é o meio utilizado para o cultivo das amebas de vida livre. Para preparar 1000 ml de meio PYG, inicialmente, em um béquer com 300 mL de água é acrescentado 8 μM de sulfato de magnésio heptahidratado ($MgSO_4.7H_2O$) (Merck, Alemanha); 0,5 μM de cloreto de cálcio ($CaCl_2$) (Merck, Alemanha); 5 nM de sulfato de ferro amoniacal hexahidratado ($Fe(NH_4)_2(SO_4).6H_2O$) (Merck, Alemanha); 1,4 mM de fosfato dibásico de sódio heptahidratado ($Na_2HPO_4.7H_2O$) (Merck, Alemanha); 2,5 mM de fosfato monobásico de potássio (KH_2PO_4) (Merck, Alemanha); 3,4 mM de citrato de sódio dihidratado ($C_6H_5Na_3O_7.2H_2O$) (Merck, Alemanha) e misturado em agitador magnético até a completa solubilização. Em outro béquer com 200ml de água, são acrescentado 20g de protease peptona (extrato bactopeptona) (Merck, Alemanha) e também agitado até se solubilizar. Em um terceiro béquer com 200 mL de água são solubilizados 9,0g de glicose (Merck, Alemanha). Posteriormente, as três soluções são misturadas em um único béquer e completadas com água destilada quantidade suficiente para 1 litro de meio. O pH deve ser ajustado em 6,5 e o meio deve ser aliquotado, autoclavado e filtrado. Após, ao meio de cultura PYG, no momento de uso, é adicionado 7% de SFB, antibióticos e antifúngico. O PYG suplementado é mantido em câmara fria até o momento de uso. Como controle, uma alíquota do meio deve ser incubada a 37ºC para verificar se o mesmo está contaminado; além disso, outra alíquota deve ser incubada em meio tioglicolato para verificação de crescimento de microorganismos.

Anexo 2 – Receita PAS

A solução salina para amebas é a solução utilizada para o cultivo das amebas de vida livre, além de ser usada em experimentos para que não haja intensa multiplicação das amebas, visto que é um mais meio pobre. Para preparar 1000 ml desta solução, inicialmente, preparam-se duas soluções chamadas de solução A e solução B. Para a solução A, adiciona-se as seguintes substâncias em 10 ml de água estéril: 0,16 µM sulfato de magnésio heptahidratado ($MgSO_4.7H_2O$) (Merck, Alemanha); 0,1 mM de fosfato dibásico de sódio (Na_2HPO_4) (Merck, Alemanha); 0,1 mM de fosfato monobásico de potássio (KH_2PO_4) (Merck, Alemanha); NaCl (2mM); Na_2HPO_4 (0,0001 mM). Para o preparo da solução B, adiciona-se 0,272 µM de cloreto de cálcio ($CaCl_2.2H_2O$) (Merck, Alemanha). As soluções A e B são filtradas em filtro de 0,22 µm a fim de deixar a solução final estéril e também eliminar possíveis cristais formados durante o preparo e posteriormente adicionadas a um volume final de 1 litro de água. Esta solução é mantida em câmara fria até o momento de uso. Como controle, uma alíquota da solução preparada deve ser incubada a 37ºC para verificar se a mesma está contaminada; além disso, outra alíquota é incubada em meio tioglicolato para verificação de crescimento de microorganismos.

Anexo 3 – Receita TS

A solução TS para amebas é a solução utilizada para o cultivo das amebas *V. vermiformis*, além de ser usada em experimentos de titulação para que não haja intensa multiplicação das amebas durante o período de observação. Para preparar 1000 ml desta solução, pesa-se 18g de glicose, 2g de extrato de levedura e 0,02 g de ferro amoniacal hexahidratado ($Fe(NH_4)_2(SO_4).6H_2O$) e adiciona-se sobre uma 1 L de solução de PAS. A solução é mantida em agitador magnético até completa solubilização e após é filtrada em filtro de 0,22 µm a fim de deixar a solução final estéril e também eliminar possíveis cristais formados durante o preparo. Esta solução é mantida em câmara fria até o momento de uso. Como controle, uma alíquota da solução preparada deve ser incubada a 37ºC para verificar se a mesma está contaminada; além disso, outra alíquota é incubada em meio tioglicolato para verificação de crescimento de microorganismos.

Anexo 4 – Tabela de códons e siglas de aminoácidos.

Código	Códon	Aminoácido
F	TTT	Fenilalanina
	TTC	
L	TTA	Leucina
	TTG	
	CTT	
	CTC	
	CTA	
	CTG	
I	ATT	Isoleucina
	ATC	
	ATA	
M	ATG	Metionina
V	GTT	Valina
	GTC	
	GTA	
	GTG	
S	TCT	Serina
	TCC	
	TCA	
	AGT	
	AGC	
	TCG	
P	CCT	Prolina
	CCC	
	CCA	
	CCG	
T	ACT	Treonina
	ACC	
	ACA	
	ACG	

A	GCT GCC GCA GCG	Alanina
Y	TAT TAC	Tirosina
H	CAT CAC	Histidina
Q	CAA CAG	Glutamina
N	AAT AAC	Asparagina
K	AAA AAG	Lisina
D	GAT GAC	Aspartina
E	GAA GAG	Glutamato
C	TGT TGC	Cisteína
W	TGG	Triptofano
R	CGT CGC CGA CGG AGA AGG	Arginina
G	GGT GGC GGA GGG	Glicina
Códon de terminação	TAA TAG	

TGA

Anexo 5 – Tabela de anticódons para os tRNA de Tupanvirus deep ocean.

tRNA - anticódons
Acido Glutaminil tRNA ctc
Acido Glutaminil tRNA tcc
Acido Glutaminil tRNA ttc x3
Alanil tRNA agc
Alanil tRNA CGC
Alanil tRNA tgc
Arginil tRNA acg
Arginil tRNA cct
Arginil tRNA gcg
Arginil tRNA tcg
Arginil tRNA tct
Asparaginil tRNA gtt x 3
Asparatil tRNA gtc x3
Cisteinil tRNA gca x2
Fenilalanil tRNA gaa
Glicil tRNA gcc
Glutamil tRNA ctg
Glutamil tRNA ttg x 4
Histidil tRNA gtg
Isoleucinil tRNA gat x2
Isoleucinil tRNA tat
Leucinil tRNA caa x2
Leucinil tRNA cag x2
Leucinil tRNA gag
Leucinil tRNA taa x2
Leucinil tRNA tag
Lisinil tRNA ctt
Lisinil tRNA ttt x2
Metionil tRNA cat

Prolinil tRNA agg
Prolinil tRNA cgg
Prolinil tRNA tgg
Serinil tRNA act
Serinil tRNA aga
Serinil tRNA cga
Serinil tRNA gct
Serinil tRNA gga
Serinil tRNA tga
Tirosinil tRNA gta x2
Treonil tRNA agt
Treonil tRNA cgt
Treonil tRNA tgt
Triptofanil tRNA cca x2
tRNA-?(Arg|Pyl)(ct)
Valinil tRNA aac
Valinil tRNA cac
Valinil tRNA gac
Valinil tRNA tac

Anexo 6 - Árvores filogenéticas para as aaRS presentes em tupanvírus. (A) Alanil-RS, (B) Arginil-RS, (C) Asparaginil-RS, (D) Aspartil-RS, (E) Cisteinil-RS, (F) Fenilalanil-RS, (G) Glicil-RS, (H) Glutamato/prolil-RS, (I) Glutaminil-RS, (J) Histidil-RS, (K) Isoleucinil-RS, (L) Leucil-RS, (M) Lisil-RS, (N) Metionil-RS, (O) Prolil-RS, (P) Seril-RS, (Q) Tirosinil-RS, (R) Treonil-RS, (S) Triptofanil-RS, (T) Valinil-RS

A

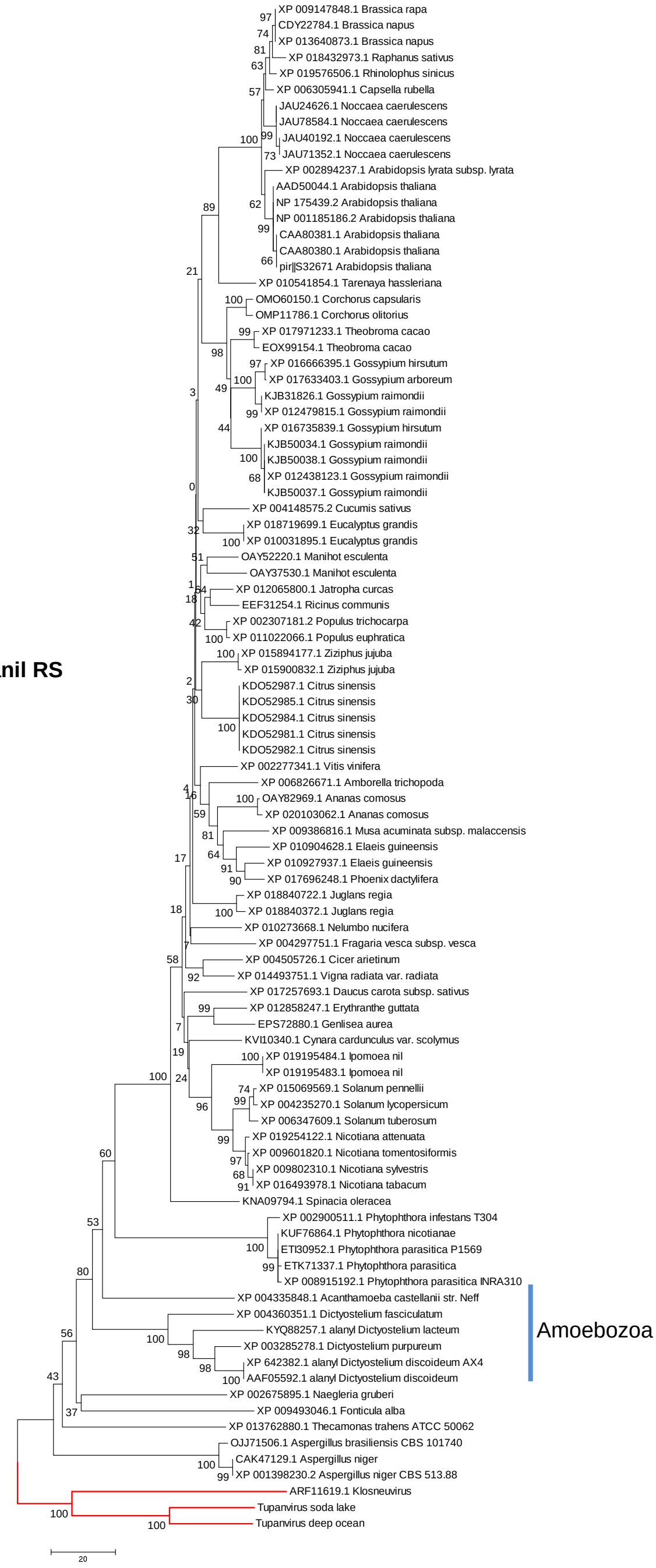

B

Arginil RS

XP014951663.1 Ovis aries
XP005683435.1 Capra hircus
XP011968917.1 Ovis aries musimon
XP005959447.1 Pantholops hodgsonii
NP001098808.1 Bos taurus
XP005904597.1 Bos mutus
XP019820926.1 Bos indicus
XP006065155.1 Bubalus bubalis
XP007110095.1 Physeter catodon
XP019801148.1 Tursiops truncatus
XP004272023.1 Orcinus orca
XP007447884.1 Lipotes vexillifer
XP007520916.1 Erinaceus europaeus
XP007077700.1 Panthera tigris altaica
XP019305791.1 Panthera pardus
XP003981378.1 Felis catus
XP014921252.1 Acinonyx jubatus
XP004679251.1 Condylura cristata
XP008053026.1 Carlito syrichta
XP003404695.1 Loxodonta africana
XP853102.1 Canis lupus familiaris
XP016006921.1 Rousettus aegyptiacus
XP006906557.1 Pteropus alecto
XP002918656.1 Ailuropoda melanoleuca
EFB14579.1 Ailuropoda melanoleuca
XP008690622.1 Ursus maritimus
XP004737703.1 Mustela putorius furo
XP006742620.1 Leptonychotes weddellii
XP004392087.1 Odobenus rosmarus divergens
XP017505806.1 Manis javanica
XP015426756.1 Myotis davidii
XP006775019.1 Myotis davidii
XP014398678.1 Myotis brandtii
EPQ10412.1 Myotis brandtii
XP014322894.1 Myotis lucifugus
XP008145858.1 Eptesicus fuscus
XP016069501.1 Miniopterus natalensis
JAV43957.1 Castor canadensis
XP004428605.1 Ceratotherium simum simum
XP004371278.1 Trichechus manatus latirostris
XP007937933.1 Orycteropus afer afer
XP003473233.1 Cavia porcellus
XP008570623.1 Galeopterus variegatus
XP006864899.1 Chrysochloris asiatica
XP006148429.1 Tupaia chinensis
XP019596507.1 Rhinolophus sinicus
XP019491524.1 Hipposideros armiger
XP004611509.1 Sorex araneus
EGV96305.1 Cricetulus griseus
XP003782010.1 Otolemur garnettii
XP010224350.1 Tinamus guttatus
XP013809153.1 Apteryx australis mantelli
XP013919571.1 Thamnophis sirtalis
XP015205528.1 Lepisosteus oculatus
XP006632005.1 Lepisosteus oculatus
XP010732880.2 Larimichthys crocea
XP017208243.1 Danio rerio
AAH83505.1 Danio rerio
XP012989983.1 Esox lucius
XP015817343.1 Nothobranchius furzeri
XP013859525.1 Austrofundulus limnaeus
XP017288225.1 Kryptolebias marmoratus
XP012728864.1 Fundulus heteroclitus
XP014868768.1 Poecilia mexicana
XP014916107.1 Poecilia latipinna
XP008426663.1 Poecilia reticulata
XP004085032.1 Oryzias latipes
XP008331579.1 Cynoglossus semilaevis
XP019964870.1 Paralichthys olivaceus
XP012673798.1 Clupea harengus
XP019725305.1 Hippocampus comes
XP008292304.1 Stegastes partitus
XP018535176.1 Lates calcarifer
XP004556889.1 Maylandia zebra
XP005472371.1 Oreochromis niloticus
XP003454001.1 Oreochromis niloticus
XP001632819.1 Nematostella vectensis
ERL94414.1 Dendroctonus ponderosae
XP017768556.1 Nicrophorus vespilloides
WP 067764355.1 Nostoc sp. NIES-3756
WP 012410352.1 Nostoc punctiforme
WP 006634878.1 Microcoleus vaginatus
WP 015176954.1 Oscillatoria nigro-viridis
WP 026222219.1 filamentous cyanobacterium ESFC-1
WP 017659013.1 Geitlerinema sp. PCC 7105
ABB57607.1 Synechococcus elongatus PCC 7942
WP 044304441.1 Richelia intracellularis
CRX38999.1 Estrella lausannensis
XP 012758544.1 Acytostelium subglobosum LB1
XP 020434534.1 Polysphondylium pallidum PN500
XP 003286138.1 Dictyostelium purpureum
KYQ91087.1 Dictyostelium lacteum
ANV79811.1 Candidatus Thalassoarchaea euryarchaeote
OIO40330.1 Candidatus Pacearchaeota archaeon CG1 02 31 27
XP 651552.1 Entamoeba histolytica HM-1:IMSS
XP 008856275.1 Entamoeba nuttalli P19
XP 001733845.1 Entamoeba dispar SAW760
XP 012752677.1 Acytostelium subglobosum LB1
XP 644926.1 Dictyostelium discoideum AX4
WP 007141601.1 Halobiforma lacisalsi
ELY62564.1 Natronobacterium gregoryi SP2
AOV94304.1 Nanohaloarchaea archaeon SG9
WP 042697884.1 Thermococcus sp. PK
WP 010878394.1 Archaeoglobus fulgidus
WP 012966459.1 Ferroglobus placidus
WP 048093472.1 Geoglobus acetivorans
ARF11619.1 Klosneuvirus
Tupanvirus soda lake
Tupan virus deep ocean
KF493711.1 Hirudo virus
KU761889.1 Bombay
KT599914.1 Niemeyer virus
KF959826.2 Samba virus
YP003987185.1 Acanthamoeba polyphaga mimivirus
JF801956.1 Mamavirus
KM982401 Oyster virus
KM982402 Kroon virus
AEX62415.1 Moumouvirus Monve
AQN68587.1 Saudi moumouvirus
YP 007354684.1 Moumovirus
AGF85004.1 Moumouvirus goulette
ANB50893.1 Powai lake megavirus
AGD92756.1 Megavirus lba
AFX92906.1 Megavirus courdo11
YP004894855.1 Megavirus chiliensis
ADX97536.1 Terra1 virus

Amoebozoa

10

C

Asparaginil RS

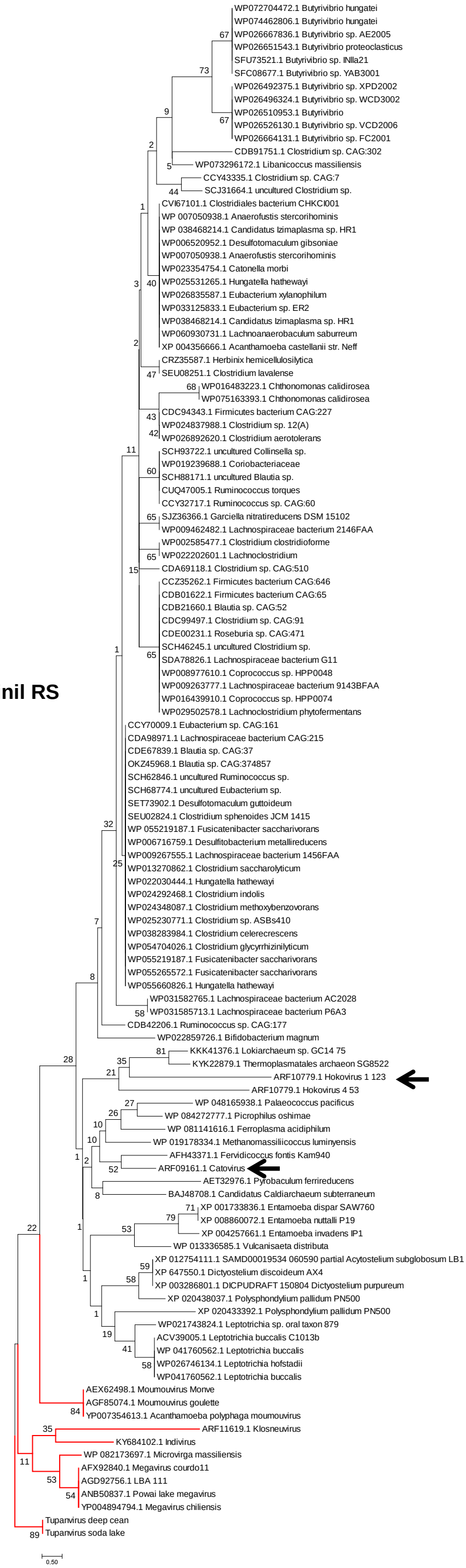

Amoebozoa and others

D

Aspartil RS

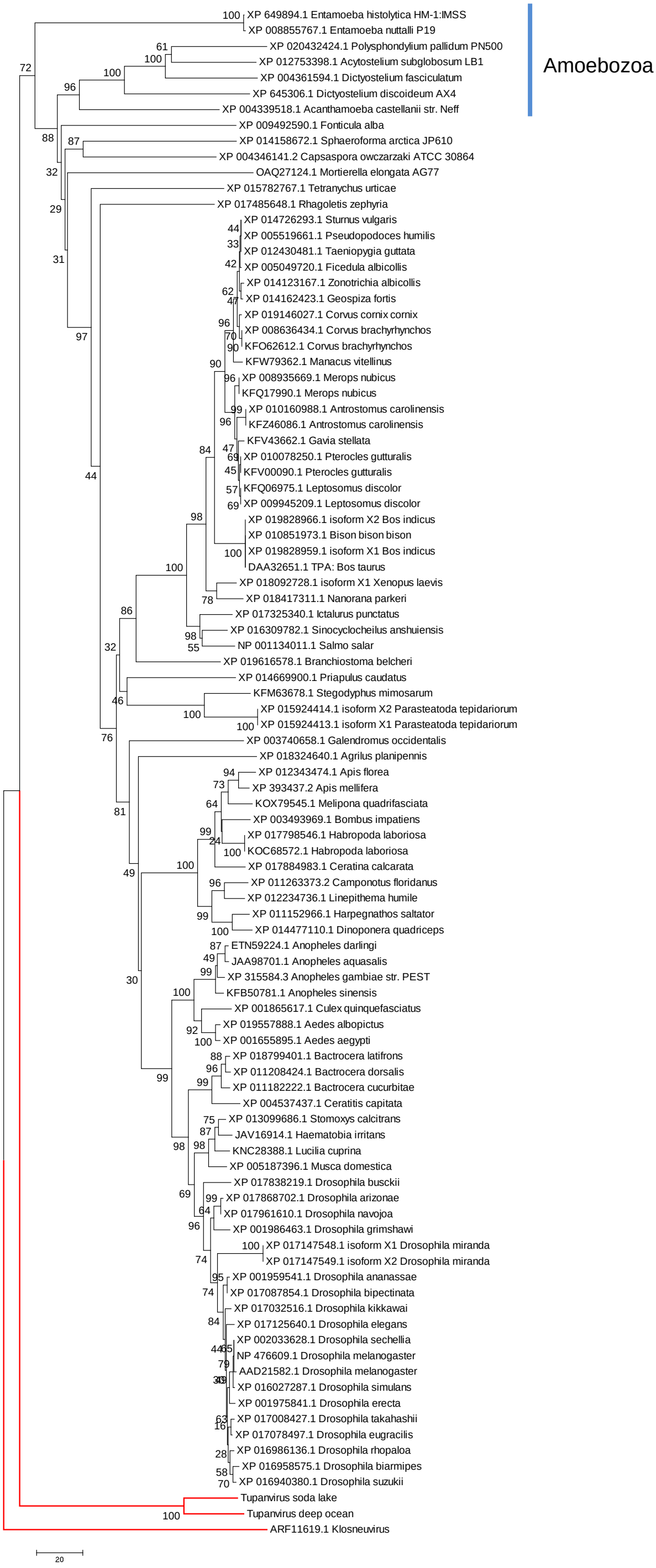

E

Cisteinil RS

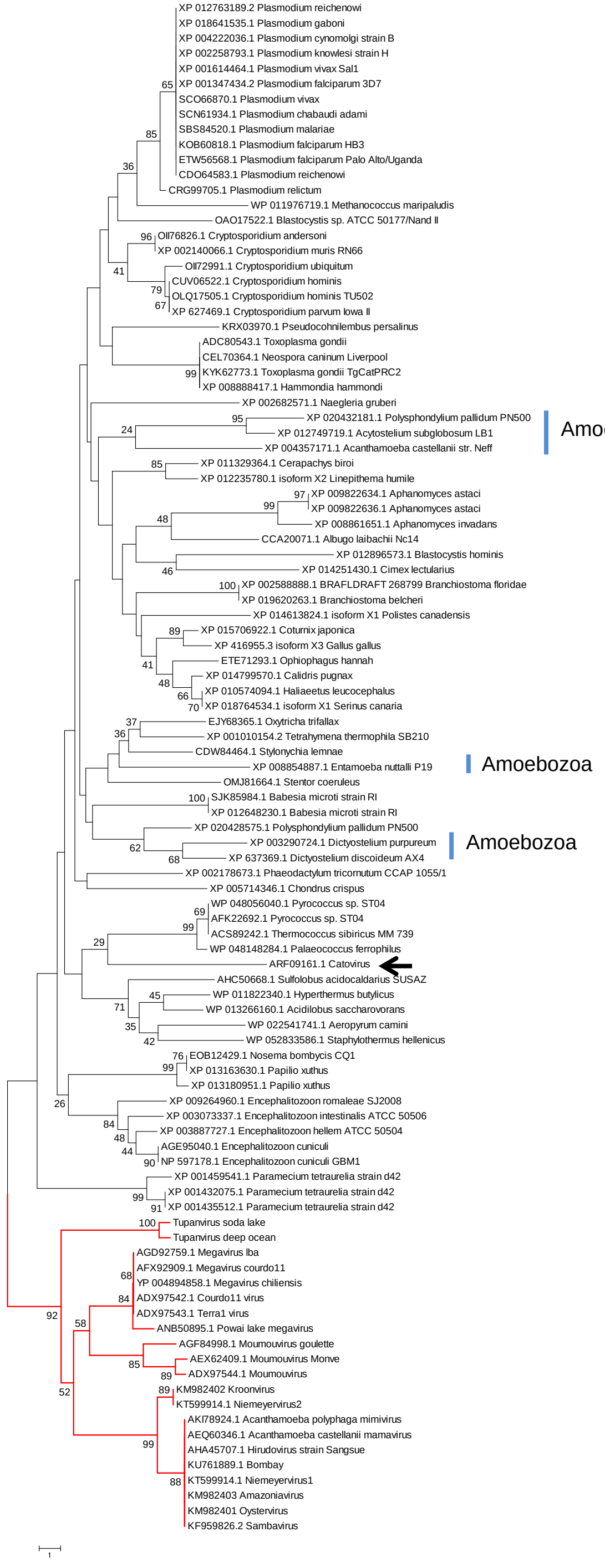

F

Fenilalanil RS

G

Glicil RS

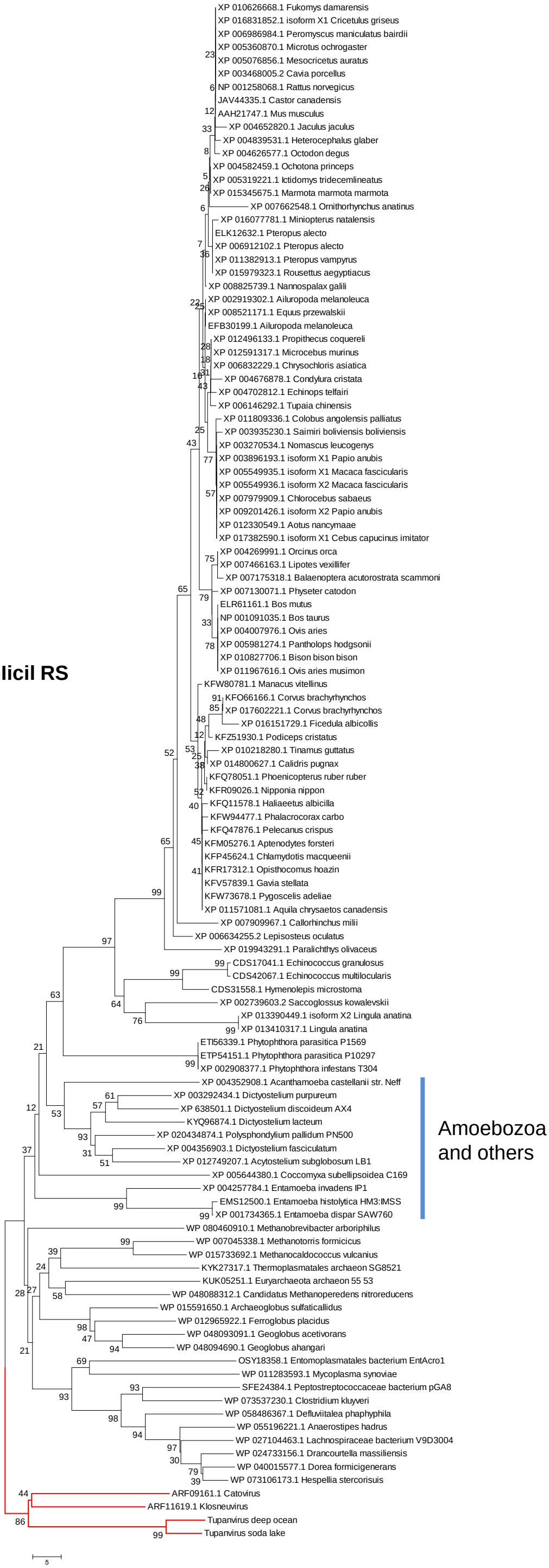
XP 010626668.1 Fukomys damarensis
XP 016831852.1 isoform X1 Cricetulus griseus
XP 006986984.1 Peromyscus maniculatus bairdii
XP 005360870.1 Microtus ochrogaster
XP 005076856.1 Mesocricetus auratus
XP 003468005.2 Cavia porcellus
NP 001258068.1 Rattus norvegicus
JAV44335.1 Castor canadensis
AAH21747.1 Mus musculus
XP 004652820.1 Jaculus jaculus
XP 004839531.1 Heterocephalus glaber
XP 004626577.1 Octodon degus
XP 004582459.1 Ochotona princeps
XP 005319221.1 Ictidomys tridecemlineatus
XP 015345675.1 Marmota marmota marmota
XP 007662548.1 Ornithorhynchus anatinus
XP 016077781.1 Miniopterus natalensis
ELK12632.1 Pteropus alecto
XP 006912102.1 Pteropus alecto
XP 011382913.1 Pteropus vampyrus
XP 015979323.1 Rousettus aegyptiacus
XP 008825739.1 Nannospalax galili
XP 002919302.1 Ailuropoda melanoleuca
XP 008521171.1 Equus przewalskii
EFB30199.1 Ailuropoda melanoleuca
XP 012496133.1 Propithecus coquereli
XP 012591317.1 Microcebus murinus
XP 006832229.1 Chrysochloris asiatica
XP 004676878.1 Condylura cristata
XP 004702812.1 Echinops telfairi
XP 006146292.1 Tupaia chinensis
XP 011809336.1 Colobus angolensis palliatus
XP 003935230.1 Saimiri boliviensis boliviensis
XP 003270534.1 Nomascus leucogenys
XP 003896193.1 isoform X1 Papio anubis
XP 005549935.1 isoform X1 Macaca fascicularis
XP 005549936.1 isoform X2 Macaca fascicularis
XP 007979909.1 Chlorocebus sabaeus
XP 009201426.1 isoform X2 Papio anubis
XP 012330549.1 Aotus nancymaae
XP 017382590.1 isoform X1 Cebus capucinus imitator
XP 004269991.1 Orcinus orca
XP 007466163.1 Lipotes vexillifer
XP 007175318.1 Balaenoptera acutorostrata scammoni
XP 007130071.1 Physeter catodon
ELR61161.1 Bos mutus
NP 001091035.1 Bos taurus
XP 004007976.1 Ovis aries
XP 005981274.1 Pantholops hodgsonii
XP 010827706.1 Bison bison bison
XP 011967616.1 Ovis aries musimon
KFW80781.1 Manacus vitellinus
KFO66166.1 Corvus brachyrhynchos
XP 017602221.1 Corvus brachyrhynchos
XP 016151729.1 Ficedula albicollis
KFZ51930.1 Podiceps cristatus
XP 010218280.1 Tinamus guttatus
XP 014800627.1 Calidris pugnax
KFQ78051.1 Phoenicopterus ruber ruber
KFR09026.1 Nipponia nippon
KFQ11578.1 Haliaeetus albicilla
KFW94477.1 Phalacrocorax carbo
KFQ47876.1 Pelecanus crispus
KFM05276.1 Aptenodytes forsteri
KFP45624.1 Chlamydotis macqueenii
KFR17312.1 Opisthocomus hoazin
KFV57839.1 Gavia stellata
KFW73678.1 Pygoscelis adeliae
XP 011571081.1 Aquila chrysaetos canadensis
XP 007909967.1 Callorhinchus milii
XP 006634255.2 Lepisosteus oculatus
XP 019943291.1 Paralichthys olivaceus
CDS17041.1 Echinococcus granulosus
CDS42067.1 Echinococcus multilocularis
CDS31558.1 Hymenolepis microstoma
XP 002739603.2 Saccoglossus kowalevskii
XP 013390449.1 isoform X2 Lingula anatina
XP 013410317.1 Lingula anatina
ETI56339.1 Phytophthora parasitica P1569
ETP54151.1 Phytophthora parasitica P10297
XP 002908377.1 Phytophthora infestans T304
XP 004352908.1 Acanthamoeba castellanii str. Neff
XP 003292434.1 Dictyostelium purpureum
XP 638501.1 Dictyostelium discoideum AX4
KYQ96874.1 Dictyostelium lacteum
XP 020434874.1 Polysphondylium pallidum PN500
XP 004356903.1 Dictyostelium fasciculatum
XP 012749207.1 Acytostelium subglobosum LB1
XP 005644380.1 Coccomyxa subellipsoidea C169
XP 004257784.1 Entamoeba invadens IP1
EMS12500.1 Entamoeba histolytica HM3:IMSS
XP 001734365.1 Entamoeba dispar SAW760
WP 080460910.1 Methanobrevibacter arboriphilus
WP 007045338.1 Methanotorris formicicus
WP 015733692.1 Methanocaldococcus vulcanius
KYK27317.1 Thermoplasmatales archaeon SG8521
KUK05251.1 Euryarchaeota archaeon 55 53
WP 048088312.1 Candidatus Methanoperedens nitroreducens
WP 015591650.1 Archaeoglobus sulfaticallidus
WP 012965922.1 Ferroglobus placidus
WP 048093091.1 Geoglobus acetivorans
WP 048094690.1 Geoglobus ahangari
OSY18358.1 Entomoplasmatales bacterium EntAcro1
WP 011283593.1 Mycoplasma synoviae
SFE24384.1 Peptostreptococcaceae bacterium pGA8
WP 073537230.1 Clostridium kluyveri
WP 058486367.1 Defluviitalea phaphyphila
WP 055196221.1 Anaerostipes hadrus
WP 027104463.1 Lachnospiraceae bacterium V9D3004
WP 024733156.1 Drancourtella massiliensis
WP 040015577.1 Dorea formicigenerans
WP 073106173.1 Hespellia stercorisuis
ARF09161.1 Catovirus
ARF11619.1 Klosneuvirus
Tupanvirus deep ocean
Tupanvirus soda lake
5
Amoebozoa and others

H

Glutamato-Prolil RS

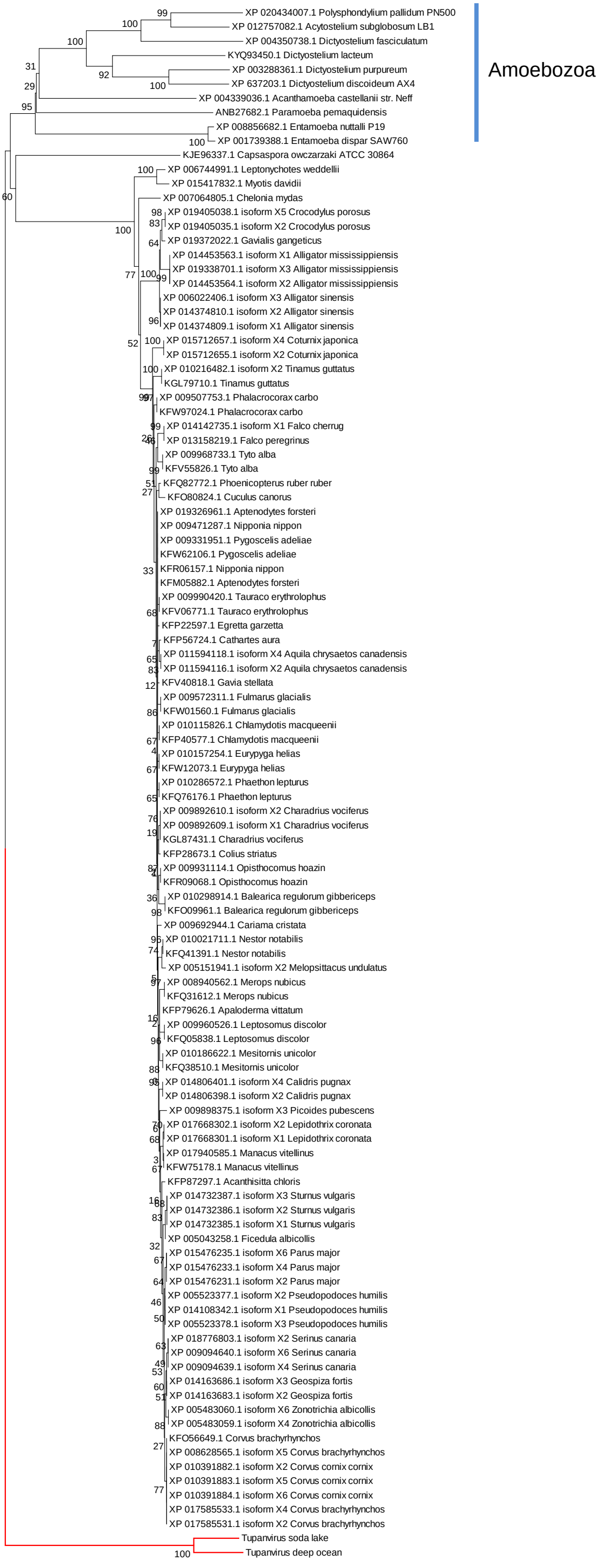

Glutaminil RS

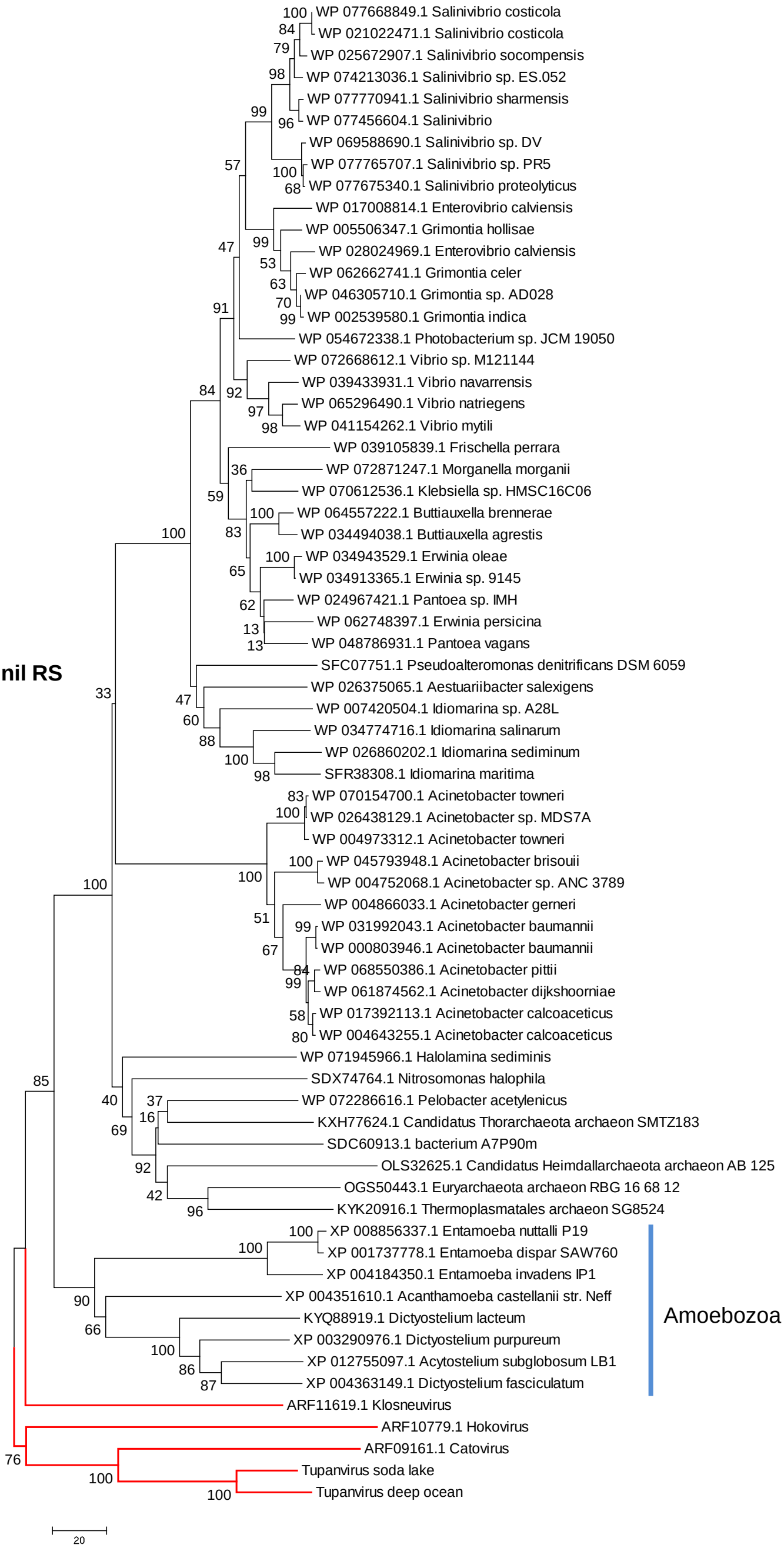

J

Histidil RS

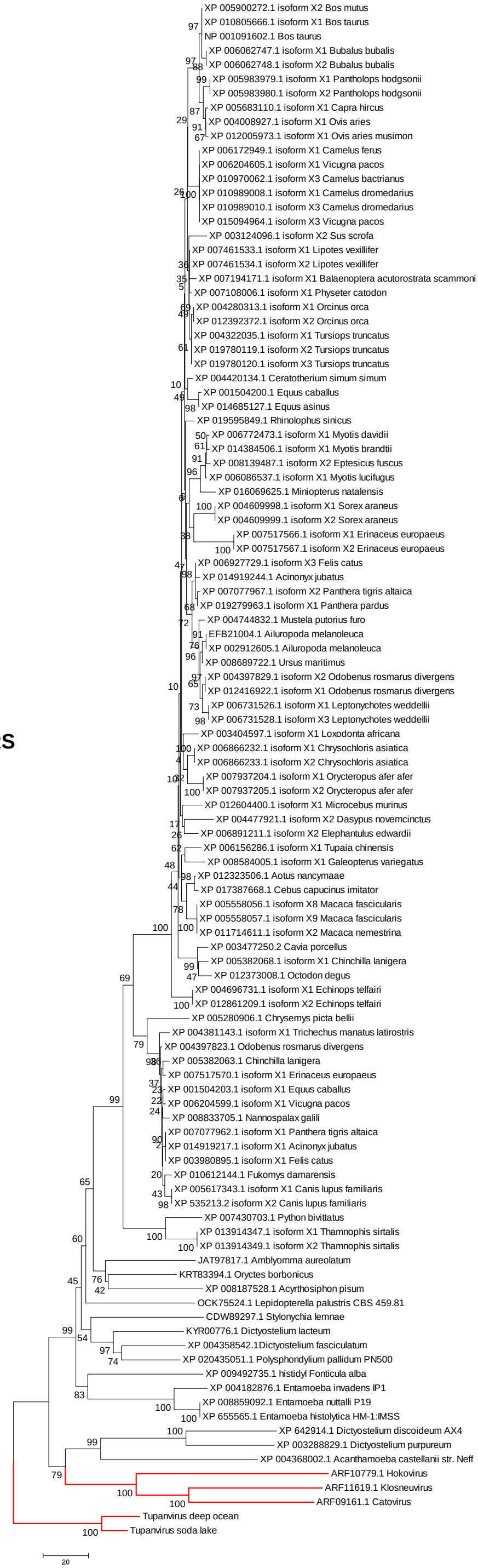

K

Isoleucil RS

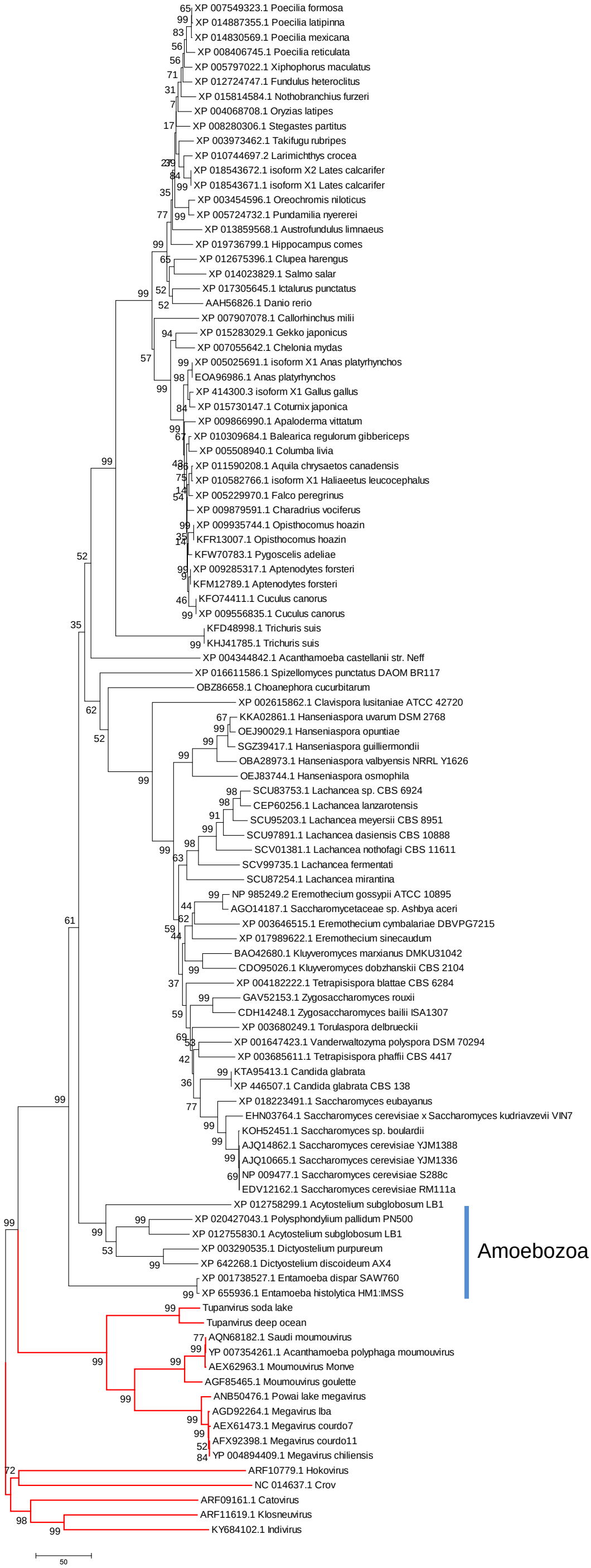

L

Leucil RS

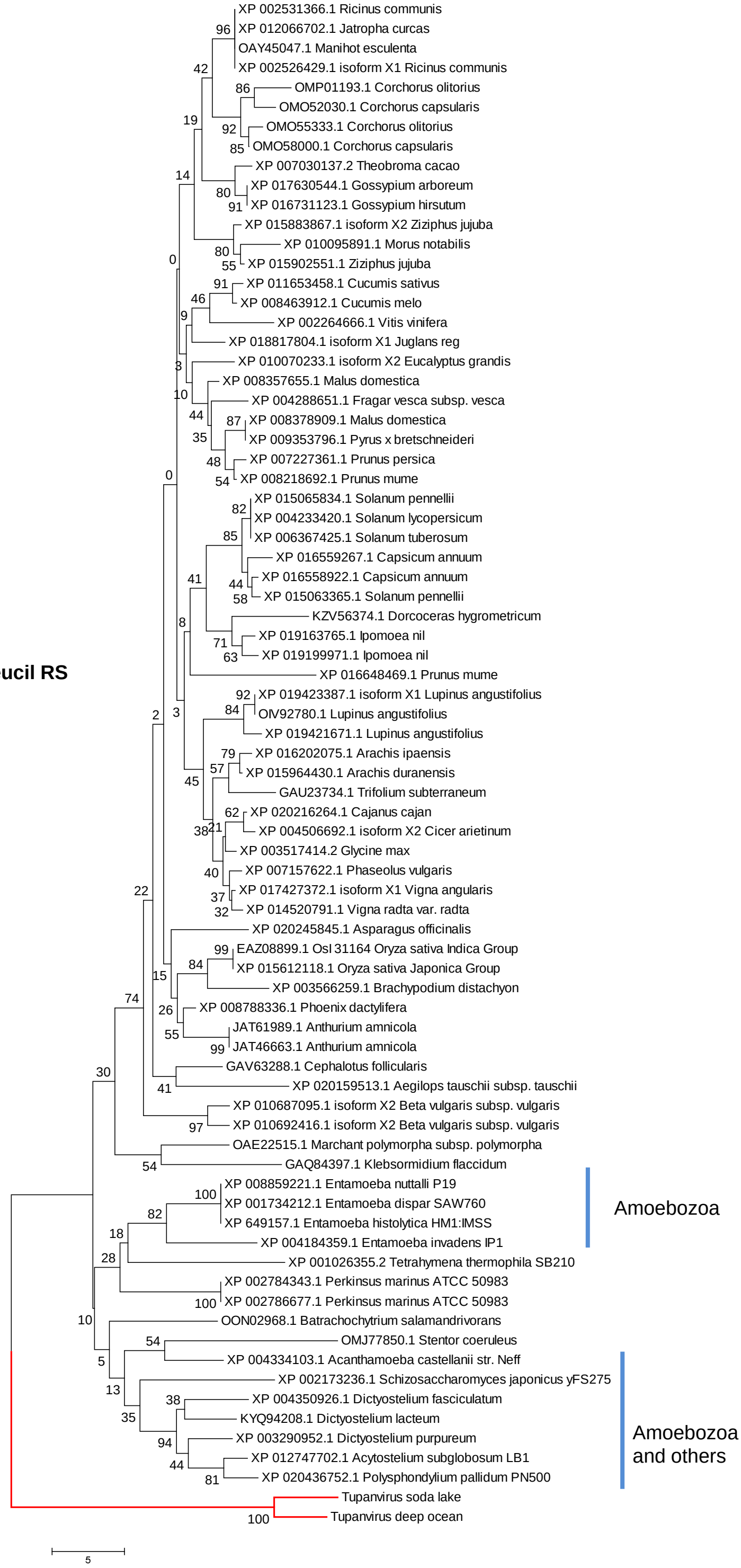
XP 002531366.1 Ricinus communis
XP 012066702.1 Jatropha curcas
OAY45047.1 Manihot esculenta
XP 002526429.1 isoform X1 Ricinus communis
OMP01193.1 Corchorus olitorius
OMO52030.1 Corchorus capsularis
OMO55333.1 Corchorus olitorius
OMO58000.1 Corchorus capsularis
XP 007030137.2 Theobroma cacao
XP 017630544.1 Gossypium arboreum
XP 016731123.1 Gossypium hirsutum
XP 015883867.1 isoform X2 Ziziphus jujuba
XP 010095891.1 Morus notabilis
XP 015902551.1 Ziziphus jujuba
XP 011653458.1 Cucumis sativus
XP 008463912.1 Cucumis melo
XP 002264666.1 Vitis vinifera
XP 018817804.1 isoform X1 Juglans reg
XP 010070233.1 isoform X2 Eucalyptus grandis
XP 008357655.1 Malus domestica
XP 004288651.1 Fragar vesca subsp. vesca
XP 008378909.1 Malus domestica
XP 009353796.1 Pyrus x bretschneideri
XP 007227361.1 Prunus persica
XP 008218692.1 Prunus mume
XP 015065834.1 Solanum pennellii
XP 004233420.1 Solanum lycopersicum
XP 006367425.1 Solanum tuberosum
XP 016559267.1 Capsicum annuum
XP 016558922.1 Capsicum annuum
XP 015063365.1 Solanum pennellii
KZV56374.1 Dorcoceras hygrometricum
XP 019163765.1 Ipomoea nil
XP 019199971.1 Ipomoea nil
XP 016648469.1 Prunus mume
XP 019423387.1 isoform X1 Lupinus angustifolius
OIV92780.1 Lupinus angustifolius
XP 019421671.1 Lupinus angustifolius
XP 016202075.1 Arachis ipaensis
XP 015964430.1 Arachis duranensis
GAU23734.1 Trifolium subterraneum
XP 020216264.1 Cajanus cajan
XP 004506692.1 isoform X2 Cicer arietinum
XP 003517414.2 Glycine max
XP 007157622.1 Phaseolus vulgaris
XP 017427372.1 isoform X1 Vigna angularis
XP 014520791.1 Vigna radta var. radta
XP 020245845.1 Asparagus officinalis
EAZ08899.1 OsI 31164 Oryza sativa Indica Group
XP 015612118.1 Oryza sativa Japonica Group
XP 003566259.1 Brachypodium distachyon
XP 008788336.1 Phoenix dactylifera
JAT61989.1 Anthurium amnicola
JAT46663.1 Anthurium amnicola
GAV63288.1 Cephalotus follicularis
XP 020159513.1 Aegilops tauschii subsp. tauschii
XP 010687095.1 isoform X2 Beta vulgaris subsp. vulgaris
XP 010692416.1 isoform X2 Beta vulgaris subsp. vulgaris
OAE22515.1 Marchant polymorpha subsp. polymorpha
GAQ84397.1 Klebsormidium flaccidum
XP 008859221.1 Entamoeba nuttalli P19
XP 001734212.1 Entamoeba dispar SAW760
XP 649157.1 Entamoeba histolytica HM1:IMSS
XP 004184359.1 Entamoeba invadens IP1
XP 001026355.2 Tetrahymena thermophila SB210
XP 002784343.1 Perkinsus marinus ATCC 50983
XP 002786677.1 Perkinsus marinus ATCC 50983
OON02968.1 Batrachochytrium salamandrivorans
OMJ77850.1 Stentor coeruleus
XP 004334103.1 Acanthamoeba castellanii str. Neff
XP 002173236.1 Schizosaccharomyces japonicus yFS275
XP 004350926.1 Dictyostelium fasciculatum
KYQ94208.1 Dictyostelium lacteum
XP 003290952.1 Dictyostelium purpureum
XP 012747702.1 Acytostelium subglobosum LB1
XP 020436752.1 Polysphondylium pallidum PN500
Tupanvirus soda lake
Tupanvirus deep ocean
Amoebozoa
Amoebozoa and others
5

M

Lisil RS

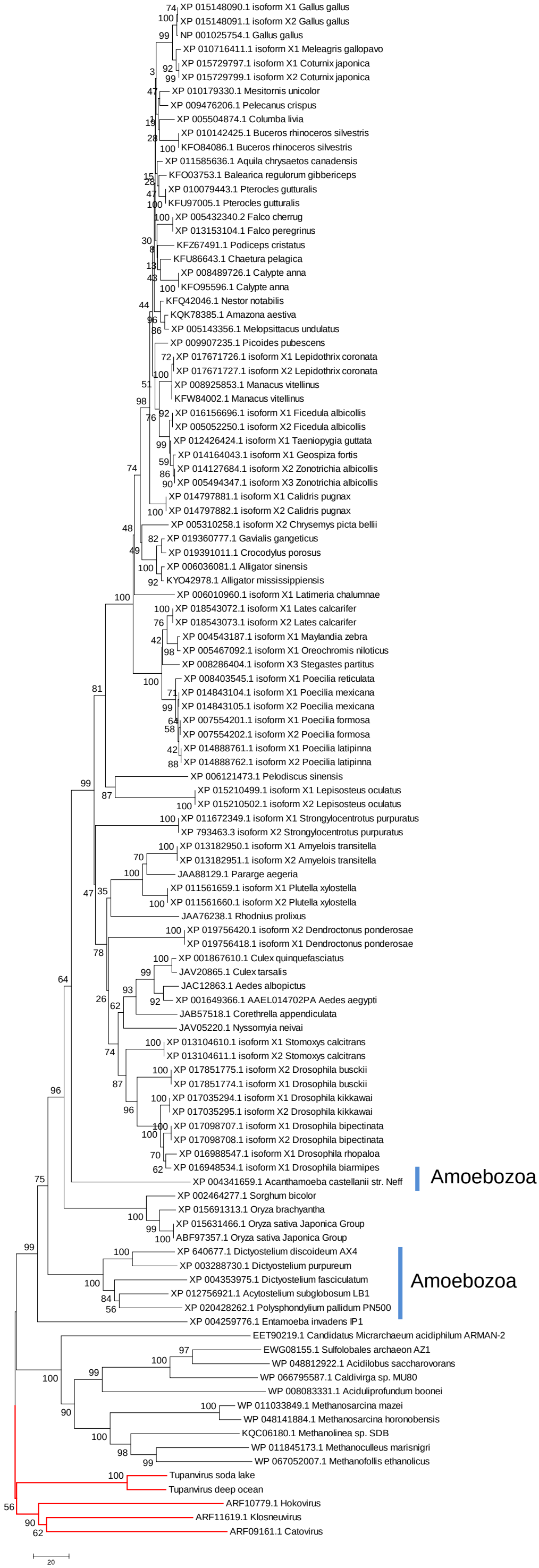
XP 015148090.1 isoform X1 Gallus gallus
XP 015148091.1 isoform X2 Gallus gallus
NP 001025754.1 Gallus gallus
XP 010716411.1 isoform X1 Meleagris gallopavo
XP 015729797.1 isoform X1 Coturnix japonica
XP 015729799.1 isoform X2 Coturnix japonica
XP 010179330.1 Mesitornis unicolor
XP 009476206.1 Pelecanus crispus
XP 005504874.1 Columba livia
XP 010142425.1 Buceros rhinoceros silvestris
KFO84086.1 Buceros rhinoceros silvestris
XP 011585636.1 Aquila chrysaetos canadensis
KFO03753.1 Balearica regulorum gibbericeps
XP 010079443.1 Pterocles gutturalis
KFU97005.1 Pterocles gutturalis
XP 005432340.2 Falco cherrug
XP 013153104.1 Falco peregrinus
KFZ67491.1 Podiceps cristatus
KFU86643.1 Chaetura pelagica
XP 008489726.1 Calypte anna
KFO95596.1 Calypte anna
KFQ42046.1 Nestor notabilis
KQK78385.1 Amazona aestiva
XP 005143356.1 Melopsittacus undulatus
XP 009907235.1 Picoides pubescens
XP 017671726.1 isoform X1 Lepidothrix coronata
XP 017671727.1 isoform X2 Lepidothrix coronata
XP 008925853.1 Manacus vitellinus
KFW84002.1 Manacus vitellinus
XP 016156696.1 isoform X1 Ficedula albicollis
XP 005052250.1 isoform X2 Ficedula albicollis
XP 012426424.1 isoform X1 Taeniopygia guttata
XP 014164043.1 isoform X1 Geospiza fortis
XP 014127684.1 isoform X2 Zonotrichia albicollis
XP 005494347.1 isoform X3 Zonotrichia albicollis
XP 014797881.1 isoform X1 Calidris pugnax
XP 014797882.1 isoform X2 Calidris pugnax
XP 005310258.1 isoform X2 Chrysemys picta bellii
XP 019360777.1 Gavialis gangeticus
XP 019391011.1 Crocodylus porosus
XP 006036081.1 Alligator sinensis
KYO42978.1 Alligator mississippiensis
XP 006010960.1 isoform X1 Latimeria chalumnae
XP 018543072.1 isoform X1 Lates calcarifer
XP 018543073.1 isoform X2 Lates calcarifer
XP 004543187.1 isoform X1 Maylandia zebra
XP 005467092.1 isoform X1 Oreochromis niloticus
XP 008286404.1 isoform X3 Stegastes partitus
XP 008403545.1 isoform X1 Poecilia reticulata
XP 014843104.1 isoform X1 Poecilia mexicana
XP 014843105.1 isoform X2 Poecilia mexicana
XP 007554201.1 isoform X1 Poecilia formosa
XP 007554202.1 isoform X2 Poecilia formosa
XP 014888761.1 isoform X1 Poecilia latipinna
XP 014888762.1 isoform X2 Poecilia latipinna
XP 006121473.1 Pelodiscus sinensis
XP 015210499.1 isoform X1 Lepisosteus oculatus
XP 015210502.1 isoform X2 Lepisosteus oculatus
XP 011672349.1 isoform X1 Strongylocentrotus purpuratus
XP 793463.3 isoform X2 Strongylocentrotus purpuratus
XP 013182950.1 isoform X1 Amyelois transitella
XP 013182951.1 isoform X2 Amyelois transitella
JAA88129.1 Pararge aegeria
XP 011561659.1 isoform X1 Plutella xylostella
XP 011561660.1 isoform X2 Plutella xylostella
JAA76238.1 Rhodnius prolixus
XP 019756420.1 isoform X2 Dendroctonus ponderosae
XP 019756418.1 isoform X1 Dendroctonus ponderosae
XP 001867610.1 Culex quinquefasciatus
JAV20865.1 Culex tarsalis
JAC12863.1 Aedes albopictus
XP 001649366.1 AAEL014702PA Aedes aegypti
JAB57518.1 Corethrella appendiculata
JAV05220.1 Nyssomyia neivai
XP 013104610.1 isoform X1 Stomoxys calcitrans
XP 013104611.1 isoform X2 Stomoxys calcitrans
XP 017851775.1 isoform X2 Drosophila busckii
XP 017851774.1 isoform X1 Drosophila busckii
XP 017035294.1 isoform X1 Drosophila kikkawai
XP 017035295.1 isoform X2 Drosophila kikkawai
XP 017098707.1 isoform X1 Drosophila bipectinata
XP 017098708.1 isoform X2 Drosophila bipectinata
XP 016988547.1 isoform X1 Drosophila rhopaloa
XP 016948534.1 isoform X1 Drosophila biarmipes
XP 004341659.1 Acanthamoeba castellanii str. Neff
XP 002464277.1 Sorghum bicolor
XP 015691313.1 Oryza brachyantha
XP 015631466.1 Oryza sativa Japonica Group
ABF97357.1 Oryza sativa Japonica Group
XP 640677.1 Dictyostelium discoideum AX4
XP 003288730.1 Dictyostelium purpureum
XP 004353975.1 Dictyostelium fasciculatum
XP 012756921.1 Acytostelium subglobosum LB1
XP 020428262.1 Polysphondylium pallidum PN500
XP 004259776.1 Entamoeba invadens IP1
EET90219.1 Candidatus Micrarchaeum acidiphilum ARMAN-2
EWG08155.1 Sulfolobales archaeon AZ1
WP 048812922.1 Acidilobus saccharovorans
WP 066795587.1 Caldivirga sp. MU80
WP 008083331.1 Aciduliprofundum boonei
WP 011033849.1 Methanosarcina mazei
WP 048141884.1 Methanosarcina horonobensis
KQC06180.1 Methanolinea sp. SDB
WP 011845173.1 Methanoculleus marisnigri
WP 067052007.1 Methanofollis ethanolicus
Tupanvirus soda lake
Tupanvirus deep ocean
ARF10779.1 Hokovirus
ARF11619.1 Klosneuvirus
ARF09161.1 Catovirus
Amoebozoa
Amoebozoa
20

N

Metionil RS

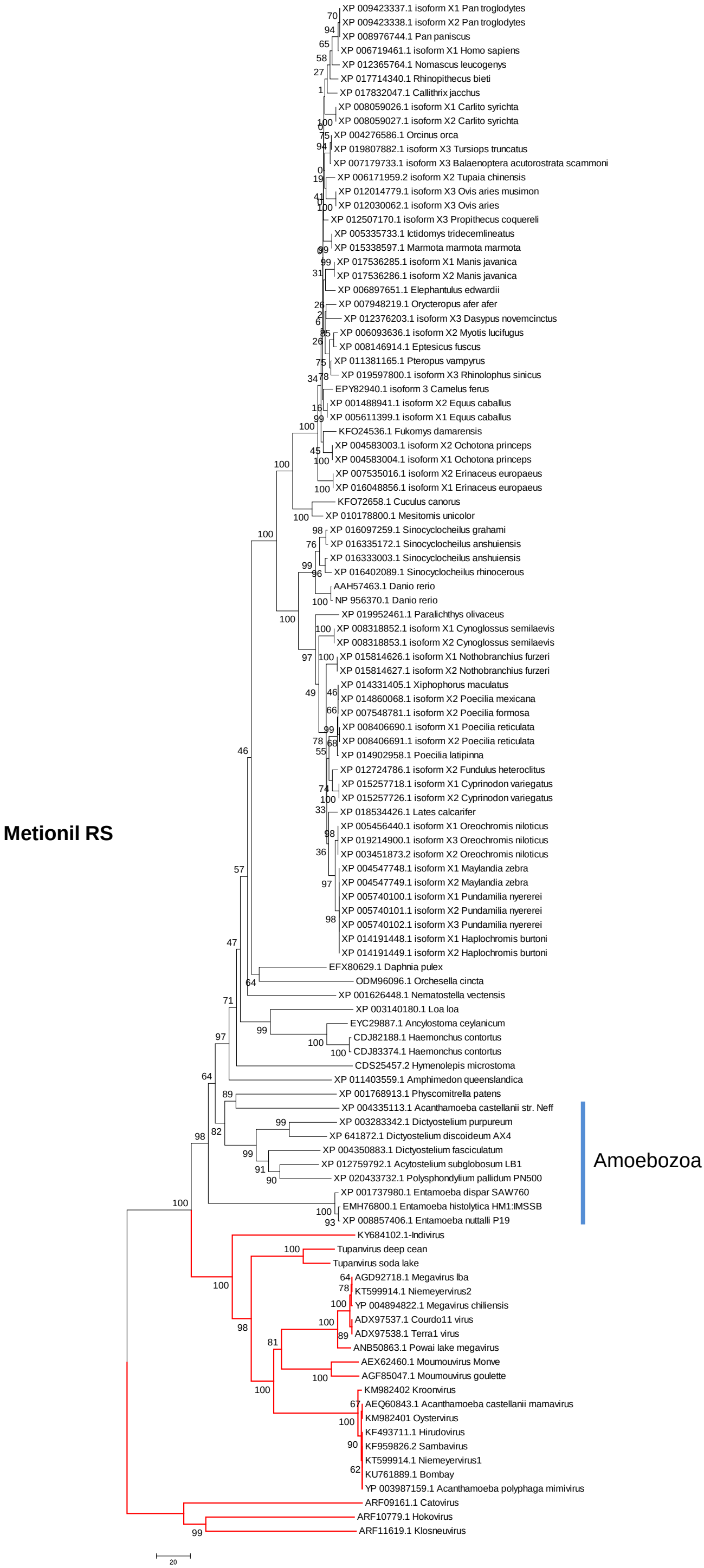

O

Prolil RS

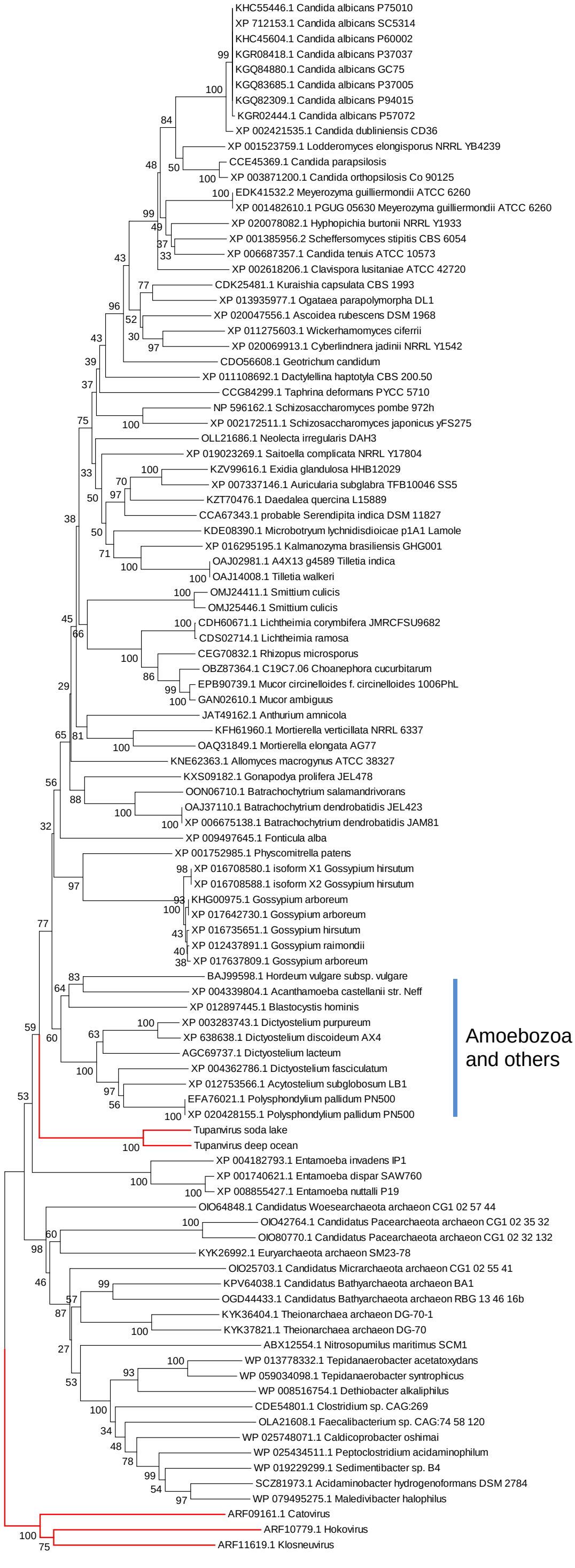
KHC55446.1 Candida albicans P75010
XP 712153.1 Candida albicans SC5314
KHC45604.1 Candida albicans P60002
KGR08418.1 Candida albicans P37037
KGQ84880.1 Candida albicans GC75
KGQ83685.1 Candida albicans P37005
KGQ82309.1 Candida albicans P94015
KGR02444.1 Candida albicans P57072
XP 002421535.1 Candida dubliniensis CD36
XP 001523759.1 Lodderomyces elongisporus NRRL YB4239
CCE45369.1 Candida parapsilosis
XP 003871200.1 Candida orthopsilosis Co 90125
EDK41532.2 Meyerozyma guilliermondii ATCC 6260
XP 001482610.1 PGUG 05630 Meyerozyma guilliermondii ATCC 6260
XP 020078082.1 Hyphopichia burtonii NRRL Y1933
XP 001385956.2 Scheffersomyces stipitis CBS 6054
XP 006687357.1 Candida tenuis ATCC 10573
XP 002618206.1 Clavispora lusitaniae ATCC 42720
CDK25481.1 Kuraishia capsulata CBS 1993
XP 013935977.1 Ogataea parapolymorpha DL1
XP 020047556.1 Ascoidea rubescens DSM 1968
XP 011275603.1 Wickerhamomyces ciferrii
XP 020069913.1 Cyberlindnera jadinii NRRL Y1542
CDO56608.1 Geotrichum candidum
XP 011108692.1 Dactylellina haptotyla CBS 200.50
CCG84299.1 Taphrina deformans PYCC 5710
NP 596162.1 Schizosaccharomyces pombe 972h
XP 002172511.1 Schizosaccharomyces japonicus yFS275
OLL21686.1 Neolecta irregularis DAH3
XP 019023269.1 Saitoella complicata NRRL Y17804
KZV99616.1 Exidia glandulosa HHB12029
XP 007337146.1 Auricularia subglabra TFB10046 SS5
KZT70476.1 Daedalea quercina L15889
CCA67343.1 probable Serendipita indica DSM 11827
KDE08390.1 Microbotryum lychnidisdioicae p1A1 Lamole
XP 016295195.1 Kalmanozyma brasiliensis GHG001
OAJ02981.1 A4X13 g4589 Tilletia indica
OAJ14008.1 Tilletia walkeri
OMJ24411.1 Smittium culicis
OMJ25446.1 Smittium culicis
CDH60671.1 Lichtheimia corymbifera JMRCFSU9682
CDS02714.1 Lichtheimia ramosa
CEG70832.1 Rhizopus microsporus
OBZ87364.1 C19C7.06 Choanephora cucurbitarum
EPB90739.1 Mucor circinelloides f. circinelloides 1006PhL
GAN02610.1 Mucor ambiguus
JAT49162.1 Anthurium amnicola
KFH61960.1 Mortierella verticillata NRRL 6337
OAQ31849.1 Mortierella elongata AG77
KNE62363.1 Allomyces macrogynus ATCC 38327
KXS09182.1 Gonapodya prolifera JEL478
OON06710.1 Batrachochytrium salamandrivorans
OAJ37110.1 Batrachochytrium dendrobatidis JEL423
XP 006675138.1 Batrachochytrium dendrobatidis JAM81
XP 009497645.1 Fonticula alba
XP 001752985.1 Physcomitrella patens
XP 016708580.1 isoform X1 Gossypium hirsutum
XP 016708588.1 isoform X2 Gossypium hirsutum
KHG00975.1 Gossypium arboreum
XP 017642730.1 Gossypium arboreum
XP 016735651.1 Gossypium hirsutum
XP 012437891.1 Gossypium raimondii
XP 017637809.1 Gossypium arboreum
BAJ99598.1 Hordeum vulgare subsp. vulgare
XP 004339804.1 Acanthamoeba castellanii str. Neff
XP 012897445.1 Blastocystis hominis
XP 003283743.1 Dictyostelium purpureum
XP 638638.1 Dictyostelium discoideum AX4
AGC69737.1 Dictyostelium lacteum
XP 004362786.1 Dictyostelium fasciculatum
XP 012753566.1 Acytostelium subglobosum LB1
EFA76021.1 Polysphondylium pallidum PN500
XP 020428155.1 Polysphondylium pallidum PN500
Tupanvirus soda lake
Tupanvirus deep ocean
XP 004182793.1 Entamoeba invadens IP1
XP 001740621.1 Entamoeba dispar SAW760
XP 008855427.1 Entamoeba nuttalli P19
OIO64848.1 Candidatus Woesearchaeota archaeon CG1 02 57 44
OIO42764.1 Candidatus Pacearchaeota archaeon CG1 02 35 32
OIO80770.1 Candidatus Pacearchaeota archaeon CG1 02 32 132
KYK26992.1 Euryarchaeota archaeon SM23-78
OIO25703.1 Candidatus Micrarchaeota archaeon CG1 02 55 41
KPV64038.1 Candidatus Bathyarchaeota archaeon BA1
OGD44433.1 Candidatus Bathyarchaeota archaeon RBG 13 46 16b
KYK36404.1 Theionarchaea archaeon DG-70-1
KYK37821.1 Theionarchaea archaeon DG-70
ABX12554.1 Nitrosopumilus maritimus SCM1
WP 013778332.1 Tepidanaerobacter acetatoxydans
WP 059034098.1 Tepidanaerobacter syntrophicus
WP 008516754.1 Dethiobacter alkaliphilus
CDE54801.1 Clostridium sp. CAG:269
OLA21608.1 Faecalibacterium sp. CAG:74 58 120
WP 025748071.1 Caldicoprobacter oshimai
WP 025434511.1 Peptoclostridium acidaminophilum
WP 019229299.1 Sedimentibacter sp. B4
SCZ81973.1 Acidaminobacter hydrogenoformans DSM 2784
WP 079495275.1 Maledivibacter halophilus
ARF09161.1 Catovirus
ARF10779.1 Hokovirus
ARF11619.1 Klosneuvirus
Amoebozoa and others
20

P

Seril RS

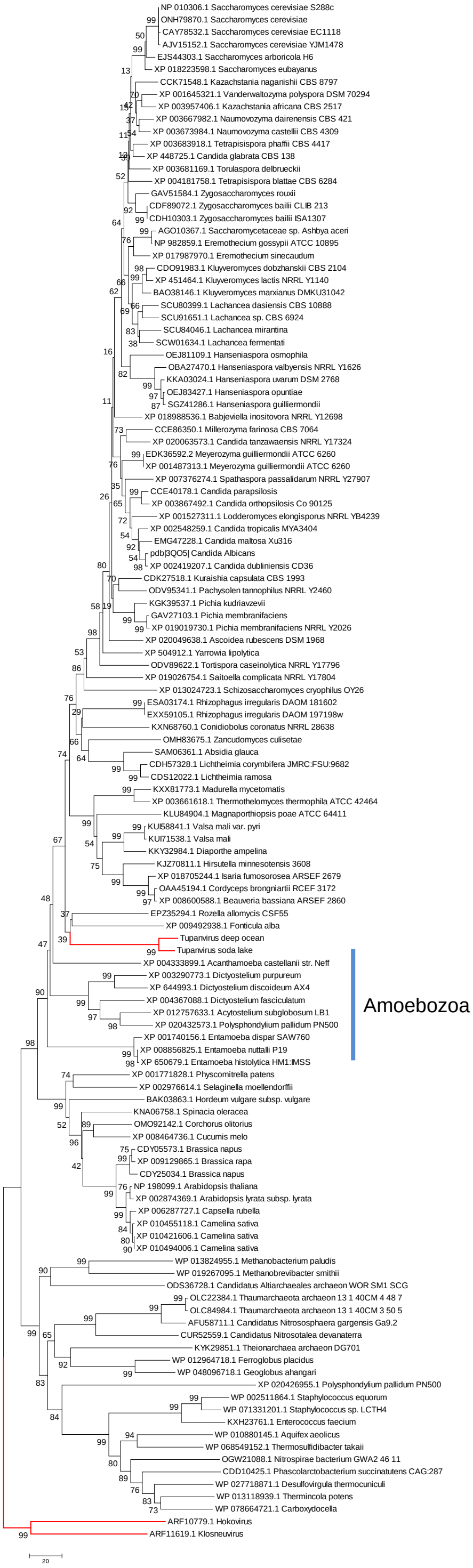
NP 010306.1 Saccharomyces cerevisiae S288c
ONH79870.1 Saccharomyces cerevisiae
CAY78532.1 Saccharomyces cerevisiae EC1118
AJV15152.1 Saccharomyces cerevisiae YJM1478
EJS44303.1 Saccharomyces arboricola H6
XP 018223598.1 Saccharomyces eubayanus
CCK71548.1 Kazachstania naganishii CBS 8797
XP 001645321.1 Vanderwaltozyma polyspora DSM 70294
XP 003957406.1 Kazachstania africana CBS 2517
XP 003667982.1 Naumovozyma dairenensis CBS 421
XP 003673984.1 Naumovozyma castellii CBS 4309
XP 003683918.1 Tetrapisispora phaffii CBS 4417
XP 448725.1 Candida glabrata CBS 138
XP 003681169.1 Torulaspora delbrueckii
XP 004181758.1 Tetrapisispora blattae CBS 6284
GAV51584.1 Zygosaccharomyces rouxii
CDF89072.1 Zygosaccharomyces bailii CLIB 213
CDH10303.1 Zygosaccharomyces bailii ISA1307
AGO10367.1 Saccharomycetaceae sp. Ashbya aceri
NP 982859.1 Eremothecium gossypii ATCC 10895
XP 017987970.1 Eremothecium sinecaudum
CDO91983.1 Kluyveromyces dobzhanskii CBS 2104
XP 451464.1 Kluyveromyces lactis NRRL Y1140
BAO38146.1 Kluyveromyces marxianus DMKU31042
SCU80399.1 Lachancea dasiensis CBS 10888
SCU91651.1 Lachancea sp. CBS 6924
SCU84046.1 Lachancea mirantina
SCW01634.1 Lachancea fermentati
OEJ81109.1 Hanseniaspora osmophila
OBA27470.1 Hanseniaspora valbyensis NRRL Y1626
KKA03024.1 Hanseniaspora uvarum DSM 2768
OEJ83427.1 Hanseniaspora opuntiae
SGZ41286.1 Hanseniaspora guilliermondii
XP 018988536.1 Babjeviella inositovora NRRL Y12698
CCE86350.1 Millerozyma farinosa CBS 7064
XP 020063573.1 Candida tanzawaensis NRRL Y17324
EDK36592.2 Meyerozyma guilliermondii ATCC 6260
XP 001487313.1 Meyerozyma guilliermondii ATCC 6260
XP 007376274.1 Spathaspora passalidarum NRRL Y27907
CCE40178.1 Candida parapsilosis
XP 003867492.1 Candida orthopsilosis Co 90125
XP 001527311.1 Lodderomyces elongisporus NRRL YB4239
XP 002548259.1 Candida tropicalis MYA3404
EMG47228.1 Candida maltosa Xu316
pdb|3QO5| Candida Albicans
XP 002419207.1 Candida dubliniensis CD36
CDK27518.1 Kuraishia capsulata CBS 1993
ODV95341.1 Pachysolen tannophilus NRRL Y2460
KGK39537.1 Pichia kudriavzevii
GAV27103.1 Pichia membranifaciens
XP 019019730.1 Pichia membranifaciens NRRL Y2026
XP 020049638.1 Ascoidea rubescens DSM 1968
XP 504912.1 Yarrowia lipolytica
ODV89622.1 Tortispora caseinolytica NRRL Y17796
XP 019026754.1 Saitoella complicata NRRL Y17804
XP 013024723.1 Schizosaccharomyces cryophilus OY26
ESA03174.1 Rhizophagus irregularis DAOM 181602
EXX59105.1 Rhizophagus irregularis DAOM 197198w
KXN68760.1 Conidiobolus coronatus NRRL 28638
OMH83675.1 Zancudomyces culisetae
SAM06361.1 Absidia glauca
CDH57328.1 Lichtheimia corymbifera JMRC:FSU:9682
CDS12022.1 Lichtheimia ramosa
KXX81773.1 Madurella mycetomatis
XP 003661618.1 Thermothelomyces thermophila ATCC 42464
KLU84904.1 Magnaporthiopsis poae ATCC 64411
KUI58841.1 Valsa mali var. pyri
KUI71538.1 Valsa mali
KKY32984.1 Diaporthe ampelina
KJZ70811.1 Hirsutella minnesotensis 3608
XP 018705244.1 Isaria fumosorosea ARSEF 2679
OAA45194.1 Cordyceps brongniartii RCEF 3172
XP 008600588.1 Beauveria bassiana ARSEF 2860
EPZ35294.1 Rozella allomycis CSF55
XP 009492938.1 Fonticula alba
Tupanvirus deep ocean
Tupanvirus soda lake
XP 004333899.1 Acanthamoeba castellanii str. Neff
XP 003290773.1 Dictyostelium purpureum
XP 644993.1 Dictyostelium discoideum AX4
XP 004367088.1 Dictyostelium fasciculatum
XP 012757633.1 Acytostelium subglobosum LB1
XP 020432573.1 Polysphondylium pallidum PN500
XP 001740156.1 Entamoeba dispar SAW760
XP 008856825.1 Entamoeba nuttalli P19
XP 650679.1 Entamoeba histolytica HM1:IMSS
Amoebozoa
XP 001771828.1 Physcomitrella patens
XP 002976614.1 Selaginella moellendorffii
BAK03863.1 Hordeum vulgare subsp. vulgare
KNA06758.1 Spinacia oleracea
OMO92142.1 Corchorus olitorius
XP 008464736.1 Cucumis melo
CDY05573.1 Brassica napus
XP 009129865.1 Brassica rapa
CDY25034.1 Brassica napus
NP 198099.1 Arabidopsis thaliana
XP 002874369.1 Arabidopsis lyrata subsp. lyrata
XP 006287727.1 Capsella rubella
XP 010455118.1 Camelina sativa
XP 010421606.1 Camelina sativa
XP 010494006.1 Camelina sativa
WP 013824955.1 Methanobacterium paludis
WP 019267095.1 Methanobrevibacter smithii
ODS36728.1 Candidatus Altiarchaeales archaeon WOR SM1 SCG
OLC22384.1 Thaumarchaeota archaeon 13 1 40CM 4 48 7
OLC84984.1 Thaumarchaeota archaeon 13 1 40CM 3 50 5
AFU58711.1 Candidatus Nitrososphaera gargensis Ga9.2
CUR52559.1 Candidatus Nitrosotalea devanaterra
KYK29851.1 Theionarchaea archaeon DG701
WP 012964718.1 Ferroglobus placidus
WP 048096718.1 Geoglobus ahangari
XP 020426955.1 Polysphondylium pallidum PN500
WP 002511864.1 Staphylococcus equorum
WP 071331201.1 Staphylococcus sp. LCTH4
KXH23761.1 Enterococcus faecium
WP 010880145.1 Aquifex aeolicus
WP 068549152.1 Thermosulfidibacter takaii
OGW21088.1 Nitrospirae bacterium GWA2 46 11
CDD10425.1 Phascolarctobacterium succinatutens CAG:287
WP 027718871.1 Desulfovirgula thermocuniculi
WP 013118939.1 Thermincola potens
WP 078664721.1 Carboxydocella
ARF10779.1 Hokovirus
ARF11619.1 Klosneuvirus
20

Q

Tirosil RS

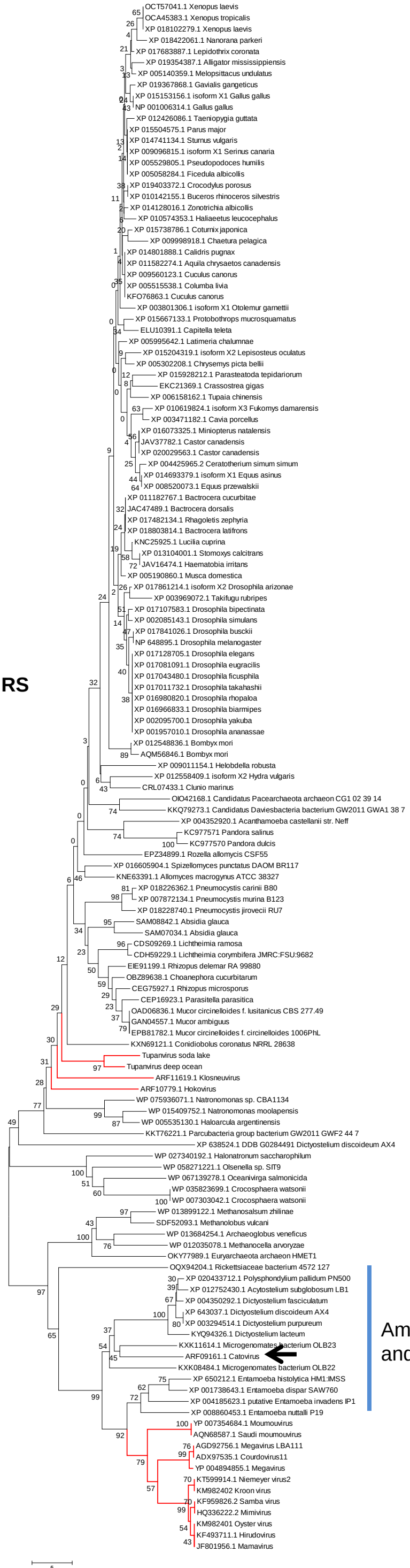

Amoebozoa and others

R

Treonil RS

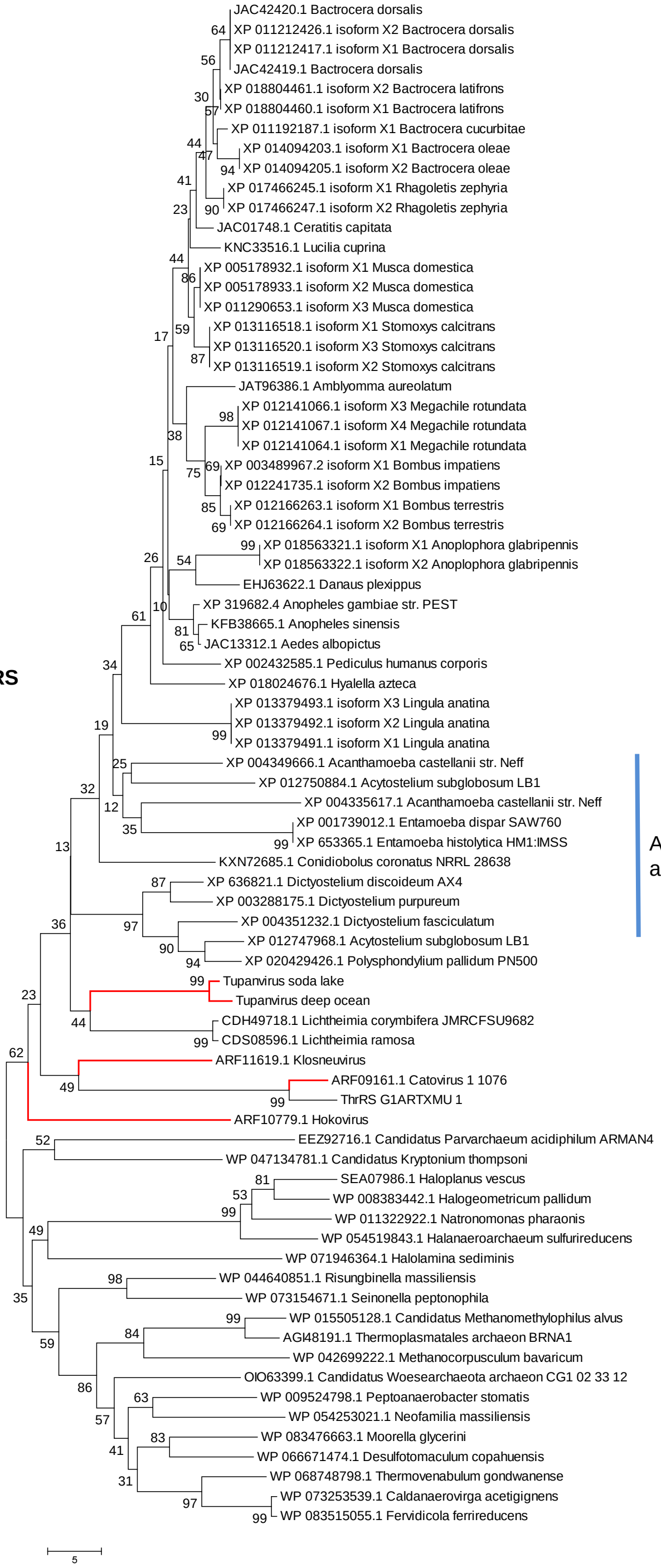
JAC42420.1 Bactrocera dorsalis
XP 011212426.1 isoform X2 Bactrocera dorsalis
XP 011212417.1 isoform X1 Bactrocera dorsalis
JAC42419.1 Bactrocera dorsalis
XP 018804461.1 isoform X2 Bactrocera latifrons
XP 018804460.1 isoform X1 Bactrocera latifrons
XP 011192187.1 isoform X1 Bactrocera cucurbitae
XP 014094203.1 isoform X1 Bactrocera oleae
XP 014094205.1 isoform X2 Bactrocera oleae
XP 017466245.1 isoform X1 Rhagoletis zephyria
XP 017466247.1 isoform X2 Rhagoletis zephyria
JAC01748.1 Ceratitis capitata
KNC33516.1 Lucilia cuprina
XP 005178932.1 isoform X1 Musca domestica
XP 005178933.1 isoform X2 Musca domestica
XP 011290653.1 isoform X3 Musca domestica
XP 013116518.1 isoform X1 Stomoxys calcitrans
XP 013116520.1 isoform X3 Stomoxys calcitrans
XP 013116519.1 isoform X2 Stomoxys calcitrans
JAT96386.1 Amblyomma aureolatum
XP 012141066.1 isoform X3 Megachile rotundata
XP 012141067.1 isoform X4 Megachile rotundata
XP 012141064.1 isoform X1 Megachile rotundata
XP 003489967.2 isoform X1 Bombus impatiens
XP 012241735.1 isoform X2 Bombus impatiens
XP 012166263.1 isoform X1 Bombus terrestris
XP 012166264.1 isoform X2 Bombus terrestris
XP 018563321.1 isoform X1 Anoplophora glabripennis
XP 018563322.1 isoform X2 Anoplophora glabripennis
EHJ63622.1 Danaus plexippus
XP 319682.4 Anopheles gambiae str. PEST
KFB38665.1 Anopheles sinensis
JAC13312.1 Aedes albopictus
XP 002432585.1 Pediculus humanus corporis
XP 018024676.1 Hyalella azteca
XP 013379493.1 isoform X3 Lingula anatina
XP 013379492.1 isoform X2 Lingula anatina
XP 013379491.1 isoform X1 Lingula anatina
XP 004349666.1 Acanthamoeba castellanii str. Neff
XP 012750884.1 Acytostelium subglobosum LB1
XP 004335617.1 Acanthamoeba castellanii str. Neff
XP 001739012.1 Entamoeba dispar SAW760
XP 653365.1 Entamoeba histolytica HM1:IMSS
KXN72685.1 Conidiobolus coronatus NRRL 28638
XP 636821.1 Dictyostelium discoideum AX4
XP 003288175.1 Dictyostelium purpureum
XP 004351232.1 Dictyostelium fasciculatum
XP 012747968.1 Acytostelium subglobosum LB1
XP 020429426.1 Polysphondylium pallidum PN500
Tupanvirus soda lake
Tupanvirus deep ocean
CDH49718.1 Lichtheimia corymbifera JMRCFSU9682
CDS08596.1 Lichtheimia ramosa
ARF11619.1 Klosneuvirus
ARF09161.1 Catovirus 1 1076
ThrRS G1ARTXMU 1
ARF10779.1 Hokovirus
EEZ92716.1 Candidatus Parvarchaeum acidiphilum ARMAN4
WP 047134781.1 Candidatus Kryptonium thompsoni
SEA07986.1 Haloplanus vescus
WP 008383442.1 Halogeometricum pallidum
WP 011322922.1 Natronomonas pharaonis
WP 054519843.1 Halanaeroarchaeum sulfurireducens
WP 071946364.1 Halolamina sediminis
WP 044640851.1 Risungbinella massiliensis
WP 073154671.1 Seinonella peptonophila
WP 015505128.1 Candidatus Methanomethylophilus alvus
AGI48191.1 Thermoplasmatales archaeon BRNA1
WP 042699222.1 Methanocorpusculum bavaricum
OIO63399.1 Candidatus Woesearchaeota archaeon CG1 02 33 12
WP 009524798.1 Peptoanaerobacter stomatis
WP 054253021.1 Neofamilia massiliensis
WP 083476663.1 Moorella glycerini
WP 066671474.1 Desulfotomaculum copahuensis
WP 068748798.1 Thermovenabulum gondwanense
WP 073253539.1 Caldanaerovirga acetigignens
WP 083515055.1 Fervidicola ferrireducens
Amoebozoa and others
5

S

Triptofanil RS

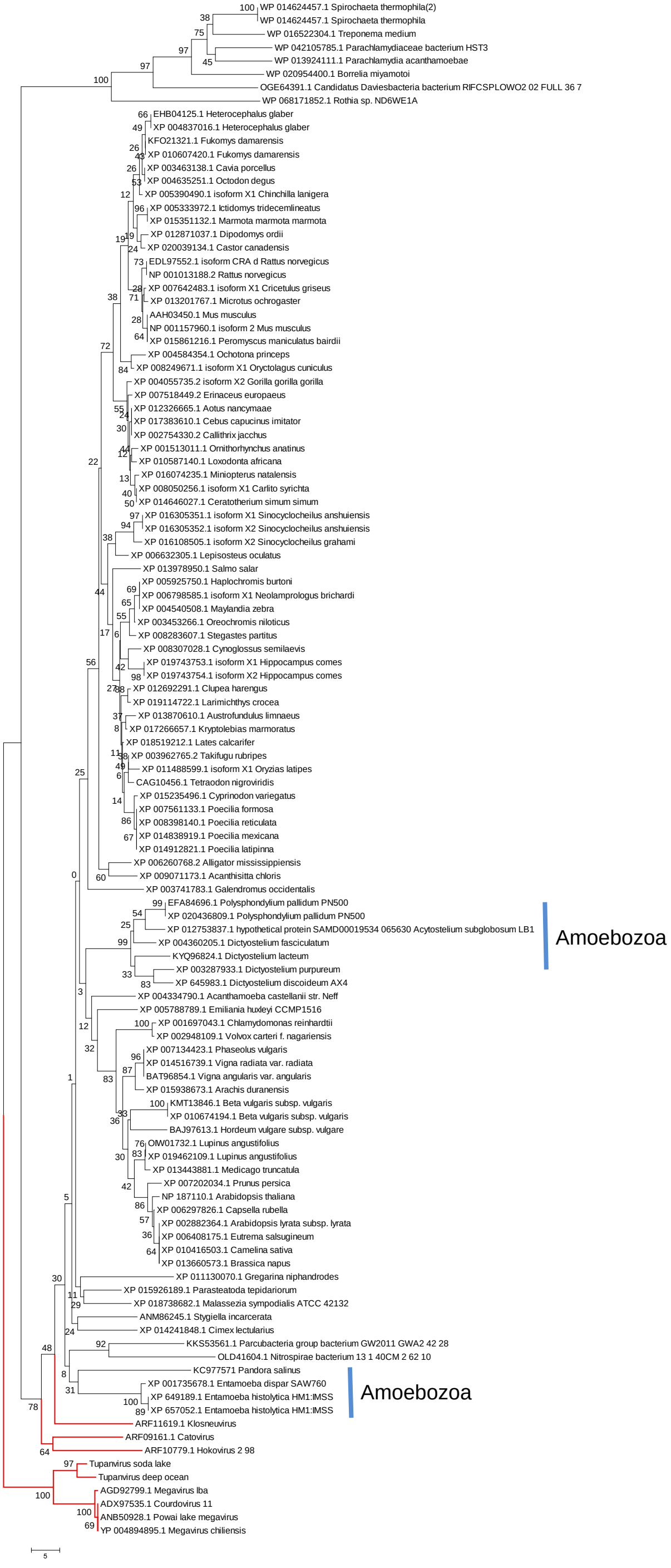

T

Valinill RS

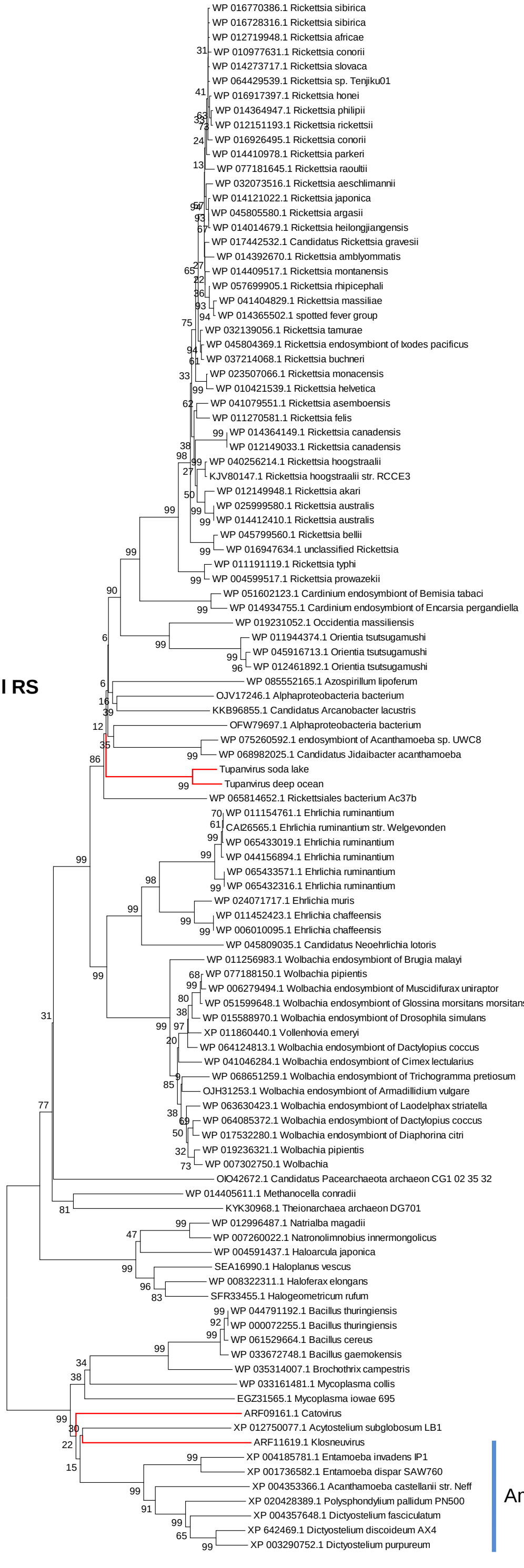

Anexo 7 – Polimorfismos apresentados nos genes de tRNA e aaRS de APMV, APMV M4, SMBV, KROV e OYTV

X Promotor precoce

XPromotor tardio

X Região codificante

X Sinal de poliadenilação

X Substituições

Histidinil tRNA

>APMV/SMBV/APMV M4

TCAATTTTTTCAA**ATG**CGTTTGAAAATAAATTAAAAA**TG**TATAATTTATTATTGTGGGTAAAACCACGGATTTCCAAAAATTC
AACAATACTATAAGATCCGTTAGTTTAGTGGTAGAACTACTGTTTGTGGGACGGTCGACACAGGTTCGATTCCTGTACGGGTC
ATTTTTGAAAATTTTGAAATCCAGTTGATTGTAGATTTACAGTCAACTGGAT

>KROV

TCAATTTTTTTTAA**ATG**CGTTTGAAAATAAATTAAAAATGTATAATCTATTTTTGTGGGTAAAACCACGGATTTCCAAAAATCC
AACAATACTATAAGATCCGTTAGTTTAGTGGTAGAACTACTGTTTGTGGGACGGTCGACACAGGTTCGATTCCTGTACGGGTC
ATCCT-GAAAATTTTGAAATCCAGTTGATTGTAGATTTACAGTCAACTGGAT

OYTV

TCAATTTTTTTAA**ATG**CGTTTGAAAATAAATTAAAAA**TG**TATAATTTATTATTGTGGATAAAACCCACGGATTTCCAAAAATT
CAACAGTATTATAAGATCCGTTAGTTTAGTGGTAGAACTACTGTTTGTGGGACGGTCGACACAGGTTCGATTCCTGTACGGGT
CATTTTTGAAAATTTTGAAATCCAGTTGATTGTAGATTTACAGTCAACTGGAT

Leucinil tRNA

>APMV/SMBV/APMV M4

TCAATTTTAATTGATACATTTATA**ATG**ATTCAA**ATG**AATCATTATAAATAGTGTGA**ATG**CAAAGGGTGGGATTCGAACCCAC
GACATCAAAAGATAGTAGATCTTAAGTCTACCGCGTTAGACCACTCCGCCACCTTTGCTTATTTAATTAATATTAAATTATTTT
TATATCATTTTGATATTTTGATATCTTGATAATTGTTGGATTGGTAATTTTTAATTGATAAAAAATTACACAATTAAAAATTAC

>KROV

TCAATTTTAATTGATACATTTATAATGATTCAATCGAATAATTATAAATAATGTGA**ATG**CAAAGGGTGGGATTCGAACCCACG
ATATCAAATGATACTAGATCTTAAGTCCACCGCGTTAGACCACTCCGCCACCTTTGCTTATTTTAATGTAATTAATTTCTTTTT
ATATCATTTTTATATTTTGATA-------ATTGTTGGATTGGTAATTTTTAATTGATAAAAAATTATACATTAAAAATTAC

>OYTV

TCAATTTTAATTGATACATTTATA**ATG**ATTCAA**ATG**AATCATTATAAATAGTGTGAATGCAAAGGGTGGGATTCGAACCCACG
ACATCAAAAGATAGTAGATCTTAAGTCTACCGCGTTAGACCACTCCGCCACCTTTGCTTATTTTAATGTAATTAATTTTCTTTTT
ATATCATTTTGAAATTTTGATAATTTGATAATTGCCAAATTGGTAATTTTTAATTGATAAAAAATTTATACACTAAAAATTAC

Cisteinil tRNA

>APMV/SMBV/APMV M4

TCAATTTTTTCAAATGCGTTTGAAAATAAATTAAAAATGTATAATTTATTATTGTGGGTAAAACCACGGATTTCCAAAAATTC
AACAATACTATAAGATCCGTTAGTTTAGTGGTAGAACTACTGTTTGTGGGACGGTCGACACAGGTTCGATTCCTGTACGGGTC
ATTTTTGAAAATTTTGAAATCCAGTTGATTGTAGATTTACAGTCAACTGGATCGTTAGCTCA**ATG**GTAGAGCGCTCGCCTGCA
GAGCGATAGGTTATCAGTTCAATTCTGATACGATCCTTTTTTAGATGTATAAATTTATGCATCTAAAAA

>KROV

TTGAAAATAAATTAAAAATGTATAATCTATTTTTGTGGGTAAAACCACGGATTTCCAAAAATGCAACAATACTATAAGATCCG
TTAGTTTAGTGGTAGAACTACTGTTTGTGGGACGGTCGACACAGGTTCGATTCCTGTACGGGTCATCCTT
zAAAATTTTGAAATCCAGTTGATTGTAGATTTACAGTCAACTGGATCGTTAGCTCA**ATG**GTAGAGCGCTCGCCTGCAGAGCGA
TAGGTTATCAGTATCAATTCTGATACGATCCTTTTTTAGATGTATATTTTTATGCATCTAAAAA

>OYTV

TCAATTTTTTTTAAATGCGTTTGAAAATAAATTAAAAATGTATAATTTATTATTGTGGATAAAACCCACGGATTTCCAAAAATTC
AACAGTATTATAAGATCCGTTAGTTTAGTGGTAGAACTACTGTTTGTGGGACGGTCGACACAGGTTCGATTCCTGTACGGGTC
ATTTTTGAAAATTTTGAAATCCAGTTGATTGTAGATTTACAGTCAACTGGATCGTTAGCTCA**ATG**GTAGAGCGCTCGCCTGCA
GAGCGATAGGTTATCAGTTCAATTCTGATACGATCCTTTTTTAGATGTATAAATTTATGCATTTTAAAAA

Triptofanil tRNA

>APVMV/SMBV

TCCATAAAACCACAATCTAAATATCACAGACAAAAAAAATTTAGAAATAATTTTTCATCACAAAATAAATTTCACCATCAAA
AAATTTTTCCTCGACAAAAATTCTCTAAATTTCACAGATAAAAATGGGTGGGAATTATATAAAAATTTTTTCTTTACTGTAAGT
GTAAAGATCTGTTGTTGCATTTAGTGCAACAATAGACCTGTTAGTTTA**ATG**GTAAAACGGTAGCCTCCAGAGTGATTGATACT
GGTTCGATTCCGGTATAGGTCCATTTAATAAAAAAAACAATTAATTAGTATTAGTTGTTTTTTT

APMV M4(deletado)

KROV (deletado)

OYTV

TCCATAAAACCACAATCTAAATATCACAGACAAAAAAAATTTAGAAATACTTTTTCATCACAAAATAAATTTCACCATC
AAAAAATTTTTCCTCGACAAAAATTCTCTAAATTTCATAGATAATAATGGTTGGAAATTATATAAAAATTTTTTCTTTAC
TGTAAGTGTATAGATCTGTTGCTGCATTTAGTGCAACAATAGACCTGTTAGTTTAATGGTAAAACGGTCGCCTCCAGAG
TGATTGATACTGGTTCGATTCCGGTACATGTCCTTTTTAATAAAAAAACAATTAATTAGTATTAGTTGTTTTTTT

Tirosil tRNA sintetase – L124

>APMV/SMBV

TAGAATCATATAAATTATTTGATGGCGGCTAAATTATTTTGAAGGTTGTTGGTAAGATTTGACATTTGATAACAATTCAGACA
ATTCTGGTTTTTTGAAGTGTTCTCTAACTAGATCAATAATAGTGTTAATATAATTGGCTACATCAGTTTTAAGTTCACGTTTATT
CATACTGGAAAAATCTTCTTGAATTGACTCGATATCTGTGTATATTTTACCACATAAGTTTAATGTACCAAACCATCTCAAAAG
CAAATATTTGATGTATTCGAAAATTGGATTGTCAAAAGTTTCATCAGTACAATATGCTCTAGATATTTTTTCACTGACTTCTTG
TTCAGTATCATCCATAAAAATTGCACCTTGAGGATCAGATTTACTCATTTTTTTTTTTGGACCAGATAGACTCATTAACATGTG
ATGTGATAGAGAAATTGGGATTTTTAATCCACGGTCATTTGCATATTCAATAGCCAACATATTGACTTTACGTTGATCAATTCC
TAGTTGACAAATGTCAATTCCTTCAGGAACTAATTCAAATACGTCTGCAGCTTGCATACAAGGATAGAAAATTTGTGAGGCTT
TTAAACAATCACTTTCATTACGACCCATGATTTGACAACATCTTTTAACTCTAGATATAGTAGAAAATTCAGCTATATCTAACA
TTCTCTCGATATAAGATGGATTAGAAGCAATGAATTCACTGGCCCAAATAAATCTTGTACCATCCAAATTAATACCACATGCT
TTGAAAACTTCAATAAAATATCTTCCAAGTTCTCTAATCTTATTAATATCTCCATTCATTTTCAAATTCATTTTGGCAAACCAAT
CGGCAATATAGATAATCATCTGTCCACCACATTCAATAATATTATTGGTGTTCATTACAGTAATAAGAGCTTGAGCAATATGA
ATACGACCACTAGGTTCAAAACCATTGTAAGCTGTAAAAATTCTTCCTGAATCAACTAATTGTTTGAGTCGATCTAATGTTTCA
CATTCTTCTGCTATTGATAGAAGTTGAGTCAAACGATGTTCATTATTGGTATGGTCTGTGTTTTC**CAT**TTGGATATGTATGATT
TGTGAATGAAGACGAATATAAATTTAGGACAAAAAATTATCAATTTT

>APMV M4 (deletado)

>KROV

ATTATTTGATAACGGTTAAATTATTTTGAAGATTGTTGGTAAGATTTGATTATTTGACAATTAAGTCAGACAATTCTGGTTTTTTA
AAGTGTTCTCTAACTAGGTCAATGATAATGTTAATATAATTGGCAACATCAGTTTTAAGTTCACGTTTATTCATACTGGAAAA
ATCTTGTTCAATTGACTTATATCTGTGTATACTTTACCACATAAGTTCAATGTACCAAACCATCTCAAAAGTAAATATTTGAT
GTATTCAAAAATTGGATTGTCAAAAATTTCATCAGTACAATATGCTCTAGATATTTTTTCATTGATTTCTTGTTCAGTATCATCC
ATAAAAATTGCACTTTGAGGATCGGATTTACTCATTTTTTTTTTTGGACCATTTAGACTCATTAACATGTGATGTGACAGAGAA
ATTGGGATTTTTAATCCACGATCATTTGCATATTCAATAGCCAACATATTAACTTTTCGTTGATCAATTCCTAGTTGACAAATA
TCAATTCCAGCAGGAACTAATTCAAATACATCAGCAGCTTGCATACAAGGATAAAAATTTGTGAGGCTTTTAAACAATCACT
TTCATTGCGACCCATGATCTGACAACATCTTTTAACTCTAGATAGAGTAGAAAATTCTGCTATGTCTAACATTCTCTCAATATA
AGATGGATTAGAAGCAATAAATTCACTCGCCCAAATAAATTTTGTACCACCCAAATTAATACCACATGCTTTGAAAACTTCAA
TAAAATATCTTCCGAGCTCTCTAATCTTCTCAATATCTCCATTCATTTTCAAATTCATTTTGGCAAACCAATCGGCAATATAAA
TAATCATTTGTCCACCACATTCAATAATCTTATTGGTATTCATTACGGTGATGAGAGCTTGAGCAATATGAATACGACCACTTG
GTTCAAAACCATTATAAGCTGTAAAAATTTTTCCTGAATCAACTAATTGTTTGAGTCGGTCTAGTGTTTCACATTCTTCGGCGA
TTAATAGAAGTTGATTTAAGCGATGTTCATTGTTGGAATAATCTGTGTTTTC**CAT**CTGAATACAAATTGATAATTTTATAAATG
AACAAGTATAAATCAAGACAATAAAATTATCAATTTT

>OYTV

TAGAATCATATAAATTATTTGATGACGGCTAAATTATTTTGAAGGTTGTTGGTAGGATTTGACATTTGATAACAATTCAGACA
ATTCTGGTTTTTTGAAGTGTTCTCTAACTAGATCAATAATAGTGTTAATATAATTGGCTACATCAGTTTTAAGTTCACGTTTATT
CATACTGGAAAAATCTTCTTGAATTGACTCGATATCTGTGTATATTTTACCACATAAATTTAATGTACCAAACCATCTCAAAAG
CAAATATTTGATGTATTCAAAAATCGGATTGTCAAAAATTTCATCAGTACAATATGCTCTAGATATTTTTTCACTGACTTCTTG
TTCAGTATCATCCATAAAAATTGCACCTTGAGGATCAGATTTACTCATTTTTTTTTTTGGACCAGATAGACTCATTAACATGTG
ATGTGATAGAGAAATTGGGATTTTTAATCCACGGTCATTTGCATATTCAATAGCCAACATATTGACTTTACGTTGATCAATTCC
TAGTTGACAAATGTCAATTCCTTCAGGAACTAATTCAAATACGTCTGCAGCTTGCATACAAGGATAGAAAATTTGTGAGGCTT
TTAAACAATCACTTTCATTACGACCCATGATTTGACAACATCTTTTAACTCTAGATATAGTAGAAAATTCAGCTATATCTAACA
TTCTCTCGATATAAGATGGATTAGAAGCAATGAATTCACTGGCCCAAATAAATCTTGTACCATCCAAATTAATGCCACATGCT
TTGAAAACTTCAATAAAATATCTTCCAAGTTCTCTAATCTTATTAATATCTCCATTCATTTTCAAATTCATTTTGGCAAACCAAT
CGGCAATATAGATAATCATCTGTCCACCACATTCAATAATCTTATTGGTGTTCATTACAGTAATAAGAGCTTGAGCAATATGA
ATACGACCACTAGGTTCAAAACCATTGTAAGCTGTAAAAATTCTTCCTGAATCAACTAATTGTTTGAGTCGATCTAATGTTTCA
CATTCTTCTGCTATTGATAAAAGTTGATTCAAACGATGTTCATTATTGGTATAGTCTGTGTTTTC**CAT**TTGGATATGTATGATTT
GTGAATGAAGACGAATATAAATTTAGGACAAAAAATTATCAATTTT

Cisteinil tRNA sintetase – L164

>APMV/SMBV/APMV M4

TGCTATTATTACCTTTATTATTGTTTAATAAAATCAATGTTTTTGACAGTTATTAACTATAGTGATGTAGTGTGTATTAAGTAGT
AGAGTGTATTACTCAGACGATTGAACACAAGAATTCTCGTACCACAAACTAGAATCTTTGGAATCTTCCAAAATAATACCTAT
GTCGGGTAATTGAATATTACGTTGACGATCCAAAATATCAAAAAGTTGCTTTTTAATTCCAGGAGAAAGATCCGGATTTCTTG
TCAATTGTCTTAATTGAGAGCGAGTCTCAATCAGAATATTCATGAGATCTTTAATTTTATGGGAACTACTACTATTTCCCACCC
TATAAATAAAACCTAATTTGTCTAATAAATCCAGTAAATAATCACGAATTTTACCAACAATAGATTCATTTGGTCTGGGCAAA
TCTAAATAAACATTTGTTGTGCCAATTAAATGCTGAATAGATCTAGCAACCATTTCAAATTTAAATTCAGTCAAATAACTGTA
AATACGTTGTTGAATTCGATAAAAATCATCATGTAGCAAAGTTTCTTTGTCATTGAATTCAACATCAGATACTTCAAATGGAT
AATTGGAAACTCTATTGACAAAATTAACTACTGTAAAATCTAATTCTTTTGCGATAGAGATTAATCCATCAGTAAAATCAACT
TGTTGTTTCCATTTTGTTGACATGAATAACCATCTAAATTGATTTGAATTAATTTTGTCAAGCATTTCTTTAATGGTTGAAAAAT
TCTTTAGAGACTTTGACATTTTCTGACCCTTGATACAAAGATGTCCAACATGAATAAACTCTCTAGTCCACGTATGAAAAATC
ATTGTGTCACTTTGATGGAGAGGATTATACATTGGATGATGATAAGCATTAGCCTGTAAACATTCATTATAATGATGAGGAAA
TTTCAAATCGATTCCACCAAAATGAATATCAATACTATTTCCTAATGTTTTCTTGATCATGGCTGAACATTCAATATGCCAACC
AGGTACACCAAATGATTTAAATGTTTGGTTATCAAAAATAAATTCCACATTAAATCCTACATCGGATTCTGATCGACCTTTCC
AAAGAGCAAAATCTTTATGGTGTTTTTTTTGGGAAACTATTTCTTTAGAAAGAAGAGATTCGTACTGTTGTTCTTCTTCATCGT
CAATTTCACTAAATTCATATCCTGCTTTTTTGTATTCAATTGAGTCAAAATAAACCGAACTATCTGATACAATATAAGCAAAAC
CGTTATTAATAATCTGTTGGATATATAACACAATATCACTGATGGATTCTGTTACTCTAATCACAGAATCTGGTCTTGTGACAT
TTAATTTAGACATACAATCAAAAAAAGAATTTTCATGGAGTCTTGCCAATTCAAGCCAAGTAATTCCTTTGTTTTTTGATTCTC
GGATAATTTTATCATCAATATCTGTAACATTCATTACTAGATGAGTAGGTTTGTTAAGGATTTTATTCATGGTTCGATTAATTA
AATCGACAATAACATAGATTCTGGCATGTCCAATATGCGCATCATTGTAAACTGTTGGACCACATACATACATTTTTGTAACA
GTGGGTAAAATAGTTTCAGATAATTCCGTCTCCATGTCAATTACTGATTGTTGTCAAAATATTATTGATTATTTAATTAGTATT
TTGTTATACATTTAATAATAAATTAAATATAACAAAATAATATTTCAATTTTTATTGGAATCAGATTTTGATGTTTTACTCCTAT
TGTAAACAGTTTTACATTTGATACATTGATAATATAACGTATTAGTTTTGTAATGTGTCTGATATTTAATATTTTTACACACCTT
ACATCGATACCAAATTACTATCATTTAAGATTTGGATTTAATATTGAATCATTAAGTTATTAAAATAATTTTAATAACGATAT

>KROV

----------ITTATTAATTATAGTGATATAGGCGTATATCAAATGGCGCAATT
ATTATTCAGACGATTGAATACAAGAATTTTCATACCATTAAACTTGAATCTTTGGAATCTTCCAAAATAATACCTATGTCGGGT
AATTGAATATTACGTTGACGATCCAAAATATCAAAAAGTTGCTTTTTAATTCCAGGAGAAATTATCTGGATTTCTTGTCAATTGT
CTTAATTGAGAGCGAGTCTCAATTAGAATATTCATGAGGTCTTTAATTTTATGGAAACTACTACTATTTCCCATTTTATAAACA
AAACCTAATTTGTCTAATAAATCCAGTAAATAATCACGGATTTTATTAACAATAGACTCATTTGGTCTGGGTAAATCTAAATA
AACATTTGTTGTGCCAATTAAATGCTGAACAGATCTAACAACCATTTCGAATTTAAATTCAGTCAAATAACTGTAAATACGTT
GTTGAATTCGATAAAAATCATCATGTAGTAAAGTTTCTTTGTCGTTAAATTCAACATCTGATACTTCAAATGGATAATTGGAA
ACTCTATTAACAAAATTAACGACTGTGGAATCTAATTCTTTTGCGGTTGAAATTAATCCATCGGTAAAATCAACTTGTTGTTTC
CATTTTGTTGACATAAATAACCATCTAAACTGATTAGAATTAATTTTGTCAAGCATTTCTTTGATGGTTGAAAAATTCTTTAAT
GACTTTGACATTTTCTGACCTTTGATACAAAGATGTCCAACATGAATAAACTCTCTAGTCCACTTATAAAAAATCATTGTGTTA
CTTTGATGAAGAGGATTATACATTGGATGATGATAAGCATTAGCTTGTAAACATTCATTATAATGGTGAGGAAATTTCAAATC
AATTCCACCGAAATGAATATCGATACTATTTCCTAATGTTTTCTTGATCATGGCTGAACACTCAATATGCCAACCAGGTACAC
CAAATGATTTAAATGTTTGGTTATCAAAAACAAATTCCACATTAAATCCTACATCAGATTCTGATCGACCTTTCCAAAGAGCA
AAATCTTTATCATGTTTGTTTTGGGAAACTATTTCCTTTGAAAGAAGAGATTCATATTGTTGTTCTTCTTCATCGTCAATTTCAC
TAAATTCATAACCAGCTTTTTTGTATTCAATTGAGTCAAAATACACTGAACCATCTGATACAATATAAGCAAAACCATTATTA
ATAATCTGTTGGATATATAACACAATATCACTAATAGATTCTGTTACTCTAATCACAGAATCTGGTCTCGCAACATTTAATTTA
GACATACAGTCAAAAAAAGAATTTTCATGGAGTCTTGCTAGTTCGAGCCAAGTAATTCCTCTATTTTTTGATTCTCGAATAATT
TTATCATCTATATCTGTAATTATTCATTACAAGATGAGTAGGTTTATCGAGGATTTTATTCATAGTTCGATTAATTAAATCGACA
ATGACATAGATTCTGGCATGTCCAATATGCGCATCATTGTAAACTGTTGGACCACATACATACATTTTTGTAACAGTTGGTAA
ATTAGTTTTGGATAATTTTGTCTCCATGTTGATTATTGATTGTTATTAAAATATTATTAAATATCAATGTAGTATTTTGTTATTT
ATTGTAGTATTTTTGTTATTTATGTGATATTTTGTTAAATATTACATAAATAATATTTCAATTTTTATTTAAACATAATTGGATTTC
AATGTTCCACTTCTATCATATGTGGTTTTACACTTGGTACATTGATAGTATAACATATTAGTTTTACCATGTATTTGATATTTAA
TATTCTTACATATTATACATCGATACCAAATTATTATCA----------

>OYTV

TGCTATTATTATCTTTATTATTGTTTAATAAAATCAATGTTTTTGACAGTTATTAACTATAGTGATGTAGTGTGTATTAAGTAGT
AGAGTGTATTACTCAGACGATTGAACACAAGAATTCTCGTACCACAAACTAGAATCTTTGGAATCTTCCAAAATAATACCTAT
GTCGGGTAATTGAATATTACGTTGACGATCCAAAATATCAAAAAGTTGCTTTTTAATTCCAGGAGAAAGATCCGGATTTCTTG
TCAATTGTCTTAATTGAGAGCGAGTCTCAATCAGAATATTCATGAGATCTTTAATTTTATGGGAACTACTACTATTTCCCACCC
TATAAATAAAACCTAATTTGTCTAATAAATCCAGTAAATAATCACGAATTTTACCAACAATAGATTCATTTGGTCTGGGCAAA
TCTAAATAAACATTTGTTGTGCCAATTAAATGCTGAACAGATCTAGCAACCATTTCAAATTTAAATTCAGTCAAATAACTGTA
AATACGTTGTTGAATTCGATAAAAATCATCATGTAGCAAAGTTTCTTTGTCATTGAATTCAACATCAGATACTTCAAATGGAT
AATTGGAAACTCTATTGACAAAATTAACTACTGTAGAATCTAATTCTTTTGCAATAGAGATTAATCCATCAGTAAAATCAACT
TGTTGTTTCCATTTTGTTGACATGAATAACCATCTAAATTGATTTGAATTAATTTTGTCAAGCATTTCTTTAATGGTTGAAAAAT
TCTTTAGAGACTTTGACATTTTCTGACCCTTGATACAAAGATGTCCAACATGAATAAATTCTCTAGTCCATTTATGAAAAATCA
TTGTGTCACTTTGATGAAGAGGATTATACATTGGATGATGATAAGCATTAGCCTGTAAACATTCGTTATAATGATGAGGAAAT

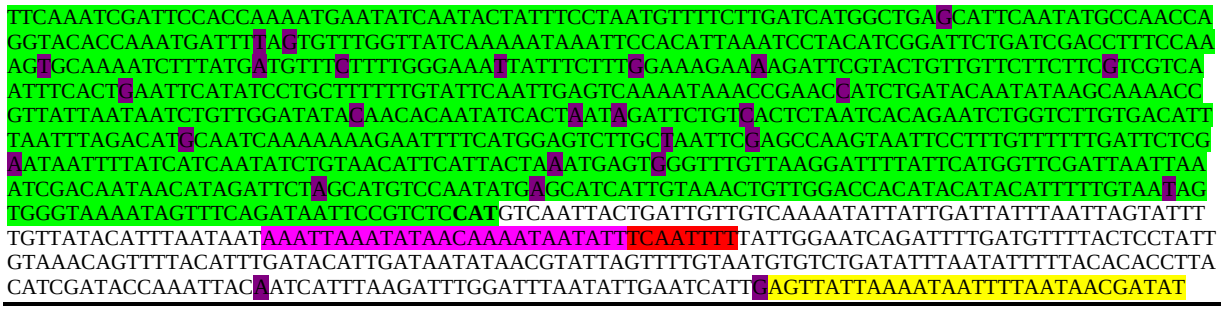

Metionil tRNA sintetase –R639

>APMV/SMB/APMV M4

>KROV

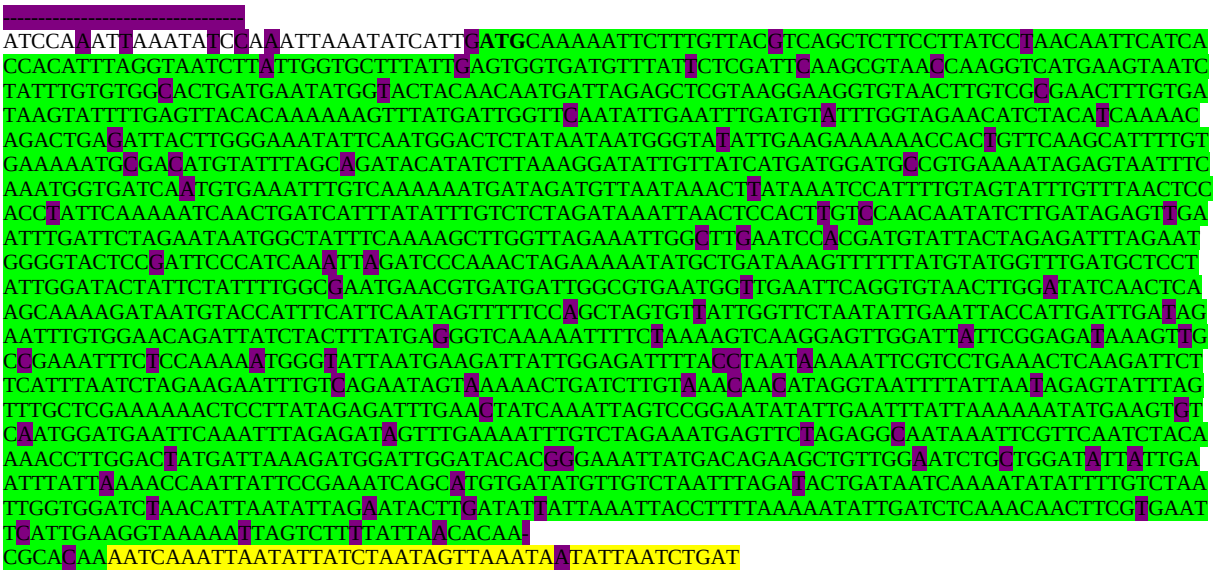

>OYTV

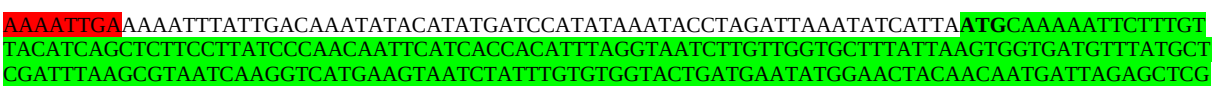

TAAGGAAGGTGTAACTTGTCGTGAACTTTGTGATAAGTATTTTGAGTTACACAAAAAAGTTTATGATTGGTTTAATATTGAAT
TTGATGTTTTTGGTAGAACATCTACAACAAAACAGACTGAAATTACTTGGGAAATATTCAATGGACTCTATAATAATGGGTAC
ATTGAAGAAAAAACCACCGTTCAAGCATTTTGTGAAAAATGTGATATGTATTTAGCGGATACATATCTTAAAGGATATTGTTA
TCATGATGGATGTCGTGAAAATAGAGTAATTTCAAATGGTGATCAGTGTGAAATTTGTCAAAAAATGATAGATGTTAATAAA
CTCATAAATCCATTTTGTAGTATTTGTTTAACTCCACCCATTCAAAAATCAACTGATCATTTATATTTGTCTCTAGATAAATTA
ACTCCACTCGTTCAACAATATCTTGATAGAGTAGAATTTGATTCTAGAATAATGGCTATTTCAAAAGCTTGGTTAGAAATTGG
TTTAAATCCGCGATGTATTACTAGAGATTTAGAATGGGGTACTCCAATTCCCATCAATTTGGATCCCAAACTAGAAAAATATG
CTGATAAAGTTTTTTATGTATGGTTTGATGCTCCTATTGGATACTATTCTATTTTGGCAAATGAACGTGATGATTGGCGTGAAT
GGCTGAATTCAGGTGTAACTTGGGTATCAACTCAAGCAAAAGATAATGTACCATTTCATTCAATAGTTTTTCCGGCTAGTGTA
ATTGGTTCTAATATTGAATTACCATTGATTGACAGAATTTGTGGAACAGATTATCTACTTTATGAAGGTCAAAAATTTTCCAAA
AGTCAAGGAGTTGGATTGTTCGGAGACAAAGTCGCTGAAATTTCCCCAAAATTGGGAATTAACGAAGATTATTGGAGATTTT
ATTTAATGAAAATTCGTCCTGAAACTCAAGAGTCTTCATTTAATCTAGAAGAATTTGTTAGAATAGTGAAAACTGATCTTGTG
AATAATATAGGTAATTTTATTAACAGAGTATTTAGTTTGCTCGAAAAAACTCATTATAGAGATTTGAATTATCAAATTAGTCC
GGAATATATTGAATTTATTAAAAAATATGAAGTATATATGGATGAATTCAAATTTAGAGATGGTTTGAAAATTTGTCTAGAAA
TGAGTTCCAGAGGTAATAAATTCGTTCAATCTACAAAACCTTGGACCATGATTAAAGATGGATTGGATACACAAGAAATTAT
GACAGAAGCTGTTGGTATCTGTTGGATTTTGTTGAATTTATTGAAACCAATTATTCCGAAATCAGTGTGTGATATGTTGTCTAA
TTTAGACACTGATAATCAAAATATATTTTGTCTAATTGGTGGATCCAACATTAATATTAGGATACTTAATATCATTAAATTACC
TTTTAAAAATATTGATCTCAAACAACTTCGCGAATTTATTGAAGGTAAAAACTAGTCTTCTATTAGCACAAACGCATAAAATC
AAATTAATATTATCTAATAGTTAAATACTATTAATCTGAT

Arginil tRNA Sintetase – R663

>APMV/SMBV/APMV M4

TCAATTTTTTTAATTAAAAAAAAATTGATAAGTGTAATATATTAGTATATTTTATACACATTAAATTTACCATCATAGTGTAAGA
TGCAAGATAATTTAATTTATTTGGCAAATTGTTTCCTTAATGAAGCAATTAAAACAACTTTACAGAATTTAAATAAGGTTAAC
ATTATAGACACTCCTGAATTATACAGTTTTGTTAAGGGAATTAATACTGATTATCAATTCAATAAATCAACTAAATTGGCAAA
TGATTGTAATCTTGATAAAGAAAAAATTGTCAACGAATTGATAACTCAACTGAAATCAAATTCATTTTTCGAAAATATTTCTA
GTGTGGAATTAGAACAAAATAAGTCGGTCAAAATTAATGGTAAGAAAACTAATACTGTTATCAAGCAAATTATGATAACATT
AAATATATCAAAATTATATTTGTCAAATAGAATTAATTTATTGTACAAAAGAATTCTTTCGGGTTCTAGTATTTATGTTCCAAA
TACTATTACAAAGAAAATTATTGTCGATTATTCTTCTCCAAATATTGCTAAAGAAATGCATATTGGACATTTAAGATCAACTAT
TATTGGTGAATCTATTTGTAGGGTATTAGAAATGTGTGGACACGATGTTTATCGTATTAATCATGTGGGTGATTGGGGAACTC
AATTCGGTATGTTAATTGCTTATATTAAAAAATAATCAAATAGAATCTTACACCATTAGTGAACTCATGAACATTTACAAAGAA
TCAAGGAAATTATTTGAATCAAGTATTGATTTTAAAAACCAATCCCGATTGGAGACCGTATCATTACAAAATGGTAATATTGA
AAGTATTACTATTTGGCAAAAAATTCACAAAATATCGATGAACTCATTTCATGAGATCTACAGTCTTCTCGGAATAAATAATC
TGATTACAAAAGGAGAATCTTTTTATCAAGATCAAATGACTGAATTAGTAAATAGTTTGACTTCGGACAACAAAATCACTGTT
GAAAATGACATGAAATTAATGTTTGTCGAAGGAATTTCCAAACCGTTTATTTTACAAAAATCTGATGGAGGATTTACTTATGA
CACGTCAGATTTGACTGCCTTGAAATATCGTTTATTTATAGAAAAGGCTGACCATATAATATATGTTGTAGATTCCAGTCAAC
AAGAACATTTTAGTCAAATGTTTCAAATTGCTGAAAAATTAGATTGGATAAAAAATCAACAACTCCAACATATTGGATTTGGT
TTAGTATTGGGATCCGATGGTTCCAAATTAAAAACTCGTTCTGGAGAAACCATTAAATTACAAGATGTTATTGATAATGTTGT
TTCTCATGCATCTAATATTACTCGAGAATTAATCAAACAAAAAAATCTTGATTGGAATGATGATGATATTTTGACTATTTCCAA
GAAAATAGCAATTAATTGCATTAAATATTCGGATCTAAATAATCCTAGACTAAACAATTACAAATTTGATATCAATAAAATGC
TTAATTCAAAAGGTAATACAGCTGTATATCTAATGTATGGATTAGCTCGTTGTAAAAGTATTTTAAGGAAAGTTCCAAATAAT
ACTGTTTTGAATGGTGATATTATTATTGAAAATGAAAATTCCAGGAATTTATTACTACATGTTCTAAAATATGTTGAAGTGATT
GATCAAACTGTCGAAACAATGTGCCCACATTATCTTTGTATTTATTTGTATGATTTGATTGGATCTCTTACTAAATTTTATACA
ACAAATAGGTGTTTGGAATATGATAATGATAATTTAATTGGATATAATGCAAATAATTTACGCATAGTAAATATGGTCAAAAT
AATAATTTCCAAAATATTCGAATTGATTGGTTTAGAAGAAATTGAACAGTTATAAATAACTTTTTGTCATGTCGATAAACATG
GCAAAAGAGTATAATGTCTGTCATAAAAAATTGAAATTATTTTTGTAGATTTAATCAATTCATTAAATCCACAAAAATAAT

>KROV

TTAATAAAAAATTGATAAACGTAATATATTAGTATATTTTATACACATTAAAATTATTATCACAGATAAAGA**TG**CAAGATAATT
TAATTTATTTGGCAAATTGTTTCCTCAATGAGGCAATTAAAACAACTTTGCAGAATTTAAATAAAGTTAATTATTATAGACACA
CCAGAATTATACAGTTTTGTTAAAGGAGTTAATACGGATTATCAATTCAATAAATCAACTAAATTGGCAAATGATTGTGATAT
TGATAAAGAAAAAATTTTGTTAACGAATTGATAATTCAACTGAAATTGAATTCATTTTTCGAAAATATTTCTAGTCTTGAATTAG
AACAAAATAAGTCAGTAAAAATTAATGGAAAAAAAACTAATACTGTTATTAAACAAATTATGATTACACGTAAATATATCAAA
ATTATATTTGTCAAATAGGATTAATTTATTGTACAAGAGAATTCTGTCAGGTTTTAGTATTTATGTTCCAAATGTTGTCGCAAA
AAAATTTATTGTCGATTATTCTTCCCCAAATATTGCCAAAGAAATGCATATTGGACATTTAAGATCGACTATTATTGGTGAATC
TATTTGTAGAGTACTAGAAATTATGTGGACACAATGTTTATCGGATCAATCATGTGGGTGATTGGGGAACACAATTTGGTATGT
TAATTGCTTATATTAAAAAATAACAAAATAGAATCTTACACCATTAGTGAACTCATGAACATTTATTAAAG-
AATCAAGGAAATTATTTGAGTCAAATATTGATTTTAAAAACCAAGCACGATTGGAGACTGTATCATTACAAAATGGTAATATT
GAAAGTATTACTATTTGGAAAAAAATTCACGAAATATCCATGAATTTCATTTTATGAGATCTACAAACTTCTTGGAATAAATAA
TCTACTTACAAAAGGAGAATCTTTTTATCAAGATCAAATGATCGAATTAGTAAATAGTTTAACTTTGGAAACAAAATCACTG
TTGAAAATGACATGAAATTAATGTTTATTGAAGGAATTTCCAAACCATTTATTTTACAAAAATCTGATGGAGGATTCACTTAT
GATACATCAGATTTGGCTGCCTTAAAATATCGTTTATTTATAGAAAAAGCCGATCGTATAATATATGTTGTAGATTCTAGTCA
ACAAGAACATTTTAGTCAAATGTTTCAAATTGCTGAAAAATTAGATTGGATAAAAAATCAACAACTTCAACATATTGGATTTG
GTTTAGTATTGGGATCTGATGGTTCCAAATTAAAAACTCGTTCGGAGAAACCATTAAACTACAAGATGTTATTGATGATGTT
GTTTCTCATGCATCTAATATTACTCGAGAATTAGTCAAACAAAAAGATCTTGATTGGAATGATGATGATATTTTGGTTATTTCC
AAGAAAATTGCCATTAATTGCATTAAATATTCGGAGCTAAATAATCCCAGATTAAATTAATTACAAGTTTGATATCAATAAAAT
GCTTAATTCAAAAGGTAATACAGCTGTATATTTAATGTATGGATTAGCTCGCTGTAAAAGTATTTTAAGGAAAGTTCCAGATA
ATACTATTTTGAATGGTGATATTATTATTGAAAATGAAAATGCTAGAAATTTATTGTTACATGTGCTAAAATATGTGGAAGTG

ATTGATCAAACTATCGAAACAATGTGTCCACATTATCTTTGTATTTATTTGTATGATTTGGTTGGATCTCTCACTAAATTTTATA
CAACAAATAGATGTTTGGAATATGATAATAGCGATTTAATTGGATATAATACAAATAATTTACGCATAATAAATATTGTCAAA
ACAATAATTTCCAAAATATTTGAATTGATTGGTTTAGAAGAAATTGAGCAGTTATAAATACTTCTTT----------
---

> OYTV

TCAATTTTTTTAATTAAAAAAAAATTGATAAGTGTAATATATTAGTATATTTTATACACATTAAATTTACCATCATAGTGTAAGA
TGCAAGATAATTTAATTTATTTGGCAAATTGTTTCCTTAATGAAGCAATTAAAACAACTTTACAGAATTTAAATAAGGTTAAC
ATTATAGACACTCCTGAATTATACAGTTTTGTTAAGGGAATTAATACTGATTATCAATTCAATAAATCAACTAAATTGGCAAA
TGATTGTAATCTTGATAAAGAAAAAATTGTCAACGAATTGATAACTCAACTGAAATCAAATTCATTTTTCGAAAATATTTCTA
GTGTGGAATTAGAACAAAATAAGTCGGTCAAAATTAATGGTAAGAAAACTAATACTGTTATCAAGCAAATTATGATAACATT
AAATATATCAAAATTATATTTGTCAAATAGAATTAATTTATTGTACAAAAGAATTCTTTCGGGTTCTAGTATTTATGTTCCAAA
TACTATTACAAAGAAAATTATTGTCGATTATTCTTCTCCAAATATTGCTAAAGAAATGCATATTGGACATTTAAGATCAACTAT
TATTGGTGAATCTATTTGTAGGGTATTAGAAATGTGTGGACACGATGTTTATCGTATTAATCATGTGGGTGATTGGGGAACTC
AATTCGGTATGTTAATTGCTTATATTAAAAAATAATCAAATAGAATCTTACACCATTAGTGAACTCATGAAGATTTAGAAAGAA
TCAAGGAAATTATTTGAATCAAGTATTGATTTTAAAAACCAATCCCGATTGGAGACGGTATCATTACAAAATGGTAATATTGA
AAGTATTACTATTTGGCAAAAAATTCACAAAATATCGATGAACTCATTTCATGAGATCTACAGTCTTCTCGGAATAAATAATC
TGATTACAAAAGGAGAATCTTTTTATCAAGATCAAATGACTGAATTAGTAAATAGTTTGACTTCGGACAACAAAATCACTGTT
GAAAATGACATGAAATTAATGTTTGTCGAAGGAATTTCCAAACCGTTTATTTTACAAAAATCTGATGGAGGATTTACTTATGA
CACGTCAGATTTGACTGCCTTGAAATATCGTTTATTTATAGAAAAGGCTGACCATATAATATATGTTGTAGATTCCAGTCAAC
AAGAACATTTTAGTCAAATGTTTCAAATTGCTGAAAAATTAGATTGGATAAAAAATCAACAACTCCAACATATTGGATTTGGT
TTAGTATTCGGATCCGATGGTTCCAAATTAAAAACTCGTTCTGGAGAAACCATTAAATTACAAGATGTTATTGATAATGTTGT
TTCTCATGCATCTAATATTACTCGAGAATTAATCAAACAAAAAAATCTTGATTGGAATGATGATGATATTTTGACTATTTCCAA
GAAAATAGCAATTAATTGCATTAAATATTCGGATCTAAATAATCCTAGACTAAACAATTACAAATTTGATATCAATAAAATGC
TTAATTCAAAAGGTAATACAGCTGTATATCTAATGTATGGATTAGCTCGTTGTAAAAGTATTTTAAGGAAAGTTCCAAATAAT
ACTCTTTTGAATGGTGATATTATTATTGAAAATGAAAATTCCAGGAATTTATTACTACATGTTCTAAAATATGTTGAAGTGATT
GATCAAACTGTCGAAACAATGTGCCCACATTATCTTTGTATTTATTTGTATGATTTGATTGGATCTCTTACTAAATTTTATACA
ACAAATAGGTGTTTGGAATATGATAATGATAATTTAATTGGATATAATGCAAATAATTTACGCATAGTAAATATGGTCAAAAT
AATAATTTCCAAAATATTCGAATTGATTGGTTTAGAAGAAATTGAACAGTTATAAATAACTTTTTGTCATGTCGATAAACATG
GCAAAAGAGTATAATGTCTGTCATAAAAAATTGAAATTATTTTTGTAGATTTAATCAATTCATTAAATCCACAAAAATAAT

nature COMMUNICATIONS

ARTICLE

DOI: 10.1038/s41467-018-03168-1 OPEN

Tailed giant Tupanvirus possesses the most complete translational apparatus of the known virosphere

Jônatas Abrahão[1,2], Lorena Silva[1,2], Ludmila Santos Silva[1,2], Jacques Yaacoub Bou Khalil[3], Rodrigo Rodrigues[2], Thalita Arantes[2], Felipe Assis[2], Paulo Boratto[2], Miguel Andrade[4], Erna Geessien Kroon[2], Bergmann Ribeiro[4], Ivan Bergier[5], Herve Seligmann[1], Eric Ghigo[1], Philippe Colson[1], Anthony Levasseur[1], Guido Kroemer[6,7,8,9,10,11,12], Didier Raoult[1] & Bernard La Scola[1]

Here we report the discovery of two Tupanvirus strains, the longest tailed *Mimiviridae* members isolated in amoebae. Their genomes are 1.44–1.51 Mb linear double-strand DNA coding for 1276–1425 predicted proteins. Tupanviruses share the same ancestors with mimivirus lineages and these giant viruses present the largest translational apparatus within the known virosphere, with up to 70 tRNA, 20 aaRS, 11 factors for all translation steps, and factors related to tRNA/mRNA maturation and ribosome protein modification. Moreover, two sequences with significant similarity to intronic regions of 18 S rRNA genes are encoded by the tupanviruses and highly expressed. In this translation-associated gene set, only the ribosome is lacking. At high multiplicity of infections, tupanvirus is also cytotoxic and causes a severe shutdown of ribosomal RNA and a progressive degradation of the nucleus in host and non-host cells. The analysis of tupanviruses constitutes a new step toward understanding the evolution of giant viruses.

[1] MEPHI, APHM, IRD 198, Aix Marseille Univ, IHU-Méditerranee Infection, 19-21 Bd Jean Moulin, 13005 Marseille, France. [2] Laboratório de Vírus, Instituto de Ciências Biológicas, Departamento de Microbiologia, Universidade Federal de Minas Gerais, Belo Horizonte 31270-901, Brazil. [3] CNRS, 13005 Marseille, France. [4] Laboratório de Microscopia Eletrônica e Virologia, Departamento de Biologia Celular, Instituto de Ciências Biológicas, Universidade de Brasília, Asa Norte, Brasília 70910-900, Brazil. [5] Lab. Biomass Conversion, Embrapa Pantanal, R. 21 de Setembro 1880, 79320-900 Corumbá/MS, Brazil. [6] Cell Biology and Metabolomics Platforms, Gustave Roussy Cancer Campus, Villejuif 94805, France. [7] Equipe 11 labellisée Ligue Nationale contre le Cancer, Centre de Recherche des Cordeliers, Paris 75006, France. [8] Institut National de la Santé et de la Recherche Médicale (INSERM), Paris 75654, France. [9] Université Paris Descartes, Sorbonne Paris Cité, Paris 75015, France. [10] Université Pierre et Marie Curie, Paris 75005, France. [11] Pôle de Biologie, Hôpital Européen Georges Pompidou, AP-HP, Paris 75015, France. [12] Department of Women's and Children's Health, Karolinska University Hospital, Stockholm SE-171 76, Sweden. Jônatas Abrahão, Lorena Silva and Ludmila Santos Silva contributed equally to this work. Correspondence and requests for materials should be addressed to D.R. (email: didier.raoult@gmail.com) or to B.S. (email: bernard.la-scola@univ-amu.fr)

Translation is one of the canonical frontiers between the cell world and the virosphere. Even the simplest non-viral obligatory intracellular parasites present a wealthy set of translation apparatus, including aminoacyl tRNA synthetases, tRNAs, peptide synthesis factors and ribosomal proteins[1–3]. The nature of the parasitism of the most of non-viral obligatory intracellular parasites relies on partial or severe deficiency of genes related to energy production. Although sharing a similar lifestyle with those organisms, the most of the virus lack not only energy production genes, but also translation-related genes[1–3].

In this context, the discovery of mimiviruses and other amoeba-infecting giant viruses surprised the scientific community due their unusual sizes and long genomes, able to encode from hundreds to thousands of genes, including tRNAs, peptide synthesis factors and, for the first time seen in the virosphere, aminoacyl tRNA synthetases (aaRS)[4]. Although the very first discovered mimivirus (*Acanthamoeba polyphaga mimivirus*) encodes four different types of aaRS (Arg, Cys, Met, TyrRS), other mimivirus isolates genomes were described, containing up to seven types of aaRS, as Megavirus chilensis and LBA111 (Arg, Asn, Cys, Ile, Met, Trp, TyrRS)[5]. While amoeba-infecting mimiviruses present up to six copies of tRNA, *Cafeteria roenbergensis virus* (CroV), a group II algae-infecting of *Mimiviridae*, encodes 22 sequences for five different tRNAs[5]. Even more surprisingly, metagenomics data reveal that klosneuvirus genome may encodes aaRS with specificities for 19 different amino acids, over 10 translation factors and several tRNA-modifying enzymes[6]. However, klosneuviruses were not isolated and therefore there is no data regarding important biological features as virus particles, morphogenesis and host-range.

Here we report the discovery of two Tupanvirus strains, the longest tailed *Mimiviridae* members isolated in amoebae. Their genomes are 1.44–1.51 Mb linear double-strand DNA coding for 1276–1425 predicted proteins. Tupanviruses share the same ancestors with mimivirus lineages and these giant viruses present the largest translational apparatus within the known virosphere, with up to 70 tRNA, 20 aaRS, 11 factors for all translation steps, and factors related to tRNA/mRNA maturation and ribosome protein modification. Moreover, two sequences with significant similarity to intronic regions of 18 S rRNA genes are encoded by the tupanviruses and highly expressed. In this translation-associated gene set, only the ribosome is lacking. Tupanvirus is also cytotoxic and causes a severe shutdown of ribosomal RNA and a progressive degradation of the nucleus in host and non-host cells. The analysis of tupanviruses constitutes a new step towards understanding the evolution of giant viruses.

Results

Tupanviruses description and cycle. While attempting to find new and distant relatives of currently known giant viruses, we performed prospecting studies in special environments. Soda lakes (Nhecolândia, Pantanal biome, Brazil) are known as environments that conserve and/or mimic ancient life conditions (extremely high salinity and pH) and are considered some of the most extreme aquatic environments on Earth[7]. We also prospected giant viruses in ocean sediments collected at a depth of 3000 m (Campos dos Goytacazes, Brazilian Atlantic Ocean).

Both in soda lake and deep ocean samples, we found optically visible *Mimiviridae* members that surprisingly harbored a long, thick tail (Fig. 1a, b) as they grew on *Acanthamoeba castellanii* and *Vermamoeba vermiformis*. We named these strains Tupanvirus soda lake and Tupanvirus deep ocean as a tribute to the South American Guarani Indigenous tribes, for whom Tupan—or Tupã—(the God of Thunder) is one of the main mythological figures. Electron microscopy analyses revealed a remarkable virion structure. Tupanviruses present a capsid similar to that of amoebal mimiviruses in size (~450 nm) and structure, including a stargate vertex and fibrils[8] (Figs. 1a–d, 2a–q). However, the Tupanvirus virion presents a large cylindrical tail (~550 nm extension; ~450 nm diameter, including fibrils) attached to the base of the capsid (Figs. 1b–d, 2a,i–k). This tail is the longest described in the virosphere[9]. Microscopic analysis suggests that the capsid and tail are not tightly attached (Figs. 1e, f, 2a, i; Supplementary Movies 1 and 2), although sonication and enzymatic treatment of purified particles were not able to separate the two parts (Fig. 2f–h). The average length of a complete virion is ~1.2 µm, although some particles can reach lengths of up to 2.3 µm because of the variation in the tail's size; this makes them the one of the longest viral particles described to date (Figs. 1, 2i–k). Furthermore, there is a lipid membrane inside the capsid, which is associated with the fusion with the cellular membrane and the release of capsid content (Fig. 1f). Tail content appears to be released after an invagination of the phagosome membrane inside the tail (Fig. 1e). In contrast

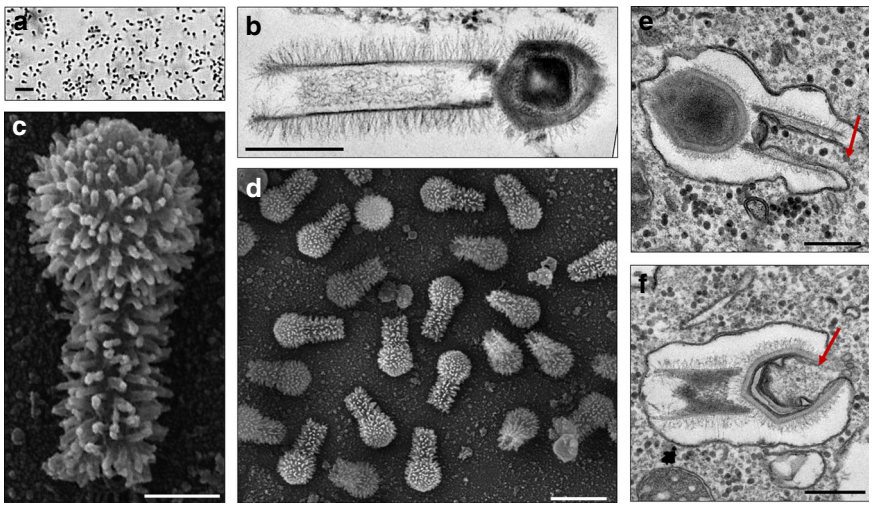

Fig. 1 Tupanvirus soda lake particles and cycle. **a** Optical microscopy of Tupanvirus particles after haemacolour staining (1000 ×). Scale bar, 2 µm. **b** Super particle (>1000 nm) observed by transmission electron microscopy (TEM). Scale bar, 500 nm. **c**, **d** Scanning electron microscopy (SEM) of Tupanvirus particles. Scale bars 250 nm and 1 µm, respectively. **e**, **f** The initial steps of infection in *A. castellanii* involve the release of both capsid (**e**) and tail (**f**) content into the amoeba cytoplasm (red arrows). Scale bars, 350 nm and 450 nm, respectively

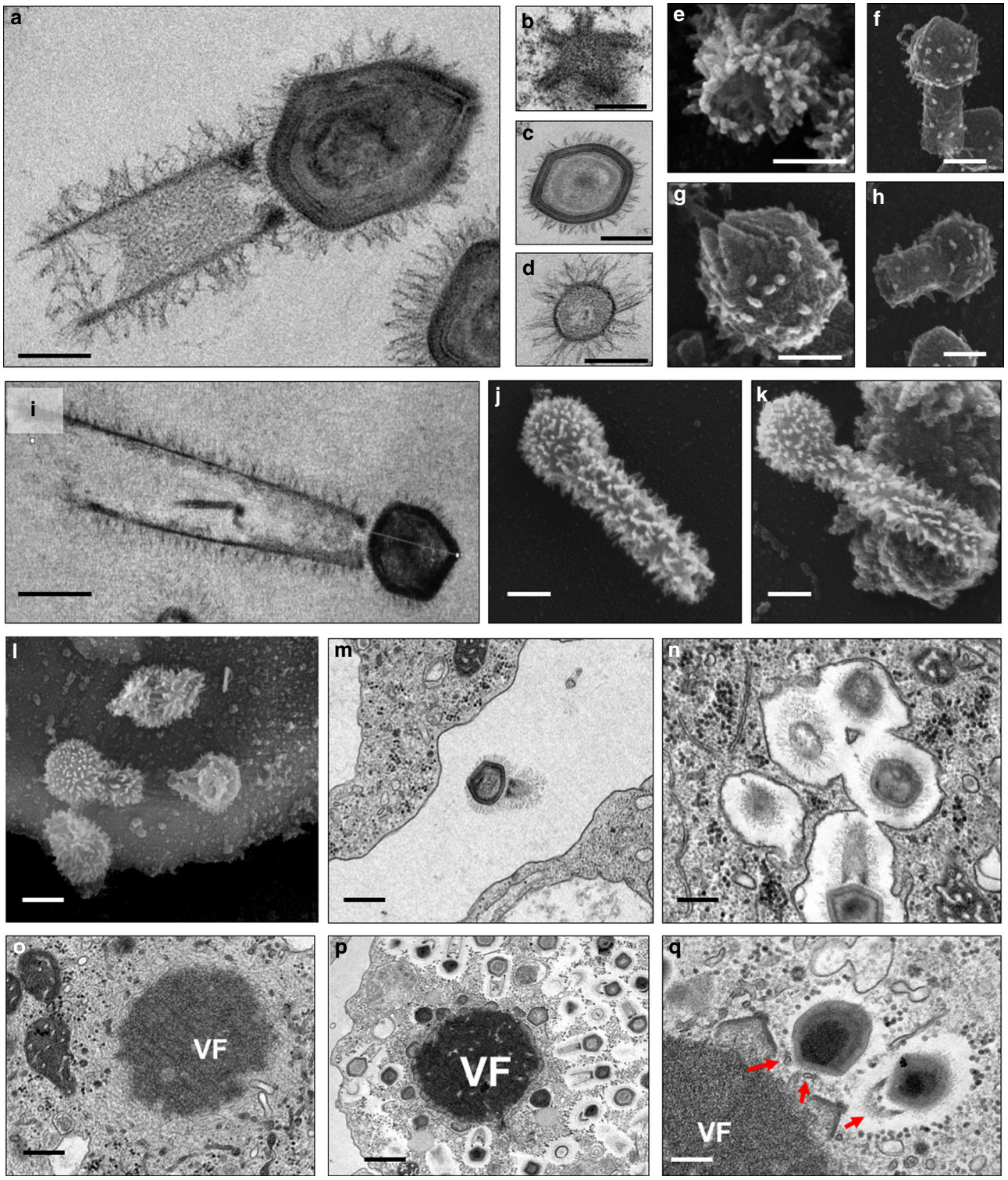

Fig. 2 Tupanvirus soda lake particles and cycle features. **a** Transmission electron microscopy (TEM) highlights the inner elements of the whole particle. Scale bar, 200 nm. **b** Star-gate vertex transversally cut. Scale bar, 100 nm. **c** Capsid transversally cut. Scale bar, 100 nm. **d** Tail transversally cut. Scale bar, 200 nm. **e**–**h** Scanning electron microscopy (SEM) of purified particles. Scale bars, 250 nm. The treatment of particles with lysozyme, bromelain and proteinase-K removed most of the fibers, revealing head and tail junction details. Super particles (>2000 nm) could be observed by TEM (**i**) and SEM (**j**, **k**). Scale bars, 400 nm. Cycle steps are shown from **l**–**r**. **l** Viral particle attachment to *Acanthamoeba castellanii* surface; scale bar, 500 nm; **m** phagocytosis; scale bar, 500 nm; **n** particles in a phagosome; scale bar, 500 nm; **o** early viral factory; scale bar, 500 nm; and **p**, **q** mature viral factories. Scale bars 1 µm and 250 nm, respectively. Arrows highlight tail formation associated with the viral factories. VF viral factory

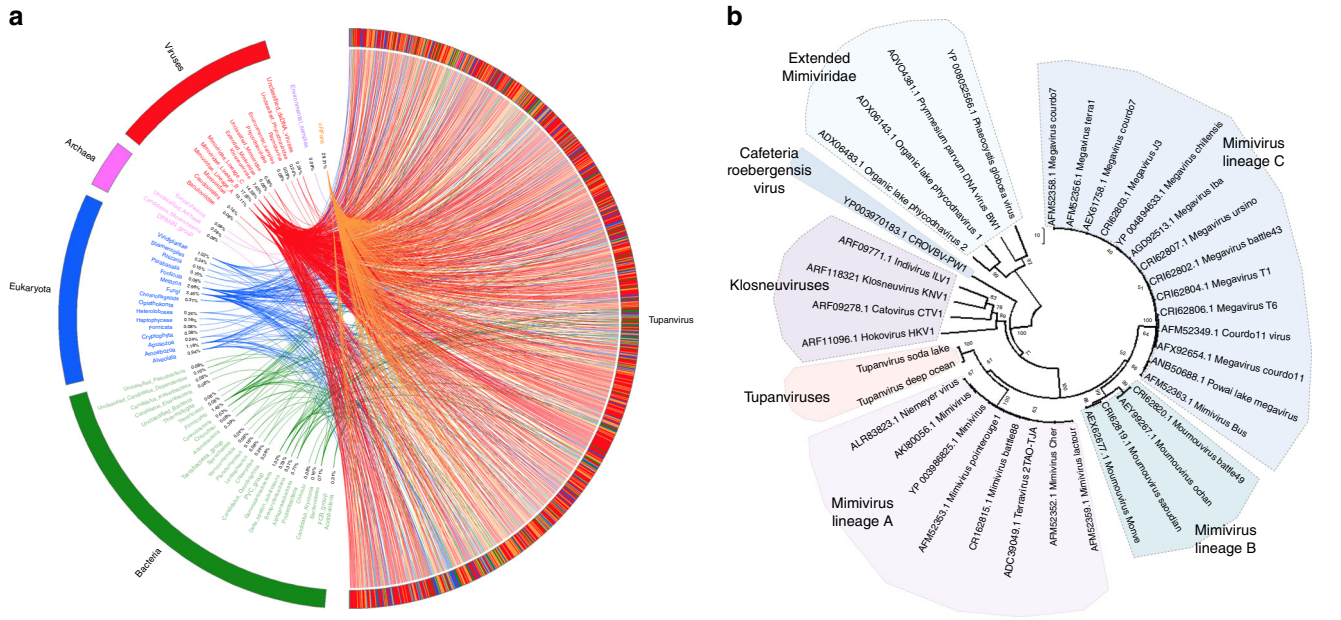

Fig. 3 Tupanvirus soda lake rhizome and Mimiviridae family B DNA polymerase tree. **a** The rhizome shows that most Tupanvirus soda lake genes have mimiviruses as best hits. However, correspondence among Tupanvirus and *Archaea*, *Eukaryota*, *Bacteria* and other viruses was also observed. **b** Family B DNA polymerase maximum likelihood phylogenetic tree demonstrating the position of Tupanvirus among *Mimiviridae* members, likely forming a new genus

to other giant viruses[10–14], Tupanviruses similarly replicate both in *A. castellanii* and *V. vermiformis*. Viral particles attach to the host-cell surface and enter through phagocytosis (1 h.p.i.) (Fig. 2 l,m,n). The inner membrane of the capsid merges with the amoebal host phagosome membrane, releasing the genome (2–6 h.p.i.) (Fig. 1f). A viral factory (VF) is then formed (7–12 h.p.i.)[15] where particle morphogenesis occurs (Fig. 2o–q; Supplementary Movies 1 and 2). During this step, the virion tail is attached to the capsid after its formation and closure. Later in the process (16–24 h.p.i.), the amoebal cytoplasm is filled with viral particles, followed by cell lysis and the release of viruses (Supplementary Fig. 1). This nucleus-like viral factory has also recently been reported in bacteria and fuels the concept of a virocell[16,17]. In that perspective, viral factories actively producing the progeny could be considered as the nuclei of virocells[16,17].

The genomes of tupanviruses. The tupanvirus soda lake and tupanvirus deep ocean genomes (GenBank accession number KY523104 and MF405918) are linear dsDNA molecules measuring 1,439,508 bp and 1,516,267 bp (GC% ~28%), respectively—the fourth largest viral genomes described to date[10,18]—containing a total of 1276 and 1425 predicted ORFs, 375 and 378 of which are ORFans (ORFs with no matches in current databases), respectively. To date, the largest genomes belong to pandoravirus isolates, and the largest one, *P. salinus*, has 2,473,870 bp and encodes 2,556 putative proteins[10]. The rhizome[19] of tupanvirus (graphical representation of gene-by-gene best hits) revealed sequences from mimiviruses of amoebae (~42%) and klosneuviruses (~8%) as their main best hits. Other best hits were mostly sequences from eukaryotes (~11%) and bacteria (~8%) (Fig. 3a; Supplementary Fig. 2A). Tupanviruses exhibited relatively close numbers of best matches to amoebal mimiviruses from lineages A (~10%), B (~18%) and C (~14%). These data and phylogenetic analyses demonstrate that they cluster with amoebal mimiviruses, suggesting that tupanviruses are distant relatives of, and comprise a sister group to, mimiviruses of amoeba (Figs. 3b, 4a). The 'AAAATTGA' promoter motif was found ~410 times in Tupanvirus deep ocean intergenic regions, a frequency similar to that of other *Mimiviridae* members, and ~600% more frequent than those coding regions ($p < 10^{-95}$, Fisher exact test)[20–22] (Fig. 4b). The pangenome of the family *Mimiviridae*, when taking into account the gene contents of tupanviruses, klosneuviruses and distant relatives to amoebal mimiviruses, was found by Proteinortho to comprise 8,753 groups of orthologues ($n = 3588$) or virus unique genes ($n = 5165$). A total of 189 groups were shared by at least one tupanvirus; one mimivirus of *Acanthamoeba* of each lineage A, B and C; and one klosneuvirus, and 100 of them were also shared with Cafeteria roenbergensis virus. In addition, a total of 757 groups were shared by a tupanvirus and at least another mimivirus: 477 were shared with Megavirus chiliensis, 434 with Moumouvirus, 431 with Mimivirus, 287 with Klosneuvirus, 126 with Cafeteria roenbergensis virus, and 59 with Phaeocystis globosa virus 12 T. Among these 757 groups, 583 corresponded to clusters of orthologous groups previously delineated for mimiviruses[19]. Finally, a total of 775 tupanvirus genes were absent from all other mimivirus genomes (Supplementary Data 1).

Proteomic analysis. Proteomic analysis of Tupanvirus soda lake particles revealed 127 proteins, nearly half (67/127 = 52.8%) of which are unknown and eight of which are encoded by ORFans (11/127 = 8.6%) (Supplementary Data 2; Supplementary Note 1). Although 62 Tupanvirus virion proteins homologous were not found by proteomics, either in Mimivirus or in *Cafeteria roenbergensis virus* particles, there are no distinct clues about which protein (s) could be associated with the tupanvirus fibrils and tail structure.

The most complete translational apparatus of the virosphere. Analyses of the tupanvirus gene sets related to energy production revealed a clear dependence of these viruses on host energy production mechanisms, similarly to other mimiviruses, because genes involved in glycolysis, the Krebs cycle and the respiratory chain are mostly lacking[22–24]. Astonishingly, Tupanvirus soda lake and Tupanvirus deep ocean exhibit the largest viral sets of genes involved in translation, with 20 ORFs related to aminoacylation (aaRS) and transport, and 67 and 70 tRNA associated with 46 and 47 codons, respectively (Fig. 5a; Supplementary

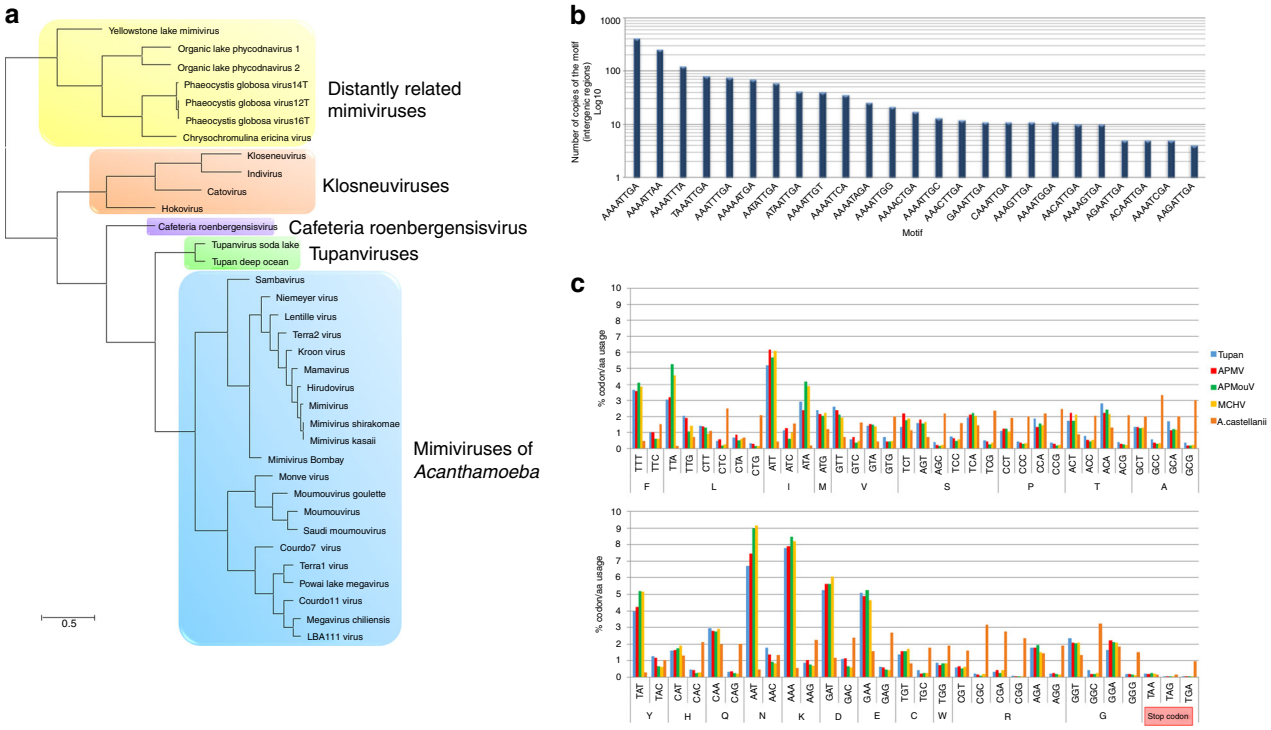

Fig. 4 Tupanvirus soda lake hierarchical clustering, promoter's motifs and amino-acid usage analysis. **a** Hierarchical clustering tree based on presence-absence matrix of cluster of orthologous genes shared by *Mimiviridae* members. **b** Frequency of mimivirus AAAATTGA canonical promoter motifs in Tupanvirus intergenic regions. We also analyzed the presence of the AAAATTGA motif with SNPs, considering each motif position. **c** Comparative amino-acid usage analysis of Tupan, *A. castellanii* and mimivirus lineages **a**, **b** and **c**. The amino-acid usage for protein sequences was calculated using the CGUA (General Codon Usage Analysis) tool

Fig. 2B, C, 3 and 7; Supplementary Datas 3 and 4). Tupanvirus deep ocean encodes an ambiguous tRNA related to the rare amino-acid pyrrolysine. Only selenocysteine-related genes are lacking, as previously observed for many cellular organisms[25]. Several translation factors were identified, including eight translation initiation factors (IF2 alpha, IF2 beta, IF2 gamma, IF4e (2 copies in Tupanvirus soda lake), IF5a (2 copies in Tupanvirus deep ocean), SUI1, IF4a), one elongation/initiation factor (GTP-binding elongation/initiation), one elongation factor (Ef-aef-2), and one release factor (ERF1) (Fig. 5a; Supplementary Fig 2B, C and 3; Supplementary Datas 3 and 4). Furthermore, we detected additional translation-related genes: factors related to tRNA maturation and stabilization (tRNA nucleotidyltransferase, tRNA guanylyltransferase, cytidine deaminase, RNA methyl transferase); mRNA maturation (poly(A) polymerase, mRNA capping enzyme) and splicing (RNA 2—phosphotransferase Tpt1 family protein); and ribosomal protein modification (ribosomal-protein-alanine N-acetyltransferase, FtsJ-like methyl transferase) (Fig. 5a; Supplementary Fig 2B; Supplementary Datas 3, 4). Phylogenies based on aaRS are acknowledged to be complex as they depend on sequence sampling, and natural and canonical taxonomical groups can be separated into different clades, as previously observed[6]. To reduce such disturbances in the trees during their construction, we selected the 100 best hits related to Tupanvirus soda lake, plus the sequences of 5–10 amoebozoa and those of klosneuviruses. In most of the trees, sequences from natural clades were clustered together, although some amoebozoa were separated into different clusters. Based on the 20 aaRS trees, it is not possible to state that the origin of most of these tupanvirus aaRS genes is cellular (Supplementary Fig. 4). Furthermore, the mosaic structure of aaRS gene reinforced the difficult to state on the origin of these genes, as illustrated in Supplementary Fig. 5. This contrasting result to that reported by Schultz et al.[6], 2017 for klosneuviruses may also be explained by the different sampling used for alignments and trees construction. In addition, the codon and amino-acid usage of tupanviruses is substantially different from that of *Acanthamoeba* spp. In tupanviruses, we observed a high correlation between tRNA isoacceptors and the most used codons, as these viruses present more tRNA isoacceptors for highly abundant codons (Fig. 4c; Supplementary Figs. 2C and 3). Surprisingly, we found two different copies of an 18 S rRNA intronic region in tupanviruses (Supplementary Fig. 6; Fig. 6a–e). In fact, such 18 S rRNA intronic regions are widespread in all mimiviruses (lineages A and B present only one copy in an intronic region and next to a self-splicing group I intron endonuclease) but are not found in klosneuviruses. Phylogenetic analyses revealed that the two copies found in tupanviruses had separate and different origins (Fig. 6f). Although Tupanvirus 18 S rRNA intronic sequences are located in intergenic regions, qPCR and FISH demonstrated that Tupanvirus soda lake 18 S rRNA intronic sequences are highly expressed during the entire replicative cycle but particularly during intermediate and late phases (6 and 12 h post-infection) (Fig. 7a; Supplementary Fig. 8). Furthermore, Tupanvirus soda lake is more tolerant to the translation-inhibiting drugs geneticin and cycloheximide than Mimivirus, an impressive characteristic considering the natural ribosomal RNA shutdown it performs in the permissive host (Fig. 8h). The functions of these 18 S rRNA intronic region sequences require further clarification. No exonic region of 18 S rRNA was found in the genomes of tupanviruses or any previously described mimivirus. The comparison between contents in translation-related categories of genes present in tupanviruses and cellular organisms reveals that tupanviruses present a richer gene set than *Candidatus Carsonella ruddii* (*Bacteria*) and *Nanoarchaeum equitans* (*Archaea*) (not considering ribosomal proteins). Tupanvirus deep ocean has even

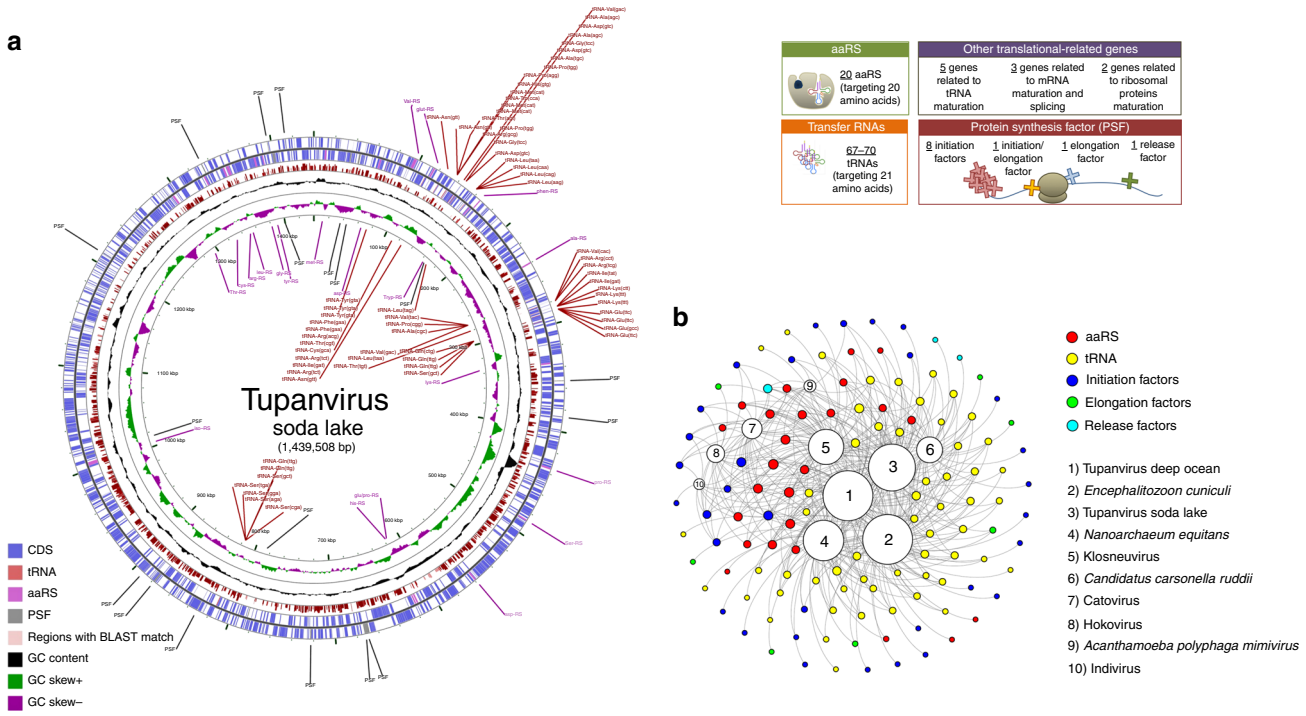

Fig. 5 Tupanvirus genome-translation-related factors. **a** Circular representation of Tupanvirus soda lake genome highlighting its translation-related factors (aaRS, tRNAs and PSF). The box (upright) summarizes this information and considers the Tupanvirus deep ocean data set. **b** Network of shared categories of translation-related genes (not considering ribosomal proteins) present in tupanviruses, Mimivirus (APMV), Klosneuvirus, Catovirus, Hokovirus, Indivirus and cellular world organism—*Encephalitozoon cuniculi* (*Eukaryota*), *Nanoarchaeum equitans* (*Archaea*) and *Candidatus Carsonella ruddii* (*Bacteria*). The diameter of the organism's circles (numbers) is proportional to the number of translation-related genes present in those genomes. CDS coding sequences, tRNA transfer RNA, aaRS aminoacyl tRNA synthetase, PSF protein synthesis factors

more such genes than *Encephalitozoon cuniculi*, a eukaryotic organism (Fig. 5b). Even if the impressive translation gene set recently described for klosneuviruses is taken into account, tupanviruses are the first viruses reported to harbor the complete set of the 20 aaRS (Fig. 5; Supplementary Figs. 3, 6 and 7).

Host range and host-ribosomal shutdown characterization. In contrast to other mimiviruses, Tupanvirus soda lake was able to infect a broad range of protist organisms in vitro. Surprisingly, we observed four distinct profiles of infectiveness: (i) productive cycle in permissive cells; (ii) abortive cycle; (iii) refractory cells; and (iv) most surprisingly, non-host cells exhibiting a cytotoxic phenotype in the presence of Tupanvirus without multiplication, a circumstance never previously reported—to the best of our knowledge (Supplementary table 1; Supplementary Notes 1). This latter profile was intriguing because toxicity was observed in *Tetrahymena* sp., a ravenous free-living protist[26]. This unusual phenotype was also observed in *A. castellanii* but only at higher multiplicities of infection (50 and 100; Fig. 8a). No such cytotoxicity was observed for Mimivirus (Fig. 8a). This toxic profile associated specifically with Tupanvirus appears to be related to shutting down host ribosomal RNA abundance, insofar that Tupanvirus leads to a reduction of host rRNA amounts by a mechanism not related to the canonical ribophagy/autophagy process (Figs. 7b–d, 8b–d; Supplementary Fig. 9). A remarkable acidification of amoebal cytoplasm is induced by Tupanvirus infection (but not mimivirus) (Fig. 7b; Supplementary Fig. 9A, B). The treatment of acanthamoeba with chloroquine, a lysosomal toxin, or bafilomycin did not prevent the Tupanvirus-induced rRNA shutdown (Supplementary Fig. 9A, C–H). Transfection with an siRNA targeting Atg8-2, a protein required for ribophagy/autophagy, failed to prevent Tupanvirus-induced ribosomal shutdown in *A. castellanii* (Fig. 7c, d). Transmission electron microscopy (TEM) of vesicles containing ribosomes after Tupanvirus infection (2 h.p.i.) revealed that these structures were formed close to the nuclear membrane after invagination and engulfment of ribosomes, mostly by single-membrane vesicles, rarely by double-membrane vesicles (Fig. 7e). These small vesicles then aggregated, accumulating more ribosomes and forming large structures containing ribosomes (Fig. 8d), which were fully depleted from the amoebal cytoplasm 6–9 h.p.i, when strong cellular rRNA shutdown could be detected (Fig. 8c). In addition, Tupanvirus infection induces nuclear/nucleolar progressive degradation, which is temporally associated with cellular rRNA shutdown (Fig. 7f). Mimivirus infection also caused changes in nucleolus architecture, but such alterations were not comparable to those observed upon Tupanvirus infection (Fig. 7e, f). Although the formation of vesicles containing ribosomes and nuclear degradation can be related to cellular rRNA shutdown during Tupanvirus infection, the mechanisms involved in cellular rRNA degradation after the formation of large vesicles containing ribosomes remain to be investigated. One possibility that should be explored is that Tupanvirus might preferentially target some ribosomes to favor the translation of its own (as opposed to cellular) proteins, as previously described for poxviruses[27].

The toxicity effect and rRNA shutdown are independent of Tupanvirus replication; instead, they are caused by the viral particle (Fig. 8e–g). UV-light-inactivated particles continued to induce the depletion of *Acanthamoeba* rRNA (Fig. 8g). Although Tupanvirus is not able to replicate within *Tetrahymena* sp., it is phagocytosed in a voracious manner (as are other available macromolecular structures) and forms large intracellular vesicles, where the capsid and tail release their content inside the protist cytoplasm (Fig. 8i–k). The virus induces gradual vacuolization (Fig. 8i), loss of motility, a decrease in the phagocytosis rate

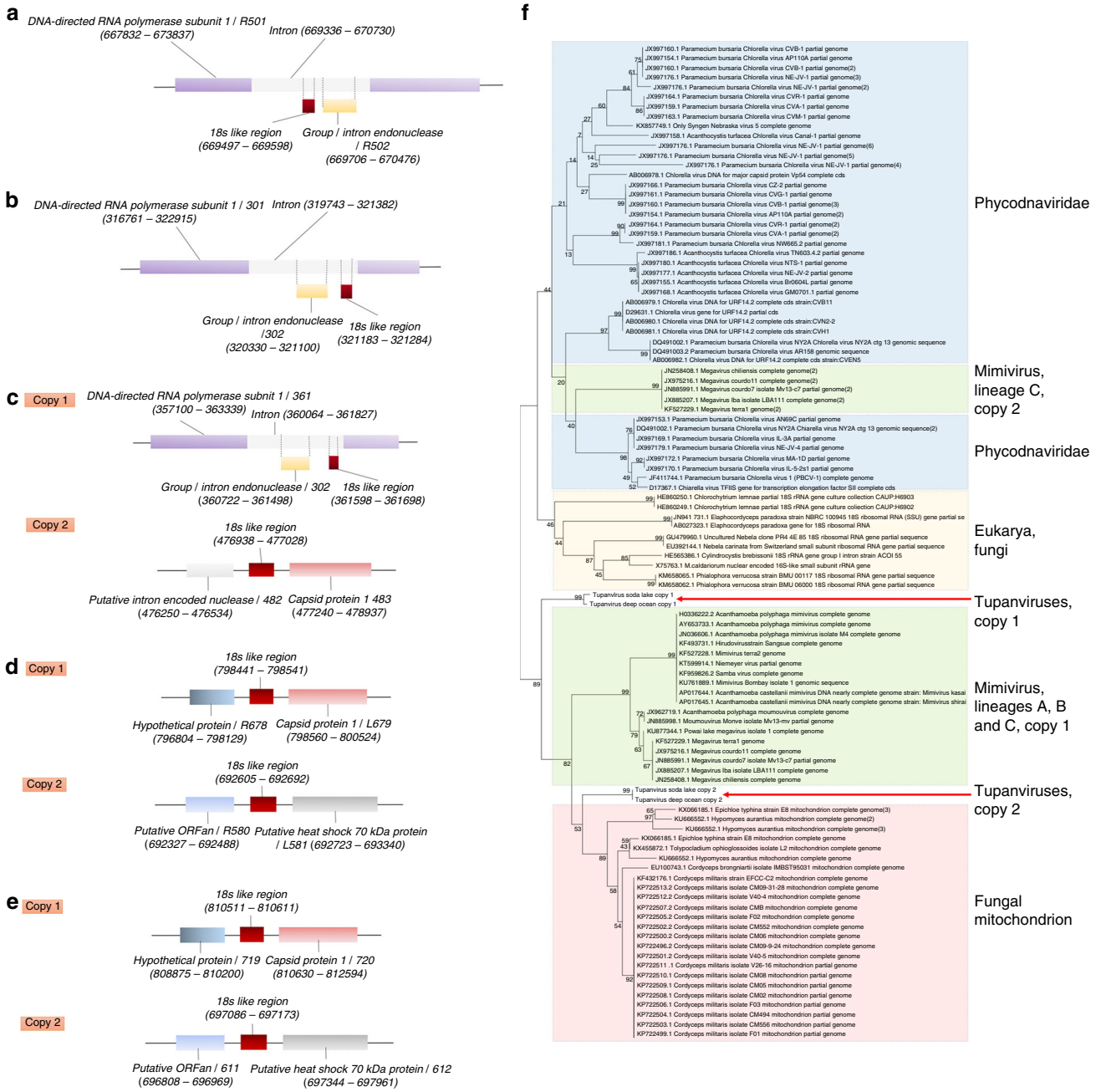

Fig. 6 Adjacent regions of 18S rRNA intronic sequences in the genus *Mimivirus* and Tupanvirus and maximum likelihood phylogenetic tree of 18S rRNA intronic region. Core sequences are represented for lineages A (**a**), B (**b**), C (**c**), Tupanvirus soda lake (**d**) and Tupanvirus deep ocean (**e**). Phylogenetic tree of 18S rRNA intronic region present in mimivirus (**e**), *Phycodnaviridae*, eukaryotes and fungi mitochondrion

(Fig. 8m), a decrease in rRNA abundance (Fig. 8l) and triggers nuclear degradation (Fig. 7g), similar to the effects observed in *A. castellanii* cells with high multiplicities of infection (Fig. 8a–d). We performed in vitro simulations to determine whether this toxicity could affect the maintenance of Tupanvirus populations in a solution containing both *Tetrahymena* and *Acanthamoeba*. Our data suggest that at M.O.I. of 10 the reduction of the physiological activity of *Tetrahymena* sp., a (non-host) predator, decreases the ingestion of Tupanvirus particles (Fig. 8n), improving their chances to find its host, *Acanthamoeba*, and keeping viral titers constant in the system. In contrast, mimivirus particles, which do not present any toxicity to *Tetrahymena* sp., are quickly predated, and the virus is eliminated from the system after some days (Fig. 8n). Although we have no clues about the hosts of tupanviruses at their original habitats nor if such high M. O.I. would be expected in nature, to our knowledge, a viral particle responsible for the modulation of host and non-host organisms independent of viral replication has not been previously described.

Discussion

Considering that tupanviruses comprise a sister group to amoebal mimiviruses, we can hypothesize that the ancestors of these clades of *Mimiviridae* could had a more generalist lifestyle and were able to infect a wide variety of hosts. In this view, the ancestors of tupanviruses (and maybe of amoebal mimiviruses) might have already been giant viruses that underwent reductive evolution,

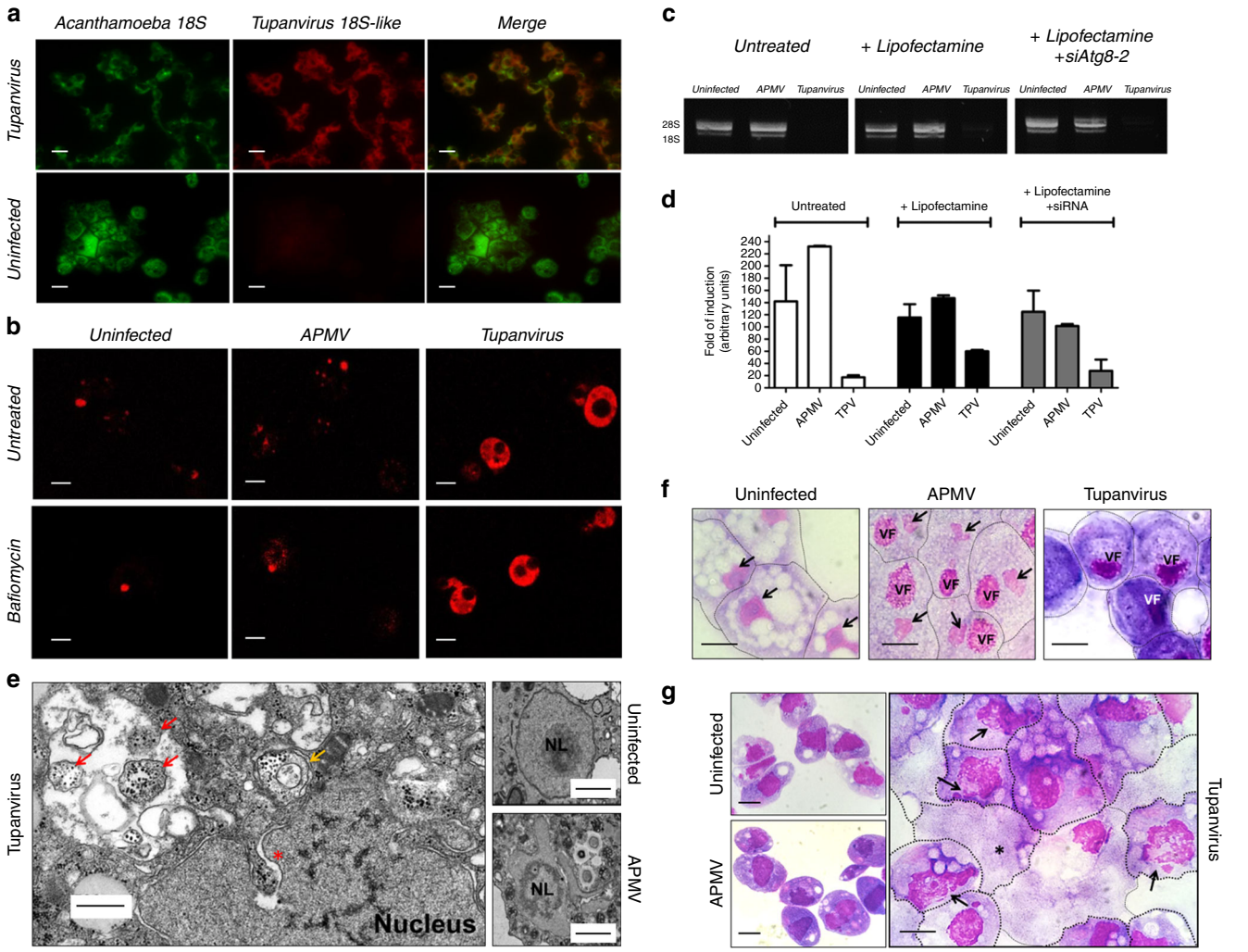

Fig. 7 Tupanvirus soda lake biological features in a host (*A. castellanii*) and non-host (*Tetrahymena* sp.). **a** Expression of Tupanvirus 18S intronic sequence-copy 1 transcript, 12 h post-infection observed by fluorescence in situ hybridization (FISH) (red). Tupanvirus-induced shutdown of *A. castellanii* ribosomal RNA18S transcripts (green). Scale bars, 10 µm. **b** Tupanvirus, but not mimivirus, induces strong acidification of *A. castellanii* cytoplasm (9 h.p.i.), even in the presence of bafilomycin A1. Scale bars, 10 µm. **c**, **d** The silencing of the canonical autophagy protein Atg8-2 does not prevent rRNA shutdown induced by Tupanvirus infection. Error bars, standard deviation. **e** Electron microscopy of *A. castellanii* infected by Tupanvirus (2 h.p.i.), highlighting the degradation of the nucleolus, nuclear disorganization and the formation of ribosome-containing vesicles near nuclear membranes. Scale bar, 500 nm. Red arrow: single-membrane vesicles containing ribosomes; orange arrow: double-membraned vesicles containing ribosomes; asterisk: ribosomes wrapping by the external nuclear membrane. Right: electron microscopy of uninfected amoebae and APMV infected cell (8 h.p.i.) showing a mild nucleolar disorganization in the presence of the virus. Scale bars: 1 µm. **f** Haemacolour staining showing the nuclear degradation of *A. castellanii* induced by Tupanvirus infection (9 h.p.i.) compared with infection by mimivirus (APMV) and uninfected cells. Tupanvirus-infected cells are purplish because of cytoplasm acidification. Scale bars, 5 µm. Arrows: nucleus, when present; VF: viral factory. **g** Haemacolour staining showing the nuclear degradation in *Tetrahymena sp.* induced by Tupanvirus infection (4 days post-inoculation) compared with mimivirus (APMV)-inoculated cells and uninfected cells. Tupanvirus-infected cells present an atypical shape and intense vacuolization, and some cells lack a nucleus (asterisk). Arrows: nucleus under degradation. Scale bars, 5 µm. The experiments were performed 3 times independently, with two replicates each

although some genes could have been acquired over time, as previously hypothesized for other mimiviruses[5,23,28,29]. A reductive evolution pattern is typical among obligatory intracellular parasites[30–32]. In these cases, the organisms lose genes related to energy production, which is one of the main reasons for their obligatory parasitic lifestyle. In an alternative scenario, a simpler ancestor could had substantially acquired genes over time and became more resourceful, being able to infect a broader host range[5,33]. Nevertheless, tupanvirus presents the most complete translational apparatus among viruses, and its discovery takes us one step forward in understanding the evolutionary history of giant viruses.

Methods

Virus isolation and host-range determination. In April 2014, a total of 12 sediment samples were collected from soda lakes in Southern Nhecolândia, Pantanal, Brazil. In 2012, 8 ocean sediments samples were collected from 3000 meters below water line surface at Bacia de Campos, in Campos dos Goytacazes, Rio de Janeiro, Brazil. The collection was performed by a submarine robot, during petroleum prospection studies performed by the Petrobras Company, and kindly provided to our group. The samples were stored at 4 °C until the inoculation process. The samples were transferred to 15 mL flasks, and 5 mL of Page's Amoebae Saline (PAS) was added. The solution was stored for 24 h to decant the sediment. The liquid was then subjected to a series of filtrations: first through paper filter and then through a 5 µm filter to remove large particles of sediment and to concentrate any giant viruses present. For co-culture, the cells used were *A. castellanii* (strain NEFF) and *V. vermiformis* (strain CDC 19), purchased from ATCC. These cell strains

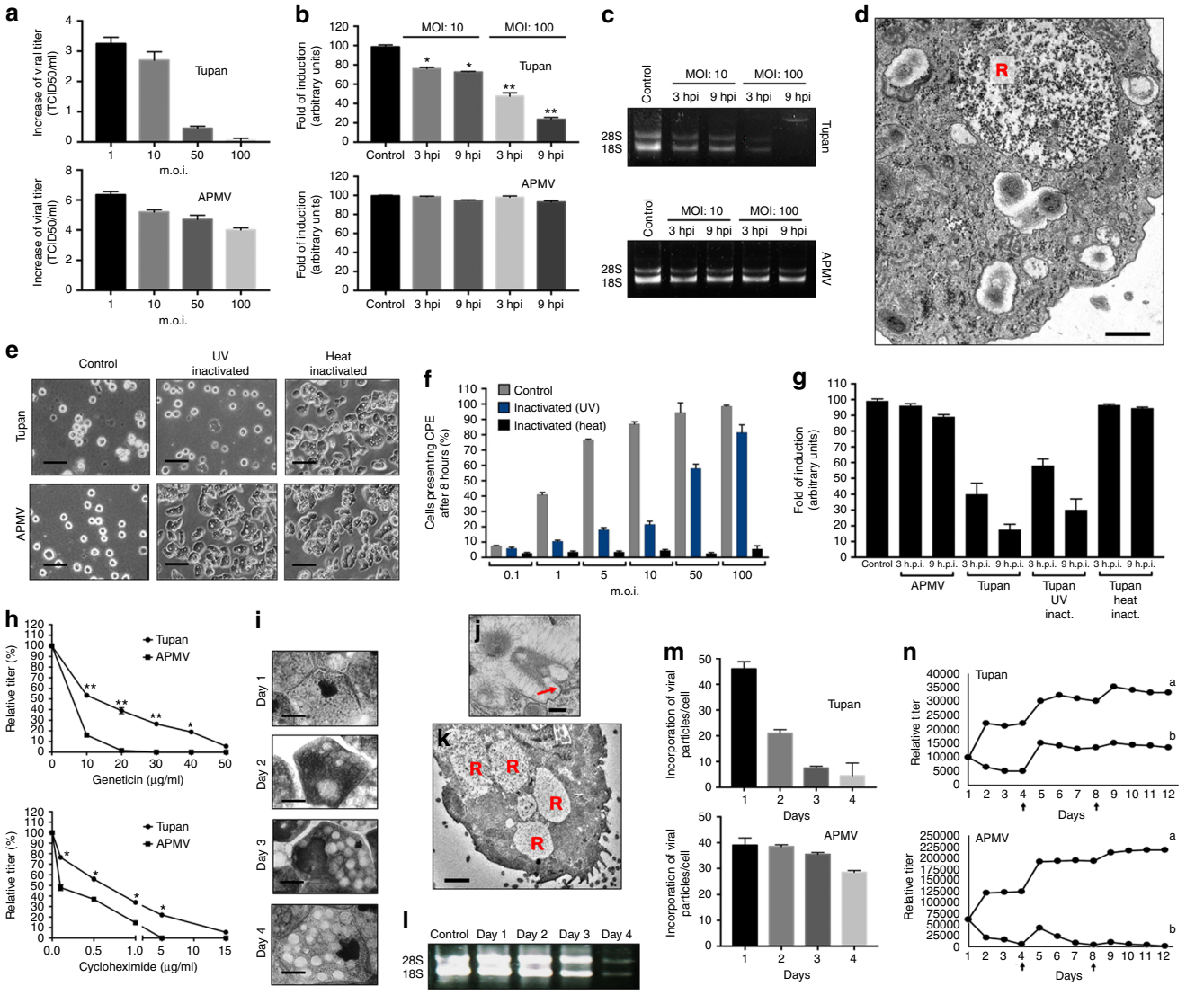

Fig. 8 rRNA shutdown induced by Tupanvirus and toxicity assays. **a** Tupanvirus and mimivirus titers (log_{10} values) 24 h.p.i. in *Acanthamoeba castellanii* at distinct MOIs. **b** Ribosomal 18S RNA relative measure by qPCR from *A. castellanii* infected by tupanvirus or mimivirus at an MOI of 10 or 100, 3 and 9 h post-infection. **c** Electrophoresis gel showing ribosomal 18S and 28S RNA from *A. castellanii* under the same conditions described in **b**. **d** Vesicle containing a large amount of *A. castellanii* ribosomes (R) 6 h after Tupanvirus infection. Scale bar, 1 μm. (**e**) Cytopathic effect of *A. castellanii* inoculated with Tupanvirus or mimivirus after UV or heat inactivation, MOI of 100, 8 h post-inoculation. Scale bar, 20 μm. **f** Counting of *A. castellanii* presenting cytopathic effect 8 h post-inoculation with tupanvirus inactivated by UV or heating under different MOIs. **g** Ribosomal 18S RNA relative measure by qPCR from *A. castellanii* infected by UV-inativated or heat-inactivated Tupanvirus, or APMV, at an MOI of 100, 3 and 9 h post-infection. **h** Dose-response of Tupanvirus and APMV in *A. castellanii* pre-treated with distinct doses of geneticin or cycloheximide. (**i**) Progressive vacuolization of tetrahymena after infection with Tupanvirus (days 1–4). Scale bars, 10 μm. **j** Tupanvirus tail content releasing in tetrahymena 1 h post-inoculation (TEM). Scale bar, 200 nm. **k** Vesicles containing large amounts of *Tetrahymena* ribosomes (R) after Tupanvirus infection. Scale bar, 3.5 μm. **l** Electrophoresis gel showing rRNA shutdown in tetrahymena inoculated with Tupanvirus at an MOI of 10 (days 1–4). **m** Rate of particles incorporation per tetrahymena cell (days 1–4). **n** Simulations showing the decrease in APMV and maintenance of Tupanvirus populations over the analyzed days after infection of a mix of *Acanthamoeba castellanii* and tetrahymena at an MOI of 10 (lines indicated by 'b' in both graphs of **n**). At days 4 and 8, fresh PYG medium and 10^5 *A. castellanii* were added to the systems (arrows). For the negative control of this experiment we pre-treated tetrahymena with 20 μg/ml of geneticin (lines indicated by 'a' in both graphs of **n**). In this case, both APMV and Tupanvirus were able to grow in the system. Statistical analyses in **b** and **h**: t-test based on control groups (**b**) or corresponding virus/drug concentrations (**h**). *:$p < 0.05$; **:$p < 0.01$. The experiments were performed 3 times independently, with two replicates each. Error bars (**a**, **b**, **f**, **g**, **h**, **m** and **n**), standard deviation

were stored in 75 cm^2 cell culture flasks containing 30 mL of peptone yeast extract glucose medium (PYG) at 28 °C. After 24 h of growth, cells were harvested and pelleted by centrifugation. The supernatant was removed, and the amoebae were resuspended three times in sterile PAS. After the third washing, 500,000 *A. castellanii* or *V. vermiformis* were resuspended in PAS or TS solutions and seeded in 24-well plates. The amoebae suspensions were added to an antibiotic mix containing ciprofloxacin (20 μg/mL; Panpharma, Z.I., Clairay, France), vancomycin (10 μg/mL; Mylan, Saint-Priest, France), imipenem (10 μg/mL; Mylan, Saint-Priest, France), doxycycline (20 μg/mL; Mylan, Saint-Priest, France), and voriconazole (20 μg/mL; Mylan, Saint-Priest, France). Each 100 μL of sample was mixed and inoculated in the numbered (1–12) wells and incubated at 30 °C in a humid chamber. A negative control was used in each plate. The wells were observed daily under an optical microscope. After 3 days, new passages of the inoculated wells were performed in the same manner until the third passage. In this passage, the content of the wells presenting lysis and cytopathic effects were collected and stored for production and analysis of the possible isolates by haemacolour staining and electron microscopy using the negative stain technique. Of the twelve tested samples from Pantanal, we found Tupanvirus (soda lake) in three. In only one

ocean sample we did isolate Tupanvirus (deep ocean). To evaluate the Tupanvirus soda lake host range, a panel of cell lines was subjected to virus infection at an multiplicity of infection (MOI) of 5: *Acanthamoeba castellanii* (ATCC30010), *Acanthamoeba royreba* (ATCC30884), *Acanthamoeba griffin* (ATCC50702), *Acanthamoeba* sp. E4 (IHU isolate), *Acanthamoeba* sp. Micheline (IHU isolate), *Vermamoeba vermiformis* (ATCC50237), *Dictyostelium discoideum* (ATCC44841), *Willartia magna* (ATCC50035), *Tetrahymena hyperangularis* (ATCC 50254), *Trichomonas tenax* (ATCC 30207), RAW264.7 (Mouse leukemic monocyte-macrophage) (ATCCTIB71) and THP-1 (human monocytic cell line) (ATCCTIB202). Cell lines were tested for mycoplasma. The assays were carried out in 24-well plates, and cells were incubated for 24 or 48 h. The tupanvirus titer was measured in *A. castellanii* by end-point and calculated by the Reed-Muench method[34]. In parallel, the samples were subjected to qPCR, targeting the tupanvirus tyrosyl RNA synthetase (5′-CGCAATGTGTGGAGCCTTTC-3′ and 5′-CCAAGA-GATCCGGCGTAGTC-3′) and aiming to verify viral genome replication (Biorad, CA, USA). Tupanvirus was propagated in 20 *A. castellanii* 175 cm^2 cell culture flasks in 50 mL PYG medium. The particles were purified by centrifugation through a sucrose cushion (50%), suspended in PAS and stored at −80 °C. Purified particles were used for genome sequencing, proteomic analysis[10], and microscopic and biological assays.

Cycle and virion characterization. All biological tests were performed with Tupanvirus soda lake only. To investigate the viral replication cycle by TEM, 25 cm^2 cell culture flasks were filled with 10×10^6 *A. castellanii* per flask, infected by Tupanvirus at a multiplicity of infection of 10 and incubated at 30 °C for 0, 2, 4, 6, 8, 12, 15, 18, and 24 h. One hour after virus-cell incubation, the amoeba monolayer was washed three times with PAS buffer to eliminate non-internalized viruses. A total of 10 mL of the infected cultures was distributed into new culture flasks. A culture flask containing only amoeba was used as the negative control. The infected cells and control sample were fixed and prepared for electron microscopy[14]. For immunofluorescence, *A. castellanii* cells were grown, infected by Tupanvirus at a multiplicity of infection of 1 as described and added to coverslips for 0, 2, 4, 6, 8, 12, 15, 18, and 24 h. After infection, the cells were rinsed in cold phosphate-buffered saline (PBS) and fixed with 4% paraformaldehyde (PFA) in PAS for 10 mins. After fixation, cells were permeabilized with 0.2% Triton X-100 in 3% bovine serum albumin (BSA)–PAS for 5 min, followed by rinsing with 3% BSA–PBS three times. Cells were then stained for 1 h at room temperature with an anti-tupanvirus antibody produced in mice (According Aix Marseille University ethics committee rules). After incubation with an anti-mouse secondary antibody, fluorescently labeled cells were viewed using a Leica DMI600b microscope. For Tupanvirus virion characterization, we also used scanning electron microscopy (SEM)[35]. Chemical treatment with proteases and sonication was performed as described elsewhere[35] to investigate fiber composition and the attachment between capsid and tail. For tomography videos, tilt series were acquired on a Tecnai G2 transmission electron microscope (FEI) operated at 200 keV and equipped with a 4096×4096 pixel resolution Eagle camera (FEI) and Explore 3D (FEI) software. The tilt range was 100°, scanned in 1° increments. The magnification ranged between 6,500 and 25,000, corresponding to pixel sizes between 1.64 and 0.45 nm, respectively. The image size was $4,096 \times 4,096$ pixels. The average thickness of the obtained tomograms was 298 ± 131 nm ($n = 11$). The tilt series were aligned using ETomo from the IMOD software package (University of Colorado, USA) by cross-correlation (http://bio3d.colorado.edu/imod/). The tomograms were reconstructed using the weighted-back projection algorithm in ETomo from IMOD. ImageJ software was used for image processing.

Genomes sequencing and analyses. The tupanviruses genomes were sequenced using an Illumina MiSeq instrument (Illumina Inc., San Diego, CA, USA) with the paired end application. The sequence reads were assembled de novo using ABYSS software and SPADES, and the resulting contigs were ordered by the Python-based CONTIGuator.py software. The obtained draft genomes were mapped back to verify the read assembly and close gaps. The best assembled genome was retained, and the few remaining gaps (three) were closed by Sanger sequencing. The gene predictions were performed using the RAST (Rapid Annotation using Subsystem Technology) and GeneMarkS tools. Transfer RNA (tRNA) sequences were identified using the ARAGORN tool. The functional annotations were inferred by BLAST searches against the GenBank NCBI non-redundant protein sequence database (nr) (e-value $< 1 \times 10^{-3}$) and by searching specialized databases through the Blast2GO platform. Finally, the genome annotation was manually revised and curated. The predicted ORFs that were smaller than 50 amino acids and had no hits in any database were ruled out. Tupanvirus codon and aa usages were compared with those of *A. castellanii* and other lineages of mimiviruses. Sequences were obtained from NCBI GenBank and subjected to CGUA (General Codon Usage Analysis). The global distribution of Tupanvirus tRNAs was analyzed and compared manually with viral aa usage considering the corresponding canonical codons related to each aa. Phylogenetic analyses were carried out based on the separate alignments of several genes, including family B DNA polymerase, 18 S rRNA intronic regions (copies 1/2) and 20 aminoacyl-tRNA synthetases (aaRS). The predicted aa sequences were obtained from NCBI GenBank and aligned using Clustal W in the Mega 7.0 software program. Trees were constructed using the maximum likelihood evolution method and 1000 replicates. The analysis of aaRS domains was carried out using NCBI Conserved Domain Search (https://www.ncbi.nlm.nih.gov/Structure/cdd/wrpsb.cgi). A search for promoter sequences was performed in intergenic regions based on a search for the mimivirus canonical AAAATTGA promoter sequence, as previously described[20]. Single-nucleotide polymorphisms (SNP) in the AAAATTGA promoter sequence were also considered for each base, considering all possibilities. Gene sets available for members of the family *Mimiviridae* and those of Tupanvirus soda lake and Tupanvirus deep ocean were used for analyses of the mimivirus pangenome. Groups of orthologues were determined using the Proteinortho tool V51 with 1*e*−3 and 50% as the *e*-value and coverage thresholds, respectively. Concurrently, BLAST searches were performed using ORFs of all mimivirus genomes available in the NCBI GenBank nucleotide sequence database against the set of clusters of orthologous groups previously delineated for mimiviruses (mimiCOGs) ($n = 898$), with 1*e*−3 and 50% as the *e*-value and coverage thresholds, respectively. For rhizome preparations, all coding sequences were blasted against the NR database, and results were filtered to retain the best hits. Taxonomic affiliation was retrieved from NCBI. For the construction of a translation-associated elements network, the different classes of translation elements of each organism included in the analysis were obtained by searching for each component within their genome, according to protein function annotation using Blastp searches against the GenBank NCBI non-redundant protein sequence database. The tRNA components were obtained using the ARAGORN tool. Different tRNA molecules were included in the analysis, considering the anti-codon sequence. Repeated elements were eliminated to avoid analysis of duplicate events. The layout of the network was generated by a force-directed algorithm—followed by local rearrangement for visual clarity, leaving the network's overall layout unperturbed—using the program Gephi (https://gephi.org).

Ribosomal RNA shutdown and toxicity assays. To investigate the toxicity of Tupanvirus particles, 1 million *A. castellanii* cells were infected with Tupanvirus or mimivirus at a multiplicity of infection of 1, 10, 50, or 100 and incubated at 32 °C. At 0 and 24 h post-infection, the cell suspensions were collected and titered as previously described. A fraction of this suspension (200 µL) was subjected to RNA extraction (Qiagen RNA extraction Kit, Hilden, Germany). The RNA was subjected to reverse transcription by using Vilo enzymes (Invitrogen, CA, USA) and then used as a template in qPCR targeting *A. castellanii* 18 S rRNA (5′-TCCAATTTTCTGCCACCGAA-3′ and 5′-ATCATTACCCTAGTCCTCGCG C-3′). The values were expressed as arbitrary units (delta-Ct). Normalized amounts of the original RNA extracted from each sample were electrophoresed in 1% agarose gel with TBE buffer and run at 150 V. TEM over the entire testing period was performed to evaluate the presence of ribosome-containing vesicles and other cytological alterations. To investigate the nature of virion toxicity, purified Tupanvirus was inactivated by UV light (1 h of exposure, 60 W/m^2) or heating (80 °C, 1 h)—inactivation was confirmed by inoculation on *Acanthamoeba castellanii*, CPE was observed for 5 days and lack of replication was confirmed by qPCR—and inoculated onto *A. castellanii* containing 500,000 cells at multiplicities of infection of 0.1, 1, 5, 10, 50, and 100. The assays were performed in PAS solution. The cytopathic effect was documented and quantified in a counting-cells chamber. Inactivated mimivirus was used for comparison. To determine whether Tupanvirus-induced shutdown of amoebal 18 S rRNA even after inactivation, 500,000 cells were infected (at a multiplicity of infection of 100) and collected at 3 and 9 h post-infection, and amoebal 18 S rRNA levels were measured by qPCR. APMV was used as the control. The sensitivity of Tupanvirus and mimivirus to the translation-inhibiting drugs geneticin and cycloheximide was tested. A total of 500,000 *A. castellanii* cells were pre-treated with different concentrations of the drugs (0–50 and 0–15 µg/ml, respectively) for 8 h and then infected at a multiplicity of infection of 10. Twenty-four hour post-infection, cells were collected, and the viral titers were measured. To investigate the toxicity effect of Tupanvirus particles in the non-host *Tetrahymena* sp., 1 million fresh cells were infected at a multiplicity of infection of 10 in a medium composed of 50% PYG and 50% PAS. The cytopathic effect was monitored for 4 days post-infection, given the reduction of cell movement and vacuolization (lysis or viral replication was not observed). Each day post-infection, 100 µL of infected cell suspension was collected and subjected to cytospin and haemacolour staining to observe vacuolization and other cytological alterations induced by the virus. Other 100 µL aliquots were used to investigate the occurrence of rRNA shutdown induced by Tupanvirus. To this end, the samples were subjected to RNA extraction and electrophoresis. Viral infection in *Tetrahymena* sp. was also observed by TEM at a multiplicity of infection of 10. To determine whether Tupanvirus particles affect the rate of *Tetrahymena* sp. phagocytosis because of toxicity, the rate of viral particle incorporation per cell was calculated during the period of infection. The ratio of TCID50 (infectious entities) and total particles was first calculated by counting the number of viral particles in a counting chamber (approximately 1 $TCID_{50}$ to 63 total particles). One million *Tetrahymena* cells were infected by Tupanvirus or mimivirus at an MOI of 10 $TCID_{50}$. Twelve hour post-infection, the number of viral particles in the medium was estimated by counting the remaining (non-phagocytized) particles. An input of 10 $TCID_{50}$ per cell was added each day post-infection (in separate flasks, one for each day), and the rate of particles phagocytosis was calculated 12 h post-input. For the calculation, the remaining particles from the day before were considered (counted immediately before the input). Considering the toxicity caused by Tupanvirus, but not APMV, in tetrahymena, we conducted an in vitro experiment

aiming to investigate the ability to maintain Tupanvirus or APMV in a system containing both *Acanthamoeba* (host) and *Tetrahymena* (non-host, predator of particles). Thus, *A. castellanii* (900,000 cells) and *Tetrahymena* (100,000 cells) were added simultaneously to the same flask, then infected by Tupanvirus or mimivirus at an MOI of 10 and observed for 12 days. One flask per observation day was prepared. At days 4 and 8, we added 500 µL of fresh medium (50% PYG and 50% PAS) and 100,000 *A. castellanii*, the permissive host. Each day post-infection, the corresponding flask was collected and subjected to titration as previously described. The same experiment was carried out by pre-treating *Tetrahymena* (8 h before infection) with 20 µg/ml of geneticin as negative controls.

Analysis involving Tupanvirus 18 S rRNA intronic region. All analyses involving the genomic environment of copies 1 and 2 were conducted based on the annotation of Tupanvirus. In the best-hits evaluation, the core sequences of copies 1 and 2 were used for nucleotide BLAST analysis using blastn. The resulting 100 best hits were tabulated, and the information was used to construct diagrams. For the phylogenetic analysis, the sequences of these best hits were also aligned, using Clustal W in the Mega 7.0 software, and constructed using the maximum likelihood evolution method of 1,000 replicates. To analyze subjacent regions of the core sequence of 18 S rRNA intronic regions in the *Mimiviridae* family, one member of the lineages A (HQ336222.2), B (JX962719.1) and C (JX885207.1) was chosen and analyzed. The expression of both copies was checked using fluorescence in situ hybridization (FISH) and qPCR. For this, *A. castellanii* cells were infected with Tupanvirus with a multiplicity of infection of 5 and collected at 30 min and at 6 and 12 h post-infection. As a control, *A. castellanii* cells were also incubated with PAS alone and collected. At the indicated times, cells and the supernatant were collected and centrifuged at 800 × g for 10 min. For FISH, the pellet was resuspended in 200 µL of PAS, submitted to cytospin and the cells were fixed in cold methanol for 5 min. Specific probes targeting the 18 S rRNA of *A. castellanii* (5′-TTCACGGTAAACGATCTGGGCC-3′-fluorophore Alexa 488), copy 1 RNA (5′-AGTGGAACTCGGGTATGGTAAAA-3′-fluorophore Alexa 555) and copy 2 RNA (5′-GGCCAAGCTAATCACTTGGG-3′-fluorophore Alexa 555) were diluted and applied at 2 µM in hybridization buffer (900 mM NaCl, 20 mM Tris/HCL, 5 mM EDTA, 0.01% SDS, 10–25% deionized-formamide in distilled-H_2O). The hybridization buffer containing the probes was added to the slides and the hybridization was carried out at 46 °C overnight in a programmable temperature-controlled slide-processing system (ThermoBrite StatSpin, IL, USA). Post-hybridization washes consisted of 0.45–0.15 M NaCl, 20 mM Tris/HCL, 5 mM EDTA, and 0.01% SDS at 48 °C for 10 min. Slides were analyzed using a DMI6000B inverted research microscope (Leica, Wetzlar, Germany). To qPCR the pellet of infected cells was also washed with PAS and then used for total RNA extraction using the RNeasy mini kit (Qiagen, Venlo, Netherlands). The extracted RNA was treated with the Turbo DNA-free kit (Invitrogen, CA, USA) and then used as a template in reverse transcription (RT) reactions carried out using SuperScript Vilo (Invitrogen, CA, USA). The resultant cDNA was used as a template for quantitative real-time PCR assays using the QuantiTect SYBr Green PCR Kit (Qiagen RNA extraction Kit, Hilden, Germany) and targeting copies 1 (primers 5′-GCATCAA GTGCCAACCCATC-3′ and 5′-CTGAAATGGGCAATCCGCAG-3′) and 2 (primers 5′-CCAAGTGATTAGCTTGGCCATAA-3′ and 5′-CGGGAAGTCCCTA AAGCTCC-3′) of the intergenic18S rRNA region in TPV. To normalize the results, primers targeting the GAPDH housekeeping gene of *Acanthamoeba* (primers 5′-GTCTCCGTCGTCGATCTCAC-3′ and 5′-GCGGCCTTAATCTCGTCGTA-3′) were also used. qPCR assays were performed in a BioRad Real-Time PCR Detection System (BioRad) using the following thermal conditions for all genes: 15 min of pre-incubation at 95 °C followed by 40 amplification cycles of 30 s at 95 °C, 30 s at 60 °C and 30 s at 72 °C. The results were analyzed using the relative quantification methodology of $2^{(-\Delta\Delta ct)}$.

Investigation of the nature of ribosomal RNA shutdown. To investigate the shutting down of the host rRNA and verify whether this phenomenon was related to the canonical ribophagy/autophagy process, tests using two acidification and lysosome-vesicle fusion inhibitors (chloroquine and bafilomycin A) were performed. The pH of infected cells and the effect of Atg8-2 silencing on shutdown were also tested. For the inhibitor assays, 5×10^5 *A. castellanii* cells cultured in PYG medium were infected with Tupanvirus or mimivirus at a multiplicity of infection of 100 and incubated at 32 °C. At 1 h post-infection, chloroquine (Sigma-Aldrich, MO, USA) at a final concentration of 100 µM or bafilomycin A (Sigma-Aldrich, MO, USA) at a final concentration of 10 nM was added to the infected cell suspensions. As a control, *A. castellanii* cells not infected were also treated with these inhibitors under the same conditions. After 3 and 9 h post-infection, cells and the supernatant were collected and centrifuged at 800 × *g* for 10 min. The supernatant was discarded, and the pellet was submitted to RNA extraction (Qiagen RNA extraction Kit, Hilden, Germany). From the extracted RNA, 10 µL of each sample was electrophoresed in 1.5% agarose gel with TBE buffer and run at 135 V, and 14 µL was submitted to reverse transcription to measure the amoebal 18 S rRNA levels by qPCR as previously described. To investigate the acidification caused by Tupanvirus or mimivirus infection, *A. castellanii* cells were also submitted to the same pattern of infection and treatment with bafilomycin A, as previously described. In addition, 1 h before the collection time, the cells were incubated with LysoTracker Red DND-99 (Thermo Fisher Scientific, Massachusetts, United States) at a final concentration of 75 nM. After 9 h post-infection, cells and the supernatant were collected and centrifuged at 800 × *g* for 10 min. The supernatant was discarded, and the pellet was resuspended in 1 mL of PAS medium containing only bafilomycin A (10 nM). A total of 20 µL of this suspension was added to glass slides and cover slipped. Analyses were performed using a confocal microscope (Zeiss, Jena, Germany). For gene silencing, small interfering RNA (siRNA) targeting the Atg8-2 gene of *A. castellanii* was synthesized by Eurogentec (Liège, Belgium) based on the cDNA sequence of the gene. The siRNA duplex with sense (5′-GAACUC AUGUCGCACAUCUTT-3′) and anti-sense (5′-AGAUGUGCGACAUGAGU UCTT-3′) sequences was used. The siRNA tagged with a fluorescence dye was transfected onto *A. castellanii* trophozoites at a density of 1×10^6 cells. The control of transfection was performed using fluorescence microscopy. The biological effect of siRNA was check by qPCR and by the observation of the inhibition of acanthamoebal encystment, which is dependent on Atg8-2. Finally, modifications of *A. castellanii* nucleus/nucleolus structure after infection with Tupanvirus and mimivirus were investigated. A total of 10^6 cells were infected with Tupanvirus or mimivirus at an MOI of 10, stained by haemacolour and treated with SYTO RNASelect Green Fluorescent cell stain (Invitrogen, USA) following the manufacturer's instructions. After 9 h.p.i., cells were observed under an immunofluorescence microscope to observe modifications to the nucleus /nucleolus of infected and control cells. In parallel, this preparation was submitted to electron microscopy.

Data availability. The Tupanvirus genome sequences have been deposited in GenBank under accession codes KY523104 (soda lake) and MF405918 (deep ocean). Proteomic data have been deposited in PRIDE archive under accession code PXD007583. All other data supporting the findings of this study are available within the article and its Supplementary Information, or from the corresponding author upon reasonable request.

Received: 3 October 2017 Accepted: 23 January 2018
Published online: 27 February 2018

References

1. Raina, M. & Ibba, M. tRNAs as regulators of biological processes. *Front. Genet.* **5**, 171 (2014).
2. Fournier, G. P., Andam, C. P., Alm, E. J. & Gogarten, J. P. Molecular evolution of aminoacyl tRNA synthetase proteins in the early history of life. *Orig. Life Evol. Biospheres.* **41**, 621–632 (2011).
3. Korobeinikova, A. V., Garber, M. B. & Gongadze, G. M. Ribosomal proteins: structure, function, and evolution. *Biochemistry* **77**, 562–574 (2012).
4. La Scola, B. et al. A giant virus in amoebae. *Science* **299**, 2033 (2003).
5. Abrahao, J. et al. The analysis of translation-related gene set boosts debates around origin and evolution of mimiviruses. *PLoS Genet.* **13**, e1006532 (2017).
6. Schulz, F. et al. Giant viruses with an expanded complement of translation system components. *Science* **356**, 82–85 (2017).
7. Sorokin, D. Y. et al. Microbial diversity and biogeochemical cycling in soda lakes. *Extremophiles* **18**, 791–809 (2014).
8. Xiao, C. et al. Structural studies of the giant mimivirus. *PLoS Biol.* **7**, e92 (2009).
9. Ageno, M., Donelli, G. & Guglielmi, F. Structure and physico-chemical properties of bacteriophage G. II. The shape and symmetry of the capsid. *Micron* **4**, 376–403 (1973).
10. Philippe, N. et al. Pandoraviruses: amoeba viruses with genomes up to 2.5 Mb reaching that of parasitic eukaryotes. *Science* **341**, 281–286 (2013).
11. Legendre, M. et al. Thirty-thousand-year-old distant relative of giant icosahedral DNA viruses with a pandoravirus morphology. *Proc. Natl. Acad. Sci. USA* **111**, 4274–4279 (2014).
12. Legendre, M. et al. In-depth study of Mollivirus sibericum, a new 30,000-y-old giant virus infecting Acanthamoeba. *Proc. Natl. Acad. Sci. USA* **112**, E5327–E5335 (2015).
13. Reteno, D. G. et al. Faustovirus, an asfarvirus-related new lineage of giant viruses infecting amoebae. *J. Virol.* **89**, 6585–6594 (2015).
14. Andreani, J. et al. Cedratvirus, a double-cork structured giant virus, is a distant relative of Pithoviruses. *Viruses* **8**, E300 (2016).
15. Suzan-Monti, M., La Scola, B., Barrassi, L., Espinosa, L. & Raoult, D. Ultrastructural characterization of the giant volcano-like virus factory of Acanthamoeba polyphaga Mimivirus. *PLoS ONE* **2**, e328 (2007).
16. Chaikeeratisak, C. et al. Assembly of a nucleus-like structure during viral replication in bacteria. *Science* **355**, 194–197 (2017).
17. Forterre, P. The virocell concept and environmental microbiology. *ISME J.* **7**, 233–236 (2013).
18. Antwerpen, M. H. et al. Whole-genome sequencing of a pandoravirus isolated from keratitis-inducing acanthamoeba. *Genome Announc.* **3**, e00136–15 (2015).

19. Raoult, D. The post-Darwinist rhizome of life. *Lancet* **375**, 104–105 (2010).
20. Suhre, K., Audic, S. & Claverie, J. M. Mimivirus gene promoters exhibit an unprecedented conservation among all eukaryotes. *Proc. Natl. Acad. Sci. USA* **102**, 14689–14693 (2005).
21. Fischer, M. G., Allen, M. J., Wilson, W. H. & Suttle, C. A. Giant virus with a remarkable complement of genes infects marine zooplankton. *Proc. Natl Acad. Sci. USA* **107**, 19508–19513 (2010).
22. Raoult, D. et al. The 1.2-megabase genome sequence of Mimivirus. *Science* **19**, 1344–1350 (2004).
23. Arslan, D., Legendre, M., Seltzer, V., Abergel, C. & Claverie, J. M. Distant mimivirus relative with a larger genome highlights the fundamental features of Megaviridae. *Proc. Natl Acad. Sci. USA* **108**, 17486–17491 (2011).
24. Assis, F. L. et al. Pan-genome analysis of Brazilian lineage A amoebal mimiviruses. *Viruses* **7**, 3483–3499 (2015).
25. Gonzales-Flores, J. N., Shetty, S. P., Dubey, A. & Copeland, P. R. The molecular biology of selenocysteine. *Biomol. Concepts* **4**, 349–365 (2013).
26. Csaba, G. Lectins and Tetrahymena—A review. *Acta Microbiol. Immunol. Hung.* **63**, 279–291 (2016).
27. Jah, S. et al. Trans-kingdom mimicry underlies ribosome customization by a poxvirus kinase. *Nature* **546**, 651–655 (2017).
28. Claverie, J. M. Viruses take center stage in cellular evolution. *Genome Biol.* **7**, 110 (2006).
29. Filée, J. Genomic comparison of closely related Giant Viruses supports an accordion-like model of evolution. *Front. Microbiol.* **6**, 593 (2015).
30. Smith, J. E. The ecology and evolution of microsporidian parasites. *Parasitology* **136**, 1901–1914 (2009).
31. Nunes, A. & Gomes, J. P. Gomes Evolution, phylogeny, and molecular epidemiology of Chlamydia. *Infect. Genet. Evol.* **23**, 49–64 (2014).
32. Raoult, D. & Forterre, P. Redefining viruses: lessons from Mimivirus. *Nat. Rev. Microbiol.* **6**, 315–319 (2008).
33. Yutin, N. et al. Origin of giant viruses from smaller DNA viruses not from a fourth domain of cellular life. *Virology* **0**, 38–52 (2014).
34. Reed, L. J. & Muench, H. A simple method of estimating fifty percent endpoints. *Am. J. Hyg.* **27**, 493–497 (1938).
35. Rodrigues, R. A. et al. Mimivirus fibrils are important for viral attachment to the microbial world by a diverse glycoside interaction repertorie. *J. Virol.* **89**, 1182–1189 (2015).

Acknowledgements

We thank our colleagues from URMITE and Laboratório de Vírus of Universidade Federal de Minas Gerais for their assistance, particularly Julien Andreani, Jean-Pierre Baudoin, Gilles Audoly, Amina Cherif Louazani, Lina Barrassi, Priscilla Jardot, Eric Chabrières, Philippe Decloquement, Nicholas Armstrong, Said Azza, Emeline Baptiste, Claudio Bonjardim, Paulo Ferreira, Giliane Trindade and Betania Drumond. In addition, we thank the Méditerranée Infection Foundation, Centro de Microscopia da UFMG, CNPq (Conselho Nacional de Desenvolvimento Científico e Tecnológico), CAPES (Coordenação de Aperfeiçoamento de Pessoal de Nível Superior) and FAPEMIG (Fundação de Amparo à Pesquisa do estado de Minas Gerais) for their financial support. We thank Petrobras for the collection of sediments from ocean. This work was also supported by the French Government under the « Investissements d'avenir » (Investments for the Future) program managed by the Agence Nationale de la Recherche (ANR, fr: National Agency for Research), (reference: Méditerranée Infection 10-IAHU-03). J.A., B.R. and E.K. are CNPq researchers. B.L.S., J.A., L.S., P.C., and E.G.K. are members of a CAPES-COFECUB project.

Author contributions

D.R., B.L.S., J.S.A., A.L., P.C., E.G.K, and E.G. designed the study and experiments. L.S., J. S.A, J.B.K., R.R., L.S., L.S.S., T.A., P.C., F.A. P.B., M.A., I.B., B.R., A.L., and H.S. performed sample collection, virus isolation, experiments and/or analyses. D.R., B.L.S., A.L., J.S.A., P.C., G.K., R.R., L.S., and L.S.S. wrote the manuscript. All authors approved the final manuscript.

Additional information

Supplementary Information accompanies this paper at https://doi.org/10.1038/s41467-018-03168-1.

Competing interests: The authors declare no competing financial interests.

Reprints and permission information is available online at http://npg.nature.com/reprintsandpermissions/

Publisher's note: Springer Nature remains neutral with regard to jurisdictional claims in published maps and institutional affiliations.

frontiers in Microbiology

ORIGINAL RESEARCH
published: 01 June 2015
doi: 10.3389/fmicb.2015.00539

Modulation of the expression of mimivirus-encoded translation-related genes in response to nutrient availability during *Acanthamoeba castellanii* infection

*Lorena C. F. Silva[1], Gabriel M. F. Almeida[2], Felipe L. Assis[1], Jonas D. Albarnaz[1], Paulo V. M. Boratto[1], Fábio P. Dornas[1], Ketyllen R. Andrade[1], Bernard La Scola[3], Erna G. Kroon[1], Flávio G. da Fonseca[1,4] and Jônatas S. Abrahão[1]**

[1] Laboratório de Vírus, Departamento de Microbiologia, Instituto de Ciências Biológicas, Universidade Federal de Minas Gerais, Belo Horizonte, Brazil, [2] AQUACEN – Laboratório Nacional de Referencia para Doenças de Animais Aquáticos, Ministério da Pesca e Aquicultura, Universidade Federal de Minas Gerais, Belo Horizonte, Brazil, [3] URMITE CNRS UMR 6236 – IRD 3R198, Aix Marseille Université, Marseille, France, [4] Laboratório de Virologia Básica e Aplicada, Departamento de Microbiologia, Instituto de Ciências Biológicas, Universidade Federal de Minas Gerais, Belo Horizonte, Brazil

The complexity of giant virus genomes is intriguing, especially the presence of genes encoding components of the protein translation machinery such as transfer RNAs and aminoacyl-tRNA-synthetases; these features are uncommon among other viruses. Although orthologs of these genes are codified by their hosts, one can hypothesize that having these translation-related genes might represent a gain of fitness during infection. Therefore, the aim of this study was to evaluate the expression of translation-related genes by mimivirus during infection of *Acanthamoeba castellanii* under different nutritional conditions. *In silico* analysis of amino acid usage revealed remarkable differences between the mimivirus isolates and the *A. castellanii* host. Relative expression analysis by quantitative PCR revealed that mimivirus was able to modulate the expression of eight viral translation-related genes according to the amoebal growth condition, with a higher induction of gene expression under starvation. Some mimivirus isolates presented differences in translation-related gene expression; notably, polymorphisms in the promoter regions correlated with these differences. Two mimivirus isolates did not encode the tryptophanyl-tRNA in their genomes, which may be linked with low conservation pressure based on amino acid usage analysis. Taken together, our data suggest that mimivirus can modulate the expression of translation-related genes in response to nutrient availability in the host cell, allowing the mimivirus to adapt to different hosts growing under different nutritional conditions.

Keywords: mimivirus, tRNA, aminoacyl-tRNA-synthetases, translation, gene expression

OPEN ACCESS

Edited by:
William Michael McShan, University of Oklahoma Health Sciences Center, USA

Reviewed by:
Hendrik Huthoff, King's College London, UK
Bin Su, Université Paris Diderot, France

****Correspondence:***
Jônatas S. Abrahão, Laboratório de Vírus, Departamento de Microbiologia, Instituto de Ciências Biológicas, Universidade Federal de Minas Gerais, Avenida Antônio Carlos, 6627, Caixa Postal 486, Bloco F4, Sala 258, 31270-901 Belo Horizonte, MG, Brazil
jonatas.abrahao@gmail.com

Specialty section:
This article was submitted to Virology, a section of the journal Frontiers in Microbiology

Received: *01 April 2015*
Accepted: *15 May 2015*
Published: *01 June 2015*

Citation:
Silva LCF, Almeida GMF, Assis FL, Albarnaz JD, Boratto PVM, Dornas FP, Andrade KR, La Scola B, Kroon EG, da Fonseca FG and Abrahão JS (2015) Modulation of the expression of mimivirus-encoded translation-related genes in response to nutrient availability during Acanthamoeba castellanii infection. Front. Microbiol. 6:539. doi: 10.3389/fmicb.2015.00539

Introduction

Acanthamoeba polyphaga mimivirus (APMV) was the first discovered representative of the *Mimiviridae* family of amoeba-associated microorganisms involved with pneumonia

(La Scola et al., 2003). Mature APMV particles are 700 nm in diameter and contain a double-stranded DNA genome of approximately 1.2 Mb that encodes approximately 1000 proteins, thereby surpassing the coding capacity of some bacteria (i.e., mycoplasma) (La Scola et al., 2003; Raoult et al., 2004; Moreira and Brochier-Armanet, 2008). The function of many of the ORFs encoded by APMV remain unknown. Some of these ORFs have never or rarely been found in other viruses, particularly components of the protein translation machinery (hereafter referred to as translation-related genes) including transfer RNAs (tRNAs), aminoacyl-tRNA-synthetases (aaRS), initiation factors, elongation factors, and release factors (Saini and Fischer, 2007; Claverie and Abergel, 2010; Legendre et al., 2010; Colson et al., 2011).

The translation of messenger RNA (mRNA) into protein in cellular organisms occurs through a complex process in the cytoplasm and consists of three main stages: initiation, elongation, and termination. Several players participate in this process, such as the ribosomes, tRNAs, and a varied enzymatic apparatus. In this context, aaRS are essential for the promotion of the correct interaction between tRNAs with their cognate amino acids. This reaction is called aminoacylation and leads to the formation of covalent bonds between the amino acid and the tRNA; once charged, the complex recognizes the respective codon in the mRNA and promotes the translation of the genetic information into a polypeptide chain (Ibba and Söll, 2004; Walsh and Mohr, 2011).

Cellular genes encoding the components of the protein translation machinery are regulated by different mechanisms. Some of the mechanisms involved in the regulation of aaRS expression are better characterized in bacteria and unicellular eukaryotes (Ryckelynck et al., 2005). The expression of aaRS in *Escherichia coli*, for example, is regulated in a manner that is dependent on the growth rate, but also by specific mechanisms induced in response to starvation of the cognate amino acid (Putzer and Laalami, 2000). In *Bacillus subtilis*, at least 16 aaRS genes are induced in response to starvation of their cognate amino acids via an uncharged tRNA-mediated transcription antitermination mechanism that appears to be conserved in Gram-positive bacteria (Putzer and Laalami, 2000; Ryckelynck et al., 2005). In budding yeast under amino acid starvation, stimulation of the translation of the transcriptional activator GCN4 in turn activates aaRS expression (Ryckelynck et al., 2005). This control is necessary to ensure the balance between the intracellular concentrations of uncharged and charged tRNAs to allow fine-tuning of not only translation, but also cellular metabolism as a whole in response to nutritional conditions in the extracellular environment. Various elements of specific amino acid biosynthetic pathways are involved in the regulation of aaRS expression and their disruption, either by raising or lowering the intracellular concentration of amino acids and other components important for the control of the expression and activity of these enzymes. Many different regulatory mechanisms allow both gene-specific control and global control of the expression of genes involved in protein translation (Neidhardt et al., 1975; Putzer and Laalami, 2000).

Although the existence of virally encoded translation-related genes is intriguing from a phylogenetic viewpoint, the functional relevance of such genes in the context of mimivirus infection is unknown. Here, we evaluated the expression of a number of mimivirus genes involved in translation during infection by APMV and other mimiviruses isolated in Brazil under different growth conditions. Our analysis revealed that mimiviruses were able to modulate the expression of viral translation-related genes according to the amoebal growth conditions during infection; for example, gene expression was increased under starvation conditions. We propose that the ability to adjust the expression of viral translation-related genes in response to nutrient availability may represent a remarkable example of viral adaptation to constantly changing conditions during infection of amoebal populations in the environment.

Materials and Methods

Virus Preparation and Cells

Acanthamoeba polyphaga mimivirus, a prototype of the *Mimiviridae* family, and APMV M4, a strain derived from APMV after 150 passages in amoeba culture (Boyer et al., 2011), were kindly provided by Dr. Didier Raoult (Aix Marseille Université, France). The Brazilian mimivirus isolates Kroon virus, Oyster virus, and Samba virus were produced and purified as previously described (La Scola et al., 2003). Briefly, *A. castellanii* (ATCC 30010) cells were grown in 75-cm^2 cell culture flasks (Nunc, USA) in peptone-yeast extract-glucose (PYG) medium (Visvesvara and Balamuth, 1975) supplemented with 7% fetal calf serum (FCS, Cultilab, Brazil), 25 mg/mL fungizone (amphotericin B, Cristalia, Brazil), 500 U/mL penicillin, and 50 mg/mL gentamicin (Schering-Plough, Brazil). After reaching confluence, the amoebas were infected and incubated at 32°C until cytopathic effects were observed. Supernatants from the infected amoebas were collected and filtered through a 0.8-μm filter to remove cell debris. The viruses were purified by centrifugation through a sucrose cushion (24%), suspended in phosphate-buffered saline (PBS), and stored at −80°C. For the gene expression experiments, *A. castellanii* was maintained in PYG medium in the absence or in the presence of 7% FCS at 32°C or in Page's amoeba saline (PAS) at 32°C to induce starvation.

Infections and Experimental Design

To investigate the expression of mimivirus translation-related genes under distinct nutritional conditions, we selected eight genes based on the APMV genome: four tRNAs (leucyl, histidyl, cysteinyl, and tryptophanyl) and four aaRSs (methionyl, arginyl, tyrosyl, and cysteinyl). Twenty-four-well plates containing 1×10^5 amoebas per well were infected with APMV, APMV M4, and the Brazilian isolates at a multiplicity of infection (MOI) of 10 and incubated at 32°C for 8 h, during which time the viral yield and expression of the selected genes are at their maxima (data not shown). We used three different amoebal growth conditions: PAS (a simple saline used for maintenance of the amoebas to induce starvation) and PYG (the growth medium commonly used to

culture these cells under laboratory conditions), in the absence (PYG 0% FCS), and in the presence of FCS (PYG 7% FCS). The rationale behind this strategy is based on a nutritional scale of growth conditions: PAS < PYG 0% FCS < PYG 7 % FCS. Cells were collected and centrifuged, and the pellet was homogenized in 400 μL of PBS, from which 50 μL was used for titration in amoebas, while the remainder was pelleted again and used for total RNA extraction, reverse transcription, and quantitative PCR. The viral titer was determined using the $TCID_{50}$ (tissue culture infective dose) method calculated with the Reed–Muench method (Reed and Muench, 1938). The titration was performed in 96-well Costar®microplates (Corning, NY, USA) containing 4×10^4 amoebas per well in 100 μL of PYG with 7% FCS. Samples were serially diluted in PBS ranging from 10^{-1} to 10^{-11}, and 100 μl of each dilution was inoculated onto amoebas (four wells per dilution, 200 μl final volume). Plates were incubated for 4 days at 32°C to determine the highest dilution that led to amoeba lysis ($TCID_{50}$/ml). The results shown are representative of two independent experiments performed in duplicate.

RNA Extraction, Reverse Transcription, and Real-Time PCR

Total RNA was extracted using the RNeasy kit (Qiagen, Germany). Reverse transcription was performed using the MMLV reverse transcriptase (Promega, USA) as recommended by the manufacturers. cDNA was used to determine the levels of tRNA and aaRS mRNA by quantitative PCR using specific primers (**Table 1**), SYBR Green Master Mix (Applied Biosystem, USA) and water in 10 μL reactions. Reactions were performed in the StepOne instrument (Applied Biosystem, USA). All reactions were previously optimized and presented high efficiency values. Relative gene expression analyses were performed using the ΔΔCt method and normalized to the expression of 18S ribosomal RNA (18S rDNA) and the viral RNA helicase mRNA.

Amino Acid Usage

To investigate the profile of amino acid usage between mimivirus isolates and *A. castellanii,* the protein sequences predicted from the Brazilian mimivirus genomes [APMV (GenBank accession HQ336222.2) and APMV M4 (GenBank accession JN036606.1)] and amoebal sequences obtained from the NCBI GenBank amino acid sequence database were subjected to amino acid composition calculation using the program CGUA (General Codon Usage Analysis). The amino acid usages were expressed as percentages and reflected the contribution made by each amino acid. The amino acid usage of *A. castellenii* was calculated from the 45,664 protein sequences available in the NCBI database.

tRNA and aaRS Gene Analysis

To investigate possible polymorphisms among translation-related gene sequences of the five mimivirus isolates analyzed, the tRNA and aaRS sequences of APMV (GenBank accession HQ336222.2), APMV M4 (GenBank accession JN036606.1), Kroon virus, Oyster virus, and Samba virus were aligned with GenBank references using ClustalW and manually aligned using MEGA software version 5.2 (Arizona State University, Phoenix, AZ, USA). Whole genome sequences of Brazilian mimivirus isolates were obtained using an Illumina MiSeq instrument (Illumina Inc., San Diego, CA, USA) with the paired-end application (unpublished data). Brazilian mimiviruses genomes were searched for translation-related genes using available sequences from giant viruses available in GenBank. After the alignment, the sequences were thoroughly analyzed and compared for similarity, promoter sequences, gaps, and polyadenylation signals. The APMV ORF with no predicted promoter regions in GenBank (methionyl-RS and tryptophanyl-tRNA), had their promoters analyzed manually.

Statistical Analyses

Statistical analyses were performed using GraphPad Prism software (San Diego, CA, USA). The significance analysis was performed by comparing the average of the obtained results within the groups. The values were subjected in different combinations to one-way ANOVA tests and Bonferroni post-tests (95% confidence intervals). Differences between groups were considered significant when the *p*-values were smaller than 0.05.

Results

Amino Acid Usage

Our results clearly showed a different profile of amino acid usage between the *Acanthamoeba* and mimiviruses isolates

TABLE 1 | Primers used for quantitative PCR.

Gene	Forward primer	Reverse primer
Leucyl-tRNA	GGGATTCGAACCCACGACAT	ATAAGCAAAGGTGGCGGAGT
Histidyl-tRNA	TTAGTGGTAGAACTACTGTTTGTGG	TTTTCAAAAATGACCCGTACAGGAA
Cysteinyl-tRNA	ACAGTCAACTGGATCGTTAGC	AGGATCGTATCAGAATTGAACTGA
Tryptophanyl-tRNA	GTGCAACAATAGACCTGTTAGTTTA	ACCGGAATCGAACCAGTATCA
Methionyl tRNA synthetase	TGATTGGCGTGAATGGCTGA	ACCAATCACACTAGCCGGAA
Arginyl tRNA synthetase	GTGGGTGATTGGGGAACTCA	TGATACGGTCTCCAATCGGG
Tyrosyl tRNA synthetase	TTTGGCAAACCAATCGGCAA	TGGTTTTGAACCTAGTGGTCGT
Cysteinyl tRNA synthetase	TGCCAACCAGGTACACCAAA	TGCTCTTTGGAAAGGTCGATCA
18S rDNA	TCCAATTTTCTGCCACCGAA	ATCATTACCCTAGTCCTCGCGC
Viral RNA helicase	ACCTGATCCACATCCCATAACTAAA	GGCCTCATCAACAAATGGTTTCT

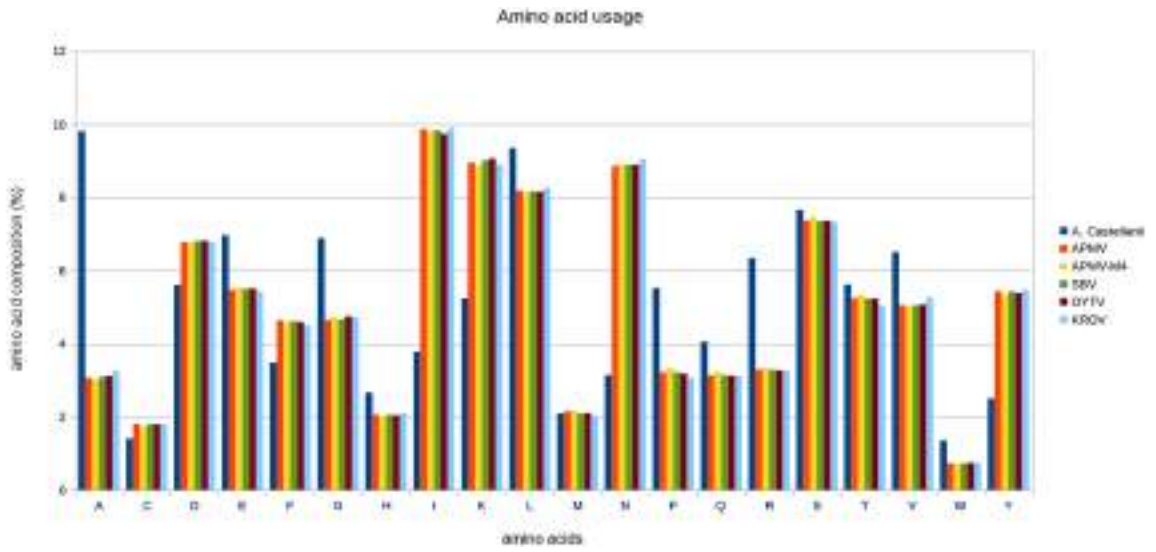

FIGURE 1 | Comparative amino acid usage analysis of *Acanthamoeba castellanii* and mimivirus strains. The amino acid usage for protein sequences of Brazilian mimivirus strains, *A. polyphaga mimivirus* (APMV) and APMV M4 strains, and the *A. castellanii* amoeba were calculated using the CGUA (General Codon Usage Analysis) tool.

(**Figure 1**). In contrast, the amino acid usage in APMV, APMV M4, and the other Brazilian mimivirus isolates was very similar (**Figure 1**). Two of the amino acids for which mimiviruses encode a cognate aaRS [cysteine (C) and methionine (M)] are less frequently found in both *A. castallanii* and the predicted proteome of the mimivirus isolates compared to arginine (R; most frequent in the host proteome) and tyrosine (Y; more frequently found in the viral proteome). The leucine, histidine, and tryptophan tRNAs were less frequently found in the viral predicted proteome compared to the host.

Expression of tRNA and aaRS Genes

To evaluate the effect of nutrient availability on the expression profile of virally encoded tRNA and aaRS during infection with different mimivirus isolates (APMV, APMV M4, Kroon virus, Oyster virus, and Samba virus), cells infected under different growth conditions were collected, processed, and assayed by quantitative PCR. The quantitative PCR results were expressed as arbitrary units, fitted to standard curves generated for each target gene (Supplementary Figure S1), and normalized using the amoebal 18S rDNA gene levels.

Our results revealed that viral tRNA and aaRS mRNA expression varied according to the viral strain and growth medium used (PAS, PYG 0% FCS, or PYG 7% FCS; **Figures 2** and **3**). Overall, mimivirus-encoded tRNA and aaRS gene expression was significantly lower in cells infected under high nutrient availability conditions (PYG 7% FCS) in comparison to cells infected under PYG 0% FCS or starvation (PAS) conditions. Viruses infecting amoeba maintained in PAS medium presented the highest viral mRNA expression for all analyzed genes ($p < 0.001$ or $p < 0.01$; **Figures 2** and **3**). The different mimivirus isolates showed some variation in translation-related gene expression profiles between them when infection was performed under the same conditions. For example, there was a distinctive expression profile was observed for Kroon virus-encoded cysteinyl-tRNA in PYG 0% FCS and arginyl- and methionyl-RS under all amoebal growth conditions (**Figures 2** and **3**). Neither Kroon virus nor M4 presented detectable levels of tryptophanyl-tRNA due to the absence of this gene in both isolates, as revealed by genomic prediction (Supplementary Figure S2). Similarly, M4 does not encode (or express the mRNA) of tyrosyl-RS. We also performed a quantification of the viral RNA helicase gene by real-time PCR. The results revealed that viruses and nutritional conditions did not significantly influence RNA helicase expression, suggesting that the effect observed for the tRNA, and aaRS mRNA expression levels cannot be generalized for all genes under starvation conditions (Supplementary Figure S3).

We also performed one-step growth curves. Our results showed that the five evaluated mimivirus strains were able to productively infect the amoebas under the three tested growth conditions (**Figure 4**). All five isolates showed a substantial increase in viral yield at 4 h post-infection (h.p.i.), with a peak at approximately 8 h.p.i. that was maintained until 24 h.p.i. (**Figure 4**). There were no significant differences between the growth curves of the tested mimivirus isolates when the infection was performed in the presence of PYG 0% FCS or PYG 7% FCS (**Figures 4A,B**). In contrast, the viral yield was approximately 1,000-fold lower under starvation conditions (PAS solution; **Figure 4C**). Although the mimivirus isolates showed a lower progeny yield in the starved amoebas, the low nutrient availability induced higher expression of the virally encoded translation-related genes compared to PYG with 0 or 7% FCS.

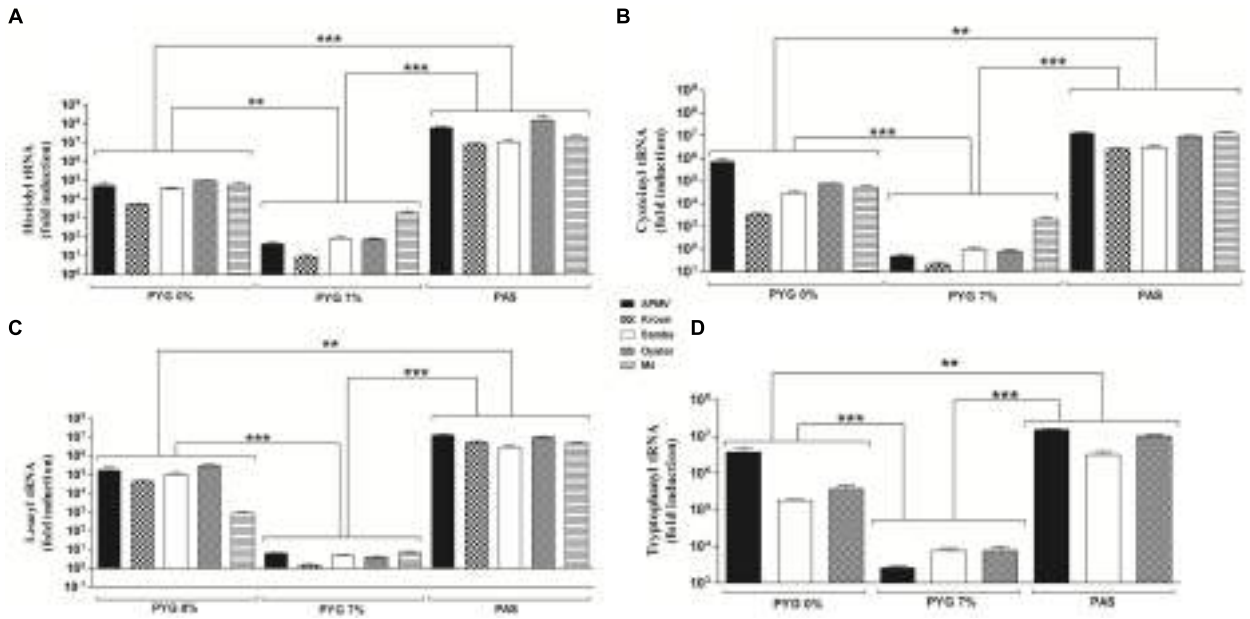

FIGURE 2 | tRNA expression by different mimivirus strains. Cells of *A. castellanii* were plated in 24-well plates (1×10^5 cells per well), infected for 8 h with different mimivirus strains in different culture medium, subjected to total RNA extraction, and reverse transcription and the resulting cDNA was used as a template for quantitative PCR. **(A)** Histidyl-tRNA. **(B)** Cysteinyl-tRNA. **(C)** Leucyl-tRNA. **(D)** Tryptophanyl-tRNA. The quantitative PCR results were expressed in arbitrary units, fitted to a standard curve, normalized to levels of the constitutive amoebal 18S rDNA gene and presented as the mean ± SD from a representative experiment conducted in duplicate. The values were subjected in different combinations to one-way ANOVA tests and Bonferroni post-tests (95% confidence intervals). Differences between groups were considered significant when the *p*-values were smaller than 0.05. $^{**}p < 0.01$; $^{***}p < 0.001$.

Polymorphisms in Mimivirus-Encoded Translation-Related Genes

To evaluate whether the differences in translation-related gene expression during infection by the different mimivirus isolates could be associated with polymorphisms in the genes, we analyzed the sequences of the eight translation-related genes investigated in this study using a nucleotide alignment constructed with the MEGA software version 5.2. The fully sequenced and annotated APMV genome (the prototype of the *Mimiviridae* family) showed the presence of tRNAs, aaRSs, and elongation factors among other elements involved in the process of protein synthesis. Thus, this virus was selected for analysis in this work and served as the source for primer design and comparison with the sequences of the other isolates studied. These comparisons showed that the APMV and Samba virus orthologs of the investigated genes under study exhibited 100% similarity. Six of the genes in APMV and M4 exhibited 100% similarity, with the exception of tyrosyl-RS and tryptophanyl-tRNA that were reported to have been deleted during the successive passages of APMV that gave rise to the M4 strain. Several polymorphisms were detected during the comparison of the translation-related genes encoded by APMV and two other Brazilian mimivirus strains (Kroon virus and Oyster virus; Supplementary Figure S2). Among the studied Brazilian isolates, Kroon virus presented the most remarkable polymorphisms, including the absence of the tryptophanyl-tRNA coding region (Supplementary Figure S2). Moreover, careful analysis of the nucleotide sequences of the translation-related genes encoded by Oyster virus and Kroon virus revealed several differences in the promoter regions and polyadenylation signals, with important nucleotide changes in genes such as the cysteinyl-tRNA and methionyl- and arginyl-RS due to the presence of gaps in these regions (Supplementary Figures S2 and S4).

Discussion

Not enough all the structural complexity presented by giant viruses, in recent years, studies showed that they also have large and complex genomes (La Scola et al., 2003; Raoult et al., 2004; Moreira and Brochier-Armanet, 2008). The fact that these viruses possess genes that encode proteins involved in protein translation is highly intriguing, but the biological essentiality and importance of these genes remains unknown (Jeudy et al., 2012; Colson et al., 2013). In this context, our study presents new data concerning the giant viruses and their translation-related genes.

Viruses are known to rely exclusively on the host cell protein synthesis machinery for the translation of viral proteins. Therefore, the discovery that giant viruses encoded translation-related genes in their genomes was quite surprising and led virologists to question the boundaries between giant viruses and cellular organisms (Raoult et al., 2004; Moreira and Brochier-Armanet, 2008). The prototype of *Mimiviridae* family, APMV, encodes six tRNAs (histidyl, cysteinyl, tryptophanyl, and leucyl, the latter of which appears in three copies in the genome) and four aaRSs (methionyl, arginyl, tyrosyl, and cysteinyl) (Colson

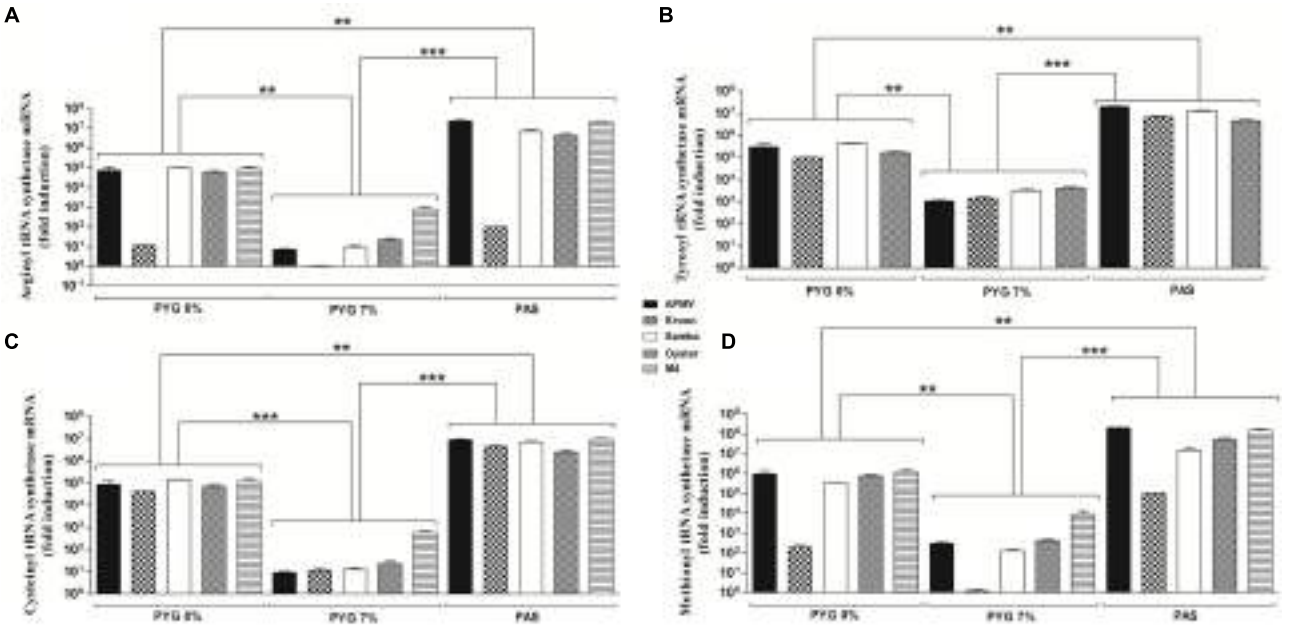

FIGURE 3 | Aminoacyl-tRNA-synthetase (aaRS), messenger RNA (mRNA) expression by different mimivirus strains. Cells of *A. castellanii* were plated in 24-well plates (1×10^5 cells per well), infected for 8 h with different mimivirus strains in different culture medium, subjected to total RNA extraction and reverse transcription and the resulting cDNA used as a template for quantitative PCR. **(A)** Arginyl-RS mRNA levels. **(B)** Tyrosyl-RS mRNA levels. **(C)** Cysteinyl-RS mRNA. **(D)** Methionyl-RS mRNA levels. The real-time PCR results were expressed arbitrary units, fitted to a standard curve, corrected using normalization with amoebal 18S rDNA gene expression levels and presented as the mean ± SD from a representative experiment conducted in duplicate. The values were subjected in different combinations to one-way ANOVA tests and Bonferroni post-tests (95% confidence intervals). Differences between groups were considered significant when the *p*-values were smaller than 0.05. $^{**}p < 0.01$; $^{***}p < 0.001$.

et al., 2013). We propose that the existence of translation-related genes encoded in the mimivirus genome suggests that they may exert some control on the cellular translational machinery in a way that cannot be performed by their cellular counterparts and is necessary for successful viral replication.

Evaluation of amino acid usage of the five mimivirus strains used in this study and *A. castellanii* suggested that the amino acid usage was very similar between viral strains but differed from *A. castellanii* (**Figure 1**), as previously suggested by Colson et al. (2013). Considering the tRNA and aaRS elements analyzed here, we hypothesize that the most used amino acids [i.e., leucine (L) and tyrosine (Y)] are important for the viral machinery. Thus, all of the analyzed viral isolates possess a leucyl-tRNA gene. Arginine (R) and methionine (M) are less used, but can be important because R is widely used by *A. castellanii,* while M is the initiating amino acid. Histidine (H) and cysteine (C) are also maintained in the viral machinery although they are used less (even by *A. castellanii*), but can be important to the process of infection of other hosts, including *Homo sapiens* (data not shown). Finally, the use of tryptophan (W) is not frequent, which accounts for the low pressure of maintenance of the viral machinery demonstrated by the lack of tryptophanyl-tRNA in Kroon virus and APMV M4.

Relative expression analysis revealed that mimivirus is able to modulate the expression of translational-related genes according to nutrient availability during amoebal infection (**Figures 2** and **3**). Under starvation conditions, mimivirus-encoded aaRS mRNA expression resembles the induction of cellular aaRS expression under the same growth condition, as previously observed for bacteria and *Saccharomyces cerevisae* (Ryckelynck et al., 2005). In the yeast, low amino acid availability is sensed by the GCN2 protein kinase that is activated by uncharged tRNAs. GCN2 phosphorylates the eIF2 initiation factor, inhibiting its function in translation initiation. Inactivation of eIF2 leads to translation of GCN4, which in turn is a transcriptional activator that activates the transcription of aaRS by binding to the aaRS gene promoters (Ryckelynck et al., 2005). Whether this amino acid availability sensor operates in *A. castellanii* awaits investigation. Furthermore, there is the possibility of an interplay between nutrient availability sensing of the host amoeba and the stimulation of the mimivirus tRNA and aaRS genes during infection under starvation conditions. Considering the reduced viral growth under starvation (as shown by the one-step-growth curve experiments in **Figure 4C**), we can hypothesize that circumventing limited nutrient availability is critical for successful mimivirus propagation in natural amoebal populations.

Some isolates presented differences in gene expression in comparison to other isolates. Genetic differences between isolates were discovered when the nucleotide and predicted amino acid sequences of translation-related genes were analyzed, revealing polymorphisms in gene promoter regions that could explain this phenomenon. Polymorphisms were detected only in Oyster virus and with high frequency in the Kroon virus-encoded translation-related genes and regulatory elements

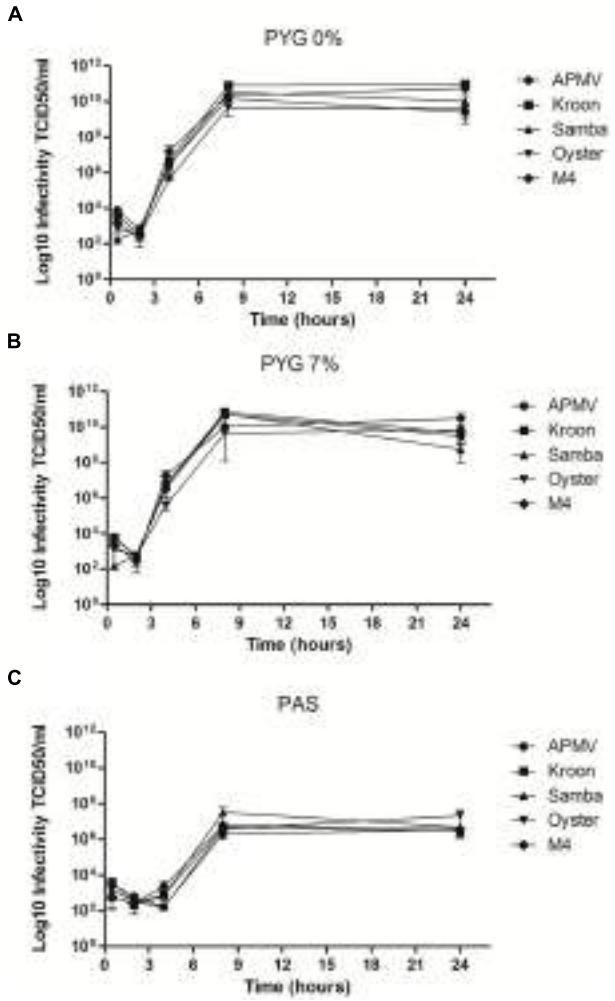

FIGURE 4 | Replication of different mimivirus strains in *A. castellanii.* Cells of *A. castellanii* were plated in 24-well plates (1×10^5 cells per well) and infected with APMV, APMV M4, Kroon virus, Oyster virus, and Samba virus at an multiplicity of infection (MOI) of 10 for the 8 h in three different culture media: **(A)** peptone-yeast extract-glucose (PYG) 0% FCS; **(B)** PYG 7% FCS and **(C)** Page's amoeba saline (PAS). The infectivity of viral particles was evaluated by titration in amoebas by $TCID_{50}$. The results are the mean ± SD of a representative experiment conducted in duplicate.

(Supplementary Figure S2). A careful analysis of these sequences from these two Brazilian isolates (especially Kroon virus) demonstrated nucleotide substitutions in the promoter regions and polyadenylation signals of some genes and the absence of these regulatory sequences in other genes, including leucyl-tRNA, cysteinyl-RS, cysteinyl-tRNA, methionyl-RS, and arginyl-RS (Supplementary Figure S2). For the arginyl-RS gene that presented the lowest expression levels during infection by Kroon virus, we observed an approximately 15% difference in the nucleotide sequence between the early promoter and the initiation codon and an approximately 8% difference in the region containing the late promoter. Furthermore, approximately 46 bp are missing in the 3′ end of the Kroon virus-encoded arginyl-RS compared to the APMV ortholog (Supplementary Figure S4). We propose that these differences may help explain the different levels of translation-related gene expression in Kroon virus compared to the other mimivirus strains (**Figures 2** and **3** and Supplementary Figure S2). APMV M4, which was obtained after successive passages of APMV under allopatric conditions, lost several ORFs including those encoding the tryptophanyl-tRNA and tyrosyl-RS, suggesting that these ORFs were not essential under these culture conditions. Therefore, these genes are likely important in sympatric growth conditions, and APMV would be able to compete better with other microorganisms associated with amoebas by encoding these ORFs and expressing them according to nutrient availability (Boyer et al., 2011; Colson and Raoult, 2012).

The tRNA and aaRS present in giant virus genomes are not pseudogenes, because they are temporally expressed (early, intermediate, and late) during the replication cycle and they are different from cellular genes. Some of these genes are expressed at high levels at different times of infection, suggesting that they are involved in protein translation from the beginning to the late phases of the cycle (Legendre et al., 2010). Moreover, two mimivirus-encoded aaRS (methionyl-RS and tyrosyl-RS) possess genuine enzymatic activity (Abergel et al., 2007; Legendre et al., 2010). Therefore, considering the fact that these viral proteins are differentially expressed depending on the mimivirus isolate and the nutrient availability during infection, we can speculate that genetic and biological differences among viral strains probably reflect their natural history in the environment and their ability to adapt to different hosts under different environmental conditions. In conclusion, our study showed that translation-related genes encoded by giant viruses are differentially expressed in response to nutrient availability during infection of the amoebal host. This finding raised three key questions that need further investigation to be answered: (i) how the regulation of viral tRNA and aaRS gene expression is coordinated with the host cell response to low nutrient availability, especially amino acid starvation; (ii) the functional relevance of these viral translation-related gene products for productive viral infection and for host range adaptation in natural populations of susceptible hosts; and (iii) the significance of the polymorphisms in the regulatory and coding regions of some Brazilian mimivirus isolates for the expression and function of the viral translation-related gene products.

Acknowledgments

We would like to thank colleagues from Gepvig, Laboratório de Vírus, and Aix Marseille Université for their excellent technical support. We also would like to thank CAPES, FAPEMIG, and CNPq for financial support.

Supplementary Material

The Supplementary Material for this article can be found online at: http://journal.frontiersin.org/article/10.3389/fmicb.2015.00539/abstract

References

Abergel, C., Rudinger-Thirion, J., Giegé, R., and Claverie, J. M. (2007). Virus-encoded aminoacyl-RNA synthetases: structural and functional characterization of mimivirus TyrRS and MetRS. *J. Virol.* 81, 12406–12417. doi: 10.1128/JVI.01107-07

Boyer, M., Azza, S., Barrassi, L., Klose, T., Campocasso, A., Pagnier, I., et al. (2011). Mimivirus shows dramatic genome reduction after intraamoebal culture. *Proc. Natl. Acad. Sci. U.S.A.* 108, 10296–10301. doi: 10.1073/pnas.1101118108

Claverie, J. M., and Abergel, C. (2010). Mimivirus: the emerging paradox of quasi-autonomous viruses. *Trends Genet.* 26, 431–437. doi: 10.1016/j.tig.2010.07.003

Colson, P., Fournous, G., Diene, S. M., and Raoult, D. (2013). Codon usage, amino acid usage, transfer RNA and amino-acyl tRNA synthetases in mimivirus. *Intervirology* 56, 364–375. doi: 10.1159/000354557

Colson, P., and Raoult, D. (2012). Lamarckian evolution of the giant Mimivirus in allopatric laboratory culture on amoebas. *Front. Cell. Infect. Microbiol.* 2:91. doi: 10.3389/fcimb.2012.00091

Colson, P., Yutin, N., Shabalina, S. A., Robert, C., Fournous, G., La Scola, B., et al. (2011). Viruses with more than 1,000 Genes: mamavirus, a new *Acanthamoeba polyphaga* mimivirus strain, and reannotation of mimivirus genes. *Genome Biol. Evol.* 3, 737–742. doi: 10.1093/gbe/evr048

Ibba, M., and Söll, D. (2004). Aminoacyl tRNA: setting the limits of the genetic code. *Genes Dev.* 18, 731–738. doi: 10.1101/gad.1187404

Jeudy, S., Abergel, C., Claverie, J. M., and Legendre, M. (2012). Translation in giant viruses: a unique mixture of bacterial and eukaryotic termination schemes. *PLoS Genet.* 8:e1003122. doi: 10.1371/journal.pgen.1003122

La Scola, B., Audic, S., Robert, C., Jungang, L., de Lamballerie, X., Drancourt, M., et al. (2003). A giant virus in amoebas. *Science* 299, 2033. doi: 10.1126/science.1081867

Legendre, M., Audic, S., Poirot, O., Hingamp, P., Seltzer, V., Byrne, D., et al. (2010). mRNA deep sequencing reveals 75 new genes and a complex transcriptional landscape in *Mimivirus*. *Genome Res.* 20, 664–674. doi: 10.1101/gr.102582.109

Moreira, D., and Brochier-Armanet, C. (2008). Giant viruses, giant chimeras: the multiple evolutionary histories of mimivirus genes. *BMC Evol. Biol.* 8:12. doi: 10.1186/1471-2148-8-12

Neidhardt, F. C., Parker, J., and McKeever, W. G. (1975). Function and regulation of aminoacyl tRNA synthetases in prokaryotic and eukaryotic cells. *Annu. Rev. Microbiol.* 29, 215–250. doi: 10.1146/annurev.mi.29.100175.001243

Putzer, H., and Laalami, S. (2000). *Regulation of the Expression of Aminoacyl tRNA Synthetases and Translation Factors. In: Madame Curie Bioscience Database* [*Internet*]. Austin, TX: Landes Bioscience. Available at: http://www.ncbi.nlm.nih.gov/books/NBK6026

Raoult, D., Audic, S., Robert, C., Abergel, C., Renesto, P., Ogata, H., et al. (2004). The 1.2-megabase genome sequence of mimivírus. *Science* 306, 1344–1350. doi: 10.1126/science.1101485

Reed, L. J., and Muench, H. (1938). A simple method of estimating fifty per cent end points. *Am. J. Hyg.* 27, 493–497.

Ryckelynck, M., Masquida, B., Giegé, R., and Frugier, M. (2005). An intricate RNA structure with two tRNA-derived motifs directs complex formation between yeast aspartyl-tRNA synthetase and its mRNA. *J. Mol. Biol.* 354, 614–629. doi: 10.1016/j.jmb.2005.09.063

Saini, H. K., and Fischer, D. (2007). Structural and functional insights into Mimivirus ORFans. *BMC Genomics* 8:115. doi: 10.1186/1471-2164-8-115

Visvesvara, G. S., and Balamuth, W. (1975). Comparative studies on related free-living and pathogenic amebae with special reference to *Acanthamoeba*. *J. Protozool.* 22, 245–256. doi: 10.1111/j.1550-7408.1975.tb05860.x

Walsh, D., and Mohr, I. (2011). Viral subversion of the host protein synthesis machinery. *Nat. Rev. Microbiol*. 9, 860–875. doi: 10.1038/nrmicro2655

Conflict of Interest Statement: The authors declare that the research was conducted in the absence of any commercial or financial relationships that could be construed as a potential conflict of interest.

Mimiviruses and the Human Interferon System: Viral Evasion of Classical Antiviral Activities, But Inhibition By a Novel…

Article *in* Journal of Interferon & Cytokine Research · January 2017

DOI: 10.1089/jir.2016.0097

CITATION
1

READS
39

4 authors, including:

Gabriel Magno de Freitas Almeida
University of Jyväskylä
31 PUBLICATIONS **343** CITATIONS
SEE PROFILE

Jônatas S Abrahão
Federal University of Minas Gerais
153 PUBLICATIONS **883** CITATIONS
SEE PROFILE

JOURNAL OF INTERFERON & CYTOKINE RESEARCH
Volume 37, Number 1, 2017

DOI: 10.1089/jir.2016.0097

REVIEW

Mimiviruses and the Human Interferon System: Viral Evasion of Classical Antiviral Activities, But Inhibition By a Novel Interferon-β Regulated Immunomodulatory Pathway

Gabriel Magno de Freitas Almeida,[1,*] Lorena C. Ferreira Silva,[2,*] Philippe Colson,[3] and Jonatas Santos Abrahao[2,3]

In this review we discuss the role of mimiviruses as potential human pathogens focusing on clinical and evolutionary evidence. We also propose a novel antiviral immunomodulatory pathway controlled by interferon-β (IFN-β) and mediated by immune-responsive gene 1 (IRG1) and itaconic acid, its product. *Acanthamoeba polyphaga* Mimivirus (APMV) was isolated from amoebae in a hospital while investigating a pneumonia outbreak. Mimivirus ubiquity and role as protist pathogens are well understood, and its putative status as a human pathogen has been gaining strength as more evidence is being found. The study of APMV and human cells interaction revealed that the virus is able to evade the IFN system by inhibiting the regulation of interferon-stimulated genes, suggesting that the virus and humans have had host–pathogen interactions. It also has shown that the virus is capable of growing on IFN-α2, but not on IFN-β-treated cells, hinting at an exclusive IFN-β antiviral pathway. Our hypothesis based on preliminary data and published articles is that IFN-β preferentially upregulates IRG1 in human macrophagic cells, which in turn produces itaconic acid. This metabolite links metabolism to antiviral activity by inactivating the virus, in a novel immunomodulatory pathway relevant for APMV infections and probably to other infectious diseases as well.

Keywords: IFN-β, interferon beta, IRG1, itaconic acid, APMV, mimivirus, immunometabolism, giant virus

Acanthamoeba polyphaga Mimivirus Discovery and the Growing Family *Mimiviridae*

The discovery of the first mimivirus came from the investigation of amoeba-associated microorganisms (AAMs) following an episode of nosocomial pneumonia in a hospital in Bradford, England in 1992. No conventional etiological agent of pneumonia was found, but *Acanthamoeba* isolated from a water cooling tower contained a strange organism inside them, which was characterized years later and shown to be a giant virus. This new virus was called *Acanthamoeba polyphaga* mimivirus (APMV) and was so unique in its size, morphology, genome, and biological characteristics that the family *Mimiviridae* was created to accommodate it (La Scola and others 2003). Currently, the family *Mimiviridae* comprises two genera: Mimivirus with APMV, and *Cafeteriavirus* with *Cafeteria roenbergensis virus* as its only species (Colson and others 2011; ICTV 2016).

However, since APMV discovery, several other related, but still unclassified giant viruses have been isolated by coculturing on amoebae, mostly *Acanthamoeba* spp., from many different environments and specimen samples (Pagnier and others 2013; La Scola 2014). For example: *A. castellanii* Mamavirus was isolated from water collected from a cooling tower in Paris and Marseillevirus was isolated from free-living amoebae (La scola and others 2008); Megavirus chilensis was isolated from a water sample collected off the coast of Chile (Arslan and others 2011); Terra1 virus, Terra2 virus, Courdo viruses, Samba virus, and Moumou virus were isolated from environmental samples

[1]Department of Biological and Environmental Sciences, University of Jyvaskyla, Jyvaskyla, Finland.
[2]Laboratorio de Virus, Departamento de Microbiologia, Universidade Federal de Minas Gerais, Belo Horizonte, Brazil.
[3]Unité de Recherche sur les Maladies Infectieuses et Tropicales Emergentes (URMITE), Aix-Marseille Universite Faculté de Médecine, Marseille, France.
*These authors contributed equally to this work.

such as soil and water (Campos and others 2014; La Scola and others 2010); Senegal virus was isolated from the feces of a healthy Senegalese man (Colson and others 2013b); LBA111 virus was isolated in a respiratory sample from a patient with pulmonary infection (Saadi and others 2013a); Lentille virus was isolated from a contact lens washing solution (Cohen and others 2011); Pandoraviruses were isolated from samples from Chile and Australia (Philippe and others 2013); Pithovirus sibericum and Mollivirus sibericum were discovered in the northeastern Siberian permafrost (Legendre and others 2014, 2015); Faustovirus E12 was isolated from sewage by coculturing on another amoeba, *Vermamoeba vermiformis* (Reteno and others 2015); and many other giant virus isolates were described.

All these isolates show that giant viruses compose a diverse group of viruses capable of infecting amoebae and that have been overlooked so far due to their large size, findings also corroborated by several metagenomic and evolutionary studies (Aherfi and others 2016b).

Evidences of Mimiviruses as Human Pathogens

Following the discovery of APMV, much has been learned about mimiviruses ubiquity in the environment and endless peculiarities that distinguish them from other viruses and microbes. However, the milieu from which APMV was originally isolated (in a hospital as an AAMs following a nosocomial pneumonia outbreak) implied that it also could have a darker side and could infect humans as well as protists. It is known that hospitalized patients, especially if immunocompromised or breathing through mechanical ventilation systems, represent a risk group for acquiring pneumonia caused by AAMs. Many studies suggested that APMV could be an amoebal virus also capable of causing disease in humans (Raoult and Boyer 2010; Kutikhin and others 2014; La Scola 2014).

It may sound unreasonable that a protist virus could also infect a vertebrate, but APMV large and uncharacterized genome allied to its ubiquity left the question opened for some time. So, as new giant viruses were being isolated and their peculiarities were being investigated, several studies describing serological, molecular, and biological data linking it to humans also appeared (Colson and others 2016). APMV's widespread presence in hospital environments was confirmed when viral DNA was detected by quantitative polymerase chain reaction (qPCR) and live viruses were isolated from inanimate surfaces in Brazil, where the location with the greatest number of positive samples was the respiratory isolation ward (Santos-Silva and others 2015). The virus has been shown to be highly resistant to chemical biocides and capable of persisting for long periods of time in different substrates (Campos and others 2012; Dornas and others 2014b).

Serological data from Canadian patients revealed that the prevalence of antibodies against APMV was $\sim$9.7% in those with pneumonia diagnostics. For French patients, antibodies against APMV were found in ill patients, but not in healthy individuals. When serum of pneumonia patients in intensive care units were tested for conventional pneumonia agents and AAMs, it was seen that antibodies against APMV and AAMs were more common among patients using mechanical ventilation, a system that provides greater exposure to these organisms, and APMV seroconversions were detected (Raoult and others 2007; Bousbia and others 2013).

In 2004, a laboratory technician who handled large amounts of mimivirus developed a subacute pneumonia that did not respond to antibiotics, and for which no pathogen was identified by routine clinical microbiology testing. Serum samples were negative by serology for pneumonia agents, except mimivirus, and seroconversion was found, therefore, this case can be considered as a laboratory-acquired mimivirus infection that led to a self-resolving pneumonia case (Raoult and others 2006). In a screening for AAMs made on pneumonia patients in France, mimivirus was the fourth most common etiological agent (Berger and others 2006). In 2010, two cases of a probable parasitic disease were associated to seroconversion and increased antibodies against APMV virophage, a virus closely associated to mimivirus (Parola and others 2012).

However, some studies have also shown a low positivity or negative association between mimivirus and disease. Molecular data from China shows that from over 3,000 samples collected from patients with respiratory problems, only one was positive for APMV (Zhang and others 2016). One study from the United States and another one from Australia did not detect mimiviruses in all nasopharyngeal aspirate samples tested (Arden and others 2006; Dare and others 2008; Vincent and others 2010), similar to another study made in Italy using bronchoalveolar lavage specimens (Costa and others 2012), and one from Austria which used respiratory or amoeba-containing water samples (Larcher and others 2006). These differences and low positivity rates in these studies might be due to the genetic diversity of the mimiviruses, its distribution worldwide, characteristics of the primers and reactions used, and also other features, such as differences on clinical samples' collection procedures (Vincent and others 2010; Colson and others 2013a).

On the other hand, molecular evidence of APMV presence was detected in bovine serum samples from Germany and also in animals from the Brazilian Amazon region (Hoffmann and others 2012; Dornas and others 2014a). Mimivirus isolations from human specimens were also described. In one occasion, isolation attempts were made from samples collected from patients in Tunisia between 2009 and 2010. One bronchoalveolar sample from a 72-year-old patient with pneumonia was positive for viral isolation (LBA111 virus) (Saadi and others 2013a). In another study, Shan virus was isolated from a stool sample collected from another Tunisian patient with pneumonia (Saadi and others 2013b).

Although controversial, collagen was shown to be present on the surface of mimivirus particles, and exposure of mice to viral collagen led to the production of anticollagen antibodies that also targeted murine collagen. A human blood sera survey revealed that 22% of rheumatoid arthritis patients were positive for mimivirus collagen against 6% in the healthy control group, pointing to mimivirus exposure as a risk factor for triggering autoimmunity against collagen (Shah and others 2014). All these data pointed to a possible role of mimiviruses as a putative human pathogen, but were not definitive and thus resulted in a lot of controversy (La Scola and others 2005; Vanspauwen and others 2012).

Interestingly, other giant viruses also have been related to infection in humans, particularly an increasing number of cases involved marseilleviruses in the blood and lymphoid tissue, where viral presence has been detected in macrophages (Colson and others 2013b; Popgeorgiev and others 2013a, 2013b; Aherfi and others 2016a, 2016b).

Besides clinical data, some studies focused on APMV biological features also gave strength to the hypothesis that this virus could be a potential vertebrate pathogen. An intracardiac infection mice model was developed and with it histopathological evidence of acute pneumonia, viral reisolation, and antigen detection were possible (Khan and others 2007). As knowledge increased concerning mimivirus entry mechanisms, it became clear that the virus do not require any specific receptor, relying on phagocytosis to enter amoebal cells, and this suggested that mimivirus may have a broad tropism. Phagocytosis is not a characteristic restricted to protists. In fact, it is an important feature of certain subsets of vertebrate immune cells that could also be used by mimiviruses as a way to enter these cells.

In 2008, molecular evidence appeared showing that APMV was able to infect macrophages through phagocytosis (Ghigo and others 2008). It was also highlighted that other microorganisms can be pathogenic for both amoebae and macrophages, and even that amoebae may represent a training field for microorganisms' survival in macrophages (Salah and others 2009). It was also shown that if APMV is cultivated exclusively on germ-free amoebal cells, it goes through a dramatic genomic reduction event after several passages (Boyer and others 2011). This reduction might be excluding genes not required in the laboratory system used, such as those required for competition with other AAMs inside the amoebal cells or even necessary for the interaction with another host species. Among the lost genes are two that code for the proteins required for the assemblage or structure of the antigenic viral fibers, which are targeted by human and mouse anti-APMV antibodies and this was associated with fiber loss (Boyer and others 2011). Maybe the antigenic fiber presence could serve as bait for macrophagic cells to internalize and then be infected by the virus.

Finally, there is the large and partially uncharacterized viral genome that may contain genes related to evasion from the vertebrate immune system. The gene cluster N232 is predicted to encode protein kinases, molecules that have potential to be regulators of cellular processes and signaling pathways (Suhre 2005).

The Virus–Host Interactions Between APMV and Humans

One aspect of the interaction between competing species is that an adaptation in one competitor leads to selection pressure that may result in a counter-adaptation on the other. When this occurs reciprocally the competition leads to an arms race, where one side is constantly changing to respond to the other adaptations (Dawkins and Krebs 1979). This type of race (biological interaction), where competitors need to be in constant movement (evolutionary changes) to remain at the same place (survive) has been called the Red Queen dynamics, using Lewis Carroll's fictional Red Queen character as an analogy (Van Valen 1973).

Red queen dynamics can happen intraspecies and interspecies, the latter in cases such as prey–predator and host–pathogen interactions. Antagonistic interactions between hosts and parasites are a strong driver of coevolution (Decaestecker and others 2007), especially on virus–host cases due to its very intimate dynamics. As in other cases of Red Queen coevolution dynamics, the arms race between viruses and their hosts is constantly shaping both sides, resulting in antiviral host strategies and viral evasion mechanisms. So, if APMV is indeed a human pathogen, we can expect to find host immune mechanisms against the viral infections and viral evasion mechanisms to escape the host immune response.

Type I interferons (IFNs) are important molecules for vertebrate antiviral responses. They are composed of several related but not identical molecules that bind to the same cellular receptor composed of two chains (IFNAR1 and IFNAR2), regulating the expression of interferon-stimulated genes (ISGs). These genes are the effectors of the IFNs biological activities, such as antiviral responses (Isaacs and Lindenmann 1957; Borden and others 2007). Each type I IFN has a specific affinity to the receptor chains, resulting in redundant but not completely identical biological responses. Among type I IFNs, IFN-β has a high affinity for the receptor and elicits stronger biological responses, while the others (like IFN-α2) have reduced affinity for the receptor and generates milder responses (Jaitin and others 2006).

Since the IFN system has been molded by evolution to be able to protect vertebrate hosts from viral infections (among other functions), most viruses of vertebrates have acquired evasion mechanisms to escape the system. So, in the right experimental conditions, it is possible to observe a given vertebrate virus evading the IFN system or having its replication being impaired by it.

In 2012, our research group decided to contribute to the APMV as a human pathogen puzzle by searching for evolutive evidence of virus–host interactions between these organisms. From the host side our choice was to use total human peripheral blood mononuclear cells (PBMCs) since these are composed of a complex mixture of primary immune cells, whereas from the pathogen side we used APMV and decided to quantify viral growth by titrations instead of qPCRs to be able to detect viable viral particles. Our first findings were that the virus was able to grow on human PBMCs and, as expected from a giant viral particle, it was recognized by the immune cells and induced the production of type I IFNs (Silva and others 2013). Then we found the first evolutive evidence of a host–pathogen interaction between APMV and humans, from the pathogen side: the IFNs produced by APMV recognition were not able to induce the expression of ISGs during the course of infection. This APMV evasion strategy was shown to be mediated by a yet unknown mechanism, which does not rely on soluble viral decoy receptors or on signal transducers and activators of transcription (STATs) dephosphorylation, and is dependent on viral replication.

However, our most surprising finding came when APMV replication was assessed on PBMCs with an active antiviral state (i.e., pretreated with type I IFNs). The virus was able to grow normally on IFN-α2-pretreated cells, but not on IFN-β-pretreated cells. IFN-β inhibition was dose dependent, whereas even higher doses of IFN-α2 did not protect the cells from APMV. Even though IFN-β is known to be stronger than IFN-α2 in its biological activities, no virus has been shown to behave in this manner (completely resistant to IFN-α2 and not to IFN-β). That makes our finding unique and led us to believe that what inhibited APMV replication in human PBMCs could be a novel IFN-β-specific biological activity.

We can summarize the results from our study as follows: APMV is able to replicate in human primary immune cells, which in turn recognize the virus and produce type I IFNs; from the virus perspective it guarantees its replication by inhibiting the regulation of ISGs by a still uncharacterized evasion

strategy; and from the host perspective it can block APMV replication by an IFN-β-specific and still unknown mechanism. In the context of a real infection it is possible to speculate that the virus would enter the host and infect its cells, which in turn would produce IFNs. How the infection proceeds will depend on several factors that will end up favoring the IFN-β protection mechanism or the viral evasion strategy.

Unfortunately, due to the large and partially uncharacterized mimivirus genome and lack of specific IFN-β antiviral mechanisms described in the literature, we could not propose a more complete hypothesis on how APMV and its human host interacted at the time (Silva and others 2013). Also due to the lack of a convenient animal model, we could not determine which pattern recognition receptors and signaling pathways were important for APMV recognition, and neither test other IFNs besides IFN-α2 and IFN-β.

IFN-β, Immune Responsive Gene 1, and Itaconic Acid: A Novel Antiviral Immunomodulatory Pathway

In 2013, two unrelated articles were published and shed some light on the matter. The first one shows that of all type I IFNs, IFN-β is unique in its ability to signal using exclusively the IFNAR1 chain of the type I IFNs receptor. This peculiar IFN-β signaling strategy results in the regulation of a distinct gene subset unrelated to the classical ISGs shared with other type I IFNs (de Weerd and others 2013). If IFN-β is indeed capable of eliciting a specific antiviral response against APMV, it may be mediated by one of these unique genes. Of all the specific IFN-β-upregulated genes shown by de Weerd and others (2013), the one with highest expression level was the immune responsive gene 1 (IRG1).

This gene, also known as aconitate decarboxylase 1 in humans, conserved among vertebrates, was originally cloned as an lipopolysaccharide (LPS)-inducible gene, and has been consistently shown to be highly upregulated in immune cells during proinflammatory conditions. Its regulation is complex and multifactorial: it is induced as a response to LPS and CpG DNA in wild-type or IFNABR and STAT-1 knockout cells; by progesterone alone or associated with estradiol in the uterus epithelium; or synergistically by tumor necrosis factor (TNF-α) and IFN-γ (Hoshino and others 2002; Chen and others 2003; Xiao and others 2011; Li and others 2013). It points to a complex regulation network, in which the gene is strongly induced by innate immune sensors activation, but can also be indirectly upregulated by alternative pathways. More recently a study focused on human immune cells stimulated by TNF-α, IFN-γ, and lipopolysaccharides revealed by computational and experimental methods that interferon regulatory factor 1 is directly related to IRG1 expression in macrophages (Tallam and others 2016).

The second article revealed that IRG1 codes for an enzyme that produces itaconic acid in mammalian cells by the decarboxylation of cis-aconitate (Michelucci and others 2013). Itaconic acid is an unsaturated dicarbonic acid traditionally produced by *Aspergillus terreus* and used industrially as a starting material for the chemical synthesis of polymers. It was only recently that its presence in mammalian tissue samples has been detected by metabolomic analysis (Steiger and others 2013). Itaconic acid production by vertebrate cells is cell type-dependent and seems to be related to stimulated macrophagic lineages, pointing to a role in macrophage activation or effector responses (Strelko and others 2011). IRG1 expression was correlated to itaconic acid levels inside mouse and human immune cells, and itaconic acid presence was shown to inhibit *Salmonella enterica* and *Mycobacterium tuberculosis* growth. IRG1 silencing in macrophages results in decreased levels of intracellular itaconic acid and in reduced antibacterial activity (Michelucci and others 2013).

IRG1 also seems to be involved in antiviral responses since microarray analysis revealed that it is upregulated in a chicken lineage susceptible to Marek's disease (caused by a herpes virus), and an single nucleotide polymorphism in its promoter was shown to be related to susceptibility by still unknown mechanisms (Smith and others 2011). IRG1 has also been shown to be a regulator on reactive oxygen species (ROS) and its suppression reduces lung injury caused by respiratory syncytial virus infections (Ren and others 2016).

By taking all the information above into account it is possible to realize that IFN-β is capable of inducing IRG1 in immune (macrophagic) cells, which in turn produces itaconic acid, a metabolite that can function as a link between metabolic processes and immune responses by acting as an antibacterial molecule. It is very tempting to speculate that this novel immunomodulatory mechanism has also implications for viral infections, and is in fact the specific IFN-β antiviral activity responsible for inhibiting APMV infections in human cells that we were seeking.

The specific induction of IRG1 by IFN-β was originally shown in IFNAR2$^{-/-}$ mice (de Weerd and others 2013), but we have preliminary data showing that IRG1 is preferentially induced by IFN-β in normal human PBMCs when compared with other ISGs. This finding hints that IRG1 expression by IFN-β in humans is also differential and relevant. We have also tested itaconic acid as a virucidal agent, and saw that it is able to inactivate APMV *in vitro* in a dose-dependent manner. It shows that itaconic acid by itself can kill the viruses, making it a potential antiviral effector molecule.

How itaconic acid could act against the virus *in vivo* is still a mystery, but since it can be found inside immune cells, a putative mode of action would be direct interaction with viral particles. This interaction could happen by the fusion of phagosomes used by APMV to enter the cells with lysosomes containing itaconic acid, or by interaction of intracellular viruses with itaconic acid-rich subcellular regions. There is also evidence that itaconic acid can be secreted (Strelko and others 2011), and in this case it could act directly upon extracellular virions.

Our hypothesis so far is that human macrophagic cells are the main target during APMV infections, being infected after phagocytosis stimulated by the viral fibers. Viral recognition by pattern recognition receptors in these cells and others lead to the production of IFNs, which in turn acts in autocrine and paracrine ways by binding to its receptors. Even with circulating IFNs APMV is able to evade classical IFN antiviral mechanisms by blocking the induction of ISGs, but is not able to grow in cells protected by an immunomodulatory pathway controlled by IFN-β. This pathway consists of IFN-β inducing IRG1, which in turn produces itaconic acid molecules that function as the final antiviral effectors (Fig. 1).

The IFN-β—IRG1—itaconic acid immunomodulatory pathway is biologically relevant in cell lineages that are potentially infected by APMV through phagocytosis, a coincidence that actually can be another hint of the linkage between

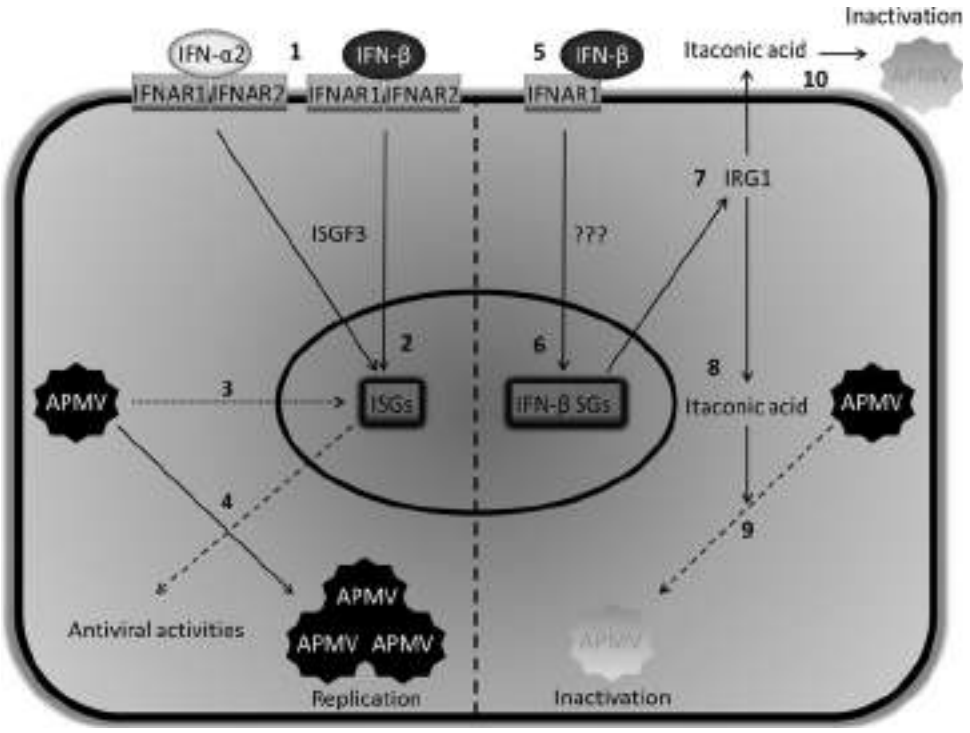

FIG. 1. The ''IFN-β—IRG1—itaconic acid'' antiviral immunomodulatory pathway hypothesis. During an APMV infection the virus is recognized by host pattern recognition receptors resulting in the production of type I IFNs. These IFNs are secreted and act in autocrine and paracrine ways by finding their cellular receptor. All type I IFNs are able to bind to both chains of its receptor, forming a trimeric structure that activates a signaling pathway mediated by ISGF3 resulting in the regulation of ''classical'' ISGs (1, 2). In APMV-infected cells, the virus is capable of inhibiting ISGs regulation by a still unknown evasion mechanism (3), probably related to disrupting ISGF3 formation or translocation to the nucleus. By impairing ISGs transcription, the virus avoids the establishment of an antiviral state in the infected cell, and is able to replicate normally (4). Of all type I IFNs, IFN-β has a high affinity for the cellular receptor and is capable of binding to the IFNAR1 chain alone forming a dimeric structure (5). The IFN-β—IFNAR1 complex regulates a different and exclusive set of genes (here called IFN-β-stimulated genes) by a still unknown signaling pathway that may be mediated by interferon regulatory factor 1 (6). One of these genes is IRG1, an enzyme responsible for itaconic acid production (7). Itaconic acid can act as a virucidal molecule by interacting with the viral particles directly, probably inside cellular vesicles such as phagosomes, phagolysosomes, or even in enriched cellular compartments (9). Itaconic acid can also be secreted from cells, and in this case can act against extracellular virions (10). APMV, *Acanthamoeba polyphaga* Mimivirus; IFN-α2, interferon-α2; IFN-β, interferon-β; IRG1, immune responsive gene 1; ISGs, interferon-stimulated genes.

this pathway and protection against APMV. It is not possible to know when or as a response to what each of these adaptations arose, but we can speculate that the inhibition of ISGs by APMV was a counter-adaptive measure to the antiviral activity of cellular ISGs, allowing these viruses to replicate in human cells. The immunomodulatory pathway mediated by IFN-β could have been selected in the hosts as another layer of IFN antimicrobial activity, complementing the immune response with a different pathway capable of inhibiting the growth of pathogens such as APMV, which are resistant to the classical antiviral mechanisms.

There is still a lot to be learned before these hypotheses can be completely proven, but so far, the information found on related literature and our preliminary data point that they can be, at least, in part, true and relevant. Immunometabolism is considered to be an emerging frontier for immunologists and cell biologists alike (Mathis and Shoelson 2011), and our hypothesis is a very solid point for starting to dissect how our immune and metabolic processes act together against infections. It also helps to focus on a novel antiviral pathway and is important for IFN biology for hinting at a specific IFN-β antiviral activity.

Conclusions

In conclusion, mimiviruses are diverse and ubiquitous giant DNA viruses that infect amoebae, but can also infect humans and possibly other vertebrates. Amoebae carrying the virus can be considered to be a source of infection especially in hospital environments, and so far it is not known if APMV must be seen as an emergent threat or an opportunistic virus. There are several studies showing serological and molecular data linking mimiviruses to pneumonia patients, and more recently viruses have been isolated from such patient's samples. It has also been shown that the virus is immunogenic, pneumonia can be induced in a mice infection model, the virus can enter human cells through phagocytosis, replicate in these cells, and it can be inhibited by and evade the human type I IFN system. The latter is an undisputed proof that both organisms are involved in a host–pathogen coevolutionary process responsible for shaping each other over time, and can be taken as a very strong argument in favor of APMV being a human pathogen.

By studying the interaction between APMV and human cells, we have not only found that the virus establishes

productive infections and that host cells recognize it, but also stumbled on an unique viral evasion strategy and on a novel antiviral immunomodulatory pathway mediated exclusively by IFN-β. Improbable as it can be, a mimivirus has led us to uncover a not yet completely understood, but highly relevant aspect of our physiology that links our metabolism to immunological processes against viruses. Further characterizing the APMV evasion mechanisms against type I IFNs will allow us to learn more about these virus remarkable features and will probably lead to even more surprising discoveries. Studying the novel immunomodulatory antiviral pathway mediated by IFN-β will certainly contribute to a better understanding of our own antiviral defenses, with biological and clinical implications.

Acknowledgments

The authors thank CAPES-COFECUB, CNPq, FAPEMIG, and the Mediterranean Infection Foundation for financial support. J.S.A. is a CNPq researcher. From March 2016 onward G.M.F.A. was funded by the Finnish Center of Excellence Program of the Academy of Finland (CoE in Biological Interactions 2012–2017, project no. 252411).

Author Disclosure Statement

No competing financial interests exist.

References

Aherfi S, Colson P, Audoly G, Nappez C, Xerri L, Valensi A, Million M, Lepidi H, Costello R, Raoult D. 2016a. Marseillevirus in lymphoma: a giant in the lymph node. Lancet Infect Dis. 16(10):e225–234.

Aherfi S, Colson P, La Scola B, Raoult D. 2016b. Giant viruses of amoebas: an update. Front Microbiol 7:349.

Arden KE, McErlean P, Nissen MD. Sloots TP, Mackay IM. 2006. Frequent detection of human rhinoviruses, paramyxoviruses, coronaviruses, and bocavirus during acute respiratory tract infections. J Med Virol 78:1232–1240.

Arslan D, Legendre M, Seltzer V, Abergel C, Claverie JM. 2011. Distant mimivirus relative with a larger genome highlights the fundamental features of Megaviridae. PNAS 108:17486–17491.

Berger P, Papazian L, Drancourt M, La Scola B, Auffray JP, Raoult D. 2006. Ameba-associated microorganisms and diagnosis of nosocomial pneumonia. Emerg Infect Dis 12:248–255.

Borden EC, Sen GC, Uze G, Silverman RH, Ransohoff RM, Foster GR, Stark GR. 2007. Interferons at age 50: past, current and future impact on biomedicine. Nat Rev Drug Discov 6:975–990.

Bousbia S, Papazian L, Saux P, Forel JM, Auffray JP, Martin C, Raoult D, La Scola B. 2013. Serologic prevalence of amoeba-associated microorganisms in intensive care unit pneumonia patients. PLoS One 8:e58111.

Boyer M, Azza S, Barrassi L, Klose T, Campocasso A, Pagnier I, Fournous G, Borg A, Robert C, Zhang X, Desnues C, Henrissat B, Rossmann MG, La Scola B, Raoult D. 2011. Mimivirus shows dramatic genome reduction after intraamoebal culture. Proc Natl Acad Sci U S A 108(25):10296–10301.

Campos RK, Andrade KR, Ferreira PCP, Bonjardim CA, La Scola B, Kroon EG, Abrahão JS. 2012. Virucidal activity of chemical biocides against mimivirus, a putative pneumonia agent. J Clin Virol 55:323–328.

Campos RK, Boratto PV, Assis FL, Aguiar ER, Silva LC, Albarnaz JD, Dornas FP, Trindade GS, Ferreira PP, Marques JT, Robert C, Raoult D, Kroon EG, La Scola B, Abrahão JS. 2014. Samba virus, the first brazillian giant virus, isolated from water of Negro River from Amazon Virol J 11:95.

Chen B, Zhang D, Pollard JW. 2003. Progesterone regulation of the mammalian ortholog of methylcitrate dehydratase (immune response gene 1) in the uterine epithelium during implantation through the protein kinase C pathway. Mol Endocrinol 17(11):2340–2354.

Cohen G, Hoffart L, La Scola B, Raoult D, Drancourt M. 2011. Ameba-associated Keratitis, France. Emerg Infect Dis 17(7):1306–1308.

Colson P, Aherfi S, La Scola B, Raoult D. 2016. The role of giant viruses of amoebas in humans. Curr Opin Microbiol 31:199–208.

Colson P, Fancello L, Gimenez G, Armougom F, Desnues C, Fournous G, Yoosuf N, Million M, La Scola B, Raoult D. 2013b. Evidence of the megavirome in humans. J Clin Virol 57:191–200.

Colson P, Gimenez G, Boyer M, Fournous G, Raoult D. 2011. The giant Cafeteria roenbergensis virus that infects a widespread marine phagocytic protist is a new member of the fourth domain of life. PLoS One 6:1–11.

Colson P, La Scola B, Raoult D. 2013a. Giant viruses of amoebae as potential human pathogens. Intervirology 56:376–385.

Costa C, Bergallo M, Astegiano S, Terlizzi ME, Sidoti F, Solidoro P, Cavallo R. 2012. Detection of Mimivirus in bronchoalveolar lavage of ventilated and nonventilated patients. Intervirology 55(4):303–305.

Dare RK, Chittaganpitch M, Erdman DD. 2008. Screening pneumonia patients for mimivirus. Emerg Infect Dis 14: 465–467.

Dawkins R, Krebs JR. 1979. Arms races between and within species. Proc R Soc Lond B 205:489–511.

de Weerd NA, Vivian JP, Nguyen TK, Mangan NE, Gould JA, Braniff SJ, Zaker-Tabrizi L, Fung KY, Forster SC, Beddoe T, Reid HH, Rossjohn J, Hertzog PJ. 2013. Structural basis of a unique interferon-β signaling axis mediated via the receptor IFNAR1. Nat Immunol 14(9):901–907.

Decaestecker E, Gaba S, Raeymaekers JAM, Stoks R, Van Kerckhoven L, Ebert D, De Meester L. 2007. Host–parasite 'Red Queen' dynamics archived in pond sediment. Nature 450:870–873.

Dornas FP, Rodrigues FP, Boratto PV, Silva LC, Ferreira PCP, Bonjardim CA, Trindade GS, Kroon EG, La Scola B, Abrahão JS. 2014a. Mimivirus circulation among wild and domestic mammals, Amazon Region, Brazil. Emerg Infect 20:469–472.

Dornas FP, Silva LC, Almeida GM, Campos RK, Boratto PV, Franco-Luiz AP, La Scola B, Ferreira PC, Kroon EG, Abrahão J.S. 2014b. Acanthamoeba polyphaga mimivirus stability in environmental and clinical substrates: implications for virus detection and isolation. PLoS One 9:e878111.

Ghigo E, Kartenbeck J, Lien P, Pelkmans L, Capo C, Mege JL, Raoult, D. 2008. Ameobal pathogen mimivirus infects macrophages through phagocytosis. PLoS Pathogens 4:1–17.

Hoffmann B, Scheuch M, Höper D, Jungblut R, Holsteg M, Schirrmeier H. 2012. Novel orthobunyavirus in cattle, Europe, 2011. Emerg Infect Dis 18:469–472.

Hoshino K, Kaisho T, Iwabe T, Takeuchi O, Akira S. 2002. Differential involvement of IFN-beta in Toll-like receptor-stimulated dendritic cell activation. Int Immunol 14(10):1225–1231.

International Committee on Taxonomy of Viruses (ICTV). Master Species List 2016. http://ictvonline.org/taxonomy Releases.asp (accessed Dec. 17, 2016).

Isaacs A, Lindenmann J. 1957. Virus interference. I. The interferon. Proc R Soc Lond B Biol Sci 147:258–267.

Jaitin DA, Roisman LC, Jaks E, Gavutis M, Piehler J, Van der Heyden J, Uze G, Schreiber G. 2006. Inquiring into the differential action of interferons (IFNs): an IFN-alpha2 mutant with enhanced affinity to IFNAR1 is functionally similar to IFN-beta. Mol Cell Biol 26(5):1888–1897.

Khan M, La Scola B, Lepidi H, Raoult D. 2007. Pneumonia in mice inoculated experimentally with *Acanthamoeba polyphaga* mimivirus. Microb Pathog 42(2–3):56–61.

Kutikhin AG, Yuzhalin AE, Brusina EB. 2014. Mimiviridae, Marseilleviridae, and virophages as emerging human pathogens causing healthcare-associated infections. GMS Hyg Infect Control 9(2):Doc16.

La Scola B. 2014. Looking at protists as a source of pathogenic viruses. Microb Pathog 77:131–135.

La Scola B, Audic S, Robert C, Jungang L, de Lamballerie X, Drancourt M, Birtles R, Claverie JM, Raoult D. 2003. A giant virus in amoebae. Science 299(5615):2033.

La Scola B, Campocasso A, N'dong R, Fournous G, Barrassi L, Flaudrops C, Raoult D. 2010. Tentative characterization of new environmental giant viruses by MALDI-TOF mass spectrometry. Intervirology 53:344–353.

La Scola B, Desnues C, Pagnier I, Robert C, Barrassi L, Fournous G, Merchat M, Suzan-Monti M, Forterre P, Koonin E, Raoult D. 2008. The virophage as a unique parasite of the giant mimivirus. Nature 455:100–104.

La Scola B, Marrie TJ, Auffray JP, Raoult D. 2005. Mimivirus in pneumonia patients. Emerg Infect Dis 11:449–452.

Larcher C, Jeller V, Fischer H, Huemer HP. 2006. Prevalence of respiratory viruses, including newly identified viruses, in hospitalised children in Austria. Eur J Clin Microbiol Infect Dis 25(11):681–686.

Legendre M, Bartoli J, Shmakova L, Jeudy S, Labadie K, Adrait A, Lescot M, Poirot O, Bertaux L, Bruley C, Couté Y, Rivkina E, Abergel C, Claverie JM. 2014. Thirty-thousand-year-old distant relative of giant icosahedral DNA viruses with a pandoravirus morphology. Proc Natl Acad Sci U S A 111:4274–4279.

Legendre M, Lartigue A, Bertaux L, Jeudy S, Bartoli J, Lescot M, Alempic JM, Ramus C, Bruley C, Labadie K, Shmakova L, Rivkina E, Couté Y, Abergel C, Claverie JM. 2015. In-depth study of Mollivirus sibericum, a new 30,000-y-old giant virus infecting Acanthamoeba. Proc Natl Acad Sci U S A 112:E5327–E5335.

Mathis D, Shoelson SE. 2011. Immunometabolism: an emerging frontier. Nat Rev Immunol 11(2):81.

Michelucci A, Cordes T, Ghelfi J, Pailot A, Reiling N, Goldmann O, Binz T, Wegner A, Tallam A, Rausell A, Buttini M, Linster CL, Medina E, Balling R, Hiller K. 2013. Immune-responsive gene 1 protein links metabolism to immunity by catalyzing itaconic acid production. Proc Natl Acad Sci U S A 110(19):7820–7825.

Pagnier I, Reteno DG, Saadi H, Boughalmi M, Gaia M, Slimani M, Ngounga T, Bekliz M, Colson P, Raoult D, La Scola B. 2013. A Decade of improvements in Mimiviridae and Marseilleviridae isolation from amoeba. Intervirology 56:354–363.

Parola P, Renvoisé A, Botelho-Nevers E, La Scola B, Desnues C, Raoult D. 2012. Acanthamoeba polyphaga mimivirus virophage seroconversion in travelers returning from Laos. Emerg Infect Dis 18(9):1500–1502.

Philippe N, Legendre M, Doutre G, Couté Y, Poirot O, Lescot M, Arslan D, Seltzer V, Bertaux L, Bruley C, Garin J, Claverie JM, Abergel C. 2013. Pandoraviruses: amoeba viruses with genomes up to 2.5 Mb reaching that of parasitic eukaryotes. Science 341:281–286.

Popgeorgiev N, Boyer M, Fancello L, Monteil S, Robert C, Rivet R, Nappez C, Azza S, Chiaroni J, Raoult D, Desnues C. 2013a. Giant blood Marseillevirus recovered from asymptomatic blood donors. J Infect Dis 208:1042–1050.

Popgeorgiev N, Michel G, Lepidi H, Raoult D, Desnues C. 2013b. Marseillevirus adenitis in an 11-month-old child. J Clin Microbiol 51(12):4102–4105.

Raoult D, Boyer M. 2010. Amoebae as genitors and reservoirs of giant viruses. Intervirology 53:321–329.

Raoult D, La Scola B, Birtles R. 2007. The discovery and characterization of Mimivirus the largest known virus and putative pneumonia agent. Clin Infect Dis 45:5–102.

Raoult D, Renesto P, Brouqui P. 2006. Laboratory infection of a technician by Mimivirus. Ann Intern Med 144:702–703.

Ren K, Lv Y, Zhuo Y, Chen C, Shi H, Guo L, Yang G, Hou Y, Tan RX, Li E. 2016. Suppression of IRG-1 reduces inflammatory cell infiltration and lung injury in respiratory syncytial virus infection by reducing production of reactive oxygen species. J Virol 90(16):7313–7322.

Reteno DG, Benamar S, Khalil JB, Andreani J, Armstrong N, Klose T, Rossmann M, Colson P, Raoult D, La Scola B. 2015. Faustovirus, an asfarvirus-related new lineage of giant viruses infecting amoebae. J Virol 89:6585–6594.

Saadi H, Pagnier I, Colson P, Cherif JK, Beji M, Boughalmi M, Azza S, Armstrong N, Robert C, Fournous G, La Scola B, Raoult D. 2013a. First isolation of Mimivirus in a patient with pneumonia. Clin Infect Dis 57:127–134.

Saadi H, Reteno DG, Colson P, Aherfi S, Minodier P, Pagnier I, Raoult D, La Scola B. 2013b. Shan virus: a new mimivirus isolated from the stool of a Tunisian patient with pneumonia. Intervirology 56:424–429.

Salah IB, Ghigo E, Drancourt M. 2009. Free-living amoebae, a training field for macrophage resistance of mycobacteria. Clin Microbiol Infect 15(10):894–905.

Santos-Silva L, Arantes TS, Andrade KR, Lima Rodrigues RA, Miranda Boratto PV, de Freitas Almeida GM, Kroon EG, La Scola B, Clemente WT, Santos Abrahão J. 2015. High positivity of mimivirus in inanimate surfaces of a hospital respiratory-isolation facility, Brazil. J Clin Virol 66:62–65.

Shah N, Hülsmeier AJ, Hochhold N, Neidhart M, Gay S, Hennet T. 2014. Exposure to mimivirus collagen promotes arthritis. J Virol 88(2):838–845.

Silva LC, Almeida GM, Oliveira DB, Dornas FP, Campos RK, La Scola B, Ferreira PCP, Kroon EG, Abrahão JS. 2013. A resourceful giant: APMV is able to interfere with the human type I interferon system. Microbes Infect 16:187–195.

Smith J, Sadeyen JR, Paton IR, Hocking PM, Salmon N, Fife M, Nair V, Burt DW, Kaiser P. 2011. Systems analysis of immune responses in Marek's disease virus-infected chickens identifies a gene involved in susceptibility and highlights a possible novel pathogenicity mechanism. J Virol 85(21):11146–11158.

Steiger MG, Blumhoff ML, Mattanovich D, Sauer M. 2013. Biochemistry of microbial itaconic acid production. Front Microbiol 4:23.

Strelko CL, Lu W, Dufort FJ, Seyfried TN, Chiles TC, Rabinowitz JD, Roberts MF. 2011. Itaconic acid is a mammalian metabolite induced during macrophage activation. J Am Chem Soc 133(41):16386–16389.

Suhre K. 2005. Gene and genome duplication in Acanthamoeba polyphaga Mimivirus. J Virol 79(22):14095–14101.

Tallam A, Perumal TM, Antony PM, Jäger C, Fritz JV, Vallar L, Balling R, Del Sol A, Michelucci A. 2016. Gene regulatory

network inference of immunoresponsive gene 1 (IRG1) identifies interferon regulatory factor 1 (IRF1) as its transcriptional regulator in mammalian macrophages. PLoS One 11(2): e0149050.

Van Valen L. 1973. A new evolutionary law. Evol Theory 1: 1–30.

Vanspauwen MJ, Franssen FM, Raoult D, Wouters EF, Bruggeman CA, Linssen C.F. 2012. Infections with mimivirus in patients with chronic obstructive pulmonary disease. Respir Med 106:1690–1694.

Vincent A, La Scola B, Papazian L. 2010. Advances in Mimivirus pathogenicity. Intervirology 53:304–309.

Xiao W, Wang L, Xiao R, Wu M, Tan J, He Y. 2011. Expression profile of human immune-responsive gene 1 and generation and characterization of polyclonal antiserum. Mol Cell Biochem 353(1–2):177–187.

Zhang XA, Zhu T, Zhang PH, Li H, Li Y, Liu EM, Liu W, Cao WC. 2016. Lack of Mimivirus detection in patients with respiratory disease, China. Emerg Infect Dis 22(11): 2011–2012.

Address correspondence to:
Dr. Jonatas Santos Abrahao
Laboratorio de Virus
Departamento de Microbiologia
Universidade Federal de Minas Gerais
Belo Horizonte CEP 31270-901
Brazil

E-mail: jonatas.abrahao@gmail.com

Received 28 September 2016/Accepted 28 October 2016

frontiers in Microbiology

ORIGINAL RESEARCH
published: 10 November 2015
doi: 10.3389/fmicb.2015.01256

Niemeyer Virus: A New Mimivirus Group A Isolate Harboring a Set of Duplicated Aminoacyl-tRNA Synthetase Genes

Paulo V. M. Boratto[1†], Thalita S. Arantes[1†], Lorena C. F. Silva[1], Felipe L. Assis[1], Erna G. Kroon[1], Bernard La Scola[2] and Jônatas S. Abrahão[1]**

[1] *Laboratório de Vírus, Departamento de Microbiologia, Instituto de Ciências Biológicas, Universidade Federal de Minas Gerais, Belo Horizonte, Brazil,* [2] *URMITE CNRS UMR 6236 – IRD 3R198, Aix Marseille Université, Marseille, France*

It is well recognized that gene duplication/acquisition is a key factor for molecular evolution, being directly related to the emergence of new genetic variants. The importance of such phenomena can also be expanded to the viral world, with impacts on viral fitness and environmental adaptations. In this work we describe the isolation and characterization of Niemeyer virus, a new mimivirus isolate obtained from water samples of an urban lake in Brazil. Genomic data showed that Niemeyer harbors duplicated copies of three of its four aminoacyl-tRNA synthetase genes (cysteinyl, methionyl, and tyrosyl RS). Gene expression analysis showed that such duplications allowed significantly increased expression of methionyl and tyrosyl aaRS mRNA by Niemeyer in comparison to APMV. Remarkably, phylogenetic data revealed that Niemeyer duplicated gene pairs are different, each one clustering with a different group of mimivirus strains. Taken together, our results raise new questions about the origins and selective pressures involving events of aaRS gain and loss among mimiviruses.

Keywords: ***Mimiviridae*, Niemeyer virus, aminoacyl-tRNA synthetase, gene duplication, giant virus isolation**

OPEN ACCESS

Edited by:
Gilbert Greub,
University of Lausanne, Switzerland

Reviewed by:
Hendrik Huthoff,
King's College London, UK
Juliana Cortines,
Universidade Federal do Rio de Janeiro, Brazil

****Correspondence:***
Bernard La Scola
bernard.la-scola@univ-amu.fr;
Jônatas S. Abrahão
jonatas.abrahao@gmail.com

[†]These authors have contributed equally to this work.

Specialty section:
This article was submitted to Virology, a section of the journal Frontiers in Microbiology

Received: *03 September 2015*
Accepted: *29 October 2015*
Published: *10 November 2015*

Citation:
Boratto PVM, Arantes TS, Silva LCF, Assis FL, Kroon EG, La Scola B and Abrahão JS (2015) Niemeyer Virus: A New Mimivirus Group A Isolate Harboring a Set of Duplicated Aminoacyl-tRNA Synthetase Genes. Front. Microbiol. 6:1256. doi: 10.3389/fmicb.2015.01256

INTRODUCTION

Since the discovery of the first member of the family *Mimiviridae*, *Acanthamoeba polyphaga mimivirus* (APMV), in 2003, more mimivirus-like viruses are being isolated with increasing frequency from phagotrophic protists (La Scola et al., 2003). Mimivirus-like particles have been detected in the most diverse environments, such as rivers, soil, oceans, hospital and animals, and from different countries, such as France, Tunisia, Chile, Australia among others (La Scola et al., 2010; Arslan et al., 2011; Boughalmi et al., 2013). Recently, Campos et al. (2014) described the discovery of the first giant virus isolated in Brazil, named *Samba virus* (SMBV), which was isolated in 2011 from surface water collected from the Negro River, in the Amazon forest (Campos et al., 2014). SMBV is biologically and molecularly related to other mimiviruses, and was isolated in association with Rio Negro virus (RNV), a novel virophage strain belonging to this new class of viruses that parasitize the viral factory during mimivirus replication (Campos et al., 2014). Currently, the family *Mimiviridae* consists of dozens of mimivirus-like isolates that are able to infect amoeba of the genus *Acanthamoeba.* These viruses have been grouped into three distinct lineages, according to their polymerase B gene sequence and other genetic markers: lineage A (containing APMV), lineage B (containing *Acanthamoeba polyphaga moumouvirus*) and lineage

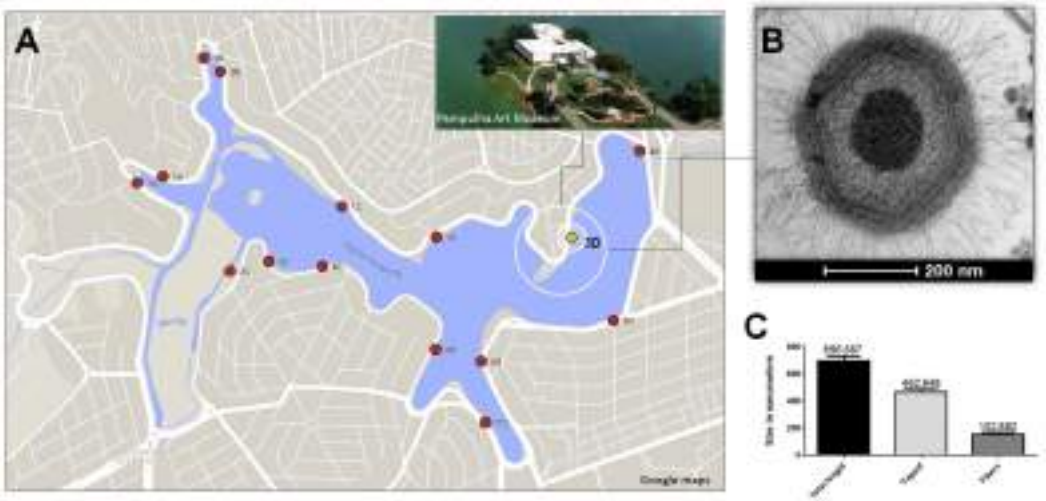

FIGURE 1 | Niemeyer virus (NYMV) collection site, morphometric analysis, and electron microscopy. (A) Shows a map of the Pampulha Lagoon, from where the samples were collected. Red dots: collection points; yellow dot: NYMV isolation site. **(B)** Shows an image of a NYMV particle, observed in electron microscopy. **(C)** Shows the size, in nanometers, of different components of the NYMV particle: only the fibers, only the capsid and the particle as a whole.

C (containing *Megavirus chilensis*) (Gaia et al., 2013). These amoeba-associated viruses have led to a paradigm shift in virus research due to their peculiar features which had never been seen in other viruses until then: large viral particles presenting a diameter of approximately 750 nm, covered by capsid associated fibers, and containing large double stranded DNA genomes of about 1.2 megabases (Mb), and approximately 1000 hypothetical proteins, many of them still uncharacterized or having functions never/rarely seen before in other viruses (La Scola et al., 2003; Raoult et al., 2004). Among the most intriguing predicted proteins in the genome of mimiviruses, it is worth highlighting those related to DNA repair and translation machinery, as well as chaperones related to DNA processing (La Scola et al., 2003; Raoult et al., 2004). Genes that encode translation related proteins, such as aminoacyl tRNA synthetases (aaRS) and translation factors, could hypothetically confer on APMV and other giant viruses a certain degree of autonomy from cellular machinery, and may be under conservative selection pressure (Raoult et al., 2004). Currently, seven aaRS have already been described among mimiviruses genomes: tyrosyl, cysteinyl, methionyl, arginyl, isoleucyl, asparaginyl, and tryptophanyl tRNA-synthetases. Among the aforementioned molecules, the first four enzymes are encoded by the genome of APMV, the prototype of the family *Mimiviridae*. However, no aaRS duplication events in the family *Mimiviridae* have been previously reported, other than in the exceptional case of the *Acanthamoeba polyphaga moumouvirus*, that possesses four orthologs of arginyl-tRNA synthetase in its genome (Yoosuf et al., 2012). In this work we describe the isolation and characterization of Niemeyer mimivirus, a new mimivirus-like virus isolated from water samples from an urban lake in Brazil. Genomic data show that Niemeyer harbors duplicated copies of three of its four aaRS genes (cysteinyl, methionyl, and tyrosyl aaRS), which are associated with increased expression of methionyl and tyrosyl aaRS mRNA by this virus in comparison to APMV. Remarkably, phylogenetic data revealed that Niemeyer duplicated genes are different from each other, each one clustering with a different group of mimivirus strains. Taken together, our results raise new questions about the origins and selective pressures involving aaRS gain and loss events among mimiviruses.

MATERIALS AND METHODS

Sample Collection and Virus Isolation

To explore the presence of giant viruses in an urban lake marked by a high concentration of organic matter, in 2011 we collected about 80 water samples, located at equidistant points, around Pampulha Lagoon (19°51′0.60″S and 43°58′18.90″W), in the city of Belo Horizonte, Brazil (**Figure 1A**). After collection, the samples were stored at 4°C overnight. Then, 500 μl of each sample was added to 4.5 mL of autoclaved rice and water medium made with 40 rice grains in 1 l of water. The samples were stored for 20 days in the dark at room temperature. Afterward, 5×10^3 *Acanthamoeba castellanii* trophozoites (ATCC 30234), kindly provided by the Laboratório de Amebíases (Departamento de Parasitologia, ICB/UFMG) were added, and the samples were re-incubated under the same conditions for 10 days (Dornas et al., 2014). After the enrichment process, samples were pooled in groups of five, and filtered through a 1.2 μm membrane to remove impurities, and a 0.2 μm membrane to retain giant viruses. The samples were then subjected in parallel to real-time PCR, targeting the RNA helicase gene (primers: 5′ACCTGATCCACATCCCATAACTAAA3′ and 5′GGCCTCATCAACAAATGGTTTCT3′) and to viral isolation from *A. castellanii*. As a control for the molecular and biological assays APMV was used. A new virus isolate, Niemeyer

TABLE 1 | Primers used for quantitative PCR.

Gene	Foward primer	Reverse primer
Leucyl-tRNA	GGGATTCGAACCCACGACAT	ATAAGCAAAGGTGGCGGAGT
Histidyl-IRNA	TTAGTGGTAGAACTACTGTTTGTGG	TTTTCAAAAATGACCCGTACAGGAA
Cysteinyl-tRNA	ACAGTCAAaGGATCGTTAGC	AGGATCGTATCAGAATTGAACTGA
Tryptophanyl-tRNA	GTG CAACAATAG ACCTGTTAGTTTA	ACCGGAATCGAACCAGTATCA
Methionyl tRNA synthetase	TGATTGGCGTGAATGGCTGA	ACCAATCACACTAGCCGGAA
Arginyl tRNA synthetase	GTGGGTGATTGGGGAAaCA	TGATACGGTCTCCAATCGGG
Tyrosyl tRNA synthetase	TTTGGCAAACCAATCGGCAA	TGGTTTTGAACCTAGTGGTCGT
Cysteinyl tRNA synthetase	TGCCAACCAGGTACACCAAA	TGCTCTTTGGAAAGGTCGATCA
18S rDNA	TCCAATTTTCTGCCACCGAA	ATCATTACCCTAGTCCTCGCGC
Viral RNA helicase	ACCTGATCCACATCCCATAAaAAA	GGCCTCATCAACAAATGGTTTCT

mimivirus, was grown and purified as described by La Scola et al. (2003) and Abrahão et al. (2014), respectively. The virus was called Niemeyer in tribute to the Brazilian architect who designed important buildings all over the world, including the Pampulha Art Museum near to where the virus was isolated (**Figure 1A**).

NYMV Virus Transmission Electron Microscopy

For the electron microscopy assays, *A. castellanii* cells were cultivated until 80–90% confluence was observed and infected with NYMV in a M.O.I of 0.01. Twelve hours post-infection (hpi), when approximately 50% of the trophozoites were presenting cytopathic effects, the medium was discarded and the monolayer gently washed twice with 0.1 M sodium phosphate buffer. Samples were fixed by adding glutaraldehyde (2.5% v/v) for 1 h at room temperature. The cells were then collected by centrifugation at 1500 *g* for 10 min, the medium was discarded and the cells were stored at 4° C until electron microscopy analysis was performed.

TABLE 2 | Best-hit analysis of proteins predicted in NYMV genome.

Compared strains	Best hits	Identity (%)	SD (%)	proteins
NYMV × APMV	One-way AAI 1	98,65	4,35	975
(group A)	One-way AAI 2	99,94	1,01	841
	Two-way AAI	99,99	0,08	836
NYMV × SMBV	One-way AAI 1	98,62	4,42	956
(group A)	One-way AAI 2	99,94	1,02	825
	Two-way AAI	99,99	0,08	820
NYMV × Moumou	One-way AAI 1	74,98	3,62	61
(group B)	One-way AAI 2	75,3	3,85	58
	Two-way AAI	75,21	3,7	53
NYMV × MCHV	One-way AAI 1	75,82	5,3	55
(group C)	One-way AAI 2	ND	ND	ND
	Two-way AAI	ND	ND	ND

NYMV, Niemeyer virus; APMV, Acanthamoeba polyphaga mimivirus; SMBV, Samba virus; MCHV, Megavirus chilensis; APMOUV, Acanthamoeba polyphaga moumouvirus; SD, standard deviation; AAI, average amino acid identity.

Evaluation of the Replication Profile of NYMV

Briefly, NYMV was inoculated in *A. castellanii* cells until appearance of cytopathic effect and purified by centrifugation on a 25% sucrose cushion as previously described (Abrahão et al., 2014). The titer was obtained by using the Reed–Muench method. To evaluate the replication profile of NYMV, the procedure was performed in 96-well Costar® microplates (Corning, NY, USA) containing 40,000 cells of *A. castellanii* maintained in 100 μl of PAS (Page's amoeba saline, PAS) culture medium per well. The cells were then infected with NYMV at a multiplicity of infection (M.O.I.) of 10. The cells were collected at different time points (0, 1, 2, 4, 8, and 24 hpi) and submitted to cell counting with a Neubauer chamber to evaluate the reduction of cells and the cytopathic effect. As a control for this experiment we used APMV, which was kept under the same conditions as NYMV.

Genome Sequencing and Annotation

The genome of NYMV was sequenced using the Illumina MiSeq instrument (Illumina Inc., San Diego, CA, USA) with the paired-end application. The sequenced reads were imported to CLC_Bio software[1] and assembled into contigs by the *de novo* method. The prediction of open reading frame (ORF) sequences was carried out using the FgenesV tool. ORFs smaller than 100aa were excluded from the annotation. Paralogous groups of genes were predicted by OrthoMCL program. The ORFs were functionally annotated using similarity analyses with sequences in the NCBI database using BLAST tools. In addition, the presence of trademark genes of the family *Mimiviridae* was evaluated, and some of them were analyzed in detail. Genbank number: KT599914.

Similarity Analysis

Viruses of the genus *Mimivirus* are divided into groups A to C. Thereby, the ORFs predicted in NYMV genome were compared to amino acid sequences available in Genebank of APMV (group A), APMOUV (Group B), and MCHV (group C), as well as sequences from SMBV (group A), a Brazilian

[1]http://www.clcbio.com/index.php?id=28

TABLE 3 | Distribution of aminoacyl-tRNA synthetases in mimiviral genomes.

Aminoacyl-tRNA sintetase	Mimivirus strains								
	NYMV	APMV	Mamavirus	SMBV	Hirudovirus	APMV-M4	MCHV	APMOUV	Terra1 virus
Tyrosyl	2	1	1	1	1	0	1	1	1
Cysteinyl	2	1	1	1	1	1	1	1	1
Methionyl	2	1	1	1	1	1	1	1	1
Argiryl	1	1	1	1	1	1	1	4	1
Isoleucyl	0	0	0	0	0	0	1	1	0
Asparaginyl	0	0	0	0	0	0	1	0	0
Tryptophanyl	0	0	0	0	0	0	1	0	0

NYMV, Niemeyer virus; APMV, Acanthamoeba polyphaga mimivirus; SMBV, Samba virus; MCHV, Megavirus chilensis; APMOUV, Acanthamoeba polyphaga moumouvirus.

mimivirus isolate. The AAI calculator program[2] Rodriguez-R and Konstantinos (2014) was used to estimate the average amino acid identity between two protein datasets using both best hits (one-way AAI) and reciprocal best hits (two-way AAI). The similarity and score thresholds for the alignments were 70 and 0%, respectively. A minimum alignment of 50% was considered.

Expression of Translation-related Genes

In order to check the expression of aaRS by NYMV, we selected four genes based on the APMV genome sequence (methionyl, tyrosyl, cysteinyl, and arginyl tRNA synthetases) to evaluate the expression profile of NYMV in comparison with APMV as previously described by Silva et al. (2015). Twenty-four-well plates containing 1×10^5 amoeba per well, kept in PAS medium were infected with NYMV and APMV at M.O.I. 10 and incubated at 32°C for 8 h. Cells were collected, centrifuged and the pellet used for total RNA extraction, reverse transcription and quantitative PCR. Briefly, total RNA was extracted using the RNeasy kit (Qiagen, Germany), and reverse transcription was performed by using the MMLV reverse transcriptase (Promega, USA), as recommended by the manufacturers. The cDNA was used to determine the levels of aaRS mRNA by quantitative PCR (primers in **Table 1**) by using specific primers, SYBR Green Master Mix (Applied Biosystem, USA) and water in 10 μL reactions. Reactions were carried out in a StepOne instrument (Applied Biosystem, USA). All reactions had been previously optimized and presented high efficiency values. Relative gene expression analyses were performed using the ΔΔCt method and normalized to the expression of 18S ribosomal RNA (18S rDNA) and the viral RNA helicase mRNA and calibrated using the lower value (=1). Statistical analysis and primers sequences were as described by Silva et al. (2015).

Phylogeny

The β-DNA polymerase sequence of NYMV was aligned with sequences from other giant viruses, previously deposited in GenBank, using the ClustalW program. After the alignment analysis, phylogeny reconstruction was performed using the maximum likelihood method implemented by the MEGA5 software. Additionally, sequences of aaRS predicted in the genome of NYMV were aligned with sequences from other giant viruses among GenBank sequences as described above, and the phylogeny reconstruction was performed using the neighbor-joining method in the MEGA5 software.

[2]http://enve-omics.ce.gatech.edu/aai/

RESULTS

Niemeyer: A New Mimivirus Group A Isolate

Here we report the isolation of Niemeyer virus (NYMV) from water samples collected in an urban lake in Brazil. The isolation was confirmed by the observation of a cytopathic effect in cells of *A. castellanii* (ATCC 30234) after 4 days of incubation and also by viral RNA helicase gene amplification in qPCR assays, a highly conserved gene amongst mimiviruses.

Electron microscopy and morphometric assays showed virus particles with average size of 616 nm in total, with fibers of about 153 nm and a capsid size of about 463 nm (**Figures 1B,C**), similar to the dimensions described for other mimivirus-like viruses. Large viral factories were observed in the amoebic cytoplasm, and these contained viral particles at distinct steps of morphogenesis. In addition, NYMV demonstrated a similar pattern of replication to APMV in one-step-growth curve assays (**Figure 5A**).

NYMV Genome Analyses and Phylogeny

The final genome assembly of NYMV yielded 69 contigs, consisting of fifteen small contigs (<2,000 bp) and fifty-four large contigs (>2,000 bp), including five contigs larger than 100 kb. The NYMV genome is a double-stranded DNA molecule composed of approximately 1,299,140 base pairs. This genome presented a mean C–G content of 27.96%, which is similar to that of other mimiviruses. A total of 1003 proteins were predicted, ranging in size from 100 to 2156 amino acids, with a mean size of 379 amino acids. Moreover, we identified 970 proteins with high similarity (coverage > 90%; identity > 80%; *e*-value < 10e-5) to mimivirus sequences available in the non-redundant NCBI protein database, as well as 27 proteins with

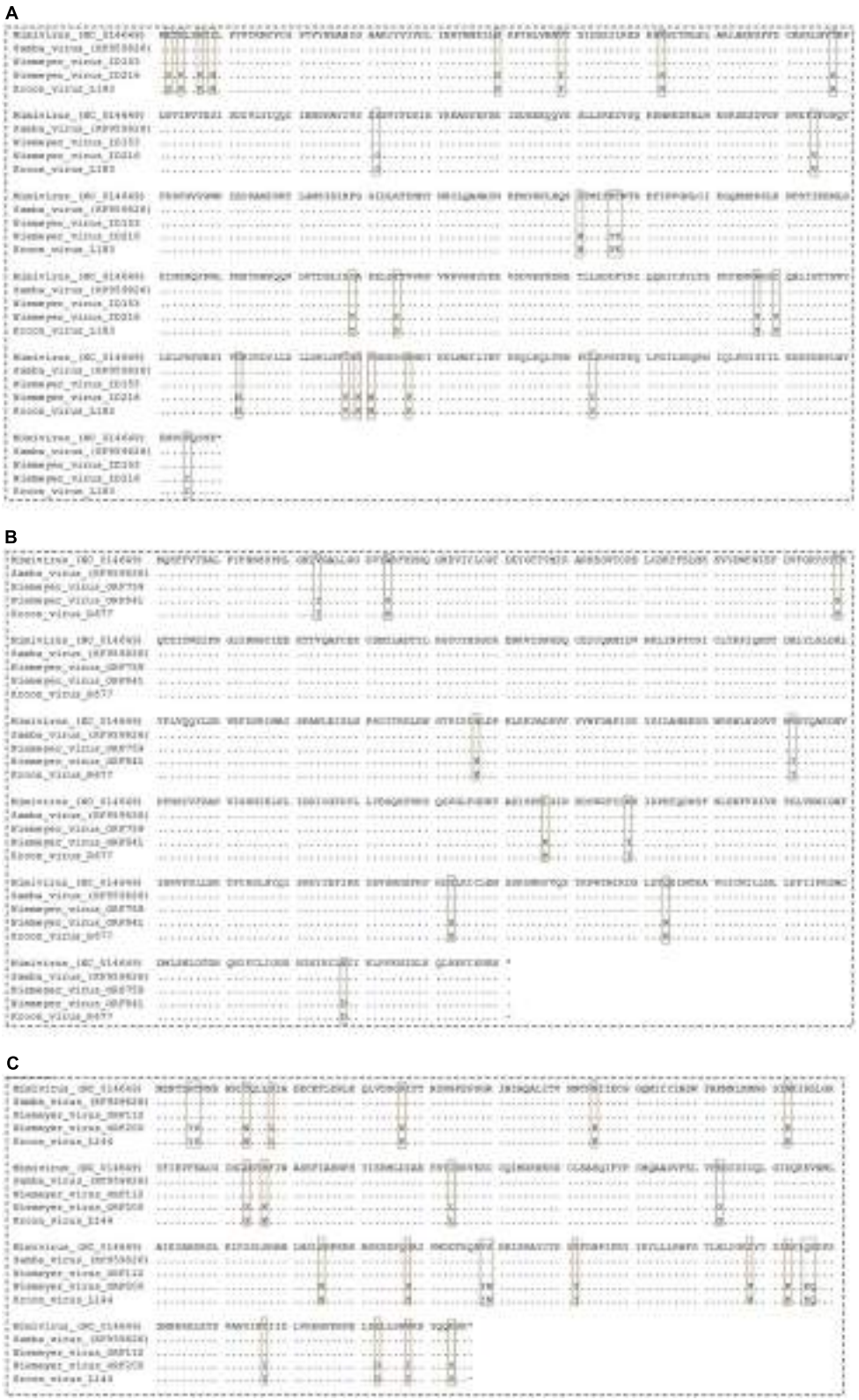

FIGURE 2 | Alignment of NYMV aaRs sequences. (A) Cysteinyl-tRNA synthetase, **(B)** methionyl-tRNA synthetase, and **(C)** tyrosyl-tRNA synthetase sequences. In this analysis sequences from *Acanthamoeba polyphaga mimivirus* (APMV), the prototype of *Mimivirus,* and sequences from Samba virus (SMBV) and Kroon virus (KROV) were used. Brown boxes highlight polymorphisms in the alignments.

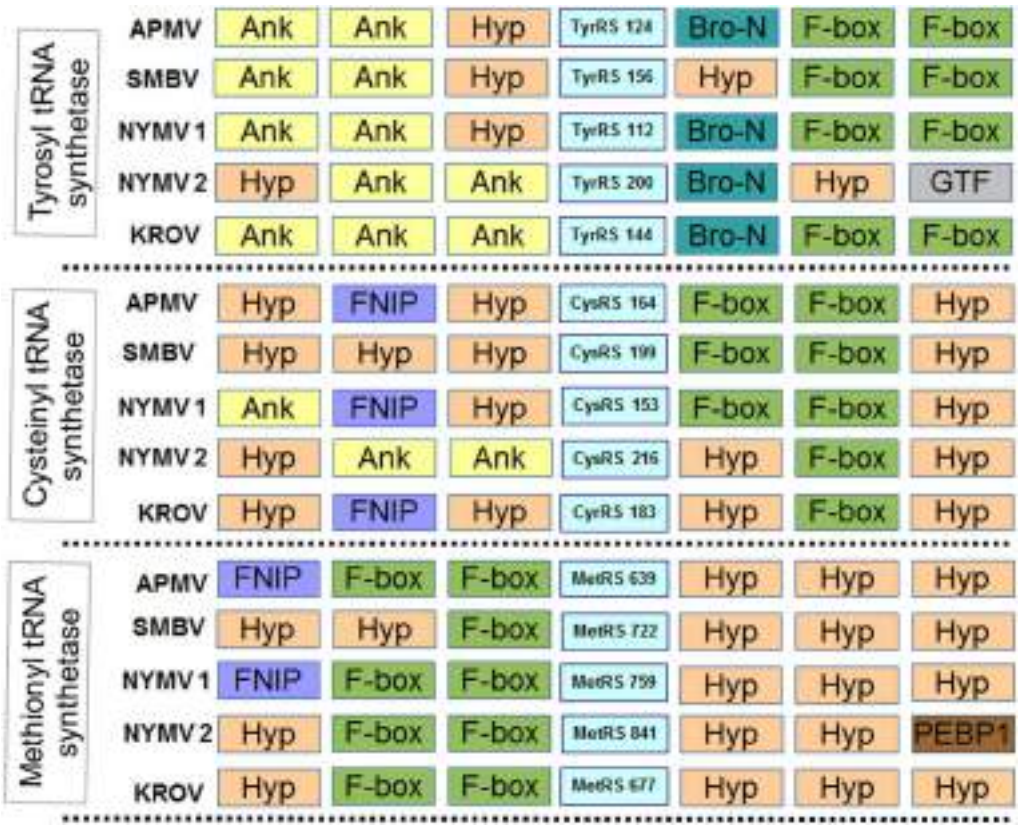

FIGURE 3 | Neighboring gene synteny analyses of aminoacyl-tRNA synthetase. Three upstream and downstream neighbor genes of each aaRS predicted in the genome of NYMV and other mimivirus were checked. Ank, ankyrin repeat family protein; Hyp, Hypothetical Protein; F-box, F-box protein family; Bro-n, bro-n family protein; GTF, glycosyltransferase; FNIP, FNIP repeat-containing protein; PEBP1, phosphatidylethanolamine-binding protein. NYMV 1 and 2 refer to each copy of the aaRS genes.

low similarity (coverage 50%; identity 35–80%; *e*-value < 10e-5) to mimivirus sequences. We identified two proteins with higher similarity to non-viral sequences (ID 80: Ankyrin repeat protein – *Trichomonas vaginalis* [coverage: 83%; identity: 29%; *e*-value: 5e-5]; ID 193: Hypothetical protein – *Volvox carteri* [coverage: 99%; Identity: 36%; *e*-value: 8e-12]). Indeed, four putative proteins of NYMV had no significant hit (*e*-value threshold 1e-2) against the NCBI non-redundant sequence database. A total of 90 clusters consisting of 269 paralogous proteins were identified in the NYMV genome, which is a remarkably higher number than that described for other mimiviruses. It is worth mentioning that neither virophage sequences nor other mobilome elements were detected in the analyzed data set.

A comparative analysis of NYMV gene content with other mimivirus sequences was performed, which showed the highest identity and bit-score distributions against mimivirus group A sequences, such as SMBV (**Supplementary Figure S1A**) and mimivirus (**Supplementary Figure S1B**). Moreover, the similarity decreased toward moumouvirus (**Supplementary Figure S1C**) and *Megavirus chilensis* (**Supplementary Figure S1D**) of groups B and C, respectively. Furthermore, the one-way and two-way best hit analysis (**Table 2**) corroborated the previous observations. This analysis showed a two-way similarity higher than 99% for NYMV with both SMBV and APMV, reinforcing its grouping with other mimiviruses in group A. During functional annotation, we identified important proteins required for virus replication: DNA polymerase, helicases, nucleases, and proteins with DNA polymerase sliding clamp activity related to replication processes; resolvases and topoisomerases related to DNA manipulation and processing; transcription and translation factors; and ATPases for DNA packaging. However, no chaperone molecules were detected in the NYMV genome, as has been described elsewhere (Yutin and Koonin, 2009, Yutin et al., 2009). Furthermore, we identified four regions encoding tRNA molecules for leucine (two sequences), histidine and cysteine amino acids. However, unlike other mimivirus genomes, no tryptophan tRNA gene was detected.

NYMV aaRS Analyses

In addition, we evaluated the presence of the landmark aaRS in NYMV genome. The analysis of such proteins is particularly interesting due to the fact that no virus outside the family *Mimiviridae* has been predicted to encode them. We identified seven aaRS sequences in NYMV genome, being two orthologs

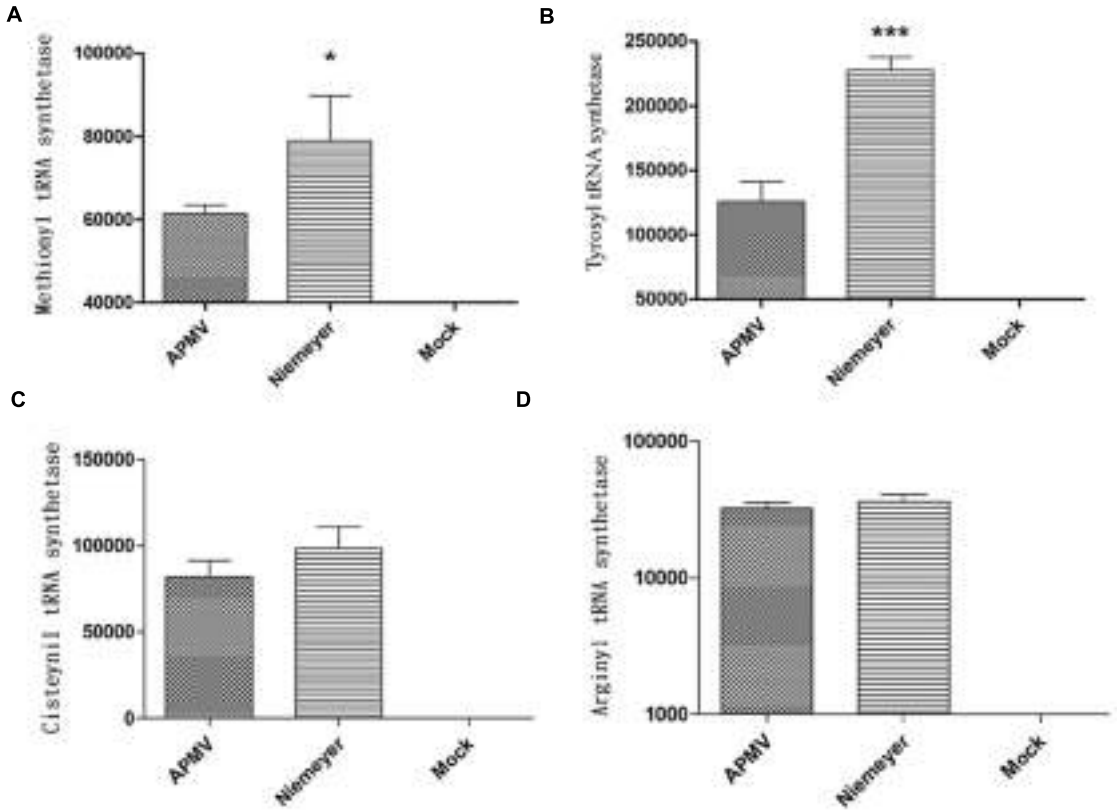

FIGURE 4 | Aminoacyl-tRNA-synthetase (aaRS) mRNA expression by NYMV. (A) Methionyl tRNA synthetase, **(B)** tyrosyl tRNA synthetase, **(C)** cysteinyl tRNA synthetase, and **(D)** arginyl tRNA synthetase. Relative gene expression analyses were performed using the $\Delta\Delta$Ct method and normalized to the expression of 18S ribosomal RNA [18S rDNA) and the viral RNA helicase mRNA (and calibrated with the lower value (=1)]. The values were subjected in different combinations to one-way ANOVA tests and Bonferroni post-tests (95% confidence intervals). Differences between groups were considered significant when the *p*-values were smaller than 0.05 (asterisks). *Y* axis represents relative abundance.

each for tyrosyl, cysteinyl, and methionyl-tRNA synthetases, as well as one sequence for arginyl-tRNA synthetase. The NYMV genome encoded similar aaRS molecules as those detected in the APMV, Mamavirus, SMBV, and Hirudovirus genomes (mimivirus group A), except for Terra1 virus (mimivirus group C). However, no aaRS duplications were observed in such genomes. The aaRS distribution in other mimivirus genomes, including NYMV, can be seen in **Table 3**. The arginyl-tRNA synthetase encoded by NYMV presented 100% identity (amino acid) with the sequences of Mimivirus and SMBV, whereas the duplicated aaRS of NYMV presented some polymorphisms when paralogs were compared with each other (**Figure 2**). Curiously, one copy of each NYMV duplicated aaRS presented 100% identity with APMV and SMBV, while the other copy had 100% identity with Kroon virus (KROV; **Figure 2**), a Brazilian mimivirus-like virus strain isolated from a water sample collected in an urban lake, at Lagoa Santa city, Brazil (approximately 30 km from Pampulha lagoon). The biological and molecular characterization of KROV is in progress, but preliminary results suggest a possible dichotomy among Brazilian mimivirus A isolates. To evaluate the distribution of duplicated aaRS genes within NYMV and other mimivirus genomes, three upstream and downstream genes neighboring aaRS from APMV, SBMV, KROV, and NYMV were analyzed (**Figure 3**). We observed that the duplicated aaRS in the genome of NYMV are not in tandemly duplicated, being located distant from each other (**Figure 3**). The methionyl-tRNA loci presented the best neighbor gene synteny, as all virus strains had two neighboring genes the same on both sides, with the exception of the SMBV strain, which had a distinct neighbor gene at second position toward the 3′ extremity. Altogether, no conservative genomic loci were observed for any aaRS, and none of the analyzed virus strains shared the same neighboring gene for all of the aaRS analyzed, reinforcing the uniqueness of each isolate (**Figure 3**).

Expression of *aaRS* Genes and NYMV Replication Profile

To evaluate the expression profile of NYMV-encoded aaRS during infection, infected *A. castellanii* cells were collected, processed and assayed by Real-time PCR. The results of quantitative PCR were expressed as arbitrary units, fitted to standard curves generated for each target gene and normalized by amoebal 18S rDNA gene levels. Our results

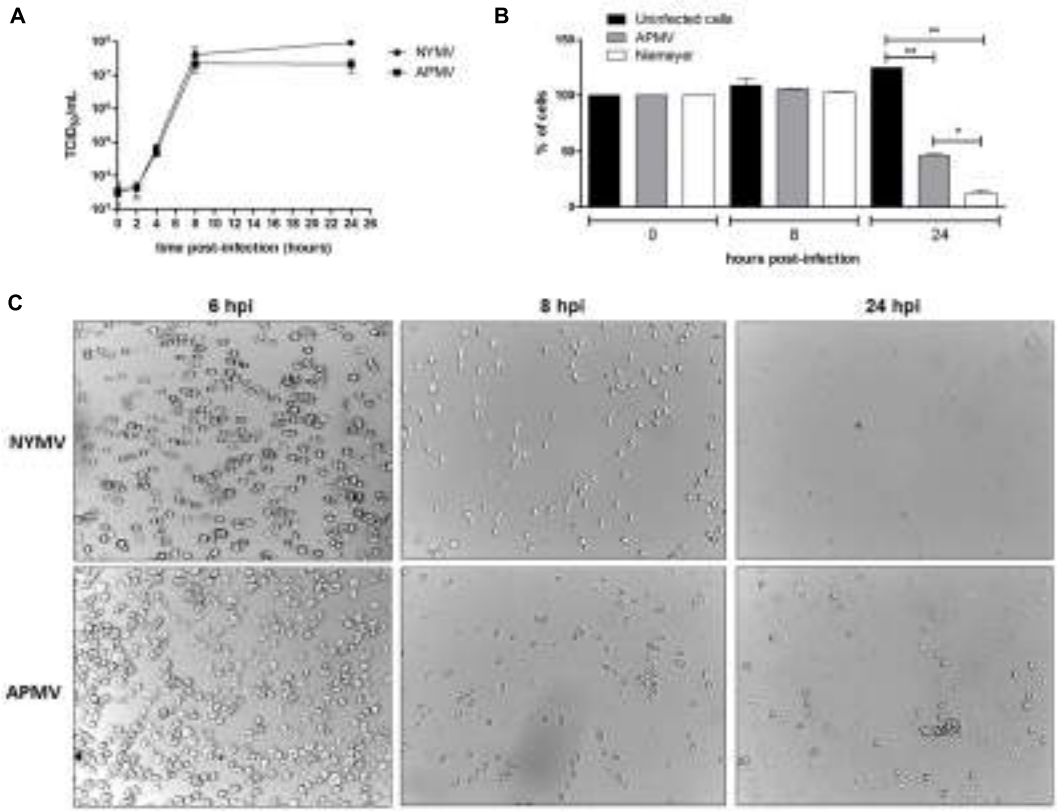

FIGURE 5 | (A) One step growth curves of NYMV and APMV in *Acanthamoeba castellanii*. At 6 hpi cells are similar negative control cell (data not shown). **(B)** *A. castellanii* cells counting at different time points (0, 8, and 24 hpi with APMV or NYMV). **(C)** Images obtained from cells of *A. castellanii* infected with NYMV and APMV at different time points after infection.

revealed that the expression of two aaRS, methionyl-RS, and tyrosyl-RS (both duplicated in NYMV), was significantly distinct between APMV and NYMV ($p < 0.001$ or $p < 0.01$; **Figures 4A,B**), while for the other two analyzed genes, cysteinyl-RS, and arginyl-RS, there was no significant difference in expression between the two viruses (**Figures 4C,D**). Evaluation of the replication profile of NYMV showed that up to 4 hpi, NYMV and APMV showed a similar replication profile. After 8 hpi it was possible to notice an increased lysis of cells infected with NYMV when compared to APMV. After 24 hpi, the lysis induced by NYMV is greater than that induced in the amoebae infected with APMV (**Figure 5**).

NYMV Phylogenetic Analysis

β-DNA polymerase-based phylogenetic analysis corroborated all of the previous observations, clustering the mimivirus NYMV strain with members of *Megavirales* order group A, which includes APMV (the prototype of the family), mamavirus, and other Brazilian mimivirus isolates, such as the SMBV and KROV strains (**Figure 6**). Additionally, we performed aaRS-based phylogenetic analyses of NYMV. The arginyl-tRNA synthetase-based tree (**Figure 7A**) grouped the NYMV within the APMV, SMBV, and Mamavirus branch, with KROV being positioned more distant from the other mimiviruses of group A. The subsequent phylogenetic trees (**Figures 7B–D**), based on duplicated aaRS, presented a peculiar feature, in which one of each doublet grouping within the mimivirus group A branch, and the other copy grouping more distantly with the sequences of the KROV (**Figures 7B–D**).

DISCUSSION

In this work we describe the isolation of NYMV, a new mimivirus group A isolate from an aquatic habitat marked by a high concentration of organic matter, the eutrophicated urban lake Pampulha Lagoon (**Figure 1A**). NYMV presented some features similar to other mimiviruses such as viral particles of approximately 696 nm and the presence of fibers around the capsid; a replication profile similar to APMV; and gene content/similarity resembling viruses belonging to the genus *Mimivirus*. However, as demonstrated by genomic data and gene expression analysis, NYMV harbors duplicated copies of three of its four aaRS genes, which may be associated with an increased expression of methionyl and tyrosyl aaRS mRNA.

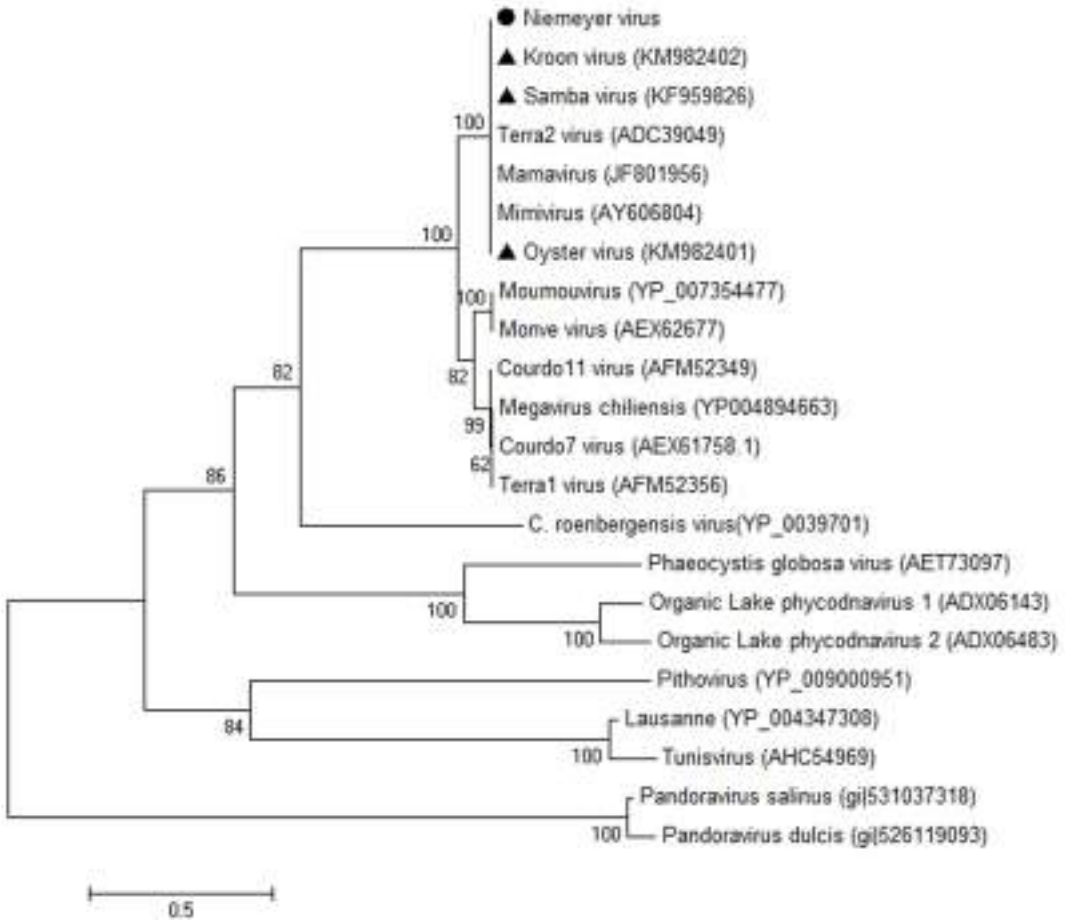

FIGURE 6 | Phylogenetic reconstruction of mimiviruses including the Brazilian Niemeyer mimivirus strain, based on the Polymerase-B amino acid sequences, using MEGA5 software (Maximum-likelihood – 1,000 bootstrap replicates). The NYMV (highlighted by black dot) clustered with other Brazilian mimivirus isolates (triangles), as well as other members of mimivirus lineage A. For each sequence, the gene identification number is indicated.

Gene duplication is an important process driving molecular evolution, allowing the formation of new genes with new or redundant biological functions, affecting the evolutionary history and/or the fitness of the organisms. This process is well described for several species in the different domains of life, especially for the eukaryotes (Zhang, 2003). Simon-Loriere et al. (2013) showed, by using comparative analysis among 55 species of RNA viruses from humans, animals, and plants, distributed across 19 viral families and 30 genera, that genetic duplication seems to have only a modest role in the evolutionary history of RNA viruses (Simon-Loriere et al., 2013). Nonetheless, this process has been described quite commonly for DNA viruses (Shackelton and Holmes, 2004). In viruses belonging to the family *Mimiviridae*, gene duplication events are an open field for new studies. It has already been shown that these processes were very important in shaping the APMV genome during its evolutionary history, with about of one-third of the viral genes having at least one other related gene in the same genome (Suhre, 2005).

Despite this, the duplication of aaRS genes related to protein translation, seems not to be a very frequent event in giant viruses, as demonstrated in **Table 3**, in which only two known viruses present duplications, *Acanthamoeba polyphaga moumouvirus* (Yoosuf et al., 2012) and NYMV. This feature could have brought important adaptive advantages for both viruses, aiding the protection against deleterious mutations in the gene, allowing the emergence of novel mimivirus-like strains during evolutionary history and even potentially endowing the capacity of infecting a larger host range. For example, in the case of the methionyl-tRNA synthetase, duplications of the gene could have brought an important evolutionary advantage since its cognate amino acid is essential for the initiation of protein synthesis. For cysteinyl-tRNA synthetase, a high level of conservation is observed among the mimiviruses in which the genomes have already been described. This could have been important in facilitating the occurrence of an event of genetic duplication. Finally, the gene duplication of tyrosyl-tRNA synthetase could represent an important advantage for NYMV in the environment since its cognate amino acid ranks

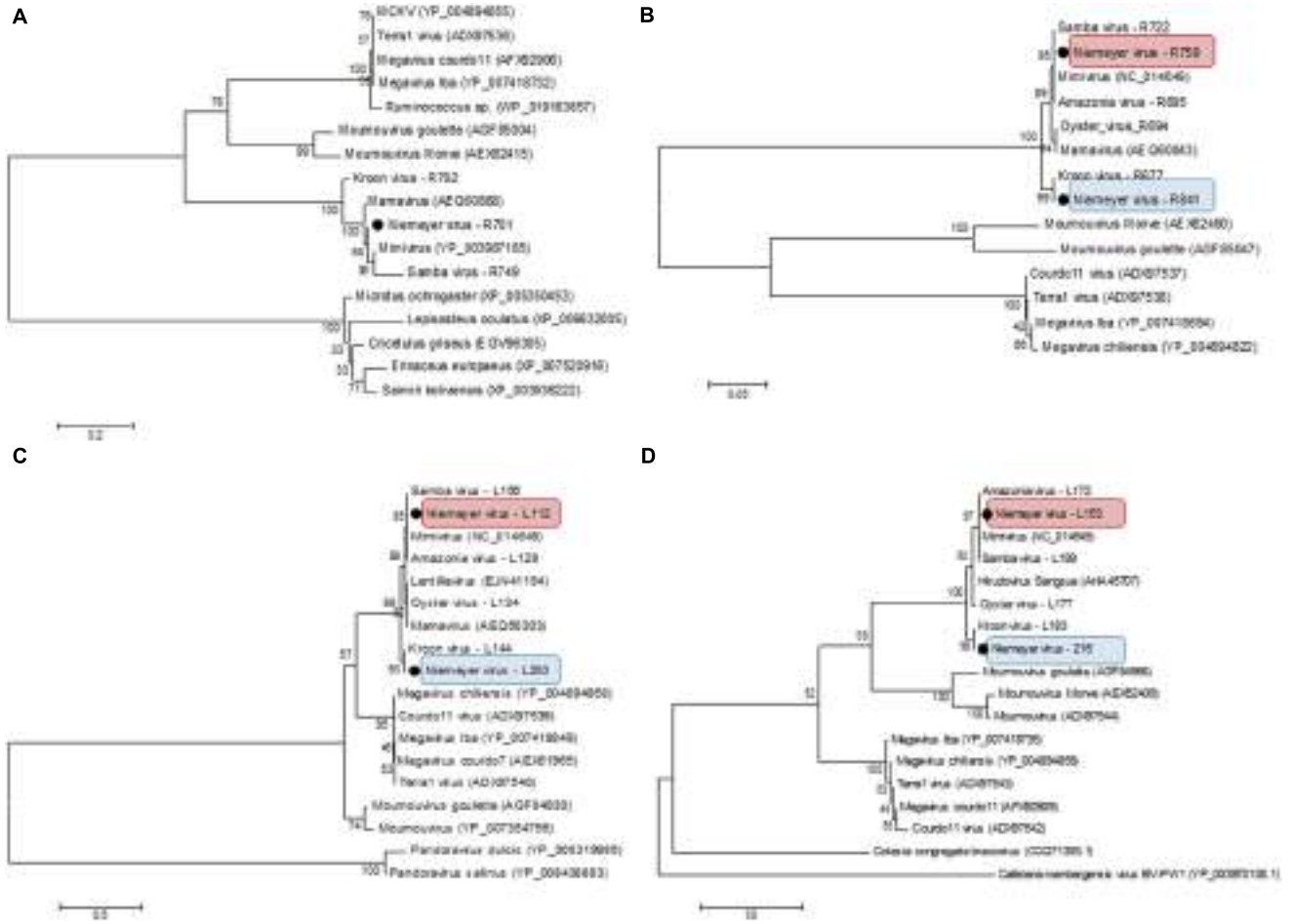

FIGURE 7 | Phylogenetic analysis based on sequences of (A) Arginyl-tRNA synthetase, (B) Methionyl-tRNA synthetase, (C) Tyrosyl-tRNA synthetase, and (D) Cysteinyl-tRNA synthetase predicted in the genome of NYMV, and orthologous sequences obtained from the NCBI database. The trees were inferred by using MEGA5 software (Neighbor-joining – 1,000 bootstrap replicates). The aaRS encoded by NYMV are highlighted by black dots. For each sequence, the gene identification number is indicated. Red and blue boxes indicates the different copies of NYMV aaRS.

highly in the composition of the amino acid usage profile of mimiviruses (Silva et al., 2015). Beyond that, it was demonstrated in another study that apart from the conserved domains presented by aaRSs, which are involved in the process of aminoacylation, these enzymes might also incorporate novel motifs related to new biological functions in different eukaryotic organisms, for example functions related to angiogenic activity, angiostatic activity, and inflammatory response (Guo et al., 2010). Considering this case, the presence of duplicated aaRSs may represent a potential role for the addition of important new biological functions in giant viruses.

Another interesting fact was that from each duplicated copy of aaRS present in NYMV, one gene showed 100% identity with the corresponding APMV and SMBV gene, and the second copy also presented a 100% identity with a giant virus called KROV, isolated by our group from a different urban lake. This result may suggest an event of gene transfer among the ancestors of these viruses (Kroon vs. NYMV and or APMV-like virus and NYMV) in the same host at some moment in their evolutionary history. Furthermore, analysis of the expression of aaRS genes in NYMV showed that methionyl (duplicated) and tyrosyl-RS (duplicated) mRNA expression was significantly higher in cells infected with NYMV in comparison with APMV (**Figures 4A,B**), while for arginyl-RS (unduplicated) and cysteinyl-RS (duplicated), there was no significant difference in the expression (**Figures 4C,D**). Given the sequence similarity observed for the promoters of all of the aaRs genes (**Supplementary Figure S2**), we believe that this differential expression may be due to the presence of the duplicated genes in NYMV in comparison with APMV. This feature could give NYMV an advantage during its replication cycle into the host, increasing in the production of its own proteins during the process of translation and could be the cause of the faster growth of NYMV in comparison to APMV (**Figure 5**). The reason that cysteinyl RS NYMV duplication does not result in significant gene expression needs to be investigated, but it could be a result of some gene specificity regarding amoebal growth conditions (Silva et al., 2015) and/or virus host range.

The results obtained in this work suggest the importance of gene duplication events during the evolutionary history of the aaRSs in mimiviruses. These translation related genes seems to present a considerable influence during replication of the giant viruses in amoebae. This theme then becomes extremely interesting for future studies trying to understand the origin, genetic exchange and evolution of the aaRSs among mimiviruses, as well as the role of these processes in the acquisition of evolutionary advantages by the giant viruses.

AUTHOR CONTRIBUTIONS

PB, TA, LS, FA performed experiments and wrote the paper.

ACKNOWLEDGMENTS

We would like to thank colleagues from Gepvig, Laboratório de Vírus, and Aix Marseille Université for their excellent technical support. Also would like to thank Pro-reitoria de pesquisa da Universidade Federal de Minas Gerais, CAPES, FAPEMIG, CNPq and Marseille Université.

SUPPLEMENTARY MATERIAL

The Supplementary Material for this article can be found online at: http://journal.frontiersin.org/article/10.3389/fmicb.2015.01256

FIGURE S1 | Comparative analysis of Niemeyer virus (NYMV) gene content with other mimivirus sequences. The analysis showed the highest identity and bit-score distributions of NYMV against mimivirus group A sequences, such as Samba virus (SMBV) **(A)** and *Acanthamoeba polyphaga mimivirus* (APMV) **(B)**. Moreover, the similarity decreased toward moumouvirus **(C)** and Megavirus chilensis **(D)** of groups B and C, respectively. At the top of figures are mean and median of each compared group, considering identity and bit score distribution.

FIGURE S2 | Promoter regions analysis of NYMV AaRS. Red arrows indicate the promoter regions. Blue arrows indicate the start-codon regions.

REFERENCES

Abrahão, J. S., Boratto, P. V. M., Dornas, F. P., Silva, L. C., Campos, R. K., Almeida, G. M., et al. (2014). Growing a giant: evaluation of the virological parameters for mimivirus production. *J. Virol. Methods* 207, 6–11. doi: 10.1016/j.jviromet.2014.06.001

Arslan, D., Legendre, M., Seltzer, V., Abergel, C., and Claverie, J. M. (2011). Distant Mimivirus relative with a larger genome highlights the fundamental features of Megaviridae. *Proc. Natl. Acad. Sci. U.S.A.* 108, 17486–17491. doi: 10.1073/pnas.1110889108

Boughalmi, M., Saadi, H., Pagnier, I., Colson, P., Fournous, G., Raoult, D., et al. (2013). High-throughput isolation of giant viruses of the Mimiviridae and Marseilleviridae families in the Tunisian environment. *Environ. Microbiol.* 15, 2000–2007. doi: 10.1111/1462-2920.12068

Campos, R. K., Boratto, P. V., Assis, F. L., Aguiar, E. R., Silva, L. C., Albarnaz, J. D., et al. (2014). Samba virus: a novel mimivirus from a giant rain forest, the Brazilian Amazon. *Virol. J.* 11, 95. doi: 10.1186/1743-422X-11-95

Dornas, F. P., Silva, L. C., de Almeida, G. M., Campos, R. K., Boratto, P. V., Franco-Luiz, A. P., et al. (2014). *Acanthamoeba polyphaga mimivirus* stability in environmental and clinical substrates: implications for virus detection and isolation. *PLoS ONE* 9:e87811. doi: 10.1371/journal.pone.0087811

Gaia, M., Pagnier, I., Campocasso, A., Fournous, G., Raoult, D., and La Scola, B. (2013). Broad spectrum of mimiviridae virophage allows its isolation using a mimivirus reporter. *PLoS ONE* 8:e61912. doi: 10.1371/journal.pone.0061912

Guo, M., Yang, X. L., and Schimmel, P. (2010). New functions of aminoacyl-tRNA synthetases beyond translation. *Nat. Rev. Mol. Cell Biol.* 11, 668–674. doi: 10.1038/nrm2956

La Scola, B., Audic, S., Robert, C., Jungang, L., de Lamballerie, X., Drancourt, M., et al. (2003). A giant virus in amoebae. *Science* 299, 2033. doi: 10.1126/science.1081867

La Scola, B., Campocasso, A., N'Dong, R., Fournous, G., Barrassi, L., Flaudrops, C., et al. (2010). Tentative characterization of new environmental giant viruses by MALDI-TOF mass spectrometry. *Intervirology* 53, 344–353. doi: 10.1159/000312919

Raoult, D., Audic, S., Robert, C., Abergel, C., Renesto, P., Ogata, H., et al. (2004). The 1.2-megabase genome sequence of Mimivirus. *Science* 306, 1344–1350. doi: 10.1126/science.1101485

Rodriguez-R, L. M., and Konstantinos, T. K. (2014). Bypassing cultivation to identify bacterial species – culture-independent genomic approaches identify credibly distinct clusters, avoid cultivation bias, and provide true insights into microbial species. *Microbe* 9, 111–118.

Shackelton, L. A., and Holmes, E. C. (2004). The evolution of large DNA viruses: combining genomic information of viruses and their hosts. *Trends Microbiol.* 12, 458–465. doi: 10.1016/j.tim.2004.08.005

Silva, L. C., Almeida, G. M., Assis, F. L., Albarnaz, J. D., Boratto, V. M., Boratto, D., et al. (2015). Modulation of the expression of mimivirus-encoded translation-related genes in response to nutrient availability during *Acanthamoeba castellanii* infection. *Front. Microbiol.* 6:539. doi: 10.3389/fmicb.2015.00539

Simon-Loriere, E., Holmes, E. C., and Pagán, I. (2013). The effect of gene overlapping on the rate of RNA virus evolution. *Mol. Biol. Evol.* 30, 1916–1928. doi: 10.1093/molbev/mst094

Suhre, K. (2005). Gene and genome duplication in *Acanthamoeba polyphaga Mimivirus*. *J. Virol.* 79, 14095–14101. doi: 10.1128/JVI.79.22.14095-14101.2005

Yoosuf, N., Yutin, N., Colson, P., Shabalina, S. A., Pagnier, I., Robert, C., et al. (2012). Related giant viruses in distant locations and different habitats: *Acanthamoeba polyphaga* moumouvirus represents a third lineage of the Mimiviridae that is close to the megavirus lineage. *Genome Biol. Evol.* 4, 1324–1330. doi: 10.1093/gbe/evs109

Yutin, N., and Koonin, E. V. (2009). Evolution of DNA ligases of nucleo-cytoplasmic large DNA viruses of eukaryotes: a case of hidden complexity. *Biol. Direct.* 4, 51. doi: 10.1186/1745-6150-4-51

Yutin, N., Wolf, Y. I., Raoult, D., and Koonin, E. V. (2009). Eukaryotic large nucleo-cytoplasmic DNA viruses: clusters of orthologous genes and reconstruction of viral genome evolution. *Virol. J.* 6. 223. doi: 10.1186/1743-422X-6-223

Zhang, J. (2003). Evolution by gene duplication: a update. *Trends Ecol. Evol.* 18, 292–298.

Conflict of Interest Statement: The authors declare that the research was conducted in the absence of any commercial or financial relationships that could be construed as a potential conflict of interest.

Oysters as hot spots for mimivirus isolation

Article *in* Archives of Virology · October 2014

DOI: 10.1007/s00705-014-2257-2

10 authors, including:

Lorena C F Silva
Federal University of Minas Gerais
11 PUBLICATIONS **126** CITATIONS
SEE PROFILE

Gabriel Magno de Freitas Almeida
University of Jyväskylä
31 PUBLICATIONS **343** CITATIONS
SEE PROFILE

Erna G Kroon
Federal University of Minas Gerais
251 PUBLICATIONS **2,913** CITATIONS
SEE PROFILE

Jônatas S Abrahão
Federal University of Minas Gerais
153 PUBLICATIONS **883** CITATIONS
SEE PROFILE

Arch Virol
DOI 10.1007/s00705-014-2257-2

BRIEF REPORT

Oysters as hot spots for mimivirus isolation

Kétyllen R. Andrade · Paulo P. V. M. Boratto · Felipe P. Rodrigues · Lorena C. F. Silva · Fábio P. Dornas · Mariana R. Pilotto · Bernard La Scola · Gabriel M. F. Almeida · Erna G. Kroon · Jônatas S. Abrahão

Received: 8 August 2014 / Accepted: 11 October 2014

Abstract Viruses are ubiquitous organisms, but their role in the ecosystem and their prevalence are still poorly understood. Mimiviruses are extremely complex and large DNA viruses. Although metagenomic studies have suggested that members of the family *Mimiviridae* are abundant in oceans, there is a lack of information about the association of mimiviruses with marine organisms. In this work, we demonstrate by molecular and virological methods that oysters are excellent sources for mimiviruses isolation. Our data not only provide new information about the biology of these viruses but also raise questions regarding the role of oyster consumption as a putative source of mimivirus infection in humans.

Viruses are ubiquitous organisms that are found in any environment where life is present. Viruses infect almost all known living organisms, from bacteria to whales, and even other viruses. It has been estimated that there are 10^{31} viral particles in the oceans, which cause the death of approximately 20 % of the marine biomass daily [31]. Despite this, little is known about the role of the viruses in most ecosystems [13, 25]. The members of one particular group of viruses, the nucleocytoplasmic large DNA viruses (NCLDV), have a wide host range, infecting a variety of hosts, including eukaryotic algae (*Phycodnaviridae*), protists (*Mimiviridae*), and metazoans (*Poxviridae, Asfarviridae, Iridoviridae, Mimiviridae*) [11, 15, 32, 35, 37]. The family *Mimiviridae* is included in the NCLDV group, with *Acanthamoeba polyphaga* mimivirus (APMV) as its prototype [17, 20, 22, 23]. APMV was first found to be associated with amoebas in a water sample collected from a cooling tower of a hospital in England. APMV has a diameter of about 700 nm and a double-stranded DNA genome of ~1.2 megabases encoding proteins not previously observed in other viruses [17, 18, 20, 34].

After the discovery of APMV, several mimiviruses from different environments were isolated, including *Acanthamoeba castellanii* mamavirus, which was also isolated from a water sample from a cooling tower [5]; megavirus chiliensis, which was recently isolated from seawater [1]; *Cafeteria roebergensis* virus, which can infect unicellular algae [12]; and lentille virus, isolated from contact lens fluids from a patient with keratitis [8]. More recently, studies have shown tangible evidence of an association between giant viruses and animals, vertebrates and invertebrates, and mimiviruses have been isolated from of bronchoalveolar lavage and stool samples from pneumonia patients [2, 4, 9, 23, 26, 29].

Due to the filtration methods previously used for virus isolation, giant viruses were trapped, and their discovery was therefore delayed. Some of the data on these viruses were obtained through metagenomic studies [16, 19]. Metagenomic studies of samples of marine origin have

Electronic supplementary material The online version of this article (doi:10.1007/s00705-014-2257-2) contains supplementary material, which is available to authorized users.

K. R. Andrade · P. P. V. M. Boratto · F. P. Rodrigues · L. C. F. Silva · F. P. Dornas · G. M. F. Almeida · E. G. Kroon · J. S. Abrahão (✉)
Laboratório de Vírus, Instituto de Ciências Biológicas, Universidade Federal de Minas Gerais, Belo Horizonte, Minas Gerais, Brazil
e-mail: jonatas.abrahao@gmail.com

M. R. Pilotto
Universidade Federal de Santa Catarina, Florianópolis, Brazil

B. La Scola
URMITE CNRS UMR 6236, IRD 3R198, Aix Marseille Universite, Marseille, France

resulted in the identification of a variety of mimivirus-like sequences, suggesting that members of the family *Mimiviridae* are abundant in this environment [13, 16, 19]. In the marine environment, oysters deserve attention when searching for viruses, because of their constant filtration behavior. By filtering water in order to feed, these organisms accumulate in their body chemical compounds and microorganisms that are present in the surrounding water. Oysters have a highly efficient filtration capacity, filtering more than 400 liters per day [28, 30]. Thus, oysters can be used as bio-indicators for water contamination, and their consumption can result in risks to human health [6, 30]. In addition, many viral and non-viral pathogens, including those of humans, can be isolated from oyster, such as norovirus [27], *Cryptosporidium parvum* [33], *Vibrio cholera* [14], and ostreid herpes virus 1 [7, 24].

In this work, we demonstrate that oysters are excellent sources for isolation of giant viruses. Isolation of mimivirus-like viruses from oysters is important not only for increasing our knowledge regarding the biology of these viruses but also for raising questions regarding the role of oyster consumption as a putative source of APMV infection in humans.

A total of 99 samples (49 oysters and 50 seawater samples) were collected between 2012 and 2013 in three distinct Brazilian coastal regions belonging to Santa Catarina, Rio Grande do Norte and Bahia States (Fig. 1A). Oysters were obtained from oyster production farms. The oyster's body and inner water were collected and transferred to sterile 50-ml tubes. Seawater samples were collected at the same sites where oysters were collected, using sterile 2-ml tubes. All samples were manipulated separately to avoid cross-contamination. Data regarding the number of samples per collection site are shown in Fig. 1A and Table 1. In order to increase the efficiency of virus recovery, samples were subjected to an enrichment process [10]. After this procedure, total DNA was extracted from the samples by the phenol-chloroform method and used as template for real-time PCR assays targeting the conserved helicase gene (primers: 5′-ACCTGATCCACATCCCATAACTAAA-3′ and 5′-GGCCTCATCAACAAATGGTTTCT-3′), using a SYBR Green Master Mix (Applied Biosystems, USA) in 10-μL reactions. The reactions were done in a Step One instrument (Applied Biosystems, USA). In parallel, samples were also used for an isolation assay in *Acanthamoeba castellanii* (ATCC 30010) monolayers. A total of three blind passages were performed, and samples showing a cytopathic effect were collected, titrated using the $TCID_{50}$ method and analyzed by transmission electron microscopy (TEM) and qPCR [10]. Also, to characterize those isolates biologically, representative viral samples from each studied area were used to make one-step-growth curves and analyzed by polyacrylamide gel electrophoresis (PAGE) [3].

A marked difference was observed between the rates of detection of mimiviruses from oysters and water samples (Table 1) regardless of the collection site. From a total of 99 samples (49 oysters and 50 seawater samples), 22 oysters (44.9 %) were positive in the qPCR assay, while

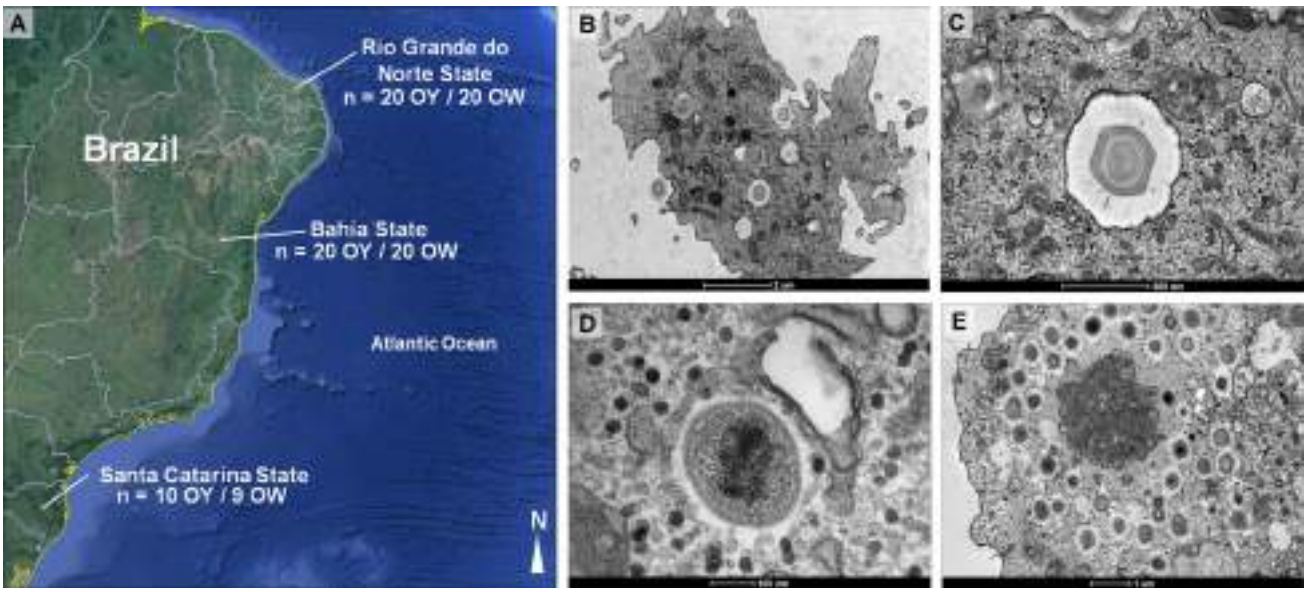

Fig. 1 **(A)** Sample collection sites. Samples were collected from three different sites: Natal (Rio Grande do Norte; 05°47′42″S 35°12′32″W); Salvador (Bahia; 12°58′16″S 38°30′39″W); Florianópolis (Santa Catarina; 27°40′14″S, 48°32′50″W). OW, ocean water sample; OY, oyster sample. **(B-E)** Transmission electron microscopy of infected *Acanthamoeba* highlighting the different steps of the mimivirus life cycle (all of these isolates were obtained from oyster samples). Entry of mimivirus particles in an *Acanthamoeba* cell by phagocytosis **(B)**. Viral particle in a vesicle **(C)**. Viral seed **(D)**. Viral factory **(E)**

Table 1 Detection of mimiviruses in oysters and ocean water - comparison between isolation and polymerase chain reaction results

State and samples	Total no. of samples	Real-time PCR, helicase gene		Isolation in *Acanthamoeba*	
		No. (%) negative samples	No. (%) positive samples	No. (%) negative samples	No. (%) positive samples
Santa Catarina					
Ocean water	10	10 (100.0)	0 (0.0)	10 (100.0)	0 (0.0)
Oyster	9	2 (22.2)	7 (77.8)	4 (44.5)	5 (55.5)
Bahia					
Ocean water	20	18 (90.0)	2 (10.0)	18 (90.0)	2 (10.0)
Oyster	20	12 (60.0)	8 (40.0)	13 (65.0)	7 (35.0)
R. Grande do Norte					
Ocean water	20	20 (100.0)	0 (0.0)	20 (100.0)	0 (0.0)
Oyster	20	13 (65.0)	7 (35.0)	12 (60.0)	8 (40.0)
Total					
Ocean water	50	48 (96.0)	**2 (4.0)**	48 (96.0)	**2 (4.0)**
Oyster	49	27 (55.1)	**22 (44.9)**	29 (59.2)	**20 (40.8)**

Main findings are in bold

only two seawater samples (4.0 %) were positive. Mimiviruses were isolated successfully from 20 of the 22 positive oyster samples (40.8 % of all of the oyster samples). All seawater samples that were positive in the qPCR assays were also positive in the isolation experiments (4.0 %). By comparing qPCR and isolation, we observed a higher positivity rate for the first method, as was expected because of its higher sensitivity. These results contrast with those from a previous study [21]. However, other factors, such as the integrity of viral particles and the differences between the natural cellular hosts and the cells used for isolation could also explain the slight difference between the qPCR and isolation results (Table 1).

In order to evaluate the morphological features of the isolated viruses and their similarity to other giant viruses, electron microscopy was performed. Briefly, *Acanthamoeba castellanii* were infected at an m.o.i. of 0.01 for 36 hours and then fixed with 2.5 % glutaraldehyde (Merck, Germany) for one hour before visualization by electron microscopy, ultrathin sections were prepared and analyzed at the Centro de Microscopia, UFMG, Brazil [10]. Images of our samples revealed the presence of typical mimivirus-like particles, with sizes ranging between 500 and 700 nm (Fig. 1B-C). In some images, it was possible to visualize the typical stargate face and long surface fibrils. Typical viral seeds were also observed in some infected *Acanthamoeba* samples (Fig. 1D). Large viral factories (>2 μM) were observed in the amoebic cytoplasm, and these contained viral particles at distinct steps of morphogenesis (Fig. 1E).

In addition, qPCR-amplified DNA from 24 positive samples (24.24 % of the total) were sequenced in both orientations and in duplicates (MegaBACE sequencer; GE Healthcare, Buckinghamshire, UK). Sequences were aligned with previously published sequences from GenBank using ClustalW and MEGA software version 4.1 (Arizona State University, Phoenix, AZ, USA) (http://www.megasoftware.net). The optimal nucleotide sequence alignment of a fragment of the mimivirus helicase gene revealed a high similarity (98.2-100 %) among our isolates and mimiviruses belonging to group A, including APMV, mamavirus, sambavirus and others [3, 5, 8]. However, some samples contained polymorphic sites in the helicase gene (Fig. 2A). Phylogenetic trees were constructed using the neighbor-joining method, and they showed a close relationship between our novel isolates and viruses of the family *Mimiviridae*, especially group A mimiviruses (Fig. 2B). The genetic diversity among strains of mimivirus may have been the cause of all our isolates belonging to group A and may have prevented detection of mimiviruses of groups B and C (moumouvirus and megavirus chiliensis relatives, respectively). However, since culture isolation was performed concurrently, it is unlikely that many mimiviruses from lineages B and C were missed [1, 5, 36]. PAGE assays also revealed similar viral particle protein profiles among the prototype APMV and oyster mimivirus isolates (Supplemental Figure A), although it was possible to observe differences in the growth profiles of the isolates in one-step growth curve assays (Supplemental Figure B).

Taken together, our data suggest that oysters are an excellent source for isolation of giant viruses, probably due to their physiology, which allows the accumulation of viruses and possibly amoebae. There is no evidence that mimiviruses can be propagated and reproduced in oysters. As mentioned above, *Acanthamoeba* are their known reservoirs. We could detect *Acanthamoeba* DNA from the most mimiviruses PCR-positive samples (70.8 % of positivity by real-time PCR) (data not shown). Since amoebas are the natural reservoirs of mimiviruses, which in turn are ubiquitous in the aquatic environment, oysters could

A

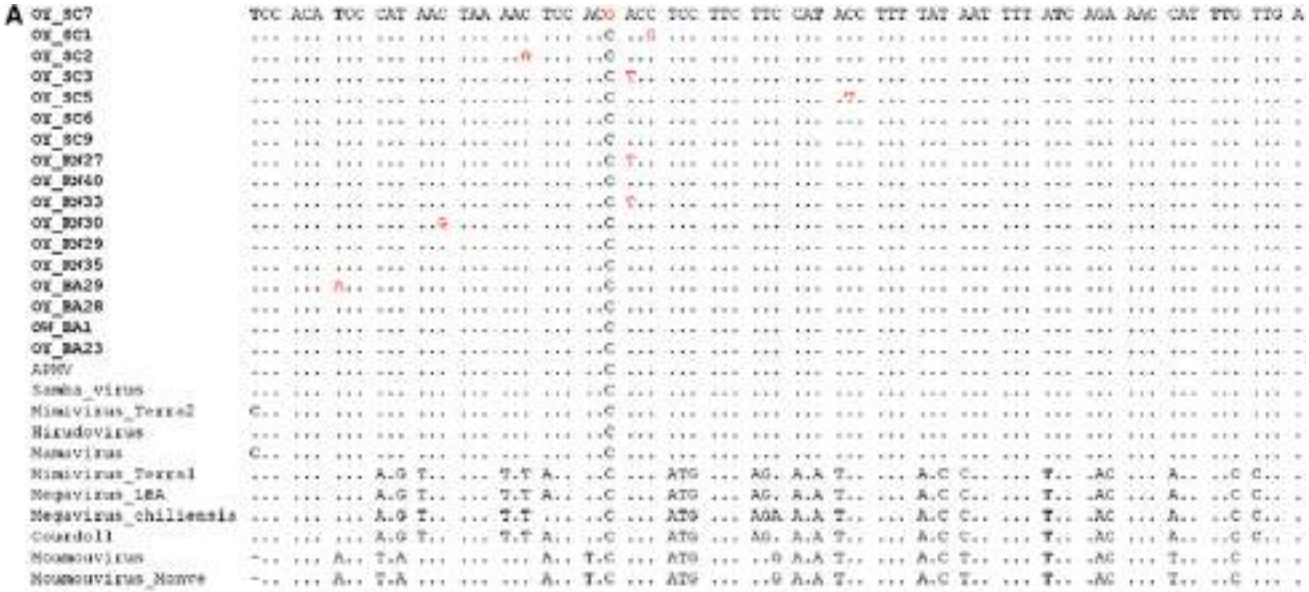
OY_SC7
OY_SC1
OY_SC2
OY_SC3
OY_SC5
OY_SC6
OY_SC9
OY_RN27
OY_RN40
OY_RN33
OY_RN30
OY_RN29
OY_RN35
OY_BA29
OY_BA28
OW_BA1
OY_BA23
APMV
Samba_virus
Mimivirus_Terra2
Hirudovirus
Mamavirus
Mimivirus_Terra1
Megavirus_LBA
Megavirus_chilliensis
Courdo11
Moumouvirus
Moumouvirus_Monve

B

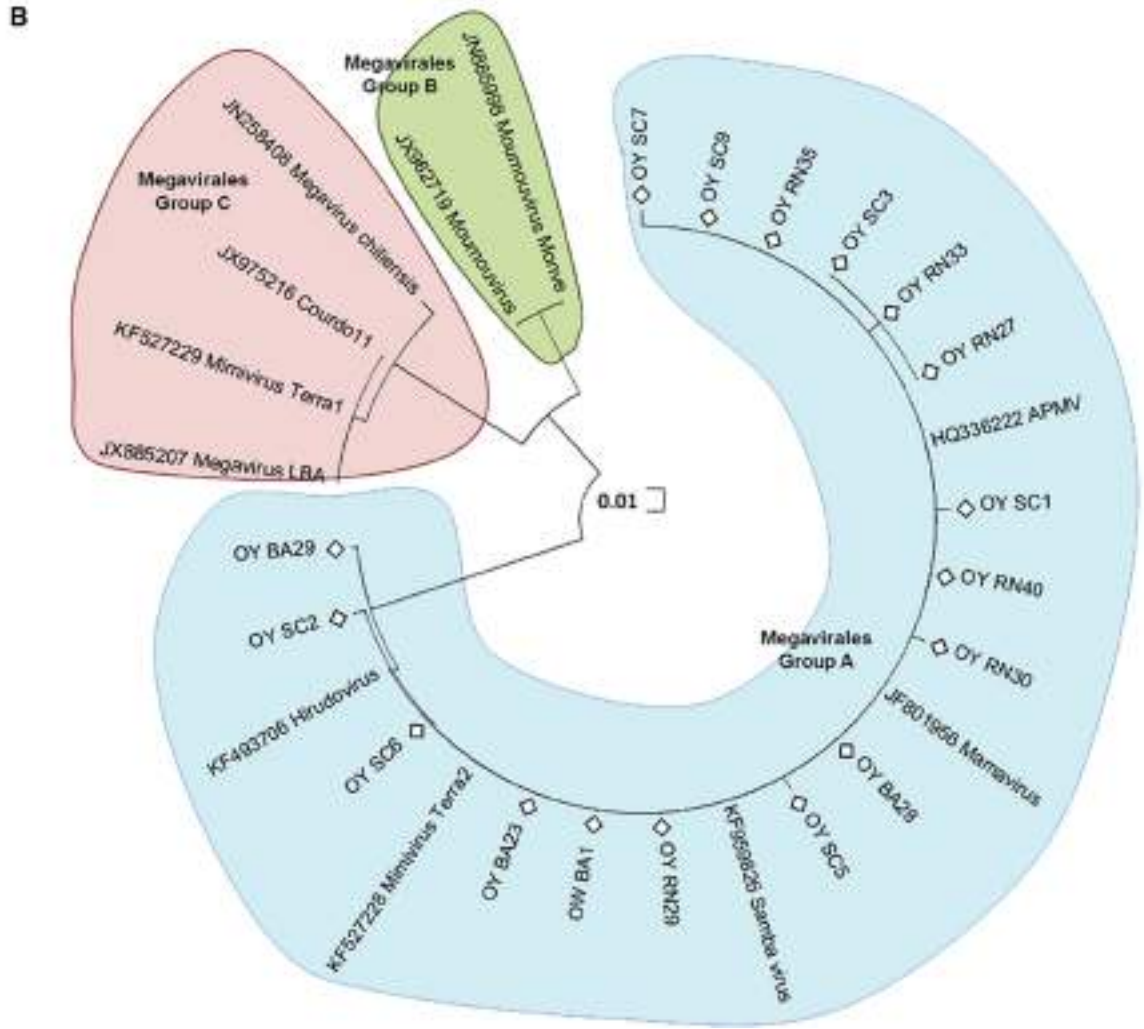
Megavirales Group B
JN850950 Moumouvirus Monve
JX962719 Moumouvirus
Megavirales Group C
JN258408 Megavirus chilliensis
JX975216 Courdo11
KF527229 Mimivirus Terra1
JX885207 Megavirus LBA
0.01
OY SC7
OY SC9
OY RN35
OY SC3
OY RN33
OY RN27
HQ336222 APMV
OY SC1
OY RN40
OY RN30
JF801956 Mamavirus
OY BA28
OY SC5
KF959826 Samba virus
OY RN29
OW BA1
OY BA23
KF527228 Mimivirus Terra2
OY SC6
KF493706 Hirudovirus
OY SC2
OY BA29
Megavirales Group A

◀**Fig. 2** **(A)** Nucleotide sequence alignment of a fragment of the nucleocytoplasmic large DNA virus helicase gene. Samples obtained in this study are shown in boldface type; nucleotides in red indicate sites that are polymorphic among isolates obtained in this study. **(B)** Neighbor-joining phylogenetic tree constructed using sequences from the amplicons obtained from the helicase gene. OW, ocean water sample; OY, oyster sample

function as an enrichment medium, favoring a high viral load of these viruses, the isolation of which will deepen our understanding of the biology and evolution of these organisms. This is also of public-health interest, since oysters are eaten by humans and have a high content of nutrients such as minerals (phosphorus, calcium, iron and iodine), glycogen, vitamins (A, B1, B2, C and D) and protein [28]. There is increasing evidence that APMV might play a role as a pathogen of humans and other vertebrate [9, 26, 29], and our results therefore raise concerns about the possibility of oysters being a possible source of APMV infection when consumed by humans.

Acknowledgments We thank Laboratório de Vírus colleagues for their excellent technical support. We also thank Coordenação de Aperfeiçoamento de Pessoal de Nível Superior (CAPES), Conselho Nacional de Desenvolvimento Científico e Tecnológico (CNPq), Fundação de Amparo à Pesquisa do estado de Minas Gerais (FAPEMIG) and the Pró -Reitoria de Pesquisa da Universidade Federal de Minas Gerais. EGK is a CNPq researcher.

Conflicts of interest The authors declare no conflicts of interest.

References

1. Arslan D, Legendre M, Seltzer V, Abergel C, Claverie JM (2011) Distant Mimivirus relative with a larger genome highlights the fundamental features of *Megaviridae*. PNAS 108:17486–17491
2. Boughalmi M, Pagnier I, Aherfi S, Colson P, Raoult D, La Scola B (2013) First Isolation of a Giant Virus from Wild *Hirudo medicinalis* Leech: *Mimiviridae* isolation in *Hirudo medicinalis*. Viruses 5:2920–29030
3. Campos RK, Boratto PV, Assis FL, Aguiar ER, Albarnaz JD et al (2014) Samba virus; a novel mimivirus from a giant rain forest, the Brazilian Amazon. Virol J 11:95
4. Claverie JM, Grzela R, Lartigue A, Bernadac A, Nitsche S, Vacelet J, Ogata H, Abergel C (2009) Mimivirus and Mimiviridae: Giant viruses with an increasing number of potential hosts, including corals and sponges. J Invertebr Pathol 101:172–180
5. Colson P, Yutin N, Shabalina SA, Robert C, Fournous G, La Scola B, Raoult D, Koonin EV (2011) Viruses with more than 1,000 genes: mamavirus, a new Acanthamoeba polyphaga mimivirus strain, and reannotation of mimivirus genes. Genome Biol Evol 3:737–742
6. Corrêa AA, Rigotto C, Moresco V, Kleemann CR, Teixeira AL, Poli CR, Simões CMO, Barardi CRM (2012) The depuration dynamics of oysters (*Crassostrea gigas*) artificially contaminated with hepatites A vírus and human adenovirus. Memorias do Instituto Oswaldo Cruz 107:11–17
7. Davison AJ, Trus BL, Cheng N, Steven AC, Watson MS, Cunningham C, Le Deuff RM, Renault T (2005) A novel class of herpesvirus with bivalve hosts. J Gen Virol 86:41–53
8. Desnues C, La Scola B, Yutin N, Fournous G, Robert C, Azza S et al (2012) Provirophages and transpovirons as the diverse mobilome of giant viruses. PNAS 109:18078–18083
9. Dornas FP, Rodrigues FP, Boratto PV, Ferreira PC, Bonjardim CA, Trindade GS, Kroon EG, Abrahão JS (2014) Mimivirus circulation among wild and domestic mammals, amazon region, Brazil. Emerg Infect Dis 3:469–472
10. Dornas FP, Silva LC, de Almeida GM, Campos RK, Boratto PV, Franco-Luiz AP, La Scola B, Ferreira PC, Kroon EG, Abrahão JS (2014) *Acanthamoeba polyphaga mimivirus* stability in environmental and clinical substrates: implications for virus detection and isolation. PLoS One 2:1–7
11. Filée J (2009) Lateral gene transfer, lineage-specific gene expansion and the evolution of nucleo cytoplasmic large DNA viruses. J Invertebr Pathol 101:169–171
12. Fischer MG, Allen MJ, Wilson WH, Suttle CA (2010) Giant virus with a remarkable complement of genes infects marine zooplankton. PNAS 107:19508–19513
13. Ghedin E, Claverie JM (2005) Mimivirus relatives in the Sargasso Sea. Virol J 2:62
14. Haley B, Choi SY, Shakur HA, Cebula TA, Huq A, Colwell RR (2013) Genome sequences of clinical *Vibrio cholerae* isolates from an oyster-borne cholera outbreak in florida. Genome Announcements 1:1–2
15. Iyer LM, Balaji S, Koonin EV, Aravind L (2006) Evolutionary genomics of nucleo-cytoplasmic large DNA viruses. Virus Res 117:156–184
16. Kristensen DM, Mushegian AR, Dolja VV, Koonin EV (2010) New dimensions of the virus world discovered through Metagenomics. Trends Microbiol 18:11–19
17. La Scola B, Audic S, Robert C, Jungang L, de Lamballerie X, Drancourt M, Birtles R et al (2003) A giant virus in amoebae. Science 299:2033
18. Legendre M, Audic S, Poirot O, Hingamp P, Seltzer V, Byrne D et al (2010) mRNA deep sequencing reveals 75 new genes and a complex transcriptional landscape in Mimivirus. Genome Res 20:664–674
19. Monier A, Claverie JM, Ogata H (2008) Taxonomic distribution of large DNA viruses in the sea. Genome Biol 9:106
20. Moreira D, Brochier-Armanet C (2008) Giant viruses, giant chimeras: the multiple evolutionary histories of Mimivirus genes. BMC Evol Biol 8:01–10
21. Pagnier I, Reteno DGI, Saadi H, Boughalmi M, Gaia M, Slimani M, Ngounga T et al (2013) A decade of improvements in mimiviridae and marseilleviridae isolation from amoeba. Intervirology 56:354–363
22. Raoult D, Audic S, Robert C, Abergel C, Renesto P, Ogata H et al (2004) The 1.2-megabase genome sequence of Mimivirus. Science 306:1344–1350
23. Raoult D, La Scola B, Birtles R (2007) The discovery and characterization of Mimivirus, the largest known virus and putative pneumonia agent. Clin Infect Dis 45:95–102
24. Renault T, Le Deuff RM, Cochennec N, Chollet B, Maffart P (1995) Herpes-like viruses associated with high mortality levels in larvae and spat of Pacific oysters, *Crassostrea gigas*: a comparative study, the thermal effects on virus detection in hatchery-reared larvae, reproduction of the disease in axenic larvae. Vet Res 26:539–543
25. Rohwer F, Prangishvili D, Lindell D (2009) Roles of viruses in the environment. Environ Microbiol 11:2771–2774
26. Saadi H, Reteno DGI, Colson P, Aherfi S, Minodier P, Pagnier I, Raoult D, La Scola B (2013) Shan virus: a new mimivirus

isolated from the stool of a Tunisian patient with pneumonia. Intervirology 56:424–429
27. Schaeffer J, Le Saux JC, Lora M, Atmar RL, Le Guyader FS (2013) Norovirus contamination on French marketed oysters. Int J Food Microbiol 166:244–248
28. Carvalho AFU, Farias DF, Barroso CX, Sombra CML, Silvino AS, Menezes MOT, Soares MO, Fernandes DAO, Gouveia ST (2007) Nutritive value of three organisms from mangrove ecosystem: Ucides cordatus (Linnaeus, 1763), Mytella sp. (Soot-Ryen, 1955) and Crassostrea rhizophorae (Guilding, 1828). Braz J Biol 67:787–788
29. Silva LC, Almeida GM, Oliveira DB, Campos RK, La Scola B, Ferreira PC, Kroon EG, Abrahão JS (2013) A resourceful giant: APMV is able to interfere with the human type I interferon system. Microbes Infect 16:187–195
30. Souza DSM, Piazza RS, Pilotto MR, Nascimento MA, Moresco V, Taniguchi S, Leal DAG et al (2013) Virus, protozoa and organic compounds decay in depurated oysters. Int J Food Microbiol 167:337–345
31. Suttle CA (2005) Viruses in the sea. Nature 4370:356–361
32. Van Etten JL (2011) Another really, really big virus. Viruses 3:32–46
33. Willis JE, McClure JT, McClure C, Spears J, Davidson J, Greenwood SJ (2014) Bioaccumulation and elimination of *Cryptosporidium parvum* oocysts in experimentally exposed Eastern oysters (*Crassostrea virginica*) held in static tank aquaria. Int J Food Microbiol 173:72–80
34. Xiao C, Kuznetsov YG, Sun S, Hafenstein SL, Kostyuchenko VA, Chipman PR et al (2009) Structural studies of the giant mimivirus. PLoS Biol 7:958–966
35. Yamada T (2011) Giant viruses in the environment: their origins and evolution. Curr Opin Virol 1:58–62
36. Yoosuf N, Yutin N, Colson P, Shabalina SA, Pagnier I, Robert C, Azza S et al (2012) Related giant viruses in distant locations and different habitats: *Acanthamoeba polyphaga moumouvirus* represents a third lineage of the Mimiviridae that is close to the *Megavirus* lineage. Genome Biol Evol 4:1324–1330
37. Yutin N, Wolf YI, Raoult D, Koonin EV (2009) Eukaryotic large nucleo-cytoplasmic DNA viruses: clusters of orthologous genes and reconstruction of viral genome evolution. Virol J 6:223

Mimivirus Circulation among Wild and Domestic Mammals, Amazon Region, Brazil

Fábio P. Dornas, Felipe P. Rodrigues, Paulo V.M. Boratto, Lorena C.F. Silva, Paulo C.P. Ferreira, Cláudio A. Bonjardim, Giliane S. Trindade, Erna G. Kroon, Bernard La Scola, and Jônatas S. Abrahão

To investigate circulation of mimiviruses in the Amazon Region of Brazil, we surveyed 513 serum samples from domestic and wild mammals. Neutralizing antibodies were detected in 15 sample pools, and mimivirus DNA was detected in 9 pools of serum from capuchin monkeys and in 16 pools of serum from cattle.

The group of nucleocytoplasmic large DNA viruses includes viruses that are able to infect different hosts, such as animals, green algae, and unicellular eukaryotes (*1*). Several members of this group are widely distributed in various environments, actively circulate in nature, and are responsible for outbreaks of medical importance (*2*,*3*). *Mimiviridae*, the newest family in this group, has been researched as a putative pneumonia agent and found in different biomes worldwide (*3*,*5*–*9*). The ubiquity of freeliving amebas and their parasitism by mimiviruses enhances the prospect that diverse environments could shelter these giant viruses (*8*–*10*). Mimiviruses can induce infection in a murine model, have had antibodies detected in patients with pneumonia, and can replicate in murine and human phagocytes (*11*,*12*). Moreover, although some authors suggest that mimivirus is a not frequent pneumonia agent (*4*), mimivirus has been isolated from a human with pneumonia (*3*).

The biomes in Brazil, particularly in the Amazon region, provide the diversity, species richness, and ecologic relationships ideal for identifying circulation of mimiviruses. Preliminary studies found *Acanthamoeba polyphaga mimivirus* (APMV) genomes in samples of bovine serum from Germany (*13*,*14*), indicating that the analysis of samples from vertebrates could be a way to explore and understand the circulation of this group of viruses in nature. We describe the detection of mimivirus antibodies and DNA in 2 mammalian species in the Amazon region of Brazil.

Author affiliations: Universidade Federal de Minas Gerais, Belo Horizonte, Brazil (F.P. Dornas, F.P. Rodrigues, P.V.M. Boratto, L.C.F. Silva, P.C.P. Ferreira, C.A. Bonjardim, G.S. Trindade, E.G. Kroon, J.S. Abrahão); and URMITE CNRS UMR 6236, IRD 3R198, Aix Marseille Université, Marseille, France (B. La Scola)

DOI: http://dx.doi.org/10.3201/eid2003.131050

The Study

We selected 321 serum samples collected from wild monkeys from the Amazon region of Brazil during 2001–2002: 91 from black howler monkeys (*Alouatta caraya*) and 230 from capuchin monkeys (*Cebus apella*). Samples were collected in an overflow area of a fauna rescue program during the construction of a hydroelectric dam in Tocantins State (Figure 1, Appendix, wwwnc.cdc.gov/EID/article/20/3/13-1050-F1.htm). The monkeys had no previous contact with humans. After blood collection, the animals were released into areas selected by environmental conservation programs. We also collected serum samples from cattle (*Bos taurus*): 147 samples from Pará and Maranhão States in the Amazon region and 45 from Bahia and Espírito Santo States in the Caatinga and Mata Atlântica biomes.

All samples underwent serologic and molecular testing for mimivirus (Figure 2). Because total serum volumes were low, the specimens were grouped into pools of 2–5 serum samples (20 μL for each sample) from animals belonging to the same species that were from the same collection area. A total of 210 pools were compiled (Table). Pools were tested by real-time PCR targeting the conserved helicase viral gene (primers 5′-ACCTGATCCACATCCCATAACTAA-3′ and 5′-GCCTCATCAACAAATGGTTTCT-3′). DNA extractions were performed by using phenol-chloroform-isoamyl alcohol, and DNA quality and concentration were checked by using a nanodrop spectrophotometer (Thermo Scientific, Waltham, MA, USA). PCRs were performed by using the One Step SYBr Green Master Mix (Applied Biosystems, Foster City, CA, USA), and real-time PCR quality and sensitivity parameters were adjusted, including efficiency (102.6%) and R^2 (0.992). APMV (kindly provided by Didier Raoult, Marseille, France) was used as a positive control. The serum pools were manipulated in a laminar flow cabinet, separate from any virus samples, to avoid cross-contamination.

Of the 210 pools, 25 (11.9%) were positive for APMV (viral loads 1.4×10^3 to 2.3×10^6 copies/mL); 9 (4.3%) pools were capuchin monkey serum and 16 (7.6%) were bovine serum, all from the Amazon region. Mimivirus DNA was not detected in serum from black howler monkeys or cattle from Bahia and Espírito Santo States (Table). Using external primers 5′-ACCTGATCCACATCCCATAACTAAA-3′ and 5′-ATGGCGAACAATATTAAAACTAAAA-3′, we amplified a larger fragment of the helicase gene (390 bp) from all 25 positive samples; 12 positive serum pools, 4 from capuchin

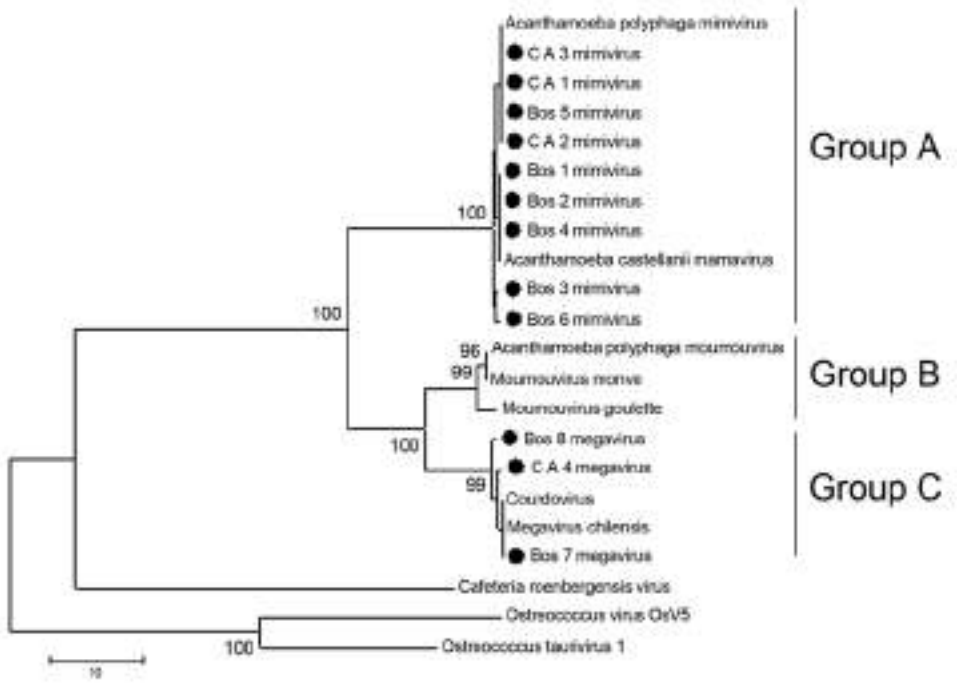

Figure 2. Consensus bootstrap phylogenetic neighbor-joining tree of helicase gene from nucleocytoplasmic large DNA viruses showing alignment of mimivirus and megavirus isolates obtained from *Cebus apella* (CA) and bovids (Bos) in Brazil. Tree was constructed by using MEGA version 4.1 (www.megasoftware.net) on the basis of the nucleotide sequences with 1,000 bootstrap replicates. Bootstrap values >90% are shown. Nucleotide sequences were obtained from GenBank. Scale bar indicates rate of evolution.

monkeys and 8 from cattle, were chosen for helicase gene sequencing and analysis. The helicase fragments were directly sequenced in both orientations and in triplicate (MegaBACE sequencer; GE Healthcare, Buckinghamshire, UK). The sequences were aligned with previously published sequences from GenBank by using ClustalW (www.clustal.org) and manually aligned by using MEGA software version 4.1 (www.megasoftware.net). Modeltest software (www.molecularevolution.org/software/phylogenetics/modeltest) was used determine which model of evolution was most appropriate for our analysis.

Optimal alignment of the predicted highly conserved helicase amino acid sequences showed several amino acid substitutions in the mimivirus amplicons we derived compared with other available sequences (Figure 3). Nine of the 12 sequenced amplicons showed high identity among themselves and with the APMV sequence (GenBank accession no. HQ336222). The other 3 amplicons showed a high identity with *Megavirus chilensis* (GenBank accession no. JN258408), a giant virus isolated in 2011 from seawater off the coast of Chile (*15*). A neighbor-joining phylogenetic tree constructed on the basis of the helicase gene revealed that all the amplicons we derived clustered with mimivirus isolates; however, according to the sequences alignment analysis, 3 of them clustered directly with the *Megavirus chilensis* group (Figure 2). The sequences have been deposited in GenBank.

Concomitantly with molecular analysis, the pools of samples were submitted to a virus neutralization (VN) test to detect mimivirus neutralizing antibodies. VN was used rather than ELISA because the secondary antibodies required for an ELISA for monkey species were unavailable. Before being arranged in pools, the serum samples were inactivated separately by heating at 56°C for 30 min. Inactivated samples were diluted 1:20, mixed with 10^7 APMV particles to a final volume of 400 μL (peptone yeast glucose medium), then incubated at 37°C for 1 h to optimize virus–antibody interaction. This solution was added to 2 × 10^5 *Acanthamoeba castellanii* cells (ATCC 30234). To improve virus–ameba contact, the adsorption step was performed while rotating for 60 min. The samples were then centrifuged at 400 × *g* for 5 min, the supernatants were discarded, and the amebas were cultivated at 32°C for 8 h in PYG medium. Afterward, the samples were titrated in *A. castellannii* cells by using the 50% tissue culture

Table. Sources and test results for serum samples from wild and domestic animals analyzed for presence of mimivirus, Brazil*

Species	States where samples were collected	Total no. samples	Total no. pools	Real-time PCR, helicase gene: No. (%) negative pools	Real-time PCR, helicase gene: No. (%) positive pools	VN >90%, no. (%) pools
Black howler monkeys	Tocantins	91	21	21 (100.0)	0	0
Capuchin monkeys	Tocantins	230	106	97 (91.5)	9 (8.5)	5 (4.72)
Cattle	Pará and Maranhão	147	63	47 (74.6)	16 (25.4)	10 (15.9)
	Espírito Santo and Bahia	45	20	20 (100.0)	0	0
Total		513	210	185 (88.1)	25 (11.9)	15 (7.14)

*VN, virus neutralization test.

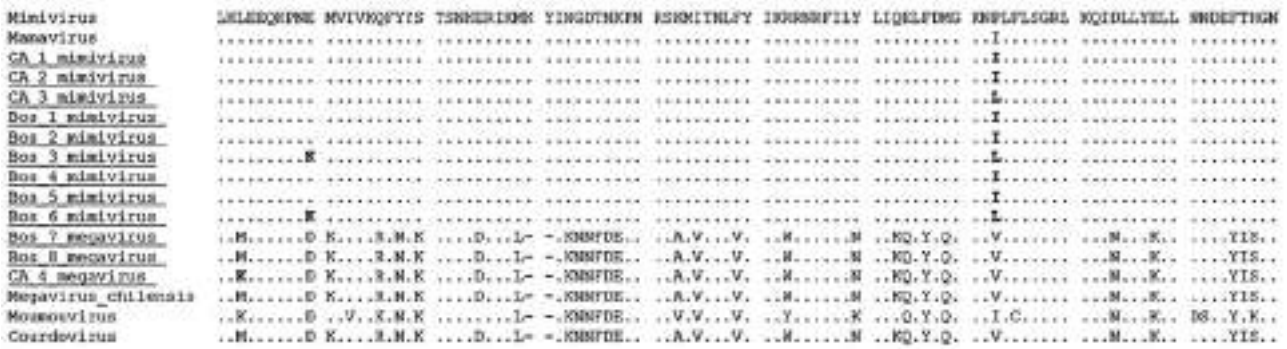

Figure 3. Amino acid inferred sequence of a fragment of the nucleocytoplasmic large DNA virus helicase gene (130 aa were inferred from the obtained 390-bp sample). Samples obtained in this study are underlined; boldface indicates polymorphic.

infective dose method. Antimimivirus serum produced in Balb/c mice was used as VN positive control, and bovine serum collected during previous studies by our group was used as VN negative control. The percentage of reduction was calculated, and the cutoff for positive serum was defined as 90% of the reduction in comparison with the negative control. VN results showed that 15 of the 25 PCR-positive pools contained neutralizing antibodies against mimivirus, 5 from *C. apella* monkeys and 10 from cattle (Table).

Conclusions

We found evidence of mimivirus circulation in wild and domestic animals in the Amazon region of Brazil. Several agents of emerging infectious diseases in humans have reservoirs in wild and domestic animals, which act as a regular source for these agents. Anthropogenic disturbance of the Amazon ecosystem and increases in agricultural and livestock areas result in more contact between wildlife and rural human populations (*2*). Therefore, although mimivirus-associated pneumonia has not been studied in human patients in Brazil, surveillance of wild and domestic animals can help predict outbreaks and lead to establishment of control measures.

Although mimiviruses are known to be present in water and soil environments, new studies are necessary to determine if these viruses are a part of a vertebrate's normal microbiota and act as opportunistic pathogens for pneumonia and to clarify whether viruses that are associated with pneumonia have any special genetic and physiologic features. Ecologic and public health studies should be designed to evaluate the risk for infection by mimiviruses during wildlife conservation efforts and to determine whether surveillance systems can predict outbreaks by monitoring mimivirus infections in wild and domestic animals.

Acknowledgments

We thank João Rodrigues dos Santos, Gisele Cirilo, and their colleagues for excellent technical support.

We also thank Milton F. Souza-Júnior for providing some samples used in this study.

This study was supported by the Conselho Nacional de Desenvolvimento Científico e Tecnológico, Coordenação de Aperfeiçoamento de Pessoal de Nível Superior, the Fundação de Amparo à Pesquisa do Estado de Minas Gerais, the Ministério da Agricultura, Pecuária e Abastecimento, and the Pro-Reitoria de Pesquisa da Universidade Federal de Minas Gerais. F.P.D. was supported by a fellowship from the Coordenação de Aperfeiçoamento de Pessoal de Nível Superior. E.G.K., C.A.B., G.S.T., and P.C.P.F. are researchers of the Conselho Nacional de Desenvolvimento Científico e Tecnológico.

Mr Dornas is a pharmacist and a PhD student at the Laboratório de Vírus, Departamento de Microbiologia, Instituto de Ciências Biológicas, Universidade Federal de Minas Gerais, Belo Horizonte, Brazil. His research interests focus on diagnosing, monitoring, controlling, and preventing emerging infectious diseases.

References

1. Yutin N, Wolf YI, Raoult D, Koonin EV. Eukaryotic large nucleo-cytoplasmic DNA viruses: clusters of orthologous genes and reconstruction of viral genome evolution. Virol J. 2009;6:223. http://dx.doi.org/10.1186/1743-422X-6-223
2. Abrahão JS, Silva-Fernandes AT, Lima LS, Campos RK, Guedes MI, Cota MM, et al. Vaccinia virus infection in monkeys, Brazilian Amazon. Emerg Infect Dis. 2010;16:976–9. http://dx.doi.org/10.3201/eid1606.091187
3. Saadi H, Pagnier I, Colson P, Cherif JK, Beji M, Boughalmi M, et al. First isolation of mimivirus in a patient with pneumonia. Clin Infect Dis. 2013;57:e127–34. http://dx.doi.org/10.1093/cid/cit354
4. Vanspauwen MJ, Schnabel RM, Bruggeman CA, Drent M, van Mook WN, Bergmans DC, et al. Mimivirus is not a frequent cause of ventilator-associated pneumonia in critically ill patients. J Med Virol. 2013;85:1836–41. http://dx.doi.org/10.1002/jmv.23655
5. Colson P, Fancello L, Gimenez G, Armougom F, Desnues C, Fournous G, et al. Evidence of the megavirome in humans. J Clin Virol. 2013;57:191–200. http://dx.doi.org/10.1016/j.jcv.2013.03.018
6. Boughalmi M, Saadi H, Pagnier I, Colson P, Fournous G, Raoult D, et al. High-throughput isolation of giant viruses of the *Mimiviridae* and *Marseilleviridae* families in the Tunisian environment. Environ Microbiol. 2013;15:2000–7. http://dx.doi.org/10.1111/1462-2920.12068

7. Colson P, Gimenez G, Boyer M, Fournous G, Raoult D. The giant *Cafeteria roenbergensis* virus that infects a widespread marine phagocytic protist is a new member of the fourth domain of Life. PLoS ONE. 2011;6:e18935. http://dx.doi.org/10.1371/journal.pone.0018935
8. La Scola B, Audic S, Robert C, Jungang L, de Lamballerie X, Drancourt M, et al. A giant virus in amoebae. Science. 2003;299:2033. http://dx.doi.org/10.1126/science.1081867
9. Fouque E, Trouilhé MC, Thomas V, Hartemann P, Rodier MH, Héchard Y. Cellular, biochemical, and molecular changes during encystment of free-living amoebae. Eukaryot Cell. 2012;11:382–7. http://dx.doi.org/10.1128/EC.05301-11
10. Greub G, Raoult D. Microorganisms resistant to free-living amoebae. Clin Microbiol Rev. 2004;17:413–33. http://dx.doi.org/10.1128/CMR.17.2.413-433.2004
11. Raoult D, La Scola B, Birtles R. The discovery and characterization of mimivirus, the largest known virus and putative pneumonia agent. Clin Infect Dis. 2007;45:95–102. http://dx.doi.org/10.1086/518608
12. Ghigo E, Kartenbeck J, Lien P, Pelkmans L, Capo C, Mege JL, et al. Ameobal pathogen mimivirus infects macrophages through phagocytosis. PLoS Pathog. 2008;4:e1000087. http://dx.doi.org/10.1371/journal.ppat.1000087
13. Berger P, Papazian L, Drancourt M, La Scola B, Auffray JP, Raoult D. Ameba-associated microorganisms and diagnosis of nosocomial pneumonia. Emerg Infect Dis. 2006;12:248–55. http://dx.doi.org/10.3201/eid1202.050434
14. Hoffmann B, Scheuch M, Höper D, Jungblut R, Holsteg M, Schirrmeier H, et al. Novel orthobunyavirus in cattle, Europe, 2011. Emerg Infect Dis. 2012;18:469–72. http://dx.doi.org/10.3201/eid1803.111905
15. Arslan D, Legendre M, Seltzer V, Abergel C, Claverie JM. Distant mimivirus relative with a larger genome highlights the fundamental features of *Megaviridae*. Proc Natl Acad Sci U S A. 2011;108:17486–91. http://dx.doi.org/10.1073/pnas.1110889108

Address for correspondence: Jônatas S. Abrahão, Universidade Federal de Minas Gerais, Microbiology, Av. Antônio Carlos, 6627 Belo Horizonte, Minas Gerais 31270-901, Brazil; email: jonatas.abrahao@gmail.co

OPEN ACCESS Freely available online

PLOS ONE

Acanthamoeba polyphaga mimivirus Stability in Environmental and Clinical Substrates: Implications for Virus Detection and Isolation

Fábio P. Dornas[1☯], Lorena C. F. Silva[1☯], Gabriel M. de Almeida[1], Rafael K. Campos[1], Paulo V. M. Boratto[1], Ana P. M. Franco-Luiz[1], Bernard La Scola[2], Paulo C. P. Ferreira[1], Erna G. Kroon[1], Jônatas S. Abrahão[1]*

1 Universidade Federal de Minas Gerais, Instituto de Ciências Biológicas, Laboratório de Vírus, Belo Horizonte, Minas Gerais, Brazil, **2** URMITE CNRS UMR 6236– IRD 3R198, Aix Marseille Universite, Marseille, France

Abstract

Viruses are extremely diverse and abundant and are present in countless environments. Giant viruses of the *Megavirales* order have emerged as a fascinating research topic for virologists around the world. As evidence of their ubiquity and ecological impact, mimiviruses have been found in multiple environmental samples. However, isolation of these viruses from environmental samples is inefficient, mainly due to methodological limitations and lack of information regarding the interactions between viruses and substrates. In this work, we demonstrate the long-lasting stability of mimivirus in environmental (freshwater and saline water) and hospital (ventilator plastic device tube) substrates, showing the detection of infectious particles after more than 9 months. In addition, an enrichment protocol was implemented that remarkably increased mimivirus detection from all tested substrates, including field tests. Moreover, biological, morphological and genetic tests revealed that the enrichment protocol maintained mimivirus particle integrity. In conclusion, our work demonstrated the stability of APMV in samples of environmental and health interest and proposed a reliable and easy protocol to improve giant virus isolation. The data presented here can guide future giant virus detection and isolation studies.

Citation: Dornas FP, Silva LCF, de Almeida GM, Campos RK, Boratto PVM, et al. (2014) *Acanthamoeba polyphaga mimivirus* Stability in Environmental and Clinical Substrates: Implications for Virus Detection and Isolation. PLoS ONE 9(2): e87811. doi:10.1371/journal.pone.0087811

Editor: Richard Joseph Sugrue, Nanyang Technical University, United States of America

Received June 27, 2013; **Accepted** January 2, 2014; **Published** February 3, 2014

Funding: Fundação de Amparo a Pesquisa de Minas Gerais (FAPEMIG)(www.fapemig.br) and the Pró-Reitoria de Pesquisa da Universidade Federal de Minas Gerais (www.ufmg.br/prpq) supported the manuscript language (English) revision. The funders had no role in study design, data collection and analysis, decision to publish, or preparation of the manuscript.

Competing Interests: The authors have declared that no competing interests exist.

* E-mail: jonatas.abrahao@gmail.com

☯ These authors contributed equally to this work.

Introduction

Viruses are extremely diverse and abundant and are present in countless environments [1]. In some extreme ecosystems, viruses are the only known microbial predators, and they are powerful agents of gene transfer and microbial evolution [1]. Although viral genomes are ubiquitous in the biosphere, very little is known regarding the ecological roles of viruses in most ecosystems [2,3]. In this context, large nucleocytoplasmic DNA viruses (NCLDVs) emerge as a fascinating research topic for virologists around the world. NCLDVs are frequently found in environmental samples, demonstrating their ubiquity and ecological impact [4]. There is still much to learn about NCLDV host-pathogen relationships and their impact on evolution, ecology and medicine [4].

Acanthamoeba polyphaga mimivirus (APMV), the prototype of the *Mimiviridae* family, was discovered in a hospital water cooling system in Bradford, England, during an outbreak of pneumonia [5]. APMV is an amoeba-associated virus with peculiar features, including a double-stranded DNA, ~1.2 megabase (Mb) genome encoding proteins not previously observed in other viruses, such as aminoacyl-tRNA synthetases and DNA repair chaperones and enzymes, a >700 nm particle diameter and capsid-associated fibers [5,6]. In 2008, a new giant virus named *A. castellanii mamavirus* (ACMV) was isolated from a cooling tower in Paris [7,8]. Other known giant viruses include *Megavirus chiliensis*, isolated from Chilean ocean water [9]; *Lentille virus*, from the contact lens fluid of a patient with keratitis [10]; and *Moumouvirus*, isolated from cooling tower water [11].

Acanthamoeba is believed to be the natural host of *Mimiviridae* [5], though there is evidence of mimivirus replication in vertebrate phagocytes. These amoebae are ubiquitous and have been isolated from aquatic environments, soil, air, hospitals and contact lens fluid. Amoebas are part of vertebrates' normal microbiota, and they are extremely resistant to pH variations, high temperatures and disinfectants [12,13]. Considering the ubiquity of *Acanthamoeba*, giant viruses could hypothetically be found everywhere. Metagenomic analysis demonstrated the presence of mimivirus-like sequences in many aquatic environments [12,14]. There are few data on APMV in animal tissues or its hypothetical role as pneumonia agent, although a recent metagenomic study found mimivirus DNA in bovine serum [15]. Free-living amoebae may potentially propagate pathogens in hospital environments, and hospitalized patients would represent a group of risk for amoeba-associated pneumonia agents, including APMV [5,16–18].

The ubiquity of APMV DNA in the environment but the lack of information about the ecological – and medical – impact of these viruses warrants their isolation and characterization. Research groups trying to "prospect" giant viruses in the laboratory [9,11,19] have difficulty recovering these viruses from environmental samples; there is also no standard protocol for the optimization of isolation techniques [19,20]. Most giant virus prospecting studies rely on direct co-culture of samples with amoebas to propagate viruses. However, the pre-enrichment of environmental samples can be useful for viral isolation, as demonstrated by the discovery of megavirus [9]. In this study, we verified the stability of APMV in hospital and environmental substrates and validated an enrichment protocol for APMV isolation. Our results suggest that the enrichment protocol improves APMV detection from different substrates but does not modify some viral genetic and biological features. Our study may be useful in future giant virus prospecting studies.

Materials and Methods

APMV Preparation

APMV particles were isolated and purified from infected amoebae as previously described [16]. Briefly, *Acanthamoeba castellanii* (ATCC 30234) were grown in 75 cm^2 cell culture flasks (Nunc, USA) in PYG (peptone-yeast extract-glucose) medium supplemented with 7% fetal calf serum (FCS, Cultilab, Brazil), 25 mg/ml Fungizone (amphotericin B, Cristalia, São Paulo, Brazil), 500 U/ml penicillin and 50 mg/ml gentamicin (Schering-Plough, Brazil). After reaching confluence, the amoebas were infected with APMV and incubated at 37°C until the appearance of cytopathic effects. APMV-rich supernatants from the infected amoeba were collected and filtered through a 0.8-micron (Millipore, USA) filter to remove amoeba debris. The viruses were then purified using a Gastrografin gradient (45–36–28%) [5], suspended in PBS and stored at −80°C.

Virus Titration

Samples were serially diluted (1/10) in PYG medium, and 100 µl was inoculated onto 10^5 amoeba seeded in a 96-well Costar® microplate (Corning, NY) on the previous day (8 wells per dilution, 200 µl final volume). Plates were incubated for 2–4 days at 32°C to determine the highest dilution that led to amoebal lysis ($TCID_{50}$/ml) [26].

Virus Recovery from Substrates, Enrichment and Stability Tests

To test the APMV recovery from the assayed substrates, a total of 10^6 $TCID_{50}$ of purified APMV was re-suspended in phosphate buffered saline (PBS) and added to autoclaved salt water (10 ml), fresh water (10 ml) and topsoil (1 g). The fresh water and soil samples were collected from three different Brazilian biomes: Amazon and Mata Atlântica, two very biodiverse rainforests, and Cerrado, a savanna-like biome. The salt water samples were collected from 3 points on the coast of South and Southeast Brazil, for a total of five samples per substrate per biome (Figure 1). The water and land collections were performed with permission of Instituto Chico Mendes (ICM) – protocol numbers: 34293-1 and 33326-2. The field studies did not involve endangered or protected species. Considering the hypothetical role of APMV as pneumonia agent associated with prolonged mechanical ventilation the viral stability in ventilator devices was evaluated. Three different brands of sterile ventilator device (tube) (VD) were used to test APMV recovery (five quadrants of 2×2 cm per brand) [21]. In this case, 10 µl of viral suspension was added to VD quadrants with or without BAV, which were maintained in sterile Petri dishes. After one hour, all the samples were titrated in *A. castellanii* by the $TCID_{50}$ method as described [26]. All the environmental and VD samples were previously tested for APMV DNA and/or infectious particles [5].

APMV stability was analyzed for 12 months in the substrates described above. Samples were maintained in 15 ml tubes at room temperature (Figure S1). Every month, 500 µl aliquots from each substrate were collected, serial diluted in PBS and titrated in amoebae. The viral titer was adjusted to the total assayed volume. The sample enrichment protocol was adapted from Arslan et al. (2011). Briefly, 500 µl of samples were added to 450 ml water-rice medium (40 grains of rice per liter of water) and kept in the dark at room temperature for 5 days. Following this incubation, 5000 pathogen-free amoebas were added to the samples, and 5000 more amoebas were added after twenty days. The samples were titrated in amoebae after thirty days and then every subsequent month for one year. All samples were used in real-time PCRs targeting the conserved hel gene (primers: 5′ACCTGATCCACATCCCA-TAACTAAA3′ and 5′GGCCTCATCAACAAATGGTTTCT-3′). Samples DNA were extracted by Phenol-ChloroformThe real-time PCR was performed with a commercial mix Power SYBr Green (Applied Biosystems, USA), primers (4 mM each) and 1 µl sample in reaction of 10 µl final volume. All reactions were performed in a StepOne thermocycler: 95°C-10 min, 40 cycles-95°C-15 s/60°-15 s, followed by a dissociation step (specific Tm = 73°C).

Transmission Electron Microscopy

A. castellanii were infected at an MOI of 10. Uninfected amoebae were used as controls. At 7 h post-infection, amoebae were washed twice with PBS and fixed with 2.5% glutaraldehyde type 1 (Merck, Germany) for one hour at room temperature. The amoebae culture was dislodged with a cell scraper and centrifuged at 900×g for 5 min. Ultrathin sections were prepared [5] by the Centro de Microscopia, UFMG, Brazil.

One-step Growth Curves

To compare the replication of APMV before and after enrichment, one-step growth curve assays were performed. *A. castellanii* were infected at an MOI of 10. The infectivity was measured by TCID50 after 25 hours (0 to 25 hours) by observing the CPE in amoeba.

Sequencing Analysis

The hel and GlcT genes were amplified by PCR from purified APMV and from samples after enrichment. The hel and GlcT genes were chosen since they have been used as markers in phylogenetic or in evolutionary studies [5,9,11]. The primers were designed based on APMV sequences available in GenBank (Accession NC 014649). The amplicons were directly sequenced in both orientations and in triplicate (Mega-BACE sequencer, GE Healthcare, Buckinghamshire, UK). The sequences were aligned with Genbank references with ClustalW and were manually aligned using MEGA software version 4.1 (Arizona State University, Phoenix, AZ, USA).

Results

APMV is Stable for Long Periods in Different Substrates

To evaluate APMV stability in environmental and hospital substrates, an initial experiment analyzed the recovery of APMV from each substrate. A total of 10^6 $TCID_{50}$ of purified APMV was re-suspended in phosphate buffered saline (PBS) and added to

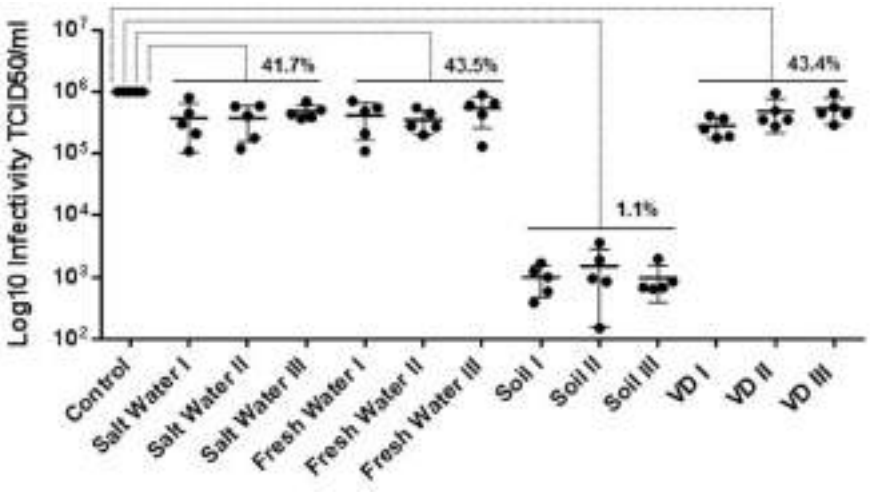

Figure 1. APMV recovery from samples after 1 hour. 10^6 $TCID_{50}$ of purified APMV were added to salt water (10 ml), fresh water (10 ml), topsoil (1 g) and three different brands of VD substrates, and after one hour, virus recovery was evaluated by titration in *A. castellanii*. The fresh water and soil samples were collected from three different Brazilian biomes: Amazon and Mata Atlântica, two highly biodiverse rainforests, and Cerrado, a savanna-like biome. The salt water samples were collected from 3 points on the coast of South and Southeast Brazil, for a total of five samples per substrate per biome. The results are the means+SD of an experiment performed in quintuplicate.
doi:10.1371/journal.pone.0087811.g001

previously autoclaved salt water (10 ml), fresh water (10 ml) and topsoil (1 g). The fresh water and soil samples were collected from three different Brazilian biomes (Amazon, Cerrado and Mata Atlântica), and the salt water samples were collected from 3 points on the coast of South and Southeast Brazil, for a total of five samples per substrate per biome (Figure 1). Three different brands of sterile ventilator device (tube) (VD) were used to test APMV recovery (five quadrants of 2×2 cm per brand) [21]. After one hour, all the samples were titrated in *A. castellanii*. The average values from quintuple replicates showed >40% virus recovery from salt water, fresh water and VD samples, regardless of the biome or brand. In contrast, viral recovery from soil was approximately 1% in all samples (Figure 1).

The stability of APMV was analyzed for 12 months in each substrate. Samples were prepared and maintained in 15 ml tubes at room temperature. Relative humidity and temperature were monitored through the experiment (relative humidity average max-72%; min 56%/temperature average max-25°C; min-19°C) (Figure S1). At monthly intervals, aliquots from each substrate were collected, serially diluted in PBS and titrated in amoebae. Titration assays revealed the long-term stability of APMV in salt and fresh water and VD, as infectious particles were detected in each substrate after 9, 12 and 10 months, respectively (Figure 2A, 2B, 2D). In general, the viral titers decreased less than 1 log until the 6^{th} month, after which time virus titers decreased eventually to undetectable levels. APMV could be isolated from soil samples until the third month, but the viral titer was decreased by >2 log after the first month (Figure 2C).

Enrichment of APMV from Different Substrates

While recovery of APMV depended on the substrate in which the virus was immersed, recovery was never complete, and the viral titer decreased over time in all substrates. To verify that an enrichment protocol following sample collection could improve viral recovery, we prepared substrates as described above containing 10^6 $TCID_{50}$ APMV and then enriched the viruses in these samples [9]. Briefly, 500 µL each sample was added to 450 ml water-rice medium (40 grains of rice per liter of water) and stored in the dark at room temperature for 5 days. Following this incubation, 5000 amoebas were added to the samples, and 5000 more amoebas were added after twenty days. After thirty days, the samples were titrated in amoebae; samples were then titrated again monthly for one year. The enrichment process improved APMV recovery from all the analyzed substrates. APMV was detected after one year in salt and fresh water (Figure 3A and 3B), seven months in soil (Figure 3C) and one year in VD samples (Figure 3D). When compared with the results shown in Figure 2, the overall viral titer and the viral recovery time were increased after the enrichment. In enriched soil samples, virus could be detected up to seven months; this duration was much improved from the unenriched maximum detection time of three months.

APMV Stability in VD Containing BAL Samples

Detection of APMV in VD is clinically relevant and could establish this virus as a human pathogen [16]. One factor that might impact viral detection in VD is the presence of bronchoalveolar lavage (BAL). To verify if BAL impairs APMV recovery from VD samples, 10^6 $TCID_{50}$ of APMV were added to VD containing BAL, which were then enriched. While BAL generally reduced APMV recovery (Figure 4A), the enrichment protocol increased the initial viral titers and allowed the isolation of APMV up to the 9^{th} month of the experiment (Figure 4B).

Real-time PCR of APMV in Environmental and Hospital Substrates

As shown above, the optimal recovery APMV results from pre-enrichment of substrates. Viral isolation from environmental samples is vital for the characterization of new giant viruses, but it is not absolutely required for some ecological, evolutionary or epidemiological studies. Molecular viral detection, e.g., PCR, is faster, cheaper and less laborious than viral isolation. To verify that enrichment improves APMV detection by PCR, the samples described in the previous experiments were used as templates for real-time PCRs designed to detect APMV helicase (hel). APMV DNA was detected in all water and VD samples, with or without enrichment. APMV DNA was detected up to the eleventh month in non-enriched salt water samples and up to the twelfth month in

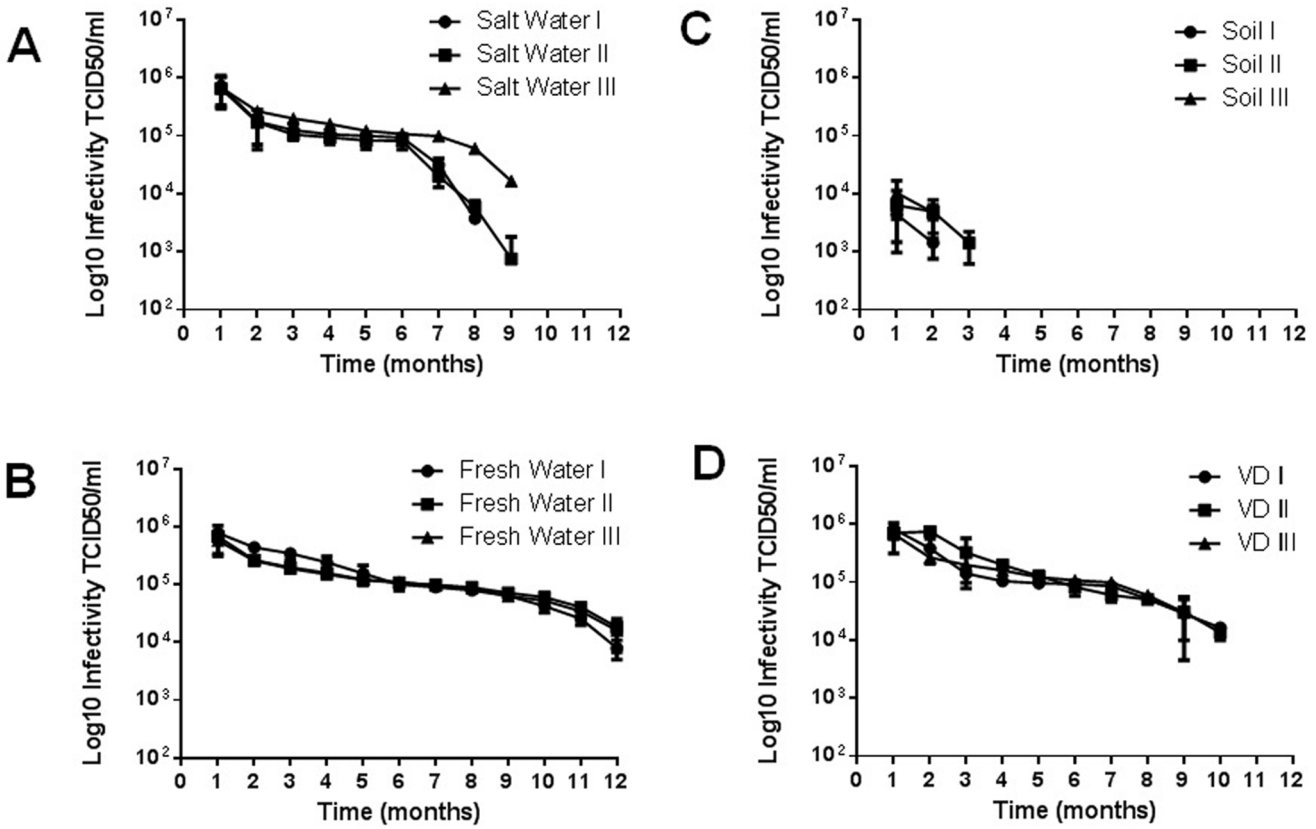

Figure 2. APMV stability in different substrates. To evaluate the long-term stability of APMV in different substrates for one year, 10^6 $TCID_{50}$ of purified APMV were added to salt water, soil, fresh water and VD substrates, which were maintained in 15 ml tubes at room temperature. At monthly intervals, the samples were titrated in amoebae. (A) Salt water; (B) Fresh water; (C) Soil; (D) VD. The results are the means+SD of an experiment performed in quintuplicate. I, II and III represent independent experiments performed with samples collected from distinct locations.
doi:10.1371/journal.pone.0087811.g002

enriched samples. In soil samples, APMV DNA was detected up to five months and nine months in unenriched and enriched samples, respectively. Enrichment also improved APMV detection in VD containing BAL samples, with a detection time shift from the eighth to the eleventh month (Table 1).

APMV Biology, Morphology and DNA Sequences are not Changed by Enrichment

Virus isolation in laboratory conditions could promote genotype and/or phenotype changes by artificial selection. Boyer et al. (2011) showed dramatic changes in APMV genomes, replication and morphology after sub-culturing APMV in a germ-free amoeba host. To evaluate possible changes in APMV caused by the enrichment process, morphological, virological and genetic assays were performed. No differences were observed in one-step growth curves of virus recovered from all assayed samples, suggesting that no biological modifications occurred during enrichment (Figure 5). These samples were also observed by electron microscopy, and no morphological changes were detected when compared to APMV images previously published [5,7]. (Figure S2). In addition, the sequences of the APMV hel and GlcT genes from enriched samples were 100% identical to the APMV reference sequences in Genbank (Figures S3 and S4).

Enrichment Applicability Tests

To test the applicability of the enrichment protocol, water samples were collected from 2 urban lakes and from a river in Southeast and North Brazil. A total of 475 samples of 5 ml each were collected from the water surface. Aliquots of the samples were enriched or directly inoculated onto *A. castellanii* monolayers for virus isolation. In parallel, real-time PCRs to detect APMV were performed.

From the 475 samples, six giant viruses were isolated with the enrichment protocol (Table 2). These viruses induced cytopathic effects in amoebas, including cell rounding and lysis, and were positive in PCR assays. In contrast, only one of the six virus isolates was propagated by direct inoculation of the water samples in amoebas. Sequencing of hel gene confirmed that all virus isolates belonged to the *Megavirales* order (data not shown).

Discussion

Virus isolation has technical limitations, and classical protocols based on filtration have delayed the detection of giant viruses [22]. Another problem for giant virus isolation is their limited known host range, which restricts the cellular systems that can be used for *in vitro* culture [22]. Thus, most information on giant viruses comes from environmental metagenomic studies and not from virus isolation [22]. This approach must be made with extreme caution, as comparing fragmented environmental sequences with those found in databases can result in false assumptions about giant virus complexity and HGT events [14]. Isolation of these viruses is imperative for understanding their roles in the environment and as potential vertebrate pathogens.

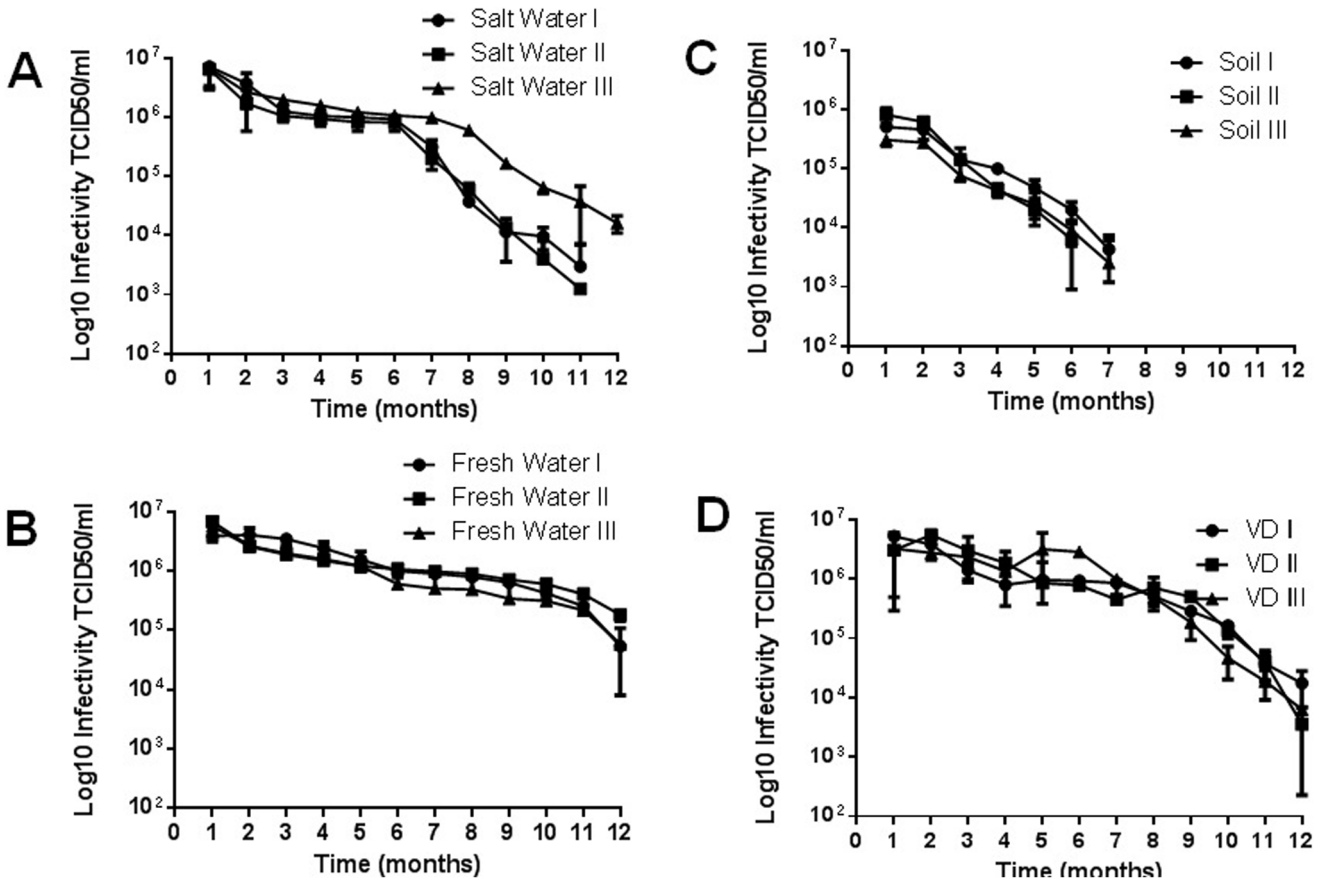

Figure 3. APMV isolation in different substrates after enrichment. As above, substrates were inoculated with APMV (10^6 viral particles) and then enriched. At one-month intervals, the samples were titrated in amoebae. (A) Salt water; (B) Fresh water; (C) Soil; (D) VD. The results are the means+SD of an experiment performed in quintuplicate. I, II and III represent independent experiments performed with samples collected from distinct locations.
doi:10.1371/journal.pone.0087811.g003

The ubiquity of amoebae implies the probable ubiquity of *Mimiviridae*, which has been confirmed by indirect viral detection methods. Despite their remarkable abundance, giant viruses are not easily isolated. Many of these viruses are unknown, and their stability in environmental samples is not determined. Furthermore, there are few described approaches for viral isolation or protocols that favor viral isolation from complex substrates. Our investigation estimates APMV stability in several relevant substrates and

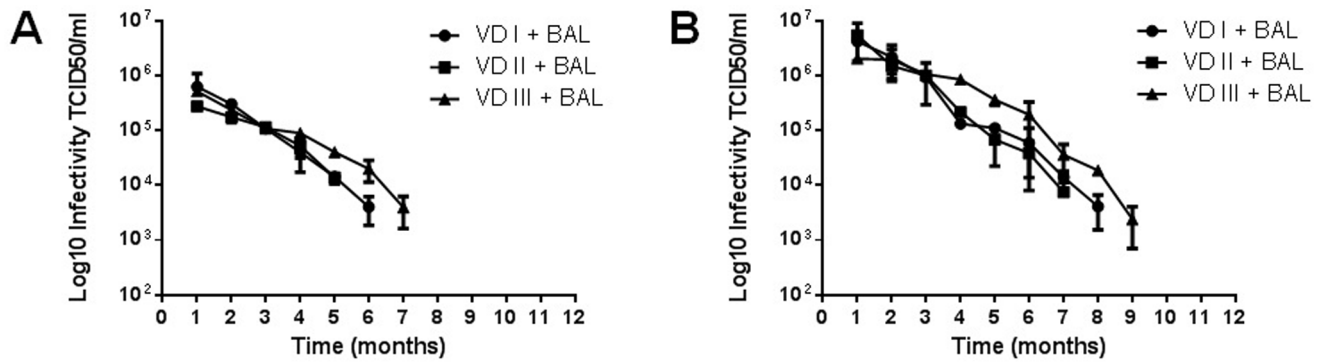

Figure 4. APMV stability in VD enriched after BAL addition. Purified APMV (10^6 viral particles) were added to VD samples, and subsequently, BAL samples were added. The BAL-VD samples were or were not enriched and maintained at room temperature. The samples were titrated in amoebae monthly. (A) Samples without enrichment; (B) Enriched samples. The results are the means+SD of an experiment performed in quintuplicate.
doi:10.1371/journal.pone.0087811.g004

Table 1. APMV detection by real-time PCR in samples with or without enrichment.

	APMV detection by PCR[a,b]	
Sample	**With no Enrichment (months)**	**Post – Enrichment (months)**
Salt Water	1st to 11th	1st to 12th
Fresh Water	1st to 12th	1st to 12th
Soil	1st to 5th	1st to 9th
VD	1st to 12th	1st to 12th
VD+BAL	1st to 8th	1st to 11th

[a]Real-time PCR – Helicase gene;
[b]Results presented considering all replicates.
doi:10.1371/journal.pone.0087811.t001

Table 2. Enrichment applicability tests: detection of giant viruses with no and post-enrichment by viral isolation and real-time PCR.

		Positive samples [total of positive (%)][a]	
Sample	**Total of samples (n)**	**With no Enrichment**	**Post – Enrichment**
Lake 1	325	1 (0.3%)	2 (0.6%)
Lake 2	88	0 (0%)	2 (2.27%)
River	35	0 (0%)	2 (5.71%)
Total	**475**	**1 (0.21%)**	**6 (1.2%)**

[a]Isolation in *A. castellani* monolayer+positivity in hel gene real-Time PCR.
doi:10.1371/journal.pone.0087811.t002

shows that enrichment prior to isolation optimizes viral stability and recovery from any substrate.

In our first analysis, APMV recovery was reduced at one hour after its addition to different substrates. Although viral recovery from fresh water, salt water or VD was approximately 40% of the initial viral load, viral recovery from soil samples was much lower, representing less than 2% of the input viruses (Figure 1). The reasons for these recovery ranges include microbial influence and physical or chemical characteristics of the substrate. These factors interfere with survival through viral particle aggregation and virucidal activity. Particularly for APMV, viral aggregation is important since through their capsid surrounded by fibrils can occurs easily aggregation and influence in the filtration process required for viral isolation [12,23,24]. Following these results, we measured the stability of APMV in the substrates mentioned above for twelve months. Virus was recovered from fresh water at all time points tested, and virus was recovered from salt water, VD and soil until the ninth, tenth and third months of the experiment, respectively (Figure 2). Viral titers dropped over time in all substrates due to the reasons stated above.

In theory, an enrichment protocol could increase the number of giant viruses in a sample (viral replication) and, thus, their likelihood of recovery. This protocol favors the proliferation of heterotrophic organisms that are consumed by amoebas, and these amoebas are used for giant virus replication. After establishing the stability of APMV in different substrates, we added an enrichment protocol prior to viral isolation. The enrichment improved the method sensitivity, as viruses were isolated at later time points compared with samples without enrichment. Furthermore, enrichment increased virus yields (Figure 3).

Among the analyzed substrates, VD is particularly interesting for the hypothetical pathogenic aspect of *Mimiviridae*, as APMV has been detected in pneumonia patients. Devices such as VD are sources of nosocomial infections and could be sources for giant virus infections as well. We showed that APMV had long-term stability in VD and that the pre-enrichment improved viral detection. In a hospital setting, VDs would most likely be filled with clinical specimens that could interfere with APMV stability and recovery. To test this possibility, we added BAL to VDs before adding APMV and then determined viral recovery and stability with or without enrichment. BAL affected APMV stability; APMV was recovered from BAL-containing VDs only up to seven months without enrichment. In this case, enrichment allowed APMV recovery at nine months (Figure 4). BAL decreased APMV stability but did not completely neutralize the virus, so these samples were still potentially infectious. As shown previously, enrichment improved APMV recovery from BAL-containing VDs and was thus useful for isolating the giant virus from these samples.

APMV in the enriched or unenriched samples was also quantified by real-time PCR, which is more sensitive than cell

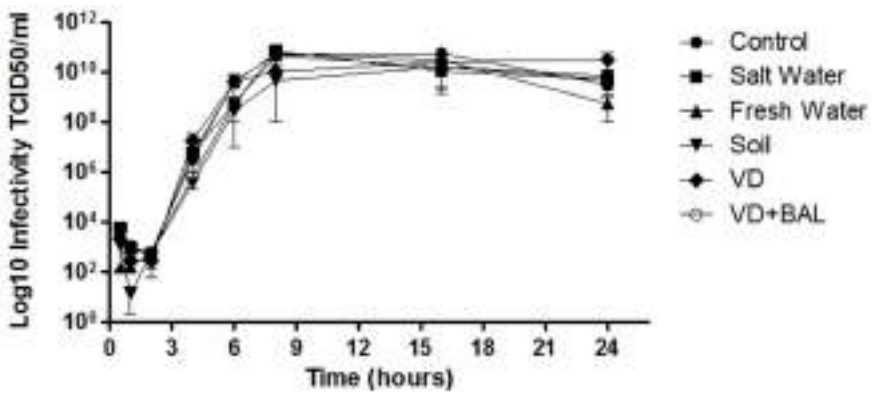

Figure 5. APMV one-step growth curves with or without enrichment. Purified APMV (10^6 viral particles) was added to salt water, soil, fresh water and VD substrates, which were then enriched. After viral isolation from each substrate, *A. castellanii* were infected at an MOI of 10. The infectivity was measured by $TCID_{50}$ after 25 hours (0 to 25 hours) by observing CPE in amoeba. The results are the means of experiments performed in duplicate.
doi:10.1371/journal.pone.0087811.g005

culture isolation and is also improved by enrichment (Table 1). While isolation needs viable viral particles in the sample, PCR detection needs viral DNA from any viral particles, whether viable, inactivated or defective. Thus, genomic studies can also benefit from the enrichment protocol described in this paper.

In allopatric conditions, successive passages of APMV in amoebae drastically reduce the viral genome, resulting in morphological and genetic changes [25]. To verify that enrichment protocol did not modify the original virus, we compared one-step growth curves from viruses obtained after enrichment to the prototype virus. The curves were similar, suggesting that the enrichment did not cause any biological alterations (Figure 5). We also verified the absence of morphological and genetic changes in APMV by electron microscopy and sequencing. All viruses were similar in size and had the characteristic APMV fibers and internal membranes (Figure S2). Analysis of hel and GlcT revealed that enrichment did not alter these genes, as they were identical to reference sequences (Figure S3).

In conclusion, our work determines the stability of APMV in samples of environmental and clinical interest and proposes a reliable and easy protocol to improve giant virus isolation. This protocol can be used for giant virus prospecting studies.

Supporting Information

Figure S1 Temperature and relative humidity averages during the 12 experimental months.
(TIF)

Figure S2 APMV do not exhibit changes in viral morphology after enrichment. Purified APMV (10^6 viral particles) were added to salt water, soil, fresh water and VD substrates, which were then enriched. After viral isolation from each substrate, *A. castellanii* were infected at an MOI of 10 and analyzed by EM at 8 hours post-infection. A, B, C and D: APMV recovery from enriched salt water, fresh water, soil and VD, respectively.
(TIF)

Figure S3 APMV do not show changes in the GlcT gene after enrichment. PCR for the GlcT gene was performed using enriched APMV samples as templates, and the resulting amplicon was sequenced. The DNA sequences were aligned with APMV reference sequences from Genbank using the ClustalW method and were manually aligned using MEGA software version 4.1 (Arizona State University, Phoenix, AZ, USA).
(TIF)

Figure S4 APMV do not show changes in the hel gene after enrichment. PCR for the hel gene was performed using enriched APMV samples as templates, and the resulting amplicon was sequenced. The DNA sequences were aligned with APMV reference sequences from Genbank using the ClustalW method and were manually aligned using MEGA software version 4.1 (Arizona State University, Phoenix, AZ, USA).
(TIF)

Acknowledgments

We thank João Rodrigues dos Santos, Gisele Cirilo dos Santos, and colleagues from Gepvig and the Laboratório de Vírus for their excellent technical support. We also thank Fundação de Amparo a Pesquisa de Minas Gerais (FAPEMIG) and the Pró-Reitoria de Pesquisa da Universidade Federal de Minas Gerais.

Author Contributions

Conceived and designed the experiments: FPD LCFS PVMB JSA. Performed the experiments: FPD LCFS GMA RKC PVMB APMFL. Analyzed the data: FPD LCFS GMA BL EGK PCPF JSA. Contributed reagents/materials/analysis tools: EGK PCPF JSA. Wrote the paper: FPD LCFS GMA BL EGK JSA.

References

1. Rohwer F, Prangishvili D, Lindell D (2009) Roles of viruses in the environment. Environ Microbiol 11: 2771–2774.
2. Breitbart M, Miyake JH, Rohwer F (2004) Global distribution of nearly identical phage-encoded DNA sequences. FEMS Microbiol Lett 236: 249–256.
3. Short CM, Suttle CA (2005) Nearly identical bacteriophage structural gene sequences are widely distributed in both marine and freshwater environments. Appl Environ Microbiol 71: 480–486.
4. Van Etten JL, Lane LC, Dunigan DD (2010) DNA viruses: the really big ones (giruses). Annu Rev Microbiol 64: 83–99.
5. La Scola B, Audic S, Robert C, Jungang L, de Lamballerie X, et al. (2003) A giant virus in amoebae. Science 299: 2033.
6. Moreira D, Brochier-Armanet C (2008) Giant viruses, giant chimeras: the multiple evolutionary histories of Mimivirus genes. BMC Evol Biol 8: 12.
7. La Scola B, Desnues C, Pagnier I, Robert C, Barrassi L, et al. (2008) The virophage as a unique parasite of the giant mimivirus. Nature 455: 100–104.
8. Desnues C, Raoult D (2010) Inside the lifestyle of the virophage. Intervirology 53: 293–303.
9. Arslan D, Legendre M, Seltzer V, Abergel C, Claverie JM (2011) Distant Mimivirus relative with a larger genome highlights the fundamental features of Megaviridae. Proc Natl Acad Sci U S A 108: 17486–17491.
10. Desnues C, La Scola B, Yutin N, Fournous G, Robert C, et al. (2012) Provirophages and transpovirons as the diverse mobilome of giant viruses. Proc Natl Acad Sci U S A 109: 18078–18083.
11. Yoosuf N, Yutin N, Colson P, Shabalina SA, Pagnier I, et al. (2012) Related giant viruses in distant locations and different habitats: Acanthamoeba polyphaga moumouvirus represents a third lineage of the Mimiviridae that is close to the megavirus lineage. Genome Biol Evol 4: 1324–1330.
12. Monier A, Larsen JB, Sandaa RA, Bratbak G, Claverie JM, et al. (2008) Marine mimivirus relatives are probably large algal viruses. Virol J 5: 12.
13. Siddiqui R, Khan NA (2012) Biology and pathogenesis of Acanthamoeba. Parasit Vectors 5: 6.
14. Ghedin E, Claverie JM (2005) Mimivirus relatives in the Sargasso sea. Virol J 2: 62.
15. Hoffmann B, Scheuch M, Höper D, Jungblut R, Holsteg M, et al. (2012) Novel orthobunyavirus in Cattle, Europe, 2011. Emerg Infect Dis 18: 469–472.
16. La Scola B, Marrie TJ, Auffray JP, Raoult D (2005) Mimivirus in pneumonia patients. Emerg Infect Dis 11: 449–452.
17. Raoult D, La Scola B, Birtles R (2007) The discovery and characterization of Mimivirus, the largest known virus and putative pneumonia agent. Clin Infect Dis 45: 95–102.
18. Ghigo E, Kartenbeck J, Lien P, Pelkmans L, Capo C, et al. (2008) Ameobal pathogen mimivirus infects macrophages through phagocytosis. PLoS Pathog 4: e1000087.
19. Boughalmi M, Saadi H, Pagnier I, Colson P, Fournous G, et al. (2012) High-throughput isolation of giant viruses of the Mimiviridae and Marseilleviridae families in the Tunisian environment. Environ Microbiol.
20. La Scola B, Campocasso A, N'Dong R, Fournous G, Barrassi L, et al. (2010) Tentative characterization of new environmental giant viruses by MALDI-TOF mass spectrometry. Intervirology 53: 344–353.
21. Campos RK, Andrade KR, Ferreira PC, Bonjardim CA, La Scola B, et al. (2012) Virucidal activity of chemical biocides against mimivirus, a putative pneumonia agent. J Clin Virol 55: 323–328.
22. Van Etten JL, Lane LC, Dunigan DD (2010) DNA viruses: the really big ones (giruses). Annu Rev Microbiol 64: 83–99.
23. Gerba CP, Schaiberger GE (1975) Effect of particulates on virus survival in seawater. J Water Pollut Control Fed 47: 93–103.
24. Wetz JJ, Lipp EK, Griffin DW, Lukasik J, Wait D, et al. (2004) Presence, infectivity, and stability of enteric viruses in seawater: relationship to marine water quality in the Florida Keys. Mar Pollut Bull 48: 698–704.
25. Boyer M, Azza S, Barrassi L, Klose T, Campocasso A, et al. (2011) Mimivirus shows dramatic genome reduction after intraamoebal culture. Proc Natl Acad Sci U S A 108: 10296–10301.
26. Raoult D, Audic S, Robert C, Abergel C, Renesto P, et al. (2004) The 1.2-megabase genome sequence of Mimivirus. Science 306: 1344–1350.

VIROLOGY JOURNAL

RESEARCH Open Access

Samba virus: a novel mimivirus from a giant rain forest, the Brazilian Amazon

Rafael K Campos[1], Paulo V Boratto[1], Felipe L Assis[1], Eric RGR Aguiar[2], Lorena CF Silva[1], Jonas D Albarnaz[1], Fabio P Dornas[1], Giliane S Trindade[1], Paulo P Ferreira[1], João T Marques[2], Catherine Robert[3], Didier Raoult[3], Erna G Kroon[1], Bernard La Scola[3*] and Jônatas S Abrahão[1*]

Abstract

Background: The identification of novel giant viruses from the nucleocytoplasmic large DNA viruses group and their virophages has increased in the last decade and has helped to shed light on viral evolution. This study describe the discovery, isolation and characterization of Samba virus (SMBV), a novel giant virus belonging to the *Mimivirus* genus, which was isolated from the Negro River in the Brazilian Amazon. We also report the isolation of an SMBV-associated virophage named Rio Negro (RNV), which is the first *Mimivirus* virophage to be isolated in the Americas.

Methods/results: Based on a phylogenetic analysis, SMBV belongs to group A of the putative *Megavirales* order, possibly a new virus related to *Acanthamoeba polyphaga mimivirus* (APMV). SMBV is the largest virus isolated in Brazil, with an average particle diameter about 574 nm. The SMBV genome contains 938 ORFs, of which nine are ORFans. The 1,213.6 kb SMBV genome is one of the largest genome of any group A *Mimivirus* described to date. Electron microscopy showed RNV particle accumulation near SMBV and APMV factories resulting in the production of defective SMBV and APMV particles and decreasing the infectivity of these two viruses by several logs.

Conclusion: This discovery expands our knowledge of *Mimiviridae* evolution and ecology.

Keywords: Mimiviridae, DNA virus, Giant virus, NCLDV, Virophage, Amazon, Brazil

Background

The discovery of the *Acanthamoeba polyphaga mimivirus* (APMV), arguably the most elusive member of the nucleocytoplasmic large DNA virus (NCLDV) group and the first discovered member of the *Mimiviridae* family, revived discussions regarding the evolution and origin of the viruses, as well as the differentiation between viruses and living organisms [1]. The complexity of NCLDVs in terms of genome size, particle size and metabolic capabilities (such as their role in photosynthesis and apoptosis) has challenged many concepts in virology [2]. However, it was the discovery of APMV that spotlighted NCLDVs [3]. This novel member of the NCLDV group, which belongs to the proposed *Megavirales* order, is extremely large and complex and contains genes related to translational activity, which were hitherto considered to be exclusive to cellular organisms [4].

The family *Mimiviridae* is comprised of double stranded DNA viruses up to 750 nm of diameter with genomes containing up to 1.2 Mb. The mimiviruses are some of the most complex viruses known to date and are important members of the NCLDV group [5]. One of this family's key members is the *Mimivirus* genus, whose type species is APMV. APMV was isolated in 1992 from a water cooling tower at a hospital in Bradford, England and was investigated as a putative etiological agent of pneumonia [6]. The APMV particle is composed of a core, internal membrane, a capsid and external fibrils. The capsid has semi-icosahedral pentagonal symmetry and with a star-shaped structure called the star gate [7,8].

To date, members of the *Mimiviridae* family have been isolated in England, France, Tunisia, Chile and a few other

* Correspondence: bernard.la-scola@univ-amu.fr; jonatas.abrahao@gmail.com
[3]Unité de Recherche sur les Maladies Infectieuses et Tropicales Emergentes (URMITE), UM63 CNRS 7278 IRD 198 INSERM U1095, Faculté de Médecine, Aix-Marseille Université, Marseille, France
[1]Departamento de Microbiologia, Universidade Federal de Minas Gerais, Laboratório de Vírus, Av. Antônio Carlos, 6627 Pampulha, Belo Horizonte, MG Zip Code 31270-901, Brazil
Full list of author information is available at the end of the article

countries [3,4,9]. Additionally, DNA from these viruses was identified in the Sargasso Sea and other ocean samples using metagenomic approaches [10-12]. While APMV was isolated from a cooling tower at a hospital in England, *Megavirus chilensis* (MCHV), a putative new species of the *Mimiviridae* family, was isolated on the coast of Chile, indicating that members of this family can be found in a range of environmental conditions [3,4].

Acanthamoeba castellanii mamavirus (ACMV), a strain of APMV, was isolated from a water cooling tower at a hospital in France, together with another virus, *Sputnik virus* (SNV) [13]. SNV decreased the infectivity of ACMV in cultured *Acanthamoeba castellanii*, leading to its classification as the first virophage [13]. Since then, other viruses with similar biological activity to SNV have been isolated from other NCLDVs, consolidating the emerging concept of virophages [14,15].

Mimiviridae family viruses have been isolated in different countries from aquatic environments that display as wide range of temperatures and salinity [3,4,8,9]. However, to date, only one *Mimivirus* has been isolated in the Americas [4]. In this work we report the isolation, biological characterization, genome sequencing and annotation of the giant Samba virus (SMBV) and its associated virophage Rio Negro virophage (RNV), both isolated from the Brazilian Amazon, known to be one of the most biodiverse ecosystems in the world.

Results and Discussion

Collection area data

We decided to explore the Brazilian Amazon with the goal of isolating giant viruses. Although the biodiversity of the Amazon is well known, there are no studies regarding the potential presence of giant viruses in this environment. We collected surface water samples in October of 2011 from the Negro River (Figure 1), an affluent of the Amazon River, which is mostly in Brazilian territory. This river is acidic due to large amounts of dissolved organic substances. Rainwater flow carries organic acids from decomposing vegetation residue to the river, resulting in its dark color ("Dark River" means "Rio Negro" in Portuguese). A total of 35 water samples were collected along a 65 km route beginning at Manaus (3°6'S 60°1'W), the capital city of Amazonas State, and stored at 4°C. The samples were collected from surface water, near aquatic plants, near indigenous tribal areas, and from small Negro River affluents.

SMBV: isolation of a giant virus from the Negro River in the Amazon, Brazil

Samples collected from the Negro River were enriched in rice water medium and filtered. Isolation was carried out by growth in *A. castellanii* monolayers. After two blind passages, a sample collected near Manaus (3°7′ 34.00" S 60°4′25.00" W) induced cytopathic effects (CPE), including cell rounding and lysis after 2 days (Figure 2A). Samples collected in parallel were assayed by real-time PCR [16] and were positive for the amplification of the mimivirus helicase gene DNA, suggesting the presence of a giant virus. This Amazonian virus was named Samba virus (SMBV).

To characterize this potential new giant virus, SMBV was grown and purified in *A. castellanii* as described previously [3], and *A. castellanii* cells infected with SMBV at a $TCID_{50}$ per cell rate of 10 were analyzed by electron microscopy (EM). Uninfected amoebae were used as controls. After seven hours of infection, EM images revealed the presence of giant viruses with multi-layered capsids

Figure 1 Location of the collections. Water samples were collected from the Negro River, which is located in the Brazilian Amazon.

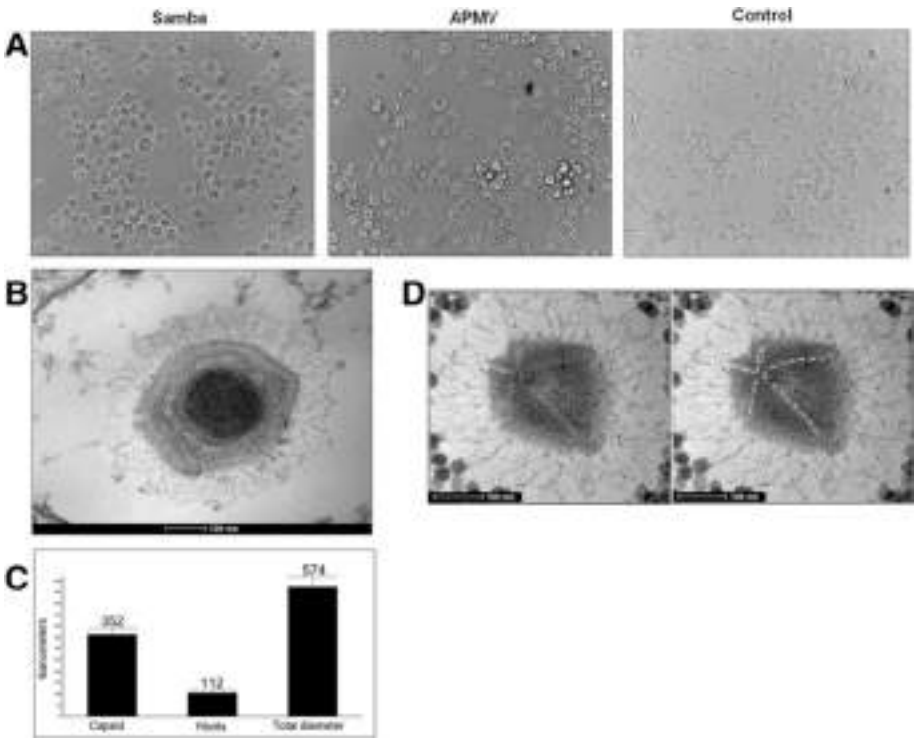

Figure 2 Isolation and characterization of SMBV. A) SMBV-induced CPEs in an ***A***. *castellanii* monolayer, which are similar to APMV-induced CPEs; **B)** SMBV particle visualized by transmission electronic microscopy; **C)** Morphometry of the SMBV particle, which has an average diameter of approximately 574 nm (a total of 50 particles images were analyzed); **D)** Detail of the star-gate structure (visualized by electronic microscopy), which is also present in APMV.

covered with fibrils (Figure 2B). The capsids averaged 352 nm in diameter, the fibrils averaged 112 nm in length, and the average diameter of the particles was 574 nm (Figure 2C), making SMBV the largest virus ever isolated in Brazil (a total of 50 particles images were analyzed) and the first mimivirus isolated in this country. Actually, the size of the particles is likely to be significantly larger since chemical preparation might be related to particles shrinkage. In some of the images we detected a hypothetical star-gate structure, which has been described in other giant viruses (Figure 2D). We next observed purified virus using a light microscope. Remarkably, we were able to detect several particles at 1000× magnification on agarose surface, similarly to APMV.

EM images obtained at different infection times suggest that SMBV entry is mediated by phagocytosis (Figure 3A). TEM images of SMBV in amoebae revealed a large viral factory occupying a large portion of the amoeba cytoplasm (Figure 3B). We observed viral morphogenesis in association with the viral factories, which presented particles in the early (Figure 3C, red arrows), intermediate (Figure 3C, green arrows) and final stages (Figure 3C, blue arrows) of assembly. Therefore, SMBV life cycle is very similar to that described to APMV.

Isolation and characterization of RNV, the virophage associated with SMBV

While analyzing the EM images, we were intrigued by the presence of a myriad of ~35 nm hexagonal-shaped particles in amoebas infected with SMBV (Figure 4A and 4B). These particles were adjacent to the SMBV viral factories, and some of them associated with the viral particles during the final assembly phase. A careful examination of infected amoebas revealed the presence of atypical SMBV particles, including defective capsids wrapped around small (roughly 35 nm) particles (Figure 4C), lemon-shaped particles (Figure 4D), and defective spiral capsids (Figure 4E). Because previous studies have described similar phenomena in amoebae co-infected with ACMV and SNV, we decided to investigate the nature of these small particles. Real-time PCR for the SNV capsid gene was performed using SMBV-infected amoeba as template, and the expected fragment was amplified from those cells, but not from the controls (water or uninfected amoebas). A primer pair was designed to amplify a large fragment of the capsid gene based on the consensus sequence of virophage capsid genes available in GenBank. An amplicon was generated from SMBV-infected amoebas and then confirmed by sequencing.

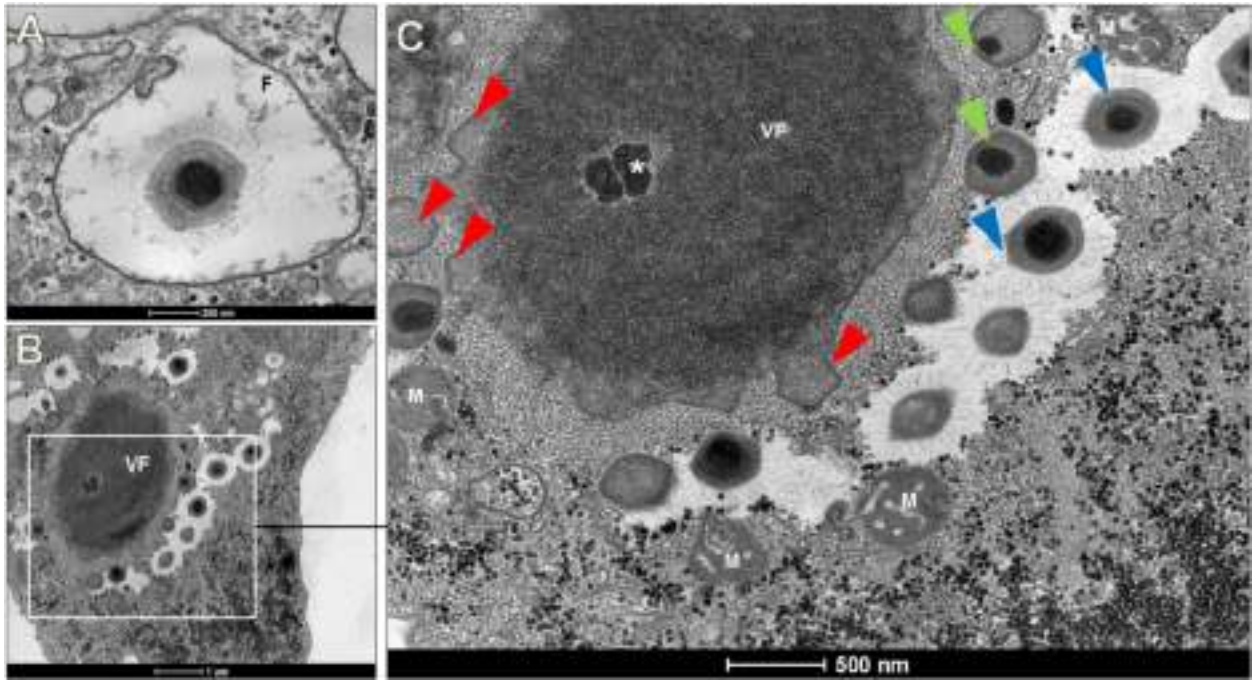

Figure 3 SMBV replication cycle. Replication of SMBV in *A. castellanii* observed by transmission electronic microcopy. **A)** SMBV enters amoebae by phagocytosis and remains within the phagosome; **B)** Giant viral factories are present within the amoebal cytoplasm; **C)** Morphology of SMBV near the viral factory: early morphogenesis (red arrows), intermediate morphogenesis (green arrows) and late morphogenesis (blue arrows). * = Viral seed; M = mitochondria, VF= Viral factory.

To analyze the influence of the virophage on giant virus replication, purified SMBV were diluted and filtered. The aliquoted virophage solution was stored at -80°C until use. An *A. castellanii* monolayer was co-infected with APMV ($TCID_{50}$ per cell rate of = 10) and 100 μl of the solution containing the undiluted virophage isolated from SMBV. After 16 hours, we analyzed the cells by EM. Remarkably, virophage particles derived from SMBV were observed in association with APMV particles during viral assembly (Figure 4F). We also observed defective APMV particles similar to those seen in SMBV and virophage co-infected amoebas. Large areas of virophage accumulation covering more area than the APMV factories themselves were observed in some of the co-infected amoebas (Figure 4G).

To quantify the SMBV virophage inhibition of giant virus replication, *A. castellanii* was infected with APMV at a $TCID_{50}$ per cell rate of 1 and superinfected with 100 μl of virophage solution, undiluted or diluted to 10^{-9}. The $TCID_{50}$ was determined after 48 hours by observing the APMV-induced CPEs in *A. castellanii* (Figure 5A). In parallel, we performed one-step growth curves (0 to 25 hours) of APMV, SMBV (naturally associated to RNV) and APMV + RNV (Figure 5B). In both assays, RNV caused a decrease in APMV titers, ranging from 2 $\log_{10}$ at early timepoints to 5 $\log_{10}$ at 25 hours post infection. The inhibitory effect of the virophage could also be observed by light microscopy. Instead of the rounding induced by APMV replication, co-infected cells exhibit milder CPEs at the same timepoint, resembling the control cells more than the APMV-infected cells (Figure 5C). No CPEs were observed in amoebas inoculated only with the virophage RNV.

SMBV genome

After sequencing, assembly and annotation, we obtained a partial SMBV genome (scaffold) of 1,213,607 bp (Figure 6A), which is comparable in size to the largest genomes described for mimiviruses to date (Figure 6B). We achieved approximately 98.8% coverage of the genome (considering APMV covered orthologous) (Genbank access number: KF959826). The SMBV genome has a GC content of 27.0% (Figure 6A) and is approximately 50,000 bp larger than the APMV genome. A total of 938 ORFs, ranging in size from 150 to 8835 bp (Figure 7A), were annotated as putative genes. The average ORF size is 1001.8 bp. Using these ORFs, a gene similarity search was conducted using the Blast2GO platform. Many of the ORFs within the SMBV genome had only been found previously in viruses from the *Mimiviridae* family, including those which putatively encode proteins with roles in protein translation or DNA repair. Overall, SMBV shared the most ORFs in common APMV (~91%), followed by ACMV (~6%), *Mimivirus pointrouge* (~0.5%), *Moumouvirus goulette* (~0.5%) and others (~2%) (Figure 7B). An analysis of the SMBV genome

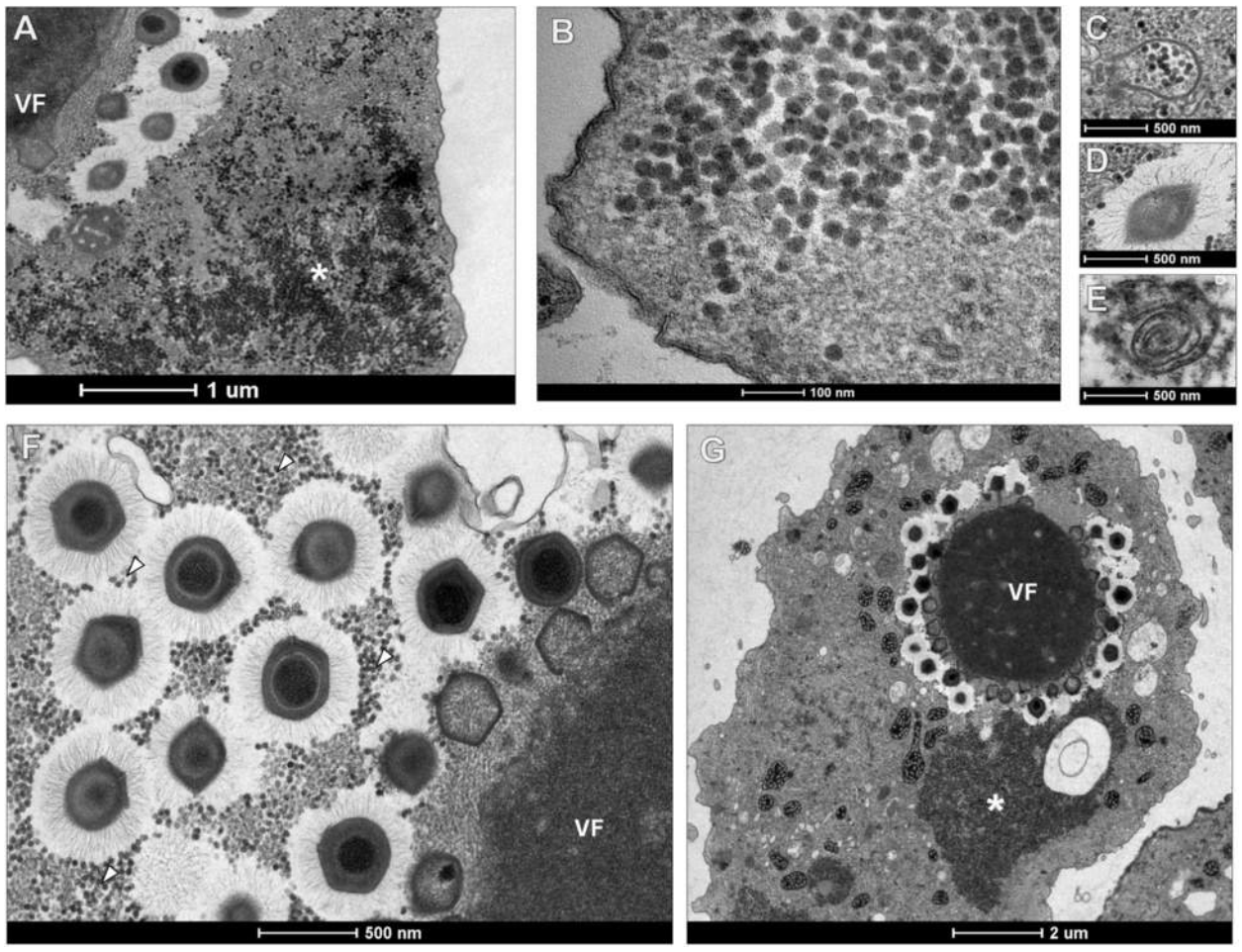

Figure 4 EM of the virophage RNV. Electron microscopy of virophage accumulation in the cytoplasm of *A. castellanii* infected with SMBV and APMV. **A**, **B)** Significant accumulation of virophage particles (indicated by an asterisk) around the viral factories and SMBV particles; **C**, **D**, **E)** SMBV particles with defective morphology as a result of infection by virophage; **F**, **G)** Virophage isolated from SMBV are also able to associate with APMV and accumulate near the viral factories, leading to the formation of defective viral progeny. VF = viral factory.

identified 19 ORFs related to DNA replication, 10 involved in DNA recombination, 14 linked to DNA repair and five related to tRNA aminoacylation, which is important for protein translation (Figure 7C). We also identified 264 domains that are putatively related to protein binding and 200 domains linked to catalytic activity (Additional file 1: Figure S1A). The sequence similarity between SMBV ORFs and the homologous genes in GenBank ranged from 35 to 100%, with many candidates showing 50 to 60% similarity, indicating that SMBV genome has many unique features (Additional file 1: Figure S1B). Although 47.1% of the predicted ORFs in the SMBV genome have homologs in other giant virus genomes, they are not homologous to other organisms and are therefore considered hypothetical proteins (Additional file 1: Figure S1C). Interestingly, a dotplot analysis of SMBV vs. APMV ORFs (gene synteny) revealed that, although the majority of SMBV genes are present in the same genome locus described for APMV, many ORFs are inverted or in distinct loci, especially those in the terminal regions (Additional file 2: Figure S2).

SMBV phylogeny

To determine which viruses SMBV is most closely related to, we performed the following analyses: [1] we constructed phylogenetic trees by aligning the ribonucleotide reductase (Figure 6B) and helicase gene (data not shown) sequences from SMBV with GenBank sequences and [2] we constructed a Venn diagram showing a presence-absence analysis of ORFs from SMBV and related viruses (Additional file 3: Figure S3). Both phylogenetic trees show that SMBV clusters with members of *Megavirales* order group A (MGA), which includes APMV (the prototype of the family) and ACMV (Figure 6B). MGA was most closely related to *Megavirales* group B (MGB), which includes *Acanthamoeba polyphaga*

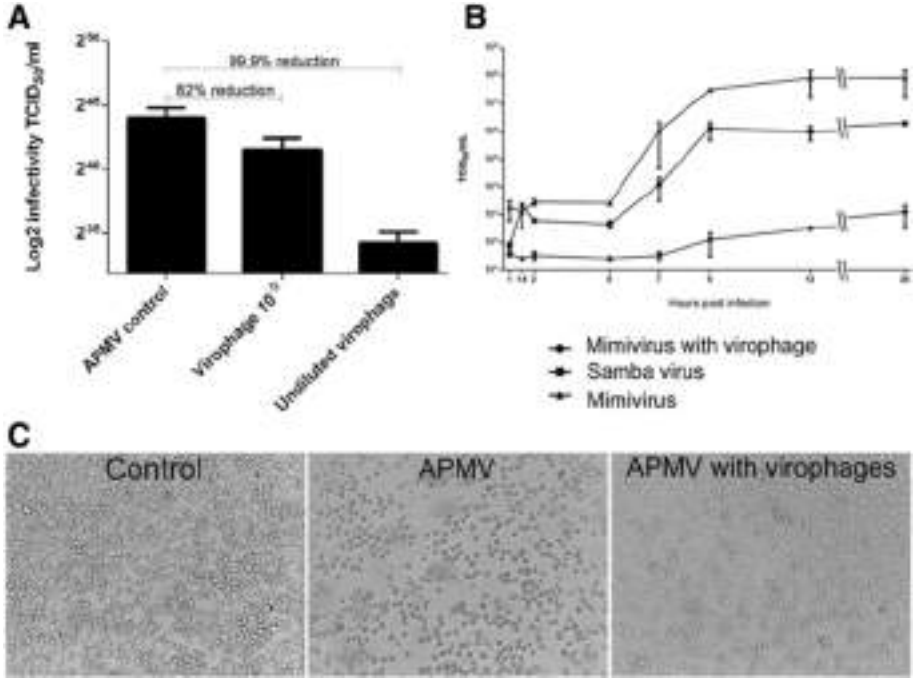

Figure 5 Reduction of viral infectivity by co-infection with virophage. Evaluation of the biological activity of virophage isolated from SMBV through viral infectivity reduction assays: **A)** Titration of APMV in *A. castellanii* after co-infection with RNV showed a reduction in viral titer by more than 80% compared to the control; **B)** A one-step growth curve of APMV in the presence of virophage showed that RNV drastically reduces the ability of APMV to multiply in *A. castellanii*, leading to a significant decrease in viral titer compared to control curves generated with SMBV naturally associated to RNV and APMV in the absence of virophage. **C)** Reduction in APMV-induced CPEs in amoeba when co-infected with virophage, visualized by light microscopy (after 12 hours).

moumouvirus (APMOUV), and was distinct from *Megavirales* group C, which includes MCHV and other viruses. Other NCLDV family members were also included in the analysis, and their position in the phylogenetic tree generated in this study corroborates previous phylogenetic studies. The phylogenetic trees were constructed by MEGA 4.1 using neighbor joining, maximum parsimony and other methods with 1,000 bootstrap replicates (n. differences model) based on the ribonucleotide reductase predicted amino acid from the SMBV and other nucleocytoplasmic large DNA viruses. The same tree topology was observed for all phylogenetic approaches.

Next, a Venn diagram (Additional file 3: Figure S3) was constructed using the predicted ORFs from SMBV and the ORF data set from its closest relatives, including APMV and ACMV (from the MGA group), APMOUV (from the MGB group) and MCHV (from the MGC group). The SMBV ORFs were aligned with the ORF data set of each viral counterpart using the Blastn all-against-all method feature of Blastall 2.2.9. Only hits with an e-value ≤ 10-5 were considered valid. The diagram (Additional file 3: Figure S3) shows that nine SMBV ORFs did not appear in other viral genomes. Of these, ORF-L331 appears to contain a signal-peptide cleavage site, and ORF-R518 exhibits a transmembrane domain. The remaining ORFans had no known function or domain. SMBV shares 925 ORFs with APMV, 909 with ACMV, 346 with MCHV and 312 with APMOUV. SMBV, APMV and ACMV (MGA strains) share 503 ORFs. SMBV, MGA and APMOUV (MGB) share 61 ORFs, while SMBV, MGA and MCHV (MGC) shared 93 ORFs. All of the viruses analyzed share a core repertoire of 249 ORFs (Additional file 3: Figure S3).

RNV virophage sequence analysis

The RNV capsid gene was also sequenced and analyzed (primers: 5'ATGTCTAATTCAGCTATTCCTCTTA3' and 5'TCACATTTTAAGTTCTTTTCTCAAT3"). We then manually aligned the sequence with conserved virophage sequences from GenBank and used Modeltest software to determine which model of evolution was most appropriate for our analysis. Phylogenetic trees based on the capsid gene sequence were constructed using MEGA 4.1 with neighbor joining, maximum parsimony and other methods with 1,000 bootstrap replicates. The RNV capsid sequence was deposited in GenBank (KJ183141). Our results show that the RNV capsid gene shares 100% identity with SNV and high identity with other SNV genes.

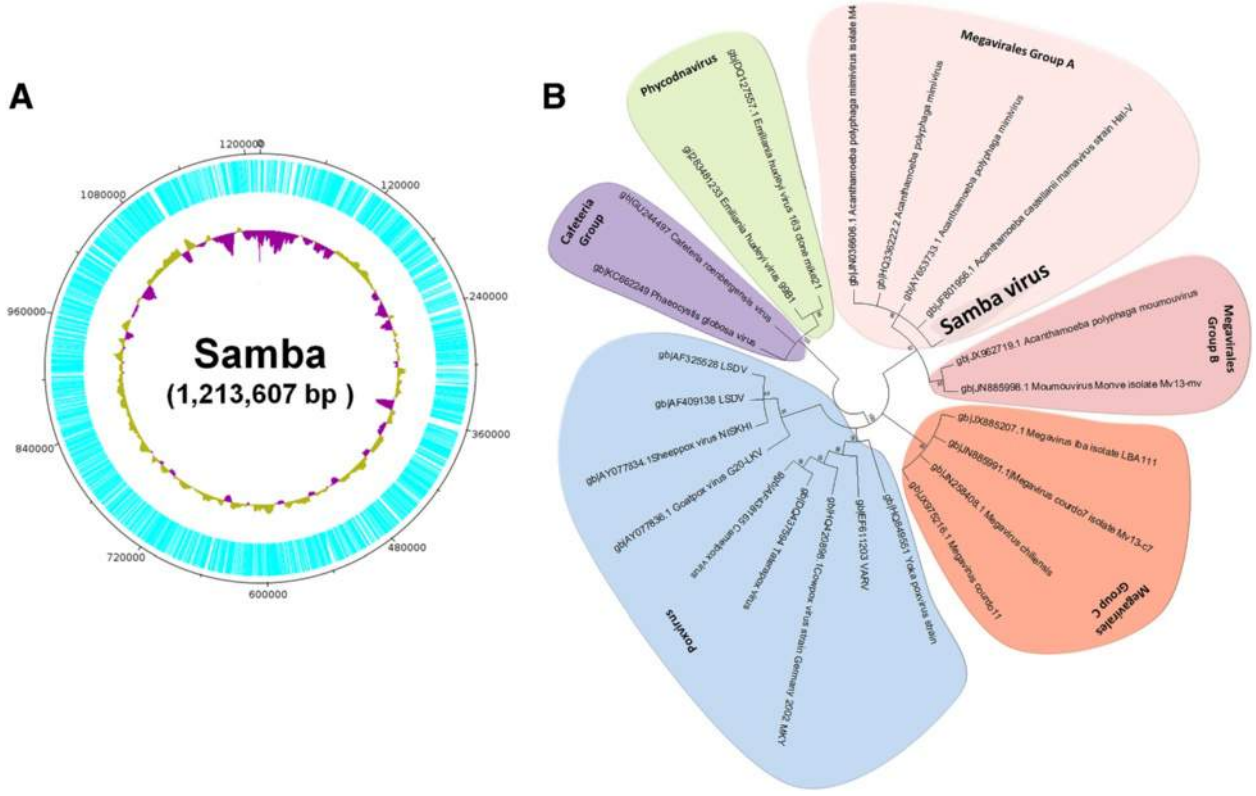

Figure 6 Samba virus genome (circular) and phylogeny: (A) Estimated Samba virus genome size assembled using the Perl-based program ABACAS 1.3.1-1. The predicted ORFs are highlighted in blue, revealing a very low proportion of noncoding DNA. The innermost circle indicates the G-C content. Regions with a G-C content higher than the average (28%) are highlighted in green, and lower than average in purple. **(B)** Phylogenetic tree (neighbor joining, 1,000 bootstrap replicates, n. differences model) based on the ribonucleotide reductase predicted amino acid from the Samba virus and other nucleocytoplasmic large DNA viruses. The Samba virus clusters with members of Megavirales group A, which is comprised of Mimivirus and Mamavirus. The tree is unrooted. The values near the branches are bootstrap values calculated using the MEGA 4 program and are used as confidence values for the tree branches.

Therefore, RNV clusters with SNV-like viruses and does not cluster with Mavirus or the Organic Lake Virophage (Additional file 4: Figure S4). Unfortunately, it was not possible to recover RNV contigs from SMBV sequencing data.

Conclusions

Giant viruses exhibit strikingly large genome and particle sizes, and have shed light on the evolution of large DNA viruses [3,4,17-25]. This study describes the discovery, isolation and characterization of Samba virus, a novel mimivirus, from the Negro River in the Brazilian Amazon. SMBV is phylogenetically related to *Megavirales* order group A, which comprises APMV and ACMV, and contains one of the the largest genome described for this group.

However, despite its close relationship to APMV, the SMBV genome is 50,000 bp longer than APMV and is unique for its ORF content. The SMBV and APMV genome alignment showed a high degree of synteny among the conserved genes, although we did observe some inversions (Additional file 2: Figure S2). Many of the SMBV ORFans exhibited homology to APMV sequences, although they did not appear to correspond to ORFs in the APMV genome. This may be explained by the use of different bioinformatics tools for ORF prediction during the genome annotation. The difference of 50,000 bp between the SMBV and APMV genomes is most likely due to intergenic regions and/or ORF size variation. Regarding the SBMV cycle of life, our data showed viral entry by phagocytosis and morphogenesis in association with the viral factories. All steps of viral morphogenesis resembled those described previously to APMV and other mimiviruses [3,4].

The presence of a *Mimiviridae* family virus and virophage in the Negro River correlates well with previous studies that indicate the presence of these viruses in aquatic ecosystems [10,11,24,25]. SMBV appeared to tolerate the virophage better than APMV, although we have not yet been able to generate virophage-free cultures. Nevertheless, these results suggest SMBV has developed mechanisms to

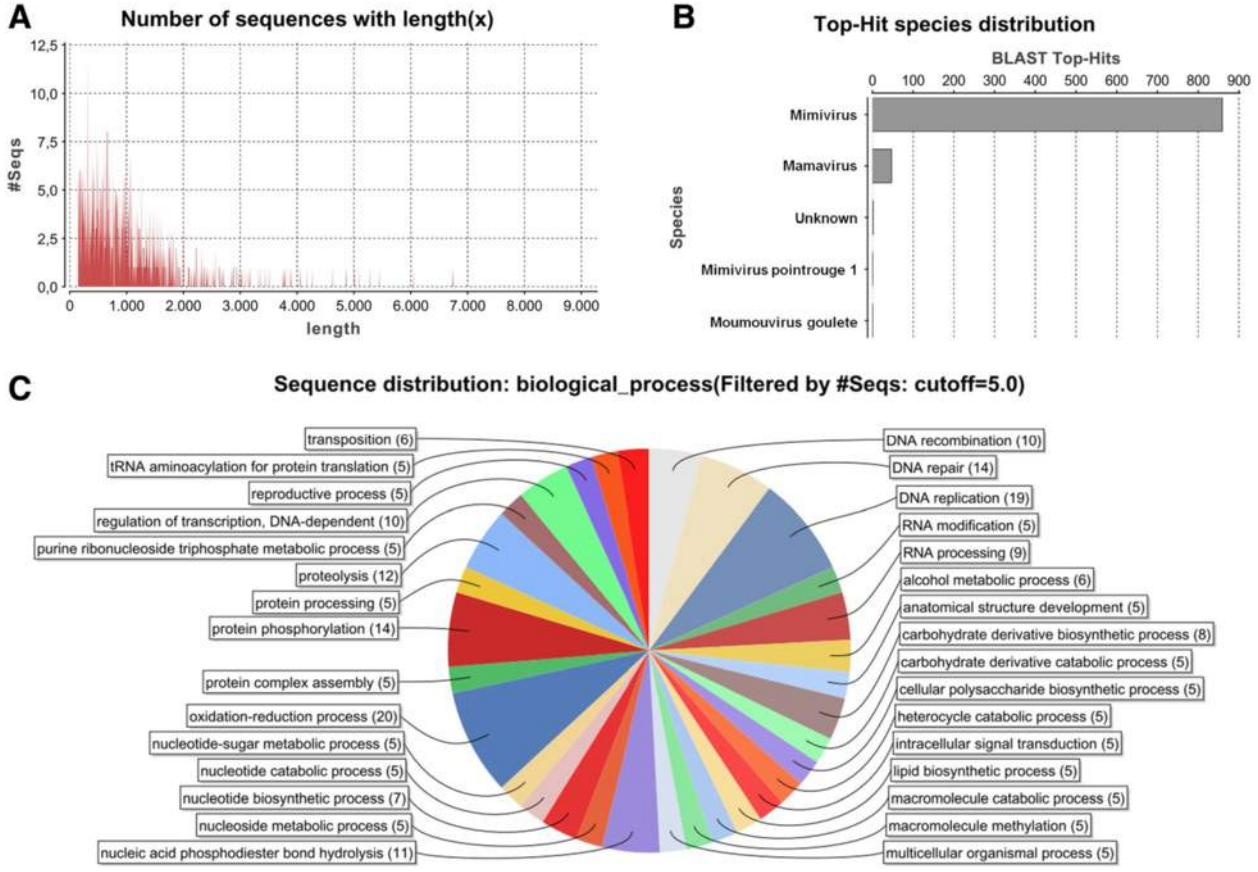

Figure 7 Genomic data. Samba virus genome characterization performed using the java-based free software Blast2go (available at http://www.blast2go.com/b2ghome): **(A)** Graphical distribution of the length of the predicted Samba virus genes, showing the predominance of small ORFs ranging mainly from 150 to 1500 nucleotides. **(B)** Graphical distribution of the sequence similarity search for the predicted Samba virus genes. The greatest number of hits were found in Mimivirus, followed by Mamavirus. **(C)** Biological processes assigned to the predicted Samba virus genes, showing a large proportion of genes involved in nucleic acid processing and cellular metabolism, as well as viral morphogenesis and intracellular regulation.

circumvent the virophage. However, future studies are necessary to confirm this hypothesis. Interestingly, recent data suggested that virophages may be important for control of giant viruses and amoeba populations [26,27].

The discovery and characterization of SMBV and its virophage raise new questions regarding the role of these viral agents in microbial ecology. The Amazon rain forest contains a striking diversity of flora and fauna, although little is known regarding the virosphere in this environment. The discovery of SMBV in the Amazon corroborates that these fascinating viruses are ubiquitous and that their isolation and characterization can yield important insights into their life cycle and complexity.

Methods

Cell line

Acanthamoeba castellanii (ATCC 30010) was kindly provided by the Laboratório de Amebíases (Departamento de Parasitologia, ICB/UFMG), and cultivated in PYG medium (Visvesvara & Balamuth, 1975) supplemented with 7% fetal bovine serum (FBS) (Cultilab, Brazil), 200 U/mL penicillin (Cristália, Brazil), 50 μg/mL gentamycin (Sigma, USA) and 2.5 μg/mL amphotericin B (Sigma, USA) at 28°C.

Virus

APMV was obtained from a cooling tower at a hospital in Bradford (England) in 1993 and characterized in 2003 [3]. APMV was used as a control for the molecular and biological assays. For viral replication, *A. castellanii* cultures were inoculated at a $TCID_{50}$ per cell rate of 0.1 and incubated in sealed bottles at 32°C.

Sample collection and virus isolation

The water samples were collected from Negro River, Amazonas and stored at 4°C overnight. The sample collections were performed with permission of Instituto Chico Mendes (ICM) – protocol numbers: 34293-1 and 33326-2. The field studies did not involve endangered or

protected species. Then, 500 μl of each sample was added to 4.5 mL of autoclaved rice and water medium made with 40 rice grains in 1 liter of water [4]. The samples were stored for 20 days in the dark at room temperature [4], then 5×10^3 *A. castellanii* trophozoites were added, and the samples were re-incubated under the same conditions for 10 days. After the enrichment process, samples were pooled in groups of five (totaling seven pools), and filtered through a 1.2 μm membrane to remove impurities and a 0.2 μm membrane to retain giant viruses. The samples were then subjected in parallel to real-time PCR and to viral isolation in *A. castellanii*.

Viral titration

The virus titration was performed in 96-well plates containing approximately 4×10^4 *A. castellanii* per well in 200 μL of PYG medium supplemented with 7% FCS. The viral samples were serially diluted (from 10^{-1} to 10^{-9}) in 50 μL of PBS, 150 μL of PYG medium with 10% FCS was added to each well, and the plates were incubated. CPEs such as rounding, loss of motility and trophozoite lysis were monitored daily in each well. After five days of incubation, the titer ($TCID_{50}$) was calculated as described by Reed and Muench [28].

Viral purification

To purify the giant viruses, cell lysates were centrifuged at 900 g for 5 minutes at 4°C. The supernatant was transferred to a fresh tube, and the pellet was subjected to three cycles of freezing and thawing to release virus trapped in the trophozoites. The lysate was homogenized in 10 mL of PBS and subjected to an additional two rounds of 50 homogenization cycles in a Dounce (Wheaton, USA). The supernatant and cell lysates were then filtered through a 2 μm filter (Millipore, USA). This filtrate was slowly dripped over 10 mL of a 22% sucrose solution (Merck, Germany) and ultra-centrifuged in a Sorvall Combi at 14,000 rpm for 30 minutes at 4°C. The pellet was homogenized in 500 μL of PBS. Aliquots of the virus were stored at -80°C and then titrated. To purify the virophages, 5 vials containing 50 μl each of previously purified infectious SMBV particles were diluted in 20 mL of PBS and filtered through 0.2 μm filters, which retain the giant viruses but not the virophages. The flow-through was collected and used in the biological assays.

Growth curve

The infectivity assays were performed by inoculating *A. castellanii* with the viral samples at an m.o.i of 10. The viruses were allowed to adsorb for 1 hour, and then the cells were washed with PBS and incubated at 32°C. At 1, 2, 4, 6, 8, 12, 24 and 48 hours, the cultures were frozen and thawed three times and titrated.

Inhibition of APMV growth after infection with isolated virophages

A. castellanii was infected with APMV at a $TCID_{50}$ per cell rate of 1 and then superinfected with 100 μl of virophages, undiluted or diluted to 10^{-9}. After 48 hours of infection, the infectivity ($TCID_{50}$) was determined by observing APMV-induced CPEs and by titration ($TCID_{50}$) in *A. castellanii* for five days.

PCR

The PCR assays were performed using primers constructed based on the helicase gene from APMV gene (primers: 5'ACCTGATCCACATCCCATAACTAAA3' and 5'GGCCTCATCAACAAATGGTTTCT3'). The PCR contained 2.0 mM $MgCl_2$, 10 mM nucleotides (dATP, dCTP, dGTP, dTTP), 2 U of Taq DNA polymerase (Promega, USA), 2.0 μl 10× Taq polymerase buffer, 4 mM primers, and 2 μl of the sample in a 20 μl total reaction volume. The amplification was performed according to the conditions recommended for StepOne (Applied Biosystems, USA) with an annealing temperature of 60°C. The PCR-amplified DNA was fractionated on a 1% agarose gel at 100 V and stained with Gel Red (Biotium, USA). The real-time PCR was performed using a commercial mix (Applied Biosystems, USA), primers (4 mM each) and 1 μl of sample in each 10 μl reaction.

Transmission electron microscopy

A. castellanii were infected at a $TCID_{50}$ per cell rate of 10. Uninfected amoebae were used as controls. After 7 hours of infection, the amoebae were washed twice with 0.1 M phosphate buffer (pH 7.4) and fixed with 2.5% glutaraldehyde (grade I) in 0.1 M phosphate buffer (pH 7.4) (Electron Microscopy Sciences, Germany) for one hour at room temperature. The amoeba monolayer was scraped from the plates and recovered by centrifugation at 900 g for 5 minutes. The amoebae were postfixed with 2% osmium tetroxide and embedded in EPON resin. Ultrathin sections were stained with 2% uranyl acetate and examined using a Tecnai G2-Spirit FEI 2006 transmission electron microscope operating at 80 kV at the Microscopy Center, UFMG, Brazil.

Sequencing analysis

The SMBV genome was sequenced using a 454 platform (Roche). For genome assembly, we used the read mapping approach implemented by the CLC Genomics Workbench 5.5.1 program to generate contig sequences, and the Perl-based genome assembly tool ABACAS.1.3.1 (algorithm-based automatic contiguation of assembled sequences) that yielded a partial genome (scaffold) of 1,213,607 bp (KF959826) (draft). The open-reading frames (ORF) were predicted using the Markov-based methods employed by Glimmer3 and FGENES. We also transferred annotations

from a closely related genome using the Rapid Annotation Transfer Tool. The predictions were manually curated, and the ORFs were assigned a final identity. ORFs smaller than 150 bp were ruled out. Finally, 938 ORFs were annotated as putative genes. A gene similarity search was conducted using Blast2GO.

Additional files

Additional file 1: Genomic data 2: Samba virus genome characterization performed using the java-based free software Blast2GO (available at http://www.blast2go.com/b2ghome). (A) Graphical distribution of the functions and domains of predicted Samba virus genes. Most of the functions are related to catalytic and binding activities. **(B)** Graphical representation of the similarity of Samba virus genes to sequences available in the data bank of the Blast2GO program. The analysis showed a broad distribution of similarity ranging between 50-60%, with a peak near 100%. **(C)** Graphical depiction of Samba virus genes with or without functional annotation (IPS – InterProScan) and Samba genes grouped into orthologous groups (GO – Gene Ontology).

Additional file 2: Dotplot of SMBV vs. APMV ORFs – MUMMER 3.0 software. Dots represent the predicted ORFs. The red dots = plus-plus ORFs, and the blue dots = inverted ORFs. Although most of the SMBV genes are present in the same genome locus described for APMV, many ORFs are inverted or located in distinct loci, especially those present in terminal regions.

Additional file 3: Venn diagram: Venn diagram of predicted Samba virus genes relative to other Mimiviridae genomes. APMV – Acanthamoeba polyphaga mimivirus; Megavirus – Megavirus chilensis; Moumouvirus - Acanthamoeba polyphaga moumouvirus; Mamavirus – Acanthamoeba castellanii mamavirus. Boxes show each gene included in the intersections. "R" (right) refers to genes that are transcribed in the positive sense, and "L" (left) refers to genes that are transcribed in the negative sense. The diagram was built using the online platform available at http://bioinformatics.psb.ugent.be/webtools/Venn/.

Additional file 4: Rio Negro virophage phylogenetic tree (A) (neighbor joining) and alignment (B) based on the predicted protein sequences of the capsid genes from RNV and other virophages.

Competing interests
The authors declare that they have no competing interests.

Authors' contributions
RKC, PVB, FLA, ERGRA, LCFS, JDA and FPD performed experiments (collection, isolation, biological and molecular characterization). GST, PCPF, JTM, CR, DR, EGK, BS and JSA designed and analyzed the results. All authors read and approved the final manuscript.

Acknowledgments
We thank João Rodrigues dos Santos and Gisele Cirilo dos Santos, colleagues from Gepvig and the Laboratório de Vírus, for their excellent technical support. We would also like to thank CNPq, CAPES, FAPEMIG, Pro-Reitoria de Pesquisa da Universidade Federal de Minas Gerais (PRPq-UFMG), and Centro de Microscopia da UFMG.

Author details
[1]Departamento de Microbiologia, Universidade Federal de Minas Gerais, Laboratório de Vírus, Av. Antônio Carlos, 6627 Pampulha, Belo Horizonte, MG Zip Code 31270-901, Brazil. [2]Departamento de Bioquímica e Imunologia, Instituto de Ciências Biológicas, Universidade Federal de Minas Gerais, Av. Antônio Carlos, 6627 Pampulha, Belo Horizonte, MG CEP 31270-901, Brazil. [3]Unité de Recherche sur les Maladies Infectieuses et Tropicales Emergentes (URMITE), UM63 CNRS 7278 IRD 198 INSERM U1095, Faculté de Médecine, Aix-Marseille Université, Marseille, France.

Received: 19 February 2014 Accepted: 1 May 2014
Published: 14 May 2014

References
1. Yamada T (2011) Giant viruses in the environment: their origins and evolution. Curr Opin Virol 1:58–62
2. Culley AI (2011) Virophages to viromes: a report from the frontier of viral oceanography. Curr Opin Virol 1:52–57
3. La Scola B, Audic S, Robert C, Jungang L, de Lamballerie X, Drancourt M, Birtles R, Claverie JM, Raoult D (2003) A giant virus in amoebae. Science 299:2033
4. Arslan D, Legendre M, Seltzer V, Abergel C, Claverie J (2011) Distant Mimivirus relative with a larger genome highlights the fundamental features of Megaviridae. Proc Natl Acad Sci U S A 108:17486–17491
5. Legendre M, Arslan D, Abergel C, Claverie JM (2012) Genomics of Megavirus and the elusive fourth domain of Life. Commun Integr Biol 5:102–106
6. La Scola B, Marrie TJ, Auffray JP, Raoult D (2005) Mimivirus in pneumonia patients. Emerg Infect Dis 11:449–452
7. Xiao C, Chipman PR, Battisti AJ, Bowman VD, Renesto P, Raoult D, Rossmann MG (2005) Cryo-electron microscopy of the giant Mimivirus. J Mol Biol 28(3):493–496, 353
8. Zauberman N, Mutsafi Y, Halevy DB, Shimoni E, Klein E, Xiao C, Sun S, Minsky A (2008) Distinct DNA exit and packaging portals in the virus Acanthamoeba polyphaga mimivirus. PLoS Biol 13;6(5):e114
9. Boughalmi M, Saadi H, Pagnier I, Colson P, Fournous G, Raoult D, La Scola B (2012) High-throughput isolation of giant viruses of the Mimiviridae and Marseilleviridae families in the Tunisian environment. Environ Microbiol 53:344–353
10. Ghedin E, Claverie JM (2005) Mimivirus relatives in the Sargasso sea. Virol J 2:62
11. Monier A, Larsen JB, Sandaa RA, Bratbak G, Claverie JM, Ogata H (2008) Marine mimivirus relatives are probably large algal viruses. Virol J 5:12
12. Williamson SJ, Allen LZ, Lorenzi HA, Fadrosh DW, Brami D, Thiagarajan M, McCrow JP, Tovchigrechko A, Yooseph S, Venter JC (2012) Metagenomic exploration of viruses throughout the Indian Ocean. PLoS One 7:e42047
13. La Scola B, Desnues C, Pagnier I, Robert C, Barrassi L, Fournous G, Merchat M, Suzan-Monti M, Forterre P, Koonin E, Raoult D (2008) The virophage as a unique parasite of the giant mimivirus. Nature 455:100–104
14. Yau S, Lauro FM, DeMaere MZ, Brown MV, Thomas T, Raftery MJ, Andrews-Pfannkoch C, Lewis M, Hoffman JM, Gibson JA, Cavicchioli R (2011) Virophage control of antarctic algal host-virus dynamics. Proc Natl Acad Sci U S A 108:6163–6168
15. Fischer MG, Suttle CA (2011) A virophage at the origin of large DNA transposons. Science 332:231–234
16. Dare RK, Chittaganpitch M, Erdman DD (2008) Screening pneumonia patients for mimivirus. Emerg Infect Dis 14:465–467
17. Philippe N, Legendre M, Doutre G, Couté Y, Poirot O, Lescot M, Arslan D, Seltzer V, Bertaux L, Bruley C, Garin J, Claverie JM, Abergel C (2013) Pandoraviruses: amoeba viruses with genomes up to 2.5 Mb reaching that of parasitic eukaryotes. Science 341:281–286
18. Xiao C, Kuznetsov YG, Sun S, Hafenstein SL, Kostyuchenko VA, Chipman PR, Suzan-Monti M, Raoult D, McPherson A, Rossmann MG (2009) Structural studies of the giant mimivirus. PLoS Biol 7:e92
19. Claverie JM, Abergel C (2010) Mimivirus: the emerging paradox of quasi-autonomous viruses. Trends Genet 26:431–437
20. Boyer M, Azza S, Barrassi L, Klose T, Campocasso A, Pagnier I, Fournous G, Borg A, Robert C, Zhang X, Desnues C, Henrissat B, Rossmann MG, La Scola B, Raoult D (2011) Mimivirus shows dramatic genome reduction after intraamoebal culture. Proc Natl Acad Sci U S A 108:10296–10301
21. Suzan-Monti M, La Scola B, Barrassi L, Espinosa L, Raoult D (2007) Ultrastructural characterization of the giant volcano-like virus factory of Acanthamoeba polyphaga Mimivirus. PLoS One 2:e328
22. Krupovic M, Cvirkaite-Krupovic V (2011) Virophages or satellite viruses? Nat Rev Microbiol 9:762–763
23. Desnues C, Raoult D (2010) Inside the lifestyle of the virophage. Intervirology 53:293–303
24. Claverie JM, Grzela R, Lartigue A, Bernadac A, Nitsche S, Vacelet J, Ogata H, Abergel C (2009) Mimivirus and Mimiviridae: giant viruses with an increasing number
of potential hosts, including corals and sponges. J Invertebr Pathol 101:172–180

25. Fischer MG, Allen MJ, Wilson WH, Suttle CA (2010) Giant virus with a remarkable complement of genes infects marine zooplankton. Proc Natl Acad Sci U S A 107:19508–19513
26. Desnues C, La Scola B, Yutin N, Fournous G, Robert C, Azza S, Jardot P, Monteil S, Campocasso A, Koonin EV, Raoult D (2012) Provirophages and transpovirons as the diverse mobilome of giant viruses. Proc Natl Acad Sci U S A 30:18078–18083
27. Slimani M, Pagnier I, Raoult D, La Scola B (2013) Amoebae as battlefields for bacteria, giant viruses, and virophages. J Virol 87(8):4783–4785
28. Reed LJ, Muench H (1938) A simple method of estimating fifty percent endpoints. Am J Hyg 27:493–497

doi:10.1186/1743-422X-11-95
Cite this article as: Campos *et al.*: Samba virus: a novel mimivirus from a giant rain forest, the Brazilian Amazon. *Virology Journal* 2014 **11**:95.

VIROLOGY JOURNAL

REVIEW Open Access

Acanthamoeba polyphaga mimivirus and other giant viruses: an open field to outstanding discoveries

Jônatas S Abrahão[1*†], Fábio P Dornas[1†], Lorena CF Silva[1†], Gabriel M Almeida[1], Paulo VM Boratto[1], Phillipe Colson[2], Bernard La Scola[2] and Erna G Kroon[1]

Abstract

In 2003, *Acanthamoeba polyphaga mimivirus* (APMV) was first described and began to impact researchers around the world, due to its structural and genetic complexity. This virus founded the family *Mimiviridae*. In recent years, several new giant viruses have been isolated from different environments and specimens. Giant virus research is in its initial phase and information that may arise in the coming years may change current conceptions of life, diversity and evolution. Thus, this review aims to condense the studies conducted so far about the features and peculiarities of APMV, from its discovery to its clinical relevance.

Keywords: Giant viruses, *Mimiviridae*, *Mimivirus*

Introduction

Viruses are remarkable organisms that have always attracted scientific interest. The study of unique viral features has been a wellspring of discovery that helped establish the foundations of molecular biology and led to in-depth evolutionary studies [1-3]. In this context, giant viruses have recently emerged as a fascinating line of research, raising important questions regarding evolution and their relationships with their hosts [4-10].

Although giant viruses offer deep ecological and clinical importance, the *Mimiviridae* group deserves special emphasis; they have been the subject of intense research in recent years, which has generated much relevant information [4-8,11-14]. *Acanthamoeba polyphaga mimivirus* (APMV) was the first known mimivirus, isolated from an amoebal co-culture present in a water sample collected from a cooling tower of a hospital in England. Its characterization revealed surprising characteristics: it was a DNA virus with a diameter of approximately 700 nm and a genome of approximately 1,2 Mb, making it the largest known virus up to then [5]. Five years later, a similar virus was isolated in amoeba from the water of a cooling tower in Paris, and since then several dozen giant viruses have been isolated from many different environments and specimens [11,15-19]. Data obtained from these viruses provoked scientific discussions regarding the nature and biological dynamics of viruses, and the intriguing features *Mimivirus* have challenged virologists and evolutionists alike. The potential existence of many other interesting and unusual unknown viruses in the biosphere makes us realize that the discovery and characterization of giant viruses is in its initial phase and that there is still much to be learned by studying these organisms. Recently, the discovery of Pandoravirus (1 μm in length and with a genome fo 2.8 Mb) and of *Pithovirus sibericum* (1.5 μm in length and a surprisingly smaller genome of 600 kb) brought even more attention to the prospection and study of giant viruses [19,20].

Discovery and taxonomy

In 1992, a pneumonia outbreak occurred in a Bradford hospital (England), and water samples from a cooling tower that contained free-living amoebae were investigated to determine the etiological agent of the pneumonia outbreak [5]. At that time, Gram-positive cocci that were visualized by light microscopy inside *Acanthamoeba polyphaga* cells

* Correspondence: jonatas.abrahao@gmail.com
†Equal contributors
[1]Universidade Federal de Minas Gerais, Instituto de Ciências Biológicas, Laboratório de Vírus, Avenida Antônio Carlos, 6627, Caixa Postal 486, Bloco F4, Sala 258, 31270-901 Belo Horizonte, Minas Gerais, Brazil
Full list of author information is available at the end of the article

were named Bradford coccus. Every attempt to isolate this microorganism and amplify its 16S rDNA failed. Moreover, treatment of amoeba cultures with antibiotics to inhibit growth of this microorganism was also unsuccessful, which led doubt whether it was indeed a bacteria [5]. After a hiatus of a few years, this organism was the subject of new studies at the *Rickettsia Unit at the School of Medicine* (Marseille, France) in the early 2000s. After a new series of unsuccessful characterization attempts, electron microscopy of *Bradfordcoccus*-infected *Acanthamoeba polyphaga* cells revealed icosahedral-like particles with an astonishing 750 nm diameter size [5]. In addition to this virus-like morphology, analysis of the replication curve of this organism in amoeba cells revealed an eclipse phase, which is an almost universal feature among viruses. Finally, when the complete sequencing and analysis of its genome was finished, it became evident that this peculiar organism clustered with other giant viruses and not with bacteria [5]. This new virus was then called *Acanthamoeba polyphaga* mimivirus (APMV), due its ability to infect the free-living amoebae *Acanthamoeba polyphaga* sp. and mimic a microbe. APMV, also known as mimivirus, had the largest viral genome known up to then, reaching approximately 1.2 Mb. Its characteristics were so different from other viruses that it was not possible to include it into any known viral family, so the *Mimiviridae* family was created [5]. APMV became the first member of the *Mimiviridae* family, *Mimivirus* genus, and its prototype.

Few years before the discovery of APMV, the genomic content of known giant viruses that replicate partly or entirely in the cytoplasm of eukaryotic cells (members from *Poxviridae*, *Asfarviridae*, *Phycodnaviridae, Ascoviridae* and *Iridoviridae* families) was analyzed in depth. Several common, and supposedly essential, genes were identified, and it was suggested that the origin of these four viral families was monophyletic [21-26]. Other common characteristics, such as a large double-stranded DNA genome, the relative independence of their host transcription machinery, and a replication cycle that occurs at least partially into the cytoplasm with the formation of inclusion bodies or viral factories, were the basis for the generic name of these viral families: the nucleocytoplasmic large DNA viruses (NCLDVs) [22-26]. Because viruses from the *Mimiviridae* family also share these characteristics, they were added to the NCLDV group as well.

After APMV was described, interest in giant viruses grew, several other giant viruses were isolated, and the *Mimiviridae* family was expanded. Currently, the *Mimiviridae* family contains two genera according to the International Committee on Taxonomy of Viruses (ICTV): *Mimivirus*, with APMV as its only member, and *Cafeteriavirus*, with *Cafeteria roenbergensis virus* as its only member (www.ictvonline.org). With the increasing number of new giant virus isolates and hypothetical species, a new viral order has been proposed [27]. The putative *Megavirales* order contains the *Mimiviridae* family and other NCLDVs, including the newly proposed *Marseilleviridae* family [28], whose founding member is Marseillevirus, another giant virus, smaller than Mimivirus, that infects amoeba isolated from cooling tower water in 2008 [18]. Mimivirus and Marseillevirus have been primarily linked to other NCLDVs, based on a set of ≈ 50 conserved core genes shared by all or by a majority of these large and giant viruses [29]. All these viruses were shown to compose a monophyletic group [21]. Nucleo cytoplasmic virus orthologous groups (NCVOGs) were defined among these viruses, including 177 proteins present in > 1 NCLDV family and five common to all viruses [30].

The discovery of new isolates of mimiviruses of amoeba revealed the existence of three different lineages (A, B and C). Lineage A of the *Mimivirus* genus contains the best known mimivirus isolates, such as the APMV species [5]. *Mimivirus* lineage B is represented by *Acanthamoeba polyphaga* moumouvirus, which was isolated from a water sample in February, 2008; genetic analysis revealed differences that placed this virus into the B lineage [15]. The first extensively described member of lineage C was *Megavirus chilensis*, isolated from a water sample collected off the coast of Chile [13]. Other previously described mimiviruses, including Courdo7, Courdo11, Terra1 and Montpellier, were also included in lineage C [31]. Other viruses, including some that are distantly related, have been obtained from environmental and clinical samples [32,33], and in the next years it will likely be possible to present an extensive depiction of the putative viral isolates, strains and species.

Amoebas as the main host of giant viruses

As mentioned above, the first mimivirus isolate was discovered from studies of the pathogenic microorganisms associated with amoebae (MPAAs) that were linked to nosocomial pneumonia [5]. Free-living amoebae of the genus *Acanthamoeba* belong to the *Protist* kingdom and can be part of the normal microbiota of some animals, including humans [34]. Amoebas from this genus are considered ubiquitous and have been isolated from various environments, including soil, air, aquatic environments, sewage treatment systems, contact lenses, hospital environments, and ventilation and air conditioning systems [34-36]. Several studies show that amoebas of this genus are very stable after treatment with disinfectants and are highly resistant to extremes of pH and temperature [34-37].

Free-living amoebae can cause severe and chronic diseases by themselves, such as granulomatous amoebic encephalitis, cutaneous acanthamoebiasis, amoebic keratitis and primary amoebic meningoencephalitis [38]. They can also carry other MPAAs that cause disease [39-41]. For example, microorganisms of the *Legionella*, *Parachlamydia*

and *Mycobacterium* genera are MPAAs considered to be causative agents of pneumonia, most of which is associated with many cases of nosocomial lung infection [37,42,43]. Even after being phagocytosed, some MPAAs are able to persist in the amoeba intracellular environment, and often manage to multiply numerously [5]. Studies have described amoebae isolation from many health institutions, revealing the presence of free living amoebae on hospital floors and objects, in intensive care units (ICUs), operating rooms, nurseries, kitchens, emergency rooms and infectious disease wards, showing that the free living amoebas may serve as potential platforms for amplification of pathogenic MPAAS in these environments [40-43]. The attention given to free living amoebas in recent years, together with the isolation and characterization of mimiviruses in amoebal samples from a cooling tower during an outbreak of pneumonia, add more importance to the role of mimiviruses as MPAAs.

Up to now, amoebae of the *Acanthamoeba* genus are the only confirmed APMV hosts; the virus was originally isolated from *A. polyphaga*, but now is also being cultivated in the laboratory in *A. castelannii*, *A. griffin* and *A. lenticulata* [5,44]. However, there is increasing evidence that these viruses have a broader host range. Some studies have indicated sponges and corals as potential hosts of mimivirus [44]. Khan (2007) described a productive APMV infection in mice after intracardiac infection [45]. The ability of APMV to enter and replicate inside human phagocytic cells and peripheral blood mononuclear cells in vitro has been reported [39]. These reports, together with the human blood isolation of the marseillevirus, another giant virus of amoeba belonging to a different family, suggests that vertebrates may also be hosts of these viruses [46]. The mimivirus genome has been detected in monkeys and bovines, supporting these findings [47,48]. Recently, it has been shown that APMV is able to interact with the human interferon system, a strong clue that both species share an evolutionary history [49]. It appears that APMV's ability to enter cells by phagocytosis without identified specific cell receptors, together with its large genome that confers a powerful array of non-essential genes, permits APMV to exploit a larger host range than initially believed [39,49]. Lastly, as described in this review, there is ample evidence associating APMV and other mimiviruses with humans, especially regarding pneumonia cases [50-57].

Viral particle structure, genome and gene expression

The remarkable size of mimiviruses and their peculiar features make them unique among viruses. First of all, their enormous size of approximately 700 nm lets them be retained on 0,2 μm filters [5] (Figure 1-A to D). APMV particles do not have an outer envelope, but fibers of approximately 120 nm can be associated with the capsid [58,59] (Figure 1-A and B). These fibers, still under investigation, may be involved in viral adsorption to substrates. APMV encodes enzymes capable of synthesizing polysaccharide complexes found in bacterial lipopolysaccharide (LPS) and/or peptidoglycan [60-63]. These polysaccharides form the viral particle's outer layer, in which the fibers are embedded, and they may also serve as a phagocytosis stimulus [58-63]. APMV has a pseudo-icosahedral symmetry, with a complex pentagonal face region named stargate [60,63]. This stargate form is a star-shaped projection from which the viral genome is released, and it can be important during early stages of the viral replication cycle [60,61,63,64] (Figure 2).

The particle also contains internal membranes surrounding the genome, likely acquired from endoplasmic reticulum [62] (Figure 1-A and B). The number of lipid membranes inside mimivirus particles is still under debate and investigation. At least three protein layers surround the internal membrane, and the fibrils are projected from the external layer in a tussock-like organization [62] (Figure 1-B). Inside the APMV membrane, a core wall envelops the viral DNA [62,63]. Some authors conjecture that APMV's unique particle structure may reflect horizontal gene transfer (HGT), especially amongst organisms that share the intracellular environment of amoeba, though adaptative convergence should also be considered. The APMV genome is found in association with a fibrous matrix, resembling the structure of most eukaryotic genomes; the genome release by the stargate mechanism is similar to genome releases in certain bacteriophages, and the peptidoglycan matrix surrounding the external fibers is similar to that found in certain bacteria [63].

This large and complex particle structure seems to be vital for viral stability and genome integrity under adverse environmental conditions [65-67]. The APMV genome consists of a double-stranded DNA molecule of approximately 1,2 Mb that encodes approximately 1000 proteins, many of them still uncharacterized or having functions never observed before in other viruses [5,68]. Four main groups of ORFs can be delineated in the APMV genome: (i) Megavirales core genes; (ii) genes involved in lateral gene transfer; (iii) duplicated genes; and (iv) ORFans [69]. Some APMV encoded proteins are involved in protein translation, DNA repair, cell motility and membrane biogenesis [68-72]. Many of these proteins are likely non-essential for viral replication, but may possibly increase viral fitness. Some APMV genomic sequences exhibit little or no homology with any other known nucleotide sequences in the current databases, and thus are called ORFans [69-72]. The presence of genes encoding proteins involved in protein translation, such as the amino-acyl tRNA synthetase (aaRS) and

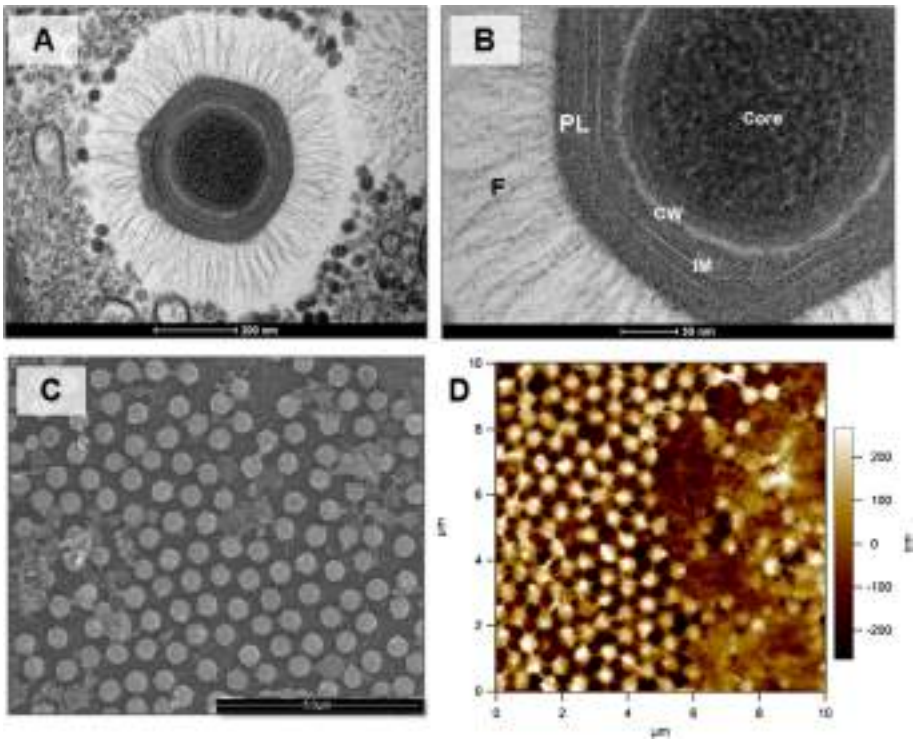

Figure 1 Mimivirus particle visualized by different microscopy methods. Transmission electron microscopy of APMV showing the complete particle **(A)** and a zoom **(B)**, highlighting the fibrils **(F)**, the capsid protein layers (PL), the internal membrane (IM), and the core wall (CW) that protects the viral genome and early factors. **(C)** and **(D)** show mimivirus isolates under scanning and atomic force microscopy, respectively. Scale in **(D)** represents the sample depth and size.

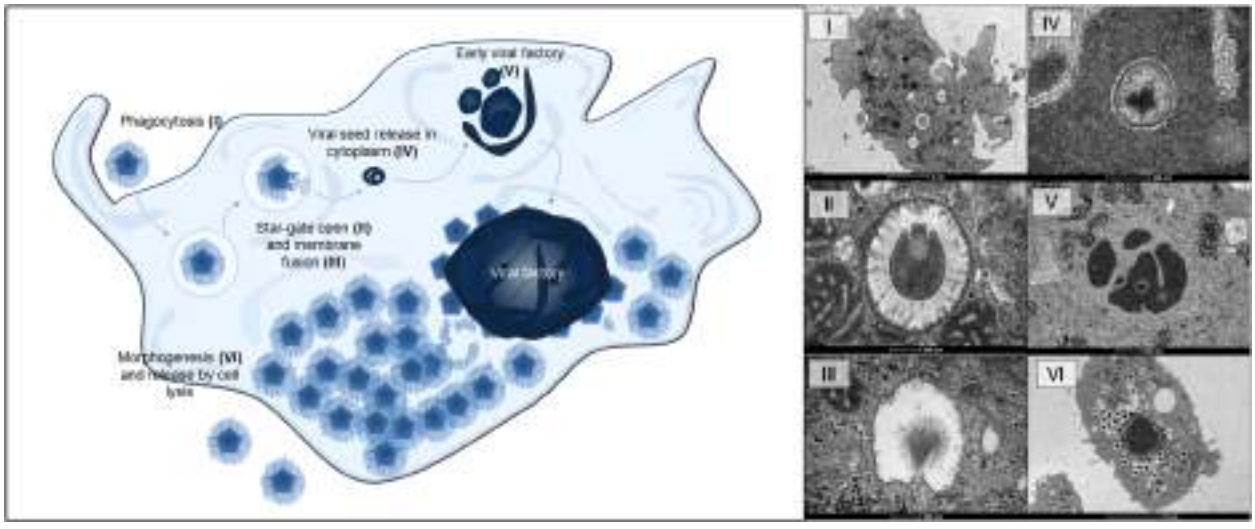

Figure 2 Mimivirus replication cycle in amoebas. (I) Phagocytosis. **(II)** Virus entry into a phagosome, followed by star-gate opening and viral membrane fusion **(III)**. **(VI)** Viral seed is released in the amoeba cytoplasm and gives start to an early viral factory **(V)**. After few hours, the viral factory grows and orchestrates the morphogenesis **(VI)** of the viral progeny, which are released by cell lysis. At the right, transmission electron microscopy of APMV at its different steps of the replication cycle.

translation factors, confers to APMV a degree of independence from their host cell machinery for genome replication [73,74].

No previously described viral genomes have shown a genetic arsenal that is able to encode elongation factors, such as tRNA and aaRS; those viruses instead must directly rely on host elongation factors. A substantial proportion of the Mimivirus, and Marseillevirus, ORFs have homologs in bacteria, archaea, eukaryotes or viruses. The large amount of chimeric genes in these viral genomes may have resulted from acquisitions by lateral gene transfer, implying sympatric bacteria and viruses with an intra-amoebal lifestyle [69].

The genomes of APMV and other mimiviruses have a high adenine-thymine (AT) content, with their most frequent codons being AAA (lysine) and AAT (asparagine). Both the codon and amino acid usages of mimiviruses are highly dissimilar to those of their amoebal host, *Acanthamoeba castellanii,* and instead are correlated with the high adenine and thymine (AT) content of the mimivirus genomes [73,75]. Additionally, it has been demonstrated that the Leu(TAA)tRNA present in several mimivirus genomes, and in multiple copies in some viral genomes, may complement the amoebal tRNA pool and may help accommodate the AT-rich viral codons [75]; remarkably, the genes most highly expressed at the beginning of the mimivirus replicative cycle have a nucleotide content more adapted to the codon usage in *A. castellanii*. Recently, an interesting study evaluated genomic alterations in APMV maintained for 150 successive passages in an axenic amoebal culture in an allopatric system. It was shown that the genome was reduced in size and morphological changes occurred in the viral particle [76]. In the allopatric system, there was no competition with other intra-amoebal micro-organisms, including bacteria and other viruses; nor were there major sources for gene gain and replacement from those micro-organisms. The passaged APMV had large deletions towards the APMV genome extremities and gene losses that were associated with: loss of fibers and their glycosylation; decreased viral ability to associate with virophages; and decreased particle antigenicity, likely due to fiber loss [76]. Excluding large deletions, 77% of the APMV genes remained intact after 150 passages in amoeba, 23% had variability and 10% were predicted to have inactivated. A majority of these inactivated genes had been previously described as weakly transcribed in APMV, prior to the laboratory culture under allopatric conditions [68,77]. In contrast, most of the genes highly transcribed before this laboratory culture were not inactivated. The major loss of weakly transcribed and weakly expressed genes in allopatric conditions suggests that the virus tends to lose or degrade its useless genes in a Lamarckian evolutionary process [77]. The loss can also be explained by the fact that DNA repair is most common in actively transcribed regions, so it is expected that genes exhibiting lower transcriptional levels undergo more changes [76,77].

Viral replication cycle

Although APMV is also unique in its replication cycle, there is a resemblance to the poxvirus replication cycle [78] (Figure 2). It has been demonstrated that APMV enters amoebas of the *Acanthamoeba* genus through phagocytosis (Figure 2-I), and the initiation of the replication cycle is marked by a typical eclipse phase, in which viral particles are not viewed in the cell [5,39]. In the early stages of replication, phagocytosed viral particles can be detected within phagosomes inside the host cell until the star-gate channels in the viral capsids (Figure 2-II) open, which is followed by membrane fusion (Figure 2-III) and release of viral seeds containing the genomes into the cytoplasm of the host cell (Figure 2-IV) [78]. DNA replication occurs exclusively in the cytoplasm, although it cannot be considered totally independent of the host nucleus because nuclear factors required for replication might participate in the process. It has been demonstrated that multiple vesicles start to appear in the cytoplasm approximately 2 hours after infection [5,78]. Their origins are unknown, but it is suspected that they are derived from the nuclear membrane or endoplasmic reticulum, and these vesicles seem responsible for nuclear factor transportation to the viral factories [78,79]. Atomic microscopy of infected amoebas revealed that the nuclear morphology does not change during the APMV infection cycle [80]. Following uncoating, the genome stabilized in viral seeds initiates the viral factories (Figure 2-V factory in formation; 2-VI mature factory). In these factories, viral DNA undergoes replication and transcription, and the DNA is prepared to be packaged in procapsids through a non-vertex portal, a transient aperture centered at an icosahedral face distal to the DNA delivery site, suggesting a pathway reminiscent of DNA segregation in bacteria [63,64,78,79].

The transcription occurs in a temporal manner: early, intermediate and late stages [80]. Interestingly, it was demonstrated that mimivirus gene promoters exhibit an unprecedented conservation among all eukaryotes [80]. After the expression of late genes, there is an increase in viral factories and structural proteins are synthesized, initiating the process of viral morphogenesis, followed by packaging of capsids with DNA (Figure 2-VI). During morphogenesis, membrane generation is accompanied by the assembly of icosahedral viral capsids, a process involving the hypothetical major capsid protein L425 that acts as a scaffolding protein [33]. An assembly model was proposed explaining how multiple mimivirus progeny can be continuously and efficiently generated. There is a high accumulation of virions in final stages of

morphogenesis [78] (Figure 2-VI). It was also demonstrated in an interesting study, that professional phagocytes such as vertebrate monocytes and macrophages are permissive for APMV replication, becoming infected via phagocytosis that leads to productive infections [39]. Ultrastructural analysis showed that protrusions were formed around the entering virus, suggesting that macropinocytosis or phagocytosis was involved in APMV entry. Reorganization of the actin cytoskeleton and activation of phosphatidylinositol 3-kinases were required for APMV entry [39]. However, although it has been shown that APMV is able to interfere with the IFN system in vertebrate cells, further studies are necessary to understand the mechanisms involved in viral replication in vertebrate phagocytes [49].

The role of giant viruses in aquatic ecosystems

The isolation of giant viruses from many different specimens, ranging from environmental samples to unicellular eukaryotic green algae and even vertebrates, reveals their ubiquitous presence on this planet. To date, we have isolated many giant viruses from aquatic environments in Brazil, especially from urban lagoons and acidic rivers, suggesting an association between a high degree of organic matter and giant virus detection [81] (unpublished data). However, discovery of mimiviruses raises questions about their ecological and evolutionary roles, especially in oceans. Carbon transfer and nutrient recycling are important biogeochemical processes that deeply involve marine zooplankton and phytoplankton [82,83]. Viruses are key regulators of these processes, due to their ability to infect and kill these populations, but the full extent of their role is still unknown [82,83]. The discovery of giant viruses in fresh and salt water provoked intense debate about the ecology of these viruses in aquatic systems, as well as their roles in structuring protist populations and even in gene exchange. In recent studies, it became evident that giant viruses can infect host protists, as in the case of the *Cafeteria roenbergensis virus* infecting marine unicellular chlorophyll flagellates [84]. It was suggested that the APMV group also contains closely related viruses capable of infecting phytoplankton, and these viruses groups phylogenetically with certain viruses of unicellular and multicellular algae [85]. Metagenomic studies, conducted in 2005 during the Global Ocean Sampling expedition in the Sargasso Sea, demonstrated through phylogenetic analysis that DNA viruses that are evolutionarily close to mimivirus exist in nature [10,86,87].

Several mimivirus-like sequences were identified, suggesting that these viruses are abundant in the marine environment. This key finding suggests that further studies of these genomic sequences can reveal the diversity of these DNA viruses and their possible roles in the evolution of eukaryotes [86]. To a lesser extent but similar to the interaction of phages and bacteria, prokaryotes that are lysed by the multiplication of marine mimiviruses could result in increased dissolved carbon and nutrients in surface waters, which might reduce sedimentation, promote microbial growth and impact local communities.

Giant viruses and the contribution to evolution knowledge

Canonically, it is considered that the genomes of most viruses do not contain sufficient information to support their classification into a domain of life. However, with the discovery of APMV and other giant viruses, this topic is being debated [24,26,88]. Giant viruses have genes that are common to the three classical Domains of life: *Archaea*, *Bacteria* and *Eukarya*, including genes involved in information storage and processing. For some researchers, this phenomenon puts them in the same definition of life that is assigned to those Domains [26]. Some APMV genes are notable due their hypothetical evolutionary importance. Recent studies have indicated the existence of a host-independent glycosylation system in APMV, likely acquired very early during evolution [89]. Collagen, one of the most abundant proteins in living cells, is found in APMV and undergoes a new type of glycosylation, showing for the first time that post-translational collagen modifications are not restricted to the canonical domains of life [90]. These results indicate that mimiviruses may have contributed to the evolution of collagen biology [90]. Genes coding for proteins involved in the replication and repair of DNA, such as DNA polymerase B and topoisomerase II, and genes for the thymidine synthetase enzymes involved in the biosynthesis of DNA oligonucleotides, are typical of eukaryotic cells but are also found in giant viruses [73]. A phylogeny based on these proteins results in an exclusive clade for the giant viruses, distinct from *Eukarya*, *Bacteria* and *Archaea* [26].

Analysis of the transcription factor II B, absent in *Bacteria*, suggests that it is highly conserved and forms a clade as old as *Eukarya* and A*r*chaea itself [88]. Analysis of the aaRS genes reveals similarity between *Mimiviridae*, *Amoebazoa* and *Eukarya*. It supports the possibility that these genes may have been transferred from a viral ancestor to amoebae, suggesting that these exchanges are common [88]. However, this specific gene has been described as involved in a lateral gene transfer. These intriguing results led some authors to question the comprehensiveness of phylogenetic trees based on analysis of ribosomal RNA because they exclude viruses and do not seem sufficient to represent all forms of life and to propose a fourth domain of life based on phylogenetic and phyletic analyses of informational genes [24,26,88]. The current classification, based on patterns of similarity of ribosomal RNA, is a prejudiced approach because it

excludes viruses from the living organisms, as viruses do not harbor ribosomal genes. However, the proposition of a fourth Domain of life to accommodate giant viruses is still much in debate. Some authors believe that the fourth domain may be artifactual, due to compositional heterogeneity and homoplasy, and the use of genes possibly acquired by the viruses from their eukaryotic hosts by horizontal gene transfer (HGT) [88].

Virophages

The isolation of *Acanthamoeba castellanii mamavirus* (ACMV) led to the discovery of one of the most intriguing and differentiating features of the *Mimiviridae* family: its close association with other small viruses called the *Sputnik virus*. *Sputnik virus* was first identified as a satellite virus [11]. Its replication, associated with the *Mimivirus* factories inside amoebas, resembled satellite viruses that affect animals and plants. However, *Sputnik virus* replication appears to impair the normal morphogenesis and production of *Mimivirus,* a process closer to true parasitism than to the previously known satellite viruses. From a biological view, the infection with *Sputnik virus* results in ~ 70% reduction of the cytopathic effect of the giant viruses in amoeba and leads to formation of some atypical viral forms, in a way never described for traditional satellite viruses [11,12]. This discovery led to the creation of the term "virophage", which means a virus able to 'infect' other viruses [11,12]. *Sputnik virus* is an icosahedral virus 50 nm in diameter and a genome of 18 kb, which contains a mosaic of genes related to bacteriophages, other viruses and amoebae. Its genome is circular double-stranded DNA that is hypothetically able to encode 21 proteins, some of which have no detectable homologues in current databases of nucleotide sequences [11,12].

Recently, we have isolated Rio Negro virophage associated with Samba virus, an APMV strain from the Brazilian Amazon [81]. Other described virophages are parasites of the giant viruses (phycodnaviruses and mimiviruses) [32] and might control the dynamics of Antarctic alga species. Mavirus is a virophage that parasitizes the giant *Cafeteria roenbergensis virus* [91]. On the basis of genetic homology, Mavirus likely represents an evolutionary link between double-stranded DNA viruses and Maverick/Polinton eukaryotic DNA transposons [91]. It has been shown that giant viruses may even have virophages inside their own mobile genetic elements. A 2013 study of the mobilome of *Lentille virus* revealed that a virophage, *Sputnik 2*, is part of this genetic element [14]. It was observed by FISH that the virus and its virophage replicate in the same viral factories and are detected in the cytoplasm of the host cell, suggesting that *Sputnik 2* was integrated into the *Lentille virus* genome [14]. This was confirmed by genome digestion of these viruses, followed by Southern blotting and 2D gel analysis. *Lentille virus* was sequenced on different platforms, and a sequence related to *Sputnik2* was integrated in its genome, thus suggesting that *Sputnik2* is a provirophage. These analyses also revealed that *Lentille virus* (and a small fraction of *Sputnik2*) contained an extrachromosomal DNA rich in CG that was called a transpoviron (an equivalent of transposon in viruses from our point of view), which can undergo recombination with *Sputnik2* and many other organisms [14]. Phylogenetic analysis of the virophages and related genetic elements is compatible with the concept of a network-like evolution in the virus world and emphasizes multiple evolutionary connections between bona fide viruses and other classes of capsid-less mobile elements. Thus, giant viruses appear to present a complex mobilome, which could contribute to gene exchanges that are common in these viruses. Further investigation of these elements will possibly lead to new discoveries, including novel classes of mobile elements, thanks to the diversity and complexity of giant viruses and their virophages [92].

Clinical significance

Hospitalized patients are a risk group for nosocomial infections, including those caused by amoeba-associated pneumonia agents [54,93]. APMV is a putative pneumonia agent and studies associating this virus with human pneumonia cases are still under investigation [51,54,55,94-97]. APMV genetic material (once) and antibodies against APMV have been detected in samples from patients who had pneumonia without any known cause (bacterial, viral or fungal); these patients came from different locations and were studied by different research groups, lending strength to the possible role of APMV as a pneumonia agent [54-57,98]. The genetic diversity among the *Mimiviridae* members needs to be considered when interpreting negative PCR tests in several studies because the diversity may have impaired detection of APMV-related DNA [29]. An animal model for mimivirus pneumonia studies has been proposed. When various routes of infection were tested, the intracardiac infection route induced pneumonia in C57/B6 mice [45]. Although this model does not exactly simulate the hypothetical natural route of mimivirus infection, it was possible to observe histopathological evidence of acute pneumonia, isolate the virus and detect antigens by indirect immunofluorescence assay [45].

The first studies in which a giant virus was successfully isolated from a human specimen were published in 2013 [50,52]. In a first study, a total of 196 samples from patients were collected in Tunisia between 2009 and 2010; virus was detected by the formation of plaques in monolayers of amoeba grown on agar plates [52]. The isolated virus (LBA111) was found in a sample obtained from a 72-year-old patient with pneumonia. Serology and real time PCR confirmed the presence of a giant virus in this

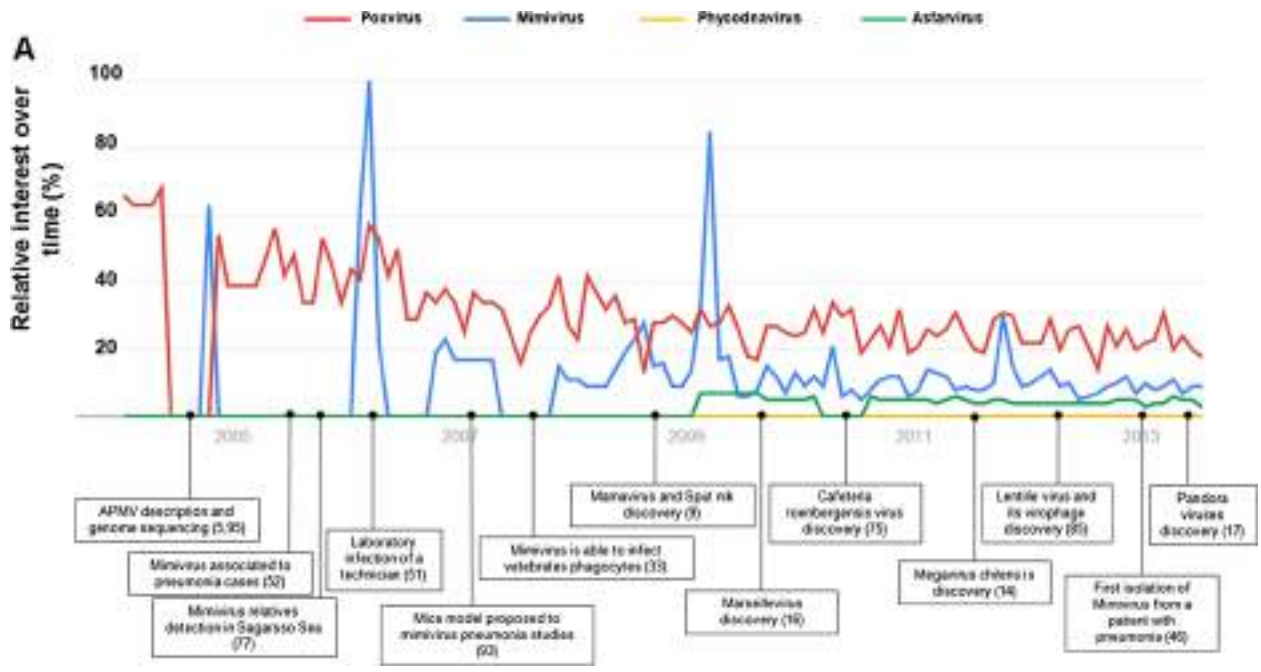

Figure 3 Timeline highlighting some hallmarks of mimivirus and related topics. Interest on the subject "Mimivirus", "Poxvirus", "Phycodnavirus" and "Asfarvirus" as a research terms in Google Search, over time. The incidence of the research for these subjects in Google Search was obtained by the use of Google Trends tool (http://www.google.com/trends/). The graphics depict relative interest over time (%). The values are in comparison to the highest number of searches at a given occasion (see "help" in Google Trends website). Google trends show available data since 2004. A timeline was set in the bottom of the figure, highlighting some hallmarks of mimivirus and related topics.

sample. LBA111 has a similar morphology to other mimiviruses, with a size of approximately 560 nm and a genome of 1,23 Mb. Western blot analysis showed positive immunoreactivity of patient sera against specific proteins of both APMV and LBA111 [52]. In another study, Shan virus was isolated from a stool sample collected from a Tunisian patient with pneumonia [50]. Metagenomic analysis of a human stool sample revealed the presence of sequences similar to those of giant viruses. From these samples, a virus was isolated and named Senegalvirus [53]. Its characteristics linked it to the *Marseilleviridae* family, representing the first detection of a marseillevirus from a human sample [53]. Additionally, a blood sample from an apparently healthy donor revealed the presence of Marseillevirus-like DNA; antigens from this virus were detected, it was visualized by microscopy and it grew in human T cell lymphocytes [46].

The potential clinical relevance of mimivirus can also be analyzed by studies involving the host-virus relationship. In 2008, it was observed that APMV is internalized by professional phagocytic cells such as macrophages, but not by non-phagocytic cells like fibroblasts, epithelial or neuronal cells [39]. This suggests that these professional phagocytic cells can be targets for APMV replication in humans. Analysis of 'infected' macrophages revealed that viral DNA

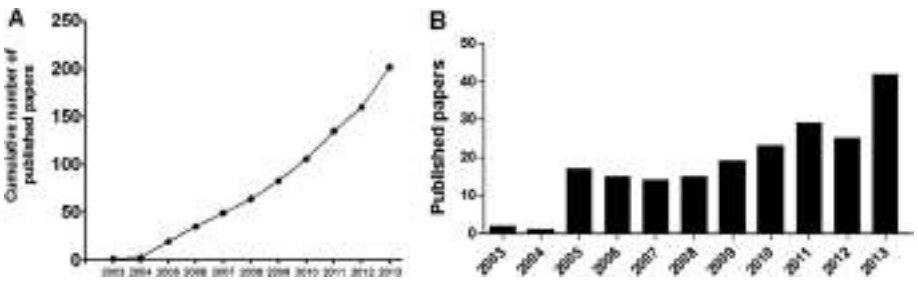

Figure 4 Cumulative number of publications relating to mimivirus and "mimivirus"/"giant viruses" over time since its discovery in 2003 (http://www.ncbi.nlm.nih.gov/pubmed)". (A) Cumulative number of publications relating to mimivirus over time. The subject was researched on Pubmed page (http://www.ncbi.nlm.nih.gov/pubmed), demonstrating the growing number of papers related to the virus since its discovery in 2003. **(B)** Published "mimivirus"/"giant viruses" papers per year since 2003, also according to the Pubmed website.

increased following infection, and APMV was seem as cytopathogenic for these cells [39]. Recently, a study investigated whether human peripheral blood mononuclear cells (PBMC) can recognize APMV presence by measuring IFN induction; whether APMV can replicate in these cells; and whether replication of the virus is affected by treatment of cells with IFN type I [49]. The results showed that APMV is able to replicate in human PBMC and induce type I IFN in these cells and that it inhibits some IFN-stimulated genes (ISG) by a mechanism that is independent of viroceptors and STAT dephosphorylation [49]. It was also seen that APMV is resistant to the antiviral action of IFN alpha2 (IFNA2), but is sensitive to the antiviral action of IFN beta (IFNB1). These results not only confirm that APMV can indeed replicate in vertebrate phagocytes but also show that it is recognized by the innate immune system and that it is likely able to at least partially evade that system [49]. This interaction is most likely the result of co-evolution between APMV and vertebrate hosts, and it is strong evidence of an ancestral relationship between these organisms [49]. Recently, mouse exposure to mimivirus collagens was shown to induce anti-collagen antibodies that also targeted mouse collagen type II, and the exposure was associated with T-cell reactivity to collagen and joint inflammation [99]. Furthermore, a serologic study found reactivities to the mimivirus collagen protein L71 in 22% of rheumatoid arthritis patients, compared to 6% of healthy-subjects. Thus, while clinical studies involving mimivirus are still a growing field, research over the past few years is strengthening the idea that mimiviruses, which are broadly distribution in our biosphere, not only have an environmental impact but are also involved in human health.

Viral resistance to chemical and physical biocides

The probable importance of APMV as a human pathogen in hospital environments has led to the need for investigating the virucidal activity of chemical biocides used for disinfection in hospitals. In a study performed in 2012, it was shown that APMV is especially resistant to alcohols but is sensitive to the action of active chlorine and glutaraldehyde, and it is able to remain stable on inanimate surfaces for 30 days, even in the absence of organic matter; this highlights the need for best strategies to control this putative pneumonia agent in hospital environments [69]. Amoebae, the hosts of several giant viruses, may act as biological platforms in the spread of pathogens such as *Legionella*, *Parachlamydia*, *Mycobacterium* and also APMV, representing a public health concern. In 2013 we investigated the APMV survival in certain adverse conditions when present in the intracellular environment of *A. castellanii* [100]. It was found that when APMV is inside an amoebal cell subjected to UV irradiation, heat or exposure to different chemical biocides, it remains more stable, showing that these hosts can act like natural bunkers for APMV, increasing its resistance to the viral agents used to disinfect hospital environments [100]. In addition, *Acanthamoeba* spp. may represent a training field for human pathogens, as several micro-organisms resisting these amoebae were concurrently found to resist human macrophages [40].

Giant viruses publication indicators

An indicator of the growth of related research fields concerning giant viruses is the recent increase in the number of publications about APMV and other giant viruses. In 2013, the number of papers related to these fields was 21-fold greater than to the number of papers published in 2003, the year of APMV discovery (Figures 3 and 4). Interest in APMV also increased in internet search tools such as Google Search (Google Trends) over the years, with peaks in 2004, 2006 and 2009 (Figure 3) that most likely are related to mimivirus research hallmarks, such as its discovery, its association to virophages and studies describing APMV as a putative pneumonia agent [5,11,57,73] (Figure 3). Currently, mimiviruses are the second group amongst NCLDVs most searched in the Google platform, and, on some occasions, even overcomes the well-known poxviruses (Figure 3).

Conclusions

As described, APMV and other giant viruses have emerged as a fascinating line of research. Each discovery regarding mimiviruses has overwhelmed scientists from different areas of expertise, which may explain why so many outstanding publications are multidisciplinary. The future of mimivirus studies might go beyond the description of bigger and more complex viruses but also may contemplate deep structural, genetic and evolutionary studies. With all this knowledge, we expect it will be possible to understand the exact role of mimiviruses in environmental dynamics and their importance as etiological agents of pneumonia in humans and other animals.

Competing interests

The authors declare that they have no competing interests.

Authors' contribution

JSA, FPD, LCS, GMA, PVB, PC, BS and EGK wrote the manuscript. PVB performed analysis in Google Trends and Pubmed. FPD performed electron microscopy analysis. JSA designed the figures. All authors read and approved the final manuscript.

Acknowledgments

We thank colleagues from Laboratório de Vírus and Aix-Marseille Université for their excellent support.

This study was supported by the Conselho Nacional de Desenvolvimento Científico e Tecnológico, Coordenação de Aperfeiçoamento de Pessoal de Nível Superior, the Fundação de Amparo à Pesquisa do Estado de Minas Gerais, Pro-Reitoria de Pesquisa da UFMG, and Centro de Microscopia da UFMG. E.G.K. is researcher of the Conselho Nacional de Desenvolvimento Científico e Tecnológico.

Author details
[1]Universidade Federal de Minas Gerais, Instituto de Ciências Biológicas, Laboratório de Vírus, Avenida Antônio Carlos, 6627, Caixa Postal 486, Bloco F4, Sala 258, 31270-901 Belo Horizonte, Minas Gerais, Brazil. [2]URMITE, UM63, CNRS 7278, IRD 198, Inserm 1095, Aix Marseille Universite, Marseille, France.

Received: 17 March 2014 Accepted: 16 June 2014
Published: 30 June 2014

References

1. Rohwer F, Prangishvili D, Lindell D: **Roles of viruses in the environment.** *Environ Microbiol* 2009, **11:**2771–2774.
2. Breitbart M, Miyake JH, Rohwer F: **Global distribution of nearly identical phage-encoded DNA sequences.** *FEMS Microbiol Lett* 2004, **236:**249–256.
3. Short CM, Suttle CA: **Nearly identical bacteriophage structural gene sequences are widely distributed in both marine and freshwater environments.** *Appl Environ Microbiol* 2005, **71:**480–486.
4. Van Etten JL, Lane LC, Dunigan DD: **DNA viruses: the really big ones (giruses).** *Annu Rev Microbiol* 2010, **64:**83–99.
5. La Scola B, Audic S, Robert C, Jungang L, de Lamballerie X, Drancourt M, Birtles R, Claverie JM, Raoult D: **A giant virus in amoebae.** *Science* 2003, **299:**2033.
6. Moreira D, Brochier-Armanet C: **Giant viruses, giant chimeras: the multiple evolutionary histories of Mimivirus genes.** *BMC Evol Biol* 2008, **8:**12.
7. Hingamp P, Grimsley N, Acinas SG, Clerissi C, Subirana L, Poulain J, Ferrera I, Sarmento H, Villar E, Lima-Mendez G, Faust K, Sunagawa S, Claverie JM, Moreau H, Desdevises Y, Bork P, Raes J, de Vargas C, Karsenti E, Kandels-Lewis S, Jaillon O, Not F, Pesant S, Wincker P, Ogata H: **Exploring nucleo-cytoplasmic large DNA viruses in Tara Oceans microbial metagenomes.** *ISME J* 2013, **7:**1678–1695.
8. Kroon EG, Mota BE, Abrahao JS, da Fonseca FG, de Souza Trindade G: **Zoonotic Brazilian Vaccinia virus: from field to therapy.** *Antiviral Res* 2011, **92:**150–163.
9. Claverie JM, Abergel C: **Mimivirus: the emerging paradox of quasi-autonomous viruses.** *Trends Genet* 2010, **26:**431–437.
10. Claverie JM, Abergel C, Ogata H: **Mimivirus.** *Curr Top Microbiol Immunol* 2009, **328:**89–121.
11. La Scola B, Desnues C, Pagnier I, Robert C, Barrassi L, Fournous G, Merchat M, Suzan-Monti M, Forterre P, Koonin E, Raoult D: **The virophage as a unique parasite of the giant mimivirus.** *Nature* 2008, **455:**100–104.
12. Desnues C, Raoult D: **Inside the lifestyle of the virophage.** *Intervirology* 2010, **53:**293–303.
13. Arslan D, Legendre M, Seltzer V, Abergel C, Claverie JM: **Distant Mimivirus relative with a larger genome highlights the fundamental features of Megaviridae.** *Proc Natl Acad Sci U S A* 2011, **108:**17486–17491.
14. Desnues C, La Scola B, Yutin N, Fournous G, Robert C, Azza S, Jardot P, Monteil S, Campocasso A, Koonin EV, Raoult D: **Provirophages and transpovirons as the diverse mobilome of giant viruses.** *Proc Natl Acad Sci U S A* 2012, **109:**18078–18083.
15. Yoosuf N, Yutin N, Colson P, Shabalina SA, Pagnier I, Robert C, Azza S, Klose T, Wong J, Rossmann MG, La Scola B, Raoult D, Koonin E: **Related giant viruses in distant locations and different habitats: Acanthamoeba polyphaga moumouvirus represents a third lineage of the Mimiviridae that is close to the megavirus lineage.** *Genome Biol Evol* 2012, **4:**1324–1330.
16. Boughalmi M, Pagnier I, Aherfi S, Colson P, Raoult D, La Scola B: **First isolation of a giant virus from wild Hirudo medicinalis leech: Mimiviridae isolation in Hirudo medicinalis.** *Viruses* 2013, **5:**2920–2930.
17. Yoosuf N, Pagnier I, Fournous G, Robert C, La Scola B, Raoult D, Colson P: **Complete genome sequence of Courdo11 virus, a member of the family Mimiviridae.** *Virus Genes* 2014, **48:**218–223.
18. Boyer M, Yutin N, Pagnier I, Barrassi L, Fournous G, Espinosa L, Robert C, Azza S, Sun S, Rossmann MG, Suzan-Monti M, La Scola B, Koonin EV, Raoult D: **Giant Marseillevirus highlights the role of amoebae as a melting pot in emergence of chimeric microorganisms.** *Proc Natl Acad Sci U S A* 2009, **106:**21848–21853.
19. Philippe N, Legendre M, Doutre G, Coute Y, Poirot O, Lescot M, Arslan D, Seltzer V, Bertaux L, Bruley C, Garin J, Claverie JM, Abergel C: **Pandoraviruses: amoeba viruses with genomes up to 2.5 Mb reaching that of parasitic eukaryotes.** *Science* 2013, **341:**281–286.
20. Legendre M, Bartoli J, Shmakova L, Jeudy S, Labadie K, Adrait A, Lescot M, Poirot O, Bertaux L, Bruley C, Couté Y, Rivkina E, Abergel C, Claverie J: **Thirty-thousand-year-old distant relative of giant icosahedral DNA viruses with a pandoravirus morphology.** *Proc Natl Acad Sci U S A* 2014, **111:**4274–4279.
21. Iyer LM, Aravind L, Koonin EV: **Common origin of four diverse families of large eukaryotic DNA viruses.** *J Virol* 2001, **75:**11720–11734.
22. Colson P, Gimenez G, Boyer M, Fournous G, Raoult D: **The giant Cafeteria roenbergensis virus that infects a widespread marine phagocytic protist is a new member of the fourth domain of Life.** *PLoS One* 2011, **6:**e18935.
23. Desnues C, Boyer M, Raoult D: **Sputnik, a virophage infecting the viral domain of life.** *Adv Virus Res* 2012, **82:**63–89.
24. Colson P, de Lamballerie X, Fournous G, Raoult D: **Reclassification of giant viruses composing a fourth domain of life in the new order Megavirales.** *Intervirology* 2012, **55:**321–332.
25. Nasir A, Kim KM, Caetano-Anolles G: **Giant viruses coexisted with the cellular ancestors and represent a distinct supergroup along with superkingdoms Archaea, Bacteria and Eukarya.** *BMC Evol Biol* 2012, **12:**156.
26. Boyer M, Madoui MA, Gimenez G, La Scola B, Raoult D: **Phylogenetic and phyletic studies of informational genes in genomes highlight existence of a 4 domain of life including giant viruses.** *PLoS One* 2010, **5:**e15530.
27. Colson P, De Lamballerie X, Yutin N, Asgari S, Bigot Y, Bideshi DK, Cheng XW, Federici BA, Van Etten JL, Koonin EV, La Scola B, Raoult D: **"Megavirales", a proposed new order for eukaryotic nucleocytoplasmic large DNA viruses.** *Arch Virol* 2013, **158:**2517–2521.
28. Colson P, Pagnier I, Yoosuf N, Fournous G, La Scola B, Raoult D: **"Marseilleviridae", a new family of giant viruses infecting amoebae.** *Arch Virol* 2013, **158:**915–920.
29. Yutin N, Koonin EV: **Hidden evolutionary complexity of Nucleo-Cytoplasmic Large DNA viruses of eukaryotes.** *Virol J* 2012, **9:**161.
30. Yutin N, Koonin EV: **Evolution of DNA ligases of nucleo-cytoplasmic large DNA viruses of eukaryotes: a case of hidden complexity.** *Biol Direct* 2009, **4:**51.
31. La Scola B, Campocasso A, N'Dong R, Fournous G, Barrassi L, Flaudrops C, Raoult D: **Tentative characterization of new environmental giant viruses by MALDI-TOF mass spectrometry.** *Intervirology* 2010, **53:**344–353.
32. Yutin N, Colson P, Raoult D, Koonin EV: **Mimiviridae: clusters of orthologous genes, reconstruction of gene repertoire evolution and proposed expansion of the giant virus family.** *Virol J* 2013, **10:**106.
33. Pagnier I, Reteno DG, Saadi H, Boughalmi M, Gaia M, Slimani M, Ngounga T, Bekliz M, Colson P, Raoult D, La Scola B: **A decade of improvements in Mimiviridae and Marseilleviridae isolation from amoeba.** *Intervirology* 2013, **56:**354–363.
34. Marciano-Cabral F, Cabral G: **Acanthamoeba spp. as agents of disease in humans.** *Clin Microbiol Rev* 2003, **16:**273–307.
35. Costa AO, Castro EA, Ferreira GA, Furst C, Crozeta MA, Thomaz-Soccol V: **Characterization of acanthamoeba isolates from dust of a public hospital in Curitiba, Parana, Brazil.** *J Eukaryot Microbiol* 2010, **57:**70–75.
36. Rohr U, Weber S, Michel R, Selenka F, Wilhelm M: **Comparison of free-living amoebae in hot water systems of hospitals with isolates from moist sanitary areas by identifying genera and determining temperature tolerance.** *Appl Environ Microbiol* 1998, **64:**1822–1824.
37. Coulon C, Collignon A, McDonnell G, Thomas V: **Resistance of Acanthamoeba cysts to disinfection treatments used in health care settings.** *J Clin Microbiol* 2010, **48:**2689–2697.
38. Visvesvara GS: **Infections with free-living amebae.** *Handb Clin Neurol* 2013, **114:**153–168.
39. Ghigo E, Kartenbeck J, Lien P, Pelkmans L, Capo C, Mege JL, Raoult D: **Ameobal pathogen mimivirus infects macrophages through phagocytosis.** *PLoS Pathog* 2008, **4:**e1000087.
40. Greub G, Raoult D: **Microorganisms resistant to free-living amoebae.** *Clin Microbiol Rev* 2004, **17:**413–433.
41. Kilvington S, Price J: **Survival of Legionella pneumophila within cysts of Acanthamoeba polyphaga following chlorine exposure.** *J Appl Bacteriol* 1990, **68:**519–525.
42. Matsuo J, Hayashi Y, Nakamura S, Sato M, Mizutani Y, Asaka M, Yamaguchi H: **Novel Parachlamydia acanthamoebae quantification method based on coculture with amoebae.** *Appl Environ Microbiol* 2008, **74:**6397–6404.
43. Harriff M, Bermudez LE: **Environmental amoebae and mycobacterial pathogenesis.** *Methods Mol Biol* 2009, **465:**433–442.
44. Claverie JM, Grzela R, Lartigue A, Bernadac A, Nitsche S, Vacelet J, Ogata H, Abergel C: **Mimivirus and Mimiviridae: giant viruses with an increasing**

number of potential hosts, including corals and sponges. *J Invertebr Pathol* 2009, **101:**172–180.
45. Khan M, La Scola B, Lepidi H, Raoult D: **Pneumonia in mice inoculated experimentally with Acanthamoeba polyphaga mimivirus.** *Microb Pathog* 2007, **42:**56–61.
46. Popgeorgiev N, Boyer M, Fancello L, Monteil S, Robert C, Rivet R, Nappez C, Azza S, Chiaroni J, Raoult D, Desnues C: **Marseillevirus-like virus recovered from blood donated by asymptomatic humans.** *J Infect Dis* 2013, **208:**1042–1050.
47. Hoffmann B, Scheuch M, Hoper D, Jungblut R, Holsteg M, Schirrmeier H, Eschbaumer M, Goller KV, Wernike K, Fischer M, Breithaupt A, Mettenleiter TC, Beer M: **Novel orthobunyavirus in Cattle, Europe, 2011.** *Emerg Infect Dis* 2012, **18:**469–472.
48. Dornas FP, Rodrigues FP, Boratto PV, Silva LC, Ferreira PC, Bonjardim CA, Trindade GS, Kroon EG, La Scola B, Abrahao JS: **Mimivirus Circulation among Wild and Domestic Mammals, Amazon Region, Brazil.** *Emerg Infect Dis* 2014, **20:**469–472.
49. Silva LC, Almeida GM, Oliveira DB, Dornas FP, Campos RK, La Scola B, Ferreira PC, Kroon EG, Abrahao JS: **A resourceful giant: APMV is able to interfere with the human type I interferon system.** *Microbes Infect* 2013, **16:**187–195.
50. Saadi H, Reteno DG, Colson P, Aherfi S, Minodier P, Pagnier I, Raoult D, La Scola B: **Shan virus: a new mimivirus isolated from the stool of a Tunisian patient with pneumonia.** *Intervirology* 2013, **56:**424–429.
51. Colson P, La Scola B, Raoult D: **Giant viruses of amoebae as potential human pathogens.** *Intervirology* 2013, **56:**376–385.
52. Saadi H, Pagnier I, Colson P, Cherif JK, Beji M, Boughalmi M, Azza S, Armstrong N, Robert C, Fournous G, La Scola B, Raoult D: **First isolation of Mimivirus in a patient with pneumonia.** *Clin Infect Dis* 2013, **57:**e127–e134.
53. Colson P, Fancello L, Gimenez G, Armougom F, Desnues C, Fournous G, Yoosuf N, Million M, La Scola B, Raoult D: **Evidence of the megavirome in humans.** *J Clin Virol* 2013, **57:**191–200.
54. Bousbia S, Papazian L, Saux P, Forel JM, Auffray JP, Martin C, Raoult D, La Scola B: **Serologic prevalence of amoeba-associated microorganisms in intensive care unit pneumonia patients.** *PLoS One* 2013, **8:**e58111.
55. Vincent A, La Scola B, Forel JM, Pauly V, Raoult D, Papazian L: **Clinical significance of a positive serology for mimivirus in patients presenting a suspicion of ventilator-associated pneumonia.** *Crit Care Med* 2009, **37:**111–118.
56. Raoult D, Renesto P, Brouqui P: **Laboratory infection of a technician by mimivirus.** *Ann Intern Med* 2006, **144:**702–703.
57. La Scola B, Marrie TJ, Auffray JP, Raoult D: **Mimivirus in pneumonia patients.** *Emerg Infect Dis* 2005, **11:**449–452.
58. Azza S, Cambillau C, Raoult D, Suzan-Monti M: **Revised Mimivirus major capsid protein sequence reveals intron-containing gene structure and extra domain.** *BMC Mol Biol* 2009, **10:**39.
59. McPherson A, Kuznetsov YG: **Atomic force microscopy investigation of viruses.** *Methods Mol Biol* 2011, **736:**171–195.
60. Klose T, Kuznetsov YG, Xiao C, Sun S, McPherson A, Rossmann MG: **The three-dimensional structure of Mimivirus.** *Intervirology* 2010, **53:**268–273.
61. Claverie JM, Abergel C: **Mimivirus and its virophage.** *Annu Rev Genet* 2009, **43:**49–66.
62. Mutsafi Y, Shimoni E, Shimon A, Minsky A: **Membrane assembly during the infection cycle of the giant Mimivirus.** *PLoS Pathog* 2013, **9:**e1003367.
63. Xiao C, Kuznetsov YG, Sun S, Hafenstein SL, Kostyuchenko VA, Chipman PR, Suzan-Monti M, Raoult D, McPherson A, Rossmann MG: **Structural studies of the giant mimivirus.** *PLoS Biol* 2009, **7:**e92.
64. Zauberman N, Mutsafi Y, Halevy DB, Shimoni E, Klein E, Xiao C, Sun S, Minsky A: **Distinct DNA exit and packaging portals in the virus Acanthamoeba polyphaga mimivirus.** *PLoS Biol* 2008, **6:**e114.
65. Dornas FP, Silva LC, de Almeida GM, Campos RK, Boratto PV, Franco-Luiz AP, La Scola B, Ferreira PC, Kroon EG, Abrahao JS: **Acanthamoeba polyphaga mimivirus stability in environmental and clinical substrates: implications for virus detection and isolation.** *PLoS One* 2014, **9:**e87811.
66. Campos RK, Andrade KR, Ferreira PC, Bonjardim CA, La Scola B, Kroon EG, Abrahao JS: **Virucidal activity of chemical biocides against mimivirus, a putative pneumonia agent.** *J Clin Virol* 2012, **55:**323–328.
67. Slimani M, Pagnier I, Boughalmi M, Raoult D, La Scola B: **Alcohol disinfection procedure for isolating giant viruses from contaminated samples.** *Intervirology* 2013, **56:**434–440.
68. Legendre M, Santini S, Rico A, Abergel C, Claverie JM: **Breaking the 1000-gene barrier for Mimivirus using ultra-deep genome and transcriptome sequencing.** *Virol J* 2011, **8:**99.
69. Colson P, Raoult D: **Gene repertoire of amoeba-associated giant viruses.** *Intervirology* 2010, **53:**330–343.
70. Renesto P, Abergel C, Decloquement P, Moinier D, Azza S, Ogata H, Fourquet P, Gorvel JP, Claverie JM: **Mimivirus giant particles incorporate a large fraction of anonymous and unique gene products.** *J Virol* 2006, **80:**11678–11685.
71. Saini HK, Fischer D: **Structural and functional insights into Mimivirus ORFans.** *BMC Genomics* 2007, **8:**115.
72. Hakim M, Ezerina D, Alon A, Vonshak O, Fass D: **Exploring ORFan domains in giant viruses: structure of mimivirus sulfhydryl oxidase R596.** *PLoS One* 2012, **7:**e50649.
73. Raoult D, Audic S, Robert C, Abergel C, Renesto P, Ogata H, La Scola B, Suzan M, Claverie JM: **The 1.2-megabase genome sequence of Mimivirus.** *Science* 2004, **306:**1344–1350.
74. Abergel C, Rudinger-Thirion J, Giege R, Claverie JM: **Virus-encoded aminoacyl-tRNA synthetases: structural and functional characterization of mimivirus TyrRS and MetRS.** *J Virol* 2007, **81:**12406–12417.
75. Colson P, Fournous G, Diene SM, Raoult D: **Codon usage, amino acid usage, transfer RNA and amino-acyl-tRNA synthetases in Mimiviruses.** *Intervirology* 2013, **56:**364–375.
76. Boyer M, Azza S, Barrassi L, Klose T, Campocasso A, Pagnier I, Fournous G, Borg A, Robert C, Zhang X, Desnues C, Henrissat B, Rossmann MG, La Scola B, Raoult D: **Mimivirus shows dramatic genome reduction after intraamoebal culture.** *Proc Natl Acad Sci U S A* 2011, **108:**10296–10301.
77. Colson P, Raoult D: **Lamarckian evolution of the giant Mimivirus in allopatric laboratory culture on amoebae.** *Front Cell Infect Microbiol* 2012, **2:**91.
78. Mutsafi Y, Zauberman N, Sabanay I, Minsky A: **Vaccinia-like cytoplasmic replication of the giant Mimivirus.** *Proc Natl Acad Sci U S A* 2010, **107:**5978–5982.
79. Kuznetsov YG, Klose T, Rossmann M, McPherson A: **Morphogenesis of mimivirus and its viral factories: an atomic force microscopy study of infected cells.** *J Virol* 2013, **87:**11200–11213.
80. Suhre K, Audic S, Claverie JM: **Mimivirus gene promoters exhibit an unprecedented conservation among all eukaryotes.** *Proc Natl Acad Sci U S A* 2005, **102:**14689–14693.
81. Campos RK, Boratto PV, Assis FL, Aguiar ERGR, Silva LCF, Albarnaz JD, Dornas FP, Trindade GS, Ferreira PCP, Marques JT, Roberts C, Raoult D, Kroon EG, La Scola B, Abrahao JS: **Samba virus: a novel mimivirus from a giant rain forest, the Brazilian Amazon.** *Virol J* 2014, **11:**95.
82. Dai W, Fu C, Raytcheva D, Flanagan J, Khant HA, Liu X, Rochat RH, Haase-Pettingell C, Piret J, Ludtke SJ, Nagayama K, Schmid MF, King JA, Chiu W: **Visualizing virus assembly intermediates inside marine cyanobacteria.** *Nature* 2013, **502:**707–710.
83. Sheik AR, Brussaard CP, Lavik G, Lam P, Musat N, Krupke A, Littmann S, Strous M, Kuypers MM: **Responses of the coastal bacterial community to viral infection of the algae Phaeocystis globosa.** *ISME J* 2014, **8:**212–225.
84. Fischer MG, Allen MJ, Wilson WH, Suttle CA: **Giant virus with a remarkable complement of genes infects marine zooplankton.** *Proc Natl Acad Sci U S A* 2010, **107:**19508–19513.
85. Monier A, Larsen JB, Sandaa RA, Bratbak G, Claverie JM, Ogata H: **Marine mimivirus relatives are probably large algal viruses.** *Virol J* 2008, **5:**12.
86. Ghedin E, Claverie JM: **Mimivirus relatives in the Sargasso sea.** *Virol J* 2005, **2:**62.
87. Claverie JM: **Giant virus in the sea: Extending the realm of Megaviridae to Viridiplantae.** *Commun Integr Biol* 2013, **6:**e25685.
88. Williams TA, Embley TM, Heinz E: **Informational gene phylogenies do not support a fourth domain of life for nucleocytoplasmic large DNA viruses.** *PLoS One* 2011, **6:**e21080.
89. Piacente F, Marin M, Molinaro A, De Castro C, Seltzer V, Salis A, Damonte G, Bernardi C, Claverie JM, Abergel C, Tonetti M: **Giant DNA virus mimivirus encodes pathway for biosynthesis of unusual sugar 4-amino-4,6-dideoxy-D-glucose (Viosamine).** *J Biol Chem* 2012, **287:**3009–3018.
90. Luther KB, Hulsmeier AJ, Schegg B, Deuber SA, Raoult D, Hennet T: **Mimivirus collagen is modified by bifunctional lysyl hydroxylase and glycosyltransferase enzyme.** *J Biol Chem* 2011, **286:**43701–43709.
91. Fischer MG, Suttle CA: **A virophage at the origin of large DNA transposons.** *Science* 2011, **332:**231–234.

92. Yutin N, Raoult D, Koonin EV: **Virophages, polintons, and transpovirons: a complex evolutionary network of diverse selfish genetic elements with different reproduction strategies.** *Virol J* 2013, **10:**158.
93. Turner P, Turner C, Watthanaworawit W, Carrara V, Cicelia N, Deglise C, Phares C, Ortega L, Nosten F: **Respiratory virus surveillance in hospitalised pneumonia patients on the Thailand-Myanmar border.** *BMC Infect Dis* 2013, **13:**434.
94. Marrie TJ, Costain N, La Scola B, Patrick W, Forgie S, Xu Z, McNeil SA: **The role of atypical pathogens in community-acquired pneumonia.** *Semin Respir Crit Care Med* 2012, **33:**244–256.
95. Vanspauwen MJ, Schnabel RM, Bruggeman CA, Drent M, van Mook WN, Bergmans DC, Linssen CF: **Mimivirus is not a frequent cause of ventilator-associated pneumonia in critically ill patients.** *J Med Virol* 2013, **85:**1836–1841.
96. Dare RK, Chittaganpitch M, Erdman DD: **Screening pneumonia patients for mimivirus.** *Emerg Infect Dis* 2008, **14:**465–467.
97. Costa C, Bergallo M, Astegiano S, Terlizzi ME, Sidoti F, Solidoro P, Cavallo R: **Detection of Mimivirus in bronchoalveolar lavage of ventilated and nonventilated patients.** *Intervirology* 2012, **55:**303–305.
98. Vanspauwen MJ, Franssen FM, Raoult D, Wouters EF, Bruggeman CA, Linssen CF: **Infections with mimivirus in patients with chronic obstructive pulmonary disease.** *Respir Med* 2012, **106:**1690–1694.
99. Shah N, Hulsmeier AJ, Hochhold N, Neidhart M, Gay S, Hennet T: **Exposure to mimivirus collagen promotes arthritis.** *J Virol* 2014, **88:**838–845.
100. Boratto PV, Dornas FP, Andrade KR, Rodrigues R, Peixoto F, Silva LC, La Scola B, Costa AO, de Almeida GM, Kroon EG, Abrahao JS: **Amoebas as mimivirus bunkers: increased resistance to UV light, heat and chemical biocides when viruses are carried by amoeba hosts.** *Arch Virol* 2013, **159:**1039–1043.

doi:10.1186/1743-422X-11-120
Cite this article as: Abrahão *et al.*: *Acanthamoeba polyphaga mimivirus* and other giant viruses: an open field to outstanding discoveries. *Virology Journal* 2014 **11**:120.

Mimiviruses: Replication, Purification, and Quantification

Article *in* Current protocols in microbiology · May 2016

DOI: 10.1002/cpmc.2

6 authors, including:

Jônatas S Abrahão
Federal University of Minas Gerais
153 PUBLICATIONS **883** CITATIONS
SEE PROFILE

Lorena C F Silva
Federal University of Minas Gerais
11 PUBLICATIONS **126** CITATIONS
SEE PROFILE

Ludmila Silva
Federal University of Minas Gerais
6 PUBLICATIONS **24** CITATIONS
SEE PROFILE

Marcelo Xavier
Federal University of Minas Gerais
56 PUBLICATIONS **136** CITATIONS
SEE PROFILE

CURRENT PROTOCOLS
The Fine Art of Experimentation

Mimiviruses: Replication, Purification and Quantification.

Jônatas Santos Abrahão
Instituto de Ciências Biológicas, Departamento de Microbiologia, Laboratório de Vírus, Universidade Federal de Minas Gerais, Belo Horizonte-Minas Gerais, Brazil- (55)3134093002.
jonatas.abrahao@gmail.com

Graziele Pereira Oliveira
Instituto de Ciências Biológicas, Departamento de Microbiologia, Laboratório de Vírus, Universidade Federal de Minas Gerais, Belo Horizonte-Minas Gerais, Brazil- (55)3134093002.
graziufmg@yahoo.com.br

Lorena Christine Ferreira da Silva
Instituto de Ciências Biológicas, Departamento de Microbiologia, Laboratório de Vírus, Universidade Federal de Minas Gerais, Belo Horizonte-Minas Gerais, Brazil- (55)3134093002.
lorena.farmacia@yahoo.com.br

Ludmila Karen dos Santos Silva
Instituto de Ciências Biológicas, Departamento de Microbiologia, Laboratório de Vírus, Universidade Federal de Minas Gerais, Belo Horizonte-Minas Gerais, Brazil- (55)3134093002.
(ludmilakaren@gmail.com)

Erna Geessien Kroon
Instituto de Ciências Biológicas, Departamento de Microbiologia, Laboratório de Vírus, Universidade Federal de Minas Gerais, Belo Horizonte-Minas Gerais, Brazil- (55)3134093002.
(kroone@icb.ufmg.br)

Bernard La Scola
[2]Unité de Recherche sur les Maladies Infectieuses et Tropicales Emergentes (URMITE) UM63 CNRS 7278 IRD 198 INSERM U1095, Aix-Marseille Univ., 13385 Marseille, France.(bernard.lascola@univ-amu.fr)

ABSTRACT

The aim of this protocol is to describe the replication, purification and titration of mimiviruses. These viruses belong to the *Mimiviridae* family and its first member was isolated in 1992 from a cooling tower water sample collected during an outbreak of pneumonia in a hospital in Bradford, England. In recent years, several new mimivirus have been isolated from different environmental conditions. These giant viruses are easily replicated in amoeba of the *Acanthamoeba* genus, its natural host. mimiviruses present peculiar features that make them unique viruses such as the particle and genome size and its complexity. The discovery of these viruses rekindled discussions about its origin and evolution and the genetic and structural complexity opened a new field of study. Here we describe some methods utilized for mimiviruses replication, purification and titration.

Keywords: Mimiviruses; replication; purification; titration.

INTRODUCTION

Mimiviruses are a group of giant viruses recently discovered that are worldwide distributed infecting amoeba of the *Acanthamoeba* genus and has been related to infections in a number of vertebrates. The first *Mimivirus* was isolated from a cooling tower water sample collected in a hospital in Bradford, England, during an outbreak of pneumonia in 1992 (La Scola et al., 2003). This isolate was named *Acanthamoeba polyphaga mimivirus* (APMV) and due to its unique morphological and molecular features it was included in a new viral family denominated *Mimiviridae*. The family *Mimiviridae* contains two genera: *Mimivirus* and *Cafeteriavirus* [International Committee on Taxonomy of Viruses(ICTV), 2014]. Mimiviruses present peculiar features that make them unique viruses. One of most notable characteristic is its 700 nm diameter sized particles, which is related to their retention on 0,2 µm filters, that are commonly used in viruses studies. The mimivirus particles are constituted of a core, an inner membrane, a capsid with semi-icosahedral symmetry and external fibrils (Xiao et al.,2005). Members of the *Mimiviridae* family are composed of double-

stranded DNA genome of approximately 1.2 Mb that encodes more than 900 proteins, there by surpassing the coding capacity of some bacteria (La Scola et al., 2003; Raoult et al., 2004; Moreira et al., 2008).

The *Mimiviridae* family was grouped with other families of giant virus known as nucleocytoplasmic large DNA viruses (NCLDVs) which includes *Poxviridae, Asfarviridae , Iridoviridae , Ascoviridae , Phycodnaviridae, and Marseilleviridae ,* leading the proposition of the putative order " Megavirales" to group these families (Arslan et al.,2011). In addition, phylogenetic studies resulted in an exclusive clade for the giant viruses, distinct from Eukarya, Bacteria and Archaea generating the proposition of a fourth domain of life composed by the giant virus (Boyer et al., 2010).

Due to unique structure and genetic complexity of the mimiviruses, a new field of study was opened, and subsequently, rekindled several debates regarding the definition of the viruses, evolution and origin (Raoult et al., 2008; Yamada et al.,2011).

Amoebae of the *Acanthamoeba* genus is the natural host of mimiviruses (La Scola et al., 2003). The APMV was first isolated from *A. polyphaga* culture, but it is also able to replicate in *A. castelannii*, *A. griffin*, *A. lenticulata* and *A. quina* (La Scola et al., 2003, Claverie et al., 2009). Nevertheless, there is an increasing evidence that these viruses have a wider host range, since APMV is internalized by different phagocyte cells (including human cells) and it has been shown that this virus can interact with the human interferon system (Ghigo et al.,2008; Silva et al., 2013). The mimivirus DNA has been detected in monkeys and bovines (Dornas et al., 2014). A number of studies proposed that APMV could be pathogenic to humans and mice and described the presence of antibodies against mimivirus in patients with nosocomial pneumonia (Raoult et al., 2006 ; Khan et al., 2007; Bousbia et al., 2013) Furthermore, mimiviruses have been isolated from samples collected from patients with pneumonia (Colson et al., 2013, Saadi et al.,2013). It was also found that environmental exposure to mimivirus represents a risk factor in triggering autoimmunity to collagens (Shah et al.,2013).

Viruses belonging to the *Mimiviridae* family have been isolated from environments such as soil, air, aquatic environments, sewage treatment

systems, hospital environments, and systems of ventilation and air conditioning, suggesting that they represent an ubiquitous group. The isolation reports occurred in England, France, Tunisia, EUA, Chile and Brazil and also from oceans (La Scola et al., 2003; Arslan et al., 2011; Legendre et al., 2012; Boughalmi et al.,2012; Campos et al., 2014; Andrade et al., 2015; Santos Silva et al., 2015). Furthermore a metagenomic study showed the presence of mimivirus DNA in Sargasso Sea and other oceanic samples. (Ghedin et al.,2005; Monier et al.,2008; Williamson et al., 2012; Yamada et al., 2011). Mimivirus and other giant viruses are an outstanding research field, and the rate of publications related to this viruses has increased since its discovery (Abrahão et al.,2014).

This unit describes the methods utilized for replication (Basic Protocol 1), purification (Basic Protocol 2) and titration (Basic Protocol 3) of mimivirus. Furthermore, it provides a procedure for *Acanthamoeba* cells maintenance (Support Protocol 1). Although there is an evidence of mimivirus replication in phagocyte human cells (Ghigo et al., 2008; Silva et al., 2013), the *Acanthamoeba sp* cell, mainly *Acanthamoeba castelaniiI,* are the preferred choice of mimiviruses replication in laboratory. The mimivirus purification is performed by sucrose cushion that are successfully used to increase the viral titer by concentrate the viral stock and remove the non-viral elements. Although sucrose gradient methodology is commonly used for virus purification, for most biological and molecular experiments involving Mimivirus this level of purification and titer obtained by sucrose cushion at 24% is sufficient. Although it is possible to titrate mimivirus by plaque forming units assay (depending on *Acanthamoeba* strain used), here we describe an end-point dilution assay.

CAUTION:

Mimiviruses has been studied for a few years and many of its relations with the environment and other hosts remain unclear. Furthermore, mimiviruses were initially associated with outbreaks of pneumonia and several studies reinforced the hypothesis of its clinical relevance. Although the role of mimivirus as etiological agents of pneumonia is still under investigation it is recommended that assays will be done using a class II biological safety cabinet. Besides, it is

important inactivate the viruses by autoclavation of lab material containing viral residues by before they will be discarded. To clean the working area a 70% ethanol solution can be used. Amoebae of the *Acanthamoeba* genus are the platform of the mimivirus propagation and titration. Although ubiquitous these protists can cause opportunistic infections. So it is important to take care such as not use contact lenses when handling these amoebas (Marciano-Cabral *et al*., 2003). Despite the mimivirus particles are very stable in environmental and clinical substrates (Dornas et al., 2014), it is recommended to keep the virus solutions in ice while working. Although mimivirus particle is very stable when stored at −20◦C, we recommend stored the purified virus stock at −80◦C to avoid viral titer decrease

BASIC PROTOCOL 1

Mimivirus replication

Mimivirus can be replicated in large amounts of *Acanthamoeba* sp culture to increase the virus stock. Mimivirus should be replicated in *Acanthamoeba* sp culture flasks cultivated in peptone-yeast extract-glucose (PYG) medium. This medium revealed to be efficient to mimivirus replication and it yielded approximately 6 logarithmical units higher titer as compared to replication made in Page's amoeba saline (PAS) (Abrahão et al., 2014). This protocol describes mimivirus replication on *Acanthamoeba castellanii* culture. However, this protocol can be applied to replicate mimivirus in other amoeba species, such as *Acanthamoeba polyphaga*. After reaching confluence, the amoebas should be infected and incubated at 28°C until induce cytopathic effects (CPE), as amoebae rounding, loss of motility and lysis. To obtain an efficient mimivirus replication a multiplicity of infection (MOI) of 0.01 is recommended since low MOIs produce higher viral titers as compared to high MOIs (Abrahão J.S., 2014). Supernatants from the infected amoebas should be collected and

submitted to three cycles of freezing and thawing to release viruses from cells (Basic Protocol 2).

It is recommended that the procedure should be performed using sterile materials in a Class II Biosafety cabin.

Acanthamoeba castellanii cells can be obtained from the American Type Culture Collection (ATCC) (ATCC 30234 and ATCC 30010).

Materials

Viral samples to be replicated previously titered (seed pool) (see Basic Protocol 3)

Acanthamoeba castellanii culture grown in tissue culture flasks (see Support Protocol 1)

Peptone-yeast extract-glucose (PYG) medium (see recipes)

Phosphate-buffered saline (PBS)(see recipe)

Incubator (28-32◦C)

Refrigerated low-speed table-top centrifuge

50mL- Conical centrifuge tubes

Pipette

Micropipette

Pipettor

Tips

Tube racks

Glassware

1.5mL microcentrifuge tubes

37◦C water bath

Inverted microscope

Mimivirus replication in *Acanthamoeba sp* culture

1. Add 7X10^6 *A.castellanii* cells in 150-cm^2 cell culture flasks using PYG medium (see Support Protocol 1).

   For biological assays, a total of six 150-cm^2 cell culture flasks is enough to mimivirus replication. However, the number of culture flasks can be increased according to the necessity (e.g. production of virus for genome sequencing usually requires about 20 flasks).

2. Incubate at 28◦C for 30 minutes to adhere the cells

   The cell culture flasks can be prepared 24hrs before infection. In this case 150-cm^2 cell culture flasks should be prepared by seeding 3 × 10^6 A. castellanii per 150-cm^2 cell culture flasks in 25mL PYG medium and before the infection cells should be counted to calculate the MOI.

3. Inoculate the viral samples to be replicated diluted in phosphate-buffered saline **(**PBS) at multiplicity MOI of 0,01.

   Low MOIs produce higher titers of infectious particles than high MOIs, since high MOIs may be related to a higher rate of defective particle formation.

4. Incubate at 28 ◦C for approximately 72 hrs.

   Check cells every day under the microscope to verify CPE (see figure 1).

5. Collect the supernatant and cell lysates when presenting approximately 80%-90% of CPE.

   Typically, at MOI of 0,01, 48 hours after infection all the cells show rounding and 72 hours after infection, 90% or more of the cells presented cell lysis and the most the cells have detached from the monolayer and lysed (see figure 1).

6. Submit the infected cells to three cycles of freezing and thawing to release virus.

To make the process faster freezing can be performed in liquid nitrogen and thawing in 37◦C water bath. Alternatively, a hypotonic lysis buffer can be used to promote the lysis of the remaining amoeba cells.

Freeze tubes in a −80◦C freezer for storage until purification (*Basic Protocol 2).*

If the virus will not be purified the supernatant and cell lysates should be centrifuged at 600 x g for 5 minutes at 4°C and the supernatant storaged at −80◦C.

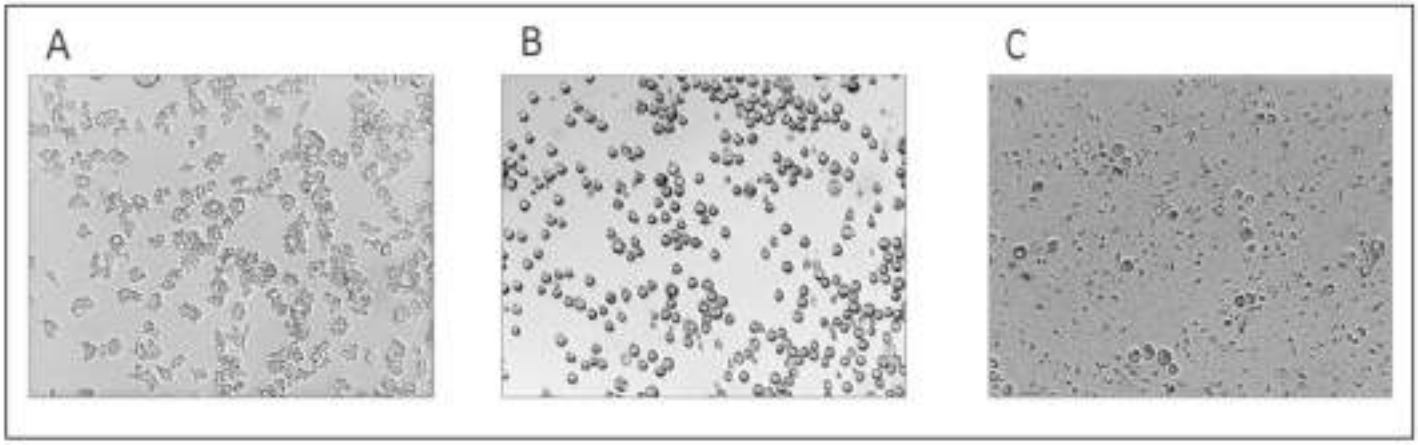

FIGURE 1. Uninfected monolayer of *A. castellanii* (A). Mimivirus replication on *A. castellanii* cells showing CPE at 48 hr (B) and 72 hr (C) post-infection.

BASIC PROTOCOL 2

Mimivirus purification

Sucrose cushion are successfully used to concentrate viral stocks, increasing the virus titer and removing the non-viral elements of the stock. For most of the biological and molecular experiments involving mimivirus, including animal experimentation this level of purification (sucrose cushion at 24%) is sufficient, and it will be presented here. Alternatively, higher sucrose concentrations may be used for mimiviruses purification (50%). Also, for host genome traces elimination, a simple filtration of containing-viruses cell lysates in 0.8µm filter was empirically tested and is indicated.

In this protocol the mimiviruses-rich supernatants from the infected amoebae obtained during the mimivirus replication (Basic Protocol 1) are submitted to several rounds in a Douncer and purified by ultracentrifugation through a sucrose cushion (24%), followed by homogenize in PBS or Page's amoeba saline (PAS), and stored at -80°C.

Materials

Viral samples to be purified (see Basic Protocol 1)

24% sucrose solution (see recipe)

Phosphate-buffered saline (PBS)(see recipe)

Dounce tissue grinder

50mL- Conical centrifuge tubes

Refrigerated low-speed table-top centrifuge

1.2-µm- pore syringe filter

Pipette

Micropipette

Pipettor

Tips

Tube racks

Glassware

Ultracentrifuge

Ultracentrifuge tubes

0.6 mL microcentrifuge tubes

Mimivirus purification by sucrose cushion

1. Submit the viral samples to be purified (see Basic Protocol 1) to 80 homogenization cycles in a Dounce tissue grinder.

Although not essential, this step is important to disrupt remaining amoebal cells and also to homogenize the solution.

2. Filter the supernatant and cell lysates through a 1.2 µm syringe filter to remove amoebal debris

   Although filtration allows to obtain of a more pure viral stocks, some particles may be retained in filter, causing a decrease of viral titer.

3. Drop slowly 25mL of the filtrate over 10 mL of a 24% sucrose cushion (see recipe) in ultracentrifuge tubes (see figure 2a)

   Despite this protocol indicate 24% sucrose cushion, the 22% sucrose cushion was also used with successful results.

4. Balance the centrifuge tubes.
5. Centrifuge at 35,250 *X* g for 30 min at 4°C in ultracentrifuge.

   An easily naked eye visualized pellet will be formed (see figure 2b)

6. Homogenize the pellet in 500 µL of PBS.

   This step should be performed on ice.

7. Storage should be made at -80°C in 0.6 mL microcentrifuge tube in 5µL to 10 µL aliquots or in an appropriate volume according to specific needs and then titrate the virus (see Basic Protocol 3).

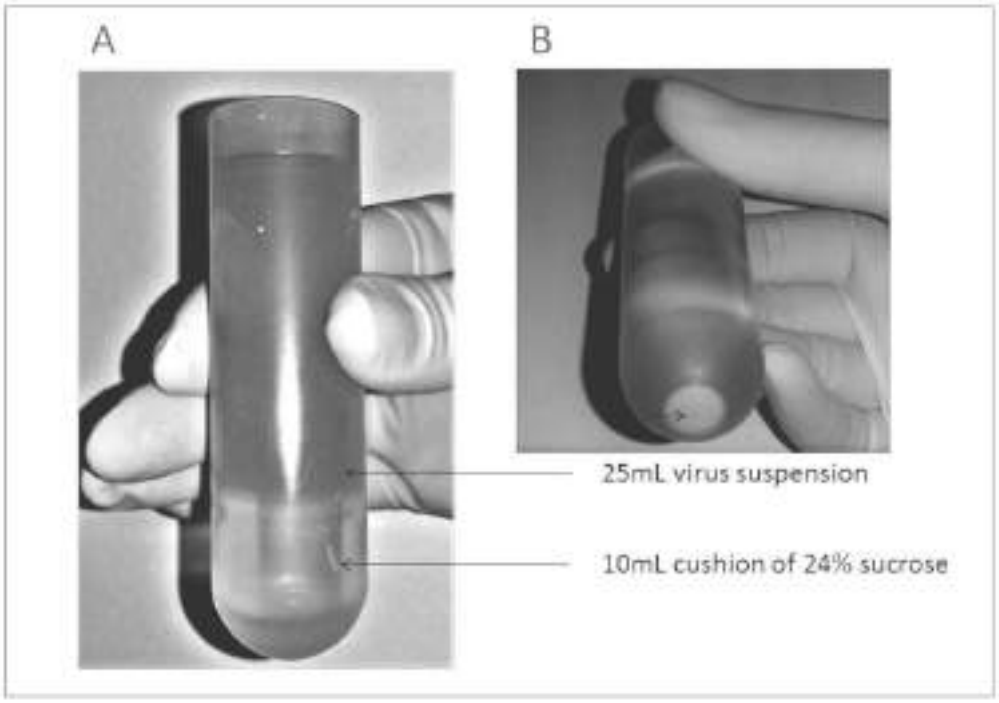

FIGURE 2.Ultracentrifuge tube with 24% sucrose cushion prepared with virus overlay prior to centrifugation (A) and mimivirus pellet after ultracentrifugation (B).

BASIC PROTOCOL 3

Mimivirus titration

End-point dilution assays are commonly performed to determine the viral titer of viruses that do not form plaques, such as mimivirus that do not form plaques in *Acanthamoeba sp* cells. This protocol describes the mimivirus the end-point dilution assays. The procedure consists in perform serial dilutions of the viral solution and inoculate in *Acanthamoeba castellanii* previously plotted on 96-well plates. After incubation, CPEs are observed in optical microscopic and the titer ($TCID_{50}$) calculated as described by Reed and Muench, 1938.

Materials

Viral samples to be quantified

Acanthamoeba castellanii culture grown in tissue culture flasks (see Support Protocol 1)

Peptone-yeast extract-glucose (PYG) medium (see recipes)

Phosphate-buffered saline (PBS; see recipe)

Incubator (28◦C)

96-well plates

Transfer pipette

Pipette

Micropipette

Pasteur pipette

Tips

Tube rack

1.5 mL microcentrifuge tubes for serial dilutions of virus.

Inverted microscope

Mimivirus titer calculation by end-point dilution assay

***Acanthamoeba castellanii* cells preparing**

1. Set up 4×10^4 *A. castellanii* cells in 96-well plates in 100 µL of PYG medium per well (see Support Protocol 1)
2. Prepare the number of cells in PYG medium to a final volume of 11mL for one 96-well plaque.
3. Pippete 100 µL of the cells mixture into each well of a 96-well tissue culture dish.

   One 75cm^2 tissue culture flasks, when confluent, contains ~1.5× 10^7 cells, and each well of the 96-well plates should be seeded with 4 × 10^4 A. castellanii. So, a single 75cm^2 tissue culture flasks is needed to prepare four 96-well plates.
4. Incubate at 28◦C for 30 minutes to adhere the cells

The 96-well plates can be prepared 24hrs before infection. In this case the 96-well plates should be prepared seeding 3×10^4 A. castellanii per well in 100 µL of PYG medium.

5. Visualize in microscope *A. castellanii* cells.

The cells should be 80% to 90% confluent.

Cell infection

6. If the sample to be titered is derived of mimivirus replication (see basic protocol 1), the samples should be submitted to three cycles of freezing and thawing to release virus trapped in the cells. But if the sample to be titered is derived of mimivirus purification (basic protocol 2) the samples should be directly diluted.

7. For each sample to be titered, perform serial 10-fold dilutions (from 10^{-1} to 10^{-11}) of the virus to final volume of 500µL in PBS or PAS, in microtubes.

During the dilution it is important to suck from surface of the sample to be diluted and following discard the sample on the tube wall in the next dilution. It is necessary to change tips between dilutions.

8. Add directly on the amoebae monolayer 100 µl of each dilution to a single well in the plate as showed in figure 3.

Each dilution is usually titered in duplicate.

9. Inoculate one row of the each plate with PBS or PAS to serve as uninfected controls as showed in figure 3.

10. Incubate at 28◦C for 96 hrs and observe CPE in an inverted microscope.

It is recommended to observe the CPE in each well daily.

For mimiviruses the CPE are amoebae rounding, loss of motility and cell lysis.

11. Calculate the titer as described by Reed and Muench, 1938.

.	1	2	3	4	5	6	7	8	9	10	11	12
A	10-1	10-2	10-3	10-4	10-5	10-6	10-7	10-8	10-9	10-10	10-11	uninfected controls
B	10-1	10-2	10-3	10-4	10-5	10-6	10-7	10-8	10-9	10-10	10-11	uninfected controls
C	10-1	10-2	10-3	10-4	10-5	10-6	10-7	10-8	10-9	10-10	10-11	uninfected controls
D	10-1	10-2	10-3	10-4	10-5	10-6	10-7	10-8	10-9	10-10	10-11	uninfected controls
E	10-1	10-2	10-3	10-4	10-5	10-6	10-7	10-8	10-9	10-10	10-11	uninfected controls
F	10-1	10-2	10-3	10-4	10-5	10-6	10-7	10-8	10-9	10-10	10-11	uninfected controls
G	10-1	10-2	10-3	10-4	10-5	10-6	10-7	10-8	10-9	10-10	10-11	uninfected controls
H	10-1	10-2	10-3	10-4	10-5	10-6	10-7	10-8	10-9	10-10	10-11	uninfected controls

FIGURE 3. Schematic figure to prepare 96-well plaque for mimivirus titration by end-point dilution assay.

SUPPORT PROTOCOL 1

Growth and splitting of *Acanthamoeba* culture

Amoebae of the *Acanthamoeba* genus are mimivirus hosts. The first mimivirus was originally isolated from *Acanthamoeba polyphaga*, but is also being isolated in the laboratory in *A. castelannii, A. griffin, A. lenticulata and A. quina* cultures. *A. polyphaga or A. castellanii* cells are the most widely used for mimivirus replication. In this protocol, the *A. castellanii* are cultivated at 28◦C in PYG medium and subcultured until confluent cell monolayers obtained. The amoebae should be counted for splitting.

Materials

Peptone-yeast extract-glucose (PYG) medium (see recipes)

Ice

Incubator (28◦C)

25- 75 and 150 cm^2 tissue culture flasks

Neubauer chamber and glass cover for cell counting

1.5 mL microcentrifuge tubes

50mL tubes

Pipette

Micropipette

Tips.

Tube rack

Inverted microscope

Preparation of *Acanthamoeba castellanii* cultures

All solutions and equipments coming into contact with A. castellanii cultures *must be sterile, and aseptic technique should be used accordingly.*

1. Maintain *A. castellanii* cultures at 28◦C in 75-cm^2 tissue culture flasks containing 15 ml of PYG medium.

Cell splitting

2. Incubate the cell culture flasks containing *A. castellanii* culture on ice bath for until 5 min to detach cells.
3. Gently knock flask to detach cells and look at inverted microscope
4. Determine the cell count by using a Neubauer chamber.

   To cell counting a dilution of the cells contained in a flask should be prepared. Typically, the concentration range for a cell count with Neubauer chamber is between 250.000 cells / ml and 2,5 million cells / ml. The Neubauer chamber should be loaded with 10 µl of the dilution with micropipette.

5. Subculture cells in a new tissue culture flask, adding 100.000; 500.000 and 1.000.000 cells to 25- 75 and 150 cm^2 tissue culture flasks with 5mL, 15 mL and 25 mL of PYG media, respectively according to requirement.

6. Incubate at 28◦C until cell confluence is reached**.**

   Perform cell splitting at least three times weekly.

Note: The same procedure should be used for cell plate preparations for titration (see basic protocol 3)

REAGENTS AND SOLUTIONS

Note: Media recipes are calculated for 1 liter but can be modified for smaller or higher volumes.

Note: Solutions should be prepared in sterile ultrapure water.

PYG medium (proteose peptone, yeast extract, glucose)

Solution A.

Dissolve the following components in 300mL ultrapure H_2O.

0,98 g $MgSO_4 . 7H_2O$

0,06 g $CaCl_2$

9,0 g $C_6H_{12}O_6$

0,02 g $Fe(NH_4)_2(SO_4) . 6H_2O$

0,40 g $Na_2HPO_4 . 7H_2O$

0,34 g KH_2PO_4

1,00 g $C_6H_5Na_3O_7 . 2H_2O$

Solution B.

Dissolve 20,0 g Bacto-peptone Extract in 200mL ultrapure H_2O.

Solution C.

Dissolve 2,0 g Yeast extract in 200mL ultrapure H_2O.

1. Mix each previous mixture on magnetic mixer;

2. Add the three solutions (A, B and C) after complete homogenization and add ultrapure H_2O to 1L final volume.

3. Check pH and adjust to pH 6.5 if necessary

4. Autoclave at 121°C for 20 min and let cool;

5. Filter the medium;

6. Add fetal bovine serum, antibiotics and antifungal to the medium at following concentrations:
    - 7% Fetal bovine serum (FBS)
    - 25 mg/mL amphotericin B
    - 500 U/mL penicillin
    - 50 mg/mL gentamicin

7. Store at 4◦C.

Page's amoebal saline (PAS) buffer

Solution A

1.20g NaCl;

0.04g $MgSO_4.7H_20$;

1.42g Na_2HPO_4;

1.36g KH2PO4

Dissolve in dH2O to 100mL final volume

Solution B

0.04g $CaCl_2.2H_2O$

Dissolve in dH2O to 100mL final volume

Per 1 liter:

Add 10 ml of solution A and 10 ml of solution B to 980 mL dH2O

Check pH and adjust to pH 6.91 if necessary

Autoclave for 20 min

Store at room temperature or at 4◦C after opening

Phosphate-buffered saline (PBS)

Per 1 liter:

8 g NaCl (137 mM)

1.44 g Na_2HPO_4 (10 mM)

0.2 g KCl (2.7 mM)

0.24 g KH_2PO_4 (2 mM)

Dissolve in 900 ml ultrapure H_2O

Check pH and adjust to pH 7.4 if necessary

Bring volume to 1 liter with ultrapure H_2O.

Autoclave in 500-ml bottles for 20 min

Store at room temperature or at 4◦C after opening

Sucrose 24% (w/v)

Per 1 liter:

240g sucrose

Dissolve in 800 ml ultrapure H_2O in a magnetic stirrer .

Then adjust volume to 1L

Prepare at moment or store in 250-ml aliquots at 4◦C

COMMENTARY

Background information

The first mimivirus was isolated in 1992 and has been investigated as a putative etiological agent of pneumonia (La Scola B et al., 2003; La Scola B et al., 2005). However its characterization as a virus occurred only in 2003. The study of this sample was delayed for a decade due difficulty in mimivirus characterization which was initially as a bacterium. In addition its size not expected for a viral particle may have prevented its isolation and consequent discovery and study due to the traditional use of 0.2 μm filters in which this virus is retained. The difficulty of characterizing the mimivirus was mainly due to the fact that these viruses have unique characteristics that differentiate them from most viruses described to date. Among these features we could highlight the extensive size of its particle (≈700 nm) and genome (≈1.2 million base pairs). Additionally, these virus show an extensive gene content that had not been attributed to any virus. These and other features makes the mimivirus one of the most complex viruses described to date. Electron microscopy was one of the main techniques responsible for solve the mystery of the mimivirus. Because of their unique morphological features the microscopy also has been a very important tool in the characterization of these viruses currently. Since the discovery and characterization of the first *Mimivirus* the prospection for mimiviruses has been conducted in different environments and clinical samples and the mimivirus replication in the laboratory can be performed in amoebae of the *Acanthamoeba* genus, its natural host, as described in this unit. The mimivirus study is an open field for basic and applied studies. However , to improve research involving the characterization of these viruses as well as elucidate their clinical and environmental significance, it is necessary, establish and improve the protocols to study these virus, for example, to test and determine the best conditions for viral isolation and replication. Analyzing

growth conditions, obtaining purified virus at high titers as well as searching for fast, efficient and not expensive viral production strategies are *sine qua non* points in the scientific routine that are directly linked to the biology of viruses (Mutsafi et al., 2013; Kuznetsov et al., 2014) but require a standardization process. Most of the newly identified mimiviruses have been successfully replicated, purified and titrated using the methods described here. However, due the increasing number of *Mimivirus* isolates it is necessary that these protocols are routinely assessed for their use in new samples that have been isolated. The interest for *Mimivirus* has become increasingly higher among researchers worldwide, creating the need to establish methods and description of them in order to improve the *Mimivirus* study and provide bases for their study in the laboratory.

Critical Parameters and Troubleshooting

As in other cell cultures, the *Acanthamoeba sp* cultures are very susceptible to contamination with bacteria, filamentous fungus and yeast. To overcome this critical parameter and to minimize contamination preventive measures such as the use of the medium containing large amounts of antimicrobial agents, mainly in viral isolation assay using environmental samples are taken. However in specific cases the antimicrobial agents can be reduced or even eliminated. All protocols described here involving cell culture must be performed in a biosafety cabinet and with aseptic technique. Furthermore it is essential that the cabinet and the work surfaces are cleaned with 70% ethanol. The PYG medium should be autoclaved and can be filtered after that to remove the salt crystals. Another critical point to consider in preparation of *Acanthamoeba* sp cultures is the procedure in step 2 of the Support Protocol 1, in which the amoeba culture are kept on an ice bath to detach. It is essential that the time of 5 minutes is complied because the amoebas cultures maintained on an ice bath for more time could encyst due to physiological stress. A second critical parameter is the cultivation atmosphere because the *Acanthamoeba* culture should be incubated without injection of CO_2. It is essential that the plates and flasks containing

Acanthamoeba sp cultures be carefully maintained completely sealed and the closed, respectively.

The mimivirus replication and titration by end-point dilution assays are very sensitive and reliable. But the success of these techniques depends among other factors of the state of *Acanthamoeba sp* cultures used. Along the *Acanthamoeba sp* cultures passages modifications may occur affecting the virus replication. So, the *Acanthamoeba sp* cultures are recommended to grow no more than 10 passages to try to reduce variability. Therefore, it is recommended to keep a stock of Acanthamoeba cysts to be desencysted when necessary.

For mimivirus replication and titration it is necessary to prepare the culture plates and flasks before and wait cell to adhere. Furthermore in this step it is essential to use a consistent cell concentration to be seed because this is a critical parameter for titration by end-point dilution assays. The seeding of 4×10^4 cells per well for the 96-well plates to mimivirus titration and $7X10^6$ cells per culture flasks to mimivirus replication is the ideal when cells are infected on the same day. If necessary the cells can be prepared approximately 24 hours before infection as described in step 2 and step 3 of the Basic Protocol 1 and Basic Protocol 3, respectively. However, in this case it is necessary to add a lower concentration of cells per well. One of the most important parameters for mimivirus replication is the MOI. Then, regarding mimivirus replication count the cells is a critical parameter to obtain MOI of 0,01.

One of the critical parameter for mimivirus purification is the quality of the sample to be purified. It is therefore very important that the viral replication has been done properly and that the viral titer is high enough. Furthermore during the procedure of the dropping de virus over sucrose solution it is important to be careful to not disturb the sucrose solution. It is important to also move carefully the ultracentrifuge tube after the addition of viral solution.

Anticipated Results

After mimivirus replication (viral seed) (Basic Protocol 1) the titers obtained in the laboratory typically range between 10^6 and 10^7 $TCID_{50}$/ml. Typically, after 48

to 72 hr of incubation, at MOI: 0,01, 90% or more of the cells presented CPE an most the cells have detached from the monolayer. The CPE most commonly observed in amoeba infected with mimivirus are amoebae rounding, loss of motility and amoeba lysis (see Figure 1). The titers can be increased by purifying the produced virus. Viral purification by sucrose cushion (Basic Protocol 2) results in formation easily naked eye visualized pellet as shown in Figure 2b. After viral purification titers typically range between 10^9 and 10^{11} $TCID_{50}$/ml. As described, mimivirus can be titrated by end-point dilution assay (Basic Protocol 3). When growth and splitting of amoebae culture are made following the conditions and amoeba concentration indicated in *support protocol 1 e*very 2 days amoebal monolayer becomes confluent and can be counted, splitted and used for preparing plaques.

Time Considerations

It generally takes 1 to 2 hours to split and to prepare the amoebae culture for infection. Preparation of the plaque to perform titration generally takes 1 to 2 hours. To PYG medium preparation a complete day is necessary, since the medium is autoclaved and only after cold it should be filtered. However, PYG medium must be prepared and stored at 4◦C until the use.

In successful experiments, it generally takes 4 days to propagated mimivirus (Basic Protocol 1), a single day to mimivirus purification (Basic Protocol 2) and another 5 days to determine the titer (Basic Protocol 3). The infection for mimivirus replication generally takes about 72 hours, since the infection is performed by the inoculation of the samples in amoebae monolayer at adequate MOI. After the mimivirus replication the sample can be purified on same day or stored at −80◦C until the purification. Amoeba cells infected with mimivirus at MOI: 0,01 generally show CPE 24 to 72 hours after infection. The time of incubation can vary among the different isolates of mimivirus. Samples with decreased rates of growth can be incubated as long as 72 hours. Then, in approximately 3 days the virus can be collected.

The mimivirus purification (Basic Protocol 2) generally takes about 8 hours to be performed. This protocol involves Douncer tissue grinder homogenizing, spins, and 30 minutes of centrifugation through a sucrose cushion. All the steps can be performed in a single day.

The mimivirus titration of the viral sample by end-point dilution assay is done over several days (5 days), but the plates can be prepared and infected about 30 minutes after on the same day (Basic Protocol 3). On day 1, cells are seeded into a 96-well dish and maintained about 30 minutes incubation, after this the virus is diluted and added to the plate. This process takes approximately 1 hour. In this case most of the time will be spent waiting for cells seeding. While the amoebae are being incubated to adhere to the plate, samples can be diluted for titration. The analyses and titer calculation can be performed in approximately 1 hour.

ACKNOWLEDGEMENT

We thank our colleagues from Laboratório de Vírus of Universidade Federal de Minas Gerais and the research team of URMITE—Aix Marseille Université for their excellent support. We would also like to thank CNPq, CAPES, FAPEMIG and Pro-Reitoria de Pesquisa da Universidade Federal de Minas Gerais (PRPq-UFMG) for financial support.

FIGURE LEGENDS

Tupanvirus, a 2.3 µm long tailed ancestor of Mimiviridae having an almost complete translational apparatus

Jônatas Abrahão[¥1,2], Lorena Silva[¥1,2], Jacques Bou Khalil[2], Rodrigo Rodrigues[2], Ludmila Santos Silva[1,2], Thalita Arantes[2], Felipe Assis[2], Paulo Boratto[2], Miguel Andrade[3], Erna Geessien Kroon[2], Bergmann Ribeiro[3], Ivan Bergier[4], Herve Seligmann[1], Eric Ghigo[1], Philippe Colson[1], Anthony Levasseur[1], Didier Raoult[1*], Bernard La Scola[1*]

Affiliations

[1] Unité de Recherche sur les Maladies Infectieuses et Tropicales Emergentes (URMITE) UM63 CNRS 7278 IRD 198 INSERM U1095, Aix-Marseille Univ., 27 boulevard Jean Moulin, Faculté de Médecine, 13385 Marseille Cedex 05, France

[2] Laboratório de Vírus, Instituto de Ciências Biológicas, Departamento de Microbiologia, Universidade Federal de Minas Gerais, Belo Horizonte, MG, 31270-901, Brazil.

[3] Laboratório de Microscopia Eletrônica e Virologia, Departamento de Biologia Celular, Instituto de Ciências Biológicas, Universidade de Brasília, Asa Norte, Brasília DF, 70910-900, Brazil.

[4] Lab. Biomass Conversion, Embrapa Pantanal, R. 21 de Setembro 1880, 79320-900, Corumbá/MS, Brazil.

¥ Contributed equally to this work

* Corresponding authors: didier.raoult@gmail.com and bernard.la-scola@univ-amu.fr

Translational is the canonical frontiers between cell-world and viruses. Cellular organisms carry ribosomal RNAs, transfer RNAs (tRNA) and genes encoding for proteins of translation such as aminoacyl-tRNA synthetases (aaRS), translation factors, ribosomal proteins, among others[1-3]. Here we report the discovery of Tupanvirus, the longest tailed *Mimiviridae* as long as 2.3 µm isolated in amoeba. Its genome is a 1.44 Mb linear double strand DNA coding for 1,276 predicted proteins. Phylogenetic analyses suggest an ancestral position among the 3 Mimivirus lineages. Remarkably, it presents the largest translational apparatus within the virosphere, even larger than several Prokaryotes and Eukaryotes, with 67 tRNA and a gene-set comprising 20 aaRS, 11 factors for all translation steps, factors related to tRNA/mRNA maturation and ribosome protein modification. Moreover, two 18S ribosomal intronic fragments (88 and 101bp) are encoded by Tupanvirus genome and expressed as demonstrated by qPCR and FISH. Finally Tupanvirus, compared to Mimivirus, partially resist translational inhibitors. Moreover, Tupanvirus is cytotoxic and causes a severe ribophagy in its host cells even without intracellular multiplication. Tupanvirus is a new step in the comprehension of evolution of giant viruses.

Attempting to find new and more distant giant viruses we performed prospecting studies in a special environment called soda lakes (Nhecolândia, Pantanal biome, Brazil). Soda lakes are known as environments that conserve and/or mimic ancient life conditions (extremely high salinity and pH), being considered some of the most extreme aquatic environments on Earth[4]. We found an optically visible mimiviridae that surprisingly harbours a thick long tail (Fig. 1A) growing on *Acanthamoeba castellanii* and *Vermamoeba vermiformis*. We named this isolate Tupanvirus as a tribute to the

South American Guarani Indian tribes, which Tupan - or Tupã - (the God of Thunder) is one of the main mythological references. Electron microscopy analyses revealed a remarkable virion structure. Tupanvirus presents a capsid similar to mimiviruses in size (~450nm) and structure, including a stargate face and fibrils[5]. However, Tupanvirus virion presents a large cylindrical tail (~550nm extension; ~450nm diameter, including fibrils) attached on the basis of the capsid (Fig. 1B,C,D). This tail is the longest described in the virosphere [6]. Microscopical analysis suggested that capsid and tail are not tightly attached (Extended data Fig. 1), although sonication and enzymatic treatment of purified particles were not able to separate both parts (Extended data Fig. 1A,B,C). The average size of complete virions is ~1.0µm, although some particles can reach up to 2.3 µm, due to plasticity in the tail's size; thus, being the longest viral particles described to date (Fig. 1; Extended data Fig. 1I,J,K). Furthermore, there is a lipid membrane inside the icosahedral and likely in the cylindrical tail, related to the fusion to cellular membrane and release of capsid and tail content (Fig.1 E,F). Different from other giant viruses[7-12], Tupanvirus was isolated both in AC and VV, wherein it exhibited very similar replication profiles. Particles attach to the host-cell surface and enter through phagocytosis (1 h.p.i.) (Extended data Fig. 1M,N,O). The inner membranes of the capsid and tail merge with the amoebal host phagosome membrane, releasing the genome and particle contents, respectively (2-6 h.p.i.) (Fig. 1 E,F). "A volcano-like" viral factory (VF) is formed (7-12 h.p.i.)[13] where morphogenesis occurs (Extended data Fig. 1, link movies). During this step, the virion tail is attached to the capsid after its formation and closure. At late times (16-24 h.p.i.), the amoebal cytoplasm is fulfilled by viral particles, followed by cell lysis and particles release (Extended data Fig. 2).

Its genome is a linear dsDNA molecule of 1,439,508 bp (GC% ~28%), the fourth largest viral genome described so far[8,14], containing a total of 1,276 predicted

ORFs, in which 425 are ORFans (ORFs with no matches in current databases). To date, the largest genomes belong to Pandoraviruses isolates and the largest one, *P. salinus*, has 2,473,870bp and encodes 2,542 putative proteins[8]. The rhizome of Tupanvirus revealed its main ancestor is a *Mimiviridae* (~65%), followed by eukaryotes (~17%) and bacteria (~14%) (Fig. 2A). Among *Mimiviridae*, Tupanvirus exhibited best matches to lineages A (~16%), B (~19%) or C (~27%) suggesting the ancestrality of Tupanvirus before the radiation of the three lineages. Phylogenetic and identity distribution analysis of Tupanvirus ORFs demonstrated that it clusters with mimiviruses but as an outgroup, suggesting its ancestry position among *Mimivirus* genus, thus being the newest member of the fourth TRUC club[15] (Fig. 2B). The 'AAAATTGA' promoter motif was found 408 times in intergenic regions, similar to other mimiviruses[16,17] (Extended data Fig. 3A). Proteomic analysis of Tupanvirus particles revealed 96 proteins, wherein nearly half of them is unknown (44/96 = 45.8%), of which eight are ORFans (8/44 = 18.2%) (SI 1). By contrast, the analysis of Tupanvirus gene-set related to energy production reveals a clear dependence of the virus to host energetic machinery, similar to other mimiviruses[18-20]. Astonishingly, Tupanvirus exhibits the largest set of genes involved in translation of a virus with 20 ORFs related to aminoacylation (aaRS) and transport with 67 tRNA comprising a total of 46 codons (Fig. 3A; Extended data Fig. 4; SI 2, 3). Only selenocysteine related genes are lacking as also seen on many other cells [21]. Several translation factors were identified such as eight translation initiation factors (IF2, IF5, IF4e (2 copies), IF5a, IF2 gamma, SUI1, IF4a), one elongation/initiation factor (GTP-binding elongation/initiation), one elongation factor (Ef-aef-2), and one release factor (ERF1) (Fig. 3A; Extended data Fig. 4; SI 3). Furthermore, other genes were observed: factors related to tRNA maturation and stabilization **(**tRNA nucleotidyltransferase, tRNA guanylyltransferase, cytidine deaminase, RNA methyltransferase); mRNA

maturation (poly(A) polymerase, mRNA capping enzyme) and splicing (RNA 2 - tpt1 family protein); and ribosomal proteins modification (ribosomal-protein-alanine n-acetyltransferase, FtsJ-like methyl transferase) (Fig. 3A; SI 3). Based on phylogenetic trees, except for leucyl-RS, phenylalanyl-RS, prolyl-RS, seryl-RS, threonyl-RS and valinyl-RS, all other translation-related genes do not seem to have been acquired recently from cellular organisms (SI 4). The codon and amino acid usage of Tupanvirus with its low GC% is quite different to *Acanthamoeba*. Remarkably, we observed a high correlation between Tupanvirus tRNA-related isoacceptors and the most used codons and presents more tRNA isoacceptors for highly abundant codons (Extended data Fig. 3B,5). Surprisingly, we found two slightly different copies of intronic 18S ribosomal region in Tupanvirus. As a matter of fact it is widespread in all mimiviruses (lineages A and B present only one copy in an intronic region also next to a self-splicing group I intron endonuclease) but was missed before. The phylogenetic analyses revealed that the two copies had separate and different origins (Extended data Fig. 6,7). Although Tupanvirus 18S-like ribosomal sequences are located in intergenic regions, we observed by qPCR and FISH that they are highly expressed during all the infection, but, especially, in intermediate and late times (6 and 12 hours post infection) (Fig 1H; Extended data Fig. 8). Furthermore, Tupanvirus is more tolerant to translation-inhibition drugs, geneticin and cycloheximide, than Mimivirus, an impressive characteristic considering the natural shutdown it performs in the permissive host (Extended data Fig. 9). The functions of these 18S-like ribosomal sequences need to be further identified. The comparison among Tupanvirus and cell-organisms shared-translation-related genes reveals that Tupanvirus presents a wealthier gene-set than *Candidatus ruddii* (Bacteria) and *Nanoarchaeum equitans* (Archaea). Tupanvirus presents even more tRNAs than *Encephalitozoon cuniculi*, an Eukaryotic organism (Fig.3B).

Different from other mimiviruses, Tupanvirus was able to infect a broad-range of protists organisms. Surprisingly, we observed four distinct profiles of infectiveness: i productive cycle in permissiveness cells; ii abortive cycle; iii refractory cells; and iv most surprisingly non-host cells exhibiting a cytotoxic phenotype in the presence of Tupanvirus without multiplication, a circumstance never reported to the best of our knowledge (Extended data Fig. 10). This latter profile was intriguing, since the toxicity was observed in *Tetrahymena* sp, a ravenous free-living protist[22], and also in the vertebrate cell lines THP-1 and RAW264.7 (Fig. 1G; Extended data Fig. 9I,J,K). This unusual phenotype was also observed in *A. castellanii*, but only in higher multiplicity of infections, 50 and 100. The same was not observed for Mimivirus (Extended data Fig. 9A). This toxic profile associated specifically to Tupanvirus is related to shut-down of host ribosomal abundance, wherein Tupanvirus leads to a reduction on host rRNA amount, by inducing ribophagy (Extended data Fig. 9B,C,D). The toxic effect and ribophagy is independent of Tupanvirus replication, but rather is caused by the viral particle (Extended data Fig. 9E,F,G) Although Tupanvirus is not able to replicate within *Tetrahymena* sp, it is phagocytosed in a voracious way, forming large intracellular vesicles, wherein occur the fusion of the internal membrane of the capsid and tail, releasing their content inside the protist cytoplasm (Extended data Fig. 9I,J,K). The virus induces gradual vacuolization, loss of motility, reduction of phagocytosis rate, decrease of rRNA and ribophagy, similar to that observed in *A. castellanii* cells (Extended data Fig. 9A-D,I-K)This reduction of physiological activity of a (non-host) predator increases the virus' fitness (Extended data Fig. 9L,M). Altogether, this data suggests for the first time that viral particles can act as active "non-alive" players favoring viral progeny maintenance, in a distinct way of their canonical role of transmitting genetic information. To our knowledge, a viral particle being responsible

for the modulation of host and non-host organisms independently of the viral replication has not been described previously.

Considering that Tupanvirus belongs to an ancestral group among the mimiviruses, we can hypothesize that the ancestor of *Mimiviridae* had a more generalist lifestyle, being able to infect a wide variety of hosts. In this view, the ancestors of mimiviruses were already giant viruses that undergone mainly through reductive evolution, although some genes could have been acquired over time. A reductive evolution pattern is usual among the obligatory intracellular parasites[23-25]. In these cases, the organisms lose genes related to energy production, being one of the main reasons of their parasitic lifestyle. However, the lack o ribosome still put Tupanvirus in the virosphere[26]. Nevertheless, Tupanvirus presents the most complete translational apparatus among the viruses, and its discovery put us one step forward in the comprehension of the evolutionary history of the giant viruses.

Methods

Samples collection, virus isolation and host-range determination

In 2014, a total of 12 soil samples were collected from soda lakes in Nhecolândia, Pantanal, Brazil. The samples were kept at 4°C until the inoculation process. The soil samples were transferred to falcons of 15 mL and added of 5 mL of Page's Amoebae Saline (PAS), the system was kept for 24 hours to sediment decantation. After this time, the liquid was submitted to a set of filtrations: first paper filter and after filter of 5 μm, to remove large particles of sediment and concentrate the possible giant viruses eventually present. To co-culture process the cells used were *A. castellanii* (strain NEFF) and *V. vermiformis* (strain CDC 19). These cells strains were kept in 75 cm^2 cell

culture flasks with 30 mL of peptone-yeast extract- glucose medium (PYG) at 28°C. After 24 hours of growth, cells were harvested and pelleted by centrifugation. The supernatant was removed and the amoebae resuspended three times in sterile PAS. After the third washing, 500,000 *A. castellanii* or *V. vermiformis* or was resuspended PAS or TS solutions and seed in 24-wells plates. The suspensions of amoebae were added of antibiotics mi containing ciprofloxacin (20 µg/mL; Panpharma, Z.I., Clairay, France), vancomycin (10 µg/mL; Mylan, Saint-Priest, France), imipenem (10 µg/mL; Mylan, Saint-Priest, France), doxycycline (20 µg/mL; Mylan, Saint-Priest, France), and voriconazole (20 µg/mL; Mylan, Saint-Priest, France). Each 100 µL of sample was mixed and inoculated in the number identified (1-12) wells and incubated at 30°C in a humid chamber. A negative control was used in each plate. Daily, the wells were observed under optical microscopy. After 3 days, new passages of the inoculated wells were done in the same way until the third passage. In this passage, the content of the wells presenting lysis and cytopathic effect were collected and stored for production and analysis of the possible isolates by hemacolor staining and electron microscopy using the negative stain technique. From the 12 tested samples, in three we found Tupanvirus. In order to evaluate Tupan host-range, a panel of cell lines was submitted to Tupanvirus infection at a multiplicity of infection (MOI) of 5: *Acanthamoeba castellanii, Acanthamoeba sp E4, Acanthamoeba sp. Micheline, Acanthamoeba royreba, Acanthamoeba griffini, Vermamoeba vermiformis, Dysctiostelium discodium, Willartia magna, Tetrahymena hyperangularis, Trichomonas tenax*, RAW264.7 and THP-1 cells. The assays were carried out in 24-wells plates, and cells were incubated for 24 or 48 hours. Tupan titer was measured in *A. castellanii* by end-point and calculated by Reed-muench method[28]. In parallel, the samples were submitted to qPCR targeting the capsid gene aiming to verify viral genome replication (Biorad, California, USA). Tupanvirus

was propagated in twenty *A. castellanii* 175-cm^2 cell culture flasks in 50 ml PYG medium. The partciles were purified by centrifugation through a sucrose cushion (50%), suspended in PAS and stored at −80°C. Purified particles were used to genome sequencing, proteomic analysis[8] microscopical and biological assays.

Cycle and virion characterization

To investigate Tupanvirus replication cycle by transmission electron microscopy, 25-cm^2 cell culture flasks were added with $10x10^6$ *A. castellanii* per flask, infected by Tupan at an multiplicity of infection of 10 and incubated at 30ºC for 0, 2, 4, 6, 8, 12, 15, 18 and 24 hours. Briefly, one hour after virus-cell incubation, the amoeba monolayer was washed 3 times with PAS buffer to eliminate non-internalized viruses. A total of 10 ml of the infected cultures were distributed into new culture flasks. A culture flask containing only amoeba was used as the negative control. Infected cells and control were fixed and prepared to electron microscopy[7]. For immunofluorescence, *A. castellanii* cells were grown, infected by Tupan at an multiplicity of infection of 1 as described and added to coverslips for 0, 2, 4, 6, 8, 12, 15, 18 and 24 hours. After infection, the cells were rinsed in cold phosphate-buffered saline (PBS) and fixed with 4% paraformaldehyde (PFA) in PAS for 10 min. After fixation, cells were permeabilized with 0.2% Triton X-100 in 3% bovine serum albumin (BSA)–PAS for 5 min, followed by a rinse with 3% BSA–PBS three times. Cells were then stained for 1h at room temperature with anti-Tupanvirus antibody produced in mouse. After incubation with secondary antibody, fluorescently labeled cells were visualized using a Leica DMI600b inverted research microscope. For Tupanvirus virions characterization we also used scanning electron microscopy (SEM)[28]. Chemical treatment with proteases and sonication was performes as described elsewhere to investigate fibers composition

and attachment between capsid and tail.

Genome sequencing, assembly and analyses

Tupanvirus genome was sequenced using the Illumina MiSeq instrument (Illumina Inc., San Diego, CA, USA) with the paired end application. The sequence reads were assembled de novo using ABYSS software and the resulting contigs were ordered by the python-based CONTIGuator.py software. Draft genomes obtained was mapped back to check the reads assembly and to close gaps. The best genome assemblage genome was kept, and the few remaining small gaps were closed by Sanger sequencing. The gene predictions were performed using RAST (Rapid Annotation using Subsystem Technology) and GeneMarkS tools. Transfer RNA (tRNA) sequences were identified using the ARAGORN tool. The functional annotations were inferred by BLAST searches against the GenBank NCBI non-redundant protein sequence database (nr) (e-value $< 1 \times 10{-}3$) and by searching specialized databases through the Blast2GO platform. Finally, the genome annotation was manually revised and curated. The predicted ORFs that were smaller than 50 amino acids and had no hit in any database were ruled out. Tupanvirus codon and aa usage were compared to *A. castellanii* and other lineages of mimiviruses. Sequences were obtained from NCBI Genbank and submitted to CGUA (General Codon Usage Analysis). The global distribution of Tupan tRNAs was analyzed and compared manually to viral aa usage considering the correspondent canonical codons related to each aa. Phylogenetic analyses were carried out based on the separated alignments of several genes, as DNA polymerase beta subunit, 10 protein synthesis related factors, 18S-like fragment copies 1/2 and 20 amynoacyl-tRNA synthetases (aaRS). The predicted aa sequences were obtained from NCBI Genbank and aligned using Clustal W in Mega 7.0 software. Trees were

constructed using maximum parsimony method and bootstrap of 1,000. The analysis of aaRS domains were carried out using NCBI Conserved Domain Search (https://www.ncbi.nlm.nih.gov/Structure/cdd/wrpsb.cgi). Search for promoter sequences was performed into intergenic regions based on the searching of mimiviruses canonical AAAATTGA promoter sequence, by using Microsoft Word search tool. Single nucleotide polymorphisms (SNP) in AAAATTGA promoter sequence were also considered for each base, considering all possibilities. For rhizome preparation, all coding sequences were blasted against the NR database and results were filtered to keep the best hits. Taxonomic affiliation was retrieved from NCBI. Finally, images was generated using Circos [29].

Ribosomal shut-down assays and ecological simulations

To investigate the toxicity of Tupanvirus particles, 1 million of *A. castellanii* cells were infected with Tupan or mimivirus at multiplicity of infection of 1, 10, 50 or 100 and incubated at 32°C. At times 0h and 24h post infection the cell suspensions were collected and tittered as described. A fraction of this suspension (200µl) were submitted to RNA extraction (Qiagen RNA extraction Kit, Hilden, Germany). The RNA was submitted to reverse transcription by using Vilo enzyme (Invitrogen, California, USA) and then used as template in qPCR targeting *A. castellanii* 18S rRNA (5-TCCAATTTTCTGCCACCGAA-3 and 5-ATCATTACCCTAGTCCTCGCGC-3). The values were expressed as arbitrary units (delta-Ct). Normalized amounts of the original extracted RNA from each sample were electrophoresed in agarose gel 1%, TBE buffer and run at 150V. Transmission electron microscopy of all time course was performed to evaluate the presence of ribophagosomes and other cytological alterations. To investigate the nature of virion toxicity, purified Tupan was inactivated by UV-ligth (1h

of exposition) or heating (80°C, 1h) and inoculated onto *A. castellanii* containing 500,000 cells, at multiplicity of infection of 0.1, 1, 5, 10, 50 and 100. The assays were performed in PAS solution. The cytopathic effect was documented and quantified in a counting-cells chamber. Inactivated mimivirus was used for comparison. To check if Tupanvirus induces shutdown of amoebal 18S rRNA even after inactivation, 500,000 cells were infected (at multiplicity of infection of 100), collected at times 3 and 9h post infection and amoebal 18S rRNA levels were measure by qPCR as previously described. APMV was used as control. The sensitivity of Tupanvirus and mimivirus to translation-inhibition drugs, geneticin or cycloheximide was assayed. A total of 500,000 *A. castellanii* cells was pre-treated with different concentrations of the drugs (0-50 µM and 0-15 µM, respectively) for 8 hours and then infected at an multiplicity of infection of 10. Twenty-four hours post infection, cells were collected and the viral titers were measured. To investigate the toxicity effect of Tupanvirus particles in the non-host *Tetrahymena* sp, 1 million fresh cells were infected at an multiplicity of infection of 10 in a medium composed by 50% PYG and 50% PAS. The cytopathic effect was monitored for 4 days post infection, considering reduction of cell movement and vacuolization (lysis was not observed). At each day post infection, 100 µl of infected cells suspension were collected and submitted to cytospin and hemacolor staining to observe vacuolization and other cytological alterations induced by the virus. Other 100 µl aliquots were used to investigate the occurrence of rRNA shutdown induced by Tupan. For this, the samples were submitted to RNA extraction and electrophoresis as described. The viral cycle in *Tetrahymena* was also observed by TEM at an multiplicity of infection of 10. To investigate if Tupanvirus particles impact the rate of *Tetrahymena* phagocytosis due its toxicity, the rate of viral particles incorporation per cell was calculated during the time-course of infection. The ratio of $TCID_{50}$ (infectious entities)

and total particles was previously calculated by counting the number of viral particles in a counting-chamber (approximately 1 TCID50 to 63 total particles). One million of *Tetrahymena* cells were infected by Tupanvirus or mimivirus at MOI of 10 $TCID_{50}$. Twelve hours post-infection the amount of viral particles was estimated in the medium, by counting the remaining (non-phagocytized particles). An input of 10 $TCID_{50}$ per cell were added after each day post infection (in separate flasks, one for each day) and the rate of particles phagocytosis was calculated 12h post-input. For the calculation, the remaining particles from day before were considered. For ecological simulations, *A. castellanii* (900,000 cells) and *Tetrahymena* (100,000 cells) were added simultaneously in the same flask, then infected by Tupanvirus or mimivirus at MOI of 10 and observed for 12 days. One flask per observation day was prepared. At days four and eigth we gave an input of 500 µl of fresh medium (50% PYG and 50% PAS) and 100,000 *A. castellanii*, the permissive host. Each day post-infection the correspondent flask was collected and submitted to titration as previously described. The same experiment was carried out pre-treating (8h before infection) *Tetrahymena* with 20 µg/ml of geneticin.

Analysis involving the tupanvirus intronic 18S ribosomal region

All the analysis involving the genomic environment of copy 1 and 2 were made based in the annotation of tupanvirus. In the best hits evaluation, the core sequences of copy 1 and 2 were used for nucleotide blast analysis, using blastn. The 100 first best hits resulting were tabulated and the information were used for the construction of Venn diagrams. For the analysis of the subjacent regions of the core sequence of 18S-like region in the family *Mimiviridae*, one member of the lineages A (Acanthamoeba polyphaga mimivirus - HQ336222.2), B (Acanthamoeba polyphaga moumouvirus - JX962719.1) and C (Megavirus lba isolate LBA111 - JX885207.1) was chosen and

analyzed. Phylogenetic analyses were carried out based on the sequences of 18S-like region from Tupanvirus and the 100 best hist obtained from NCBI Genbank and aligned using Clustal W in Mega 7.0 software. The trees were constructed using maximum parsimony method and bootstrap of 1,000. For detection of the RNA sequences of copy 1 and copy 2 we used fluorescence in situ hybridization (FISH) analysis. For this assay, $2x10^5$ *A. castellanii* cells were infected with tupanvirus multiplicity of infection of 5 and collected at 30 minutes, 6 and 12h hours post infection. As control, $2x10^5$ *A. castellanii* cells were also incubated only with PAS and collected. At the indicate times, cells and supernatant were collected and centrifuged at 800g per 10 minutes. The pellet was resuspended in 200µL of PAS and used for the preparation of cytospin slides. The cells contained in the slides were fixed in cold methanol for 5 minutes. Specific probes targeting the 18S of *A. castellanii* (TTCACGGTAAACGATCTGGGCC-fluorophore Alexa 488) [1], copy 1 (AGTGGAACTCGGGTATGGTAAAA - fluorophore Alexa 555) and copy 2 (GGCCAAGCTAATCACTTGGG-fluorophore Alexa 555) were diluted and applied at 2µM in hybridization buffer (900 mM NaCl, 20 mM Tris/HCL, 5 mM EDTA, 0,01% SDS, 10%–25% deionized-formamide in distilled-H2O). The hybridization buffer containing the probes was added to the slides, cover slipped and sealed with rubber cement. The hybridization was carried out at 46°C overnight in programmable temperature controlled slide processing system (ThermoBrite StatSpin, Illinois, USA). Post-hybridization washes consisted of 0.45-0.15 M NaCl, 20 mM Tris/HCL, 5 mM EDTA, 0,01% SDS at 48°C for 10 minutes. Slides were air dried in a dark chamber followed by cover slipped. Analyses were performed by using DMI6000B inverted research microscope (Leica, Wetzlar, Germany). For analysis of the expression of the both copies, $5x10^5$ *A. castellanii* cells were infected with Tupanvirus at an multiplicity of infection of 5 and collected at different times (30

minutes, 6 and 12 hours) post infection. As control, $5x10^5$ *A. castellanii* cells were also incubated only with PAS and collected in the same times of infected cells. At the indicated times, cells and supernatant were collected and centrifuged at 800 g per 10 minutes. The resultant pellet was washed twice with PAS and after was used for total RNA extraction using the RNeasy mini kit (Qiagen, Venlo, Netherlands). The extracted RNA was submited to treatment with Turbo DNA-free kit (Invitrogen, California, USA) and after used as template in reverse transcription reactions (RT) carried out using SuperScript Vilo (Invitrogen, California, USA). The resultant cDNA was used as template for quantitative real-time PCR assays using QuantiTect SYBr Green PCR Kit (Qiagen RNA extraction Kit, Hilden, Germany) and targeting the copy 1 (primers 5'-GCATCAAGTGCCAACCCATC-3' and 5'-CTGAAATGGGCAATCCGCAG-3') and 2 (primers 5'- CCAAGTGATTAGCTTGGCCATAA-3' and 5'-CGGGAAGTCCCTAAAGCTCC-3') of the intergenic18S-like region in TPV. In order to normalize the results, primers targeting the GAPDH housekeeping gene of *Acanthamoeba* (primers 5'- GTCTCCGTCGTCGATCTCAC-3' and 5'-GCGGCCTTAATCTCGTCGTA-3') were also used. qPCR assays were performed in a BioRad Real-Time PCR Detection Systems (BioRad) and the results were analyzed using the relative quantification methodology of $2^{(-\Delta\Delta ct)}$.

References:

1. Raina, M. & Ibba, M. tRNAs as regulators of biological processes. *Front Genet.* **5**, 171 (2014).

2. Fournier, G. P., Andam, C. P., Alm, E. J. & Gogarten, J. P. Molecular evolution of aminoacyl tRNA synthetase proteins in the early history of life. *Orig Life Evol Biosph.* **41**, 621-632 (2011).

3. Korobeinikova, A. V., Garber, M. B. & Gongadze, G. M. Ribosomal proteins: structure, function, and evolution. *Biochemistry*. **77**, 562-74 (2012).

4. Sorokin, D. Y. *et al*. Microbial diversity and biogeochemical cycling in soda lakes. *Extremophiles*. **18**, 791-809 (2014).

5. Xiao, C. *et al*. Structural studies of the giant mimivirus. *PLoS Biol*. **7**, e92 (2009).

6. Ageno, M., Donelli, G. & Guglielmi, F. Structure and physico-chemical properties of bacteriophage G. II. The shape and symmetry of the capsid. *Micron.* **4**, 376-403 (1973).

7. La Scola, B. *et al.* A giant virus in amoebae. *Science.* **299**: 2033 (2003).

8. Philippe, N. *et al*. Pandoraviruses: amoeba viruses with genomes up to 2.5 Mb reaching that of parasitic eukaryotes. *Science*. **341**, 281-6 (2013).

9. Legendre, M. *et al*. Thirty-thousand-year-old distant relative of giant icosahedral DNA viruses with a pandoravirus morphology. *Proc Natl Acad Sci U S A.* **111**, 4274-9 (2014).

10. Legendre, M. *et al.* In-depth study of Mollivirus sibericum, a new 30,000-y-old giant virus infecting Acanthamoeba. *Proc Natl Acad Sci U S A.* **112**, E5327-35 (2015).

11. Reteno, D. G. *et al*. Faustovirus, an asfarvirus-related new lineage of giant viruses infecting amoebae. *J Virol*. **89**, 6585-94 (2015).

12. Andreani, J. *et al*. Cedratvirus, a double-cork structured giant virus, is a distant relative of Pithoviruses. *Viruses*. **8**, E300 (2016).

13. Suzan-Monti, M., La Scola, B., Barrassi, L., Espinosa, L. & Raoult, D. Ultrastructural characterization of the giant volcano-like virus factory of Acanthamoeba polyphaga Mimivirus. *PLoS One.* **2**, e328 (2007).

14. Antwerpen, M. H. *et al*. Whole-genome sequencing of a pandoravirus isolated from keratitis-inducing acanthamoeba. *Genome Announc*. **3**, e00136-15 (2015).

15. Raoult, D. TRUC of the need for a new microbial classification. *Intervirology*. **56**, 349-53 (2013).

16. Suhre, K., Audic, S. & Claverie, J. M. Mimivirus gene promoters exhibit an unprecedented conservation among all eukaryotes. *Proc Natl Acad Sci U S A.* **102**, 14689-93 (2005).

17. Fischer, M. G., Allen, M. J., Wilson, W. H. & Suttle, C. A. Giant virus with a remarkable complement of genes infects marine zooplankton. *Proc Natl Acad Sci U S A.* **107**, 19508-13 (2010).

18. Raoult, D. *et al*. The 1.2-megabase genome sequence of Mimivirus. *Science*. **19**, 1344-50 (2004).

19. Arslan, D., Legendre, M., Seltzer, V, Abergel, C. & Claverie, J. M. Distant mimivirus relative with a larger genome highlights the fundamental features of Megaviridae. *Proc Natl Acad Sci U S A.* **108**, 17486-91 (2011).

20. Assis, F. L. *et al*. Pan-Genome Analysis of Brazilian Lineage A Amoebal Mimiviruses. *Viruses*. **7**, 3483-99 (2015).

21. Gonzales-Flores, J. N., Shetty, S. P., Dubey, A. & Copeland, P. R. The molecular biology of selenocysteine. *Biomol Concepts*. **4**, 349-65 (2014).

22. Csaba, G. Lectins and Tetrahymena – A review. *Acta Microbiol Immunol Hung.* **63**, 279-291 (2016).

23. Smith, J. E. The ecology and evolution of microsporidian parasites. *Parasitology*. **136**, 1901-14 (2009).

24. Merhej, V. & Raoult, D. Rickettsial evolution in the light of comparative genomics. *Biol Rev Camb Philos Soc*. **86**, 379-405 (2011).

25. Nunes, A. & Gomes, J. P. Gomes Evolution, phylogeny, and molecular epidemiology of Chlamydia. *Infect Genet Evol.* **23**, 49-64 (2014).

26. Raoult, D. & Forterre, P. Redefining viruses: lessons from Mimivirus. *Nature Revi Microb.* **6**, 315-319 (2008)

27. Reed L.J. & Muench H. A simple method of estimating fifty percent endpoints. *Am. J. Hyg.* **27**, 493-497 (1938)

28. Rodrigues R.A., dos Santos Silva L.K., Dornas F.P. de Oliveira D.B., Magalhaes T.F., Santos D.A., Costa A.O., de Macedo Farias L., Magalhaes P.P., Bonjardim C.A., Kroon E.G., La Scola B.L., Cortines J.R., Abrahao J.S. Mimivirus fibrils are important for viral attachment to the microbial world by a diverse glycoside interaction repertorie. *J Virol*. **89**, 1182-9 (2015)

29. Krzywinski M., Schein J., Birol I., Connors J., Gascoyne R., Horsman D., Jones S.J., Marra M.A. Circos: An information aesthetic for comparative genomics. *Genome Res* 1**9**: 1639–1645 (2009)

Supplementary Information is linked to online version of the paper at www.nature.com/nature.

Acknowledgments

We would like to thank our colleagues from URMITE and Laboratório de Vírus of Universidade Federal de Minas Gerais for their excellent support, in special Julien Andreani, Jean-Pierre Baudoin, Gilles Audoly, Amina Cherif Louazani, Lina Barrassi, Priscilla Jardot, Eric Chabrières, Nicholas Armstrong, Said Azza, Claudio Bonjardim, Paulo Ferreira, Giliane Trindade and Betania Drumond. In addition, we thank the financial support from Méditerranée Infection Foundation, Centro de Microscopia da UFMG, CNPq (Conselho Nacional de Desenvolvimento Científico e Tecnológico), CAPES (Coordenação de Aperfeiçoamento de Pessoal de Nível Superior) and

FAPEMIG (Fundação de Amparo à Pesquisa do estado de Minas Gerais). J.A. and E.K. are CNPq researchers. B.L.S., J.A. and E.G.K. are members of a CAPES-COFECUB project.

Author Information

The authors declare no competing financial interests. Correspondence and request for material should be addressed to didier.raoult@gmail.com and bernard.la-scola@univ-amu.fr.

Author Contributions

D.R., B.L.S., J.S.A., A.L., P.C., E.G.K, E.G. designed the study and experiments. L.S., J.S.A, J.B.K., R.R., L.S., L.S.S., T.A., F.A. P.B., M.A., I.B. B.R. A.L. H.S., performed sample collection, virus isolation, experiments and/or analyses. D.R., B.L.S., A.L., J.S.A., R.R., L.S, L.S.S. wrote the manuscript. All authors approved the final manuscript.

Figures Legends

Figure 1: Tupanvirus particles and cycle special features. Optical microscopy of Tupanvirus particles after hemacolor staining (1000x) (a). Super particle (>1000nm) observed by transmission electron microscopy (TEM) (b). Scanning electron microscopy (SEM) of Tupanvirus particles (c,d). Initial steps of infection in AC involve the release both of tail (e) and capsid (f) content in amoeba cytoplasm (red arrows). Ribophagy induced by Tupanvirus in *Tetrahymena* (TEM) (g) 72 hours post-inoculation. (h) Expression of Tupanvirus 18S-like-copy 1 transcript, 12 hours post infection observed by fluorescence in situ hybridization (FISH) (red). Tupanvirus-induced shut-down of *A. castellanii* ribosomal 18S transcripts is observed in green.

Figure 2: Tupanvirus rhizome (a) and DNA polymerase beta tree (b). The rhizome shows that most of Tupanvirus genes have mimiviruses as best-hits. However, correspondence among Tupanvirus and Archaea, Eukaryota and Bacteria was also observed. (b) DNA polymerase beta subunit maximum parsimony phylogenetic tree demonstrating the position of Tupanvirus among *Mimiviridae* members, likely forming a new genus.

Figure 3: Tupanvirus genome translation related factors. (a) Circular representation of Tupanvirus genome highlighting its translational-related factors (aaRS, tRNAs and PSF). The box (upright) summarizes this information. (b) Network of translational-related genes shared by Tupanvirus, mimivirus (APMV) and cell-world organisms - *Encephalitozoon cuniculi* (Eukaryota), *Nanoarchaeum equitans* (Archaea) and *Candidatus Carsonella ruddii* (Bacteria). The diameter of organism's circles (numbers) is proportional to the number of translational-related genes present in those genomes.

Extended Data Legends

Extended Data Figure 1: Tupanvirus particles and cycle special features. Scanning electron microscopy (SEM) of purified particles (a-d). The treatment of particles with lysozyme, bromelain and proteinase-K remove the most of fibers, revealing details of head and tail junction (a-c). Transmission electron microscopy (TEM) highlights the inner elements of the whole particle (e), star-gate face (f), capsid (g) and tail (h) transversally cut. Super particles (>2000nm) could be observed by TEM (i) and SEM (j and k). Immunofluorescence of Tupanvirus particles using anti-particle mouse-produced antibody (1000x zoom) (l). Cycle steps are showed from m to r. (m) Viral particles

attachment in AC surface; (n) phagocytosis; (o) particles in a phagosome; (p) early viral factor; (q and r) mature viral factories. Arrows highlight tail formation associated to the viral factories. VF: viral factory

Extended Data Figure 2: Tupanvirus cycle in A. castellanii observed by imunnofluorescence. Cells were infected at multiplicity of infection of 1 and observed at different time points post-infection. In green, viral particles detected by anti-tupan particles antibody produced in mouse. In red, amoeba cytoskeleton. H: hours post infection.

Extended Data Figure 3: Tupanvirus promoter's motifs and amino acid usage analysis. (a) Frequency of mimivirus AAAATTGA canonical promoter motifs in Tupanvirus intergenic regions. We also analyzed the presence of AAAATTGA motif with SNPs, considering each motif position. (b) Comparative amino acid usage analysis of Tupan, *A. castellanii* and mimivirus lineages A, B and C. The amino acid usage for protein sequences was calculated using CGUA (General Codon Usage Analysis) tool.

Extended Data Figure 4: Maximum parsimony phylogenetic trees of Tupanvirus peptide synthesis related genes.

Extended Data Figure 5: Analysis of Tupan 67 tRNAs distribution among amino acids (aa) categories, isoaceptors and their relation to viral aa usage. Bars represent the perceptual of use of a given codon (isoaceptor) related to a given aa. Dots above bars represent codons in which Tupanvirus presents one or more related tRNAs. Numbers above the squares represent the perceptual of codon occurrence covered by

Tupan tRNA, considering each aa. These numbers determined the colors, according the legend right-down in the figure.

Extended Data Figure 6: Genomic environment and best hits analyses of Tupanvirus 18S-like ribosomal region. Genomic environment of copy 1 (a) and copy 2 (b). The 100 best hits for copy 1 (c) and 2 (d).

Extended Data Figure 7: Subjacent regions of 18S-like core sequences in the genus *Mimivirus* and maximum parsimony phylogenetic tree of of 18S-like region. Core sequences are represented for lineages A (a), B (b), C (c) and Tupanvirus (d). Phylogenetic tree 18S-like region present in mimivirus (e), *Phycodnaviridae*, eukaryotes and fungi mitochondrion.

Extended Data Figure 8: Analysis of Tupanvirus 18S-like ribosomal regions (copies 1 or 2) expression in infected *Acanthamoeba castellanii* cells at times 30 minutes, 6 and 12 hours post infection. Fluorescence in situ hybridization (FISH) (a and b) and qPCR (c – copy 1 and d – copy 2). In red, viral 18S-like copies; in green *Acanthamoeba* 18S ribosomal region (a and b). FISH analysis related to time 24h post-infection, copy 1, is showed at Figure 1h.

Extended Data Figure 9: Ribophagy induced by Tupanvirus and ecological simulations. (a) Increasing of Tupan and APMV titers 24hpi in AC at distinct M.O.I.s. The titers are represented in log10. (b) Ribosomal 18S RNA relative measure by real-time PCR from AC infected by Tupan or APMV at M.O.Is of 10 or 100, after 3 and 9 hours post-infection. (c) Agarose electrophoresis gel showing ribosomal 18S and 28S

RNA from AC in the same conditions described in B. (d) Ribophagosome (R) containing a large amount of AC ribosomes under degradation after infection by Tupan. (e) Cytopathic effect of AC inoculated with Tupan or APMV after UV or heat inactivation, M.O.I. of 100, 8 hours post inoculation. (f) Counting of AC presenting cytopathic effect 8 hours post inoculation with Tupan inactivated by UV or heating under different M.O.I.s. (g) Ribosomal 18S RNA relative measure by real-time PCR from AC infected by Tupan UV or heat inactivated, or APMV, at M.O.I. of 100, after 3 and 9 hours post-infection. (h) Dose-response of Tupan and APMV titers in AC pre-treated with distinct doses of geneticin or cycloheximide. (i) Progressive vacuolization of tetrahymena cytoplasm after infection with Tupan from day 1 to day 4 post infection. (j) Tupan tail content release in tetrahymena 1 hour post infection (TEM). (k) Agarose electrophoresis gel showing ribosomal 18S and 28S RNA shut-down in tetrahymena infected with Tupan at MOI of 10 from day 1 to day 4. (l) Rate of incorporation of Tupan and APMV viral particles per tetrahymena cell from day 1 to day 4 post infection. (m) Ecological simulations showing the decrease of APMV, and maintenance of Tupan, titers through analyzed days after infection of a mix of AC and tetrahymena at M.O.I. of 10. At days 4 and 8 a input of fresh PYG medium and 10^5 AC were added to the systems.

Extended Data Table 1: Permissiveness profile of Tupanvirus in different cells.

Supplementary Information Legends

SI1: Excel file containing proteomics data-set of Tupanvirus particles and its comparison to mimivirus particles proteomics.

SI2: 2D predicted structure of Tupanvirus 67 tRNAs. This file was generated by ARAGORN tRNA prediction website (http://mbio-serv2.mbioekol.lu.se/ARAGORN/)

SI3: Detailed list of Tupanvirus translation-related factors. We present in this file best-hits analyses for each translation related factor (general, considering only nucleocytoplasmatic large DNA viruses – NCLDVs – or only other viruses).

SI4: Maximum parsimony phylogenetic trees of the 20 Tupanvirus aminoacyl tRNA synthetases (aaRS).

Title: Ribosomal sequences in viruses: what can they tell us?

Running title (5 words):

Jônatas Santos Abrahão[1,2], Lorena Christine Ferreira da Silva[1,2], Anthony Levasseur[1],

Philippe Colson[1] and Bernard La Scola[1,*]

1 Unité de Recherche sur les Maladies Infectieuses et Tropicales Emergentes (URMITE) UM63 CNRS 7278 IRD 198 INSERM U1095, Aix-Marseille Univ., 27 boulevard Jean Moulin, Faculté de Médecine, 13385 Marseille Cedex 05, France; philippe.colson@univ-amu.fr, anthony.levasseur@univ-amu.fr; bernard.la-scola@univ-amu.fr

2 Instituto de Ciências Biológicas, Departamento de Microbiologia, Laboratório de Vírus, Universidade Federal de Minas Gerais, Belo Horizonte, Minas Gerais, Brazil; jonatas.abrahao@gmail.com ; lorena.farmacia@yahoo.com.br

*** Correspondence:**
Dr Bernard La Scola
bernard.la-scola@univ-amu.fr

Abstract: The giant viruses astonished the scientific community not only by their particle size, but also due to their remarkable genome content. Among a wealthy arsenal of metabolic, transcriptional and DNA repair genes, giant viruses also encode translation-related genes; some of them (e.g. aminoacyl-tRNA-synthetases) have been seen for the first time in the virosphere. However, although exhaustive searches were made by many research groups, to the best of our knowledge, no ribosomal subunit sequences were found in giant viruses hitherto. Indeed, the presence of ribosomal sequences is considered an exclusive characteristic of cellular-world organisms' genomes. In this work we demonstrate that complete or partial 16S ribosomal sequences can be found in viral genomes available in Genbank. Most of these ribosomal sequences are related to phages genomes, although they were also found in Tokyovirus (a putative new marseillevirus) and Stealth virus 1. Based on similarity, synteny and phylogenetic analysis, our data suggest that, if these sequences are not artefacts of sequencing or contamination, they likely were acquired by mechanisms involving viral genome integration, by gene transfer from host mitochondria or from sympatric bacteria (which inhabit/parasite the same host). In this work we discuss the reasons to believe or not in the existence of ribosomal sequences in these viruses.

Keywords: ribosome; 16S ribosomal; translation; giant viruses; bacteriophages

1. Introduction

Viruses are well known to be obligatory intracellular parasites, deeply dependent on their hosts. Despite the fact that viruses are not a monophyletic group, they share a common lifestyle, exploiting metabolical, transcriptional and translational host pathways to produce their progeny [Lwoff, 1957; ICV, 2016]. However, some groups of DNA viruses present, in various diversity and abundance, key genes related to protein/nucleotide/lipid synthesis/carbohydrates pathways, transcription and even translation [Raoult et al, 2004; Boyer et al, 2009; Fischer et al, 2010; La Scola et al., 2013; Philippe et al, 2013 ; Legendre et al, 2015; Reteno et al, 2015].

Giant viruses of amoebas, including mimiviruses and viruses subsequently discovered using amoebal co-culture, represent an atypical example of genome complexity and ability to encode a number of proteins related to the aforementioned biological process, some of them being experimentally demonstrated as able to improve viral fitness [Raoult et al, 2004; Boyer et al, 2009; Fischer et al, 2010; Jeudy et al, 2012; La Scola et al., 2013; Philippe et al, 2013 ; Legendre et al, 2015; Reteno et al, 2015; Silva et al, 2015].

However, although exhaustive searches were made by many research groups, to the best of our knowledge, no ribosomal sequences were found in giant viruses hitherto. Indeed, the presence of ribosomal sequences is considered an exclusive characteristic of cellular-world organisms' genomes. It is quite curious that several host genes and genomic fragments have been described in viruses but one of the most highly expressed host transcripts, the ribosomal ones, are not found in viral genomes [Raoult et al, 2004; Boyer et al, 2009; Reteno et al, 2015]. In this work we demonstrate that complete or partial 16S ribosomal sequences can be found in viral genomes available in GenBank. Most of these ribosomal sequences are related to phage genomes, although they were also found in Tokyovirus (a putative new marseillevirus isolate) and Stealth virus 1, as previously published. Our data suggest that, if these sequences are not artefacts of sequencing or genome assembly, they were likely acquired via mechanisms involving genomic integration (in the case of phages), by gene transfer from host mitochondria or from sympatric bacteria inhabiting a common host.

2. Materials and Methods

2.1 Dataset preparation and selection criteria

The search for ribosomal sequences in the viruses' database available sequences in Genbank [Genbank, 2016] was focused on the 16S ribosomal subunit due to the larger availability of sequences of 16S than other ribosomal subunits. Searches for eukaryotic and other bacterial subunits (23S and 5S subunits) were performed but the results did not meet our criteria (see below), except for a *Dickeya phage* isolate that will be presented here. For the search, we collected 16S sequences from GenBank to prepare a dataset containing representatives from 14 bacterial/archaeal distinct groups: Acidobacteria, Actinobacteria, Chlamydiae, Chloroflexi, Cyanobacteria, Fusobacteria, Planctomycetes, Proteobacteria, Spirochaete, Gram-positive bacteria, Thermophile (bacterial groups); Crenarcheota, Euryarchaeota, Korarchaeota (archaea groups). A total of 10-20 sequences of each group was collected, belonging to distinct species and isolates. Each individual sequence from this dataset was used as query for BLAST

searches [BLAST, 2016] against viruses' taxid sequences using BLASTn default parameters to obtain a list of 16S-like viral sequence candidates.

The selection criteria used was: I) e-value should be <1e-4; II) fragments should be larger than 50 base pairs (bp); III) 16S-like environment (neighbor genes) should be related to translation process as previously described for cellular organisms (translational gene islands); IV) the 16S-like sequence should not overlap or disturb a known essential gene; V) the 16S-like sequence content and environment should be unique (to decrease the risk for this sequence to be obtained from a contaminant or due to genome misassembly). We select these criteria to improve the quality of analyses and to go as far as possible in terms of prediction of artefacts and contaminations.

2.2 Sequences analysis: environment, coverage, polymorphisms and phylogeny

After obtaining a list of viral 16S-like candidates, the environments of each 16S-like viral sequences were analyzed. In case of short length contigs/genomes (until 10,000 bp) the whole sequence was examined, while in case of long length contigs/genomes we analyzed ~15,000 bp upstream and downstream from 16S-like sequence. The nearby genes were examined by I) considering the original annotation; II) by BLASTing the fragments and analyzing manually each found gene; III) by searching for tRNA sequences using ARAGORN tRNA scan [Laslett and Canback, 2004].

The coverage (extension) of each obtained 16S-like sequence was first obtained from BLASTn and then analyzed using as reference a unique bacterial 16S sequence (*Escherichia coli* - gi556503834 - NC_000913.3). The common and exclusive covered regions were carefully analyzed as follows: the search for polymorphisms (SNPs, duplications and deletions) between viral and bacterial/eukaryotic sequences was also performed by using BLASTn (against the whole GenBank database) and by the preparation and analysis of alignments in MEGA 7.0 [Kumar et al, 2016]. Phylogenetic trees were constructed from the alignment of each taxonomical group aforementioned, using the maximum likelihood method and 1,000 replicates in the bootstrap test (MEGA 6.0). For Tokyovirus phylogenetic analysis, mitochondrial 16S sequences from different *Acanthamoeba* species were incorporated to the alignment and used for tree reconstruction.

3. Results

3.1 Viral 16S-like candidates selection, e-values and coverage

The prospecting of 16S ribosomal-like sequences in viruses resulted in the selection of six candidate hits from GenBank: *Dickeya phage* phiDP10.3 clone pD10 (KM209255.1), *Dickeya phage* phiDP23.1 clone pD23.contig.39_1 (KM209313.1), *Dickeya phage* phiDP23.1 clone pD23.contig.14_1 (KM209288.1) [*Dickeya* sp., these phage hosts, are associated with potato roots] [Czajkowski et al, 2015]; *Moraxella* pro-*phage* Mcat16 (KR093640.1) [*Moraxella catarrhalis*, the host, is commonly associated with infections in humans] [Ariff et al, 2015]; *Stealth virus 1* clone 3B43 (AF191073.1) [a cytomegalovirus associated with immunosuppressed patients] [Martin, 1999]; and Tokyovirus A1 DNA (AP017398.1) [a recently described marseillevirus] [Takemura,

2016]. This list of candidates was obtained by performing BLASTn searches using our 16S dataset against viruses' taxid (10239). The BLASTing of bacterial/archaeal/mitochondrial 16S sequences resulted in those six candidates, although the BLAST of some groups, especially archaea, resulted in fewer candidates (data not shown). Other viral 16S-like sequences were also obtained but were eliminated because they were declared as possible contaminants (e.g. *Bluetongue virus* - AY397620.1) or presented low quality (e.g. *Stealth virus* 1 clone 3B43 T3 - AF065755.1). Curiously, bacterial hits also appeared among viral ones in BLASTn results list, even after selecting exclusive search into "viruses" taxid. Nevertheless, bacterial sequences were also eliminated from our analysis. Considering that *Proteobacteria* group BLAST resulted in all those six candidates, we selected an *E.coli* (gi556503834) sequence to comparatively analyze the 16S-like obtained hits in terms of score, e-value, coverage, identity and other parameters (Table 1).

Unequivocal 16S ribosomal sequences were found in those available viral hits, with e-values ranging from 2E-20 (Tokyovirus) to 0 (others). The identity of these viral 16S hits with *E.coli (*gi556503834*)* ranged from 75% (*Moraxella phage*) to 97% (*Dickeya phage* clone pD23). Curiously, some viral 16S hits resulted in more than one piece that match the *E.coli* reference sequence (Table 1). The coverage of phage sequences was remarkably high. *Dickeya phage* phiDP10.3 clone pD10 presented 100% of 16S coverage. Considering that KM209313.1 and KM209288.1 are two contigs related to a same species/clone, *Dickeya phage* phiDP23.1 clone pD23, total coverage reached 93%, with a small gap between positions 561 and 656. In addition, *Moraxella phage* Mcat16 presented 78% of coverage (position: 21 to 1233). The coverages of eukaryotic viruses were lower: 56% for Stealth virus 1 (position: 674 to 1541) and 18% for Tokyovirus, considering the three obtained fragments (positions: 11 to 68; 296 to 390; 860 to 985) (Figure 1).

3.2 Analysis of 16S-like sequences' environment

The next step was to investigate the environment of viral 16S, to check the occurrence of other translation-related genes or elements, since it is common in genomes of cellular organisms. Also, it could give more clues about how the fragment acquisition happened and can indicate unique genomic arranges in the analyzed viral sequences. We observed that *Dickeya phage* phiDP10.3 clone pD10 complete 16S sequence (position 197 to 1914) contain not only a tRNA-Glu (2001-1076) but, more surprisingly, a 23S ribosomal sequence (2273-5179), likely acquired from its host after integration and lytic reactivation (Figure 2A). For *Dickeya phage* phiDP23.1 clone pD23, we observed that both partial 16S sequences (1-887; 2-563) overlap with hypothetical protein encoded genes. In addition, a tRNA-Glu (974-1049) was found close to the 16S fragment in contig 39 (Figure 2B). Similarly, we found a tRNA-Leu (8496-8580) downstream to 16S fragment (3450-4630) in *Moraxella phage* Mcat16 and an integrase gene (14731-15924) (Figure 2C). *Stealth virus* 1 contains two tRNAs (Ala:2217-2292; Ile: 2407-2483) close to its partial 16S sequence (2754-3620) (Figure 2D). Finally, Tokyovirus 16S fragments (6380-6438; 6768-6861; 7737-7861) presented upstream two tRNAs (His: 5265-5336; Pseudo :5345-5419) and downstream a gene annotated in GenBank (AP017398.1) as ribosomal protein L22 (10212-10751), although we were not able to find evidence that could link this ORF to L22 (Figure 2E).

3.3 Search for special features in 16S-like sequences and in their environments

A main concern during our analysis was if these candidate sequences were artefacts of sequencing or contamination with host sequences. Therefore we looked for special features in viral 16S-like sequences and their nearby genes/elements that could indicate their uniqueness. The analysis of *Dickeya phage* phiDP10.3 clone pD10 16S like sequence revealed that although the almost-whole contig can be found in its host *Dickeya solani* (gb|CP015137.1) there is a 175 bp unique duplication in *Dickeya phage* pD10 16S (positions 567-741/743-917), interestingly located in ribosomal variable region 3 (V3). Although very similar, the copies of this duplication are not identical, since there is an A/G substitution in downstream copy. For *Dickeya phage* phiDP23.1 clone pD23 (considering both contigs), the search for viral 16S-like special features also revealed variation, restricted to 6 or 64 unique mismatches in comparison to *Dickeya solani* (gb|CP015137.1) homologous region (the number of mismatches is variable amongst many *Dickeya solani* 16S paralogos) (Table 2).

Regarding *Moraxella phage* Mcat16, it presented a 16S partial sequence environment unique organization. Although other *Moraxella phage* Mcat clones also present the downstream region from 16S, no one presented 16S as found in Mcat16clone. As expected, the canonical host *Moraxella catarrhalis* presented a similar 16S environment, however the analyzed sequence (1-15924) presented >60 mismatches. More interestingly, the 16S upstream region was not found in *M. catarrhalis*, but fragments of this region were found in other bacteria, especially in *Helicobacter pylori* (gb|CP006889.1) (Table 2).

We analyzed the *Stealth virus* 1 clone 3B43 environment special features using the whole sequence (3620bp). The BLAST of this sequence against the complete GenBank database revealed as best hit the bacterium *Ochrobactrum pseudogrignonense* strain K8. It was observed an almost complete coverage of the fragment, except for region from 2302 to 2403 (101 bp), which did not match any sequence among the best hits. Even related to *Ochrobactrum sp., Stealth virus 1* clone 3B43 (AF191073.1) presented 77 and 28 mismatches related to the first and second fragments that matched with this bacterium, respectively (Table 2).

Finally, Tokyovirus 16S-like fragments environment's special features were analyzed. Considering the position 1 to 10751 in Tokyovirus genome (AP017398.1), where the 16S-like fragments (6380-6438; 6768-6861; 7737-7861) and L22 are present, it was possible to observe a predominance of regions with high similarity to *Acanthamoeba* sp. mitochondrial genomic fragments (coverage ~50%), including the Tokyovirus 16S-like region. However, the order and arrangement of these fragments (synteny) are highly variable, not keeping the same order and/or orientation in both genomes (Figure 3). The GC% content of region 1-8225 in Tokyovirus (where we found the most downstream mitochondrial piece in 5' end of Tokyovirus genome – Figure 3) is 33.86%, being more similar to mitochondrial GC% content (29.39%) than to the rest of Tokyovirus genome (44.4%). Interestingly, we also found another region with high similarity to *Acanthamoeba* sp. mitochondrial genomic fragments in 3' end of Tokyovirus genome, not related to 16S. It is important to highlight that marseilleviruses' genomes are usually circular and 3'-end might be a continuation of 5'-end, where 16S environment analysis were performed (Figure 3). Although a first examination of 16S-like region may suggest

that this specific Tokyovirus genomic region might be an artefact, possibly a contamination from amoebal mitochondria, the lack of synteny between these elements is intriguing and indicates that Tokyovirus is worthy to be re-sequenced to confirm or discard this potential important finding. To date, this region is not totally found in other marseilleviruses.

3.4 Phylogenetic and best hits analysis

Phylogenetic analysis based on 16S regions present in each viral sequence (Figure 2) suggest 16S acquisition from cellular organisms. Regardless the 16S analyzed region, all bacterial/archaeal/mitochondrial hits clustered in the expected phylum. However, in some trees we could observe variation in the positions of these intra and inter clades. Therefore our trees were useful to investigate the closest high clade (e.g. bacterial phyla) to each viral 16S-like sequence, but not to infer about 16S transfer in species level. Our strategy to infer 16S transfer in species level was to check the best hits after BLASTing viral 16S-like regions (BLAST n).

As expected, the most related clade to 16S of *Dickeya phage* phi clones is *Proteobacteria*, in which *Dickeya* sp. belongs to (Figure 4 A and B). *Dickeya* sp. isolates are the best hits of *Dickeya phage* phi clones analyzed here (BLASTn). Together, these results would reinforce the theory of 16S acquisition from the host through mechanisms involving phage reactivation after genome integration.

For *Moraxella phage* Mcat16 we observed an interesting result: the phylogenetic tree shows the clustering of viral 16S-like with Proteobacteria, the phyla of *Moraxella* sp (Figure 4D). However, the best hit (BLAST n) of *Moraxella phage* Mcat16 16S-like region is *Helicobacter* sp., which is also a Proteobacteria, but from a distinct intra-clade (*Moraxella* is a Gammaproteobacteria, while *Helicobacter* is an Epsilon proteobacteria). This result could indicate a different/unknown host or a convergent evolution in 16S regions. Regarding the eukaryotic viruses, *Stealth- virus 1* 16S fragment also clustered with Proteobacteria (Figure 4E) and as observed in the whole available fragment analysis (Table 2), the BLASTing of 16S fragment shows *Ochrobactrum sp.*, an opportunistic emerging Proteobacteria, as the best hit. At last, we constructed a tree for Tokyovirus 16S largest fragment, since the other fragments are very short (58 and 93bp) and attempts of tree construction using only 16S respective regions showed instability amongst bacterial clades. The tree showed Tokyovirus 16S largest fragment clustering into acanthamoebal mitochondrial 16S group (Figure 4F). The best hits of the three fragments (Figure 2) are also acanthamoebal mitochondrial 16S.

4. Discussion

Ribosomes are well known to be trademarks of cellular organisms [Raoult and Forterre, 2008]. Their complex operation requires much more than rRNA subunits, but also dozens of associated proteins [Rodnina et al, 2011]. To carry all this information seems not to belong to natural history of viruses and certainly would require a very large piece of their usually reduced genomes. In this work we demonstrate that complete or partial 16S ribosomal sequences can be found in viral genomes available in GenBank. This finding can be considered surprising, although its biological meaning remains to be investigated. To contain a complete or partial 16S sequence in a genome does not mean

that a "viral ribosome" is under transcription and associated to improvements in viral fitness. But, if those 16S-like sequences are not artefacts of sequencing, assembly or contamination, they could raise questions about the involvement of ribosomal sequences in host-virus or virus-host gene exchange and in the dynamics of rhizome of life [Raoult, 2010].

Despite questions related to the biological meaning of viral 16S-like sequences, we believe that it is important to discuss the technical aspects that support or discard the possibility that these sequences are no more than artefacts. Indeed, we believe that all viral 16S-like sequences here analyzed deserve more investigation and the results should be taken with caution. However, it is at least intriguing that the 16S-like sequences presented here were observed in viral species well known to be "masters of gene exchange" [Ariff et al, 2015; Czajkowsk et al, 2015; Martin, 1999; Takemura, 2016]. Still in the classical age of bacteriophage biological studies, the phenomenon of transduction was discovered, in which a phage promotes gene exchange among bacteria [McGrath and Van Sinderen, 2007]. Studies showed that phage genomic integration can be site-directed, however the integration followed by acquisition of genes (or gene fragments) by phages from bacteria can be random and can involve or not fitness improvement to phages, or even to the new bacterial host after lysogenic infection [Christiansen, 1996]. Indeed, considering the diversity of still unknown bacteria and phages, it is reasonable to admit that sometimes ribosomal sequences could be incorporated by phages genomes. For stealth virus and Tokyovirus we hypothesize that the mechanisms of heterologous gene acquisition would be very likely different to those described for phages, probably involving the incorporation of host mitochondria/sympatric bacteria sequences after reverse transcription of available mRNAs/rRNAs or by homologous recombination during viral genome replication [Ariff et al, 2015; Czajkowsk et al, 2015; Martin, 1999; Takemura, 2016]. Nevertheless, both viral groups, particularly marseilleviruses, are well known to contain a large number of genes acquired from gene transfer from amoeba or sympatric bacteria or viruses [Boyer et al, 2009]. At least in theory, the more bacterial sequences a given virus contains in its genome, the more the occurrence of adequate conditions for new homologous recombination with bacterial genomes is probable.

Another evidence that could indicate that viral 16S-like sequences are not artefacts is the moderate to high number of mutations observed in these sequences in comparison to their best hits (except for Tokyovirus). *Dickeya phage* clone pD10 presents a unique duplication in a 16S-like, not seen in any available sequence from its host; while clone pD23 contains unique mutations in the largest fragment. Similarly, *Moraxella phage* Mcats16 and *Stealth virus* 1 16S-like fragments presented a very high number of mismatches in comparison to their respective best hits. In all cases, it might indicate an independent evolution after 16S incorporation. At last, another important point to be considered regards 16S sequences' environments. All viruses here analyzed presented unique gene-set configuration in 16S region, in terms of content and/or organization. This also would indicate independent evolution after 16S and weakens the hypothesis of sequence contamination. Tokyovirus 16S-region for example, showed a lack of syntheny with fragments hypothetically acquired from an amoebal mitochondria genome. An important fact about Tokyovirus 16S environment is the presence of a gene predicted to resemble a ribosomal protein L22, downstream of 16S fragments. Ribosomal proteins (as rRNA) are exclusive of cellular organisms, therefore it would be an important finding. However, we were not able to find clear evidence that might link

this gene to a ribosomal protein. A carefully analysis of Tokyovirus annotation could elucidate this question.

Despite evidence that might suggest the uniqueness of viral 16S sequences, we can point to a number of reasons to be suspicious about them, including: (I) the lack of 16S sequences in other viral isolates available in GenBank; (II) and for this reason, those sequences were not obtained by other research groups; (III) in the case of *Dickeya phage* clones, the 16S-like sequences were obtained from contigs in which the authors were not able to insert a final version of the genome during the assembly; (IV) except for Stealth virus, in all systems a possible source of contamination was present in the system (host genome or its mitochondria); (V) unknown or unavailable technical issues (in which all available sequences in Genbank are subject), like low coverage, mistakes during assembly, etc.

In conclusion, our data demonstrates that 16S ribosomal fragments are present in viral sequences available in GenBank, with specific and/or exclusive features in their content and environments. If not artefacts, theses sequences were likely acquired from their hosts or sympatric organisms, although the biological meaning of this phenomenon remains to be investigated. We believe that these findings are important, especially if we consider the canonical natural history of viruses. However, the re-sequencing of these viruses would be a *sine qua non* condition for the confirmation of these data and for further biological conclusions related to the presence of ribosomal sequences in viral genomes.

Conflicts of Interest

The authors declare no conflict of interest.

Author Contributions: J.S.A. and L.C.F.S. performed dataset preparation; J.S.A. performed sequence alignments, environment and polymorphisms analysis, phylogenetic constructions; J.S.A., A.L., P.C. and B.L. designed the study and defined the selection criteria; all authors wrote and approved the manuscript.

Acknowledgments and Funding

We thank CNPq, CAPES-COFECUB, FAPEMIG and Mediterranean Foundation Infection for their financial support.

Figure Legends

Figure 1: Position and coverage of viral 16S-like sequences in comparison to E.coli 16S (gi556503834).

Figure 2: Environment of viral 16S-like sequences. The environments of viral 16S-like sequences were investigated to evaluate the presence of other translation-related genes or elements. The positions indicated correspond to genes/elements in viral hits.

For A and B schemes, the whole contigs are represented; for C, D and E we represented only the 16S neighborhood area.

Figure 3: Synteny between Tokyovirus (AP017398.1, region from 1 to 10751) and *A. castellanii* mitochondria complete genome (U12386.1). These sequences were BLASTed (n) and all the "ranges" with e-value <E-4 and identity>99% were plotted in the diagram considering their positions in both genomes. In Tokyovirus partial genome scheme (above) are highlighted regions corresponding to tRNAs, 16S (regions 1, 2 and 3), an uncharacterized protein (Unc. Prot.) and the predicted ribosomal protein (L22). For more details about these regions, please see Figure 2. RC: regions that match as reverse complement.

Figure 4: Phylogenetic trees based on 16S regions present in each viral sequence. For more information about these regions please see figure 2. Phylogenetic trees were constructed from the alignment of each taxonomical group aforementioned, using maximum likelihood method, 1,000 bootstrap (MEGA 6.0). For Tokyovirus phylogenetic analysis, mitochondrial 16S sequences from different *Acanthamoeba* species were incorporated to the alignment and used for trees construction. A: *Dickeya phage* phiDP10.3 clone pD10 (KM209255.1); B: *Dickeya phage* phiDP23.1 clone pD23.contig.14_1 (concatenated tree of KM209288.1 and KM209313.1); C: *Moraxella phage*Mcat16 (KR093640.1); D: *Stealth virus 1* clone 3B43 (AF191073.1); E: Tokyovirus A1 DNA (AP017398.1), largest 16S fragment.

Tables

Table 1: Viral 16S-like sequences. This list of candidates was obtained by BLASTing *E. coli*16S sequence (gi556503834) against GenBank viruses' taxid (10239).

Organism	Max Score	Total Score	Coverage	E-value*	Identity	Access Number	Number of pieces	Position (s) in viral hit
Dickeya phage phiDP10.3 clone pD10.contig.26_1	1862	2693	100%	0.0	95%	KM209255.1	2	743-1914 197-741
Dickeya phage phiDP23.1 clone pD23.contig.39_1	1474	1474	57%	0.0	97%	KM209313.1	1	1-887
Dickeya phage phiDP23.1 clone pD23.contig.14_1	848	848	36%	0.0	94%	KM209288.1	1	2-563
Moraxella phage Mcat16	812	812	78%	0.0	75%	KR093640.1	1	3450-4630
Stealth virus 1 clone 3B43	810	810	56%	0.0	81%	AF191073.1	1	2754-3620
Tokyovirus A1 DNA	107	225	18%	2,00E-20	79%	AP017398.1	3	7737-7861 6768-6861 6380-6438

*e-value of the best fragment (piece).

Table 2: viral 16S-like sequences and neighbor genes special features

Organism/contig	Access number	Length*	Observation
Dickeya phage phiDP10.3 clone pD10	KM209255.1	5269bp	Unique duplication (position 567-741/743-917) in 16S sequence
Dickeya phage phiDP23.1 clone pD23 (contigs 14 and 39)	KM209313.1 KM209288.1	1090/888bp	A total of 6 to 64 mismatches in comparison to *Dickeya solani* (host)
Moraxella phage Mcat16	KR093640.1	46782bp (analyzed from 1 to 15924)	More than 60 mismatches in comparison to the expected host *Moraxella catarrhalis*
Stealth virus 1 clone 3B43	AF191073.1	3620 bp	A total of 105 mismatches in comparison to *Ochrobactrum pseudogrignonense* strain K8v(gb|CP015775.1), the best hit
Tokyovirus A1 Marseillevirus	AP017398.1	372707 bp (analyzed from 1 to 10751)	Similar to *A.castellanii* mitochondria, but with a different organization

* In cases of large genomes (Moraxella and Tokyovirus) the analysis were made on the region related to the 16S neighborhood

References

Ariff, A., Wise, M.J., Kahler, C.M., Tay, C.Y., Peters, .F, Perkins, T.T., Chang, B.J. (2015). Novel Moraxella catarrhalisprophages display hyperconserved non-structural genes despite their genomic diversity BMC Genomics. 16, 860.

Blast website. Available online: http://blast.ncbi.nlm.nih.gov/Blast.cgi

Boyer, M., Yutin, N., Pagnier, I., Barrassi, L., Fournous, G., Espinosa, L., et al. (2009). Giant Marseillevirus highlights the role of amoebae as a melting pot in emergence of chimeric microorganisms. Proc. Natl. Acad. Sci. USA. 106, 21848-21853.

Christiansen, B., Brøndsted, L., Vogensen, F.K., Hammer, K. (1996). A resolvase-like protein is required for the site-specific integration of the temperate lactococcal bacteriophage. J. Bacteriol. 178, 5164–5173.

Czajkowski, R., Ozymko, Z., de Jager, V., Siwinska, J., Smolarska, A., et al. (2015). Genomic, proteomic and morphological characterization of two novel broad host lytic bacteriophages ΦPD10.3 and PD23.1 infecting pectinolytic Pectobacterium spp. and Dickeya spp. *PLoS One*. 10(3), e0119812.

Fischer, M.G., Allen, M.J., Wilson, W.H., Suttle, C.A. (2010) Giant virus with a remarkable complement of genes infects marine zooplankton. Proc. Natl. Acad. Sci. USA. 107, 19508-19513.

Genbank website. Available online: http://www.ncbi.nlm.nih.gov/genbank/

ICTV (2016): Last taxonomic release. Available online: http://www.ictvonline.org/

Jeudy, S., Abergel, C., Claverie, J.M., Legendre, M. (2012). Translation in Giant Viruses: A Unique Mixture of Bacterial and Eukaryotic Termination Schemes. PLoS Genet. 8, e1003122.

Kumar, S., Stecher, G., Tamura, K. (2016). MEGA7: Molecular Evolutionary Genetics Analysis Version 7.0 for Bigger Datasets. Mol. Biol. Evol. 33(7),1870-4.

La Scola, B., Audic, S., Robert, C., Jungang, L., de Lamballerie, X., Drancourt, M., et al. (2003). A giant virus in amoebae. Science. 299, 2033.

Laslett, D., Canback, B. (2004). ARAGORN,
a program to detect tRNA genes and tmRNA genes in nucleotide sequences. Nucleic Acids. Res. 32(1), 11-6.

Legendre, M., Lartigue, A., Bertaux, L., Jeudy, S., Bartoli, J., Lescot, M., et al. (2015). In-depth study of Mollivirus sibericum, a new 30,000-y-oldgiant virus infecting Acanthamoeba. Proc. Natl. Acad. Sci. USA. 112, E5327-5335.

Lwoff, A. (1957). The concept of virus. J Gen Microbiol. 17, 239-253.

Martin, W.J. (1999). Bacteria-related sequences ina simian cytomegalovirus derived stealth virus culture. Exp. Mol. Pathol. 66(1), 8-14.

McGrath, S. and Van Sinderen, D. (2007). *Bacteriophage: Genetics and Molecular Biology*. Caister Academic Press: e-book.

Philippe, N., Legendre, M., Doutre, G., Couté, Y., Poirot, O., Lescot, M., et al. (2013). Pandoraviruses: amoebae viruses with genomes up to 2.5 Mb reaching that of parasitic eukaryotes. Science. 341, 281-286.

Raoult, D. (2010). The post-Darwinist rhizome of life. Lancet. 9709, 104-5.

Raoult, D., Audic, S., Robert, C., Abergel, C., Renesto, P., Ogata, H., et al. (2004). The 1.2-Megabase Genome Sequence of Mimivirus. Science. 306, 1344-1350.

Raoult, D., Forterre, P. (2008). Redefining viruses: lessons from Mimivirus. Nat. Rev. Microbiol. 6(4), 315-9.

Reteno, D.G., Benamar, S., Khalil, J.B., Andreani, J., Armstrong, N., Klose, T., et al. (2015). Faustovirus, an asfavirus-related new lineage of giant viruses infecting amoebae. J Virol. 89, 6585-6594.

Rodnina, M.V., Wintermeyer, W., Green, R. (2011). *Ribosomes Structure, Function, and Dynamics*. Springer: e-book.

Silva, L.C., Almeida, G.M., Assis, F.L., Albarnaz, J.D., Boratto, P.V., Dornas, F.P., et al. (2015). Modulation of the expression of mimivirus-encoded translation-related genes in response to nutrient availability during Acanthamoeba castellanii infection. Front. Microbiol. 6, 539-543.

Takemura, M.G. (2016). Draft Genome Sequence of Tokyovirus, a Member of the Family Marseilleviridae Isolated from the Arakawa River of Tokyo, Japan. Genome Announc. 4(3), e00429-16.